Masked 2-Furylcarbinol Derivatives: A Modular and General Platform for Mechanically Triggered Molecular Release

Thesis by

Tian Zeng

In Partial Fulfillment of the Requirements for

the degree of

Doctor of Philosophy

CALIFORNIA INSTITUTE OF TECHNOLOGY

Pasadena, California

2024

(Defended Jan 24, 2024)

Tian Zeng
ORCID: 0000-0001-5957-3442

ACKNOWLEDGEMENTS

My research journey started when I met Prof. Keary Engle in the summer of 2016 at a research mixer in UCSD, where he explained that an alkene could act as an electrophile when activated by a transition metal. Having just completed my organic chemistry classes, this blew my mind. I worked in the Engle lab for the remaining two years of my undergraduate career, gained organic chemistry skills, experienced what conducting research was like, and learned how to have fun as a lab.

The person who challenged and supported me to mature, not just as a researcher but also as a person, is my advisor Prof. Maxwell Robb. Over the last 5.5 years, he has taught me to think deeply about a problem, to be organized with planning projects and experiments, to communicate and ask for help, and to not be afraid to fail. He encouraged me in the face of opportunities, adapted his mentoring style when I struggled, and celebrated my small accomplishments. My committee members Prof. Gregory Fu, Prof. Sarah Reisman, and Dr. Lu Wei were also instrumental to my graduate career. They witnessed and supported my growth, shared valuable advice for working in academia, and helped me in my post-doc finding process. Other members of the Caltech community were also very important in my completing grad school. Prof. Henry Lester was always kind and encouraging to me and lent an ear when I was uncertain about my future after grad school, Dr. Scott Virgil was always patient and helpful with my purification and separation problems, Dr. David Vander Velde is a wizard with NMRs, and Dr. Mona Shahgholi not only assisted me in so many HRMS experiments but also provided encouraging words when I was down. Caltech is a very special place to me. I am appreciative of all the free meals at events, all the opportunities to network and dine with visiting faculties and scientists, and all the friendly faces in the entire CCE department. It's always fun to stop and chat with Annette Luymes, Joe Drew, Alison Ross.

The Robb group is a small family to me. My mentor Dr. Xiaoran Hu, taught me how to troubleshoot problems and think creatively. Without you I wouldn't have had such a fulfilling graduate career. I am so grateful for my mentees Yu-Ling Tseng (Debbie), Jolly Patro, and Liam Ordner. You all taught me efficiency, effective communication, and the art

of mentoring. I can't wait to see you all continue to flourish. To my cohort, Dr. Anna Overholts, Dr. Brooke Versaw and Dr. Corey Husic, I've learned so much from each of you and thank you for always being there with compassion and open arms. Graduate school was much easier with you all by my side. To my friends Dr. Jessica Beard and Dr. Peng Liu. I'm sad that our time together was so short, but I'm thankful I met you and look forward to more future times together. Dr. Molly McFadden, thank you for our late-night talks, teary conversations, and phone calls. Dr. Ross Barber, and Skylar Osler, thank you for game nights and fun times in the lab. Meng Luo (Stella) and Yan Sun, thank you for great times at dumpling parties, hot pot, and karaoke. Dr. Quan Gan, thank you for welcoming me to Caltech and introducing me to the Chinese community in CCE. Analiese Wiedenbeck and Nathan Ballinger, thank you for bringing a breath of fresh air and new energy to my last year in the group. Wendy Granados Razo, thank you for being a constant source of joy.

I am also fortunate to have had support from people outside of the Robb group. Dr. Yujia Tao has been there for me since our Caltech visit weekend. Dr. Jeong Hoon Ko was always there when I needed wisdom and a chat. Dr. Yuxing Yao is constantly overfilled with research ideas, encouragement and a fun time. Gracie Zhang and Drew Honson, the DND world we created together with Anna is one that I don't want to leave. Tim Csernia, our lunches always brought me joy and peace. Dr. Kun Miao, Dr. Jiajun Du, Dr. Weilai Yu, Ziyang Qin, Dongkwan Lee, Dr Xinhong Chen, Hailan Yu, Arshiyan Alam Laaj, thank you for all the fun we've had together, whether it's spending holidays together, going out for food, playing basketball, watching shows, playing mahjong or singing with Stella and Yuxing. Dr. Isabel Klein, Dr. Bryce Hickam, and Dr. Jonathan Michelsen, thank you for our game nights and pool parties. Anna's mom and Isabel's mom, thank you for your encouragement and our conversations. You all made my time at Caltech fun and memorable.

Outside of Caltech I am grateful to have people I can escape to. Pearl Lee and her parents have known me since 18, and 10 years later still provide a space of comfort. Pearl, thank you for all these years of support. For encouraging my ventures into art, always being there when I need someone to talk to, and helping me maintain my silliness. Hilary Taylor

and Rosina Gelormino, thank you for being your warm and silly selves. I cherish our times experiencing LA together, our road trips, night beach times and dance parties.

None of this would be possible without my family. Thank you to my mom and dad for giving me the space to fly and a place to land. Your unconditional love and constant support form my strongest backbone. To my aunt, thank you for taking care of my grandparents, allowing me to have a peace of mind while I am abroad. I may feel guilty for not visiting home enough, but seeing videos and photos of my grandparents healthy and happy brings me the warmest feeling. Finally, to my partner, Dr. Zhen Liu. Thank you for the past 7.5 years together. Your encouragement, respect and understanding through my happiest and most challenging times have been what got me through it all.

In closing, I again extend my deepest gratitude to all of you. Your support, encouragement, and love have made a lasting impact on my life. As I move forward, I carry the lessons and warmth you've provided. Thank you for being a part of my journey.

ABSTRACT

Stimuli-responsive polymers that undergo chemical transformations when exposed to external stimuli are attractive materials for a wide range of applications, such as targeted drug delivery, sensing, and catalysis. Within the emerging field of polymer mechanochemistry, *mechanical force* is harnessed to promote productive chemical transformations in stress-responsive molecules known as mechanophores. My research over the past several years has focused on the development of a modular and general mechanophore platform capable of releasing covalently-bound payloads in response to mechanical force. I envision that the further advancement of this design will not only aid in a deeper understanding of the design principles of mechanophores, but also enable new technologies, including non-invasive spatiotemporal delivery of bioactivate small molecules and self-healing materials.

Chapter 1 reviews the recent process of the development of small molecule-releasing mechanophores and provide an overview of the masked 2-furylcarbinol derivatives we developed that enables a mechanically gated release cascade. Chapter 2 describes our initial demonstration of mechanically gated small molecule release from our mechanophore and the subsequent structural-property investigation to optimize for faster release rates. In Chapter 3, an alternative mechanophore design is introduced that has a shortened synthetic sequence while maintaining a fast release kinetics. In Chapter 4, we address the challenge of low release capacity from previous designs with a novel mechanophore that can be incorporated into multimechanophore polymers. Finally, Chapter 5 demonstrates the use of our modular and general release platform to trigger the depolymerization of a self-immolative polymer.

PUBLISHED CONTENT AND CONTRIBUTIONS

Portions of the work described herein were disclosed in the following publications:

1. Versaw, B. A.; Zeng, T.; Hu, X.; Robb, M. J. "Harnessing the Power of Force: Development of Mechanophore for Molecular Release" *J. Am. Chem. Soc.* **2021**, *143*, 21461–21473, DOI:10.1021/jacs.1c11868.

   T.Z. participated in partial writing of the manuscript.

2. Hu, X.; Zeng, T.; Husic, C. C.; Robb, M. J. "Mechanically Triggered Small Molecule Release from a Masked Furfuryl Carbonate," *J. Am. Chem. Soc.* **2019**, *141*, 15018–15023, DOI:10.1021/jacs.9b08663.

   T.Z. participated in the design of the project, synthesized materials, ran experiments, and analyzed data.

3. Hu, X.; Zeng, T.; Husic, C. C.; Robb, M. J. "Mechanically Triggered Release of Functionally Diverse Molecular Payloads from Masked 2-Furylcarbinol Derivatives," *ACS Cent. Sci.* **2021**, *7*, 1216–1224, DOI: 10.1021/acscentsci.1c00460.

   T.Z. participated in the design of the project, synthesized materials, ran experiments, and analyzed data.

4. Zeng, T.; Hu, X.; Robb, M. J. "5-Aryloxy Substitution Enables Efficient Mechanically Triggered Release from a Synthetically Accessible Masked 2-Furylcarbinol Mechanophore," *Chem. Commun.* **2021**, 57, 11173–11176, DOI: 10.1039/d1cc04886d

   T.Z. participated in the conception and design of the project, synthesized materials, ran experiments, analyzed data, and wrote the manuscript.

5. Zeng, T.; Ordner L. A.; Liu, P.; Robb, M. J. "Multimechanophore Polymers for Mechanically Triggered Small Molecule Release with Ultrahigh Payload Capacity" *J. Am. Chem. Soc.* **2023**, DOI: 10.1021/jacs.3c11927.

   T.Z. participated in the conception and design of the project, synthesized materials, ran experiments, analyzed data, and wrote the manuscript.

TABLE OF CONTENTS

Chapter 1

INTRODUCTION: DEVELOPMENT OF MECHANOPHORES FOR MOLECULAR RELEASE

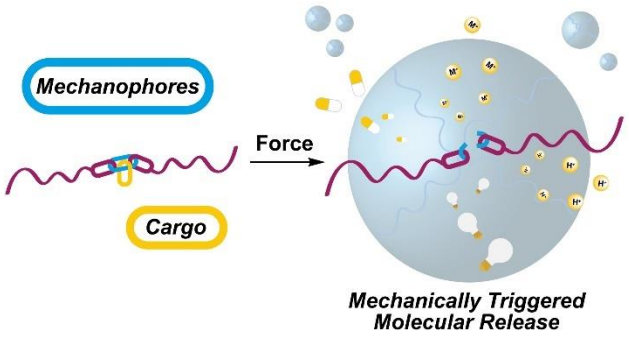

Abstract: Polymers that release small molecules in response to mechanical force are promising materials for a variety of applications ranging from sensing and catalysis to targeted drug delivery. Within the rapidly growing field of polymer mechano-chemistry, stress sensitive molecules known as mechanophores are particularly attractive for enabling the release of covalently-bound payloads with excellent selectivity and control. Here, we review recent progress in the development of mechanophore-based molecular release platforms and provide an optimistic, yet critical perspective on the fundamental and technological advancements that are still required for this promising research area to achieve significant impact.

This chapter has been adapted with permission from
Versaw, B. A., Zeng, T., Hu, X., Robb, M. J. *J. Am. Chem. Soc*. **2021**, *143*, 21461-21473.

1.1 Polymer Mechanochemistry: Enabling Productive Reactivity Using Mechanical Force.

In the rapidly growing field of polymer mechanochemistry, mechanical force is used to activate the chemical transformations of stress-sensitive molecules termed mechanophores.[1,2] Polymers maintain the important role of transducing mechanical force to the mechanophore via covalent connectivity. In contrast to nonspecific bond scission commonly associated with the mechanical degradation of polymers, mechanophores respond to force chemoselectively to elicit productive chemical changes.[3] Theoretical studies have revealed that the unique mechanochemical activity of mechanophores arises from a distortion of the potential energy surface under large forces, fundamentally changing the reaction landscape.[4–6] Mechanical force has been shown to promote remarkable transformations such as formally forbidden electrocyclic ring-opening reactions of benzocyclobutene and *gem*-dihalocyclopropanes.[7,8] The force-coupled activation of specific covalent bonds in mechanophores has also been harnessed to afford a wide range of productive chemical reactions and responsive materials.[9,10] Examples include, but are certainly not limited to, conductivity switching[11] and the generation of colored,[12–17] fluorescent,[18–20] or chemiluminescent species,[21] enabling the visual detection of stress and strain. Mechanochemical reactions have also been used to activate latent catalysts[22,23] and generate reactive functional groups,[7,24–26] imbuing polymers with self-healing properties or the ability to strengthen under typically destructive shear forces.[27] Research in the last two decades has produced an impressive library of more than one hundred mechanophores that spans an incredibly diverse range of structure and function.[28]

In a pioneering report from 2005, Moore and coworkers described the site-specific chain scission of polymers containing a mechanically weak azo group near the chain midpoint under the application of force. Mechanochemical fragmentation of the azo-linked polymers was putatively accompanied by the liberation of dinitrogen, which also makes it the first example of mechanically triggered molecular release in polymer mechanochemistry.[29] In the last few years, the topic of mechanically triggered release has gained significant attention. A quickly expanding collection of mechanophores and different mechanochemical reaction strategies are being devised to advance this important research

area, which promises applications ranging from remote controlled drug delivery to catalysis and sensing. Here, we review current progress in the development of mechanophore-based platforms for molecular release with the aim of summarizing notable contributions to the field and providing insight for future development.

1.2 Mechanically Triggered Molecular Release from Specialized Mechanophores

Several different mechanophores have been developed enabling the force-triggered release of small molecules. Unlike the more generalized platforms discussed later, each approach discussed in this section leverages a judiciously designed mechanophore to release a specific compound upon mechanochemical activation. As a result, these mechanophore design strategies are relatively limited in their modularity and the scope of molecules that can be released. Nonetheless, the mechanically triggered release of a small but relatively diverse collection of molecular payloads has been demonstrated through a range of distinct reaction manifolds.

Following their pivotal report on a dinitrogen-evolving azo mechanophore, Moore and coworkers described the mechanically triggered release of another simple diatomic molecule, HCl. As one of the simplest possible reagents and catalysts, the mechanically coupled generation of HCl is promising for the design of stress responsive polymeric materials in which self-healing, degradation, pH-driven optical signals, and other property changes are triggered with acid. The design is based on the mechanically-promoted electrocyclic ring-opening reaction of an indene-derived *gem*-dichlorocyclopropane (*g*DCC) mechanophore and spontaneous aromatization to drive HCl elimination (Scheme 1.1a).[30]

Scheme 1.1. The mechanically triggered release of HCl is achieved through ring opening and spontaneous elimination of specialized gDCC mechanophores.

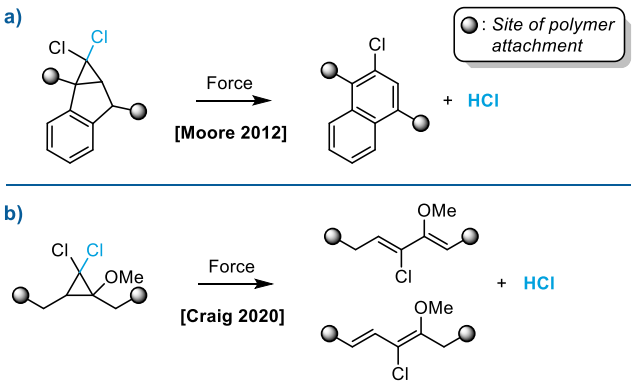

Compression of a poly(methyl acrylate) (PMA) network covalently crosslinked with the *g*DCC derivative resulted in mechanochemical activation of the mechanophore and HCl generation as demonstrated colorimetrically using a methyl red indicator as well as several other analytical techniques. Control experiments in which the mechanophore was physically incorporated into a PMA network and subjected to the same compression did not result in the same immediate color change, supporting the mechanochemical origin of the reactivity. More recently, Craig and coworkers also reported the mechanically triggered release of HCl from a methoxy-substituted *g*DCC (MeO-*g*DCC) mechanophore (Scheme 1.1b).[31] The *g*DCC mechanophore scaffold popularized by the Craig group has been extensively studied.[32] In the absence of an additional driving force like aromatization in the example above, the electrocyclic ring-opening reaction occurs with chlorine migration to form a stable 2,3-dichloroalkene product. Here, the addition of an electron-donating methoxy group was proposed to stabilize the cationic character that develops during chloride dissociation and ultimately promote the spontaneous elimination of HCl. Consistent with this hypothesis, the ring-opening reaction of the MeO-*g*DCC mechanophore was found to occur at a force of ~900 pN compared to ~1300 pN for the unsubstituted analog based on SMFS experiments. In addition, ultrasound-induced mechanochemical activation of polymers containing multiple MeO-*g*DCC units in the backbone generated, on average, 67 equivalents of HCl per chain scission event. Mechanically triggered release of HCl was also demonstrated in bulk crosslinked polydimethylsiloxane (PDMS) materials under tension and compression. Compared to the earlier indene derivative that exhibits only modest thermal stability, the MeO-*g*DCC mechanophore is also quite stable with no reaction observed after heating at 110 °C for 1 day.

The mechanical activation of metal complexes through force-induced metal–ligand bond dissociation has also received substantial interest, particularly for applications in catalysis.[33] Polymers containing Ag, Co, Cu, Eu, Fe, Pd, Pt, and Ru complexes have all been found to activate selectively at the metal–ligand bond under mechanical force.[22,34–41,23,42–47] However, only a few studies performed recently on metallocenes have demonstrated and characterized the complete dissociation of a metal ion from the parent polymer. In 2018, Giannantonio *et al.* sonicated solutions of polymers containing ferrocene units in the

backbone and characterized metal ion release by complexation with KSCN and $K_4[Fe(CN)_6]$.[42] Formation of the red $[Fe(SCN)_n(H_2O)_{6-n})]^{(3-n)+}$ complex and Prussian blue from their respective potassium salts suggested that Fe^{2+} was released upon mechanochemical activation and rapidly oxidized by air to form Fe^{3+} (Scheme 1.2a). These

Scheme 1.2. Release of metal ions is achieved through the mechanochemical scission of the metal–ligand bonds in ferrocene mechanophores.

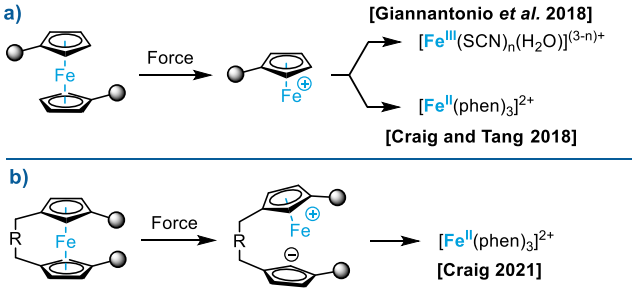

conclusions were further supported by studies of chain scission kinetics indicating that polymer cleavage occurs selectively at the embedded ferrocene moieties. In close succession, Craig, Tang, and coworkers reported a similar investigation into ferrocene mechanochemistry, successfully trapping the released Fe^{2+} ion with phenanthroline to form the stable $[Fe(phen)_3]^{2+}$ complex (Scheme 1.2a).[43] In this work and in a subsequent study,[44] the authors characterized the relative mechanical strengths of the Fe–cyclopentadienyl bond in ferrocene as well as the Ru–cyclopentadienyl bond in ruthenocene according to established protocols using the competitive reactivity of a *g*DCC mechanophore as an internal reference.[48] Interestingly, they found that despite the high thermodynamic stability of ferrocene and ruthenocene, their mechanochemical lability is similar to that of the relatively weak C–N bond of azobisdialkylnitrile (BDE < 30 kcal/mol) and the C–S bond of a thioether (BDE = 71–74 kcal/mol), respectively.[43,44] Data also suggest that the mechanochemical dissociation of both metallocenes occurs predominately via a heterolytic mechanism.

The mismatch in thermodynamic stability and mechanical susceptibility prompted further investigation into structure–mechanochemical activity relationships for metallocene mechanophores. In 2021, Craig and coworkers demonstrated that the mechanism of ferrocene dissociation under mechanical force could be biased by a distal conformational restraint between the two cyclopentadienyl ligands (Scheme 1.2b).[45] Polymers containing these *ansa*-bridged ferrocene mechanophores were shown to dissociate by peeling, rather

than shearing, of the cyclopentadienyl ligands from the metal center. Significantly, this change in mechanism leads to a substantial increase in mechanochemical activity for the *ansa*-bridged ferrocene complex, dissociating at a transition force of ~800 pN compared to the > 1600 pN of force required for reaction of the unbridged ferrocene mechanophore in SMFS experiments. The investigation of metallocene mechanochemistry has also recently been extended to cobaltocenium mechanophores that were demonstrated to react selectively under mechanical force via a peeling-type mechanism that, in this case, is driven by interactions between the metal center and the counterion.[46]

In contrast to the conventional mode of mechanophore activation in which mechanical force is coupled to the scission of a weak bond, small molecule release has also been achieved through a unique "flex activation" manifold where extrinsic force promotes bond-bending motions consistent with geometric changes in the overall transformation that direct reactivity along a particular coordinate. Larsen and Boydston introduced this strategy in 2013 by designing an oxanorbornadiene mechanophore that undergoes a retro-[4+2] cycloaddition reaction resulting in the liberation of a small molecule furan derivative (Scheme 1.3a).[49] In this work and a subsequent report by the same authors,[50] polymer

Scheme 1.3. The release of small molecules is achieved through a putative flex activation manifold in which mechanical force promotes bond-bending motions consistent with the geometric changes in the overall transformation without chain scission.

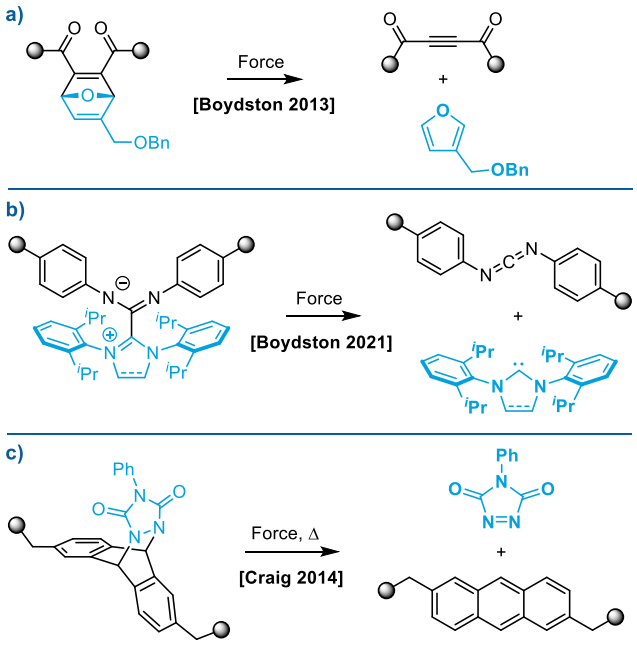

networks incorporating the oxanorbornadiene mechanophore were subjected to compression, achieving small molecule release albeit with a maximum mechanophore activation of < 10%. More recently, Boydston and coworkers expanded this strategy to the mechanically triggered release of *N*-heterocyclic carbenes (NHCs) from carbodiimide adducts (Scheme 1.3b).[51] Using phenyl isothiocyanate as a trapping agent, the mechanochemical generation of two different NHC compounds was observed from bulk samples of crosslinked PMA subjected to uniaxial compression. Mechanophore activation increased monotonically with increasing number of compression cycles, ultimately plateauing at ~1% activation. In 2014, Craig and coworkers also investigated the formal retro-[4+2] cycloaddition reaction of an anthracene–triazolinedione Diels–Alder adduct in crosslinked PDMS elastomers under tension where mechanical activation was proposed to proceed via an analogous force-induced planarization process (Scheme 1.3c).[52] Heating the material to 125 °C, however, was required to achieve ~1% mechanophore activation under a strain of 175%.

The low mechanochemical reactivity of the anthracene–triazolinedione and NHC–carbodiimide adducts is consistent with computational studies performed by Roessler and Zimmerman on the mechanochemical reactivity of the oxanorbornadiene mechanophore.[6] For that system, the flex activation mechanism was shown to be less sensitive to mechanical perturbation, likely due to the poor alignment between the direction of applied force and the nearly orthogonal scissile bonds in the mechanophore, which results in weak mechanochemical coupling. While mechanical force decreases the reaction barrier, significant thermal energy is still required under relatively large forces to move along the force modified potential energy surface. In addition to the mechanophore structure, the polymer matrix also contributes to activation efficiency. Recently, Kilian and coworkers investigated the mechanochemical activation of a similar oxanorbornadiene mechanophore in double network hydrogels of polyacrylamide and alginate, achieving ~20% activation upon compression under relatively moderate stress.[53] The improved reactivity is attributed to the enhanced toughness of the material that enables greater deformation prior to failure and adds to other recent insights into mechanophore activation in multinetwork materials.[54–56] Finally, it is notable that the use of solution state ultrasonication methods to probe the reactivity of mechanophores designed for flex activation has not been reported in the

literature. Such studies may shed light on whether the low mechanophore activation efficiencies observed for this class of compounds are due primarily to their molecular design, or rather limitations of solid-state force transduction.

In addition to the azo mechanophore discussed above, a relatively large collection of diverse mechanophores has been developed that react via homolytic fragmentation pathways.[28] Although not recognized as a mechanophore at the time, the mechanical susceptibility of the peroxide functional group was identified by Encina in 1980 through investigations of the ultrasound-induced chain fragmentation of polyvinylpyrrolidone containing several peroxide linkages distributed throughout the polymer backbone.[57] However, the mechanochemistry of organic peroxides has since received little attention, with a possible exception being the dioxetane mechanophores developed by Sijbesma and coworkers that contain a peroxo linkage within the four-membered ring but exhibit significantly different reactivity.[21] In a recent investigation of peroxide mechanochemistry, Otsuka and coworkers designed a mechanophore based on the bis(9-methylphenyl-9-fluorenyl) peroxide (BMPF) scaffold that undergoes homolytic fragmentation of the O–O bond under mechanical force to ultimately release the fluorescent small molecule 9-fluorenone via β-scission (Scheme 1.4).[58] The BMPF mechanophore was converted into a

Scheme 1.4. The force-induced homolysis of a mechanically labile peroxide bond triggers the release of the fluorescent molecule 9-fluorenone.

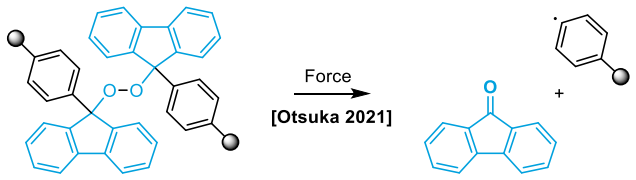

crosslinker and incorporated into both a glassy poly(butyl methacrylate) and rubbery poly(hexyl methacrylate) network via free radical polymerization where mechanical activation was evaluated using ball-milling and compression, respectively. In both cases, a fluorogenic response was observed under UV light and the release of 9-fluorenone was further confirmed through chromatographic and spectroscopic analyses performed on soluble extracts. The BMPF mechanophore was also demonstrated to be thermally stable up to 110 °C. Another peroxo containing mechanophore based on an anthracene–endoperoxide was also recently reported to liberate singlet oxygen in polymers subjected to ball-milling.[59] However, we cautiously note that without control experiments to rule out a thermal activation

pathway, additional investigation is warranted to elucidate the reactivity. Further exploration of the mechanochemistry of organic peroxides is certain to contribute to new fundamental understanding of reactivity and enable additional tools for the construction and applications of force-responsive materials.

The mechanically triggered release of small molecules has also been accomplished through depolymerization. In 2014, Moore and coworkers demonstrated the ultrasound-induced mechanochemical unzipping reaction of poly(*o*-phthalaldehyde) to produce *o*-phthalaldehyde monomers (Scheme 1.5).[60] The results of trapping experiments and steered

Scheme 1.5. Mechanical force triggers the heterolytic chain scission poly(o-phthalaldehyde) resulting in complete depolymerization above its ceiling temperature to regenerate monomer.

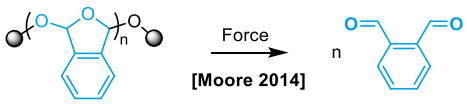

molecular dynamics simulations support a mechanism in which mechanochemical chain cleavage via heterolytic fragmentation of a C–O bond in the polymer backbone reveals reactive hemiacetalate and oxocarbenium end groups. At temperatures above the low ceiling temperature of poly(*o*-phthalaldehyde), which is around −40 °C,[61] these polymer chain fragments undergo rapid head-to-tail depolymerization to regenerate monomer. Proof-of-concept experiments were also successfully performed to demonstrate the repolymerization of recovered *o*-phthalaldehyde monomer by treating a sonicated solution of poly(*o*-phthalaldehyde) with an anionic initiator. The molecular weight-dependent kinetics associated with the mechanochemical activation of poly(*o*-phthalaldehyde) were further investigated by Peterson and Boydston by taking advantage of the rapid depolymerization that occurs following mechanical activation.[62] More broadly, the mechanically triggered degradation of polymers has recently attracted significant research interest because of the opportunities it presents for chemical recycling strategies that address the sustainable end-of-life management of plastics.[63] As discussed briefly in the next section, several reports have leveraged mechanophores to introduce chemically labile functional groups into previously inert polymer backbones;[64–67] however, mechanically triggered end-to-end depolymerization has only been demonstrated for poly(*o*-phthalaldehyde). Expanding mechanically triggered depolymerization strategies to additional self-immolative polymers[68] with greater thermal

and chemical stability while ideally also maintaining desirable physical properties for useful materials will be important for advancing these technologies. Beyond polymer degradation, the mechanically triggered depolymerization of self-immolative polymers also presents tremendously exciting opportunities to capitalize on the unique chemical amplification[69] process for stress sensing and other applications.

1.3 Mechanically gated Cascade Reactions for Molecular Release

In chemistry, gating generally refers to the use of a specific regulatory stimulus to control a secondary chemical transformation. For example, gated reactivity is an established concept in the context of photoswitching, where a photochemical transformation reveals a new structure with unique reactivity,[70] or alternatively, a photochemically active molecule is produced after a chemical reaction.[71–75] As a pertinent example of the former case of photogated reactivity, Otsuka and coworkers designed an elegant system that uses light to modulate the susceptibility of polymers toward thermal[76] and mechanochemical chain scission.[77] The related concept of mechanically gated reactivity has recently emerged as a powerful approach for the modular design of mechanophores and complex mechanochemically active systems.[64–67,78,79] As discussed this section, the same design concept derived from mechanically gated reactivity have been successfully implemented in the development of more generalized and highly modular mechanophore platforms for molecular release.

Adapting the design strategy employed in our earlier demonstration of mechanically gated photoswitching,[80] we developed a mechanophore platform for molecular release that leverages the instability of 2-furylcarbinol derivatives,[81–84] a structural motif that has also been investigated for the design of prodrugs[85] and self-immolative polymers.[86,87] The following chapters will describe our efforts of the initial mechanophore design (Chapter 2), structural optimizations for faster release rates and a more streamed-lined synthesis (Chapters 2,3), development of a novel mechanophore and the synthesis of multimechanophore polymers to achieve high capacity cargo releasing (Chpter 4), as well as using the modular mechanophore platform to achieve mechanically triggered self-immolative polymer depolymerization (Chapter 5).

The initial mechanophore design was based on a mechanically triggered cascade reaction in which the mechanochemical retro-[4+2] cycloaddition reaction of a furan–maleimide Diels–Alder adduct unmasks a latent furfuryl carbonate, which subsequently decomposes to release a covalently bound small molecule (Scheme 1.6a).[88] Hydroxycoumarin was used as a model payload due to its fluorogenic properties to facilitate the straightforward characterization of molecular release by photoluminescence spectroscopy in addition to other analytical methods. Judicious substitution of the 2-furylcarbinol scaffold was key to the success of this approach, enabling the decomposition of the furfuryl carbonate to proceed relatively quickly following mechanochemical activation of the Diels–Alder adduct. Density functional theory (DFT) calculations indicated that a combination of alkyl substituents at the 5-position of the furan and at the α-position significantly suppressed the activation barrier for carbonate fragmentation, reducing $\Delta G^{\ddagger}$

Scheme 1.6. Mechanically triggered molecular release from masked 2-furylcarbinol derivatives is accomplished via a retro-Diels–Alder/fragmentation cascade.

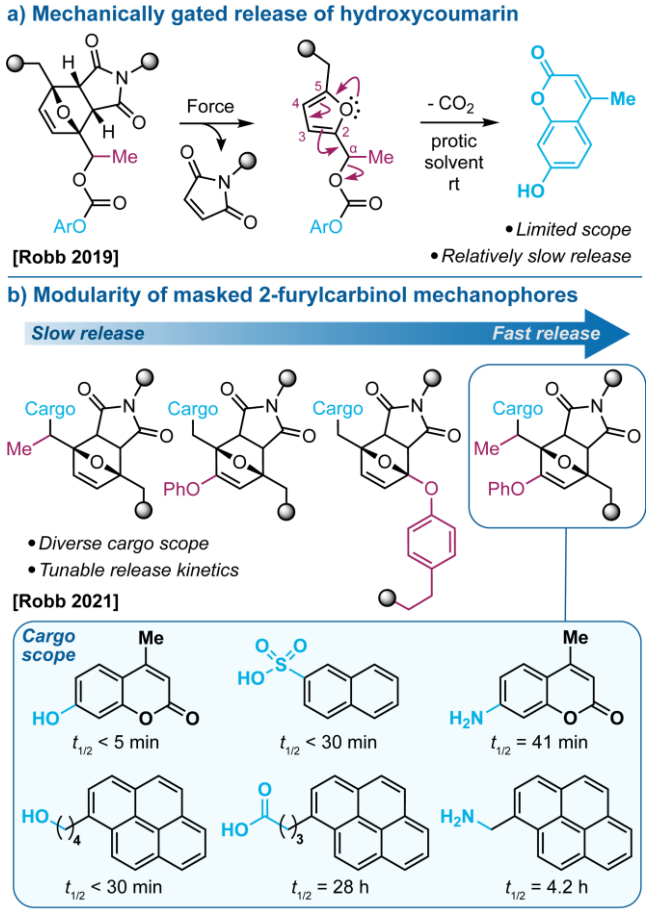

from 29.4 kcal/mol for the unsubstituted compound to 22.0 kcal/mol for the dialkyl derivative. In particular, small molecule model experiments confirmed the importance of the α-methyl substituent, which presumably stabilizes the developing positive charge in the transition state leading to the secondary furfuryl cation intermediate, as depicted by the arrow pushing mechanism in Scheme 1.6. In a polar protic mixture of acetonitrile and methanol, the furfuryl carbonate decomposes at room temperature with a half-life on the order of ~1 h to cleanly release hydroxycoumarin. Notably, release occurred ~10-fold faster in an aqueous acetonitrile mixture. The mechanically triggered release of hydroxycoumarin was successfully demonstrated by ultrasound-induced mechanochemical activation of a polymer containing a chain-centered furan–maleimide mechanophore, achieving approximately 64% release after 150 min of sonication. By fitting the sonication time-dependent photoluminescence response to an expression of first-order kinetics, the yield of hydroxycoumarin was projected to plateau at a maximum value of ~87%, indicating that mechanophore activation and subsequent payload release occurs efficiently.

While the mechanophore described above offered a promising design platform, molecular release was found to be largely limited to phenols. Kinetic studies performed on small molecule 2-furylcarbinol derivatives with the same substitution pattern demonstrated that the release of a primary alcohol is approximately 100× slower than hydroxycoumarin, with the release of aminocoumarin from the analogous furfuryl carbamate occurring approximately 60× slower than that of the primary alcohol.[89] We envisioned that an additional electron donating substituent on the furan would further suppress the activation barrier for fragmentation through resonance stabilization of the furfuryl cation intermediate, enabling the release of more challenging payloads on reasonable time scales (Scheme 1.6b). DFT calculations were performed to establish structure–activity relationships and further assess the impact of substitution on the reactivity of 2-furylcarbinol derivatives. In particular, the addition of an electron-donating phenoxy group at the 3-position of the furan, in combination with the α-methyl substituent, was found to significantly lower the activation energy and provide a highly active substrate for molecular release. Mechanochemical activation experiments corroborated the predictions from DFT and demonstrated that release kinetics could be modulated by several orders of magnitude by varying the substitution on

the masked 2-furylcarbinol derivatives. Importantly, this tunability allows release rates to be preprogrammed into the mechanophore through independent structural modifications based on the identity of the molecular payload and the desired response. The mechanically triggered release of cargo molecules bearing alcohol, phenol, alkylamine, arylamine, carboxylic acid, and sulfonic acid functional groups was successfully demonstrated using ultrasonication, illustrating the generality of the molecular design strategy (half-lives for cargo release in 3:1 acetonitrile/methanol are illustrated in Scheme 1.6b). We note, however, that less efficient release of the alkylamine payload was observed compared to the other cargo molecules, which was attributed to a side reaction involving attack of the furfuryl cation intermediate by the liberated nucleophilic amine. These results suggest a potential challenge for achieving the efficient release of cargo molecules possessing strongly nucleophilic functional groups with this mechanophore design.

Our group has also investigated an alternative mechanophore design that incorporates an aryloxy substituent at the 5-position of the masked 2-furylcarbinol scaffold, which serves as both the site of polymer attachment and an electron donating group to accelerate release (Scheme 1.6b).[90] Installation of the aryloxy group at the 5-position of the furan preserves the proximal pulling geometry in the furan–maleimide mechanophore, which leads to greater mechanochemical activity compared to the regioisomer with distal connectivity.[91] This mechanophore is prepared through a considerably more efficient four-step synthesis while still facilitating the mechanically triggered release of both phenol and arylamine payloads with rates that are comparable to those of the phenoxy-substituted mechanophore. Similar to the effects of phenoxy substitution in the prior design, the aryloxy substituent was also demonstrated to significantly improve the thermal stability of the Diels–Alder adduct without adversely affecting mechanochemical activity.

Interestingly, small molecule model experiments suggested that decomposition of the 5-aryloxy mechanophore proceeds through a fragmentation mechanism distinct from previously studied 2-furylcarbinol derivatives, involving secondary fragmentation at the aryloxy connection. Our group thusly designed a mechanophore equipped with a self-immolative spacer as the aryloxy substituent to achieve dual payload release.[92] In this design, the mechanically triggered retro-Diels–Alder reaction unveils a 5-aryloxy-substituted 2-

furfuryl carbinol species, which releases the first cargo at the 2-position as well as the 5-aryloxy spacer. The liberated self-immolative 5-aryloxy linker then undergoes further elimination to release the second cargo (Scheme 1.7). The putative stepwise fragmentation mechanism was further investigated and utilized to control the two cargos' relative release profiles. When the first cargo is a relatively poor leaving group (carbamate) while the second is a good leaving group (carbonate), the two cargos are expelled simultaneously. However, when the cargos attachments are swapped, a sequential release was observed. The ability to release two small molecules with tunable release kinetics and profiles is an attractive attribute for potential applications in combination drug-deliveries to enhance therapeutic efficacy.[93,94]

Scheme 1.7. Mechanically triggered dual-releasing mechanophore enabled by the incorporation of a self-immolative spacer.

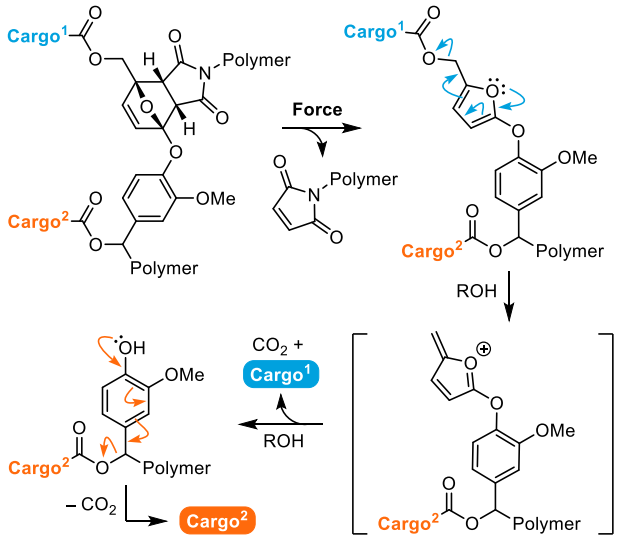

More recently, we dramatically increased the amount of payload capacity, achieving the release of hundreds of small molecule cargos per chain by designing multimechanophore polymers incorporating non-scissile mechanophores (Scheme 1.8).[95] An intramolecular Diels–Alder reaction of a furfuryl fumarate ester renders the masked 2-furyl carbinol mechanophore non-scissile. A macrocyclic alkene is designed to allow polymerization via ring-opening metathesis polymerization (ROMP) to afford multimechanophore polymers. In this design, the 3-phenoxy substituent on the furan is selected not only to provide fast release kinetics and adduct thermal stability, but also to protect the Diels–Alder alkene against undesired olefin metathesis. Interestingly, density functional theory (DFT)

Scheme 1.8. Multimechanophore polymer design for achieving high capacity cargo release.

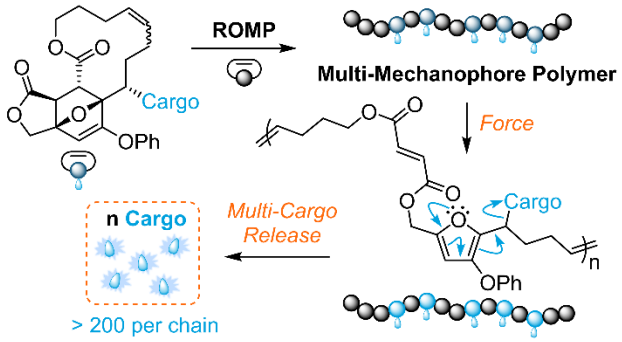

calculations using the constrained geometries simulate external force (CoGEF) method predicted that the formal retro-Diels–Alder reaction occurs with a rupture force of 3.4 nN, much lower than the furan maleimide Diels–Alder adduct which usually range from 4.0–4.4 nN.[89,90] This was also observed experimentally, with the non-scissile mechanophore reaching maximum mechanical activation after ~ 35 mins of ultrasonication as opposed to the 2–5 hours required for previous mechanophore designs. We further demonstrated that the amount of mechanophore incorporation in a polymer could be varied by changing the feeding ratio of comonomers, subsequently controlling the number of cargos released. Using a 295 kDa multimechanophore polymer with 40% mechanophore incorporation, we successfully achieved a maximum of 60% release of cargos, corresponding to ~203 cargo molecules per chain after only ~ 10 min of ultrasonication.

The mechanically triggered cascade reactions also present a unique opportunity for triggering the depolymerization of self-immolative polymers (SIPs) using mechanical force (Scheme 1.9, Chapter 5). Utilizing the modularity of the mechanophore for cargo release, we synthesized a poly (carboxy pyrrole) SIP capped with a 3-phenoxy substituted mechanophore and a fluorogenic reporter molecule, and subsequently a PMA-SIP conjugate. When exposed

Scheme 1.9. Mechanically triggered self-immolative polymer depolymerization.

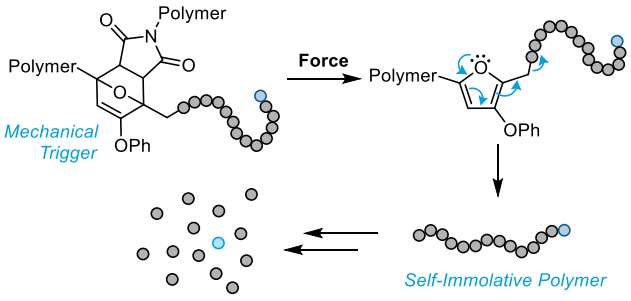

to ultrasonication, the PMA-SIP conjugate resulted in fluorescence signal increase, signifying the end-to-end depolymerization of a mechanically released SIP. The SIP, with its molecular weight below the threshold for mechanical activation, did not lead to significant reporter molecule release, indicating the mechanical origin of the SIP degradation.

Another system that leverages a mechanically triggered cascade reaction to achieve molecular release was reported by Göstl, Herrmann, and coworkers in 2020.[96] The mechanophore is based on an elegantly designed disulfide motif with payloads attached via β-carbonate linkages. Mechanically activated reduction[97,98] of the disulfide bond is followed by a 5-*exo-trig* cyclization to release a pair of alcohol-based cargo molecules (Scheme 1.10).

Scheme 1.10. The mechanochemical reduction of a disulfide mechanophore triggers cargo release via a 5-*exo-trig* cyclization.

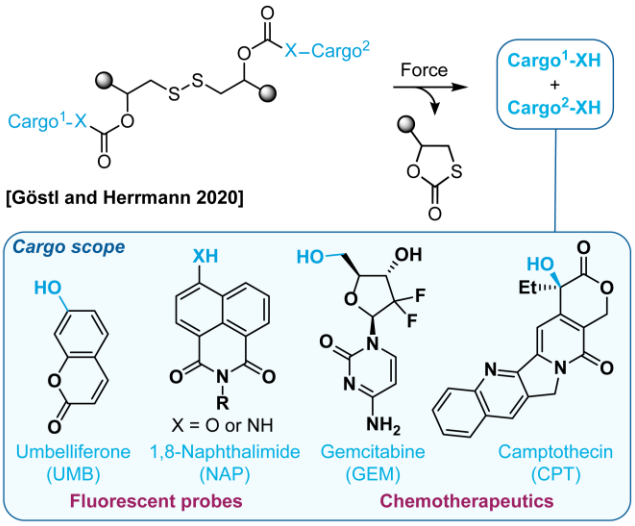

The bifunctional character of this platform enables a theranostic approach with the concurrent release of a therapeutic compound and a fluorescent reporter molecule for following drug release and biodistribution in real time. Model experiments performed on small molecule disulfide initiators dually conjugated with a reporter/drug combination of umbelliferone (UMB)/gemcitabine (GEM) or *N*-butyl-4-hydroxy-1,8-naphthalimide (NAP)/camptothecin (CPT) exhibited efficient and concomitant release of both payloads upon chemical reduction. The mechanically triggered release of NAP/CPT payloads from a polymer chain-centered mechanophore was demonstrated using ultrasonication methods. The release of NAP (and by inference, CPT) was characterized by fluorescence spectroscopy, reaching ~56% after 180 min of sonication. A series of *in vitro* experiments

were performed by treating Hela cells with sonicated polymer solutions, which demonstrated the successful release and cellular uptake of NAP. To demonstrate the generality of the platform, the mechanically triggered release of the UMB/GEM fluorophore/drug pair was also investigated, achieving comparable amounts of release to the NAP/CPT system. In this case, however, the release of UMB proceeded at a faster rate than that of GEM. A paper from the same groups that appeared later demonstrated the ultrasound-induced mechanochemical activation of polymers containing symmetrical disulfide mechanophores loaded with two equivalents of UMB or CPT with qualitatively similar results as this earlier study.[99]

A more recent investigation comparing the mechanically triggered release of NAP (X = OH) and the amine analog *N*-alkyl-4-amino-1,8-naphthalimide (X = NH_2) revealed significantly diminished release efficiency for the amine payload conjugated to the disulfide mechanophore via carbamate linkers (Scheme 1.10).[99] While ~50% release of the hydroxyl-functional payload was released after 240 min of sonication, < 3% release of the amine cargo was observed after being subjected to the same ultrasonication conditions. As for the 2-furylcarbinol platform discussed above, these results highlight the importance of the leaving group on molecular release.[100] Moreover, for the disulfide mechanophore, release is coupled to the equilibrium established between the β-mercapto carbonate/carbamate and the cyclic thiocarbonate, with the more nucleophilic amines expected to shift the equilibrium toward the former state. The susceptibility of the disulfide mechanophore to nonspecific activation via chemical reduction or thiol exchange presents another potential challenge. Studies also confirmed that ultrasound-induced mechanophore activation must occur *ex situ* to avoid loss of viability for mammalian cells,[99] identifying a substantial barrier to translational applications. As discussed in greater detail below, the sonication conditions used here are representative of those employed ubiquitously in polymer mechanochemistry research. Therefore, new remote activation strategies are needed to facilitate the application of mechanophore-based molecular release platforms in biological settings.[102] Interestingly, the same 20 kHz ultrasonication was found to have no considerable effect on the viability of *S. aureus* bacteria.[99]

1.4 Outlook

The rapidly growing field of polymer mechanochemistry has captivated the attention of organic chemists and polymer scientists and engineers alike by revealing fundamentally new concepts in chemical reactivity and unprecedented opportunities for the design of stimuli-responsive materials. Over the last decade—and the last several years, in particular—the development of force-sensitive molecules known as mechanophores that enable the mechanically triggered release of covalently bound payloads has attracted significant interest. This research has added new tools to an already active area of investigation into the development of stimuli-responsive polymers that release functional small molecules under stress for a wide variety of applications. Unlike most materials-based approaches, however, mechanophores are constructed with atomic precision and leverage the principles of organic chemistry to modulate their activity for molecularly programmed responsive behavior. Diverse strategies for harnessing mechanical force to facilitate productive chemical transformations have furnished a quickly expanding library of mechanophores enabling small molecule release. Ongoing efforts to create specialized mechanophores capable of releasing specific cargo molecules are joined by research toward the development of more modular and generalized platforms that take advantage of mechanical gating and mechanically triggered cascade reactions. While the collective intuition of mechanochemical reactivity has advanced substantially in a relatively short period of time, the continued advancement of structure–activity relationships is paramount to establish a thorough understanding of the design rules underpinning mechanically selective bond activation, and to expand the cargo scope and capabilities of mechanophore-based molecular release strategies.

As mechanophore-based molecular release platforms continue to improve and evolve, the desire to seek practical applications in areas like catalysis, autonomous materials, and controlled drug delivery will prompt further innovation. Systems that enable the release of multiple payloads per mechanical activation event by leveraging multicargo designs or multimechanophore polymers are needed to overcome limitations in cargo loading capacity and enhance the utility of mechanophore-based release strategies. Novel approaches are also required to expand beyond small molecule release to develop systems

for mechanically triggered depolymerization, a relatively unexplored area of polymer mechanochemistry with substantial promise for the design of adaptable materials with self-repairing or remodeling capabilities as well as emerging chemical recycling and stress sensing technologies. Molecular and materials design concepts for improving the efficiency of mechanically triggered release in bulk materials and in diverse solution environments will also expand the reach of mechanophore-based molecular release chemistry. Lastly, the integration of mechanophores with complementary approaches for achieving force-responsive functionality, such as microcapsule-based methods, will provide new multifaceted platforms for creating complex responsive polymeric materials that operate on multiple size and length scales.

Targeted drug delivery is one of the most compelling applications to emerge from research into mechanophore-based molecular release platforms. The ability to activate mechanophores remotely using ultrasound presents unique opportunities for translational applications of polymer mechanochemistry to benefit human health. From a technological perspective, however, the development of strategies using biomedically relevant ultrasound to activate mechanophores is still a potentially formidable challenge. With few exceptions, the sonication probes routinely employed to study mechanophore activation in the laboratory are the same devices commonly used for cell lysis,[101] illustrating their mutual incompatibility. Some existing clinical applications use ultrasound in this 20 kHz frequency range, but are generally limited to procedures where tissue disruption is desirable due to the strong cavitation effects.[102] On the other hand, many of the paradigms underpinning the current understanding of ultrasound-induced mechanochemical activation are based on models of polymer chain extension induced by cavitation,[103] thus establishing a notable dichotomy between mechanophore activation in the laboratory and physiological constraints. New methodologies will be required, particularly for *in vivo* applications, that effectively couple the mechanical activation of mechanophores with the acoustic energy from ultrasound at higher frequencies where cavitation is suppressed.[104] Fortunately for the field, experiments demonstrating the mechanical activation of mechanophores in micellar systems[105] and bulk elastomers[106] provide a promising example that focused ultrasound operating within biocompatible frequencies and pressure

amplitudes will be an important technology for advancing biomedical applications of polymer mechanochemistry. Future innovations in the technologies that enable remote mechanical activation, together with advances in the design of mechanophores for molecular release, promise to help realize the translational potential of polymer mechanochemistry while further galvanizing important fundamental discoveries in this quickly evolving arena.

1.5 References

(1) Beyer, M. K.; Clausen-Schaumann, H. Mechanochemistry: The Mechanical Activation of Covalent Bonds. *Chem. Rev.* **2005**, *105*, 2921–2948.

(2) Caruso, M. M.; Davis, D. A.; Shen, Q.; Odom, S. A.; Sottos, N. R.; White, S. R.; Moore, J. S. Mechanically-Induced Chemical Changes in Polymeric Materials. *Chem. Rev.* **2009**, *109*, 5755–5798.

(3) Li, J.; Nagamani, C.; Moore, J. S. Polymer Mechanochemistry: From Destructive to Productive. *Acc. Chem. Res.* **2015**, *48*, 2181–2190.

(4) Ribas-Arino, J.; Shiga, M.; Marx, D. Understanding Covalent Mechanochemistry. *Angew. Chem. Int. Ed.* **2009**, *48*, 4190–4193.

(5) Stauch, T.; Dreuw, A. Quantum Chemical Strain Analysis For Mechanochemical Processes. *Acc. Chem. Res.* **2017**, *50*, 1041–1048.

(6) Roessler, A. G.; Zimmerman, P. M. Examining the Ways To Bend and Break Reaction Pathways Using Mechanochemistry. *J. Phys. Chem. C* **2018**, *122*, 6996–7004.

(7) Hickenboth, C. R.; Moore, J. S.; White, S. R.; Sottos, N. R.; Baudry, J.; Wilson, S. R. Biasing reaction pathways with mechanical force. *Nature* **2007**, *446*, 423–427.

(8) Wang, J.; Kouznetsova, T. B.; Niu, Z.; Ong, M. T.; Klukovich, H. M.; Rheingold, A. L.; Martinez, T. J.; Craig, S. L. Inducing and quantifying forbidden reactivity with single-molecule polymer mechanochemistry. *Nat. Chem.* **2015**, *7*, 323–327.

(9) Chen, Y.; Mellot, G.; Luijk, D. van; Creton, C.; P. Sijbesma, R. Mechanochemical tools for polymer materials. *Chem. Soc. Rev.* **2021**, *50*, 4100–4140.

(10) Ghanem, M. A.; Basu, A.; Behrou, R.; Boechler, N.; Boydston, A. J.; Craig, S. L.; Lin, Y.; Lynde, B. E.; Nelson, A.; Shen, H.; Storti, D. W. The role of polymer mechanochemistry in responsive materials and additive manufacturing. *Nat. Rev. Mater.* **2021**, *6*, 84–98.

(11) Chen, Z.; Mercer, J. A. M.; Zhu, X.; Romaniuk, J. A. H.; Pfattner, R.; Cegelski, L.; Martinez, T. J.; Burns, N. Z.; Xia, Y. Mechanochemical unzipping of insulating polyladderene to semiconducting polyacetylene. *Science* **2017**, *357*, 475–479.

(12) Davis, D. A.; Hamilton, A.; Yang, J.; Cremar, L. D.; Gough, D. V.; Potisek, S. L.; Ong, M. T.; Braun, P. V.; Martínez, T. J.; White, S. R.; Moore, J. S.; Sottos, N. R. Force-induced activation of covalent bonds in mechanoresponsive polymeric materials. *Nature* **2009**, *459*, 68–72.

(13) Wang, Z.; Ma, Z.; Wang, Y.; Xu, Z.; Luo, Y.; Wei, Y.; Jia, X. A Novel Mechanochromic and Photochromic Polymer Film: When Rhodamine Joins Polyurethane. *Adv. Mater.* **2015**, *27*, 6469–6474.
(14) Imato, K.; Irie, A.; Kosuge, T.; Ohishi, T.; Nishihara, M.; Takahara, A.; Otsuka, H. Mechanophores with a Reversible Radical System and Freezing-Induced Mechanochemistry in Polymer Solutions and Gels. *Angew. Chem. Int. Ed.* **2015**, *54*, 6168–6172.
(15) Robb, M. J.; Kim, T. A.; Halmes, A. J.; White, S. R.; Sottos, N. R.; Moore, J. S. Regioisomer-Specific Mechanochromism of Naphthopyran in Polymeric Materials. *J. Am. Chem. Soc.* **2016**, *138*, 12328–12331.
(16) McFadden, M. E.; Robb, M. J. Force-Dependent Multicolor Mechanochromism from a Single Mechanophore. *J. Am. Chem. Soc.* **2019**, *141*, 11388–11392.
(17) Qian, H.; Purwanto, N. S.; Ivanoff, D. G.; Halmes, A. J.; Sottos, N. R.; Moore, J. S. Fast, reversible mechanochromism of regioisomeric oxazine mechanophores: Developing in situ responsive force probes for polymeric materials. *Chem* **2021**, *7*, 1080–1091.
(18) Göstl, R.; Sijbesma, R. P. π-extended anthracenes as sensitive probes for mechanical stress. *Chem. Sci.* **2016**, *7*, 370–375.
(19) Sumi, T.; Goseki, R.; Otsuka, H. Tetraarylsuccinonitriles as mechanochromophores to generate highly stable luminescent carbon-centered radicals. *Chem. Commun.* **2017**, *53*, 11885–11888.
(20) Baumann, C.; Stratigaki, M.; Centeno, S. P.; Göstl, R. Multicolor Mechanofluorophores for the Quantitative Detection of Covalent Bond Scission in Polymers. *Angew. Chem. Int. Ed.* **2021**, *60*, 13287–13293.
(21) Chen, Y.; Spiering, A. J. H.; Karthikeyan, S.; Peters, G. W. M.; Meijer, E. W.; Sijbesma, R. P. Mechanically induced chemiluminescence from polymers incorporating a 1,2-dioxetane unit in the main chain. *Nat. Chem.* **2012**, *4*, 559–562.
(22) Piermattei, A.; Karthikeyan, S.; Sijbesma, R. P. Activating catalysts with mechanical force. *Nat. Chem.* **2009**, *1*, 133–137.
(23) Michael, P.; Binder, W. H. A Mechanochemically Triggered "Click" Catalyst. *Angew. Chem. Int. Ed.* **2015**, *54*, 13918–13922.
(24) Robb, M. J.; Moore, J. S. A Retro-Staudinger Cycloaddition: Mechanochemical Cycloelimination of a beta-Lactam Mechanophore. *J. Am. Chem. Soc.* **2015**, *137*, 10946–10949.
(25) Wang, J.; Piskun, I.; Craig, S. L. Mechanochemical Strengthening of a Multi-mechanophore Benzocyclobutene Polymer. *ACS Macro Lett.* **2015**, *4*, 834–837.
(26) Zhang, H.; Gao, F.; Cao, X.; Li, Y.; Xu, Y.; Weng, W.; Boulatov, R. Mechanochromism and Mechanical Force-Triggered Cross-Linking from a Single Reactive Moiety Incorporated into Polymer Chains. *Angew. Chem. Int. Ed.* **2016**, *55*, 3040–3044.
(27) Ramirez, A. L. B.; Kean, Z. S.; Orlicki, J. A.; Champhekar, M.; Elsakr, S. M.; Krause, W. E.; Craig, S. L. Mechanochemical strengthening of a synthetic polymer in response to typically destructive shear forces. *Nat Chem* **2013**, *5*, 757–761.

(28) Klein, I. M.; Husic, C. C.; Kovács, D. P.; Choquette, N. J.; Robb, M. J. Validation of the CoGEF Method as a Predictive Tool for Polymer Mechanochemistry. *J. Am. Chem. Soc.* **2020**, *142*, 16364–16381.
(29) Berkowski, K. L.; Potisek, S. L.; Hickenboth, C. R.; Moore, J. S. Ultrasound-Induced Site-Specific Cleavage of Azo-Functionalized Poly(ethylene glycol). *Macromolecules* **2005**, *38*, 8975–8978.
(30) Diesendruck, C. E.; Steinberg, B. D.; Sugai, N.; Silberstein, M. N.; Sottos, N. R.; White, S. R.; Braun, P. V.; Moore, J. S. Proton-Coupled Mechanochemical Transduction: A Mechanogenerated Acid. *J. Am. Chem. Soc.* **2012**, *134*, 12446–12449.
(31) Lin, Y.; Kouznetsova, T. B.; Craig, S. L. A Latent Mechanoacid for Time-Stamped Mechanochromism and Chemical Signaling in Polymeric Materials. *J. Am. Chem. Soc.* **2020**, *142*, 99–103.
(32) Lenhardt, J. M.; Black, A. L.; Craig, S. L. gem-Dichlorocyclopropanes as Abundant and Efficient Mechanophores in Polybutadiene Copolymers under Mechanical Stress. *J. Am. Chem. Soc.* **2009**, *131*, 10818–10819.
(33) Groote, R.; Jakobs, R. T. M.; Sijbesma, R. P. Mechanocatalysis: forcing latent catalysts into action. *Polym. Chem.* **2013**, *4*, 4846.
(34) Paulusse, J. M. J.; Sijbesma, R. P. Reversible Mechanochemistry of a PdII Coordination Polymer. *Angew. Chem. Int. Ed.* **2004**, *43*, 4460–4462.
(35) Yount, W. C.; Loveless, D. M.; Craig, S. L. Small-Molecule Dynamics and Mechanisms Underlying the Macroscopic Mechanical Properties of Coordinatively Cross-Linked Polymer Networks. *J. Am. Chem. Soc.* **2005**, *127*, 14488–14496.
(36) Kersey, F. R.; Yount, W. C.; Craig, S. L. Single-Molecule Force Spectroscopy of Bimolecular Reactions: System Homology in the Mechanical Activation of Ligand Substitution Reactions. *J. Am. Chem. Soc.* **2006**, *128*, 3886–3887.
(37) Paulusse, J. M. J.; Sijbesma, R. P. Selectivity of mechanochemical chain scission in mixed palladium(ii) and platinum(ii) coordination polymers. *Chem. Commun.* **2008**, No. 37, 4416.
(38) Karthikeyan, S.; Potisek, S. L.; Piermattei, A.; Sijbesma, R. P. Highly Efficient Mechanochemical Scission of Silver-Carbene Coordination Polymers. *J. Am. Chem. Soc.* **2008**, *130*, 14968–14969.
(39) Wei, K.; Gao, Z.; Liu, H.; Wu, X.; Wang, F.; Xu, H. Mechanical Activation of Platinum–Acetylide Complex for Olefin Hydrosilylation. *ACS Macro Lett.* **2017**, *6*, 1146–1150.
(40) Jakobs, R. T. M.; Ma, S.; Sijbesma, R. P. Mechanocatalytic Polymerization and Cross-Linking in a Polymeric Matrix. *ACS Macro Lett.* **2013**, *2*, 613–616.
(41) Balkenende, D. W. R.; Coulibaly, S.; Balog, S.; Simon, Y. C.; Fiore, G. L.; Weder, C. Mechanochemistry with Metallosupramolecular Polymers. *J. Am. Chem. Soc.* **2014**, *136*, 10493–10498.
(42) Di Giannantonio, M.; Ayer, M. A.; Verde-Sesto, E.; Lattuada, M.; Weder, C.; Fromm, K. M. Triggered Metal Ion Release and Oxidation: Ferrocene as a Mechanophore in Polymers. *Angew. Chem. Int. Ed.* **2018**, *57*, 11445–11450.

(43) Sha, Y.; Zhang, Y.; Xu, E.; Wang, Z.; Zhu, T.; Craig, S. L.; Tang, C. Quantitative and Mechanistic Mechanochemistry in Ferrocene Dissociation. *ACS Macro Lett.* **2018**, *7*, 1174–1179.
(44) Sha, Y.; Zhang, Y.; Xu, E.; McAlister, C. W.; Zhu, T.; Craig, S. L.; Tang, C. Generalizing metallocene mechanochemistry to ruthenocene mechanophores. *Chem. Sci.* **2019**, *10*, 4959–4965.
(45) Zhang, Y.; Wang, Z.; Kouznetsova, T. B.; Sha, Y.; Xu, E.; Shannahan, L.; Fermen-Coker, M.; Lin, Y.; Tang, C.; Craig, S. L. Distal conformational locks on ferrocene mechanophores guide reaction pathways for increased mechanochemical reactivity. *Nat. Chem.* **2021**, *13*, 56–62.
(46) Cha, Y.; Zhu, T.; Sha, Y.; Lin, H.; Hwang, J.; Seraydarian, M.; Craig, S. L.; Tang, C. Mechanochemistry of Cationic Cobaltocenium Mechanophore. *J. Am. Chem. Soc.* **2021**, *143*, 11871–11878.
(47) Razgoniaev, A. O.; Glasstetter, L. M.; Kouznetsova, T. B.; Hall, K. C.; Horst, M.; Craig, S. L.; Franz, K. J. Single-Molecule Activation and Quantification of Mechanically Triggered Palladium–Carbene Bond Dissociation. *J. Am. Chem. Soc.* **2021**, *143*, 1784–1789.
(48) Lee, B.; Niu, Z.; Wang, J.; Slebodnick, C.; Craig, S. L. Relative Mechanical Strengths of Weak Bonds in Sonochemical Polymer Mechanochemistry. *J. Am. Chem. Soc.* **2015**, *137*, 10826–10832.
(49) Larsen, M. B.; Boydston, A. J. "Flex-Activated" Mechanophores: Using Polymer Mechanochemistry To Direct Bond Bending Activation. *J. Am. Chem. Soc.* **2013**, *135*, 8189–8192.
(50) Larsen, M. B.; Boydston, A. J. Successive Mechanochemical Activation and Small Molecule Release in an Elastomeric Material. *J. Am. Chem. Soc.* **2014**, *136*, 1276–1279.
(51) Shen, H.; Larsen, M. B.; Roessler, A.; Zimmerman, P.; Boydston, A. J. Mechanochemical Release of N-heterocyclic Carbenes from Flex-Activated Mechanophores. *Angew. Chem. Int. Ed.* **2021**, *60*, 13559–13563.
(52) Gossweiler, G. R.; Hewage, G. B.; Soriano, G.; Wang, Q.; Welshofer, G. W.; Zhao, X.; Craig, S. L. Mechanochemical Activation of Covalent Bonds in Polymers with Full and Repeatable Macroscopic Shape Recovery. *ACS Macro Lett.* **2014**, *3*, 216–219.
(53) Jayathilaka, P. B.; Molley, T. G.; Huang, Y.; Islam, M. S.; Buche, M. R.; Silberstein, M. N.; Kruzic, J. J.; Kilian, K. A. Force-mediated molecule release from double network hydrogels. *Chem. Commun.* **2021**, *57*, 8484–8487.
(54) Ducrot, E.; Chen, Y.; Bulters, M.; Sijbesma, R. P.; Creton, C. Toughening Elastomers with Sacrificial Bonds and Watching Them Break. *Science* **2014**, *344*, 186–189.
(55) Qiu, W.; Gurr, P. A.; Qiao, G. G. Regulating Color Activation Energy of Mechanophore-Linked Multinetwork Elastomers. *Macromolecules* **2020**, *53*, 4090–4098.
(56) Chen, Y.; Sanoja, G.; Creton, C. Mechanochemistry unveils stress transfer during sacrificial bond fracture of tough multiple network elastomers. *Chem. Sci.* **2021**, *12*, 11098–11108.

(57) Encina, M. V.; Lissi, E.; Sarasúa, M.; Gargallo, L.; Radic, D. Ultrasonic degradation of polyvinylpyrrolidone: Effect of peroxide linkages. *J. Polym. Sci. B Polym. Lett. Ed.* **1980**, *18*, 757–760.
(58) Lu, Y.; Sugita, H.; Mikami, K.; Aoki, D.; Otsuka, H. Mechanochemical Reactions of Bis(9-methylphenyl-9-fluorenyl) Peroxides and Their Applications in Cross-Linked Polymers. *J. Am. Chem. Soc.* **2021**, *143*, 17744–17750.
(59) Turksoy, A.; Yildiz, D.; Aydonat, S.; Beduk, T.; Canyurt, M.; Baytekin, B.; Akkaya, E. U. Mechanochemical generation of singlet oxygen. *RSC Adv.* **2020**, *10*, 9182–9186.
(60) Diesendruck, C. E.; Peterson, G. I.; Kulik, H. J.; Kaitz, J. A.; Mar, B. D.; May, P. A.; White, S. R.; Martínez, T. J.; Boydston, A. J.; Moore, J. S. Mechanically triggered heterolytic unzipping of a low-ceiling-temperature polymer. *Nat. Chem.* **2014**, *6*, 623–628.
(61) Aso, C.; Tagami, S.; Kunitake, T. Polymerization of aromatic aldehydes. II. Cationic cyclopolymerization of phthalaldehyde. *J. Polym. Sci., Part A: Polym. Chem.* **1969**, *7*, 497–511.
(62) Peterson, G. I.; Boydston, A. J. Kinetic Analysis of Mechanochemical Chain Scission of Linear Poly(phthalaldehyde). *Macromol. Rapid Commun.* **2014**, *35*, 1611–1614.
(63) Coates, G. W.; Getzler, Y. D. Y. L. Chemical recycling to monomer for an ideal, circular polymer economy. *Nat. Rev. Mater.* **2020**, *5*, 501–516.
(64) Lin, Y.; Kouznetsova, T. B.; Craig, S. L. Mechanically Gated Degradable Polymers. *J. Am. Chem. Soc.* **2020**, *142*, 2105–2109.
(65) Hsu, T.-G.; Zhou, J.; Su, H.-W.; Schrage, B. R.; Ziegler, C. J.; Wang, J. A Polymer with "Locked" Degradability: Superior Backbone Stability and Accessible Degradability Enabled by Mechanophore Installation. *J. Am. Chem. Soc.* **2020**, *142*, 2100–2104.
(66) Yang, J.; Xia, Y. Mechanochemical generation of acid-degradable poly(enol ether)s. *Chem. Sci.* **2021**, *12*, 4389–4394.
(67) Lin, Y.; Kouznetsova, T. B.; Chang, C.-C.; Craig, S. L. Enhanced polymer mechanical degradation through mechanochemically unveiled lactonization. *Nat. Commun.* **2020**, *11*, 4987.
(68) Yardley, R. E.; Kenaree, A. R.; Gillies, E. R. Triggering Depolymerization: Progress and Opportunities for Self-Immolative Polymers. *Macromolecules* **2019**, *52*, 6342–6360.
(69) Roth, M. E.; Green, O.; Gnaim, S.; Shabat, D. Dendritic, Oligomeric, and Polymeric Self-Immolative Molecular Amplification. *Chem. Rev.* **2016**, *116*, 1309–1352.
(70) Kathan, M.; Hecht, S. Photoswitchable molecules as key ingredients to drive systems away from the global thermodynamic minimum. *Chem. Soc. Rev.* **2017**, *46*, 5536–5550.
(71) Yokoyama, Y.; Yamane, T.; Kurita, Y. Photochromism of a protonated 5-dimethylaminoindolylfulgide: a model of a non-destructive readout for a photon mode optical memory. *J. Chem. Soc., Chem. Commun.* **1991**, No. 24, 1722–1724.

(72) Lemieux, V.; Branda, N. R. Reactivity-Gated Photochromism of 1,2-Dithienylethenes for Potential Use in Dosimetry Applications. *Org. Lett.* **2005**, *7*, 2969–2972.
(73) Kühni, J.; Belser, P. Gated Photochromism of 1,2-Diarylethenes. *Org. Lett.* **2007**, *9*, 1915–1918.
(74) Ohsumi, M.; Fukaminato, T.; Irie, M. Chemical control of the photochromic reactivity of diarylethene derivatives. *Chem. Commun.* **2005**, 3921–3923.
(75) Kawai, S. H.; Gilat, S. L.; Lehn, J.-M. Photochemical pKa-Modulation and Gated Photochromic Properties of a Novel Diarylethene Switch. *Eur. J. Org. Chem.* **1999**, *1999*, 2359–2366.
(76) Kida, J.; Imato, K.; Goseki, R.; Morimoto, M.; Otsuka, H. Photoregulation of Retro-Diels–Alder Reaction at the Center of Polymer Chains. *Chem. Lett.* **2017**, *46*, 992–994.
(77) Kida, J.; Imato, K.; Goseki, R.; Aoki, D.; Morimoto, M.; Otsuka, H. The photoregulation of a mechanochemical polymer scission. *Nat. Commun.* **2018**, *9*, 3504.
(78) Wang, J.; Kouznetsova, T. B.; Boulatov, R.; Craig, S. L. Mechanical gating of a mechanochemical reaction cascade. *Nat. Commun.* **2016**, *7*, 13433.
(79) Barber, R. W.; Robb, M. J. A modular approach to mechanically gated photoswitching with color-tunable molecular force probes. *Chem. Sci.* **2021**, *12*, 11703–11709.
(80) Hu, X.; McFadden, M. E.; Barber, R. W.; Robb, M. J. Mechanochemical Regulation of a Photochemical Reaction. *J. Am. Chem. Soc.* **2018**, *140*, 14073–14077.
(81) v. Braun, J.; Köhler, Z. Ungesättigte Reste in chemischer und pharmakologischer Beziehung. (I. Mitteilung.). *Ber. Dtsch. Chem. Ges.* **1918**, *51*, 79–96.
(82) Gilman, H.; Vernon, C. C. 2-Chloromethyl-furan from 2-Furancarbinol. *J. Am. Chem. Soc.* **1924**, *46*, 2576–2579.
(83) Zanetti, J. E. Alpha Furfuryl Iodide (2-Iodomethyl furan). *J. Am. Chem. Soc.* **1927**, *49*, 1061–1065.
(84) Zanetti, J. E.; Bashour, J. T. α-Furfuryl Bromide (2-Bromomethyl furan). *J. Am. Chem. Soc.* **1939**, *61*, 2249–2251.
(85) Berry, J. M.; Watson, C. Y.; Whish, W. J. D.; Threadgill, M. D. 5-Nitrofuran-2-ylmethyl group as a potential bioreductively activated pro-drug system. *J. Chem. Soc., Perkin Trans. 1* **1997**, No. 8, 1147–1156.
(86) Fan, B.; Trant, J. F.; Hemery, G.; Sandre, O.; Gillies, E. R. Thermo-responsive self-immolative nanoassemblies: direct and indirect triggering. *Chem. Commun.* **2017**, *53*, 12068–12071.
(87) Nichol, M. F.; Clark, K. D.; Dolinski, N. D.; Alaniz, J. R. de. Multi-stimuli responsive trigger for temporally controlled depolymerization of self-immolative polymers. *Polym. Chem.* **2019**, *10*, 4914–4919.
(88) Hu, X.; Zeng, T.; Husic, C. C.; Robb, M. J. Mechanically Triggered Small Molecule Release from a Masked Furfuryl Carbonate. *J. Am. Chem. Soc.* **2019**, *141*, 15018–15023.

(89) Hu, X.; Zeng, T.; Husic, C. C.; Robb, M. J. Mechanically Triggered Release of Functionally Diverse Molecular Payloads from Masked 2-Furylcarbinol Derivatives. *ACS Cent. Sci.* **2021**, *7*, 1216–1224.
(90) Zeng, T.; Hu, X.; Robb, M. J. 5-Aryloxy substitution enables efficient mechanically triggered release from a synthetically accessible masked 2-furylcarbinol mechanophore. *Chem. Commun.* **2021**, *57*, 11173–11176.
(91) Stevenson, R.; De Bo, G. Controlling Reactivity by Geometry in Retro-Diels–Alder Reactions under Tension. *J. Am. Chem. Soc.* **2017**, *139*, 16768–16771.
(92) Tseng, Y.-L.; Zeng, T.; Robb, M. J. Incorporation of a self-immolative spacer enables mechanically triggered dual payload release. *Chem. Sci.* **2024**, 10.1039.D3SC06359C.
(93) Braakhuis, B. J. M.; Haperen, V. W. T. R. van; Welters, M. J. P.; Peters, G. J. Schedule-dependent therapeutic efficacy of the combination of gemcitabine and cisplatin in head and neck cancer xenografts. *Eur. J. Cancer* **1995**, *31*, 2335–2340.
(94) Lee, M. J.; Ye, A. S.; Gardino, A. K.; Heijink, A. M.; Sorger, P. K.; MacBeath, G.; Yaffe, M. B. Sequential Application of Anticancer Drugs Enhances Cell Death by Rewiring Apoptotic Signaling Networks. *Cell* **2012**, *149*, 780–794.
(95) Zeng, T.; Ordner, L. A.; Liu, P.; Robb, M. J. Multimechanophore Polymers for Mechanically Triggered Small Molecule Release with Ultrahigh Payload Capacity. *J. Am. Chem. Soc.* **2023**, jacs.3c11927.
(96) Shi, Z.; Song, Q.; Göstl, R.; Herrmann, A. Mechanochemical activation of disulfide-based multifunctional polymers for theranostic drug release. *Chem. Sci.* **2021**, *12*, 1668–1674.
(97) Wiita, A. P.; Ainavarapu, S. R. K.; Huang, H. H.; Fernandez, J. M. Force-dependent chemical kinetics of disulfide bond reduction observed with single-molecule techniques. *Proc. Natl. Acad. Sci. U.S.A.* **2006**, *103*, 7222–7227.
(98) Dopieralski, P.; Ribas–Arino, J.; Anjukandi, P.; Krupicka, M.; Marx, D. Unexpected mechanochemical complexity in the mechanistic scenarios of disulfide bond reduction in alkaline solution. *Nat. Chem.* **2017**, *9*, 164–170.
(99) Shi, Z.; Song, Q.; Göstl, R.; Herrmann, A. The Mechanochemical Release of Naphthalimide Fluorophores from β-Carbonate and β-Carbamate Disulfide-Centered Polymers. *CCS Chem.* **2021**, *3*, 2333–2344.
(100) Alouane, A.; Labruère, R.; Le Saux, T.; Schmidt, F.; Jullien, L. Self-Immolative Spacers: Kinetic Aspects, Structure–Property Relationships, and Applications. *Angew. Chem. Int. Ed.* **2015**, *54*, 7492–7509.
(101) Suslick, K. S. Sonochemistry. *Science* **1990**, *247*, 1439–1445.
(102) Mitragotri, S. Healing sound: the use of ultrasound in drug delivery and other therapeutic applications. *Nat. Rev. Drug. Discov.* **2005**, *4*, 255–260.
(103) May, P. A.; Moore, J. S. Polymer mechanochemistry: techniques to generate molecular force via elongational flows. *Chem. Soc. Rev.* **2013**, *42*, 7497–7506.
(104) Basedow, A. M.; Ebert, K. H. Ultrasonic degradation of polymers in solution. In *Physical Chemistry*; Advances in Polymer Science; Springer: Berlin, Heidelberg, 1977; pp 83–148.

(105) Tong, R.; Lu, X.; Xia, H. A facile mechanophore functionalization of an amphiphilic block copolymer towards remote ultrasound and redox dual stimulus responsiveness. *Chem. Commun.* **2014**, *50*, 3575–3578.
(106) Kim, G.; Lau, V. M.; Halmes, A. J.; Oelze, M. L.; Moore, J. S.; Li, K. C. High-intensity focused ultrasound-induced mechanochemical transduction in synthetic elastomers. *Proc. Natl. Acad. Sci. USA* **2019**, *116*, 10214–10222.

Chapter 2

MECHANICALLY TRIGGERED SMALL MOLECULE RELEASE FROM MASKED 2-FURYLCARBINOL DERRIVATIVES

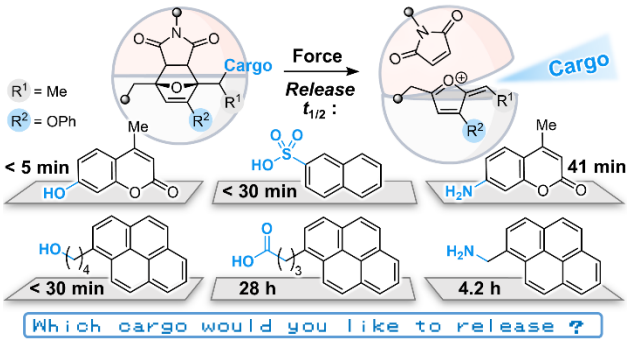

Abstract: Polymers that release functional small molecules in response to mechanical force are appealing targets for drug delivery, sensing, catalysis, and many other applications. Mechanically sensitive molecules called mechanophores are uniquely suited to enable molecular release with excellent selectivity and control. Here, we describe a general and highly modular mechanophore platform based on masked 2-furylcarbinol derivatives that spontaneously decompose under mild conditions upon liberation via a mechanically triggered reaction, resulting in the ultimate release of a covalently installed molecular payload. We identify key structure–property relationships for the reactivity of 2-furylcarbinol derivatives that enable the mechanically triggered release of functionally diverse molecular cargo with release kinetics being tunable over several orders of magnitude. The generality and efficacy of this molecular design platform is demonstrated using ultrasound-induced mechanical force to trigger the efficient release of a broad scope of cargo molecules including those bearing alcohol, phenol, alkylamine, arylamine, carboxylic acid, and sulfonic acid functional groups.

This chapter has been adapted with permission from
Hu, X.; Zeng, T.; Husic, C. C.; Robb, M. J. *J. Am. Chem. Soc.* **2019**, *141*, 15018–15023, and Hu, X.; Zeng, T.; Husic, C. C.; Robb, M. J. *ACS Cent. Sci.* **2021**, *7*, 1216–1224.

2.1 Investigation

Polymers that release functional molecules in response to a specific stimulus are desirable for a variety of applications including sensing, catalysis, self-healing, and targeted drug delivery.[1–3] Mechanically triggered release is a particularly appealing target. To this end, several different approaches have been demonstrated including physically entrapped payloads within a polymeric matrix,[4] dissociation of supramolecular assemblies,[5,6] and the use of fluid-filled microcapsules[7] or vascular networks[8] embedded within a material that release their payload after being ruptured. Recently, the use of mechanical force as an external stimulus to drive covalent chemical transformations has emerged as an attractive strategy.[9] Force is typically transduced via polymer chains to mechanically sensitive molecules known as mechanophores that respond in a chemoselective fashion, resulting in a productive chemical reaction.[10,11] In the context of targeted drug delivery, for example, ultrasound is capable of penetrating deep within biological tissues to stimulate mechanochemical transformations noninvasively and with spatial and temporal precision.[12] In light of these advantages, the field of polymer mechanochemistry has attracted significant interest for the design of autonomous materials that respond innately to mechanically dynamic environments,[3] as well as abundant opportunities to advance fundamental understanding of mechanochemical reactivity, which is underdeveloped compared to other areas of organic chemistry.[13]

Several mechanophores have been designed to achieve the mechanically triggered release of functional organic molecules, although the scope of molecules that can be released is still relatively limited. Moore and Craig have designed mechanophores based on *gem*-dichlorocyclopropane motifs that undergo mechanochemical rearrangement reactions with subsequent release of HCl.[14,15] Boydston has developed mechanophores based on a flex-activation manifold demonstrating release of a benzyl furfuryl ether molecule via a mechanically induced cycloelimination reaction[16,17] and the release of N-heterocyclic carbenes.[18] Notably, each approach uses a judiciously designed mechanophore to release a specific compound upon mechanical activation, which consequently limits the scope of molecules that can be released. Small molecule release has also been achieved through the mechanically triggered heterolytic scission and subsequent depolymerization of poly(*ortho*-

phthalaldehyde) to regenerate its constituent monomers.[19,20] Finally, Herrmann and Göstl have introduced an elegant mechanophore design that relies on the mechanically activated reduction[21,22] of a chain-centered disulfide unit and ensuing 5-*exo*-*trig* cyclization to release an alcohol attached via a β-carbonate linker.[5,23] While the release of several different alcohols has been successfully demonstrated using this disulfide mechanophore platform, it is susceptible to nonspecific activation via chemical reduction or thiol exchange and cargo scope appears to be somewhat limited, as indicated by the low release efficiency observed for amine payloads.[24]

Here we report a mechanophore platform based on a furan–maleimide Diels–Alder adduct that leverages the instability of a judiciously designed furfuryl carbonate for small molecule release via a mechanically gated reaction cascade. As illustrated in Scheme 2.1, mechanochemical activation of the kinetically stable adduct results in a retro-Diels–Alder reaction, revealing a metastable furfuryl carbonate that quickly decomposes in polar protic media to release carbon dioxide and a covalently bound alcohol molecule. The secondary furfuryl carbonate structure is a key design feature that significantly increases the rate of decomposition and small molecule release, enabling the transformation to proceed spontaneously under mild conditions, but only after the prerequisite mechanochemical cycloelimination reaction.

Scheme 2.1. Mechanically Triggered Reaction Cascade Resulting in Small Molecule Release.

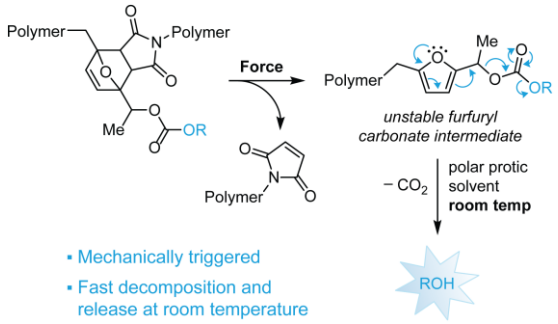

To initate the study, we synthesized fluorogenic furfuryl carbonate model compound **1** and investigated its reactivity experimentally (Figure 2.1). The coumarin payload exhibits enhanced photoluminescence (PL) upon release, allowing reaction progress to be tracked using fluorescence spectroscopy in addition to NMR spectroscopy. Furfuryl carbonate **1** is relatively stable in chloroform and acetonitrile (Figure 2.2); however, the addition of

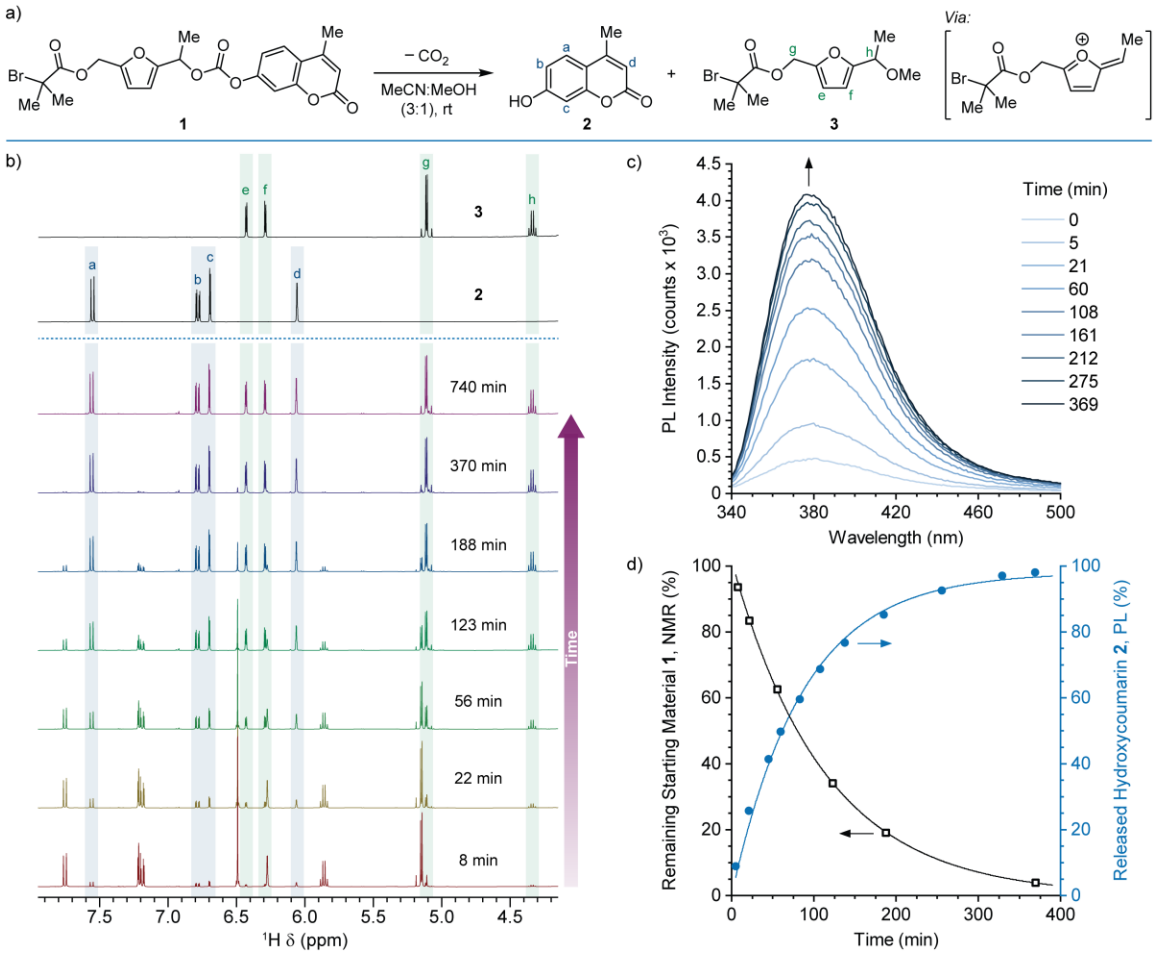

Figure 2.1. Characterization of the room temperature decomposition reaction of furfuryl carbonate **1**. (a) Decomposition of **1** in 3:1 MeCN:MeOH generates fluorescent hydroxycoumarin **2** and furfuryl methyl ether **3** via a putative furfuryl cation intermediate. (b) ^{1}H NMR spectra (3:1 MeCN-d_3:MeOH) demonstrating the clean conversion of **1** to products ($[1]_0$ = 12 mM). (c) Photoluminescence spectra ($[1]_0$ = 6.1 μM in 3:1 MeCN:MeOH, λ_{ex} = 330 nm) monitoring the generation of hydroxycoumarin 2 over time. (d) Quantification of data from panels *b* and *c* illustrating the time-dependent conversion of furfuryl carbonate **1** and the generation of hydroxycoumarin **2** as measured by NMR and fluorescence spectroscopy, respectively.

methanol to an acetonitrile solution of **1** leads to fast decomposition at room temperature and clean formation of hydroxycoumarin **2** and furfuryl ether **3** (Figure 2.1a). The generation of furfuryl ether **3** under these conditions is consistent with a mechanism involving initial fragmentation of the carbonate group to form a furfuryl cation, which is subsequently attacked by methanol followed by proton transfer. Figure 2.1b shows the decomposition of furfuryl carbonate **1** in a 3:1 (v/v) mixture of acetonitrile-d_3 and methanol monitored by ^{1}H NMR spectroscopy. Signals corresponding to **1** fully disappear in a few hours with the

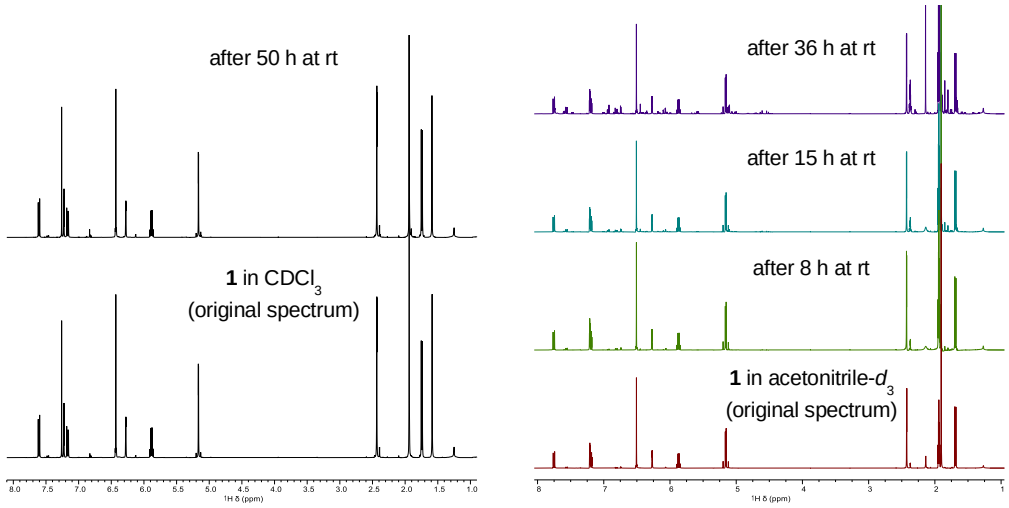

Figure 2.2. ^{1}H NMR spectra (400 MHz) of model compound **1** in (a) $CDCl_3$ at room temperature acquired 50 h apart where no reaction was observed, (b) acetontrile-d_3 at room temperature acquired over 36 h, where some degradation occurs after extended times under these conditions.

concomitant formation of two new sets of resonances that match the spectra of the isolated hydroxycoumarin and furfuryl methyl ether products. The generation of hydroxycoumarin **2** from a room temperature solution of furfuryl carbonate **1** in MeCN:MeOH (3:1) was also monitored over time using fluorescence spectroscopy (Figure 2.1c). Excitation at 330 nm revealed an emission peak around 380 nm that increased in intensity over time and matches

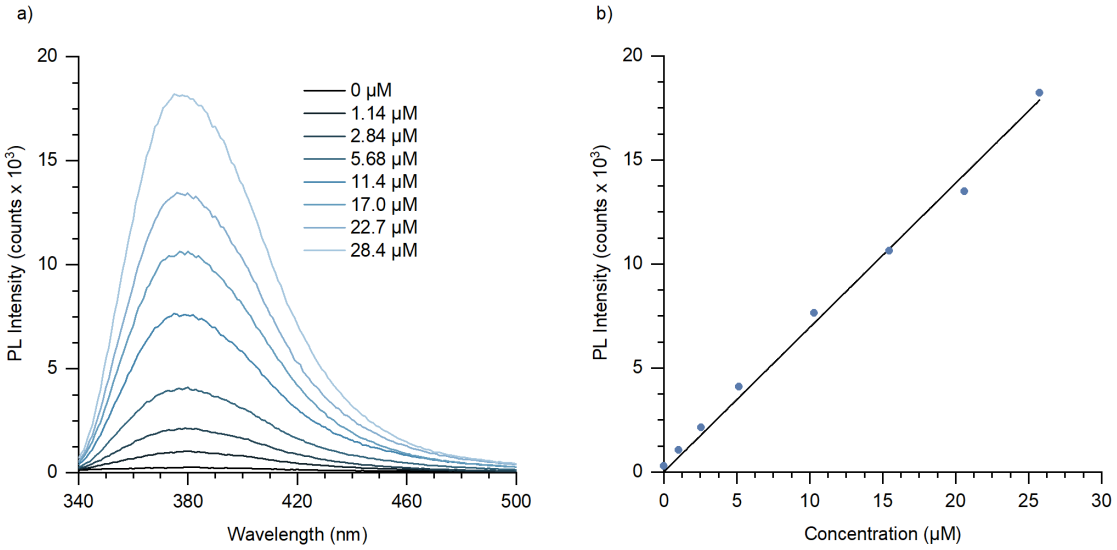

Figure 2.3. Construction of a calibration curve for experimental determination of the concentration of hydroxycoumarin **2**. (a) Fluorescence emission spectra (λ_{ex} = 330 nm) and (b) intensity at 380 nm for solutions of 7-hydroxy-4-methylcoumarin (**2**) in acetonitrile/methanol (3:1 v/v) as a function of concentration. A linear regression of the data in (b) gives the calibration function, Y = 0.694*X.

the emission spectrum of hydroxycoumarin **2** (Figure 2.3). Approximately 98% of the theoretical yield of hydroxycoumarin **2** is released over about 6 h (Figure 2.1d). The conversion of furfuryl carbonate **1** and the generation of hydroxycoumarin **2** follow exponential decay under these conditions with the reaction half-life estimated from NMR measurements to be $t_{1/2}$ = 79 min.

Scheme 2.2. Synthesis of Poly(Methyl Acrylate) (PMA) Containing a Chain-Centered Mechanophore Equipped with a Fluorogenic Coumarin Probe and a Chain-End Functional Control Polymer.

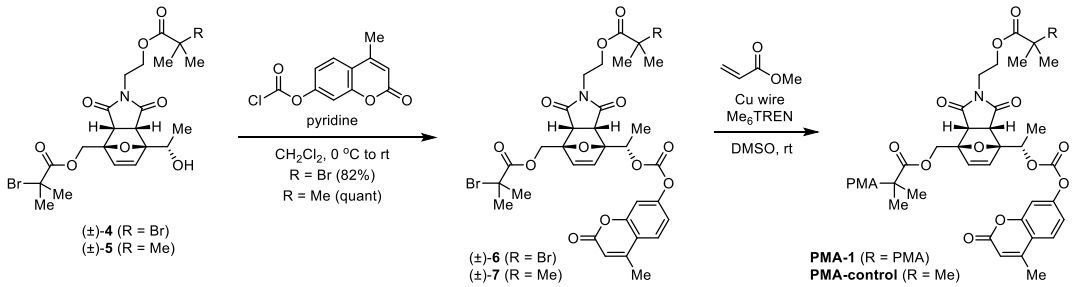

Having identified a suitable furfuryl carbonate structure for small molecule release we next set out to synthesize a furan–maleimide Diels–Alder adduct and incorporate it into a polymer to study its mechanochemical behavior. Polymers containing a chain-centered mechanophore are mechanically activated in solution using ultrasonication, which produces elongational forces that are maximized near the chain midpoint.[25] Furan–maleimide adduct (±)-**4** equipped with two α-bromoester initiating sites and a modular alcohol functional group for cargo attachment was prepared on gram scale in four steps from commercially available reagents (Scheme 2.2). Starting from a racemic mixture of α-methylfurfuryl alcohol resulted in four diastereomeric Diels–Alder adducts. Although both *endo* and *exo* isomers exhibited mechanochemical reactivity in an initial screening as expected from previous studies of furan–maleimide mechanophores,[26] here we focus on one particular *endo* racemate shown in Scheme 2.2. The absolute configuration of the Diels–Alder adduct was confirmed by single crystal X-ray diffraction. Precursor (±)-**4** was converted to mechanophore bis-initiator (±)-**6** via installation of the fluorogenic coumarin payload by reaction with the corresponding chloroformate, and then subsequently employed in the controlled radical polymerization of methyl acrylate using Cu wire/Me_6TREN in DMSO to afford the chain-centered polymer **PMA-1** (M_n = 100 kg/mol; $Đ$ = 1.06). Chain-end functional control polymer **PMA-control**

(M_n = 86 kg/mol; $Đ$ = 1.14) was synthesized similarly starting from (±)-**5** containing a single α-bromoester initiating group.

Mechanically triggered molecular release from **PMA-1** was evaluated using pulsed ultrasonication (1s on/2s off, 0 °C, 20 kHz, 8.2 W/cm^2) in the same polar protic solvent mixture employed in the small molecule model studies (3:1 MeCN/MeOH). Aliquots were periodically removed from the sonicated polymer solution and measured with gel permeation chromatography (GPC) to determine changes in molecular weight and fluorescence spectroscopy to monitor the generation of hydroxycoumarin **2** (Figure 2.4). The M_n decreased steadily over 150 min of ultrasonication, with the GPC chromatograms exhibiting characteristic features of midchain scission (Figures 2.4a, 2.5). Photoluminescence measurements also showed a predictable increase in intensity indicating the successful release of hydroxycoumarin **2**, reaching approximately 64% of the theoretical yield after 150 min (Figure 2.4a). By fitting the time-dependent PL data to a first-order rate expression, the extent of release is projected to plateau at a maximum value of approximately 87% (Figure 2.6). The reduced efficiency compared to the small molecule decomposition study likely stems from the inherent competition between mechanophore activation and

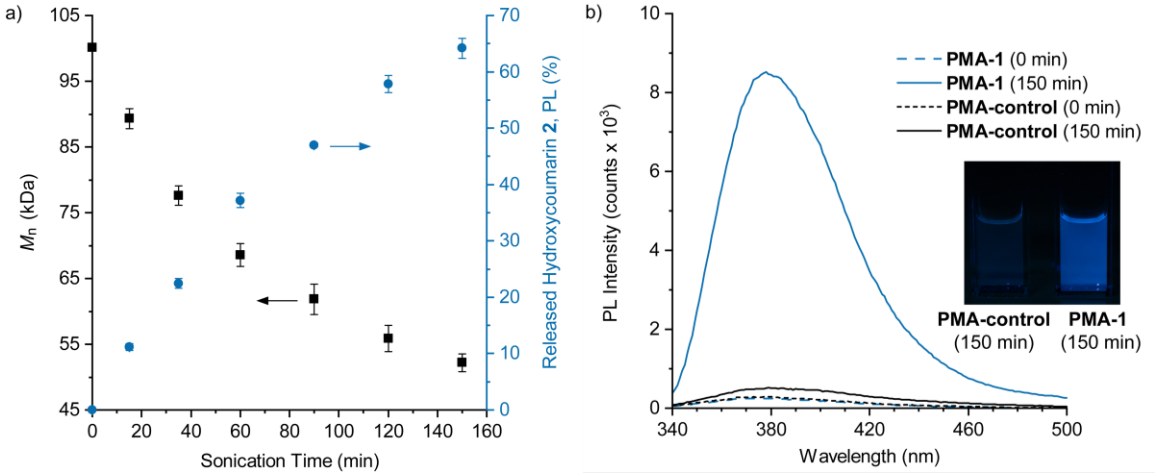

Figure 2.4. Characterization of mechanically triggered small molecule release. (a) Time-dependent evolution of number-average molecular weight (M_n) monitored by GPC-MALLS and release of hydroxycoumarin **2** monitored using fluorescence spectroscopy for **PMA-1** subjected to ultrasound-induced mechanochemical activation (2 mg/mL polymer in 3:1 MeCN:MeOH). λ_{ex} = 330 nm. (b) Fluorescence spectra of **PMA-1** and **PMA-control** before and after ultrasonication for 150 min. The inset shows photographs of sonicated solutions excited with 365 nm UV light after 6x dilution and addition of 5% water. Error bars represent standard deviation from three replicate experiments.

nonspecific chain scission, resulting in part from a distribution in the position of mechanophores in the polymer backbones.[27] The fluorescence data presented in Figure 2.4 was acquired after incubating each aliquot at room temperature for approximately 20 h to ensure complete decomposition of the mechanically generated furfuryl carbonate. However, PL measurements taken immediately after sample removal from the sonicated solution exhibit appreciable fluorescence, indicating that a significant degree of release occurs

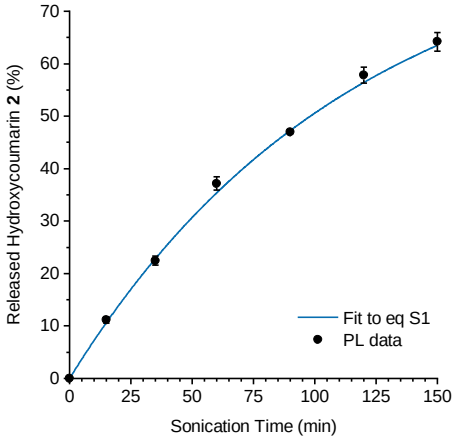

Equation S1	A*(1-e^(-k*t))
k	0.00867 ± 7.75E-04
A	87.3 ± 5.16
Reduced Chi-Sqr	0.8603
R-Square (COD)	0.9997
Adj. R-Square	0.9997

Figure 2.5. Release of hydroxycoumarin **2** from **PMA-1** as a function of sonication time (2 mg/mL polymer in 3:1 MeCN:MeOH) monitored using fluorescence spectroscopy (λ_{ex} = 330 nm, λ_{em} = 380 nm). Aliquots were removed from the sonicated solution and kept at room temperature for 20 h to allow complete decomposition of the mechanically generated furfuryl carbonate prior to measurement. Error bars represent standard deviation from three replicate experiments. Fitting the data to a first-order rate expression (eq S1) gives a projected maximum release of approximately 87%.

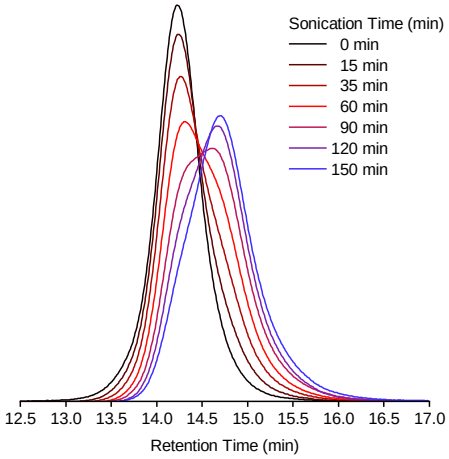

Figure 2.6. GPC traces as a function of ultrasonication time for **PMA-1** monitored with a refractive index (RI) detector. Ultrasound-induced mechanochemical activation causes chain scission near the polymer midpoint, resulting in attenuation of the initial polymer peak (M_p = 101 kg/mol) and an increase in a new peak (M_p = 55 kg/mol) at approximately one-half the original molecular weight.

quickly even at lower temperatures (Figure 2.7). Importantly, chain-end functional control polymer **PMA-control** subjected to the same ultrasonication conditions exhibits negligible changes in fluorescence compared to **PMA-1** (Figure 2.4b). These results indicate that ultrasound-induced release of hydroxycoumarin **2** from **PMA-1** is indeed a mechanically triggered cascade reaction process.

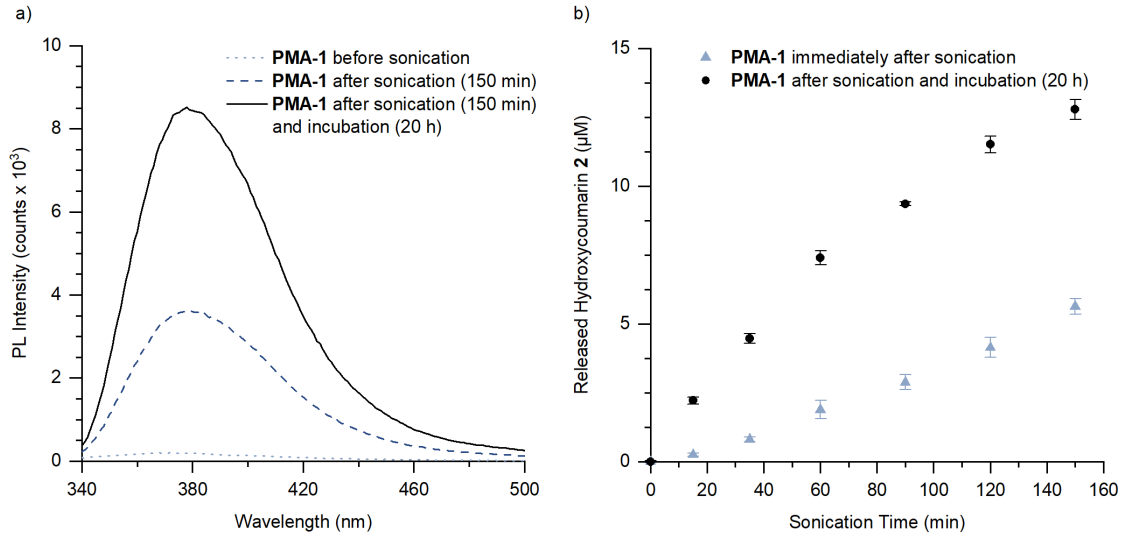

Figure 2.7. (a) Representative fluorescence spectra of a 2.0 mg/mL solution of **PMA-1** in acetonitrile/methanol (3:1 v/v) before ultrasonication (dotted line), immediately after 150 min ultrasonication at 0 °C (dashed line), and after 150 min ultrasonication followed by incubation at room temperature for 20 h (solid line). (b) Concentrations of **2** released from **PMA-1** measured by fluorescence spectroscopy as a function of ultrasonication time. Aliquots were removed from the sonicated solution and immediately measured, and then subsequently remeasured after being kept at room temperature for 20 h to allow complete decomposition of the mechanically generated furfuryl carbonate. Error bars represent standard deviation from three replicate experiments.

This paradigm offers a powerful approach for the design of highly modular systems, as the mechanochemical behavior of the mechanophore and the functional properties of the masked intermediate can be controlled independently. While the molecular design strategy is promising, our first-generation mechanophore is nevertheless limited to the release of phenols and a more general platform capable of releasing functionally diverse molecular cargo on reasonable time scales is desired. Therefore, we next investigateed the impact of substitution on the reactivity of 2-furylcarbinol derivatives, identifying structure–activity relationships (SAR) that enable the mechanically triggered release of functionally diverse molecular payloads from a second-generation mechanophore platform.

Furfuryl carbonates decompose in polar protic media by the mechanism depicted in Scheme 2.1a via a putative furfuryl cation intermediate.[28] Primary furfuryl carbonates possessing only an alkyl group at the 5-position of the furan ring are relatively unreactive and decompose slowly at room temperature; however, installation of an additional α-methyl group significantly reduces the activation barrier for carbonate fragmentation. While this substitution pattern is sufficient to enable the release of a phenolic cargo molecule with a half-life of approximately 1 h, the rate of fragmentation is still prohibitively slow for alcohol and amine-derived furfuryl carbonates and carbamates, respectively. For example,

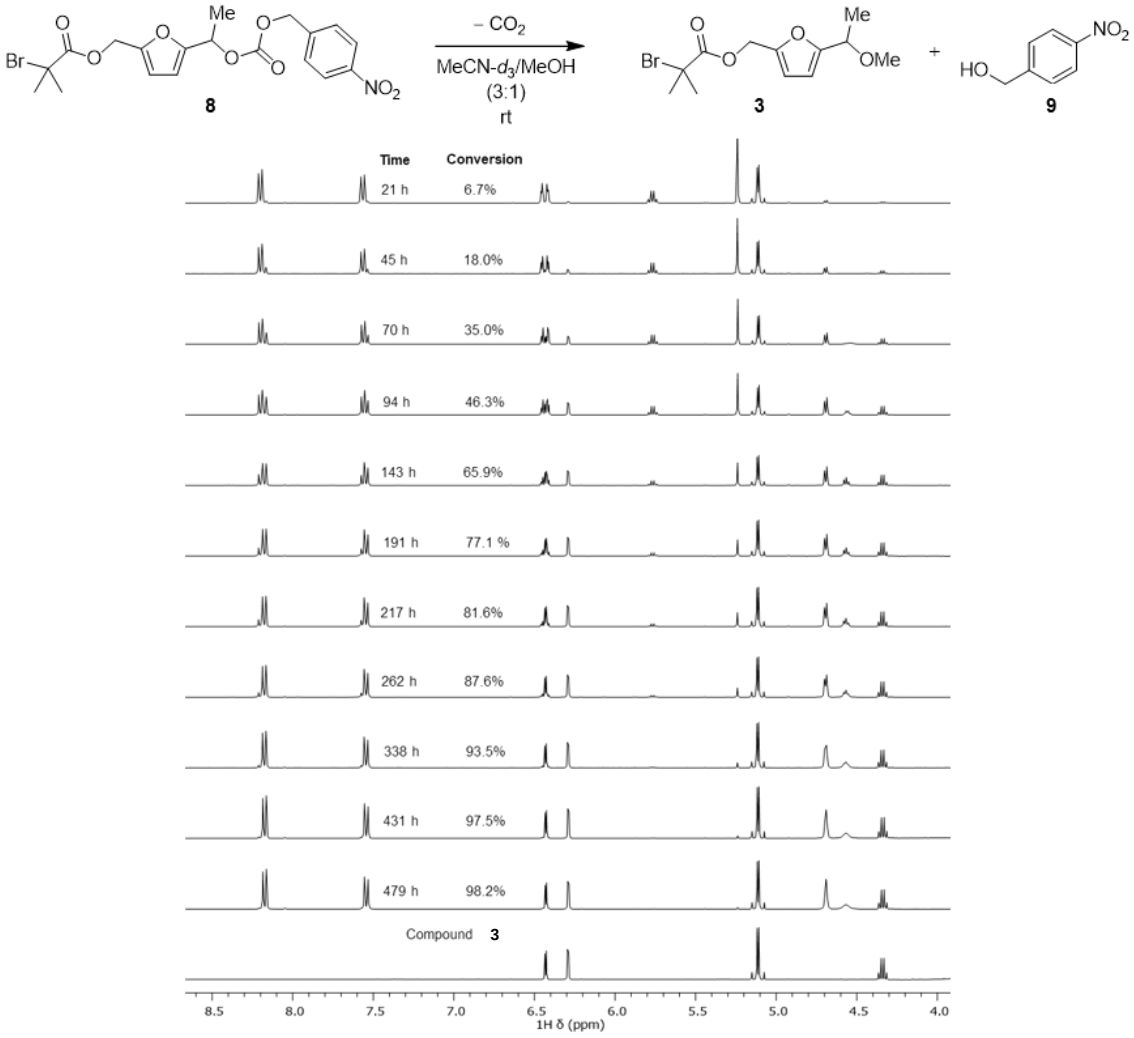

Figure 2.8. Partial ^{1}H NMR spectra (400 MHz) of a 42 mM solution of **8** in MeCN-d_3/MeOH (3:1) at room temperature. The starting material was cleanly converted over a period of approximately 500 h, with a new set of peaks emerging matching with the spectrum of furfuryl methyl ether **3** (bottom trace). The reaction half-life is approximately 4.1 days.

preliminary kinetic studies performed on a small molecule model compound reveal that the release of a primary alcohol from our earlier furfuryl carbonate substrate occurs with a half-life of approximately 4 days, or nearly 100× slower than the release of hydroxycoumarin (Figure 2.8). We reasoned that the addition of an electron-donating substituent[29] at the 3-position of the furan would further suppress the activation barrier for fragmentation since this substituent is in resonance with the furfuryl carbocation, potentially enabling the efficient release of even more challenging payloads including amines[30] under mild conditions.

To validate this hypothesis, we synthesized fluorogenic furfuryl carbamate model compound **10** containing α-methyl and 3-phenoxy substituents and investigated its reactivity experimentally (Figure 2.9). The coumarin payload exhibits a fluorescence turn-on after release, allowing the reaction to be conveniently monitored using photoluminescence (PL), in addition to NMR spectroscopy. The addition of methanol to a room temperature solution

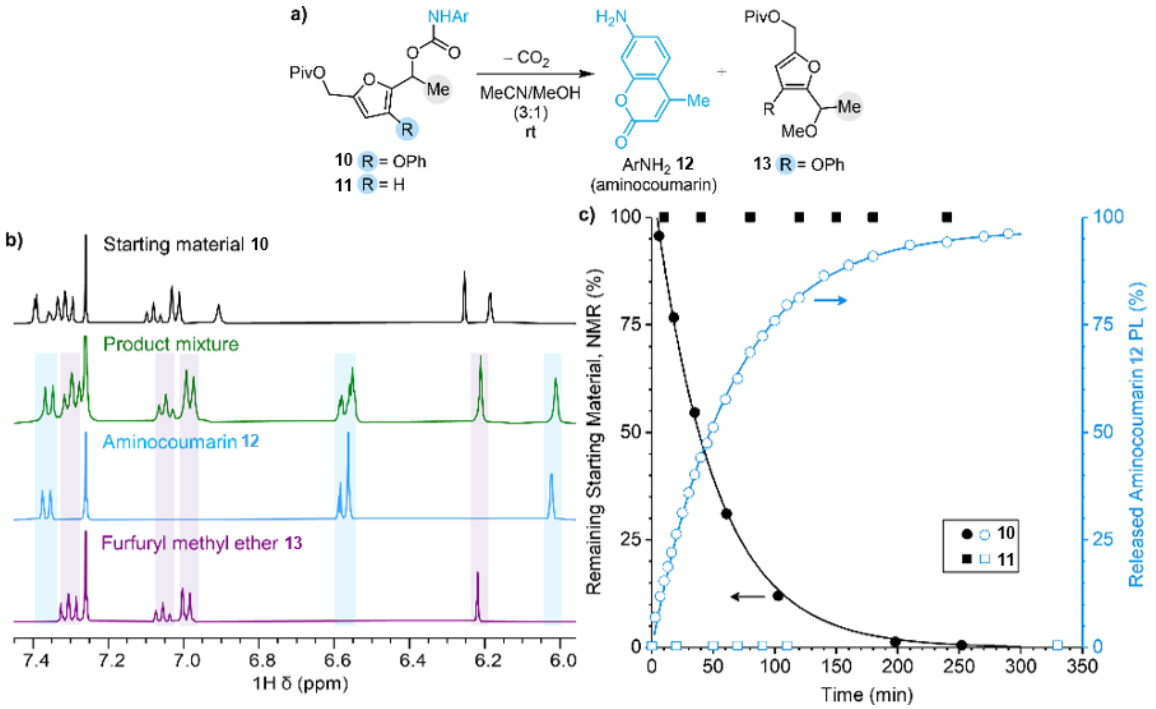

Figure 2.9. Characterization of the decomposition reactions of model furfuryl carbamates **10** and **11**. (a) Decomposition of **10** in MeCN/MeOH (3:1) at room temperature generates fluorescent aminocoumarin **12** and furfuryl methyl ether **13** via a putative furfuryl cation intermediate. (b) Partial ^{1}H NMR spectra (400 MHz, $CDCl_3$) demonstrating the clean conversion of **10** to products ($[\mathbf{10}]_0$ = 19 μM). (c) Time course experiments following the conversion of furfuryl carbamates **10** and **11** by NMR spectroscopy (in 3:1 MeCN-d_3/MeOH; $[\mathbf{10}]_0$, $[\mathbf{11}]_0$ = 14 mM) and the generation of **12** by PL spectroscopy (3:1 MeCN/MeOH; λ_{ex} = 365 nm; λ_{em} = 424 nm; $[\mathbf{10}]_0$, $[\mathbf{11}]_0$ = 7.6 μM).

of **10** in acetonitrile-d_3 (19 μM, 3:1 MeCN/MeOH) triggers decomposition and results in clean conversion to aminocoumarin **12** and furfuryl methyl ether **13** as evidenced by NMR spectroscopy (Figure 2.9b). The formation of furfuryl methyl ether **13** is consistent with the transient formation of a furfuryl cation intermediate that is intercepted by methanol. Interestingly, when the reaction is performed at significantly higher concentrations, another set of peaks was observed in the ^{1}H NMR spectra corresponding to the formation of a side product that was identified to be the furfuryl amine derived from nucleophilic attack of the furfuryl cation intermediate by liberated aminocoumarin **12** (Figures 2.10 and 2.11). A similar reaction was not observed for the furfuryl carbonate studied previously, highlighting the increased nucleophilicity of the amine cargo. Importantly, however, this furfuryl amine side product is formed in < 2% yield in reactions with a substrate concentration of 19 μM, which is similar to the concentration of mechanophores in typical ultrasonication experiments (*vide infra*). These results confirm that at these relatively low substrate concentrations, the reaction depicted in Figure 2.9 is sufficiently descriptive. The kinetics of furfuryl carbamate decomposition were further studied by monitoring the conversion of starting material and the generation of aminocoumarin **12** as a function of time using NMR and PL spectroscopy, respectively (Figure 2.9c). Furfuryl carbamate **10** is fully converted to products in approximately 5 h, with concomitant increase in fluorescence corresponding to the generation of aminocoumarin **12** (Figure 2.12). The data from both time course experiments were fitted to first-order rate expressions, providing half-lives of $t_{1/2}$ = 34 and 45 min from NMR and PL measurements, respectively. In direct contrast, secondary furfuryl carbamate model compound **11**, which does not contain a 3-phenoxy substituent but is otherwise identical to the furfuryl carbonate reported previously that is active toward phenol release, is completely unreactive under the same conditions (Figures 2.9c and 2.13). The striking difference in decomposition behavior between model compounds **10** and **11** highlights the impact of an electron-donating phenoxy substituent on the furan ring and supports the molecular design for a second-generation mechanophore platform enabling the molecular release of previously inaccessible payloads.

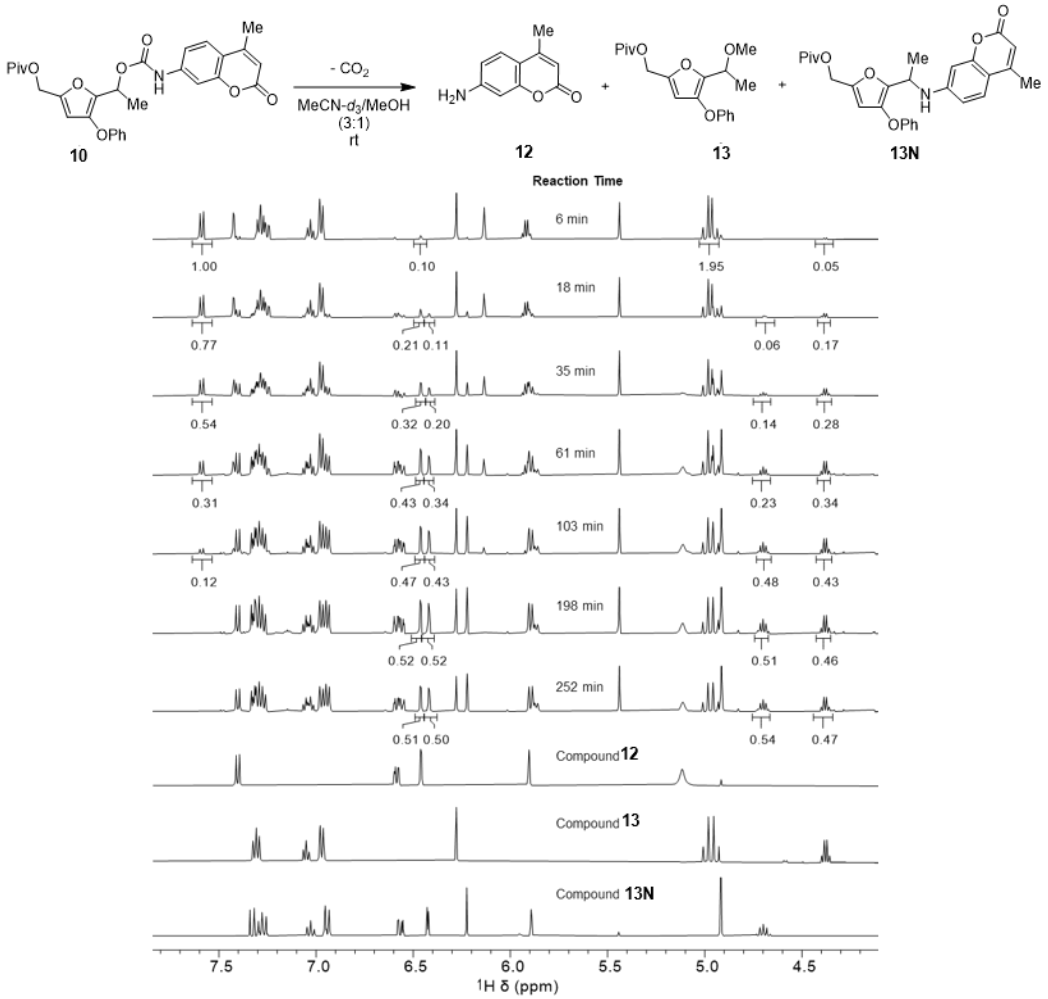

Figure 2.10. Partial ^{1}H NMR spectra (500 MHz) of a 14.0 mM solution of compound **10** in MeCN-d_3/MeOH (3:1) at room temperature, compared to spectra of compounds **12**, **13**, and **13N** (400 MHz) in the same solvent mixture. Decomposition of **10** at this relatively high concentration generates aminocoumarin **12** and furfuryl methyl ether **13**, as well as side product furfuryl amine **13N**.

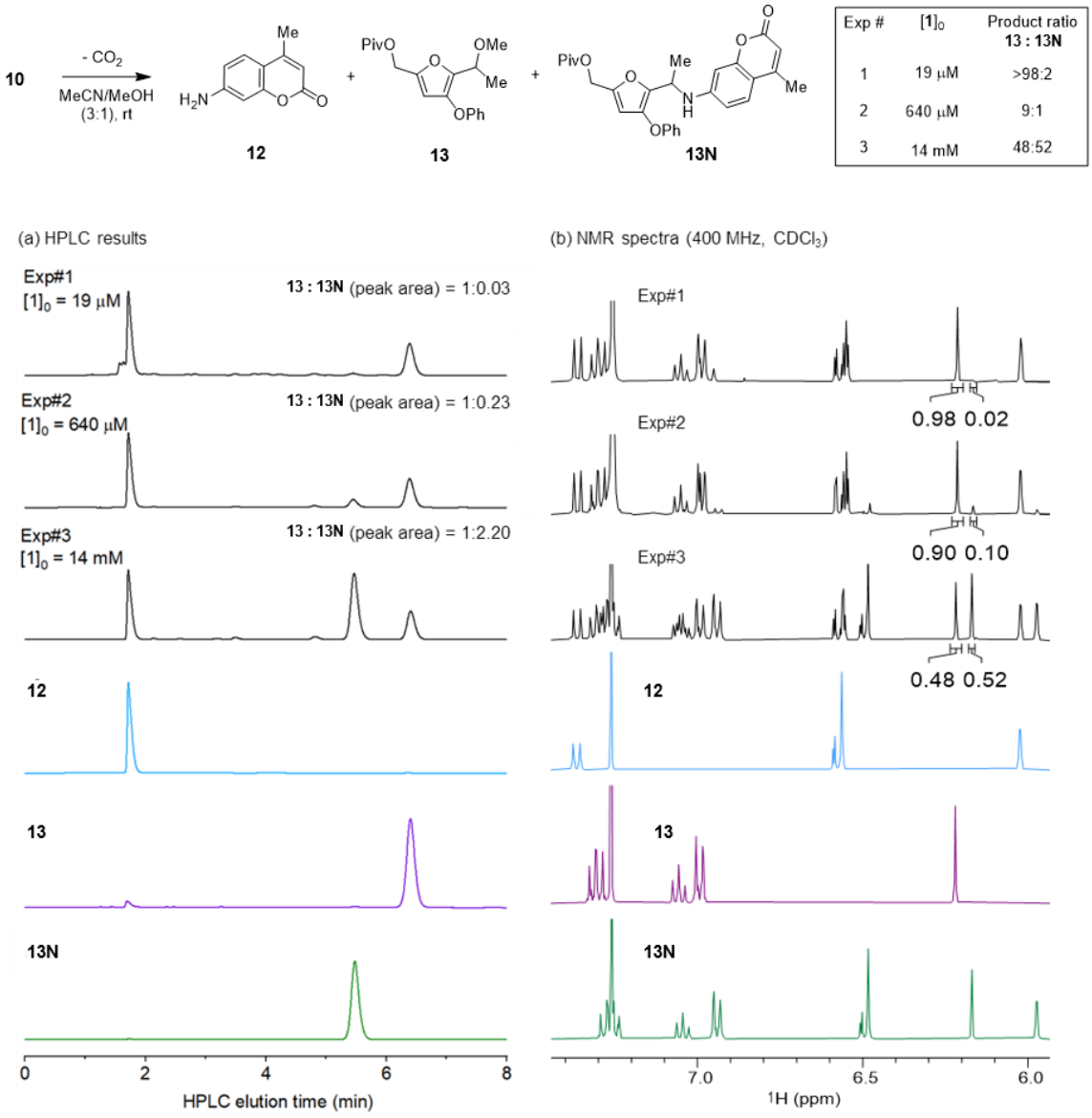

Figure 2.11. Quantification of products from the decomposition of model compound **10** under varying reaction concentrations by (a) HPLC and (b) ^{1}H NMR spectroscopy. Three separate experiments were performed with solutions of **10** at different initial concentrations in 3:1 MeCN/MeOH (19 μM, 640 μM, and 14 mM). Solutions were kept at room temperature for a minimum of 10 h to ensure complete conversion, then dried, dissolved in $CDCl_3$, and analyzed by HPLC equipped with a UV-vis detector (λ = 233 nm) and ^{1}H NMR spectroscopy. The reaction mixtures from each trial were compared to isolated aminocoumarin **12**, furfuryl methyl ether **13**, and furfuryl amine **13N**. HPLC conditions: MeCN/water (70:30), C8 column, 25°C, 1 mL/min.

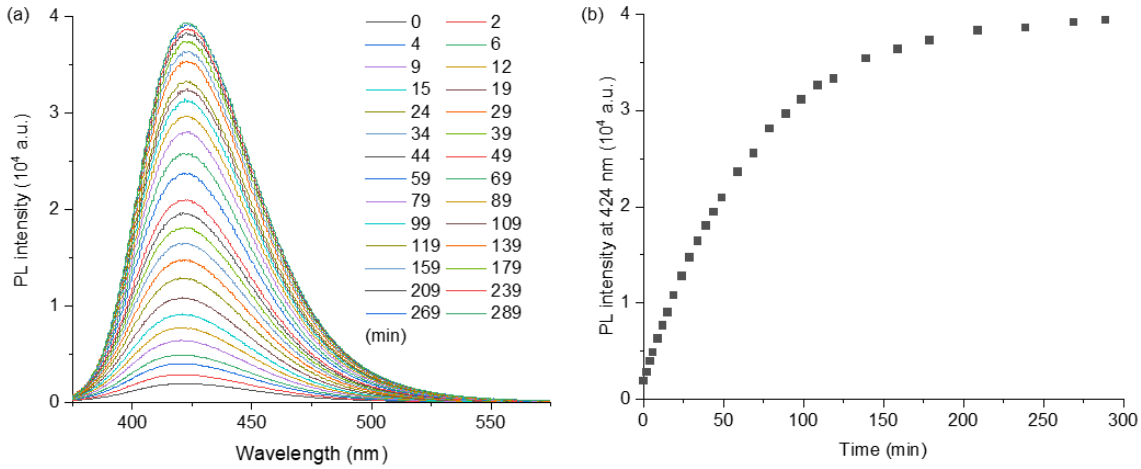

Figure 2.12. Photoluminescence characterization of the release of fluorogenic payload **12** from compound **10**. (a) Fluorescence emission spectra of a solution of compound **10** in 3:1 MeCN:MeOH (7.6 μM) at room temperature. (b) Fluorescence intensity at 424 nm as a function of time. The theoretical PL intensity of a 7.6 μM solution of **12** is calculated to be 4.09 x 10^4 a.u. based on the calibration curve in Figure S9. λ_{ex} = 365 nm.

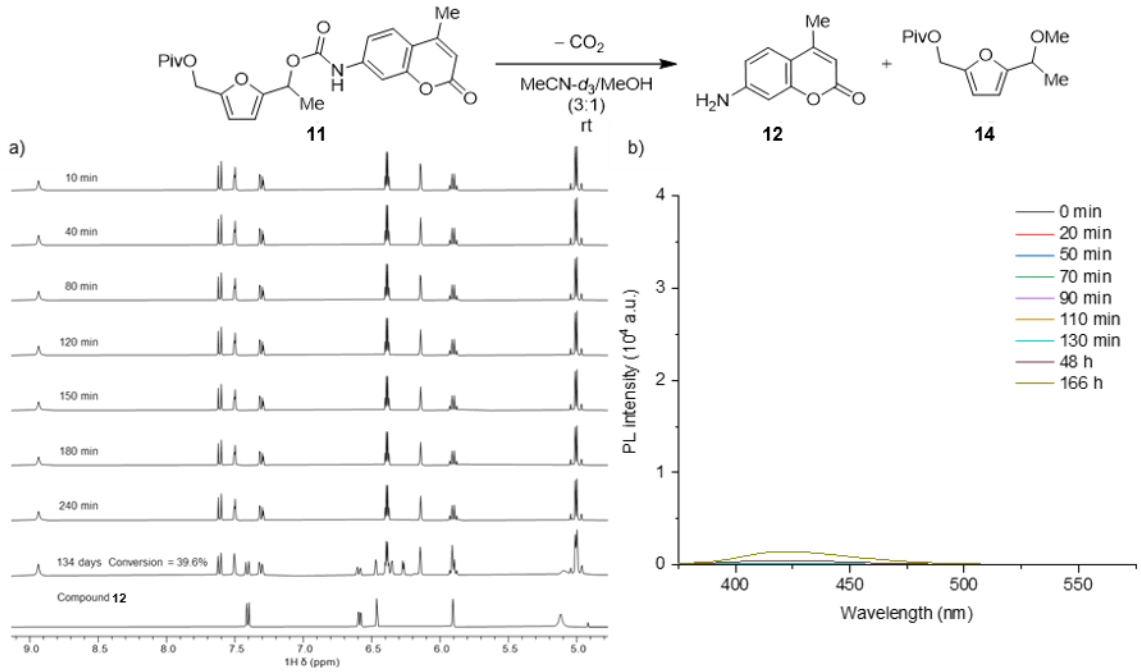

Figure 2.13. (a) Partial ^{1}H NMR spectra (400 MHz) of a 19.6 mM solution of compound **11** in MeCN-d_3:MeOH (3:1) at room temperature. Approximately 40% conversion is observed after 134 days. (b) Fluorescence emission spectra of a solution of compound **11** in 3:1 MeCN:MeOH (7.6 μM) at room temperature. The expected PL intensity from a 7.6 μM solution of aminocoumarin **12** is approximately 4.09 x 10^4 based on the calibration curve. λ_{ex} = 365 nm.

We next synthesized a series of furan−maleimide Diels−Alder adducts serving as masked furfuryl carbonates/carbamates with varying substitution and incorporated them into polymers to study their mechanochemical behavior. Polymers containing a chain-centered mechanophore are mechanically activated in solution using ultrasonication, which produces elongational forces that are maximized near the chain midpoint.[25] We synthesized polymers containing a masked phenoxy-substituted secondary furfuryl carbonate/carbamate (Scheme 2.3), polymers containing a masked phenoxy-substituted primary furfuryl carbonate/carbamate (1º, 3-*OPh*) as well as a secondary furfuryl carbonate/carbamate without a phenoxy substituent (2º, 3-*H*) matching our first-generation molecular design. Starting from 3-bromofurfural, a phenoxy group was installed via a nucleophilic substitution reaction with phenol, followed by Grignard addition and protection to yield furfuryl silyl ether **16**. Next, a formylation reaction and subsequent desilylation with TBAF yielded 2,3,5-trisubstituted furfuryl alcohol **17**. Reduction of the aldehyde with sodium borohydride and a [4+2] cycloaddition reaction with a pre-functionalized maleimide dienophile in a two-step sequence furnished an isomeric mixture of Diels−Alder adducts, from which *endo* diastereomer (±)-**17** was isolated by silica gel chromatography. Esterification of the primary alcohol proceeded with reasonable selectivity using α-bromoisobutyryl bromide to give the modular bis-initiator (±)-**19** containing a secondary alcohol for cargo attachment. The

Scheme 2.3. Synthesis of Poly(Methyl Acrylate) (PMA) Polymers Containing a Chain-Centered Mechanophore with α-Methyl/Phenoxy Substitution and a Fluorogenic Coumarin Payload.

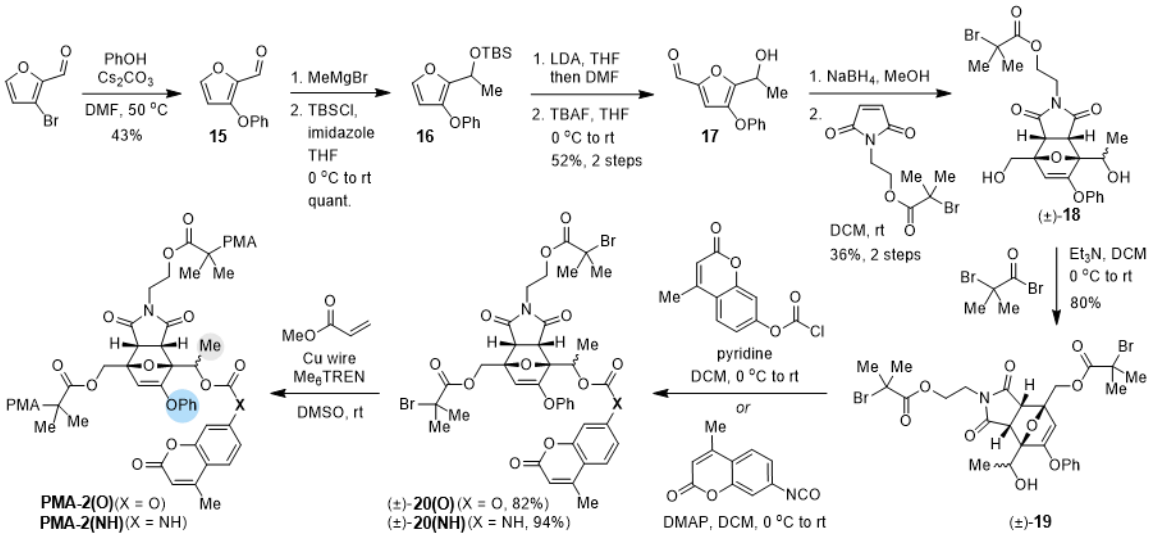

precursor bis-initiator (±)-**19** was then conveniently elaborated to carbonate (±)-**20(O)** and carbamate (±)-**20(NH)** containing fluorogenic coumarin payloads via reaction with the corresponding chloroformate or isocyanate, respectively. After cargo installation, the bis-initiators were employed in the controlled radical polymerization of methyl acrylate with Cu wire/Me_6TREN in DMSO[31] to afford poly(methyl acrylate) (PMA) polymers **PMA-2(O)** and **PMA-2(NH)** containing a chain-centered mechanophore. An analogous synthetic approach enabled the preparation of chain-centered polymers **PMA-3(X)** (1º, 3-*OPh*) and **PMA-4(X)** (2º, 3-*H*) with differing mechanophore substitution. The structure of each polymer is illustrated in Scheme 2.4 along with the number average molecular weight (M_n), which was determined to be in the range 94.7–102 kDa with $Đ \leq 1.06$ by gel permeation chromatography (GPC) equipped with refractive index and multiangle light scattering detectors. In addition, chain-end functional control polymers were synthesized similarly starting from the masked furfuryl carbonates/carbamates containing a single α-bromoester initiating group.

Scheme 2.4. Ultrasound-Induced Mechanical Activation of Substituted Mechanophores and Release of Fluorescent Hydroxycoumarin or Aminocoumarin Cargo.[a]

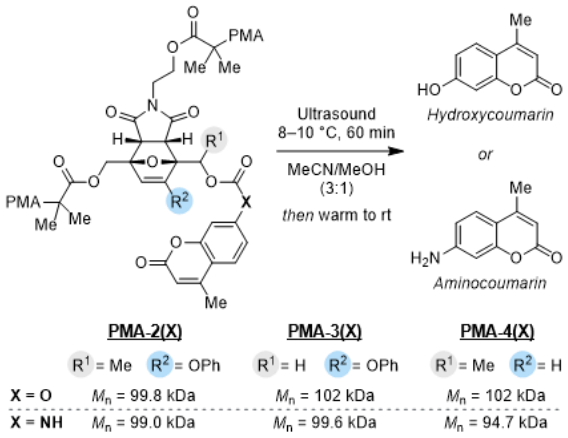

[a]$Đ$ = 1.03–1.06 for all polymers.

Mechanically triggered release of hydroxycoumarin or aminocoumarin from **PMA-2(X)**–**PMA-4(X)** in 3:1 MeCN/MeOH was evaluated using pulsed ultrasonication (1 s on/1 s off, 8–10 °C, 20 kHz, 8.2 W/cm^2) and the impact of substitution on the rate of coumarin release from the mechanically liberated 2-furylcarbinol derivatives was measured using photoluminescence spectroscopy (Scheme 2.4). Each polymer solution was subjected to 60 min of ultrasonication, and then allowed to warm to room temperature and fluorescence was

monitored over time. Kinetic data for the release of hydroxycoumarin from **PMA-2(O)**–**PMA-4(O)** is illustrated in Figure 2.14a, while the data for release of aminocoumarin from **PMA-2(NH)**–**PMA-4(NH)** is illustrated in Figure 2.14b. For clarity and to account for slight differences in average polymer molecular weight and dispersity that influence the extent of mechanophore conversion during ultrasonication,[32–34] the initial fluorescence intensity (t = 0) is subtracted from each measurement and the data are normalized to emphasize the relative rates of molecular release. The fluorescence emission from solutions of **PMA-2(O)** and **PMA-3(O)** reached a maximum prior to the first measurement and remained essentially constant over time, indicating that the release of hydroxycoumarin from both primary and secondary furfuryl carbonates containing a 3-phenoxy substituent completed nearly instantaneously upon formation ($t_{1/2}$ < 5 min). These results are contrasted by the release of hydroxycoumarin from mechanically activated **PMA-4(O)** containing our first-generation mechanophore, which occurs steadily and predictably over several hours post-activation. Fitting the time-dependent photoluminescence data for release of hydroxycoumarin from

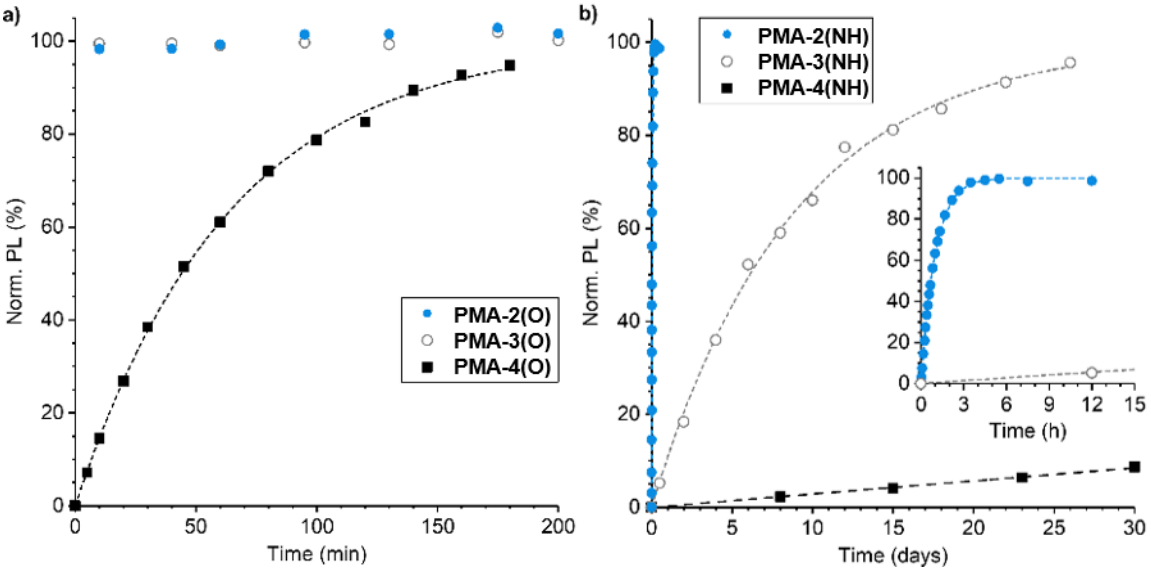

Figure 2.14. Mechanically triggered release of (a) hydroxycoumarin and (b) aminocoumarin from polymers as a function of mechanophore substitution. Polymer solutions (2 mg/mL in 3:1 MeCN/MeOH) were sonicated for 60 min, warmed to room temperature, and release of coumarin cargo from the mechanically liberated 2-furylcarbinol derivatives was monitored by photoluminescence spectroscopy. PL parameters: λ_{ex} = 330 nm, λ_{em} = 378 nm (hydroxycoumarin); λ_{ex} = 365 nm, λ_{em} = 424 nm (aminocoumarin). The initial PL intensity was subtracted from each measurement and the data were normalized to the plateau value. For **PMA-4(NH)**, the data were normalized assuming 36% mechanophore activation and the black dashed line represents a first-order reaction with a half-life of 240 days.

PMA-4(O) to a first-order rate expression gives an estimated half-life for decomposition of the 3*H* secondary furfuryl carbonate of 46 min (average of two trials).

The release of aminocoumarin from mechanically activated **PMA-2(NH)**–**PMA-4(NH)** provides an even clearer demonstration of the impact of substitution on the kinetics of furfuryl carbamate decomposition with reaction half-lives spanning four orders of magnitude (Figure 2.14b). The time-dependent photoluminescence of the sonicated solution of **PMA-2(NH)** is described by a first-order rate expression and reaches a maximum intensity after approximately 4 h post-activation, corresponding to the release of aminocoumarin with an average half-life of 41 min from two replicate experiments. In comparison, the release of aminocoumarin from mechanically activated **PMA-3(NH)** containing a masked primary furfuryl carbamate with a 3-phenoxy substituent is over 200× slower with an average half-life of 6.5 days, again highlighting the stabilizing effect of the α-methyl substituent identified previously. For **PMA-4(NH)** containing a chain-centered mechanophore analogous to our first-generation molecular design with an α-methyl substituent and no phenoxy group, only 8% release of aminocoumarin was observed after 30 days post-activation. This calculation assumes a mechanophore conversion of 36% as determined previously for our original masked furfuryl carbonate under nearly identical conditions. The time-dependent photoluminescence data for release of aminocoumarin from **PMA-4(NH)** fall on the line for

Table 2.1. Characterization of polymers PMA-2(O)–PMA-4(O) and PMA-2(NH)–PMA-4(NH), and release of hydroxycoumarin or aminocoumarin upon ultrasound-induced mechanochemical activation.[a]

Polymer	M_n (kg/mol)	M_p (kg/mol)	$Đ$	Half-Life	Ultimate payload release[b]
PMA-2(O)	99.8	95.4	1.04	< 5 min	34%
PMA-3(O)	102	103	1.05	< 5 min	36%
PMA-4(O)	102	95.7	1.03	46 min	38%
PMA-2(NH)	99.0	93.7	1.04	41 min	35%
PMA-3(NH)	99.6	104	1.06	6.5 days	39%
PMA-4(NH)	94.7	89.1	1.05	240 days	8%[c]

[a]Polymer solutions (2 mg/mL in 3:1 MeCN/MeOH) were sonicated for 60 min ("on" time) then warmed to room temperature. [b]Yield of payload release relative to mechanophore concentration estimated from photoluminescence measurements, reported as the average of two trials. [c]Calculated yield after 30 days post-sonication assuming a mechanophore activation of 36%.

a first-order reaction with a half-life of approximately 240 days. It is worth noting that the yield of hydroxycoumarin or aminocoumarin released from each polymer studied, with the exception of **PMA-4(NH)**, was 34–39% relative to the mechanophore concentration in each experiment, which is consistent with the anticipated mechanophore conversion after a relatively short exposure to ultrasound (Table 2.1).

The results above illustrate the ability to control the rate of mechanically triggered release by fine-tuning the molecular structure of the furan–maleimide mechanophore, and in particular, highlight the potential for releasing diverse chemical payloads from masked secondary 2-furylcarbinol derivatives containing a 3-phenoxy group. Therefore, we sought to further investigate the scope of molecular cargo that can be effectively released upon mechanical activation of the second-generation mechanophore (Scheme 2.5). Starting again

Scheme 2.5. Scope of Mechanically Triggered Cargo Release from the Second-Generation Mechanophore with α-Methyl/Phenoxy Substitution.[a]

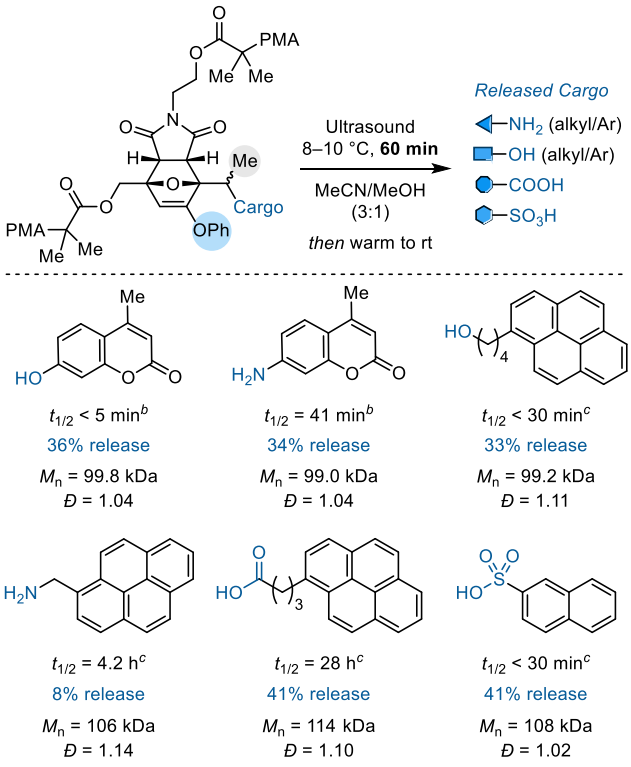

[a]Values of percent release and half-lives are averages from two replicate experiments. Percent release is reported relative to the initial mechanophore concentration and does not account for incomplete mechanopohore conversion after 60 min of ultrasonication. Values of percent release were determined by HPLC. [b]Half-life for cargo release was measured by photoluminescence spectroscopy. [c]Half-life for cargo release was measured by HPLC.

from modular bis-initiator precursor (±)-**19** containing a secondary alcohol, a variety of molecular cargo were installed via different functional group connectivity and the mechanophores were incorporated into polymers following the same protocol as before (Table 2.2). In addition to the hydroxycoumarin (phenol) and aminocoumarin (arylamine) payloads attached via carbonate and carbamate groups, respectively, four other cargo molecules were installed including those bearing alcohol, alkylamine, carboxylic acid, and sulfonic acid functional groups. Conjugation of the alcohol and alkylamine-functional cargo molecules was achieved using carbonate and carbamate spacers, respectively, where a decarboxylation step is required for molecular release similar to the coumarin-based phenol and arylamine payloads. On the other hand, cargo molecules bearing carboxylic acid and sulfonic acid functional groups were conjugated directly to the mechanophore substrate through carboxylate and sulfonate linkages. Each payload molecule was chosen to be strongly absorbing in the UV region to facilitate the characterization of their release using high-performance liquid chromatography (HPLC) equipped with a UV detector. For each derivative, a corresponding chain-end functional control polymer was also synthesized and evaluated under the same conditions to confirm the mechanical origin of molecular release (Table 2.3).[9]

Similar to the kinetic studies performed above and following the same ultrasonication procedures, solutions of each polymer (2.0 mg/ml in 3:1 MeCN/MeOH) were subjected to pulsed ultrasonication (60 min "on" time), and then payload release from the mechanically liberated 2-furylcarbinol derivative was monitored at room temperature by HPLC and quantified using an internal standard. The identity of each cargo molecule, the average half-life and yield of payload release measured from two replicate experiments, and the M_n and $Đ$ of the parent chain-centered polymers are summarized in Scheme 2.5. Similar to hydroxycoumarin, the mechanically triggered release of 1-pyrenebutanol was sufficiently rapid such that it completed prior to the first HPLC measurement ($t_{1/2}$ < 30 min). Release of 1-pyrenemethylamine from the corresponding furfuryl carbamate occurred with a moderate half-life of 4.2 h, albeit approximately 6× slower than the release of aminocoumarin. The difference in release kinetics between the alkyl and arylamines is ascribed to the difference

Table 2.2. Characterization of polymers containing functionally diverse cargo molecules and molecular release upon ultrasound-induced mechanochemical activation.[a]

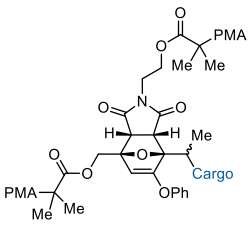

Cargo	M_n (kg/mol)	M_p (kg/mol)	$Đ$	Half-Life	Ultimate payload release[c]
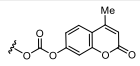	99.8	95.4	1.04	< 5 min[b]	36%
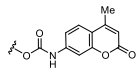	99.0	93.7	1.04	41 min[b]	34%
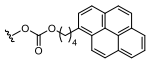	99.2	96.1	1.11	< 30 min	33%
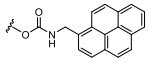	106	96.1	1.14	4.2 h	8%
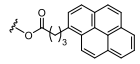	114	110	1.10	28 h	41%
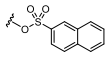	108	108	1.02	< 30 min	41%

[a]Polymer solutions (2 mg/mL in 3:1 MeCN/MeOH) were sonicated for 60 min ("on" time) then warmed to room temperature and immediately monitored by photoluminescence spectroscopy or HPLC. [b]Half-lives for the release of hydroxycoumarin and aminocoumarin from photoluminescence measurements, with all others calculated using HPLC. [b]Yield of payload release relative to mechanophore concentration calculated from HPLC measurements. Half-lives and payload release are reported as the average of two trials.

Table 2.3. Characterization of chain-end functional control polymers containing functionally diverse cargo molecules.

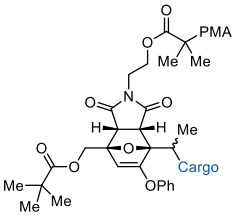

Cargo	M_n (kg/mol)	$Đ$	Cargo	M_n (kg/mol)	$Đ$
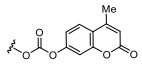	95.6	1.16	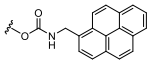	82.7	1.19
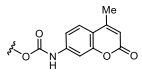	93.2	1.12	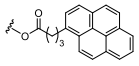	106	1.32
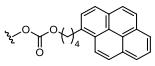	110	1.14	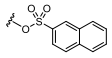	87.4	1.08

in pK_a of the conjugate acids,[35] with the aniline derivative being a better leaving group. The second-generation mechanophore design not only enables successful release of alcohols and amines via carbonate and carbamate linkages, but is also capable of effecting the release of payloads incorporating carboxylic acid and sulfonic acid functional groups conjugated to the mechanophore via carboxylate and sulfonate linkages. The mechanically triggered release of 1-pyrenebutanoic acid proceeded with a half-life of approximately 28 h, while the release of

2-naphthalenesulfonic acid completed before the first HPLC measurement ($t_{1/2}$ < 30 min). Again, this trend is consistent with the significantly lower pK_a value of the sulfonic acid compared to the carboxylic acid, reflecting the relative stabilities of sulfonate and carbonate leaving groups. The mechanically triggered release of organic acids enabled by this second-generation platform significantly expands upon the limited repertoire of mechanophores that generate HCl[14,15] and is also highly modular in nature owing to the generality of the mechanophore design.

The percent release for each cargo molecule determined by HPLC is reported in Scheme 2.5 relative to the initial concentration of mechanophore. It is important to note, however, that only a fraction of mechanophores is converted after 60 min of ultrasonication, which again is expected to be ~36% based on the experimental conditions and the average molecular weight of the polymers ($M_n \approx 100$ kDa). As demonstrated previously, increasing the sonication time to 150 min results in 64% release of hydroxycoumarin from **PMA-4(O)**. Among other factors,[36] the rate of mechanophore activation is particularly sensitive to the length of the attached polymer chains, with longer chains producing faster mechanochemical reactions.[33,34] Here the duration of ultrasonication was selected on the basis of experimental expediency. With the exception of the alkylamine cargo, the yields for payload release after 60 min of ultrasonication are within the range of 33–41%. These results suggest that payload release from the mechanochemically generated 2-furylcarbinol derivative in each case is highly efficient. Release of the alkylamine plateaus at approximately 8%, and we tentatively attribute the reduced yield to a reaction between the amine and polymer-bound furfuryl cation intermediate, similar to the side reaction observed in the decomposition of model compound **10** at relatively high concentrations. In this case, the enhanced nucleophilicity of the alkylamine is anticipated to promote this reaction pathway to a greater extent compared to aminocoumarin. On the other hand, the higher yield of 41% measured for the release of both organic acid payloads is consistent with the slightly higher average molecular weight of those polymers, which results in increased mechanophore conversion during the same period of ultrasonication. Finally, we note that payload release was not observed from any of the chain-end functional control polymers under identical experimental conditions, confirming

that molecular release from polymers bearing a chain-centered mechanophore was indeed triggered by mechanical force.[9]

In summary, we have demonstrated a mechanophore platform for release of small molecules via a mechanically triggered cascade reaction. The strategy relies on the mechanochemically activated retro-Diels–Alder reaction of a furan–maleimide adduct, which reveals a latent furfuryl carbonate that subsequently decomposes in polar protic solvents to release a covalently bound cargo molecule. We have also demonstrated the mechanically triggered release of functionally diverse small molecules with tunable release kinetics from a second-generation mechanophore platform. Changing the substitution on the masked 2-furylcarbinol derivatives allows the rates of molecular release to be varied by several orders of magnitude, while the combination of α-methyl and 3-phenoxy substitution results in a highly active substrate for the triggered release of functionally diverse molecular payloads. Starting from a modular precursor mechanophore initiator, a variety of molecular cargo were conveniently installed and then incorporated into polymers by controlled radical polymerization. The mechanically triggered release of functionally diverse cargo molecules bearing alkyl/aryl alcohols and amines as well as carboxylic acid and sulfonic acid functional groups was demonstrated using ultrasonication, exhibiting fast rates of release and high reaction efficiencies. The generality and efficacy of the mechanophore design makes it a promising platform for the mechanically triggered release of a wide variety of functional molecules to address applications in catalysis, sensing, drug delivery, and many other areas.

This research was supported by Caltech, the Arnold and Mabel Beckman Foundation through a Beckman Young Investigator Award, and the Dow Next Generation Educator Fund. We thank the Center for Catalysis and Chemical Synthesis of the Beckman Institute at Caltech and the CCE Multiuser Mass Spectrometry Laboratory for access to equipment and Larry Henling for assistance with X-ray crystallography.

2.2 Experimental Details

Reagents from commercial sources were used without further purification unless otherwise stated. Methyl acrylate was passed through a short plug of basic alumina to remove inhibitor immediately prior to use. Dry THF, diethyl ether, MeCN, and DMF were obtained

from a Pure Process Technology solvent purification system. All reactions were performed under a N_2 atmosphere unless specified otherwise. Column chromatography was performed on a Biotage Isolera system using SiliCycle SiliaSep HP flash cartridges.

NMR spectra were recorded using a 400 MHz Bruker Avance III HD with Prodigy Cryoprobe, a 400 MHz Bruker Avance Neo, or Varian Inova 500 MHz spectrometers. All ^{1}H NMR spectra are reported in δ units, parts per million (ppm), and were measured relative to the signals for residual chloroform (7.26 ppm), dichloromethane (5.32 ppm), methanol (3.31 ppm), acetone (2.05 ppm), or acetonitrile (1.94 ppm) in deuterated solvent. All ^{13}C NMR spectra were measured in deuterated solvents and are reported in ppm relative to the signals for chloroform (77.16 ppm). Multiplicity and qualifier abbreviations are as follows: s = singlet, d = doublet, t = triplet, q = quartet, dd = doublet of doublets, dq = doublet of quartets, ABq = AB quartet, m = multiplet, br = broad.

High resolution mass spectra (HRMS) were analyzed by an Agilent 6200 series time-of-flight mass spectrometer equipped with an Agilent G1978A multimode source (ESI+). Some were obtained by direct infusion electrospray ionization (ESI) in the positive ion mode using a Waters LCT Premier XE time-of-flight (TOF) mass spectrometer operated in the V mode. The instrument was externally calibrated with NaI clusters. Some samples were analyzed by Fast Atom Bombardment (FAB) using a JEOL JMS-60H Double-focusing high resolution magnetic sector mass spectrometer operated in the positive ion mode. The instrument was calibrated with PEG clusters over the mass range of interest. One sample was analyzed by GC-MS using an Agilent 6890N gas chromatograph interfaced to a JEOL double-focusing magnetic sector instrument using electron ionization (EI) in the positive ion mode. The instrument was calibrated with perfluorokerosene.

Analytical gel permeation chromatography (GPC) was performed using an Agilent 1260 series pump equipped with two Agilent PLgel MIXED-B columns (7.5 x 300 mm), an Agilent 1200 series diode array detector, a Wyatt 18-angle DAWN HELEOS light scattering detector, and an Optilab rEX differential refractive index detector. The mobile phase was THF at a flow rate of 1 mL/min. Molecular weights and molecular weight distributions were calculated by light scattering using a dn/dc value of 0.062 mL/g (25 °C) for poly(methyl acrylate).

Photoluminescence spectra were recorded on a Shimadzu RF-6000 spectrofluorophotometer using a quartz microcuvette (Starna Cells 18F-Q-10-GL14-C, 10 x 2 mm). Excitation and emission slit widths were 5 nm and 3 nm, respectively.

High-Performance Liquid Chromatography (HPLC) measurements were performed with an Agilent Eclipse Plus C18 column (959961-902) or a C8 column (993967-906) using a single-wavelength UV-vis detector.

Ultrasound experiments were performed using a 500 watt Vibra Cell 505 liquid processor (20 kHz) equipped with a 0.5-inch diameter solid probe (part #630-0217), sonochemical adapter (part #830-00014), and a Suslick reaction vessel made by the Caltech glass shop (analogous to vessel #830-00014 from Sonics and Materials).

LCMS measurements were performed with an Agilent 6140 Series Quadrupole LCMS Spectrometer System equipped with an Agilent Eclipse Plus C18 column using MeCN/water as the eluent.

Safety Statement

No unexpected or unusually high safety hazards were encountered. Chemical synthesis operations were performed with the operator wearing proper PPE (including safety glasses, labcoat, and appropriate gloves) at all times and with proper engineering controls. Triphosgene is toxic and should be handled exclusively inside of a fume hood.[37] Care should be taken when using n-butyllithium. For example, using a luer lock syringe for transferring solutions of n-butyllithium; using a syringe with double the capacity of the volume to be transferred; and avoiding use of n-butyllithium while working alone. Ultrasound experiments using a 20 kHz probe sonicator were performed inside of a sound abating enclosure. Personal hearing protection is recommended if ultrasonication is performed without the use of a sound abating enclosure.

2.3 Characterization of Molecular Release Using PL Spectroscopy

Aliquots from the sonication experiments were added to a quartz microcuvette (Starna 18F-Q-10-GL14-S) and emission spectra were recorded at 340–500 nm using an excitation wavelength of λ_{ex} = 330 nm for hydroxycoumarin and 365 nm for aminocoumarin.

The photograph of the sonicated samples, shown in the inset of Figure 2.4b in the main text, was acquired using a Canon 5D Mark IV DSLR camera at a focal length of 70 mm using the following settings: 1/4 s exposure, f/4.0, ISO 4000. The photograph was taken in a dark room with the samples illuminated by a 365 nm UV lamp. In order to capture visible photoluminescence of the released coumarin **2**, each ultrasonicated sample was diluted 6x with a mixture of acetonitrile/methanol/water 3:1:0.2 (by volume) prior to imaging. Addition of water to solutions of hydroxycoumarin **2** in alcoholic solvents shifts the fluorescence emission to visible wavelengths.[38]

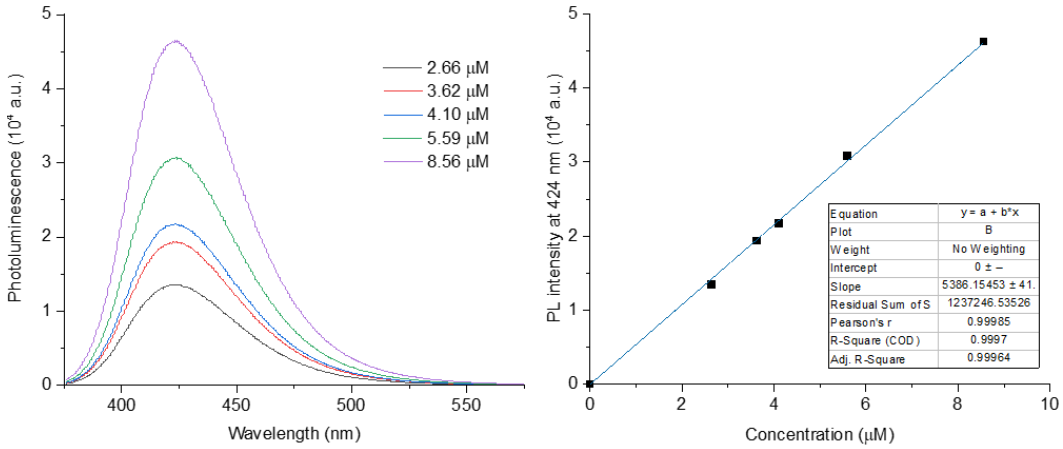

Figure 2.15. Construction of a calibration curve for experimental determination of the concentration of aminocoumarin **3**. (a) Fluorescence emission spectra (λ_{ex} = 365 nm) and (b) intensity at 424 nm for solutions of aminocoumarin 3 in MeCN/MeOH (3:1 v/v) as a function of concentration. A linear regression of the data in (b) gives the calibration function: Y = 5386X**.**

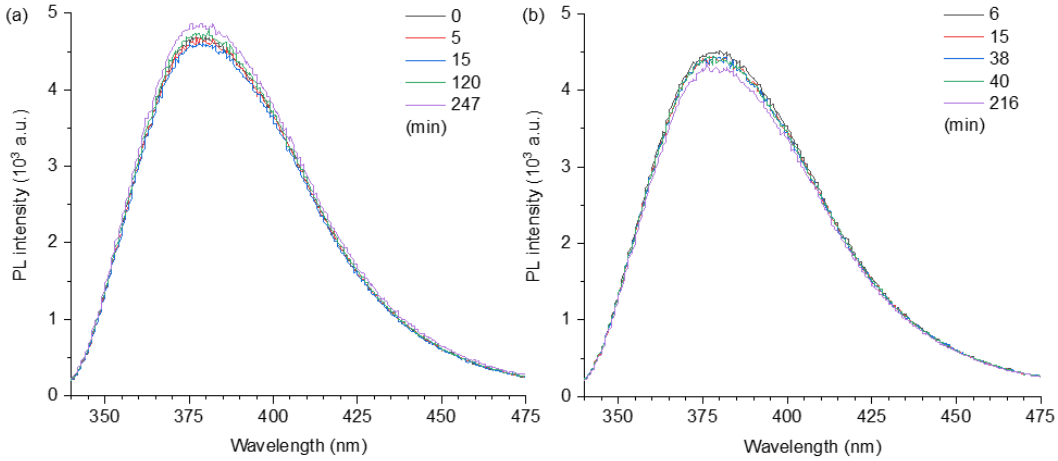

Figure 2.16. Fluorescence emission spectra of a 2.0 mg/ml solution of (a) **PMA-2(O)** and (b) **PMA-3(O)** in 3:1 MeCN/MeOH at room temperature monitored immediately after ultrasonication for 60 min. λ_{ex} = 330 nm.

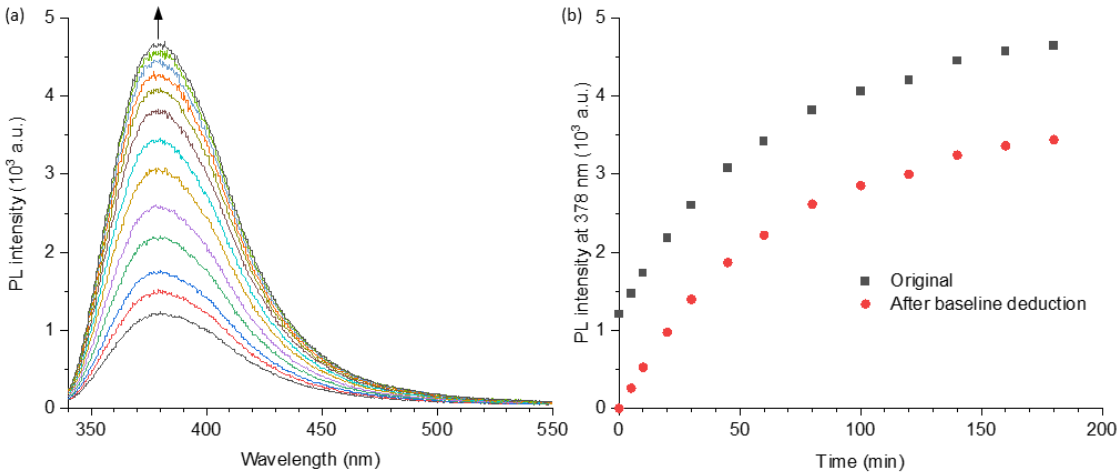

Figure 2.17. Characterization of hydroxycoumarin release from a 2.0 mg/ml solution of **PMA-4(O)** in 3:1 MeCN/MeOH immediately after ultrasonication for 60 min. (a) Fluorescence emission spectra of the solution acquired over time at room temperature. (b) Fluorescence intensity at 378 nm as a function of time. The background fluorescence at the start of the monitoring experiment (resulting from the release of hydroxycoumarin cargo during ultrasonication) was subtracted from each measurement. λ_{ex} = 330 nm.

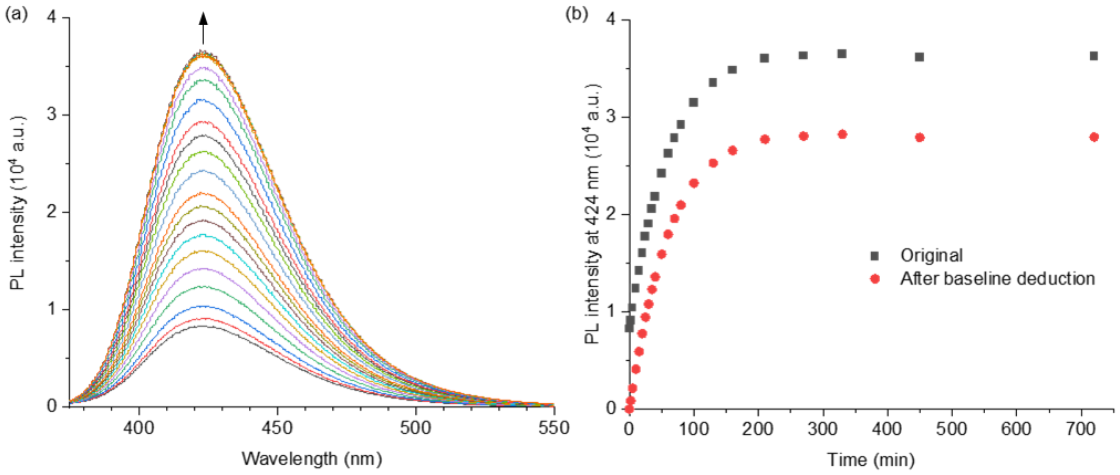

Figure 2.18. Characterization of aminocoumarin release from a 2.0 mg/ml solution of **PMA-2(NH)** in 3:1 MeCN/MeOH immediately after ultrasonication for 60 min. (a) Fluorescence emission spectra of the solution acquired over time at room temperature. (b) Fluorescence intensity at 424 nm as a function of time. The background fluorescence at the start of monitoring experiment (resulting from the release of aminocoumarin cargo during ultrasonication) was subtracted from each measurement. λ_{ex} = 365 nm.

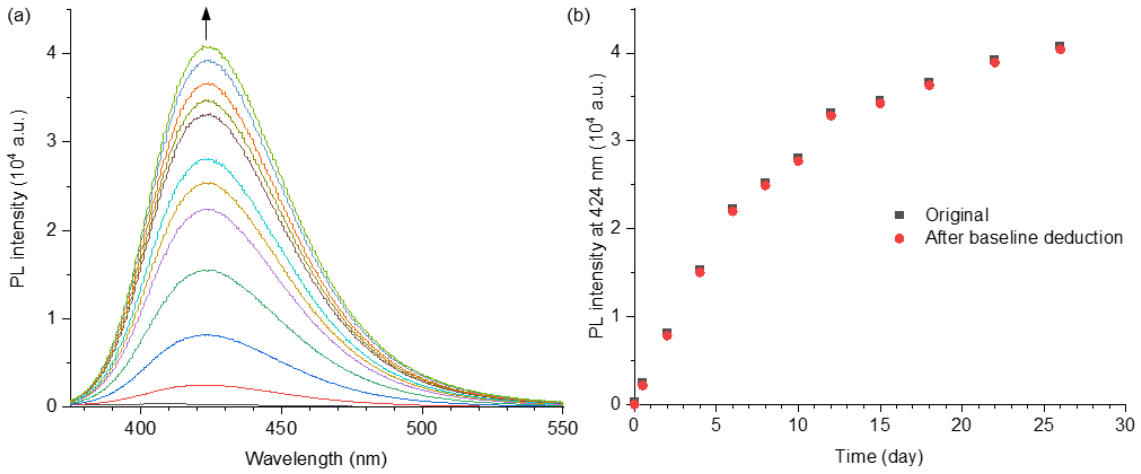

Figure 2.19. Characterization of aminocoumarin release from a 2.0 mg/ml solution of **PMA-3(NH)** in 3:1 MeCN/MeOH immediately after ultrasonication for 60 min. (a) Fluorescence emission spectra of the solution acquired over time at room temperature. (b) Fluorescence intensity at 424 nm as a function of time. The background fluorescence at the start of monitoring experiment (resulting from the release of aminocoumarin cargo during ultrasonication) was subtracted from each measurement. λ_{ex} = 365 nm.

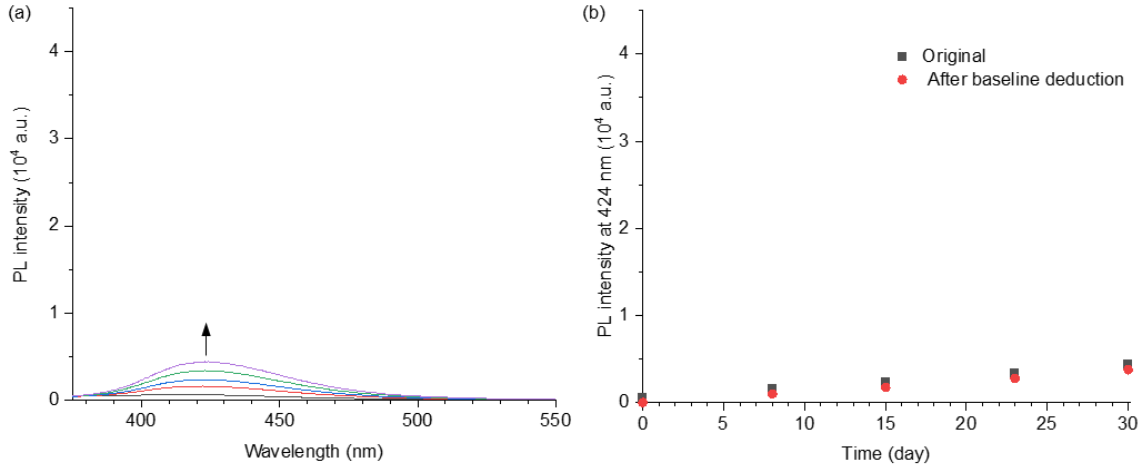

Figure 2.20. Characterization of aminocoumarin release from a 2.0 mg/ml solution of **PMA-4(NH)** in 3:1 MeCN/MeOH immediately after ultrasonication for 60 min. (a) Fluorescence emission spectra of the solution acquired over time at room temperature. (b) Fluorescence intensity at 424 nm as a function of time. The background fluorescence at the start of monitoring experiment (resulting from the release of aminocoumarin cargo during ultrasonication) was subtracted from each measurement. Assuming 36% mechanophore activation, the total concentration of aminocoumarin released is calculated to be 7.6 □M. The expected PL intensity from a 7.6 mM solution of aminocoumarin **3** is approximately 4.09 x 10^4 based on the calibration curve. λ_{ex} = 365 nm.

2.4 Characterization of Molecular Release Using HPLC and LCMS

Calculation of Relative Response Factors (RRF).

A standard solution with known concentrations of the internal standard (IS) molecule and the small molecule analyte was prepared and analyzed by HPLC equipped with a UV detector. The RRF is calculated from the HPLC results of the standard solution using the following equation:

$$RRF = \frac{Response\ Factor\ of\ the\ analyte}{Response\ Factor\ of\ the\ IS} = \left(\frac{Peak\ Area\ of\ the\ analyte}{Concentration\ of\ the\ analyte}\right)/\left(\frac{Peak\ Area\ of\ the\ IS}{Concentration\ of\ the\ IS}\right)$$

Table 2.4. Determination of relative response factors (RRF)

Entry	Payload	Internal Standard (IS)	Payload Peak Area (%)	IS Peak Area (%)	[Payload] (μM)	[IS] (μM)	RRF
1	7-Hydroxy-4-methyl-coumarin	3-Cyano-7-hydroxy-4-methylcoumarin	68.5	31.5	158	126	1.74
2	1-Pyrenebutanol	1-Pyrenebutanoic acid	43.0	57.0	59.3	79.5	1.01
3	7-Amino-4-methylcoumarin	Quinoline	45.5	54.5	100	400	3.32
4	1-Pyrenemethylamine hydrochloride	4-Methyl-7-hydroxycoumarin	69.6	30.4	67.2	112	3.82
5	1-Pyrenebutanoic acid	1-Pyrenebutanol	57.0	43.0	79.5	59.3	0.989
6	Naphthalene-2-sulfonic acid	7-hydroxy-4-methylcoumarin	59.4	40.6	600	336	0.819

Determination of the concentration of released payload molecules from polymers after ultrasound-induced mechanical activation.

After 60 min of ultrasonication, a known concentration of internal standard (IS) was added into the solution of sonicated polymer. The solution was then kept at room temperature and analyzed by HPLC at various time intervals. The concentration of the released payload molecule (the analyte) in the solution was calculated using the following relationship:

$$Concentration\ of\ analyte = \frac{Peak\ area\ of\ analyte}{Peak\ area\ of\ IS} * \frac{1}{RRF} * Concentration\ of\ IS$$

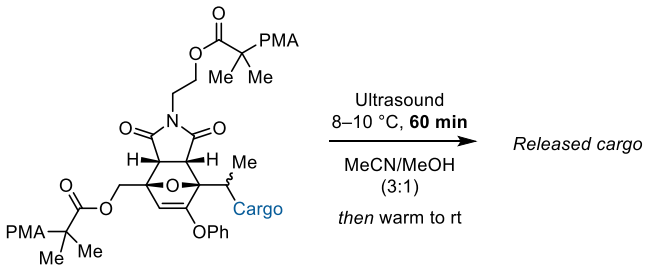

Table 2.5. Characterization of mechanically triggered payload release from polymers with a chain-centered second-generation mechanophore.

Cargo	M_n (kg/mol)	[Polymer] (mg/mL)	[Polymer] (μM)	Half-Life	[Released Payload][a] (μM)	Ultimate Payload Release[a]
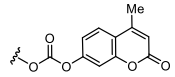	99.8	2.0	20	< 5 min[b]	7.26	36%
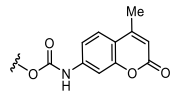	99.0	2.0	20	41 min[b]	6.91	34%
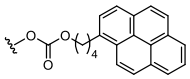	99.2	2.0	20	< 30 min	6.67	33%
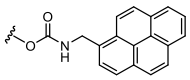	106	2.0	19	4.2 h	1.46	8%
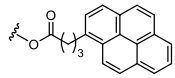	114	2.0	17	28 h	7.14	41%
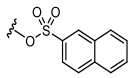	108	2.0	19	< 30 min	7.62	41%

[a]Average of two replicate experiments determined by HPLC. [b]Half-lives for the release of hydroxycoumarin and aminocoumarin are from photoluminescence measurements, with all others from HPLC measurements.

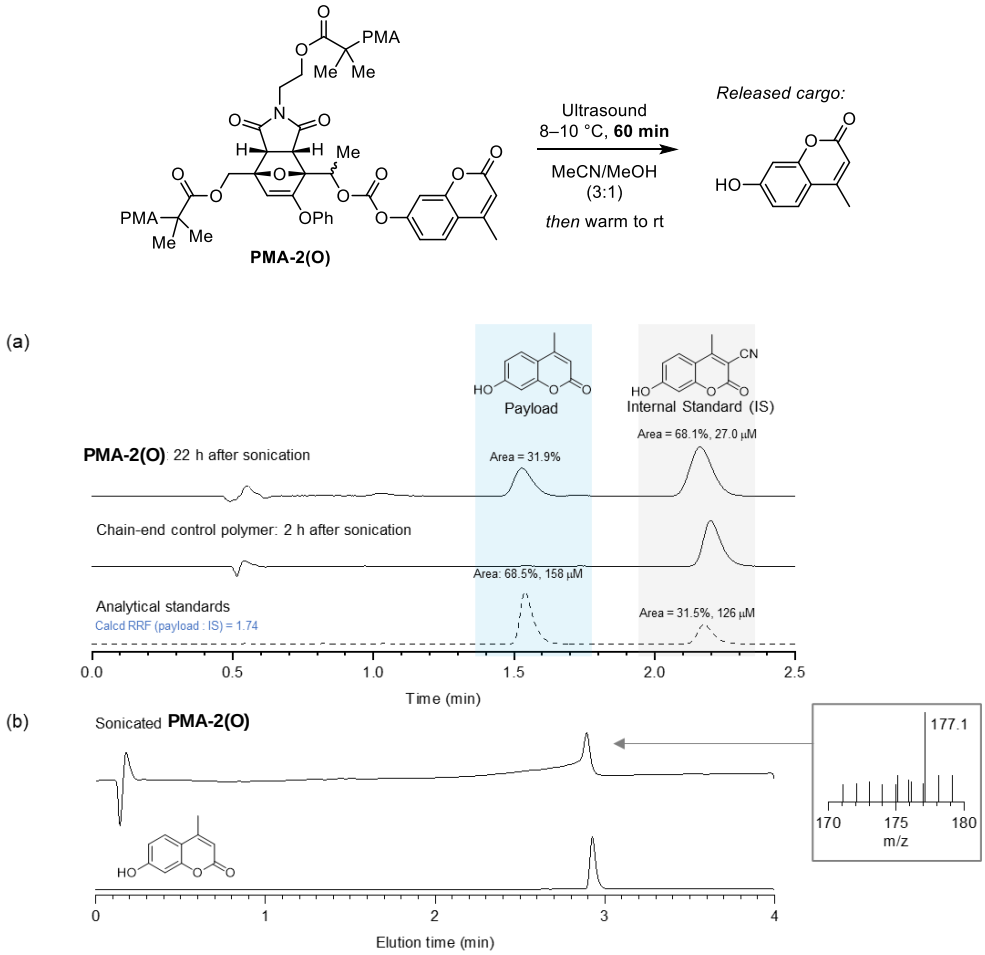

Figure 2.21. (a) Representative HPLC chromatograms for the analysis of mechanically triggered molecular release of hydroxycoumarin from the polymer containing a chain-centered mechanophore, and a chain-end control polymer (30:70 MeCN/water (with 0.1% acetic acid) isocratic, 2 ml/min, λ = 320 nm). (b) LCMS measurements further support the identity of the released molecule. The mass of the analyte (*m/z* = 177.1 amu) matches the calculated *m/z* for 7-hydroxy-4-methylcoumarin, $[C_{10}H_9O_3]^+$ $(M+H)^+$ (177.1). LCMS conditions: positive ion mode, 4 min (0–30% MeCN in water).

Table 2.6. Release of 7-hydroxy-4-methylcoumarin payload monitored by HPLC[a]

Trial 1				Trial 2			
Time Post-Sonication	Payload Peak Area (%)	IS Peak Area (%)	Released Payload, Calcd (μM)	Time Post-Sonication	Payload Peak Area (%)	IS Peak Area (%)	Released Payload, Calcd (μM)
22 h	31.9	68.1	7.27	22 h	31.9	68.2	7.25

[a]IS: 3-Cyano-7-hydroxy-4-methylcoumarin (27.0 μM). RRF = 1.74.

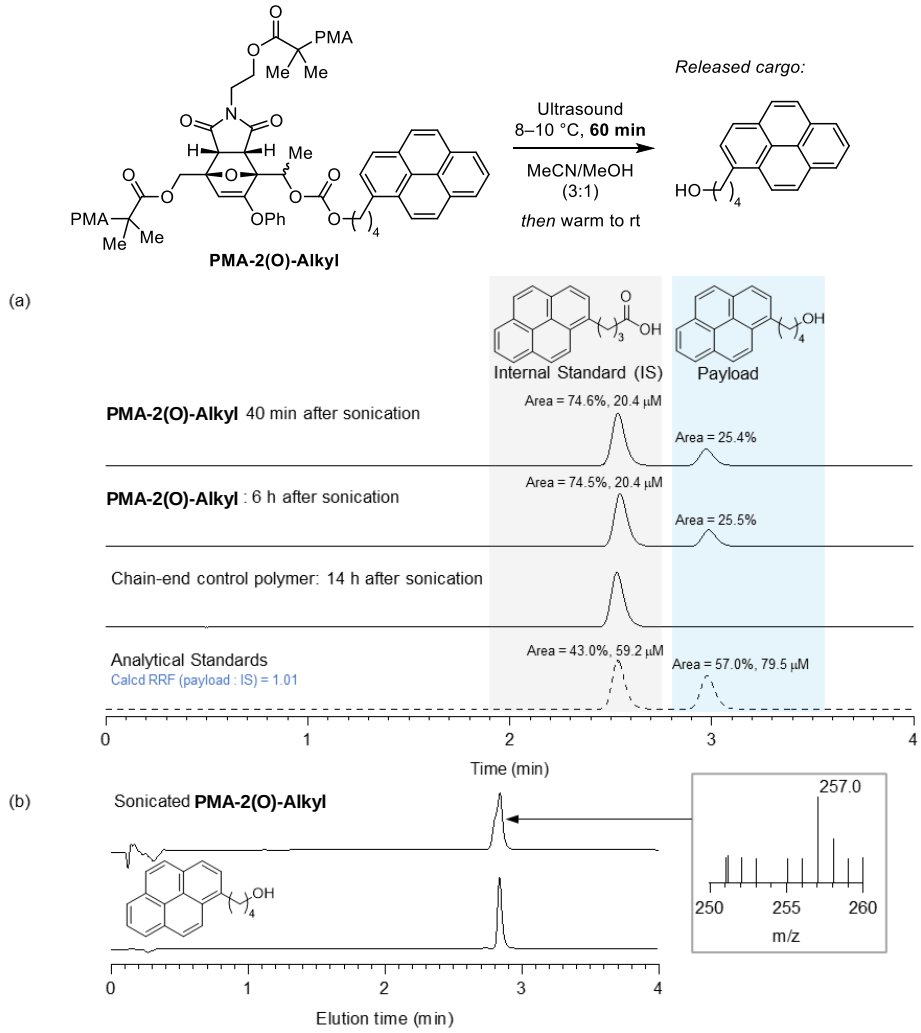

Figure 2.22. (a) Representative HPLC chromatograms for the analysis of mechanically triggered molecular release of 1-pyrenebutanol from the polymer containing a chain-centered mechanophore, and a chain-end control polymer (60:40 MeCN/water (with 0.1% acetic acid) isocratic, 2 ml/min, λ = 340 nm). (b) LCMS measurements further support the identity of the released molecule. The mass of the analyte (*m/z* = 257.0 amu) matches the calculated *m/z* for 1-pyrenebutanol, $[C_{20}H_{17}]^+$ $(M-OH)^+$(257.1). LCMS conditions: positive ion mode, 4 min (25–75% MeCN in water).

Table 2.7. Release of 1-pyrenebutanol payload monitored by HPLC [a]

Trial 1				Trial 2			
Time Post-Sonication	Payload Peak Area (%)	IS Peak Area (%)	Released Payload, Calcd (μM)	Time Post-Sonication	Payload Peak Area (%)	IS Peak Area (%)	Released Payload, Calcd (μM)
40 min	25.4	74.6	6.88	1 h	24.0	76.0	6.39
6 h	25.5	74.5	6.91	2 h	24.2	75.8	6.44

[a] IS: 1-Pyrenebutyric acid (20.4 μM). RRF = 1.01.

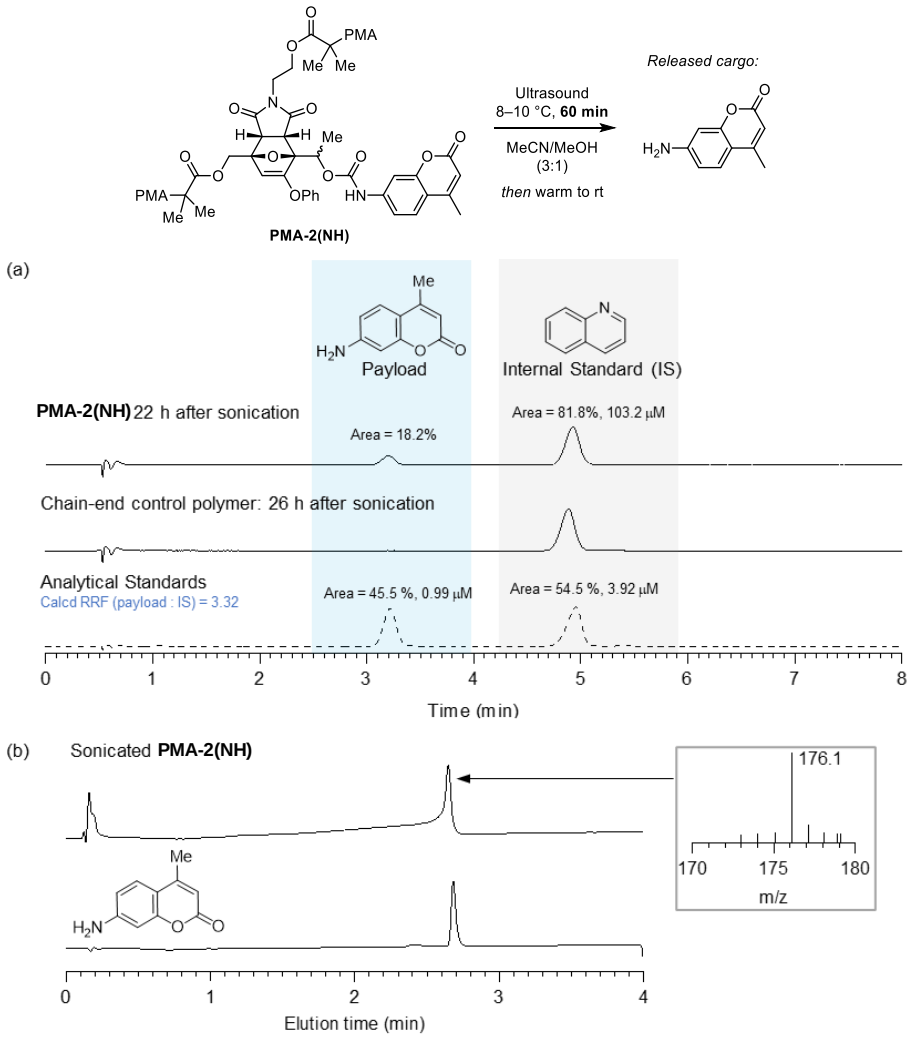

Figure 2.23. (a) Representative HPLC chromatograms for the analysis of mechanically triggered molecular release of aminocoumarin from the polymer containing a chain-centered mechanophore, and a chain-end control polymer (20:80 MeCN/water (with 0.1% acetic acid) isocratic, 2 ml/min, λ = 315 nm). (b) LCMS measurements further support the identity of the released molecule. The mass of the analyte (*m/z* = 176.1 amu) matches the calculated *m/z* for 7-amino-4-methylcoumarin, $[C_{10}H_{10}NO_2]^+$ $(M+H)^+$ (176.1). LCMS conditions: positive ion mode, 4 min (0–30% MeCN in water).

Table 2.8. Release of 7-amino-4-methylcoumarin payload monitored by HPLC [a]

Trial 1				Trial 2			
Time Post-Sonication	Payload Peak Area (%)	IS Peak Area (%)	Released Payload, Calcd (mM)	Time Post-Sonication	Payload Peak Area (%)	IS Peak Area (%)	Released Payload, Calcd (mM)
22 h	18.2	81.8	6.90	22 h	18.2	81.8	6.93

[a] IS: Quinoline (103.2 μM). RRF = 3.32.

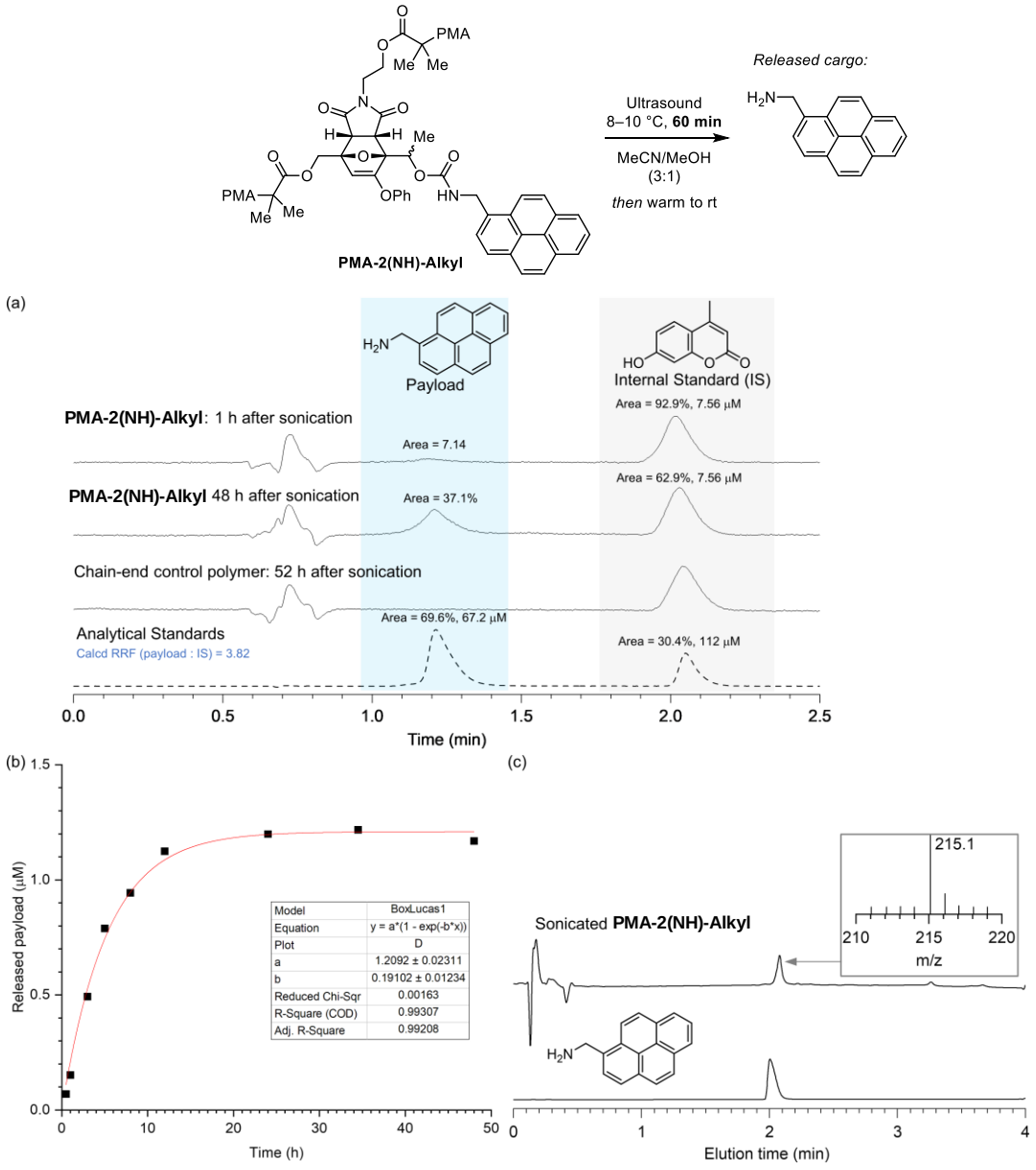

Figure 2.24. (a) Representative HPLC chromatograms for the analysis of mechanically triggered molecular release of 1-pyrenemethylamine from the polymer containing a chain-centered mechanophore, and a chain-end control polymer (30:70 MeCN/water (with 0.1% acetic acid) isocratic, 1.5 ml/min, λ = 340 nm). (b) Payload release from sonicated **PMA-2(NH)-Alkyl** as a function of time post-sonication. (c) LCMS measurements further support the identity of the released molecule. The mass of the analyte (*m/z* = 215.1 amu) matches the calculated *m/z* for 1-pyrenemethylamine, $[C_{17}H_{11}]^+$ $(M-NH_2)^+$ (215.1). LCMS conditions: positive ion mode, 4 min (5–50% MeCN in water).

Table 2.9. Release of 1-pyrenemethylamine payload monitored by HPLC[a]

Trial 1				Trial 2			
Time Post-Sonication	Payload Peak Area (%)	IS Peak Area (%)	Released Payload, Calcd (μM)	Time Post-Sonication	Payload Peak Area (%)	IS Peak Area (%)	Released Payload, Calcd (μM)
0.5	3.40	96.6	0.0697	1	7.28	92.7	0.155
1	7.14	92.9	0.152	3	17.7	82.3	0.425
3	19.9	80.1	0.492	6	31.7	68.3	0.920
5	28.5	71.5	0.788	9.5	39.3	60.7	1.28
8	32.3	67.7	0.943	21	45.1	54.9	1.63
12	36.2	63.8	1.12	31.5	46.2	53.8	1.70
24	37.7	62.3	1.20	45	45.1	54.9	1.63
34.5	38.1	61.9	1.22	Plateau value: 1.71 μM; $t_{1/2}$ = 5.4 h			
48	37.1	62.9	1.17				
Plateau value: 1.21 μM; $t_{1/2}$ = 3.6 h							

[a]IS: 4-Methyl-7-hydroxycoumarin (7.56 μM). RRF = 3.82.

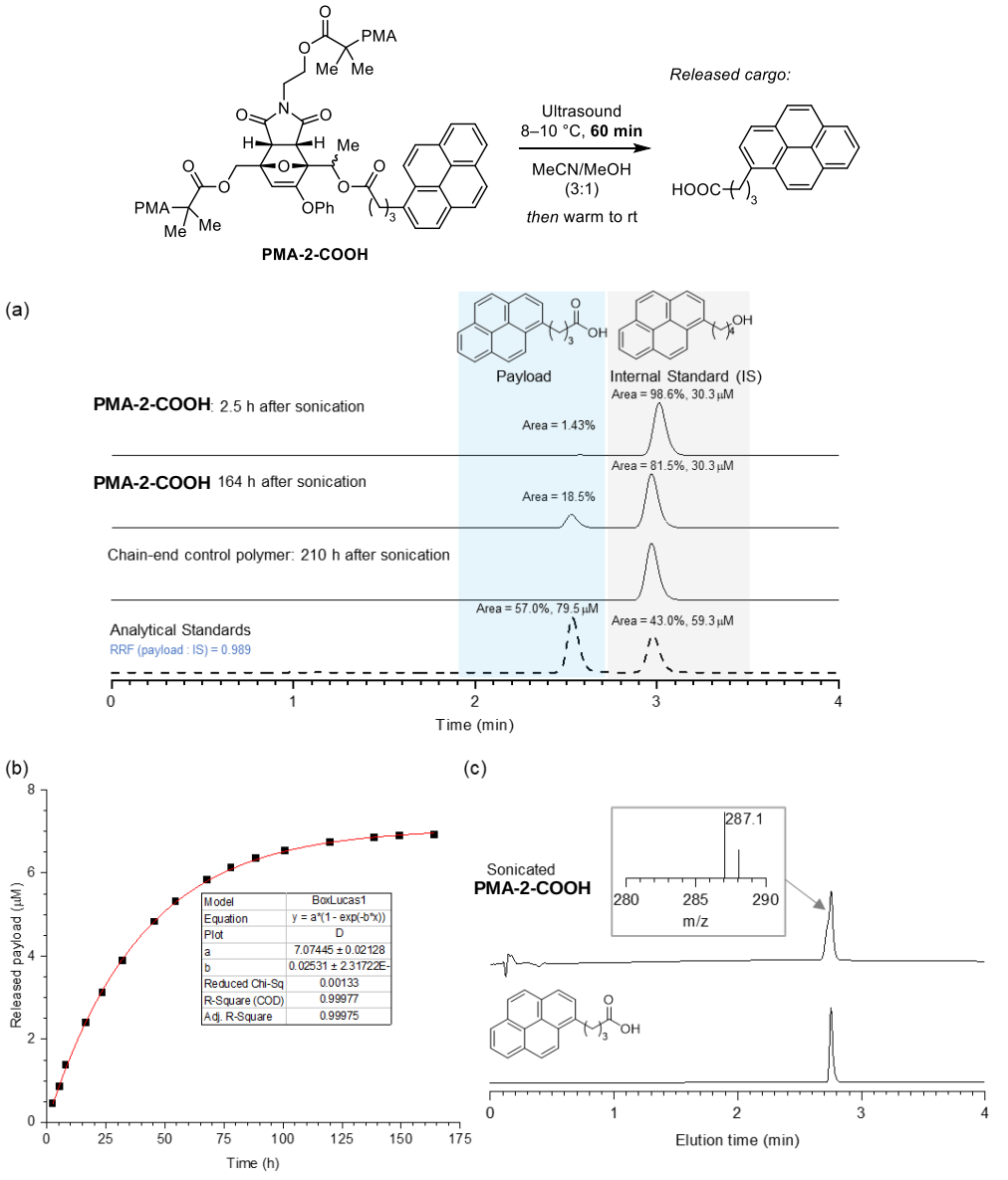

Figure 2.25. (a) Representative HPLC chromatograms for the analysis of mechanically triggered molecular release of 1-pyrenebutanoic acid from the polymer containing a chain-centered mechanophore, and a chain-end control polymer (60:40 MeCN/water (with 0.1% acetic acid) isocratic, 2 ml/min, λ = 340 nm). (b) Payload release from sonicated **PMA-2-COOH** as a function of time post-sonication. (c) LCMS measurements further support the identity of the released molecule. The mass of the analyte (*m/z* = 287.1 amu) matches the calculated *m/z* for 1-pyrenebutanoic acid $[C_{20}H_{15}O_2]^-$ $(M–H)^-$ (287.1). LCMS conditions: negative ion mode, 4 min (0–100% MeCN in water).

Table 2.10. Release of 1-pyrenebutanoic acid payload monitored by HPLC[a]

Trial 1				Trial 2			
Time Post-Sonication	Payload Peak Area (%)	IS Peak Area (%)	Released Payload, Calcd (μM)	Time Post-Sonication	Payload Peak Area (%)	IS Peak Area (%)	Released Payload, Calcd (μM)
2.5	1.43	98.6	0.443	2	0.739	99.3	0.228
5.5	2.75	97.3	0.866	5.5	2.58	97.4	0.811
8	4.30	95.7	1.37	14	6.09	93.9	1.99
16.5	7.27	92.7	2.40	21	8.35	91.7	2.79
23.5	9.25	90.8	3.12	27.5	10.6	89.4	3.63
32	11.3	88.7	3.89	43	13.2	86.9	4.63
45.5	13.6	86.4	4.83	52	14.4	85.6	5.17
54.5	14.8	85.2	5.32	65.5	15.9	84.1	5.77
68	16.0	84.0	5.83	75.5	16.5	83.5	6.07
78	16.7	83.3	6.13	98	17.6	82.4	6.54
88.5	17.2	82.8	6.35	117.5	18.1	81.9	6.75
101	17.6	82.4	6.53	136	18.4	81.6	6.91
120	18.0	82.0	6.74	147	18.6	81.4	6.97
138.5	18.3	81.7	6.85	Plateau value: 7.20 μM; $t_{1/2}$ = 28.6 h			
149.5	18.4	81.6	6.90				
164	18.5	81.5	6.92				
Plateau value: 7.07 μM; $t_{1/2}$ = 27.4 h							

[a]IS: 1-Pyrenebutanol (30.3 mM). RRF = 0.989.

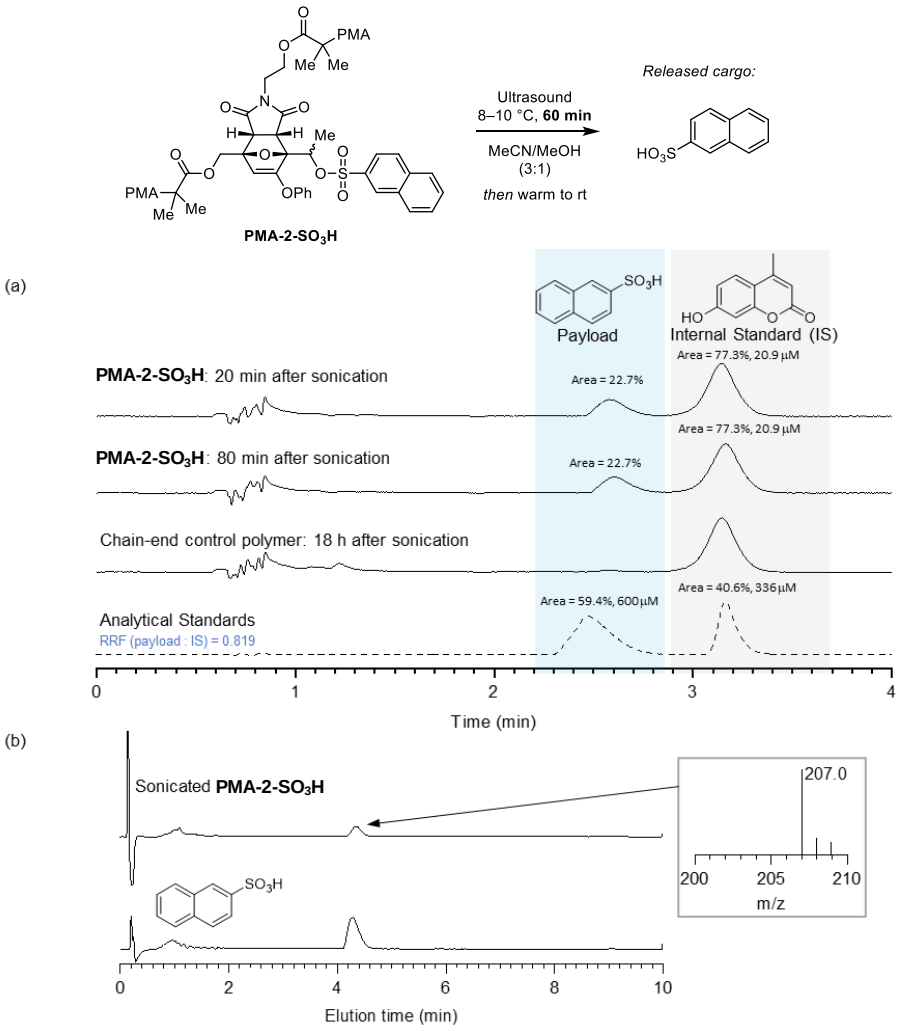

Figure 2.26. (a) Representative HPLC chromatograms for the analysis of mechanically triggered molecular release of 2-naphthalenesulfonic acid from the polymer containing a chain-centered mechanophore, and a chain-end control polymer (40:60 MeOH/water (with 0.1% acetic acid) isocratic, 1.5 ml/min, λ = 280 nm). (b) LCMS measurements further support the identity of the released molecule. The mass of the analyte (*m/z* = 207.0 amu) matches the calculated *m/z* for 2-naphthalenesulfonic acid, $[C_{10}H_7O_3S]^-$ $(M-H)^-$ (207.0). LCMS conditions: negative ion mode, 10 min (0–30% MeCN in water).

Table 2.11. Release of 2-naphthalenesulfonic acid payload monitored by HPLC[a]

Trial 1				Trial 2			
Time Post-Sonication	Payload Peak Area (%)	IS Peak Area (%)	Released Payload, Calcd (μM)	Time Post-Sonication	Payload Peak Area (%)	IS Peak Area (%)	Released Payload, Calcd (μM)
20 min	22.7	77.3	7.49	1 h	23.0	77.0	7.61
80 min	22.7	77.3	7.49	2 h	23.0	77.0	7.60

[a]IS: 7-hydroxy-4-methylcoumarin (20.9 μM). RRF = 0.818.

2.5 Synthetic Details

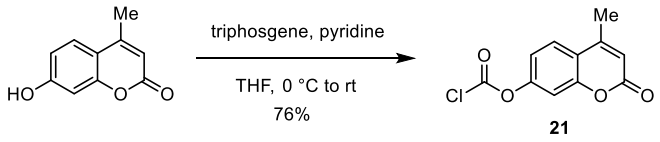

4-methylcoumarin 7-chloroformate (21). A flame-dried round bottom flask equipped with a stir bar under nitrogen was charged with triphosgene (0.50 g, 1.7 mmol) and anhydrous THF (20 mL). The solution was cooled to 0 °C in an ice bath, followed by the dropwise addition of a solution of 7-hydroxy-4-methylcoumarin (0.88 g, 5.0 mol) and anhydrous pyridine (0.40 mL, 5.0 mmol) dissolved in anhydrous THF (35 mL). A white precipitate formed quickly upon addition. The reaction was allowed to warm to rt and stirred for 18 h. The slurry was filtered through a silica plug under an inert atmosphere of nitrogen to remove the insoluble bis-coumarin carbonate byproduct. The crude mixture was dried, taken up into DCM (20 mL), and filtered twice under nitrogen to remove insoluble solids comprising mostly the hydroxycoumarin starting material. The filtrate was concentrated under reduced pressure to provide the title compound as a white powder (0.91 g, 76%), which was stored in a glovebox under nitrogen. ^{1}H NMR (400 MHz, $CDCl_3$) δ: 7.66 (d, *J* = 8.7 Hz, 1H), 7.27–7.25 (m, 1H), 7.22 (d, *J* = 2.4 Hz, 1H), 6.33 (q, *J* = 1.2 Hz, 1H), 2.45 (d, *J* = 1.3 Hz, 3H) ppm. $^{13}C\{^{1}H\}$ NMR (100 MHz, $CDCl_3$) δ: 160.1, 154.3, 153.2, 151.7, 149.2, 126.1, 119.2, 116.8, 115.5, 109.8, 18.9 ppm. HRMS (ESI, *m/z*): calcd for $[C_{11}H_8ClO_4]^+$ $(M+H)^+$, 239.0106; found, 239.0097.

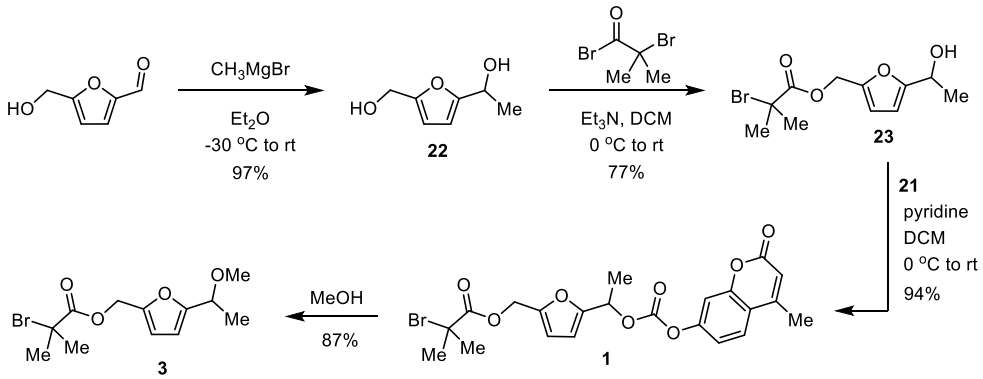

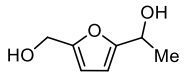

22

1-(5-(hydroxymethyl)furan-2-yl)ethan-1-ol (22). A 1 L round bottom flask equipped with a stir bar was charged with 5-(hydroxymethyl)furan-2-carbaldehyde (6.92 g, 54.9 mmol) and diethyl ether (300 mL). The solution was cooled to −30 °C, followed by the slow addition of methylmagnesium bromide (3 M in diethyl ether, 42 mL, 130 mmol). The mixture was allowed to warm to rt and stirred for 12 h, after which the reaction was cooled to 0 °C and quenched with 10% NH_4Cl (200 mL). The reaction mixture was extracted with EtOAc (3 x 100 mL) and the combined organic phase was dried over $MgSO_4$, filtered, and concentrated under reduced pressure to provide the title compound as a viscous yellow oil (7.60 g, 97%). ^{1}H NMR (400 MHz, $CDCl_3$) δ: 6.23 (d, *J* = 3.1 Hz, 1H), 6.18 (d, *J* = 3.2 Hz, 1H), 4.87 (q, *J* = 6.7 Hz, 1H), 4.59 (d, *J* = 2.9 Hz, 2H), 1.97 (br s, 1H), 1.78 (br s, 1H), 1.54 (d, *J* = 6.5 Hz, 3H) ppm. ^{13}C{^{1}H} NMR (100 MHz, $CDCl_3$) δ: 157.8, 153.5, 108.6, 106.1, 63.8, 57.7, 21.3 ppm. HRMS (ESI, *m/z*): calcd for $[C_7H_9O_2]^+$ $(M-OH)^+$, 125.0597; found, 125.0595.

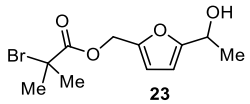

23

(5-(1-hydroxyethyl)furan-2-yl)methyl 2-bromo-2-methylpropanoate (23). A 500 mL three neck flask was equipped with a stir bar was charged with **22** (2.74 g, 19.3 mmol), triethylamine (3.00 mL, 21.6 mmol), and DCM (150 mL). The mixture was cooled to 0 °C in an ice bath followed by the dropwise addition of a solution of α-bromoisobutyryl bromide (2.60 mL, 21.0 mmol) dissolved in DCM (50 mL) over 2 h. The reaction mixture was stirred under nitrogen and allowed to warm to rt slowly. After 20 h, the reaction mixture was filtered through a plug of silica gel, washed with 1:1 EtOAc:hexanes, concentrated, then purified by column chromatography (2–35% EtOAc/hexanes) to yield the title compound as a viscous colorless liquid (4.35 g, 77%). R_f = 0.33 (1:4 EtOAc:hexanes). ^{1}H NMR (400 MHz, $CDCl_3$) δ: 6.38 (d, *J* = 3.2 Hz, 1H), 6.21 (d, *J* = 3.4 Hz, 1H), 5.13 (s, 2H), 4.87 (q, *J* = 6.6 Hz, 1H), 1.93 (s, 6H), 1.54 (d, *J* = 6.6 Hz, 3H) ppm. ^{13}C{^{1}H} NMR (100 MHz, $CDCl_3$) δ: 171.5, 158.7,

148.3, 111.7, 106.3, 63.8, 59.8, 55.8, 30.8, 21.4 ppm. HRMS (ESI, *m/z*): calcd for $[C_{11}H_{14}BrO_3]^+$ $(M\text{-}OH)^+$, 273.0121; found, 273.0119.

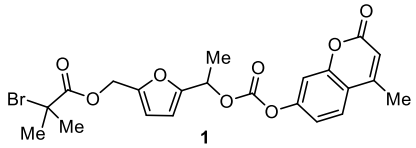

1

(5-(1-((((4-methyl-2-oxo-2H-chromen-7-yl)oxy)carbonyl)oxy)ethyl)furan-2-yl)methyl 2-bromo-2-methylpropanoate (1). A two-neck round bottom flask equipped with a stir bar was charged with **23** (58.5 mg, 0.201 mmol), pyridine (19.0 μL, 0.236 mmol), and DCM (4 mL). The solution was cooled to 0 °C in an ice bath followed by the dropwise addition of a solution of coumarin chloroformate **21** (53.5 mg, 0.224 mmol) dissolved in DCM (6 mL). The reaction was allowed to warm slowly to rt and stirred for 3 h. The reaction mixture was washed quickly with brine, dried over Na_2SO_4, filtered, and concentrated under reduced pressure to yield a viscous oil. The crude oil was dispersed in DCM/hexanes (1:2, 3 mL), then filtered to remove insoluble byproducts consisting mostly of 7-hydroxy-4-methylcoumarin and the bis-coumarin carbonate. The filtrate was concentrated under reduced pressure to provide the title compound as a viscous colorless liquid (93 mg, 94%). Compound **1** is relatively stable in solvents such as DCM, chloroform, and hexanes, but decomposes quickly in acidic and protic solvents. ^{1}H NMR (400 MHz, $CDCl_3$) δ: 7.61 (d, *J* = 8.7 Hz, 1H), 7.23 (d, *J* = 2.3 Hz, 1H), 7.17 (dd, *J* = 8.7, 2.4 Hz, 1H), 6.43 (s, 2H), 6.28 (d, *J* = 1.3 Hz, 1H), 5.88 (q, *J* = 6.7 Hz, 1H), 5.17 (ABq, $\Delta\nu_{AB}$ = 5.8 Hz, J_{AB} = 13.6 Hz, 2H), 2.43 (d, *J* = 1.3 Hz, 3H), 1.94 (s, 6H), 1.74 (d, *J* = 6.8 Hz, 3H) ppm. ^{13}C{^{1}H} NMR (100 MHz, $CDCl_3$) δ: 171.4, 160.6, 154.3, 153.3, 152.6, 152.3, 152.0, 149.6, 125.6, 118.1, 117.5, 114.8, 111.7, 110.2, 110.1, 70.7, 59.6, 55.7, 30.8, 18.9, 18.1 ppm. HRMS (ESI, *m/z*): calcd for $[C_{22}H_{25}BrNO_8]^+$ $(M+NH_4)^+$, 501.0758; found, 501.0750.

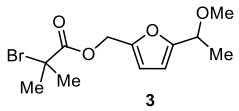

3

(5-(1-methoxyethyl)furan-2-yl)methyl 2-bromo-2-methylpropanoate (3). Compound **1** (80.2 mg, 0.163 mmol) was dissolved in methanol (1 mL) in a 2 ml vial and stirred at rt. After 16 h, the reaction mixture was concentrated under reduced pressure and the crude product was purified by flash chromatography (1–25% EtOAc/hexanes) to provide

the title compound as a colorless viscous oil (43 mg, 87%). R_f = 0.31 (1:19 EtOAc:hexanes). ^{1}H NMR (500 MHz, $CDCl_3$) δ: 6.38 (d, J = 3.2 Hz, 1H), 6.23 (d, J = 3.2 Hz, 1H), 5.13 (ABq, $\Delta\nu_{AB}$ = 7.5 Hz, J_{AB} = 13.0 Hz, 2H), 4.34 (q, J = 6.6 Hz, 1H), 3.28 (d, J = 1.0 Hz, 3H), 1.92 (d, J = 0.8 Hz, 6H), 1.49 (dd, J = 6.6, 0.9 Hz, 3H) ppm. ^{13}C{^{1}H} NMR (125 MHz, $CDCl_3$) δ: 171.4, 156.5, 148.4, 111.5, 108.0, 72.1, 59.8, 56.3, 55.7, 30.8, 30.8, 19.5 ppm. HRMS (ESI, *m/z*): calcd for $[C_{12}H_{21}BrNO_4]^+$ $(M+NH_4)^+$, 322.0648; found, 322.0654.

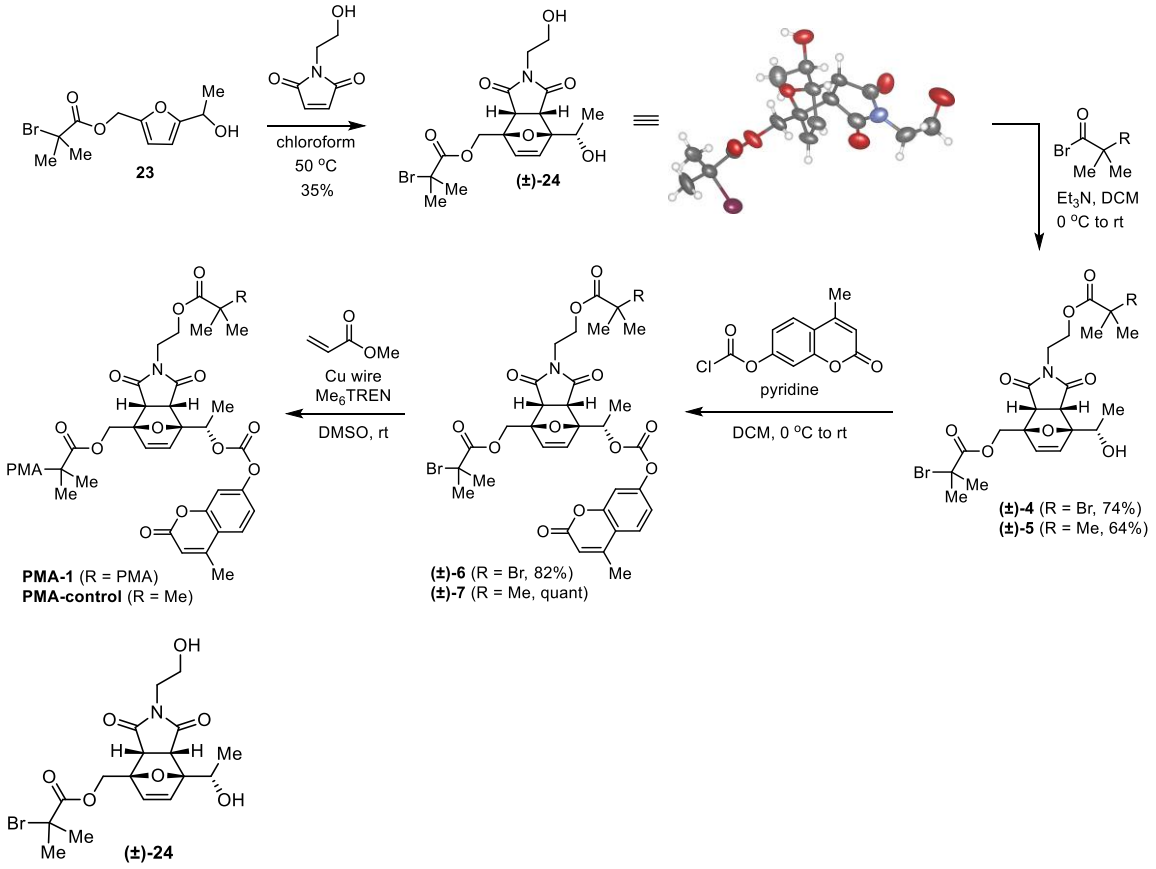

7-(1-hydroxyethyl)-2-(2-hydroxyethyl)-1,3-dioxo-1,2,3,3a,7,7a-hexahydro-4H-4,7-epoxyisoindol-4-yl)methyl 2-bromo-2-methylpropanoate ((±)-24). Compound **23** (4.15 g, 14.3 mmol) was combined with *N*-(2-hydroxyethyl)maleimide[39] (3.51 g, 24.9 mmol) and chloroform (4 mL) in a 20 mL vial and stirred at 55 °C for 14 h. The crude reaction mixture was separated by column chromatography (2–4% methanol/DCM) and a single diastereomer of the title compound was isolated as a white solid (2.19 g, 35%). The absolute configuration of compound **24** was confirmed by single crystal X-ray diffraction. R_f = 0.28 (1:24 methanol:DCM). ^{1}H NMR (400 MHz, $CDCl_3$) δ: 6.43 (d, J = 5.8 Hz, 1H), 6.38 (d, J =

5.8 Hz, 1H), 4.81 (ABq, $\Delta\nu_{AB}$ = 78 Hz, J_{AB} = 12.8 Hz, 2H), 4.34 (q, J = 7.1 Hz, 1H), 3.73–3.50 (m, 6H), 1.95 (s, 6H), 1.43 (d, J = 6.6 Hz, 3H) ppm. $^{13}C\{^1H\}$ NMR (100 MHz, $CDCl_3$) δ: 175.5, 175.0, 171.2, 135.7, 135.0, 95.0, 89.4, 66.7, 63.2, 60.6, 55.5, 49.5, 47.7, 41.5, 30.8, 30.8, 18.7 ppm. HRMS (ESI, *m/z*): calcd for $[C_{17}H_{22}BrNO_7Na]^+$ $(M+Na)^+$, 454.0472; found, 454.0470.

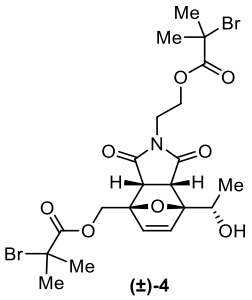

(±)-4

2-(2-((2-bromo-2-methylpropanoyl)oxy)ethyl)-7-(1-hydroxyethyl)-1,3-dioxo-1,2,3,3a,7,7a-hexahydro-4H-4,7-epoxyisoindol-4-yl)methyl 2-bromo-2-methylpropanoate ((±)-4). A three-neck round bottom flask equipped with a stir bar was charged with **24** (1.08 g, 2.50 mmol), triethylamine (0.39 mL, 2.8 mmol), and DCM (50 mL). The solution was cooled to 0 °C in an ice bath followed by the dropwise addition of α-bromoisobutyryl bromide (0.33 mL, 2.7 mmol). The solution was allowed to warm to rt slowly and stirred for an additional 16 h. The reaction mixture was washed with NH_4Cl (100 mL) and brine (100 mL), dried over Na_2SO_4, filtered, and the organic fraction was concentrated under reduced pressure. The crude product was purified by column chromatography (35–55% EtOAc/hexanes) to provide the title compound as a colorless, sticky oil (1.07 g, 74%). R_f = 0.29 (1:1 EtOAc/hexanes). ^1H NMR (400 MHz, $CDCl_3$) δ: 6.46 (d, J = 5.7 Hz, 1H), 6.41 (d, J = 5.8 Hz, 1H), 4.80 (ABq, $\Delta\nu_{AB}$ = 84 Hz, J_{AB} = 12.8 Hz, 2H), 4.33 (q, J = 6.6 Hz, 1H), 4.22 (dd, J = 5.7, 4.7 Hz, 2H), 3.73–3.62 (m, 3H), 3.58 (d, J = 7.7 Hz, 1H), 1.96 (s, 5H), 1.90 (s, 6H), 1.44 (d, J = 6.6 Hz, 3H) ppm. $^{13}C\{^1H\}$ NMR (100 MHz, $CDCl_3$) δ: 174.5, 174.0, 171.5, 171.2, 135.7, 135.1, 95.0, 89.4, 66.8, 63.2, 62.6, 55.6, 55.5, 49.6, 47.8, 37.6, 30.81, 30.80, 30.79, 30.77, 18.7 ppm. HRMS (ESI, *m/z*): calcd for $[C_{21}H_{31}Br_2N_2O_8]^+$ $(M+NH_4)^+$, 599.0421; found, 599.0420.

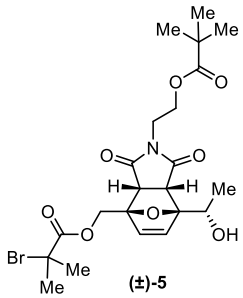

(±)-5

2-(-4-(((2-bromo-2-methylpropanoyl)oxy)methyl)-7-(-1-hydroxyethyl)-1,3-dioxo-1,3,3a,4,7,7a-hexahydro-2H-4,7-epoxyisoindol-2-yl)ethyl pivalate ((±)-5). A two-neck round bottom flask equipped with a stir bar was charged with **24** (410 mg, 0.95 mmol), triethylamine (0.21 mL, 1.5 mmol), and DCM (15 mL). The solution was cooled to 0 °C in an ice bath followed by the dropwise addition of pivaloyl chloride (0.18 mL, 1.5 mmol). The solution was allowed to warm to rt slowly and stirred for an additional 23 h. The reaction mixture was filtered through a plug of silica gel and the filtrate was concentrated under reduced pressure. The crude product was purified by column chromatography (30–55% EtOAc/hexanes) to provide the title compound as a colorless viscous oil (315 mg, 64%). R_f = 0.56 (1:1 EtOAc:hexanes). ^{1}H NMR (500 MHz, $CDCl_3$) δ: 6.42 (d, J = 5.7 Hz, 1H), 6.37 (d, J = 5.8 Hz, 1H), 4.80 (ABq, $\Delta\nu_{AB}$ = 106 Hz, J_{AB} = 12.5 Hz, 2H), 4.33 (q, J = 6.6 Hz, 1H), 4.11 (t, J = 5.3 Hz, 2H), 3.66 (d, J = 7.7 Hz, 1H), 3.63 – 3.59 (m, 2H) , 3.57 (d, J = 7.8 Hz, 1H), 1.96 (s, 6H), 1.44 (d, J = 6.6 Hz, 3H), 1.17 (s, 8H) ppm. ^{13}C{^{1}H} NMR (125 MHz, $CDCl_3$) δ: 178.3, 174.5, 174.0, 171.2, 135.7, 135.0, 94.9, 89.3, 66.8, 63.2, 61.0, 55.5, 49.5, 47.7, 38.8, 38.0, 30.80, 30.75, 27.3, 18.6 ppm. HRMS (ESI, *m/z*): calcd for $[C_{22}H_{31}BrN_2O_8]^+$ $(M+H)^+$, 516.1228; found, 516.1228.

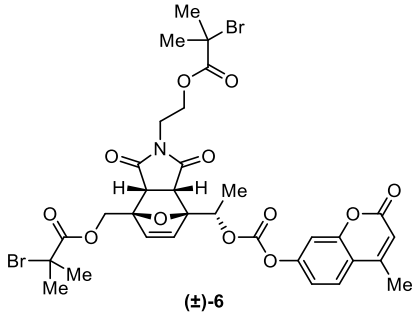

(±)-6

(2-(2-((2-bromo-2-methylpropanoyl)oxy)ethyl)-7-(-1-((((4-methyl-2-oxo-2H-chromen-7-yl)oxy)carbonyl)oxy)ethyl)-1,3-dioxo-1,2,3,3a,7,7a-hexahydro-4H-4,7-

epoxyisoindol-4-yl)methyl 2-bromo-2-methylpropanoate ((±)6). A two-neck round bottom flask equipped with a stir bar was charged with **4** (68.8 mg, 0.118 mmol), pyridine (30.0 μL, 0.372 mmol), and DCM (25 mL). The solution was cooled to 0 °C in an ice bath followed by the dropwise addition of a solution of coumarin chloroformate **21** (81.0 mg, 0.339 mmol) dissolved in DCM (5 mL). The reaction was allowed to warm slowly to rt and stirred for 20 h. The reaction mixture was washed with brine, dried over Na_2SO_4, filtered, and concentrated under reduced pressure. The crude produce was purified by column chromatography (35–55% EtOAc/Hexanes) to provide the title compound as a white foaming solid (76 mg, 82%). R_f = 0.35 (1:1 EtOAc:hexanes). ^{1}H NMR (400 MHz, $CDCl_3$) δ: 7.62 (d, *J* = 8.7 Hz, 1H), 7.26 (s, 1H), 7.21 (dd, *J* = 8.7, 2.3 Hz, 1H), δ 6.53–6.46 (m, 2H), 6.28 (q, *J* = 1.3 Hz, 1H), 5.46 (q, *J* = 6.6 Hz, 1H), 4.82 (ABq, $\Delta\nu_{AB}$ = 95 Hz, J_{AB} =12.8 Hz, 2H), 4.24 (t, *J* = 5.1 Hz, 2H), 3.77–3.56 (m, 4H), 2.44 (d, *J* = 1.3 Hz, 3H), 1.95 (d, *J* = 1.9 Hz, 6H), 1.91 (s, 6H), 1.64 (d, *J* = 6.7 Hz, 3H) ppm. ^{13}C{^{1}H} NMR (100 MHz, $CDCl_3$) δ: 173.7, 173.5, 171.5, 171.2, 160.5, 154.3, 153.3, 152.2, 151.9, 135.6, 135.2, 125.6, 118.2, 117.5, 114.9, 110.1, 92.6, 89.5, 73.9, 63.1, 62.5, 55.7, 55.5, 49.4, 48.4, 37.8, 30.80, 30.78, 18.9, 16.0 ppm. HRMS (ESI, *m/z*): calcd for $[C_{32}H_{37}Br_2N_2O_{12}]^+$ $(M+NH_4)^+$, 801.0687; found, 801.0684.

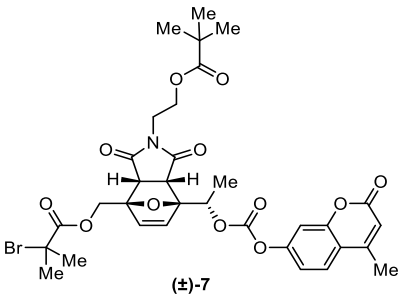

(±)-7

2-(-4-(((2-bromo-2-methylpropanoyl)oxy)methyl)-7-(-1-((((4-methyl-2-oxo-2H-chromen-7-yl)oxy)carbonyl)oxy)ethyl)-1,3-dioxo-1,3,3a,4,7,7a-hexahydro-2H-4,7-epoxyisoindol-2-yl)ethyl pivalate ((±)-7). A two-neck round bottom flask equipped with a stir bar was charged with **5** (74.6 mg, 0.144 mmol), pyridine (23.4 μL, 0.291 mmol), and DCM (25 mL). The solution was cooled to 0 °C in an ice bath followed by the dropwise addition of a solution of coumarin chloroformate **21** (69.0 mg, 0.289 mmol) dissolved in DCM (10 mL). The reaction was allowed to warm slowly to rt and stirred for 16 h. The

reaction mixture was washed with 10% NH_4Cl, dried over Na_2SO_4, filtered, and concentrated under reduced pressure. The crude produce was purified by column chromatography (35–60% EtOAc/Hexanes) to provide the title compound as a white foaming solid (103 mg, quant). R_f = 0.56 (1:1 EtOAc:hexanes). ^{1}H NMR (500 MHz, $CDCl_3$) δ: 7.62 (d, J = 8.7 Hz, 1H), 7.27–7.25 (m, 1H), 7.21 (dd, J = 8.7, 2.4 Hz, 1H), 6.47–6.42 (m, 2H), 6.29 (q, J = 1.3 Hz, 1H), 5.46 (q, J = 6.6 Hz, 1H), 4.82 (ABq, $\Delta\nu_{AB}$ = 120 Hz, J_{AB} = 12.5 Hz, 2H), 4.13 (t, J = 5.2 Hz, 2H), 3.76–3.55 (m, 4H), 2.45 (d, J = 1.3 Hz, 3H), 1.96 (d, J = 2.7 Hz, 6H), 1.65 (d, J = 6.6 Hz, 3H), 1.18 (s, 9H) ppm. $^{13}C\{^1H\}$ NMR (100 MHz, $CDCl_3$) δ: 178.4, 173.7, 173.5, 171.2, 160.5, 154.3, 153.3, 152.2, 151.9, 135.5, 135.1, 125.6, 118.2, 117.5, 114.9, 110.0, 92.6, 89.5, 73.9, 63.2, 61.0, 55.5, 49.3, 48.3, 38.9, 38.2, 30.79, 30.76, 27.3, 18.9, 16.0 ppm. HRMS (ESI, *m/z*): calcd for $[C_{33}H_{37}BrNO_{12}]^+$ $(M+H)^+$, 718.1494; found, 718.1500.

Poly(methyl acrylate) containing a chain-centered mechanophore (PMA-1). A 10 mL Schlenk flask equipped with a stir bar was charged with bis-initiator **6** (7.2 mg, 9.2 μmol), DMSO (1.2 mL), methyl acrylate (1.2 mL, 13 mmol), and Me_6TREN (4.6 mg, 20 μmol). The flask was sealed, the solution was deoxygenated with three freeze-pump-thaw cycles, and then backfilled with nitrogen. The flask was opened briefly under a flow of N_2, and freshly cut copper wire (1.0 cm length, 20 gauge) was added on top of the frozen mixture. The flask was resealed, evacuated for an additional 15 min, warmed to rt, and then backfilled with nitrogen. After stirring at rt for 90 min, the flask was opened to air and the solution was diluted with DCM. The polymer solution was precipitated into cold methanol (2x) and the isolated material was dried under vacuum to yield 0.60 g of **PMA-1** (52%). M_n = 100 kg/mol, $Đ$ = 1.06.

Poly(methyl acrylate) control polymer containing the mechanophore at the end of the polymer chain (PMA-control). A 10 mL Schlenk flask equipped with a stir bar was charged with initiator **7** (8.5 mg, 11.8 μmol), DMSO (1.6 mL), methyl acrylate (1.6 mL, 18 mmol), and Me_6TREN (5.1 mg, 22 μmol). The flask was sealed, the solution was deoxygenated with three freeze-pump-thaw cycles, and then backfilled with nitrogen. The flask was opened briefly under a flow of N_2, and freshly cut copper wire (1.1 cm length, 20 gauge) was added on top of the frozen mixture. The flask was resealed, evacuated for an additional 15 min, warmed to rt, and then backfilled with nitrogen. After stirring at rt for 2

h, the flask was opened to air and the solution was diluted with DCM. The polymer solution was precipitated into cold methanol (2x) and the isolated material was dried under vacuum to yield 0.82 g of **PMA-control** (54%). *M*n = 86 kg/mol, *Đ* = 1.14.

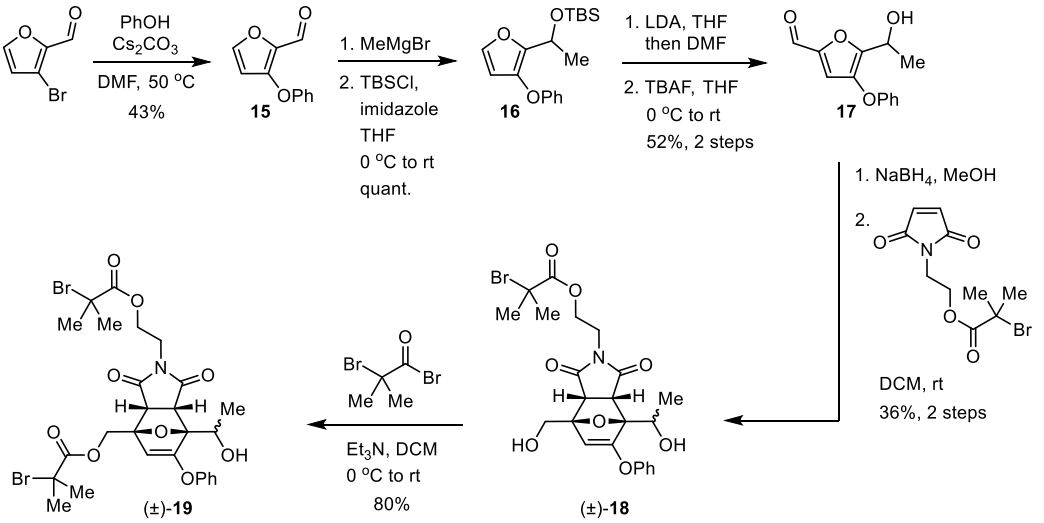

3-phenoxyfuran-2-carbaldehyde (15). A round bottom flask equipped with a stir bar was charged with phenol (16.1 g, 0.171 mol), cesium carbonate (55.7 g, 0.171 mol) and DMF (500 mL). The solution was heated to 80 °C until cesium carbonate had dissolved. The mixture was then cooled to 60 °C before adding 3-bromo-2-furfural[40] (6.30 g, 0.0360 mol), and vigorously stirred for 1 day. The reaction mixture was then cooled to room temperature before pouring into a sat. Na_2CO_3 solution (1 L), extracted with Et_2O (4 x 300 mL), and washed with copious sat. Na_2CO_3 and brine. The organic layer was dried over $MgSO_4$, filtered, and concentrated under reduced pressure. The crude product was purified by column chromatography (5–20% EtOAc/Hexanes) to yield the title compound as a light-yellow solid (2.90 g, 43%). ^{1}H NMR (500 MHz, $CDCl_3$) δ: 9.67 (s, 1H), 7.52 (d, *J* = 2.1, 1H), 7.43 – 7.37 (m, 2H), 7.25 – 7.20 (m, 1H), 7.19 – 7.13 (m, 2H), 6.22 (d, *J* = 2.1 Hz, 1H) ppm. ^{13}C{^{1}H} NMR (100 MHz, $CDCl_3$) δ: 174.9, 156.1, 155.6, 147.9, 139.5, 130.3, 125.4, 119.0, 105.4 ppm. HRMS (ESI, *m/z*): calcd for $[C_{11}H_9O_3]^+$ $(M+H)^+$, 189.0546; found, 189.0568.

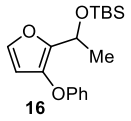

16

***Tert*-butyldimethyl(1-(3-phenoxyfuran-2-yl)ethoxy)silane (16).** A flame-dried round bottom flask was charged with **15** (1.50 g, 7.98 mmol) and anhydrous Et_2O (50 mL). The solution was cooled to −30 °C in an acetonitrile/dry ice bath followed by the dropwise addition of MeMgBr (3 M in Et_2O, 4.00 mL, 12.0 mmol). The solution was allowed to warm to room temperature and stirred for 1 h before being quenched with 10% NH_4Cl (50 mL) and extracted with Et_2O (2 x 50 mL). The combined organic phase was dried over Na_2SO_4, filtered, concentrated under reduced pressure to yield 1-(3-phenoxyfuran-2-yl)ethan-1-ol as a colorless oil, which was used in the next step without further purification.

A round bottom flask equipped with a stir bar was charged with 1-(3-phenoxyfuran-2-yl)ethan-1-ol (1.60 g, 7.84 mmol), imidazole (1.60 g, 23.5 mmol), and DCM (15 mL), followed by addition of tert-butylchlorodimethylsilane (2.40 g, 16.0 mmol). The reaction was allowed to stir at room temperature overnight before filtering the mixture through a cotton pad. The filtrate was concentrated under reduced pressure, and the crude product was purified by column chromatography (0–15% EtOAc/Hexanes) to yield the title compound as a light yellow oil (2.49 g, 98% over two steps). ^{1}H NMR (400 MHz, $CDCl_3$) δ: 7.33 – 7.27 (m, 3H), 7.06 – 7.01 (m, 1H), 7.00 – 6.95 (m, 2H), 6.19 (d, J = 2.1 Hz, 1H), 4.93 (q, J = 6.6 Hz, 1H), 1.47 (d, J = 6.6 Hz, 3H), 0.85 (s, 9H), 0.04 (s, 3H), −0.05 (s, 3H) ppm. ^{13}C{^{1}H} NMR (100 MHz, $CDCl_3$) δ: 158.4, 145.2, 140.7, 137.7, 129.7, 122.5, 116.2, 106.3, 61.6, 25.9, 25.8, 22.2, 18.3, -4.9, -5.0 ppm. HRMS (ESI, *m/z*): calcd for $[C_{12}H_{11}O_2]^+$ $(M\text{-}OTBS)^+$, 187.0754; found, 187.0732.

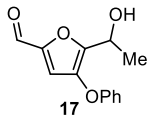

17

5-(1-hydroxyethyl)-4-phenoxyfuran-2-carbaldehyde (17). A flame-dried round bottom flask equipped with a stir bar was charged with diisopropylamine (0.80 mL, 5.7 mmol) and THF (70 mL). The solution was cooled to −78 °C in an acetone/dry ice bath before adding n-butyllithium (2.5 M in hexanes, 2.30 mL, 5.75 mmol) dropwise. After stirring the mixture for 5 min, a solution of **16** (1.06 g, 5.02 mmol) in THF (10 ml) was added

to the mixture dropwise at −78 °C. The mixture was kept at −78 °C for 30 mins before adding DMF (0.52 mL, 6.7 mmol) dropwise. The mixture was then allowed to slowly warm up to room temperature for ~1 h before 10% NH_4Cl (100 mL) was added slowly to the mixture to quench the reaction. The mixture was then extracted with Et_2O (2 x 100 mL), and the organic layer was dried over $MgSO_4$, filtered, and concentrated under reduced pressure. The crude mixture was purified by column chromatography (0–20% EtOAc/Hexanes) to yield the crude product of 5-(1-((tert-butyldimethylsilyl)oxy)ethyl)-4-phenoxyfuran-2-carbaldehyde as a colorless oil. Approximately 10% of the crude product was identified to be the regioisomer resulting from formylation at the 4-position of the furan. The crude product was used in the next step without further purification.

The crude product from above was dissolved in THF (25 mL) and cooled to 0 °C before adding TBAF (1 M in THF, 3.8 mL, 3.8 mmol) dropwise. The mixture was allowed to slowly warm up to room temperature and stirred for 1 h. The reaction mixture was then diluted with Et_2O (25 mL) washed with NH_4Cl (25 mL) and brine (25 mL), and the organic fraction was dried over Na_2SO_4, filtered, and concentrated under reduced pressure. The crude product was purified by column chromatography (25–50% EtOAc/Hexanes) to yield compound **17** as a yellow waxy solid (602 mg, 52% over two steps). ^{1}H NMR (400 MHz, $CDCl_3$) δ: 9.57 (s, 1H), 7.35 (dd, *J* = 8.7, 7.4 Hz, 2H), 7.19 – 7.08 (m, 1H), 7.05 – 6.96 (m, 3H), 5.04 (q, *J* = 6.7 Hz, 1H), 1.62 (d, *J* = 6.7 Hz, 3H). $^{13}C\{^1H\}$ NMR (101 MHz, $CDCl_3$) δ: 178.0, 157.4, 150.9, 149.4, 140.9, 130.1, 123.8, 116.8, 115.2, 61.9, 20.9 ppm. HRMS (ESI, *m/z*): calcd for $[C_{13}H_{13}O_4]^+$ $(M+H)^+$, 233.0808; found, 233.0808.

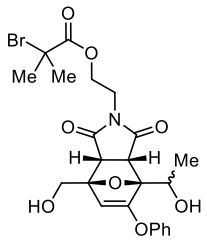

(±)-**18**

2-(-4-(1-hydroxyethyl)-7-(hydroxymethyl)-1,3-dioxo-5-phenoxy-1,3,3a,4,7,7a-hexahydro-2*H*-4,7-epoxyisoindol-2-yl)ethyl 2-bromo-2-methylpropanoate ((±)-18). A round bottom flask equipped with a stir bar was charged with **7** (350.0 mg, 1.509 mmol), THF (3 mL) and MeOH (10 mL). The solution was cooled to 0 °C in an ice bath before

slowly adding $NaBH_4$ (82.0 mg, 2.17 mmol). The mixture was kept at 0 °C for 1 h before adding 10% NH_4Cl (10 mL), extracted with EtOAc (2 x 10 mL), and washed with brine (10 mL). The organic layer was dried over Na_2SO_4, and filtered. Maleimide[41] (527 mg, 2.77 mmol) was then added and the solution was concentrated under reduced pressure until about 2 mL viscous solution remained. The solution was then stirred at room temperature for 4 h, and the crude mixture was purified by column chromatography (72–90% EtOAc/Hexanes). A single diastereomer of the title compound was isolated as a colorless oil (285 mg, 36% yield). ^{1}H NMR (400 MHz, $CDCl_3$) δ: 7.38 – 7.30 (m, 2H), 7.22-7.16 (m, 1H), 7.00 – 6.94 (m, 2H), 4.96 (s, 1H), 4.59 (s, 1H), 4.32-3.97 (m, 5H), 3.78 – 3.53 (m, 3H), 2.04 (m, 2H), 1.87 (d, J = 0.8 Hz, 6H), 1.54 (d, J = 6.6 Hz, 3H) ppm. ^{13}C{^{1}H} NMR (100 MHz, $CDCl_3$) δ: 175.1, 174.1, 171.5, 163.5, 154.8, 130.2, 126.1, 119.9, 100.9, 92.3, 90.4, 65.0, 62.5, 62.4, 55.7, 50.9, 48.0, 37.5, 30.7, 30.7, 19.0 ppm. HRMS (ESI, *m/z*): calcd for $[C_{23}H_{27}BrNO_8]^+$ $(M+H)^+$, 524.0915; found, 524.0928.

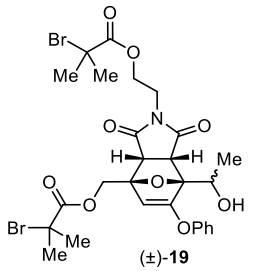

(±)-**19**

(2-(2-((2-bromo-2-methylpropanoyl)oxy)ethyl)-7-(1-hydroxyethyl)-1,3-dioxo-6-phenoxy-1,2,3,3a,7,7a-hexahydro-4H-4,7-epoxyisoindol-4-yl)methyl 2-bromo-2-methylpropanoate ((±)-19). A flame-dried round bottom flask equipped with a stir bar was charged with **(±)-18** (263 mg, 0.502 mmol), Et_3N (84 μL, 0.60 mmol) and DCM (15 mL). The solution was cooled to 0 °C before adding α-bromoisobutyryl bromide (68 μL, 0.55 mmol) dropwise. The reaction was then allowed to warm to room temperature and stirred overnight until the reaction had completed, as determined by TLC. The reaction mixture was then washed with NH_4Cl (30 mL) and brine (30 mL), and the organic fraction was dried over Na_2SO_4, filtered, and concentrated under reduced pressure. The crude product was purified by column chromatography (35–50% EtOAc/Hexanes) to yield the title compound as a colorless oil (270 mg, 80% yield). ^{1}H NMR (400 MHz, $CDCl_3$) δ: 7.39 – 7.30 (m, 2H), 7.23 – 7.15 (m, 1H), 7.01 – 6.91 (m, 2H), 4.95 (s, 1H), 4.68 (ABq, $\Delta\nu_{AB}$ = 126.4 Hz, J_{AB} = 58.0

Hz, 2H), 4.63 – 4.57 (m, 1H), 4.33-4.11 (m, 2H), 4.00 (d, *J* = 7.8 Hz, 1H), 3.79-3.52 (m, 3H), 1.96 (m, 7H), 1.86 (s, 6H), 1.52 (d, *J* = 6.6 Hz, 3H) ppm. $^{13}C\{^{1}H\}$ NMR (100 MHz, $CDCl_3$) δ: 174.1, 173.7, 171.4, 171.0, 163.5, 154.6, 130.1, 126.0, 119.7, 100.8, 92.1, 88.2, 64.8, 63.5, 62.3, 55.5, 55.5, 51.1, 47.5, 37.3, 30.7, 30.6, 18.7 ppm. HRMS (ESI, *m/z*): calcd for $[C_{27}H_{32}Br_2NO_9]^+$ $(M+H)^+$, 672.0438; found, 672.0462.

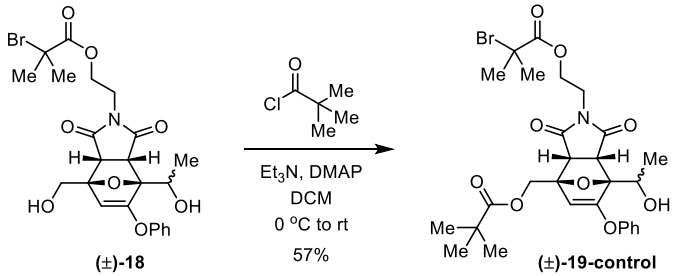

(2-(2-((2-bromo-2-methylpropanoyl)oxy)ethyl)-7-(1-hydroxyethyl)-1,3-dioxo-6-phenoxy-1,2,3,3a,7,7a-hexahydro-4H-4,7-epoxyisoindol-4-yl)methyl pivalate ((±)-19-control). A flame-dried round bottom flask equipped with a stir bar was charged with (±)-**18** (137 mg, 0.261 mmol), Et_3N (52.3 μL, 0.376 mmol), DMAP (41.7 mg, 0.342 mmol) and DCM (5 mL). The solution was cooled to 0 °C before adding pivaloyl chloride (46.3 μL, 0.376 mmol) dropwise. The reaction was then allowed to warm to room temperature and stirred overnight until the reaction completed, as determined by TLC. The reaction mixture was then diluted with DCM (20 mL), washed with NH_4Cl (30 mL) and brine (30 mL), and the organic fraction was dried over Na_2SO_4, filtered, and concentrated under reduced pressure. The crude product was purified by column chromatography (10–50% EtOAc/Hexanes) to yield the title compound as a white waxy solid (90 mg, 57% yield). ^{1}H NMR (400 MHz, $CDCl_3$) δ: 7.40 – 7.29 (m, 2H), 7.24 – 7.15 (m, 1H), 6.99 – 6.90 (m, 2H), 4.90 (s, 1H), 4.57 (ABq, $\Delta\nu_{AB}$ = 113.0 Hz, J_{AB} = 12.7 Hz, 2H), 4.55 (dt, *J* = 7.6, 6.4 Hz, 1H), 4.33-4.12 (m, 2H), 3.99 (d, *J* = 7.8 Hz, 1H), 3.79 – 3.51 (m, 3H), 1.96 (d, *J* = 7.9 Hz, 1H), 1.87 (d, *J* = 1.3 Hz, 6H), 1.52 (d, *J* = 6.6 Hz, 3H), 1.22 (s, 9H) ppm. $^{13}C\{^{1}H\}$ NMR (100 MHz, $CDCl_3$) δ: 177.9, 174.3, 173.9, 171.5, 163.5, 154.8, 130.2, 126.1, 119.8, 101.1, 92.1, 88.6, 64.9, 62.5, 62.3, 55.7, 51.2, 47.7, 39.1, 37.5, 30.7, 27.3, 18.8 ppm. HRMS (ESI, *m/z*): calcd for $[C_{28}H_{35}BrNO_9]^+$ $(M+H)^+$, 608.1490; found, 608.1479.

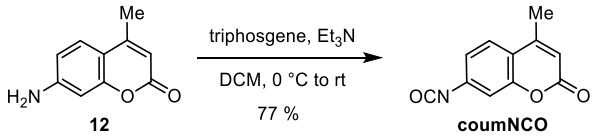

7-isocyanato-4-methyl-2H-chromen-2-one (coumNCO). A flame-dried round bottom flask equipped with a stir bar under nitrogen was charged with triphosgene (0.59 g, 2.0 mmol) and anhydrous DCM (30 mL). **CAUTION: TRIPHOSGENE IS TOXIC. ALL OPERATIONS ARE CARRIED OUT EXCLUSIVELY INSIDE A FUME HOOD.** The solution was cooled to 0 °C in an ice bath, followed by the addition of **12** (0.97 g, 5.5 mmol). Triethylamine (1.5 mL, 11 mmol) was added dropwise into the reaction. The reaction was allowed to warm to room temperature and stirred for 18 h. Hexane (30 mL) and DCM (60 mL) were added into the reaction mixture and the suspension was filtered to remove the pale yellow precipitate. The filtrate was washed with HCl (50 mL, 1 M), dried over $MgSO_4$, and filtered. The solid was discarded and the filtrate was concentrated under reduced pressure. The solid was dispersed in hexane (10 mL) and DCM (20 mL), filtered, and the filtrate was concentrated. The solid was dissolved in DCM (5 mL), and the solution was precipitated into hexane (30 mL). The fluffy white solid was collected by filtration and dried under reduced pressure to provide the title compound (0.85 g, 77%). ^{1}H NMR (400 MHz, $CDCl_3$) δ: 7.54 (dd, *J* = 8.0, 0.8 Hz, 1H), 7.09 – 6.99 (m, 2H), 6.26 (q, *J* = 1.3 Hz, 1H), 2.42 (d, *J* = 1.3 Hz, 3H) ppm. ^{13}C{^{1}H} NMR (100 MHz, $CDCl_3$) δ: 160.4, 154.4, 151.8, 136.9, 125.8, 125.7, 121.3, 118.0, 114.8, 113.1, 18.8 ppm. HRMS (ESI, *m/z*): calcd for $[C_{11}H_8NO_3]^+$ $(M+H)^+$, 202.0499; found, 202.0495.

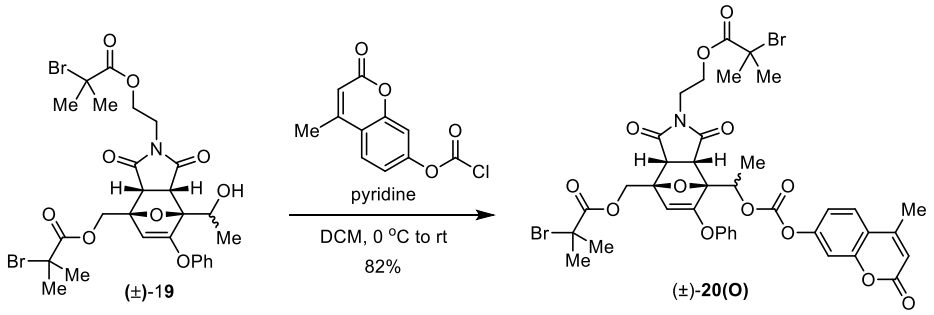

(2-(2-((2-bromo-2-methylpropanoyl)oxy)ethyl)-7-(1-((((4-methyl-2-oxo-2H-chromen-7-yl)oxy)carbonyl)oxy)ethyl)-1,3-dioxo-6-phenoxy-1,2,3,3a,7,7a-hexahydro-4H-4,7-epoxyisoindol-4-yl)methyl 2-bromo-2-methylpropanoate ((±)-20(O)). A two-

neck round bottom flask equipped with a stir bar was charged with (±)-**19** (20.4 mg, 0.0303 mmol)**,** dry pyridine (3.2 µL, 0.040 mmol), and DCM (0.5 mL). The solution was cooled to 0 °C in an ice bath followed by the dropwise addition of a solution of coumarin chloroformate (9.4 mg, 0.039 mmol) in 0.5 mL DCM. The reaction was allowed to warm slowly to room temperature and stirred for 20 h. The reaction mixture was washed with brine, dried over Na_2SO_4, filtered, and concentrated under reduced pressure. The crude product was purified by column chromatography (35–55% EtOAc/Hexanes) to afford the title compound as a white foamy solid (21.7 mg, 82%). ^{1}H NMR (400 MHz, $CDCl_3$) δ: 7.63 (d, J = 8.7 Hz, 1H), 7.39 – 7.32 (m, 2H), 7.28 (d, J = 2.3 Hz, 1H), 7.26 – 7.17 (m, 2H), 6.29 (q, J = 1.3 Hz, 1H), 5.66 (q, J = 6.5 Hz, 1H), 5.04 (s, 1H), 4.71 (ABq, $\Delta\nu_{AB}$ = 107.6 Hz, J_{AB} = 12.6 Hz, 2H), 4.34 – 4.12 (m, 2H), 3.89 (d, J = 7.9 Hz, 1H), 3.77 – 3.53 (m, 3H), 2.45 (d, J = 1.3 Hz, 3H), 1.96 (d, J = 2.2 Hz, 6H), 1.86 (d, J = 1.4 Hz, 6H), 1.72 (d, J = 6.6 Hz, 3H) ppm. ^{13}C{^{1}H} NMR (100 MHz, $CDCl_3$) δ: 173.7, 173.0, 171.5, 171.1, 162.5, 160.5, 154.6, 154.3, 153.3, 152.1, 151.9, 130.3, 126.3, 125.7, 119.7, 118.2, 117.5, 114.9, 110.0, 101.2, 90.3, 88.5, 72.5, 63.6, 62.4, 60.5, 55.7, 55.6, 51.4, 48.1, 37.6, 30.8, 30.7, 30.7, 21.2, 18.9, 15.8, 14.3 ppm. HRMS (ESI, *m/z*): calcd for $[C_{38}H_{37}Br_2NO_{13}]^+$ $(M)^+$, 873.0626; found, 873.0610.

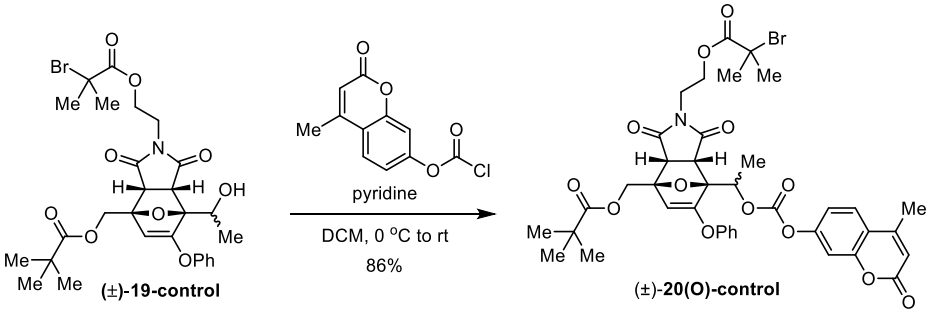

(2-(2-((2-bromo-2-methylpropanoyl)oxy)ethyl)-7-(1-((((4-methyl-2-oxo-2H-chromen-7-yl)oxy)carbonyl)oxy)ethyl)-1,3-dioxo-6-phenoxy-1,2,3,3a,7,7a-hexahydro-4H-4,7-epoxyisoindol-4-yl)methyl pivalate ((±)-20(O)-control). The title compound was prepared following a similar procedure as that for compound (±)-**20(O)**, with compound (±)-**19-control** (35.0 mg, 0.0576 mmol)**,** coumarin chloroformate (54.8 mg, 0.230 mmol), dry pyridine (18.6 µL, 0.230 mmol), and DCM (0.5 mL). The crude product was purified by column chromatography (35–55% EtOAc/Hexanes) to afford the title compound as a white foamy solid (43.4 mg, 86%). ^{1}H NMR (400 MHz, $CDCl_3$) δ: 7.63 (d, J = 8.7 Hz, 1H), 7.41 –

7.31 (m, 2H), 7.29 – 7.27 (m, 1H), 7.25 – 7.18 (m, 2H), 7.01 – 6.92 (m, 2H), 6.29 (d, J = 1.3 Hz, 1H), 5.65 (q, J = 6.5 Hz, 1H), 4.99 (s, 1H), 4.60 (ABq, $\Delta\nu_{AB}$ = 119.4 Hz, J_{AB} = 12.0 Hz, 2H), 4.34 – 4.24 (m, 1H), 4.23 – 4.11 (m, 1H), 3.89 (d, J = 7.8 Hz, 1H), 3.71 (ddd, J = 14.2, 6.7, 4.0 Hz, 1H), 3.66 – 3.57 (m, 2H), 2.45 (d, J = 1.3 Hz, 3H), 1.87 (s, 6H), 1.71 (d, J = 6.6 Hz, 3H), 1.23 (s, 9H). $^{13}C\{^{1}H\}$ NMR (100 MHz, $CDCl_3$) δ: 177.9, 173.8, 173.1, 171.6, 162.5, 160.5, 154.7, 154.3, 153.3, 152.2, 151.9, 130.3, 126.3, 125.7, 119.7, 118.2, 117.5, 114.9, 110.0, 101.4, 90.2, 88.8, 72.5, 62.4, 62.3, 55.7, 51.4, 48.1, 39.1, 37.6, 30.7, 30.7, 27.3, 18.9, 15.7 ppm. HRMS (FAB, *m/z*): calcd for $[C_{39}H_{41}BrNO_{13}]^+$ $(M+H)^+$, 810.1756; found, 810.1764.

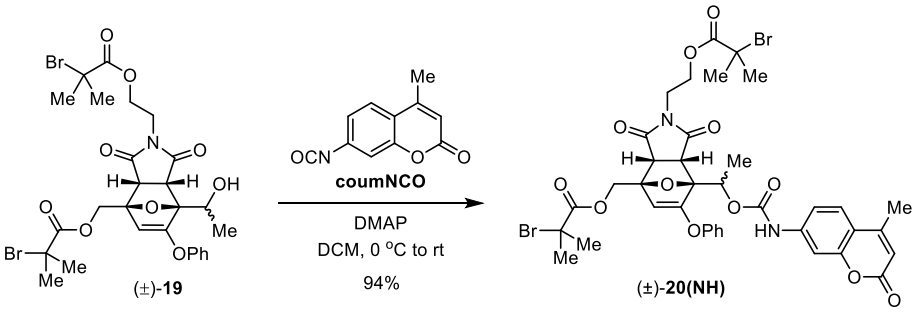

(2-(2-((2-bromo-2-methylpropanoyl)oxy)ethyl)-7-(1-(((4-methyl-2-oxo-2H-chromen-7-yl)carbamoyl)oxy)ethyl)-1,3-dioxo-6-phenoxy-1,2,3,3a,7,7a-hexahydro-4H-4,7-epoxyisoindol-4-yl)methyl 2-bromo-2-methylpropanoate ((±)-20(NH)). A two-neck round bottom flask equipped with a stir bar was charged with (±)-**19** (31.5 mg, 0.0468 mmol), **coumNCO** (36.0 mg, 0.179 mmol) and DCM (3 mL). The mixture was cooled to 0 °C in ice bath before adding DMAP (21.9 mg, 0.179 mmol). The reaction was allowed to warm to room temperature and its progress was monitored by ^{1}H NMR spectroscopy until completion (~2 h). The mixture was then washed with brine, dried over Na_2SO_4, filtered, and concentrated under reduced pressure. The crude produce was purified by column chromatography (35–55% EtOAc/Hexanes) to provide the title compound as a white foamy solid (38.5 mg, 94%). ^{1}H NMR (400 MHz, $CDCl_3$) δ: 7.57-7.50 (m, 1H), 7.48-7.41 (m, 2H), 7.39 – 7.30 (m, 2H), 7.25 – 7.17 (m, 2H), 7.01 – 6.92 (m, 2H), 6.20 (q, J = 1.2 Hz, 1H), 5.77 (q, J = 6.5 Hz, 1H), 5.02 (s, 1H), 4.70 (ABq, $\Delta\nu_{AB}$ = 99.8 Hz, J_{AB} = 12.6 Hz, 2H), 4.33-4.10 (m, 2H), 3.82 (d, J = 7.9 Hz, 1H), 3.76 – 3.53 (m, 3H), 2.41 (d, J = 1.3 Hz, 3H), 1.96 (s, 6H), 1.85 (s, 6H), 1.60 (d, J = 6.6 Hz, 3H) ppm. $^{13}C\{^{1}H\}$ NMR (100 MHz, $CDCl_3$) δ: 173.8,

173.0, 171.6, 171.1, 162.9, 161.1, 154.7, 154.6, 152.3, 151.9, 141.3, 130.3, 126.2, 125.6, 119.6, 115.8, 114.5, 113.5, 106.1, 100.8, 90.5, 88.5, 63.6, 62.4, 55.7, 55.6, 51.3, 48.1, 37.6, 30.8, 30.7, 30.7, 18.7, 16.1 ppm. HRMS (ESI, *m/z*): calcd for $[C_{38}H_{38}Br_2N_2O_{12}]^+$ $(M)^+$, 872.0786; found, 872.0792.

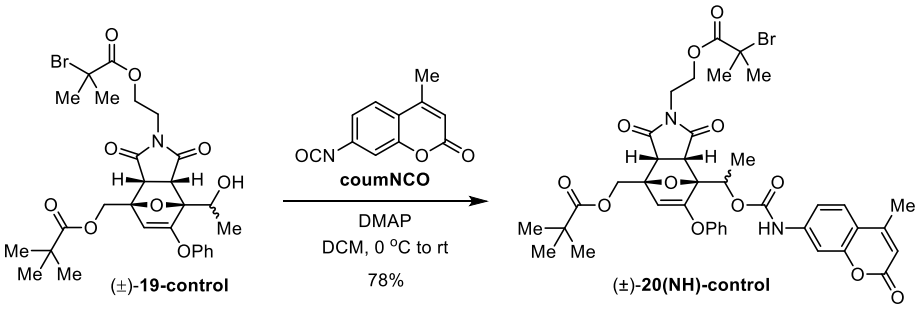

(2-(2-((2-bromo-2-methylpropanoyl)oxy)ethyl)-7-(1-(((4-methyl-2-oxo-2H-chromen-7-yl)carbamoyl)oxy)ethyl)-1,3-dioxo-6-phenoxy-1,2,3,3a,7,7a-hexahydro-4H-4,7-epoxyisoindol-4-yl)methyl pivalate ((±)-20(NH)-control). The title compound was prepared following a similar procedure as that for compound (±)-**20(NH)**, with compound (±)-**19-control** (24.4 mg, 0.0401 mmol)**, coumNCO** (16.0 mg, 0.0796 mmol), DMAP (9.8 mg, 0.080 mmol), and DCM (0.5 mL). The crude product was purified by column chromatography (35–55% EtOAc/Hexanes) to afford the title compound as a white foamy solid (25.1 mg, 78%). ^{1}H NMR (400 MHz, $CDCl_3$) δ: 7.50 – 7.37 (m, 4H), 7.31 – 7.22 (m, 2H), 7.17 – 7.08 (m, 1H), 6.93 – 6.84 (m, 2H), 6.12 (s, 1H), 5.70 (q, J = 6.5 Hz, 1H), 4.91 (s, 1H), 4.52 (ABq, $\Delta\nu_{AB}$ = 102.8 Hz, J_{AB} = 16.0 Hz, 2H), 4.25 – 4.15 (m, 1H), 4.14 – 4.02 (m, 1H), 3.77 (d, J = 7.8 Hz, 1H), 3.68 – 3.44 (m, 3H), 2.34 (d, J = 1.3 Hz, 3H), 1.78 (d, J = 1.3 Hz, 7H), 1.53 (d, J = 6.5 Hz, 3H), 1.15 (d, J = 1.5 Hz, 9H). ^{13}C{^{1}H} NMR (100 MHz, $CDCl_3$) δ: 177.9, 173.8, 173.1, 171.5, 162.8, 161.2, 154.7, 154.5, 152.4, 152.0, 141.5, 130.2, 130.1, 126.1, 125.5, 119.6, 115.7, 114.6, 113.3, 106.4, 101.0, 90.4, 88.8, 68.1, 62.4, 62.4, 55.8, 51.3, 48.1, 39.0, 37.6, 30.7, 30.7, 27.3, 18.7, 16.1.ppm. HRMS (ESI, *m/z*): calcd for $[C_{39}H_{42}BrN_2O_{12}]^+$ $(M+H)^+$, 809.1916; found, 809.1948.

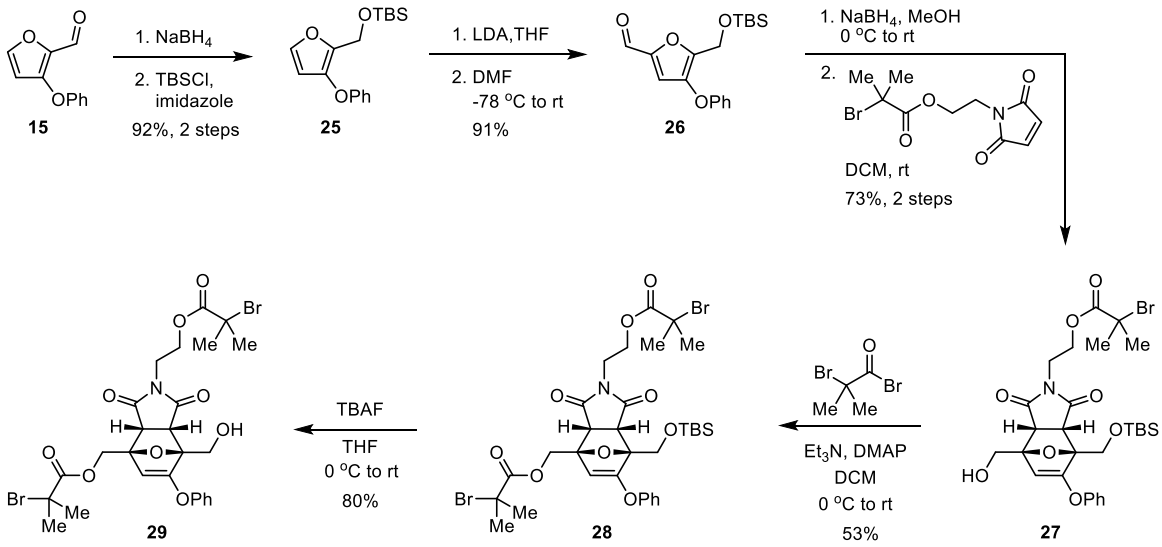

***Tert*-butyldimethyl((3-phenoxyfuran-2-yl)methoxy)silane (25).** A round bottom flask equipped with a stir bar was charged with MeOH (10 mL) and cooled to 0 °C in an ice bath before adding $NaBH_4$ (111 mg, 2.92 mmol), followed by the slow addition of **5** (303 mg, 1.61 mmol). The mixture was kept at 0 °C for 1 h before adding 10% NH_4Cl (50 mL), and extracted with EtOAc (2 x 50 mL). The organic layer was dried over Na_2SO_4, filtered, and concentrated under reduced pressure to yield (3-phenoxyfuran-2-yl)methanol as a light yellow oil (300 mg, 98%) which was used in the next step without further purification.

A round bottom flask equipped with a stir bar was charged with (3-phenoxyfuran-2-yl)methanol (300 mg, 1.58 mmol), imidazole (191 mg, 2.81 mmol), and DCM (10 mL), followed by addition of *tert*-butylchlorodimethylsilane (265 mg, 1.76 mmol). The reaction was allowed to stir at room temperature overnight before filtering the mixture through a cotton pad. The filtrate was concentrated under reduced pressure, and the crude product was purified by column chromatography (0–20% EtOAc/Hexanes) to yield the title compound as a light-yellow oil (447 mg, 92% over two steps). ^{1}H NMR (400 MHz, $CDCl_3$) δ: 7.34 – 7.26 (m, 3H), 7.08 – 6.97 (m, 3H), 6.22 (d, J = 2.1 Hz, 1H), 4.61 (s, 2H), 0.87 (s, 9H), 0.04 (s, 6H) ppm. $^{13}C\{^1H\}$ NMR (100 MHz, $CDCl_3$) δ: 158.3, 142.4, 141.4, 139.8, 129.7, 122.6, 116.4, 106.3, 54.7, 26.0, 18.6, −5.2 ppm. HRMS (EI, *m/z*): calcd for $[C_{17}H_{23}O_3Si]^+$ $(M-H)^+$, 303.1411; found, 303.1407.

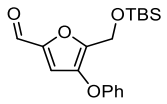

26

5-(((tert-butyldimethylsilyl)oxy)methyl)-4-phenoxyfuran-2-carbaldehyde (26). A flame-dried round bottom flask equipped with a stir bar was charged with diisopropylamine (0.30 mL, 2.1 mmol) and THF (10 mL). The solution was cooled to −78 °C in an acetone/dry ice bath before adding n-butyllithium (0.70 mL, 1.8 mmol, 2.5 M in hexanes) dropwise. After stirring the mixture for 5 mins, a solution of **25** (354 mg, 1.16 mmol) in THF (10 ml) was added dropwise at −78 °C. The mixture was kept at −78 °C for 30 mins before adding DMF (1.0 mL, 13 mmol) dropwise. The mixture was then allowed to slowly warm up to room temperature over an hour before 10% NH_4Cl (50 mL) was added slowly to quench the reaction. The mixture was extracted with Et_2O (2 x 50 mL), and the organic layer was dried over $MgSO_4$, filtered, and concentrated under reduced pressure. The crude product was purified by column chromatography (0–10% EtOAc/Hexanes) to yield the title compound as a light-yellow oil (351 mg, 91%). ^{1}H NMR (400 MHz, $CDCl_3$) δ: 9.59 (s, 1H), 7.39 – 7.29 (m, 2H), 7.15 – 7.06 (m, 1H), 7.05 – 6.97 (m, 3H), 4.70 (s, 2H), 0.88 (s, 9H), 0.07 (s, 6H) ppm. ^{13}C{^{1}H} NMR (100 MHz, $CDCl_3$) δ: 178.2, 157.3, 149.8, 148.3, 142.0, 129.8, 123.5, 116.7, 114.2, 54.9, 25.8, 18.4, -5.4 ppm. HRMS (ESI, *m/z*): calcd for $[C_{18}H_{25}O_4Si]^+$ $(M+H)^+$, 333.1517; found, 333.1543.

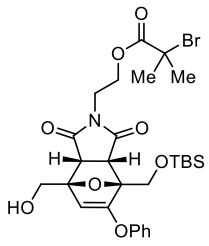

27

2-(4-(((tert-butyldimethylsilyl)oxy)methyl)-7-(hydroxymethyl)-1,3-dioxo-5-phenoxy-1,3,3a,4,7,7a-hexahydro-2H-4,7-epoxyisoindol-2-yl)ethyl 2-bromo-2-methylpropanoate (27). A round bottom flask equipped with a stir bar was charged with **26** (350 mg, 1.05 mmol), THF (4 mL), and MeOH (1 mL). The solution was cooled to 0 °C in an ice bath before slowly adding $NaBH_4$ (52.0 mg, 1.38 mmol). The mixture was kept at 0 °C for 1 h before adding 10% NH_4Cl (10 mL) and extracting with DCM (2 x 10 mL). The

organic layer was dried over Na_2SO_4 and filtered. Maleimide[2] was added to the solution, and then the mixture was concentrated under reduced pressure until about 2 mL viscous solution remaining. The mixture was then stirred at room temperature for 2 h to allow the Diels–Alder reaction to run to completion, and the crude mixture was purified by column chromatography (10–30% EtOAc/Hexanes). A single *endo* isomer of the title compound was isolated as a colorless oil (478 mg, 73%). ^{1}H NMR (400 MHz, $CDCl_3$) δ: 7.37 – 7.28 (m, 2H), 7.23 – 7.14 (m, 1H), 7.00 – 6.93 (m, 2H), 4.95 (s, 1H), 4.35 (ABq, $\Delta\nu_{AB}$ = 5.3 Hz, J_{AB} = 12.5 Hz, 2H), 4.30 – 3.98 (m, 4H), 3.86 (d, *J* = 7.8 Hz, 1H), 3.74 (m, 1H), 3.65 – 3.49 (m, 2H), 2.02 (t, *J* = 6.5 Hz, 1H), 1.87 (d, *J* = 2.4 Hz, 6H), 0.94 (s, 9H), 0.16 (d, *J* = 7.2 Hz, 6H) ppm. ^{13}C{^{1}H} NMR (100 MHz, $CDCl_3$) δ: 175.2, 174.0, 171.5, 163.3, 154.9, 130.1, 125.9, 119.9, 100.6, 90.6, 90.5, 62.6, 62.5, 59.7, 55.7, 50.8, 47.4, 37.4, 30.7, 30.7, 26.1, 18.7, -5.1, -5.2 ppm. HRMS (ESI, *m/z*): calcd for $[C_{28}H_{39}NO_8Si]^+$ $(M+H)^+$, 624.1623; found, 624.1642.

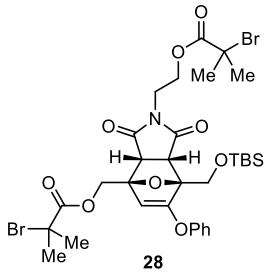

28

(2-(2-((2-bromo-2-methylpropanoyl)oxy)ethyl)-7-(((tert-butyldimethylsilyl)oxy)methyl)-1,3-dioxo-6-phenoxy-1,2,3,3a,7,7a-hexahydro-4H-4,7-epoxyisoindol-4-yl)methyl 2-bromo-2-methylpropanoate (28). A flame-dried round bottom flask equipped with a stir bar was charged with **27** (237 mg, 0.380 mmol), Et_3N (132 μL, 0.950 mmol) and DCM (10 mL). The solution was cooled to 0 °C before adding α-bromoisobutyryl bromide (0.11 mL mg, 0.89 mmol) dropwise. The reaction was then allowed to slowly warm to room temperature and stirred overnight until the reaction had completed, as determined by TLC. The reaction mixture was then diluted with DCM (10 mL), washed with NH_4Cl (25 mL) and brine (20 mL), and the organic fraction was dried over Na_2SO_4, filtered, and concentrated under reduced pressure. The crude product was purified by column chromatography (10–30% EtOAc/hexanes) to yield the title compound as a viscus colorless oil (155 mg, 53% yield). ^{1}H NMR (400 MHz, $CDCl_3$) δ: 7.36 – 7.29 (m, 2H), 7.21 – 7.15 (m, 1H), 6.99 – 6.92 (m, 2H), 4.92 (s, 1H), 4.67 (ABq, $\Delta\nu_{AB}$ = 124.7Hz,

J_{AB} = 12.5 Hz, 2H), 4.34 (ABq, $\Delta\nu_{AB}$ = 11.9 Hz, J_{AB} = 12.4 Hz, 2H), 4.30-4.10 (m, , 2H), 3.85 (d, *J* = 7.8 Hz, 1H), 3.78-3.68 (m, 1H), 3.63 (d, *J* = 7.8 Hz, 1H), 3.60-3.52 (m, 1H), 1.95 (d, *J* = 4.0 Hz, 6H), 1.87 (d, *J* = 1.9 Hz, 6H), 0.93 (s, 9H), 0.14 (d, *J* = 9.4 Hz, 6H) ppm. $^{13}C\{^1H\}$ NMR (100 MHz, $CDCl_3$) δ: 174.4, 173.8, 171.5, 171.2, 163.5, 154.9, 130.1, 126.0, 119.8, 100.4, 90.5, 88.3, 63.8, 62.6, 59.6, 55.7, 55.6, 50.9, 47.1, 37.4, 30.9, 30.8, 30.7, 30.7, 26.0, 18.6, -5.1, -5.2 ppm. HRMS (ESI, *m/z*): calcd for $[C_{32}H_{44}Br_2NO_9Si]^+$ $(M+H)^+$, 772.1147; found, 772.1168.

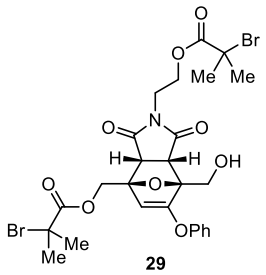

29

(2-(2-((2-bromo-2-methylpropanoyl)oxy)ethyl)-7-(hydroxymethyl)-1,3-dioxo-6-phenoxy-1,2,3,3a,7,7a-hexahydro-4H-4,7-epoxyisoindol-4-yl)methyl 2-bromo-2-methylpropanoate (29). A flame-dried round bottom flask equipped with a stir bar was charged with **28** (155 mg, 0.200 mmol) and THF (3 mL). The solution was cooled to 0 °C before adding TBAF (1 M in THF, 0.26 mL, 0.26 mmol) dropwise. The mixture was allowed to slowly warm up room temperature and stirred for 1 h. The reaction mixture was washed with NH_4Cl (10 mL), extracted with EtOAc (10 mL), washed with brine (10 mL), and the organic fraction was dried over Na_2SO_4, filtered, and concentrated under reduced pressure. The crude product was purified by column chromatography (40–65% EtOAc/hexanes) to yield the title compound as a white foamy solid (105 mg, 80% yield). ^1H NMR (400 MHz, $CDCl_3$) δ: 7.38 – 7.30 (m, 2H), 7.23 – 7.14 (m, 1H), 7.01 – 6.94 (m, 2H), 4.97 (s, 1H), 4.69 (ABq, $\Delta\nu_{AB}$ = 113.7 Hz, J_{AB} = 12.6 Hz, 2H), 4.44 (d, *J* = 13.1 Hz, 1H), 4.35 – 4.22 (m, 2H), 4.2-4.12 (m, 1H), 3.81 – 3.63 (m, 3H), 3.57 (m, 1H), 1.96 (d, *J* = 4.2 Hz, 6H), 1.86 (s, 6H) ppm. $^{13}C\{^1H\}$ NMR (100 MHz, $CDCl_3$) δ: 174.0, 173.4, 171.4, 171.1, 163.1, 154.7, 130.0, 126.0, 119.7, 100.6, 90.0, 88.6, 63.4, 62.3, 59.6, 55.5, 55.5, 50.7, 47.8, 37.4, 30.7, 30.6 ppm. HRMS (ESI, *m/z*): calcd for $[C_{26}H_{30}Br_2NO_9]^+$ $(M+H)^+$, 658.0281; found, 658.0287.

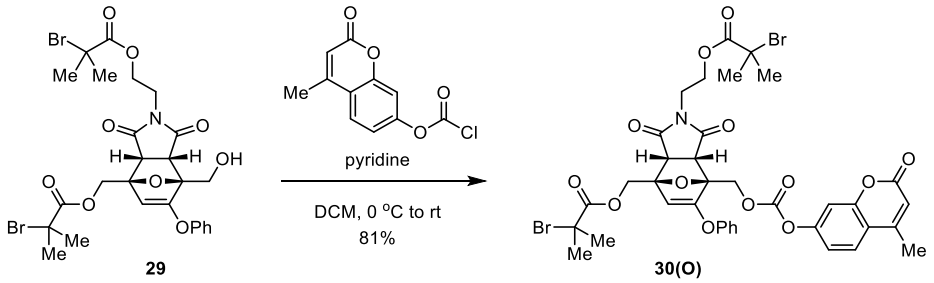

(2-(2-((2-bromo-2-methylpropanoyl)oxy)ethyl)-7-(((((4-methyl-2-oxo-2H-chromen-7-yl)oxy)carbonyl)oxy)methyl)-1,3-dioxo-6-phenoxy-1,2,3,3a,7,7a-hexahydro-4H-4,7-epoxyisoindol-4-yl)methyl 2-bromo-2-methylpropanoate (30(O)). The title compound was prepared following the same procedure as that for compound (±)-**20(O)**, with compound **29** (20 mg, 0.030 mmol), dry pyridine (3.2 μL, 0.040 mmol), coumarin chloroformate (9.4 mg, 0.039 mmol) and DCM (5 mL). The crude product was purified by column chromatography (20–50% EtOAc/hexanes) to provide the title compound as a white foamy solid (21 mg, 81%). ^{1}H NMR (400 MHz, $CDCl_3$) δ: 7.62 (d, J = 8.7 Hz, 1H), 7.36 (dd, J = 8.4, 7.4 Hz, 2H), 7.25 – 7.16 (m, 3H), 7.04 – 6.95 (m, 2H), 6.3-6.26 (m, 1H), 5.04 (s, 1H), 5.01 (ABq, $\Delta\nu_{AB}$ = 75.3 Hz, J_{AB} = 12.6 Hz, 2H), 4.71 (ABq, $\Delta\nu_{AB}$ = 110.7 Hz, J_{AB} = 12.7 Hz, 2H), 4.35-4.25 (m, 1H), 4.23-4.11 (m, 1H), 3.86 – 3.68 (m, 3H), 3.66-3.55 (m, 1H), 2.43 (d, J = 1.2 Hz, 3H), 1.96 (d, J = 3.8 Hz, 6H), 1.87 (d, J = 1.2 Hz, 6H) ppm. ^{13}C{^{1}H} NMR (100 MHz, $CDCl_3$) δ: 173.7, 172.9, 171.5, 171.2, 162.2, 160.5, 154.7, 154.3, 153.2, 152.5, 151.9, 130.3, 126.3, 125.7, 119.7, 118.3, 117.5, 114.9, 110.1, 100.8, 89.1, 87.2, 64.5, 63.4, 62.4, 55.7, 55.5, 50.7, 48.5, 37.6, 30.8, 30.7, 18.9 ppm. HRMS (ESI, *m/z*): calcd for $[C_{37}H_{36}Br_2NO_{13}]^+$ $(M+H)^+$, 860.0548; found, 860.0553.

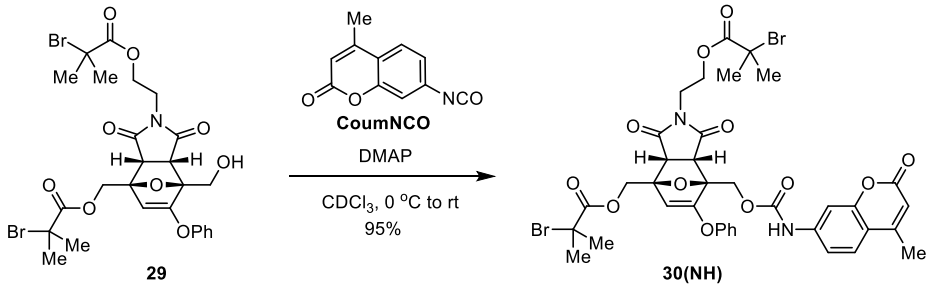

(2-(2-((2-bromo-2-methylpropanoyl)oxy)ethyl)-7-((((4-methyl-2-oxo-2H-chromen-7-yl)carbamoyl)oxy)methyl)-1,3-dioxo-6-phenoxy-1,2,3,3a,7,7a-hexahydro-4H-4,7-epoxyisoindol-4-yl)methyl 2-bromo-2-methylpropanoate (30(NH)). The title

compound was prepared following the same procedure as that for compound (±)-**20(NH)**, with compound **29** (40 mg, 0.061 mmol), DMAP (1.0 mg, 0.0082 mmol), **coumNCO** (18 mg, 0.089 mmol) and $CDCl_3$ (3 mL). The crude produce was purified by column chromatography (20–40% Et_2O in 1:1 Hexanes/DCM) to provide the title compound as a white foamy solid (50 mg, 95%). ^{1}H NMR (400 MHz, $CDCl_3$) δ: 7.53 (d, J = 8.6 Hz, 1H), 7.50 – 7.38 (m, 2H), 7.38 – 7.30 (m, 2H), 7.23 – 7.17 (m, 1H), 7.14 (s, 1H), 7.03-6.95 (m, 2H), 6.22-6.16 (m, 1H), 5.03 (s, 1H), 4.95 (ABq, $\Delta\nu_{AB}$ = 59.3 Hz, J_{AB} = 12.7 Hz, 2H), 4.70 (ABq, $\Delta\nu_{AB}$ = 108.0 Hz, J_{AB} = 12.7 Hz, 2H), 4.34-4.11 (m, 2H), 3.80 – 3.67 (m, 3H), 3.64-3.54 (m, 1H), 2.41 (d, J = 1.3 Hz, 3H), 1.95 (d, J = 3.6 Hz, 6H), 1.86 (d, J = 0.8 Hz, 6H) ppm. ^{13}C{^{1}H} NMR (100 MHz, $CDCl_3$) δ: 173.8, 172.9, 171.6, 171.2, 162.5, 161.1, 154.7, 154.6, 152.3, 152.2, 141.1, 130.2, 126.2, 125.6, 119.6, 115.9, 114.6, 113.5, 106.3, 100.7, 88.9, 87.7, 63.5, 62.4, 61.5, 55.7, 55.6, 50.7, 48.9, 37.6, 30.8, 30.7, 18.7 ppm. HRMS (ESI, *m/z*): calcd for $[C_{37}H_{37}Br_2N_2O_{12}]^+$ $(M+H)^+$, 859.0708; found, 859.0704.

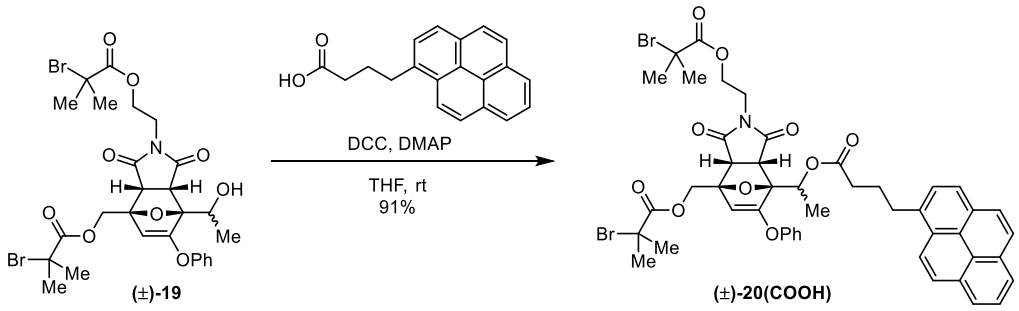

1-(2-(2-((2-bromo-2-methylpropanoyl)oxy)ethyl)-7-(((2-bromo-2-methylpropanoyl)oxy)methyl)-1,3-dioxo-5-phenoxy-1,2,3,3a,7,7a-hexahydro-4H-4,7-epoxyisoindol-4-yl)ethyl 4-(pyren-4-yl)butanoate ((±)-20(COOH)). A 2 dram vial equipped with a stir bar was charged with (±)-**19** (34.0 mg, 0.0505 mmol), DMAP (1.5 mg, 0.012 mmol), 1-pyrenebutanoic acid (16 mg, 0.056 mmol) and THF (0.5 mL). N,N′-Dicyclohexylcarbodiimide (11.5 mg, 0.0558 mmol) was then added to the reaction mixture slowly. The reaction was stirred at room temperature overnight until the reaction completed, as determined by ^{1}H NMR spectroscopy. The reaction mixture was filtered and then diluted with Et_2O (15 mL), washed with NH_4Cl (15 mL) and brine (15 mL), and the organic fraction was dried over Na_2SO_4, filtered, and concentrated under reduced pressure. The crude product was purified by column chromatography (20–40% EtOAc/hexanes) to yield the title

compound as a white foamy solid (43.6 mg, 91% yield). ^{1}H NMR (400 MHz, $CDCl_3$) δ: 8.35 – 8.28 (m, 1H), 8.21 – 8.14 (m, 2H), 8.14 – 8.08 (m, 2H), 8.05 – 8.02 (m, 2H), 8.02 – 7.97 (m, 1H), 7.91 – 7.85 (m, 1H), 7.35 – 7.28 (m, 2H), 7.20 – 7.14 (m, 1H), 6.97 – 6.91 (m, 2H), 5.77 (q, J = 6.5 Hz, 1H), 4.98 (s, 1H), 4.66 (ABq, $\Delta\nu_{AB}$ = 119.3 Hz, J_{AB} = 12.6 Hz, 2H), 4.28-4.07 (m, 2H), 3.73 – 3.62 (m, 2H), 3.62 – 3.50 (m, 2H), 3.44 (t, J = 7.7 Hz, 2H), 2.56 (t, J = 7.3 Hz, 2H), 2.32 – 2.20 (m, 2H), 1.90 (d, J = 4.2 Hz, 6H), 1.79 (d, J = 4.0 Hz, 6H), 1.55 (d, J = 6.6 Hz, 3H) ppm. ^{13}C{^{1}H} NMR (100 MHz, $CDCl_3$) δ: 173.8, 172.9, 172.4, 171.5, 171.1, 162.9, 154.7, 135.7, 131.5, 131.0, 130.2, 130.2, 128.9, 127.6, 127.6, 126.9, 126.1, 126.0, 125.2, 125.1, 125.1, 125.0, 124.9, 123.5, 119.7, 100.9, 90.8, 88.3, 66.8, 63.7, 62.4, 55.7, 55.6, 51.4, 47.9, 37.5, 34.1, 32.9, 30.8, 30.7, 30.6, 27.0, 16.0 ppm. HRMS (ESI, *m/z*): calcd for $[C_{47}H_{46}Br_2NO_{10}]^+$ $(M+H)^+$, 942.1483; found, 942.1509.

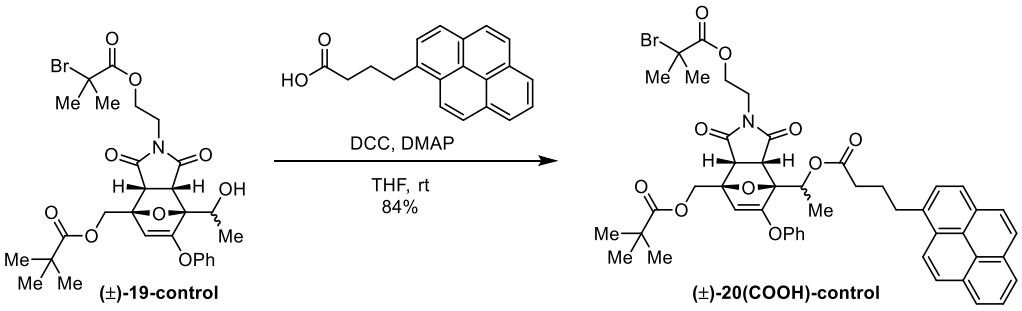

1-(2-(2-((2-bromo-2-methylpropanoyl)oxy)ethyl)-1,3-dioxo-5-phenoxy-7-((pivaloyloxy)methyl)-1,2,3,3a,7,7a-hexahydro-4H-4,7-epoxyisoindol-4-yl)ethyl 4-(pyren-1-yl)butanoate ((±)-20(COOH)-control). The title compound was prepared following a similar procedure as that for compound (±)-**20(COOH)**, with compound (±)-**19-control** (23.0 mg, 0.0378 mmol)**,** 1-pyrenebutanoic acid (21.8 mg, 0.0757 mmol), N,N′-dicyclohexylcarbodiimide (15.6 mg, 0.0757 mmol), DMAP (2.3 mg, 0.019 mmol), and THF (0.5 mL). Column chromatography (10–25% EtOAc/Hexanes) followed by preparative thin layer chromatography (4:1 toluene/acetone) afforded the title compound as a white foamy solid (28 mg, 84%). ^{1}H NMR (500 MHz, $CDCl_3$) δ: 8.34 – 8.29 (m, 1H), 8.19 – 8.14 (m, 2H), 8.14 – 8.08 (m, 2H), 8.06 – 8.02 (m, 2H), 8.02 – 7.96 (m, 1H), 7.89 – 7.86 (m, 1H), 7.35 – 7.28 (m, 2H), 7.21 – 7.14 (m, 1H), 6.95 – 6.90 (m, 2H), 5.78 (q, J = 6.5 Hz, 1H), 4.93 (s, 1H), 4.57 (ABq, $\Delta\nu_{AB}$ = 166.4 Hz, J_{AB} = 12.7 Hz, 2H), 4.28-4.10 (m, 2H), 3.74 – 3.61 (m, 2H), 3.61 – 3.47 (m, 2H), 3.44 (t, J = 7.7 Hz, 2H), 2.57 (t, J = 7.3 Hz, 2H), 2.32 – 2.20 (m,

2H), 1.80 (d, *J* = 6.0 Hz, 6H), 1.56 (d, *J* = 6.6 Hz, 3H), 1.18 (s, 9H) ppm. $^{13}C\{^{1}H\}$ NMR (100 MHz, $CDCl_3$) δ: 177.8, 173.9, 172.9, 172.4, 171.5, 162.8, 154.7, 135.7, 131.5, 131.0, 130.2, 130.1, 128.9, 127.6, 127.6, 126.9, 126.1, 126.0, 126.0, 125.2, 125.1, 125.1, 125.0, 124.9, 123.5, 119.7, 119.6, 101.1, 90.7, 88.6, 66.8, 62.5, 62.4, 55.7, 51.4, 48.0, 39.0, 37.4, 34.1, 32.9, 30.6, 30.6, 27.3, 27.2, 27.0, 16.0 ppm. HRMS (ESI, *m/z*): calcd for $[C_{48}H_{49}BrNO_{10}]^+$ $(M+H)^+$, 878.2534; found, 878.2541.

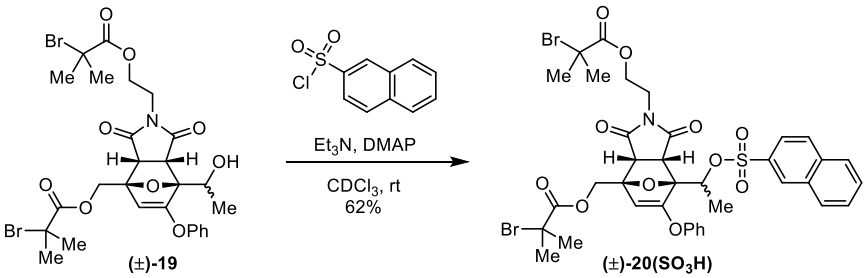

(2-(2-((2-bromo-2-methylpropanoyl)oxy)ethyl)-7-(1-((naphthalen-2-ylsulfonyl)oxy)ethyl)-1,3-dioxo-6-phenoxy-1,2,3,3a,7,7a-hexahydro-4H-4,7-epoxyisoindol-4-yl)methyl 2-bromo-2-methylpropanoate ((±)-20(SO_3H)). A 2 dram vial equipped with a stir bar was charged with (±)-**19** (22 mg, 0.033 mmol), DMAP (4.2 mg, 0.035 mmol) and $CDCl_3$ (0.3 mL). Naphthalene-2-sulfonyl chloride (7.8 mg, 0.034 mmol) dissolved in $CDCl_3$ (0.2 mL) was then added to the reaction mixture slowly. The solution was then stirred at room temperature until the reaction completed, as determined by ^{1}H NMR spectroscopy (~2 h). The reaction mixture was then diluted with DCM (10 mL), washed with NH_4Cl (15 mL) and brine (15 mL), and the organic fraction was dried over Na_2SO_4, filtered, and concentrated under reduced pressure. The crude product was purified by column chromatography (20–40% EtOAc/hexanes) to yield the title compound as a white foamy solid (17.6 mg, 62% yield). ^{1}H NMR (400 MHz, $CDCl_3$) δ: 8.62 (d, *J* = 1.8 Hz, 1H), 8.07 – 7.99 (m, 2H), 7.99 – 7.92 (m, 2H), 7.60-7.73 (m, 2H), 7.38 – 7.29 (m, 2H), 7.22 – 7.15 (m, 1H), 6.96 – 6.89 (m, 2H), 5.55 (q, *J* = 6.6 Hz, 1H), 4.94 (s, 1H), 4.60 (ABq, $\Delta\nu_{AB}$ = 107.3 Hz, J_{AB} = 12.6 Hz, 2H), 4.21 – 4.04 (m, 2H), 3.75 (d, *J* = 7.9 Hz, 1H), 3.68 – 3.49 (m, 3H), 1.92 (d, *J* = 4.6 Hz, 6H), 1.84 (d, *J* = 1.6 Hz, 6H), 1.57 (d, *J* = 6.6 Hz, 3H) ppm. $^{13}C\{^{1}H\}$ NMR (100 MHz, $CDCl_3$) δ: 173.6, 172.7, 171.4, 171.1, 162.4, 154.5, 135.5, 133.8, 132.1, 130.2, 130.0, 129.9, 129.6, 129.6, 128.2, 128.0, 126.3, 122.7, 119.6, 101.1, 90.4, 88.4, 75.2,

63.5, 62.3, 55.7, 55.5, 51.3, 47.9, 37.4, 30.8, 30.7, 30.7, 17.2 ppm. HRMS (ESI, *m/z*): calcd for $[C_{37}H_{38}Br_2NO_{11}S]^+$ $(M+H)^+$, 862.0527; found, 862.0546.

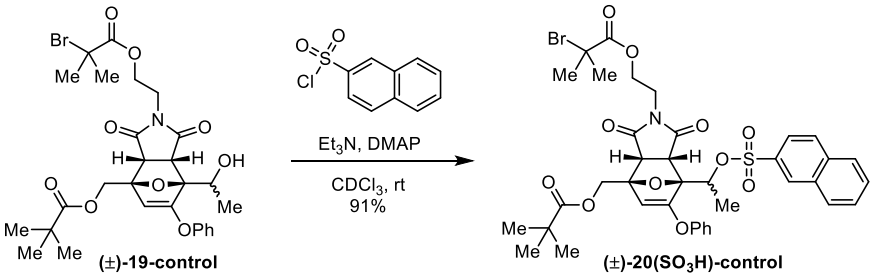

(2-(2-((2-bromo-2-methylpropanoyl)oxy)ethyl)-7-(1-((naphthalen-2-ylsulfonyl)oxy)ethyl)-1,3-dioxo-6-phenoxy-1,2,3,3a,7,7a-hexahydro-4H-4,7-epoxyisoindol-4-yl)methyl pivalate ((±)-20(SO$_3$H)-control). The title compound was prepared following the same procedure as that for compound (±)-**20(SO$_3$H)**, with compound (±)-**19-control** (20 mg, 0.033 mmol), DMAP (6.3 mg, 0.052 mmol), naphthalene-2-sulfonyl chloride (11.7 mg, 0.052 mmol, and $CDCl_3$ (0.5 mL). Column chromatography (25–45% EtOAc/Hexanes) afforded the title compound as a white foamy solid (24 mg, 91%). ^{1}H NMR (400 MHz, $CDCl_3$) δ: 8.62 (d, J = 1.8 Hz, 1H), 8.05 –7.91 (m, 4H), 7.72 – 7.61 (m, 2H), 7.38 – 7.28 (m, 2H), 7.23 – 7.16 (m, 1H), 6.95 – 6.88 (m, 2H), 5.56 (q, J = 6.5 Hz, 1H), 4.89 (s, 1H), 4.50 (ABq, $\Delta\nu_{AB}$ = 122.8 Hz, J_{AB} = 12.7 Hz, 2H), 4.22 – 4.06 (m, 2H), 3.75 (d, J = 7.9 Hz, 1H), 3.68 – 3.46 (m, 3H), 1.85 (s, 6H), 1.63 – 1.52 (m, 3H), 1.19 (s, 9H) ppm. ^{13}C{^{1}H} NMR (100 MHz, $CDCl_3$) δ: 177.8, 173.7, 172.8, 171.4, 162.4, 154.6, 135.5, 133.8, 132.1, 130.2, 130.0, 129.8, 129.6, 129. 6, 128.1, 127.9, 126.2, 122.7, 119.6, 101.2, 90.3, 88.7, 75.2, 62.3, 62.2, 55.7, 51.2, 48.0, 39.0, 37.4, 30.7, 30.6, 27.3, 27.2, 17.2 ppm. HRMS (ESI, *m/z*): calcd for $[C_{38}H_{40}BrNO_{11}SNa]^+$ $(M+Na)^+$, 820.1398; found, 820.1392.

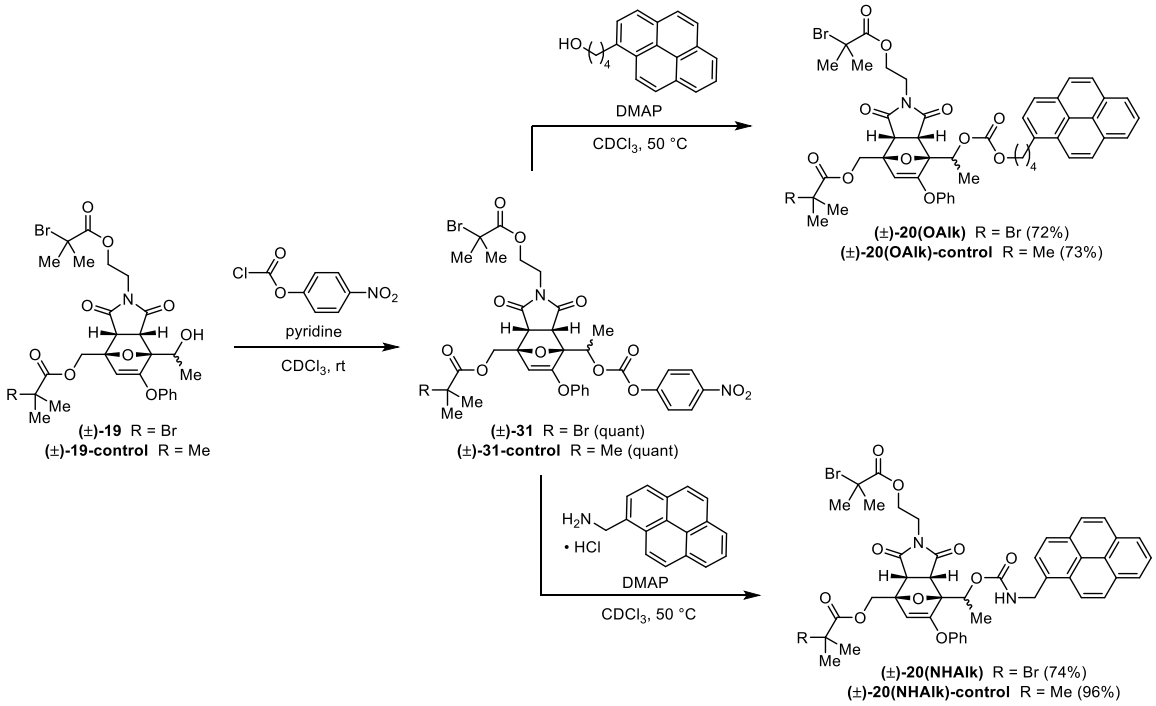

(2-(2-((2-bromo-2-methylpropanoyl)oxy)ethyl)-7-(1-(((4-nitrophenoxy)carbonyl)oxy)ethyl)-1,3-dioxo-6-phenoxy-1,2,3,3a,7,7a-hexahydro-4H-4,7-epoxyisoindol-4-yl)methyl 2-bromo-2-methylpropanoate ((±)-31). A 2 dram vial equipped with a stir bar was charged with (±)-**19** (101 mg, 0.150 mmol), pyridine (14.6 μL, 0.181 mmol) and $CDCl_3$ (1 mL). 4-nitrophenyl chloroformate (33.3 mg, 0.166 mmol) dissolved in $CDCl_3$ was then added to the reaction mixture slowly. The reaction was then stirred at room temperature until the reaction had completed, as determined by ^{1}H NMR spectroscopy (~2 h). The reaction mixture was then diluted with DCM (20 mL), washed with NH_4Cl (25 mL) and brine (25 mL), and the organic fraction was dried over Na_2SO_4, filtered, and concentrated under reduced pressure. The crude product was purified by column chromatography (20–45% EtOAc/Hexanes) to yield the title compound as a white foamy solid (125 mg, quant). ^{1}H NMR (400 MHz, $CDCl_3$) δ: 8.34 – 8.26 (m, 2H), 7.49 – 7.41 (m, 2H), 7.36 (dd, J = 8.5, 7.3 Hz, 2H), 7.21 (t, J = 7.5 Hz, 1H), 7.01 – 6.94 (m, 2H), 5.66 (q, J = 6.5 Hz, 1H), 5.03 (s, 1H), 4.71 (ABq, $\Delta\nu_{AB}$ = 106.7 Hz, J_{AB} = 12.6 Hz, 2H), 4.34 – 4.12 (m, 2H), 3.87 (d, J = 7.8 Hz, 1H), 3.78 – 3.54 (m, 3H), 1.96 (d, J = 2.0 Hz, 6H), 1.86 (d, J = 1.2 Hz, 6H), 1.72 (d, J = 6.5 Hz, 3H) ppm. ^{13}C{^{1}H} NMR (100 MHz, $CDCl_3$) δ: 173.7, 172.9, 171.5, 171.1, 162.5, 155.6, 154.6, 151.8, 145.6, 130.3, 126.3, 125.5, 121.9, 119.7,

101.2, 90.3, 88.5, 72.9, 63.5, 62.4, 55.7, 55.5, 51.4, 48.1, 37.6, 30.8, 30.7, 30.7, 15.7 ppm. HRMS (ESI, *m/z*): calcd for $[C_{34}H_{34}Br_2N_2O_{13}Na]^+$ $(M+Na)^+$, 859.0320; found, 859.0325.

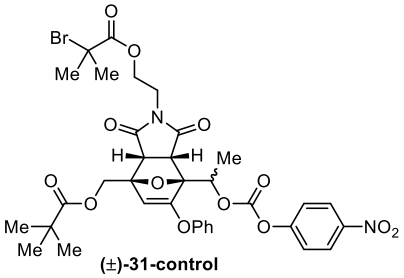

(±)-31-control

(2-(2-((2-bromo-2-methylpropanoyl)oxy)ethyl)-7-(1-(((4-nitrophenoxy)carbonyl)oxy)ethyl)-1,3-dioxo-6-phenoxy-1,2,3,3a,7,7a-hexahydro-4H-4,7-epoxyisoindol-4-yl)methyl pivalate ((±)-31-control). The title compound was prepared following a similar procedure as that for compound (±)-**31**, with compound (±)-**19-control** (75.0 mg, 0.123 mmol)**,** pyridine (12.0 μL, 0.149 mmol), 4-nitrophenyl chloroformate (27.3 mg, 0.136 mmol), and $CDCl_3$ (0.7 mL). Column chromatography (20–45% EtOAc/hexanes) afforded the title compound as a white foamy solid (94.5 mg, quant). ^{1}H NMR (500 MHz, $CDCl_3$) δ: 8.33 – 8.27 (m, 2H), 7.48 – 7.42 (m, 2H), 7.40 – 7.32 (m, 2H), 7.25 – 7.18 (m, 1H), 6.99 – 6.93 (m, 2H), 5.66 (q, J = 6.5 Hz, 1H), 4.99 (s, 1H), 4.61 (ABq, $\Delta\nu_{AB}$ = 151.1 Hz, J_{AB} = 12.8 Hz, 2H), 4.34 – 4.14 (m, 2H), 3.87 (d, J = 7.9 Hz, 1H), 3.75 – 3.58 (m, 3H), 1.87 (s, 6H), 1.72 (d, J = 6.5 Hz, 3H), 1.23 (s, 9H) ppm. ^{13}C{^{1}H} NMR (100 MHz, $CDCl_3$) δ: 177.8, 173.7, 173.0, 171.6, 162.5, 155.6, 154.7, 151.9, 145.6, 130.3, 126.3, 125.5, 121.9, 119.7, 101.4, 90.1, 88.8, 72.8, 62.4, 62.2, 55.7, 51.4, 48.2, 39.1, 37.6, 30.7, 27.3, 15.7 ppm. HRMS (ESI, *m/z*): calcd for $[C_{35}H_{37}BrN_2O_{13}Na]^+$ $(M+Na)^+$, 795.1371; found, 795.1377.

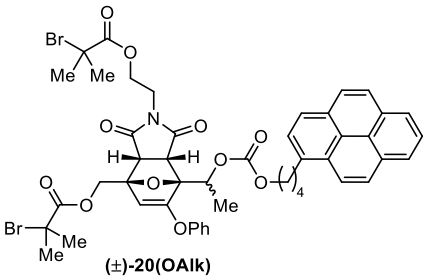

(±)-20(OAlk)

(2-(2-((2-bromo-2-methylpropanoyl)oxy)ethyl)-1,3-dioxo-6-phenoxy-7-(1-(((4-(pyren-1-yl)butoxy)carbonyl)oxy)ethyl)-1,2,3,3a,7,7a-hexahydro-4H-4,7-

epoxyisoindol-4-yl)methyl 2-bromo-2-methylpropanoate ((±)-20(OAlk)). A 2 dram vial equipped with a stir bar was charged with (±)-**31** (21.7 mg, 0.0259 mmol), DMAP (3.5 mg, 0.029 mmol) and $CDCl_3$ (0.5 mL), followed by the addition of 1-pyrenebutanol (7.8 mg, 0.028 mmol) dissolved in $CDCl_3$ (0.2 mL). The reaction was stirred at 50 °C overnight until the reaction had completed, as determined by ^{1}H NMR spectroscopy. The reaction mixture was then diluted with DCM (15 mL), washed with NH_4Cl (15 mL) and brine (15 mL), and the organic fraction was dried over Na_2SO_4, filtered, and concentrated under reduced pressure. The crude product was purified by column chromatography (35–50% EtOAc/hexanes) to yield the title compound as a white foamy solid (18 mg, 72% yield). ^{1}H NMR (400 MHz, $CDCl_3$) δ: 8.30 – 7.85 (m, 9H), 7.39 – 7.29 (m, 2H), 7.21 – 7.13 (m, 1H), 7.01 – 6.91 (m, 2H), 5.57 (q, J = 6.5 Hz, 1H), 4.99 (s, 1H), 4.66 (ABq, $\Delta\nu_{AB}$ =109.8 Hz, J_{AB} = 12.6 Hz, 2H), 4.36 – 4.17 (m, 3H), 4.16 – 4.08 (m, 1H), 3.81 (d, J = 7.9 Hz, 1H), 3.70 – 3.51 (m, 3H), 3.40 (t, J = 7.5 Hz, 2H), 2.13 – 1.85 (m, 10H), 1.82 (s, 6H), 1.58 (d, J = 6.5, 3H) ppm. ^{13}C{^{1}H} NMR (100 MHz, $CDCl_3$) δ: 173.7, 172.9, 171.4, 171.0, 162.5, 154.6, 154.5, 136.2, 131.4, 130.9, 130.1, 129.9, 128.6, 127.5, 127.4, 127.3, 126.7, 126.0, 125.9, 125.1, 125.0, 124.9, 124.8, 124.8, 123.3, 119.5, 101.0, 90.5, 88.2, 70.3, 68.3, 63.6, 62.3, 55.5, 55.5, 51.3, 47.7, 37.3, 33.0, 30.7, 30.6, 30.5, 28.7, 27.9, 15.8 ppm. HRMS (ESI, *m/z*): calcd for $[C_{48}H_{48}Br_2NO_{11}]^+$ $(M+H)^+$, 972.1589; found, 972.1597.

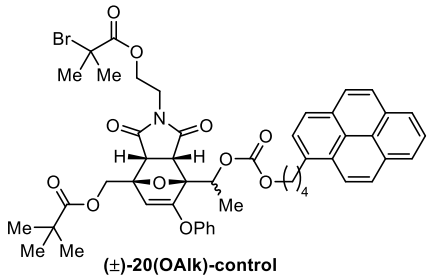

(±)-20(OAlk)-control

(2-(2-((2-bromo-2-methylpropanoyl)oxy)ethyl)-1,3-dioxo-6-phenoxy-7-(1-(((4-(pyren-1-yl)butoxy)carbonyl)oxy)ethyl)-1,2,3,3a,7,7a-hexahydro-4H-4,7-epoxyisoindol-4-yl)methyl pivalate ((±)-20(OAlk)-control). The title compound was prepared following a similar procedure as that for compound (±)-**20(OAlk)**, with compound (±)-**31-control** (30.0 mg, 0.0388 mmol)**,** DMAP (9.5 mg, 0.078 mmol), 1-pyrenebutanol (21.3 mg, 0.777 mmol), and $CDCl_3$ (0.5 mL). Column chromatography (20–50% EtOAc/Hexanes) afforded the title compound as a white foamy solid (25.9 mg, 73%). ^{1}H

NMR (400 MHz, $CDCl_3$) δ: 8.30 – 7.85 (m, 9H), 7.37 – 7.29 (m, 2H), 7.22 – 7.15 (m, 1H), 7.00 – 6.91 (m, 2H), 5.56 (q, J = 6.5 Hz, 1H), 4.94 (s, 1H), 4.56 (ABq, $\Delta\nu_{AB}$ = 123.5 Hz, J_{AB} = 12.7 Hz, 2H), 4.34 – 4.19 (m, 3H), 4.17 – 4.08 (m, 1H), 3.80 (d, J = 7.9 Hz, 1H), 3.70 – 3.49 (m, 3H), 3.40 (t, J = 7.5 Hz, 2H), 2.15 – 1.73 (m, 10H), 1.58 (d, J = 6.5 Hz, 3H), 1.20 (s, 9H) ppm. $^{13}C\{^1H\}$ NMR (125 MHz, $CDCl_3$) δ: 177.9, 173.9, 173.1, 171.5, 162.6, 154.7, 136.3, 131.6, 131.0, 130.2, 130.0, 128.8, 127.6, 127.5, 127.4, 126.8, 126.1, 126.0, 125.2, 125.1, 125.1, 125.0, 124.9, 123.4, 119.7, 101.2, 90.5, 88.7, 70.5, 68.4, 62.4, 55.7, 51.4, 47.8, 39.0, 37.4, 33.2, 30.7, 28.8, 28.0, 27.2, 27.2, 15.9 ppm. HRMS (ESI, *m/z*): calcd for $[C_{49}H_{51}BrNO_{11}]^+$ $(M+H)^+$, 908.2640; found, 908.2626.

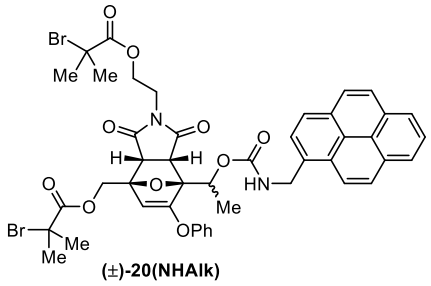

(±)-20(NHAlk)

(2-(2-((2-bromo-2-methylpropanoyl)oxy)ethyl)-1,3-dioxo-6-phenoxy-7-(1-(((pyren-1-ylmethyl)carbamoyl)oxy)ethyl)-1,2,3,3a,7,7a-hexahydro-4H-4,7-epoxyisoindol-4-yl)methyl 2-bromo-2-methylpropanoate ((±)-20(NHAlk)). A 2 dram vial equipped with a stir bar was charged with (±)-**31** (24.1 mg, 0.0289 mmol), DMAP (8.4 mg, 0.069 mmol) and $CDCl_3$ (0.5 mL). Pyren-1-ylmethanamine hydrochloride (8.5 mg, 0.032 mmol) dissolved in $CDCl_3$ (0.5 mL) was then added to the reaction mixture. The reaction was stirred at 50 °C overnight until the reaction had completed, as determined by ^1H NMR spectroscopy. The reaction mixture was then diluted with DCM (10 mL), washed with NH_4Cl (15 mL) and brine (15 mL), and the organic fraction was dried over Na_2SO_4, filtered, and concentrated under reduced pressure. The crude product was purified by column chromatography (20–60% EtOAc/hexanes) to yield the title compound as a white foamy solid (20 mg, 74% yield). ^1H NMR (500 MHz, $CDCl_3$) δ: 8.34 – 7.97 (m, 9H), 7.32 -7.26 (m, 2H), 7.19 – 7.13 (m, 1H), 6.93 (d, J = 7.9 Hz, 2H), 5.77 (q, J = 6.5 Hz, 1H), 5.38 – 5.30 (m, 1H), 5.16 (d, J = 5.6 Hz, 2H), 4.96 (s, 1H), 4.63 (ABq, $\Delta\nu_{AB}$ = 137.0 Hz, J_{AB} = 12.6 Hz, 2H), 4.34 – 4.19 (m, 1H), 4.18 – 4.08 (m, 1H), 3.77 (d, J = 7.9 Hz, 1H), 3.71 – 3.41 (m, 3H), 1.91 (d, J = 3.7 Hz, 6H), 1.82 (s, 6H), 1.57 (d, J = 6.5 Hz, 3H) ppm. $^{13}C\{^1H\}$ NMR (100

MHz, $CDCl_3$) δ: 173.9, 172.9, 171.5, 171.1, 163.1, 155.3, 154.7, 131.4, 131.2, 130.9, 130.1, 129.1, 128.4, 127.7, 127.5, 127.0, 126.3, 126.0, 125.6, 125.5, 125.2, 125.0, 124.9, 122.9, 119.7, 100.7, 90.9, 88.3, 67.3, 63.7, 62.5, 55.7, 55.6, 51.3, 47.8, 43.7, 37.5, 30.8, 30.7, 30.7, 16.3 ppm. HRMS (ESI, *m/z*): calcd for $[C_{45}H_{43}Br_2N_2O_{10}]^+$ $(M+H)^+$, 929.1279; found, 929.1268.

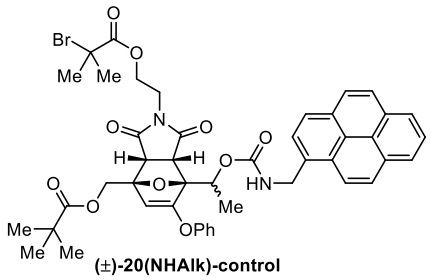

(±)-20(NHAlk)-control

(2-(2-((2-bromo-2-methylpropanoyl)oxy)ethyl)-1,3-dioxo-6-phenoxy-7-(1-(((pyren-1-ylmethyl)carbamoyl)oxy)ethyl)-1,2,3,3a,7,7a-hexahydro-4H-4,7-epoxyisoindol-4-yl)methyl pivalate ((±)-20(NHAlk)-control). The title compound was prepared following a similar procedure as that for compound (±)-**20(NHAlk)**, with compound (±)-**31-control** (38.0 mg, 0.0491 mmol)**,** DMAP (13.2 mg, 0.108 mmol), pyren-1-ylmethanamine hydrochloride (14.5 mg, 0.0542 mmol), and $CDCl_3$ (0.5 mL). Column chromatography (20–40% EtOAc/hexanes) afforded the title compound as a white foamy solid (41 mg, 96%). ^{1}H NMR (400 MHz, $CDCl_3$) δ: 8.35 – 7.92 (m, 9H) 7.29 (t, *J* = 7.7 Hz, 2H), 7.16 (t, *J* = 7.4 Hz, 1H), 6.92 (d, *J* = 7.9 Hz, 2H), 5.77 (q, *J* = 6.4 Hz, 1H), 5.34 (t, *J* = 5.6 Hz, 1H), 5.15 (d, *J* = 5.5 Hz, 2H), 4.91 (s, 1H), 4.53 (ABq, $\Delta\nu_{AB}$ = 124.2 Hz, J_{AB} = 12.7 Hz, 2H), 4.30 – 4.19 (m, 1H), 4.20 – 4.08 (m, 1H), 3.76 (d, *J* = 7.9 Hz, 1H), 3.72 – 3.50 (m, 2H), 3.46 (d, *J* = 7.9 Hz, 1H), 1.82 (d, *J* = 0.9 Hz, 6H), 1.56 (d, *J* = 6.5 Hz, 3H), 1.17 (s, 9H) ppm. ^{13}C{^{1}H} NMR (100 MHz, $CDCl_3$) δ: 177.8, 173.9, 173.0, 171.5, 163.0, 155.3, 154.8, 131.4, 131.2, 130.9, 130.1, 129.0, 128.4, 127.7, 127.5, 127.0, 126.2, 126.0, 125.6, 125.5, 125.1, 124.9, 124.8, 122.9, 119.6, 100.8, 90.8, 88.6, 67.4, 62.5, 62.4, 55.7, 51.3, 47.9, 43.7, 39.0, 37.4, 30.7, 30.7, 27.2, 16.3 ppm. HRMS (ESI, *m/z*): calcd for $[C_{46}H_{46}BrN_2O_{10}]^+$ $(M+H)^+$, 865.2330; found, 865.2338.

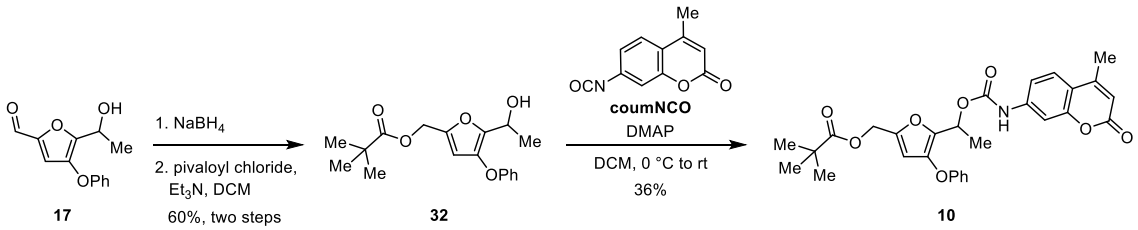

(5-(1-hydroxyethyl)-4-phenoxyfuran-2-yl)methyl pivalate (32). A round bottom flask equipped with a stir bar was charged with **17** (0.916 g, 3.95 mmol) and methanol (10 mL). The solution was cooled to 0 °C in an ice bath followed by the slow addition of $NaBH_4$ (0.246 g, 6.47 mmol). The reaction mixture was allowed to slowly warm to room temperature and stirred for 1 h. The mixture was then washed with 10% NH_4Cl (20 mL) and extracted with DCM (2 x 20 mL). The organic layer was dried over Na_2SO_4, filtered, and concentrated under reduced pressure to yield 1-(5-(hydroxymethyl)-3-phenoxyfuran-2-yl)ethan-1-ol as a colorless oil, which was used in the next step without further purification. The intermediate diol is stable for approximately one month when stored at −20°C.

A flame-dried round bottom flask equipped with a stir bar was charged with 1-(5-(hydroxymethyl)-3-phenoxyfuran-2-yl)ethan-1-ol (365.2 mg, 1.559 mmol), Et_3N (228μL, 1.64 mmol) and DCM (10 mL). The solution was cooled to 0 °C before adding pivaloyl chloride (202 μL, 1.64 mmol) dropwise. The reaction was then allowed to slowly warm to room temperature and stirred for approximately 4 h. The reaction mixture was then washed with NH_4Cl (10 mL) and brine (10 mL), and the organic fraction was dried over Na_2SO_4, filtered, and concentrated under reduced pressure. The crude product was purified by column chromatography using 3:1 hexanes/EtOAc to yield the title compound as a colorless oil (315 mg, 60% yield over two steps). A small amount of pivalic anhydride coeluted with the product. ^{1}H NMR (400 MHz, $CDCl_3$) δ: 7.33 – 7.24 (m, 2H), 7.07 – 7.01 (m, 1H), 7.02 – 6.93 (m, 2H), 6.19 (s, 1H), 4.97 (ABq, $\Delta\nu_{AB}$ = 8.19 Hz, J_{AB} = 14.2 Hz, 2H), 4.92 (q, J = 6.7 Hz, 1H), 2.36 (s, 1H), 1.53 (d, J = 6.8 Hz, 3H), 1.20 (s, 9H) ppm. $^{13}C\{^1H\}$ NMR (100 MHz, $CDCl_3$) δ: 178.2, 158.0, 147.9, 145.1, 138.8, 129.7, 122.8, 116.2, 106.5, 61.3, 58.6, 38.9, 27.2, 20.7 ppm. HRMS (ESI, *m/z*): calcd for $[C_{18}H_{21}O_4]^+$ $(M-OH)^+$, 301.1434; found, 301.1455.

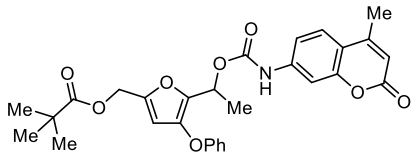

10

(5-(1-(((4-methyl-2-oxo-2H-chromen-7-yl)carbamoyl)oxy)ethyl)-4-phenoxyfuran-2-yl)methyl pivalate (10). A flamed-dried two-neck round bottom flask equipped with a stir bar was charged with **32** (77.2 mg, 0.243 mmol), **coumNCO** (81.8 mg, 0.407 mmol), and DCM (8 mL). DMAP (8.1 mg, 0.066 mmol) was then added into the stirred mixture at 0°C, and the reaction was allowed to warm to room temperature. After 3 h, the reaction was quenched by adding a solution of glucose (35.0 mg, 0.194 mmol) in 3 mL DMF. The mixture was stirred at room temperature for 2 h to consume the excess **coumNCO** completely, then diluted with diethyl ether (20 mL) and hexane (5 mL). A precipitate appeared immediately and the suspension was filtered to remove the excess glucose and any other insoluble products. The filtrate was washed with aqueous $NaHCO_3$ solution and brine, dried over Na_2SO_4, then concentrated. The crude material was again dispersed into a mixture of diethyl ether (5 mL) and hexane (10 mL), and then filtered to remove insoluble 7-amino-4-methylcoumarin. The filtrate was concentrated, dissolved in a small amount of DCM (0.3 mL), and then added into a mixture of diethyl ether (3 mL) and hexane (7 mL). The mixture was slowly concentrated to around half of its original volume using a rotary evaporator causing a white precipitate to form. The white solid was collected carefully by removing the solution using a pipet, then washed with hexane, and finally dried under high vacuum to yield metastable compound **10** as a fluffy white solid (45.5 mg, 36%). ^{1}H NMR (500 MHz, $CDCl_3$) δ: 7.49 (d, J = 8.6 Hz, 1H), 7.36 – 7.27 (m, 4H), 7.05 (t, J = 7.4 Hz, 1H), 7.00 (d, J = 8.1 Hz, 2H), 6.73 (s, 1H), 6.23 (s, 1H), 6.18 (d, J = 1.3 Hz, 1H), 6.02 (q, J = 6.7 Hz, 1H), 5.00 (ABq, $\Delta\nu_{AB}$ = 17.7 Hz, J_{AB} = 13.5 Hz, 2H), 2.41 (d, J = 1.2 Hz, 3H), 1.67 (d, J = 6.7 Hz, 3H), 1.22 (s, 9H) ppm. ^{13}C{^{1}H} NMR (125 MHz, $CDCl_3$) δ: 178.2, 161.2, 157.9, 154.6, 152.3, 152.0, 148.9, 141.4, 141.0, 140.9, 129.8, 125.5, 123.1, 116.6, 115.7, 114.4, 113.3, 106.5, 106.0, 65.0, 58.6, 39.0, 27.2, 18.7, 18.2 ppm. HRMS (FAB, *m/z*): calcd for $[C_{29}H_{30}NO_8]^+$ $(M+H)^+$, 520.1966; found, 520.1950.

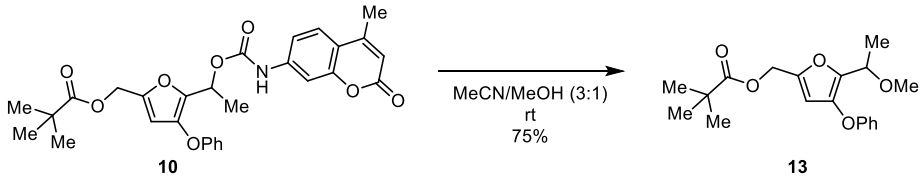

10 13

(5-(1-methoxyethyl)-4-phenoxyfuran-2-yl)methyl pivalate (13). Compound **10** (6.2 mg, 0.012 mmol) was dissolved in a mixture of MeOH (155 mL) and MeCN (465 mL) and stirred at room temperature. After 16 h, the reaction mixture was concentrated under reduced pressure and the crude product was purified by flash chromatography (0–20% EtOAc/hexanes) to provide the title compound as a colorless oil (3.0 mg, 75%). ^{1}H NMR (400 MHz, $CDCl_3$) δ: 7.39 – 7.27 (m, 2H), 7.08 – 7.03 (m, 1H), 7.02 – 6.96 (m, 2H), 6.22 (d, J = 0.6 Hz, 1H), 5.00 (ABq, $\Delta\nu_{AB}$ = 11.6 Hz, J_{AB} = 13.4 Hz, 2H), 4.44 (q, J = 6.7 Hz, 1H), 3.24 (s, 3H), 1.51 (d, J = 6.7 Hz, 3H), 1.20 (s, 9H) ppm. ^{13}C{^{1}H} NMR (100 MHz, $CDCl_3$) δ: 178.2, 158.1, 148.5, 142.8, 141.0, 129.8, 122.9, 116.4, 106.0, 69.2, 58.7, 56.3, 39.0, 27.2, 18.8 ppm. HRMS (FAB, *m/z*): calcd for $[C_{19}H_{24}O_5]^+$ $(M)^+$, 332.1624; found, 332.1645.

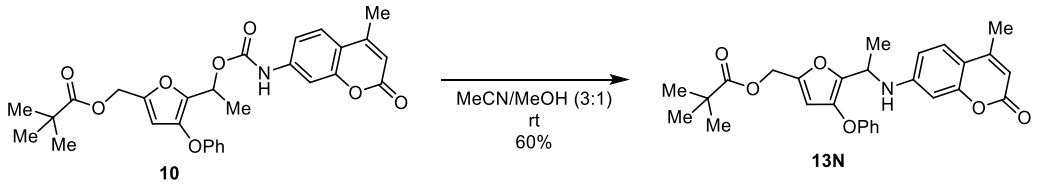

10 13N

(5-(1-((4-methyl-2-oxo-2H-chromen-7-yl)amino)ethyl)-4-phenoxyfuran-2-yl)methyl pivalate (13N). Compound **10** (22 mg, 0.066 mmol) was dissolved in a mixture of MeOH (0.15 mL) and MeCN (0.45 mL) and kept at room temperature. After 16 h, the reaction mixture was concentrated under reduced pressure and the crude product was purified by flash chromatography (0–50% EtOAc/hexanes) to provide the title compound as a white solid (19 mg, 60%). ^{1}H NMR (400 MHz, $CDCl_3$) δ: 7.30 – 7.27 (m, 2H), 7.26 – 7.22 (m, 1H), 7.09 – 7.00 (m, 1H), 6.98 – 6.90 (m, 2H), 6.53 – 6.46 (m, 2H), 6.17 (s, 1H), 5.97 (q, J = 1.2 Hz, 1H), 4.94 (ABq, $\Delta\nu_{AB}$ = 6.6 Hz, J_{AB} = 13.2 Hz, 2H), 4.74 (dq, J = 8.3, 6.8 Hz, 1H), 4.45 (d, J = 8.2 Hz, 1H), 2.30 (d, J = 1.2 Hz, 3H), 1.58 (d, J = 6.8 Hz, 3H), 1.16 (s, 9H) ppm. ^{13}C{^{1}H} NMR (100 MHz, $CDCl_3$) δ: 178.1, 162.0, 157.9, 155.8, 152.9, 150.1, 147.9, 143.4, 139.0, 129.8, 125.5, 123.0, 116.3, 111.2, 110.7, 110.0, 106.5, 99.5, 58.5, 44.6, 38.9, 27.2, 20.2, 18.6 ppm. HRMS (ESI, *m/z*): calcd for $[C_{28}H_{29}NO_6Na]^+$ $(M+Na)^+$, 498.1887; found, 498.1893.

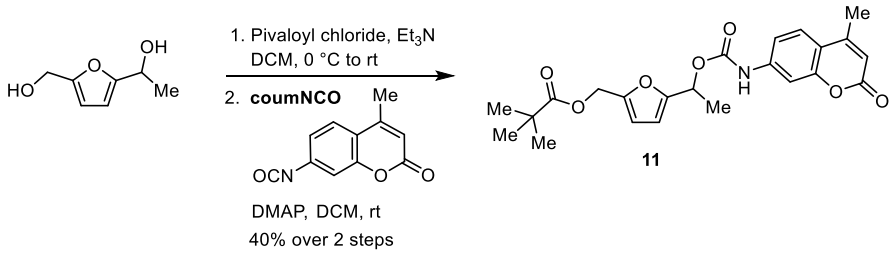

(5-(1-(((4-methyl-2-oxo-2H-chromen-7-yl)carbamoyl)oxy)ethyl)furan-2-yl)methyl pivalate (11). A flame-dried round bottom flask equipped with a stir bar was charged with 1-(5-(hydroxymethyl)furan-2-yl)ethan-1-ol[3] (1.00 g, 7.04 mmol), Et_3N (1.30 mL, 9.44 mmol) and DCM (10 mL). The solution was cooled to 0 °C before adding pivaloyl chloride (1.0 mL, 8.13 mmol) dropwise. The reaction was then allowed to slowly warm to room temperature and stirred overnight until the reaction completed, as determind by ^{1}H NMR spectroscopy. The reaction mixture was then washed with NH_4Cl (10 mL) and brine (10 mL), and the organic fraction was dried over Na_2SO_4, filtered, and concentrated under reduced pressure to afford (5-(1-hydroxyethyl)furan-2-yl)methyl pivalate as a light-yellow oil (0.79 g) which was used in the next step without further purification.

A flame-dried two-neck round bottom flask equipped with a stir bar was charged with (5-(1-hydroxyethyl)furan-2-yl)methyl pivalate (195.8 mg, 0.865 mol), **coumNCO** (233.0 mg, 1.159 mol), DCM (10 mL), and then DMAP (11.2 mg, 0.0918 mmol). The reaction was kept at room temperature for 3 h. The mixture was then washed with 10% NH_4Cl, brine, dried over Na_2SO_4, filtered, and concentrated under reduced pressure. The crude produce was purified by column chromatography (25–45% EtOAc/hexanes) to provide the title compound as a white solid (296 mg, 40% yield over two steps). ^{1}H NMR (400 MHz, $CDCl_3$) δ: 7.51 (d, J = 8.6 Hz, 1H), 7.42 (d, J = 2.3 Hz, 1H), 7.35 (dd, J = 8.6, 2.2 Hz, 1H), 6.87 (broad, 1H), 6.36 – 6.32 (m, 2H), 6.19 (q, J = 1.3 Hz, 1H), 5.96 (q, J = 6.7 Hz, 1H), 5.05 (ABq, $\Delta\nu_{AB}$ = 12.6 Hz, J_{AB} = 13.3 Hz, 2H), 2.40 (d, J = 1.2 Hz, 3H), 1.66 (d, J = 6.7 Hz, 3H), 1.19 (s, 9H) ppm. ^{13}C{^{1}H} NMR (100 MHz, $CDCl_3$) δ: 178.3, 161.2, 154.6, 153.5, 152.3, 152.3, 150.3, 141.5, 125.5, 115.7, 114.5, 113.3, 110.7, 109.2, 106.1, 66.7, 58.3, 39.0, 27.2, 18.7, 18.5 ppm. HRMS (FAB, *m/z*): calcd for $[C_{23}H_{26}NO_7]^+$ $(M+H)^+$, 428.1704; found, 428.1723.

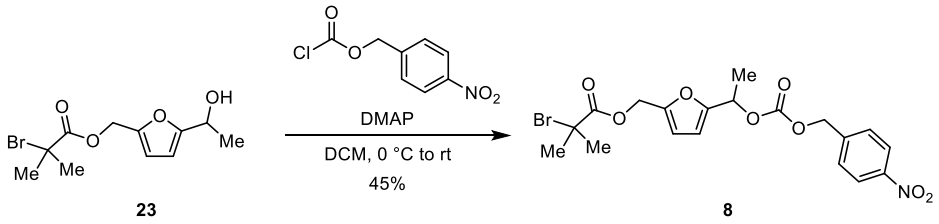

(5-(1-((((4-nitrobenzyl)oxy)carbonyl)oxy)ethyl)furan-2-yl)methyl 2-bromo-2-methylpropanoate (8). A 20 mL septum-capped vial equipped with a stir bar was charged with **23** (59.5 mg, 0.204 mmol), DMAP (24.9 mg, 0.204 mmol), and DCM (2 mL). The solution was cooled to 0 °C in an ice bath followed by the dropwise addition of a solution of 4-nitrobenzyl chloroformate (45.4 mg, 0.210 mmol) in DCM (1 mL). The reaction mixture was allowed to warm to room temperature and stirred for 5 h. A saturated solution of NH_4Cl (3 mL) was added and the mixture was extracted with DCM (3 x 10 mL). The combined organic phase was dried over Na_2SO_4, filtered, and concentrated under reduced pressure. The crude product was purified by column chromatography (10–40% EtOAc/hexanes) to provide the title compound as a colorless oil (43.4 mg, 45% yield). ^{1}H NMR (400 MHz, $CDCl_3$) δ: 8.25 – 8.19 (m, 2H), 7.56 – 7.50 (m, 2H), 6.40 (d, J = 3.3 Hz, 1H), 6.36 (d, J = 3.3 Hz, 1H), 5.80 (q, J = 6.7 Hz, 1H), 5.25 (ABq, $\Delta\nu_{AB}$ = 10.2 Hz, J_{AB} = 13.3 Hz, 2H), 5.13 (ABq, $\Delta\nu_{AB}$ = 6.4 Hz, J_{AB} = 13.0 Hz, 2H), 1.92 (s, 6H), 1.66 (d, J = 6.7 Hz, 3H) ppm. ^{13}C{^{1}H} NMR (100 MHz, $CDCl_3$) δ: 171.4, 154.3, 153.1, 149.4, 148.0, 142.5, 128.5, 124.0, 111.6, 109.7, 69.9, 68.1, 59.6, 55.7, 30.8, 18.3 ppm. HRMS (FAB, *m/z*): calcd for $[C_{11}H_{14}BrO_3]^+$ $(M-OCO_2CH_2C_6H_4NO_2)^+$, 273.0121; found, 273.0151. LCMS (ESI, *m/z*): calcd for $[C_{19}H_{20}BrNO_8Na]^+$ $(M+Na)^+$, 492.0; found, 492.0.

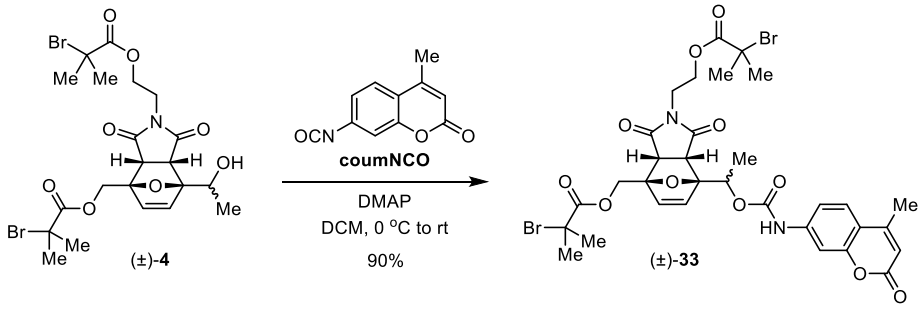

(2-(2-((2-bromo-2-methylpropanoyl)oxy)ethyl)-7-(1-(((4-methyl-2-oxo-2H-chromen-7-yl)carbamoyl)oxy)ethyl)-1,3-dioxo-1,2,3,3a,7,7a-hexahydro-4H-4,7-epoxyisoindol-4-yl)methyl 2-bromo-2-methylpropanoate ((±)-33). The title compound

was prepared following a similar procedure as that for compound (±)-**12(NH)**, with compound (±)-**4** (46.1 mg, 79.3 mmol)**,** DMAP (1.0 mg, 8.2 mmol), **coumNCO** (31.8 mg, 158.1 mmol) and DCM (1 mL). Column chromatography (20–40% Et_2O in 1:1 Hexanes/DCM) afforded the title compound as a white foamy solid (55.6 mg, 90%). ^{1}H NMR (400 MHz, $CDCl_3$) δ: 7.53 (d, *J* = 8.7 Hz, 1H), 7.47 – 7.36 (m, 2H), 7.10 (s, 1H), 6.53 – 6.40 (m, 2H), 6.19 (q, *J* = 1.3 Hz, 1H), 5.57 (q, *J* = 6.6 Hz, 1H), 4.80(ABq, $\Delta\nu_{AB}$ = 86.5 Hz, J_{AB} = 12.6 Hz, 2H), 4.22 (t, *J* = 5.1 Hz, 2H), 3.80 – 3.61 (m, 3H), 3.56 (d, *J* = 7.8 Hz, 1H), 2.41 (d, *J* = 1.3 Hz, 3H), 1.93 (d, *J* = 6.8 Hz, 6H), 1.90 (s, 6H), 1.53 (d, *J* = 6.6 Hz, 3H) ppm. ^{13}C{^{1}H} NMR (100 MHz, $CDCl_3$) δ: 173.7, 173.6, 171.5, 171.2, 161.1, 154.6, 152.3, 152.0, 141.2, 135.7, 135.3, 125.6, 115.8, 114.5, 113.5, 106.1, 92.8, 89.4, 69.6, 63.2, 62.6, 55.7, 55.5, 49.4, 48.1, 37.7, 30.8, 30.8, 18.7, 16.2 ppm. HRMS (ESI, *m/z*): calcd for $[C_{32}H_{34}Br_2N_2O_{11}Na]^+$ $(M+Na)^+$, 803.0422; found, 803.0427.

General Polymerization Procedures. A 10 mL Schlenk flask equipped with a stir bar was charged with the initiator (1 equiv), methyl acrylate (~1,500 equiv), Me_6TREN (2 equiv), and DMSO (equal volume to methyl acrylate). The flask was sealed, the solution was deoxygenated with three freeze-pump-thaw cycles, and then backfilled with nitrogen. The flask was opened briefly under a flow of N_2, and freshly cut copper wire (1.0 cm length, 20 gauge) was added on top of the frozen mixture. The flask was resealed, evacuated for an additional 15 min, warmed to room temperature, and then backfilled with nitrogen. The mixture was stirred at room temperature until the solution became sufficiently viscous, indicating that the desired monomer conversion was reached (1–6 h). The flask was then opened to air and the solution was diluted with DCM. The polymer was precipitated into cold methanol (2x) and the isolated polymer was thoroughly dried under vacuum.

2.6 Sonication Experiments and Fluorescence Spectroscopy

An oven-dried sonication vessel was fitted with rubber septa, placed onto the sonication probe, and allowed to cool under a stream of dry argon. The vessel was charged with a solution of the polymer in anhydrous acetonitrile/methanol (3:1 v/v, 2.0 mg/mL, 20 mL) and submerged in an ice bath. The solution was sparged continuously with argon

beginning 20 min prior to sonication and for the duration of the sonication experiment. Pulsed ultrasound (1 s on/2 s off, 20% amplitude, 20 kHz, 8.2 W/cm^2) was then applied to the system. Aliquots (1.0 mL) were removed and filtered through a 0.45 μm syringe filter prior to analysis by GPC and fluorescence spectroscopy. Ultrasonic intensity was calibrated using the method described by Berkowski *et al*.[25]

2.7 CoGEF calculations.

CoGEF calculations were performed using Spartan ′18 Parallel Suite according to previously reported methods.[42,43] Ground state energies were calculated using DFT at the B3LYP/6-31G* level of theory. Starting from the equilibrium geometry of the unconstrained molecule (relative energy = 0 kJ/mol), the distance between the terminal methyl groups of the truncated structure was increased in increments of 0.05 Å and the energy was minimized at each step. The maximum force associated with the retro-Diels–Alder reaction was calculated from the slope of the curve immediately prior to bond cleavage.

2.8 Single Crystal X-Ray Diffraction

Crystals for X-ray diffraction analysis were grown by slow diffusion of hexanes into a solution of compound **12** in chloroform/toluene (1:9 v:v). A crystal was mounted on a polyimide MiTeGen loop with STP Oil Treatment and placed under a nitrogen stream. Low temperature (200K; there were crystal issues at lower temperatures) X-ray data were collected with a Bruker AXS D8 VENTURE KAPPA diffractometer running at 50 kV and 1mA (Cu K_α = 1.54178 Å; PHOTON II CPAD detector and Helios focusing multilayer mirror optics). All diffractometer manipulations, including data collection, integration, and scaling were carried out using the Bruker APEX3 software. An absorption correction was applied using SADABS. The space group was determined and the structure solved by intrinsic phasing using XT. Refinement was full-matrix least squares on F^2 using XL. All non-hydrogen atoms were refined using anisotropic displacement parameters. Hydrogen atoms were placed in idealized positions and refined using a riding model. The water molecule was refined as a rigid body. The isotropic displacement parameters of all hydrogen atoms were fixed at 1.2 times (1.5 times for methyl groups) the U_{eq} value of the bonded atom. Special refinement details: Compound **12** crystallizes in the orthorhombic space group

Pna2_1(#33) with two molecules and one water molecule in the asymmetric unit. The structure was refined as a two component (0.55:0.45) inversion twin. In one molecule the Br is disordered with a CH_3 group (0.69:0.31).

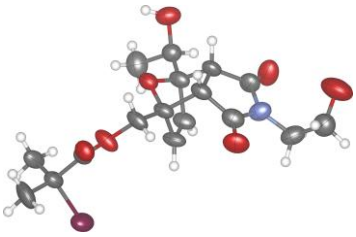

Identification code	v19226	
Empirical formula	C17 H23 Br N O7.50	
Formula weight	441.27	
Temperature	200 K	
Wavelength	1.54178 Å	
Crystal system	Orthorhombic	
Space group	$Pna2_1$	
Unit cell dimensions	a = 12.858(2) Å	α= 90°
	b = 10.2977(15) Å	β= 90°
	c = 29.000(4) Å	γ = 90°
Volume	3839.8(10) $Å^3$	
Z	8	
Density (calculated)	1.527 g/cm^3	
Absorption coefficient	3.291 mm^{-1}	
F(000)	1816	
Crystal size	0.25 x 0.10 x 0.10 mm^3	
Theta range for data collection	3.048 to 81.319°.	
Index ranges	$-16 \le h \le 13$, $-11 \le k \le 13$, $-36 \le l \le 36$	
Reflections collected	31123	
Independent reflections	8177 [R(int) = 0.0720]	
Completeness to theta = 67.679°	99.9 %	
Absorption correction	Semi-empirical from equivalents	
Max. and min. transmission	1.0000 and 0.7949	

Refinement method	Full-matrix least-squares on F^2
Data / restraints / parameters	8177 / 6 / 500
Goodness-of-fit on F^2	1.076
Final R indices [I>2sigma(I)]	R1 = 0.0667, wR2 = 0.1871
R indices (all data)	R1 = 0.0870, wR2 = 0.2044
Absolute structure parameter [Flack]	0.45(4)
Absolute structure parameter [Hooft]	0.46(1)
Extinction coefficient	n/a
Largest diff. peak and hole	0.713 and -0.691 e.$Å^{-3}$

2.9 References

(1) Swager, T. M. Sensor Technologies Empowered by Materials and Molecular Innovations. *Angew. Chem. Int. Ed.* **2018**, *57*, 4248–4257.

(2) Roth, M. E.; Green, O.; Gnaim, S.; Shabat, D. Dendritic, Oligomeric, and Polymeric Self-Immolative Molecular Amplification. *Chem. Rev.* **2016**, *116*, 1309–1352.

(3) Patrick, J. F.; Robb, M. J.; Sottos, N. R.; Moore, J. S.; White, S. R. Polymers with autonomous life-cycle control. *Nature* **2016**, *540*, 363–370.

(4) Lee, K. Y.; Peters, M. C.; Mooney, D. J. Controlled Drug Delivery from Polymers by Mechanical Signals. *Adv. Mater.* **2001**, *13*, 837–839.

(5) Huo, S.; Zhao, P.; Shi, Z.; Zou, M.; Yang, X.; Warszawik, E.; Loznik, M.; Göstl, R.; Herrmann, A. Mechanochemical bond scission for the activation of drugs. *Nature Chemistry* **2021**, *13*, 131–139.

(6) Küng, R.; Pausch, T.; Rasch, D.; Göstl, R.; Schmidt, B. M. Mechanochemical Release of Non-Covalently Bound Guests from a Polymer-Decorated Supramolecular Cage. *Angew. Chem. Int. Ed.* **2021**, *60*, 13626–13630.

(7) White, S. R.; Sottos, N. R.; Geubelle, P. H.; Moore, J. S.; Kessler, M. R.; Sriram, S. R.; Brown, E. N.; Viswanathan, S. Autonomic healing of polymer composites. *Nature* **2001**, *409*, 794–797.

(8) Toohey, K. S.; Sottos, N. R.; Lewis, J. A.; Moore, J. S.; White, S. R. Self-healing materials with microvascular networks. *Nat. Mater.* **2007**, *6*, 581–585.

(9) Li, J.; Nagamani, C.; Moore, J. S. Polymer Mechanochemistry: From Destructive to Productive. *Acc. Chem. Res.* **2015**, *48*, 2181–2190.

(10) Beyer, M. K.; Clausen-Schaumann, H. Mechanochemistry: The Mechanical Activation of Covalent Bonds. *Chem. Rev.* **2005**, *105*, 2921–2948.

(11) Caruso, M. M.; Davis, D. A.; Shen, Q.; Odom, S. A.; Sottos, N. R.; White, S. R.; Moore, J. S. Mechanically-Induced Chemical Changes in Polymeric Materials. *Chem. Rev.* **2009**, *109*, 5755–5798.

(12) Kim, G.; Lau, V. M.; Halmes, A. J.; Oelze, M. L.; Moore, J. S.; Li, K. C. High-intensity focused ultrasound-induced mechanochemical transduction in synthetic elastomers. *Proc. Natl. Acad. Sci. USA* **2019**, *116*, 10214–10222.

(13) Akbulatov, S.; Boulatov, R. Experimental polymer mechanochemistry and its interpretational frameworks. *ChemPhysChem* **2017**, *18*, 1422–1450.
(14) Diesendruck, C. E.; Steinberg, B. D.; Sugai, N.; Silberstein, M. N.; Sottos, N. R.; White, S. R.; Braun, P. V.; Moore, J. S. Proton-Coupled Mechanochemical Transduction: A Mechanogenerated Acid. *J. Am. Chem. Soc.* **2012**, *134*, 12446–12449.
(15) Lin, Y.; Kouznetsova, T. B.; Craig, S. L. A Latent Mechanoacid for Time-Stamped Mechanochromism and Chemical Signaling in Polymeric Materials. *J. Am. Chem. Soc.* **2020**, *142*, 99–103.
(16) Larsen, M. B.; Boydston, A. J. "Flex-Activated" Mechanophores: Using Polymer Mechanochemistry To Direct Bond Bending Activation. *J. Am. Chem. Soc.* **2013**, *135*, 8189–8192.
(17) Larsen, M. B.; Boydston, A. J. Successive Mechanochemical Activation and Small Molecule Release in an Elastomeric Material. *J. Am. Chem. Soc.* **2014**, *136*, 1276–1279.
(18) Shen, H.; Larsen, M. B.; Roessler, A.; Zimmerman, P.; Boydston, A. J. Mechanochemical Release of N-heterocyclic Carbenes from Flex-Activated Mechanophores. *Angew. Chem. Int. Ed.* **2021**, *60*, DOI: 10.1002/anie.202100576.
(19) Diesendruck, C. E.; Peterson, G. I.; Kulik, H. J.; Kaitz, J. A.; Mar, B. D.; May, P. A.; White, S. R.; Martínez, T. J.; Boydston, A. J.; Moore, J. S. Mechanically triggered heterolytic unzipping of a low-ceiling-temperature polymer. *Nat. Chem.* **2014**, *6*, 623–628.
(20) Peterson, G. I.; Boydston, A. J. Kinetic Analysis of Mechanochemical Chain Scission of Linear Poly(phthalaldehyde). *Macromol. Rapid Commun.* **2014**, *35*, 1611–1614.
(21) Wiita, A. P.; Ainavarapu, S. R. K.; Huang, H. H.; Fernandez, J. M. Force-dependent chemical kinetics of disulfide bond reduction observed with single-molecule techniques. *Proc. Natl. Acad. Sci. U.S.A.* **2006**, *103*, 7222–7227.
(22) Dopieralski, P.; Ribas–Arino, J.; Anjukandi, P.; Krupicka, M.; Marx, D. Unexpected mechanochemical complexity in the mechanistic scenarios of disulfide bond reduction in alkaline solution. *Nat. Chem.* **2017**, *9*, 164–170.
(23) Shi, Z.; Song, Q.; Göstl, R.; Herrmann, A. Mechanochemical activation of disulfide-based multifunctional polymers for theranostic drug release. *Chem. Sci.* **2020**.
(24) Shi, Z. Ultrasound-mediated activation of drugs. Ph.D. Dissertation, RWTH Aachen University: Aachen, Germany, 2021.
(25) Berkowski, K. L.; Potisek, S. L.; Hickenboth, C. R.; Moore, J. S. Ultrasound-Induced Site-Specific Cleavage of Azo-Functionalized Poly(ethylene glycol). *Macromolecules* **2005**, *38*, 8975–8978.
(26) Stevenson, R.; De Bo, G. Controlling Reactivity by Geometry in Retro-Diels–Alder Reactions under Tension. *J. Am. Chem. Soc.* **2017**, *139*, 16768–16771.
(27) Kean, Z. S.; Gossweiler, G. R.; Kouznetsova, T. B.; Hewage, G. B.; Craig, S. L. A coumarin dimer probe of mechanochemical scission efficiency in the sonochemical activation of chain-centered mechanophore polymers. *Chem. Commun.* **2015**, *51*, 9157–9160.

(28) Fan, B.; Trant, J. F.; Hemery, G.; Sandre, O.; Gillies, E. R. Thermo-responsive self-immolative nanoassemblies: direct and indirect triggering. *Chem. Commun.* **2017**, *53*, 12068–12071.
(29) Schmid, K. M.; Jensen, L.; Phillips, S. T. A Self-Immolative Spacer That Enables Tunable Controlled Release of Phenols under Neutral Conditions. *J. Org. Chem.* **2012**, *77*, 4363–4374.
(30) Nichol, M. F.; Clark, K. D.; Dolinski, N. D.; Alaniz, J. R. de. Multi-stimuli responsive trigger for temporally controlled depolymerization of self-immolative polymers. *Polym. Chem.* **2019**, *10*, 4914–4919.
(31) Nguyen, N. H.; Rosen, B. M.; Lligadas, G.; Percec, V. Surface-Dependent Kinetics of Cu(0)-Wire-Catalyzed Single-Electron Transfer Living Radical Polymerization of Methyl Acrylate in DMSO at 25 °C. *Macromolecules* **2009**, *42*, 2379–2386.
(32) Kryger, M. J.; Munaretto, A. M.; Moore, J. S. Structure–Mechanochemical Activity Relationships for Cyclobutane Mechanophores. *J. Am. Chem. Soc.* **2011**, *133*, 18992–18998.
(33) May, P. A.; Munaretto, N. F.; Hamoy, M. B.; Robb, M. J.; Moore, J. S. Is Molecular Weight or Degree of Polymerization a Better Descriptor of Ultrasound-Induced Mechanochemical Transduction? *ACS Macro Lett.* **2016**, *5*, 177–180.
(34) Schaefer, M.; Icli, B.; Weder, C.; Lattuada, M.; Kilbinger, A. F. M.; Simon, Y. C. The Role of Mass and Length in the Sonochemistry of Polymers. *Macromolecules* **2016**, *49*, 1630–1636.
(35) Alouane, A.; Labruère, R.; Le Saux, T.; Schmidt, F.; Jullien, L. Self-Immolative Spacers: Kinetic Aspects, Structure–Property Relationships, and Applications. *Angewandte Chemie International Edition* **2015**, *54*, 7492–7509.
(36) Lenhardt, J. M.; Black Ramirez, A. L.; Lee, B.; Kouznetsova, T. B.; Craig, S. L. Mechanistic Insights into the Sonochemical Activation of Multimechanophore Cyclopropanated Polybutadiene Polymers. *Macromolecules* **2015**, *48*, 6396–6403.
(37) Cotarca, L.; Geller, T.; Répási, J. Bis(trichloromethyl)carbonate (BTC, Triphosgene): A Safer Alternative to Phosgene? *Org. Process Res. Dev.* **2017**, *21*, 1439–1446.
(38) Cohen, B.; Huppert, D. Excited State Proton-Transfer Reactions of Coumarin 4 in Protic Solvents. *J. Phys. Chem. A* **2001**, *105*, 7157–7164.
(39) Heo, Y.; Sodano, H. A. Self-Healing Polyurethanes with Shape Recovery. *Adv. Funct. Mater.* **2014**, *24*, 5261–5268.
(40) Ronn, M.; Lim, N.-K.; Hogan, P.; Zhang, W.-Y.; Zhu, Z.; Dunwoody, N. An Expedient Route to 3-Methoxy-2-furaldehyde. *Synlett* **2012**, *2012*, 134–136.
(41) Deng, G.; Chen, Y. A Novel Way To Synthesize Star Polymers in One Pot by ATRP of N-[2-(2-Bromoisobutyryloxy)ethyl]maleimide and Styrene. *Macromolecules* **2004**, *37*, 18–26.
(42) Beyer, M. K. The mechanical strength of a covalent bond calculated by density functional theory. *J. Chem. Phys.* **2000**, *112*, 7307–7312.
(43) Klein, I. M.; Husic, C. C.; Kovács, D. P.; Choquette, N. J.; Robb, M. J. Validation of the CoGEF Method as a Predictive Tool for Polymer Mechanochemistry. *J. Am. Chem. Soc.* **2020**, *142*, 16364–16381.

2.10 ^{1}H and ^{13}C NMR spectra

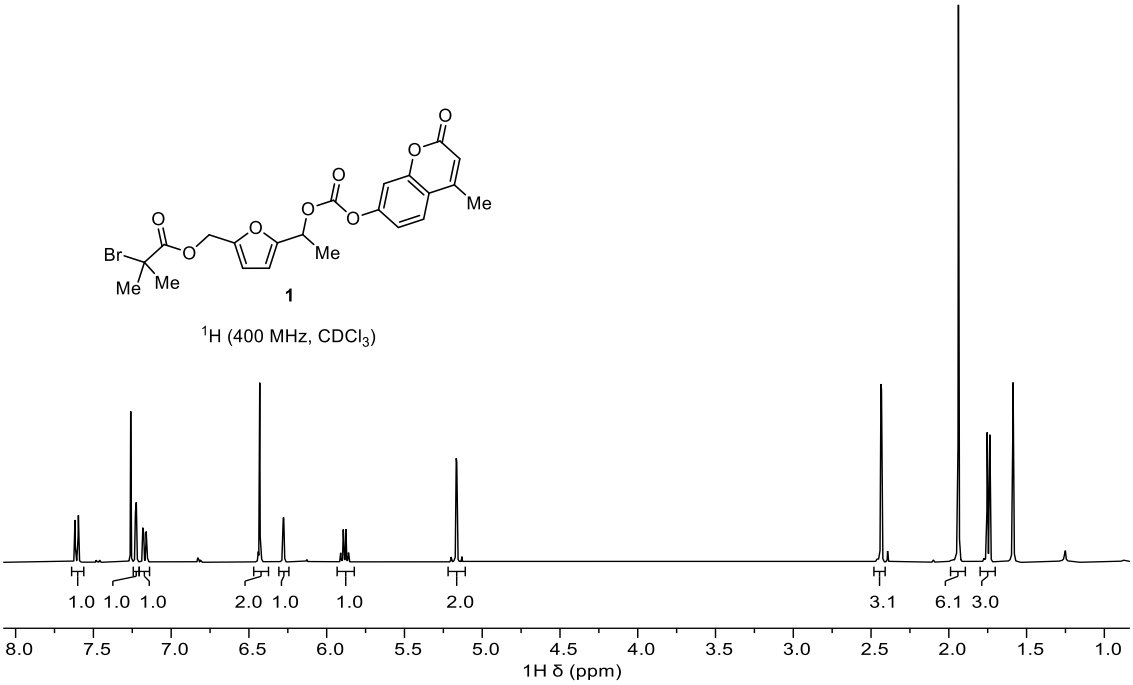

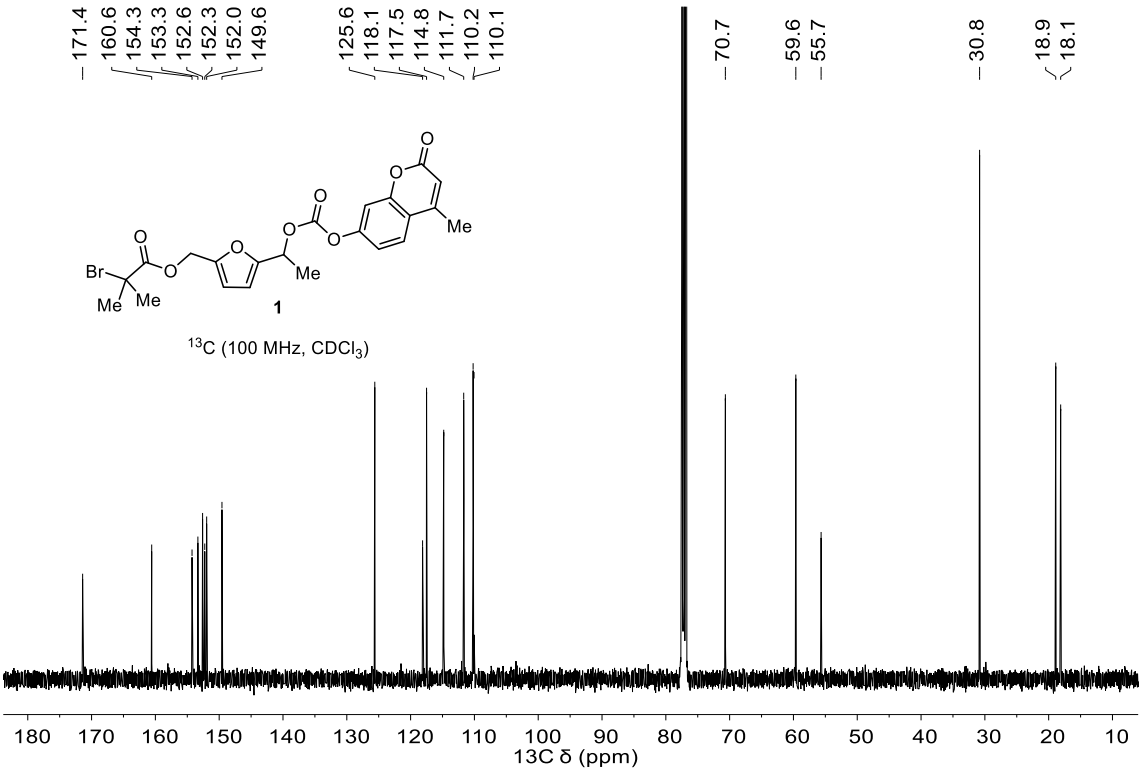

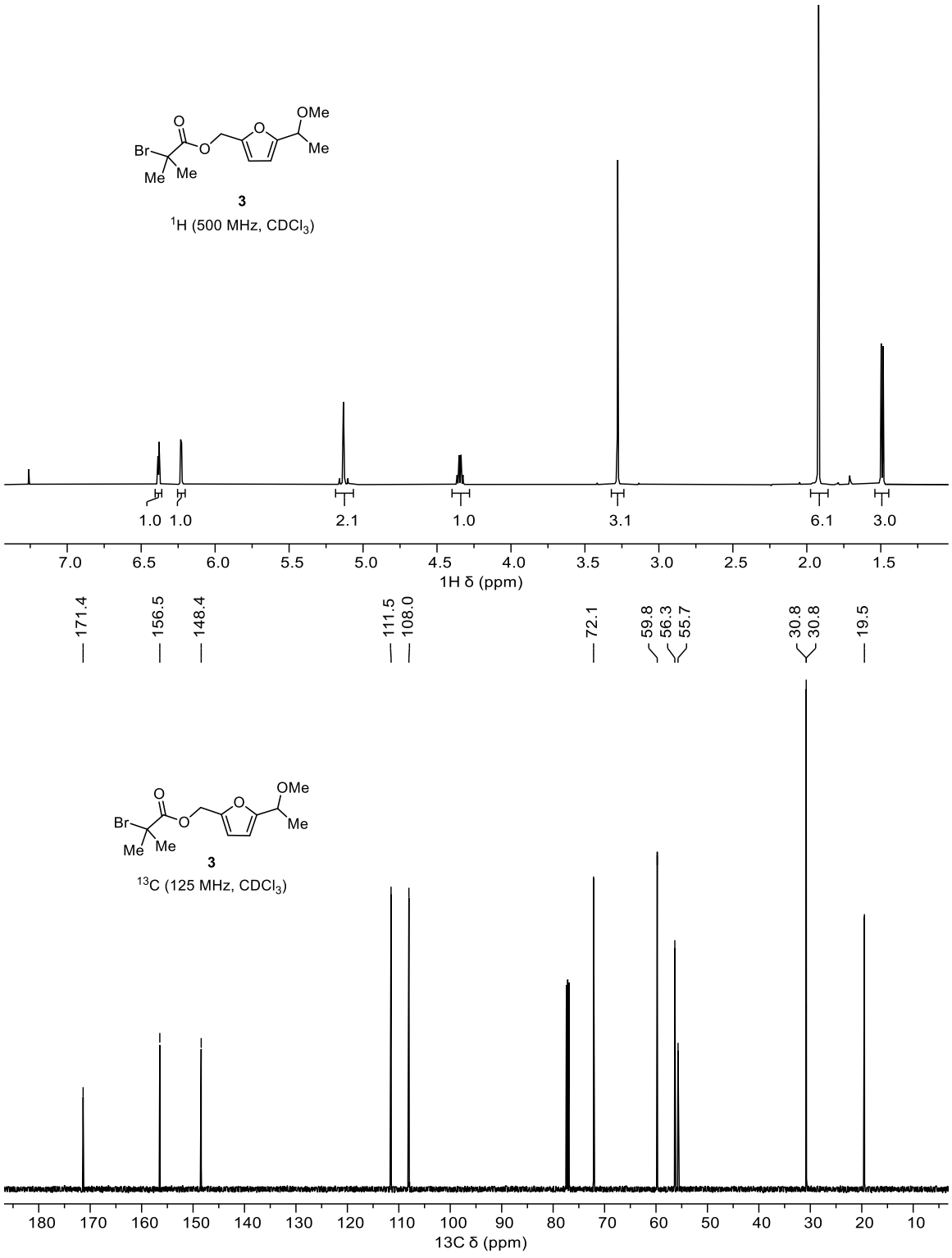
3
1H (500 MHz, CDCl3)
1.0 1.0 2.1 1.0 3.1 6.1 3.0
7.0 6.5 6.0 5.5 5.0 4.5 4.0 3.5 3.0 2.5 2.0 1.5
1H δ (ppm)
171.4 156.5 148.4 111.5 108.0 72.1 59.8 56.3 55.7 30.8 30.8 19.5
3
13C (125 MHz, CDCl3)
180 170 160 150 140 130 120 110 100 90 80 70 60 50 40 30 20 10
13C δ (ppm)

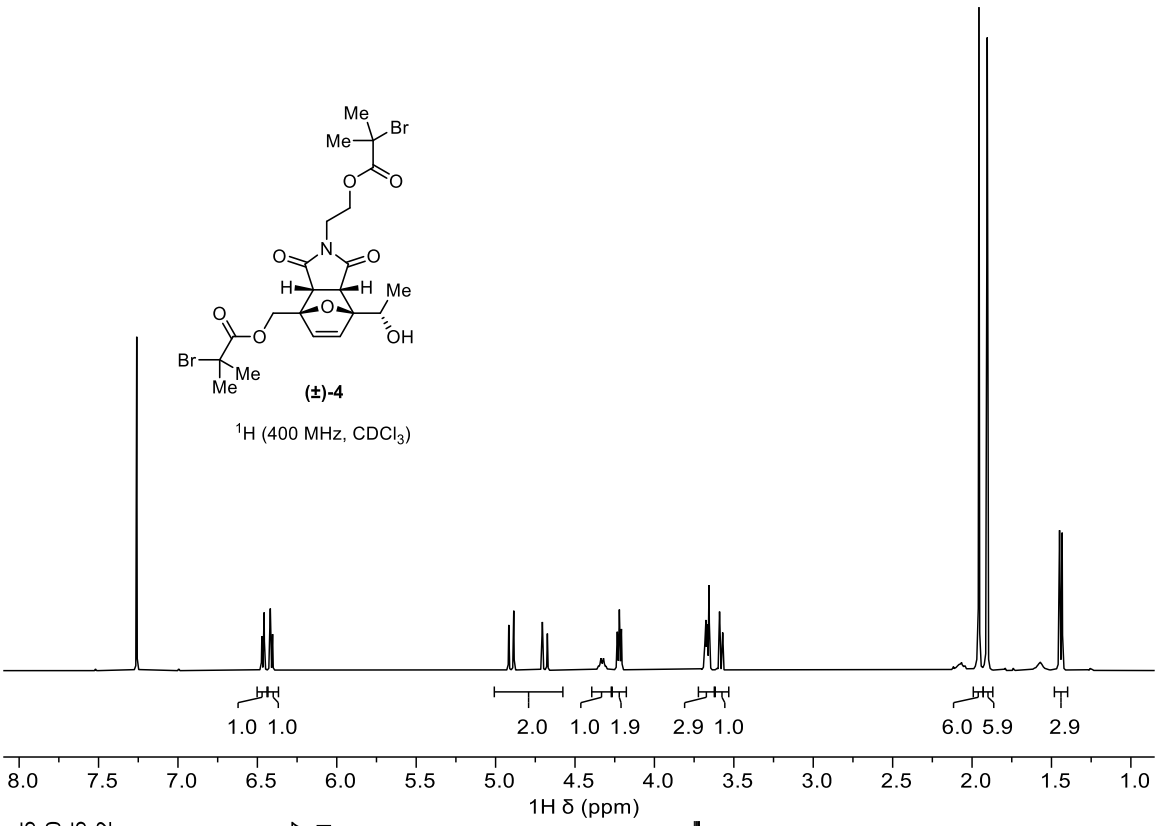
(±)-4
^{1}H (400 MHz, $CDCl_3$)
1.0 1.0 2.0 1.0 1.9 2.9 1.0 6.0 5.9 2.9
8.0 7.5 7.0 6.5 6.0 5.5 5.0 4.5 4.0 3.5 3.0 2.5 2.0 1.5 1.0
1H δ (ppm)

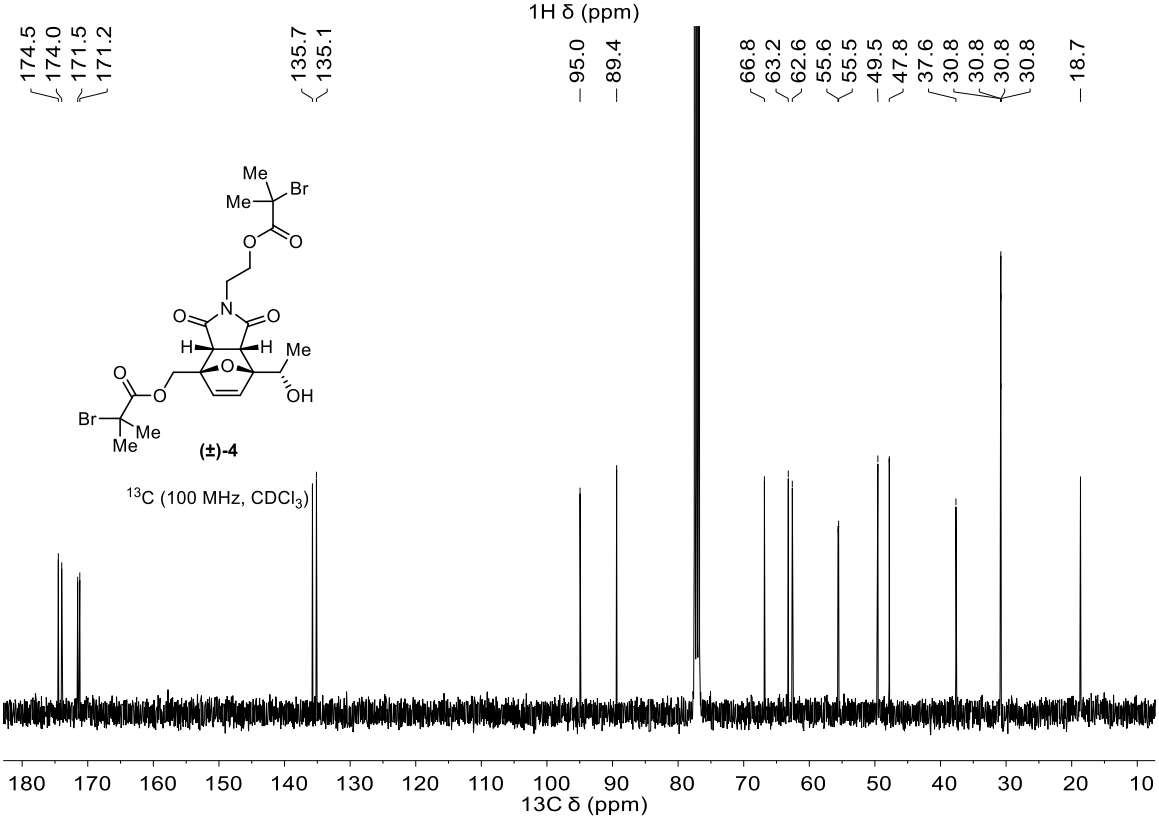
174.5 174.0 171.5 171.2 135.7 135.1 95.0 89.4 66.8 63.2 62.6 55.6 55.5 49.5 47.8 37.6 30.8 30.8 30.8 30.8 18.7
(±)-4
^{13}C (100 MHz, $CDCl_3$)
180 170 160 150 140 130 120 110 100 90 80 70 60 50 40 30 20 10
13C δ (ppm)

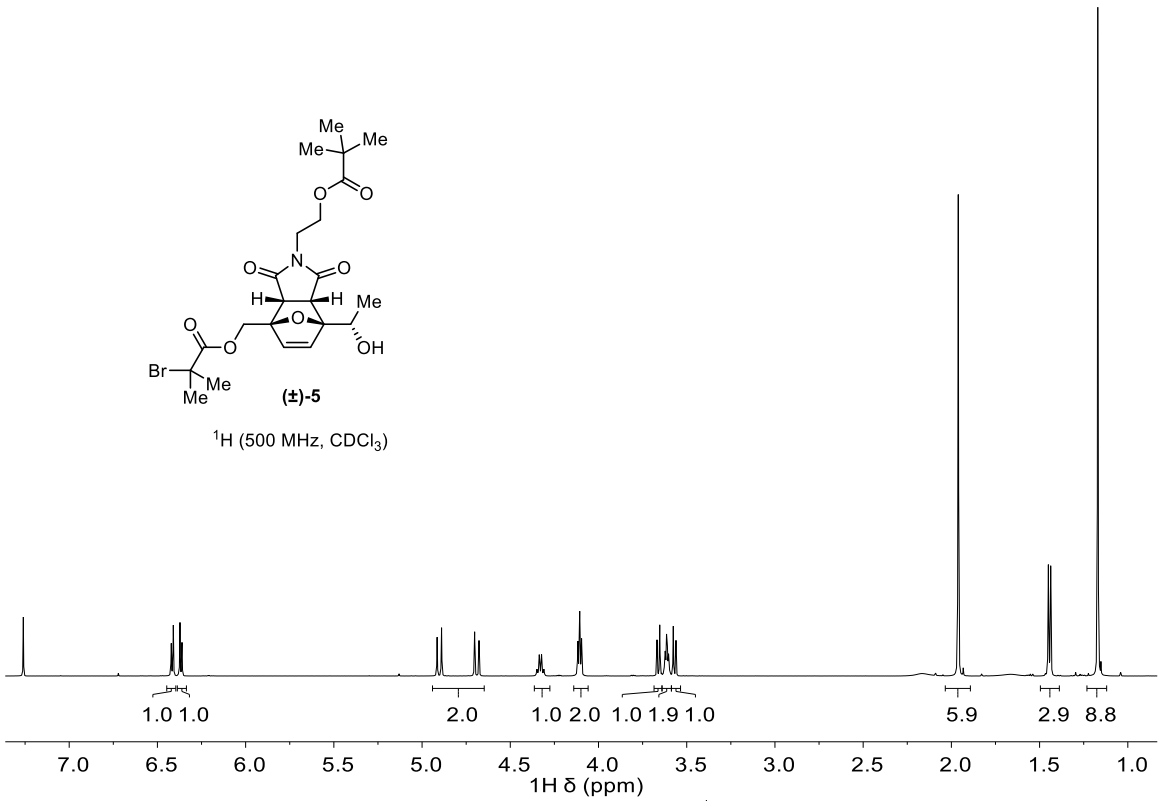
(±)-5
^{1}H (500 MHz, CDCl$_3$)
1.0 1.0
2.0
1.0 2.0 1.0 1.9 1.0
5.9
2.9 8.8
1H δ (ppm)

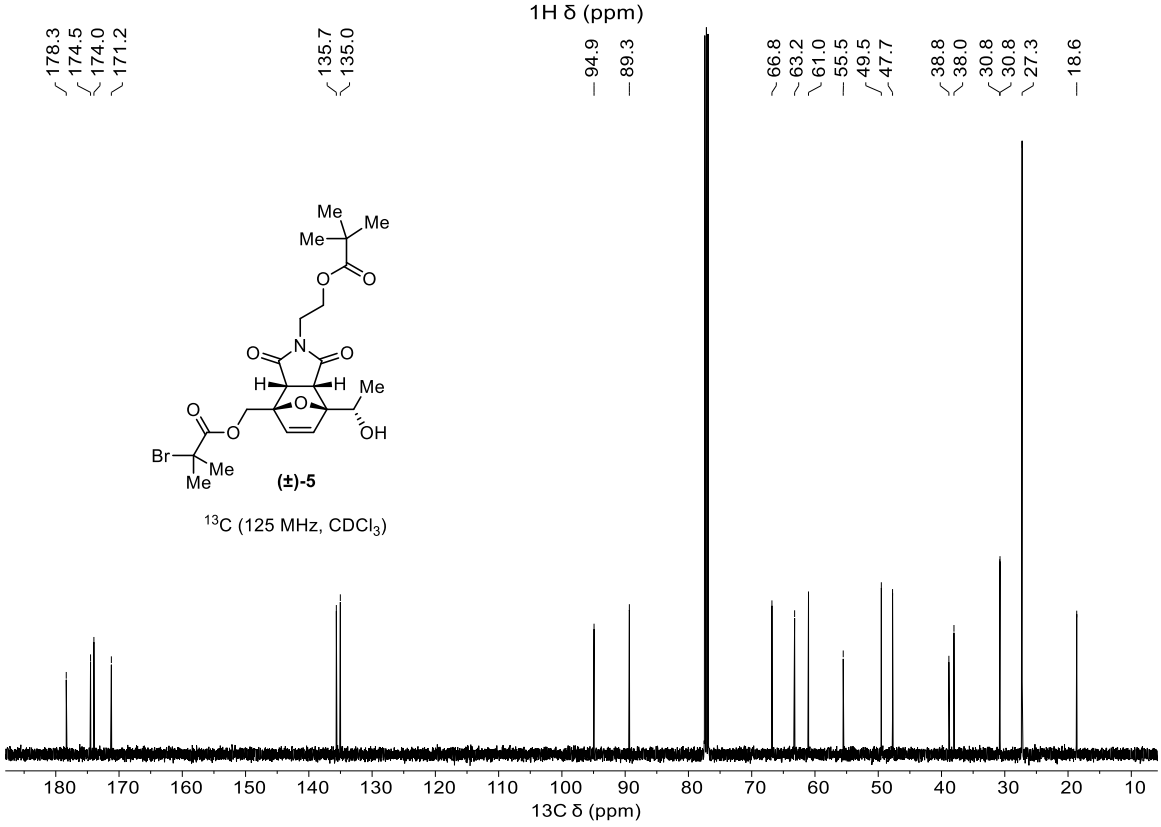
178.3
174.5
174.0
171.2
135.7
135.0
94.9
89.3
66.8
63.2
61.0
55.5
49.5
47.7
38.8
38.0
30.8
30.8
27.3
18.6
(±)-5
^{13}C (125 MHz, CDCl$_3$)
13C δ (ppm)

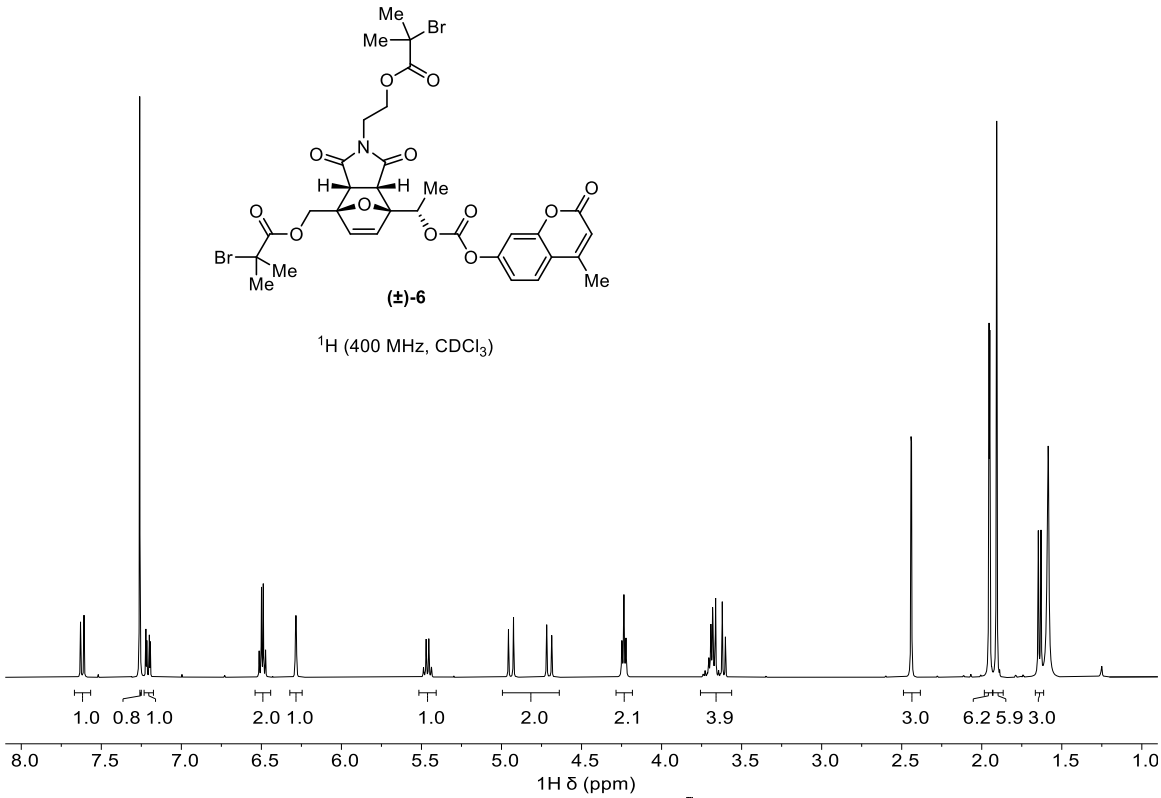
(±)-6
^{1}H (400 MHz, $CDCl_3$)
1.0 0.8 1.0 2.0 1.0 1.0 2.0 2.1 3.9 3.0 6.2 5.9 3.0
8.0 7.5 7.0 6.5 6.0 5.5 5.0 4.5 4.0 3.5 3.0 2.5 2.0 1.5 1.0
1H δ (ppm)

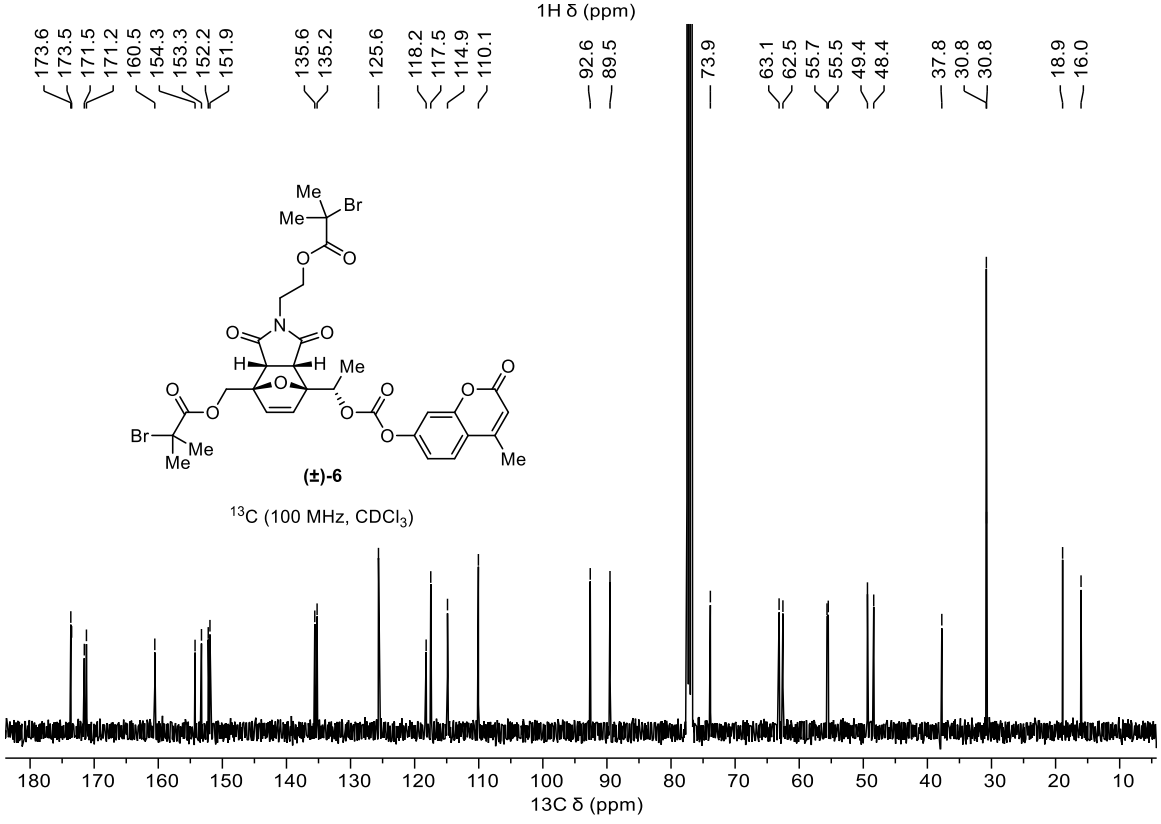
173.6 173.5 171.5 171.2 160.5 154.3 153.3 152.2 151.9 135.6 135.2 125.6 118.2 117.5 114.9 110.1 92.6 89.5 73.9 63.1 62.5 55.7 55.5 49.4 48.4 37.8 30.8 30.8 18.9 16.0
(±)-6
^{13}C (100 MHz, $CDCl_3$)
180 170 160 150 140 130 120 110 100 90 80 70 60 50 40 30 20 10
13C δ (ppm)

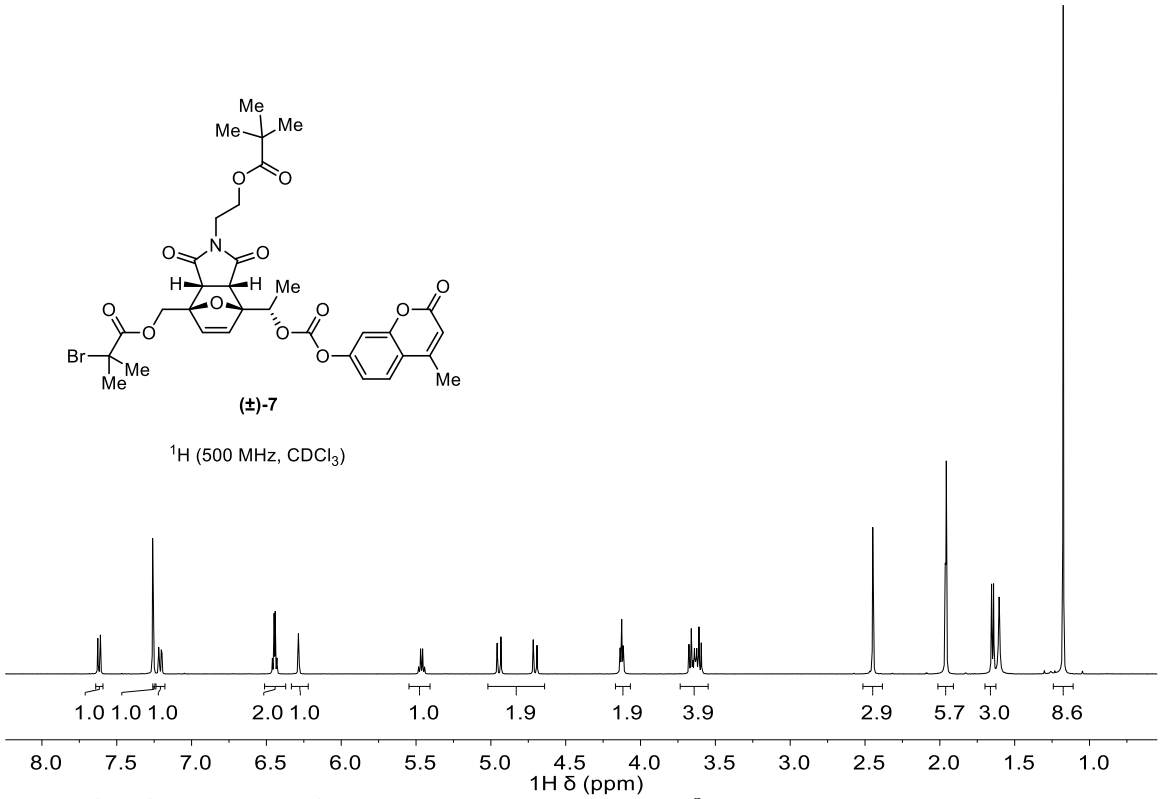
(±)-7
^{1}H (500 MHz, $CDCl_3$)
1.0 1.0 1.0 2.0 1.0 1.0 1.9 1.9 3.9 2.9 5.7 3.0 8.6
1H δ (ppm)

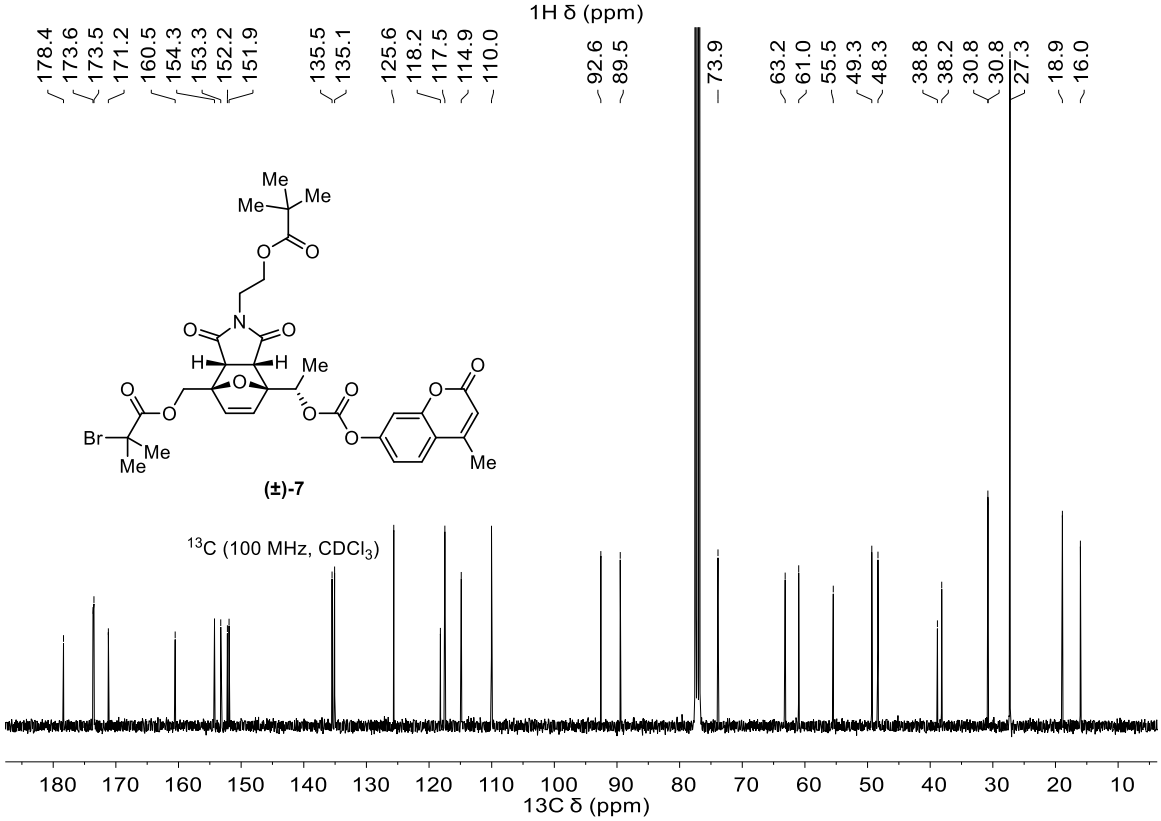
178.4 173.6 173.5 171.2 160.5 154.3 153.3 152.2 151.9 135.5 135.1 125.6 118.2 117.5 114.9 110.0 92.6 89.5 73.9 63.2 61.0 55.5 49.3 48.3 38.8 38.2 30.8 30.8 27.3 18.9 16.0
(±)-7
^{13}C (100 MHz, $CDCl_3$)
13C δ (ppm)

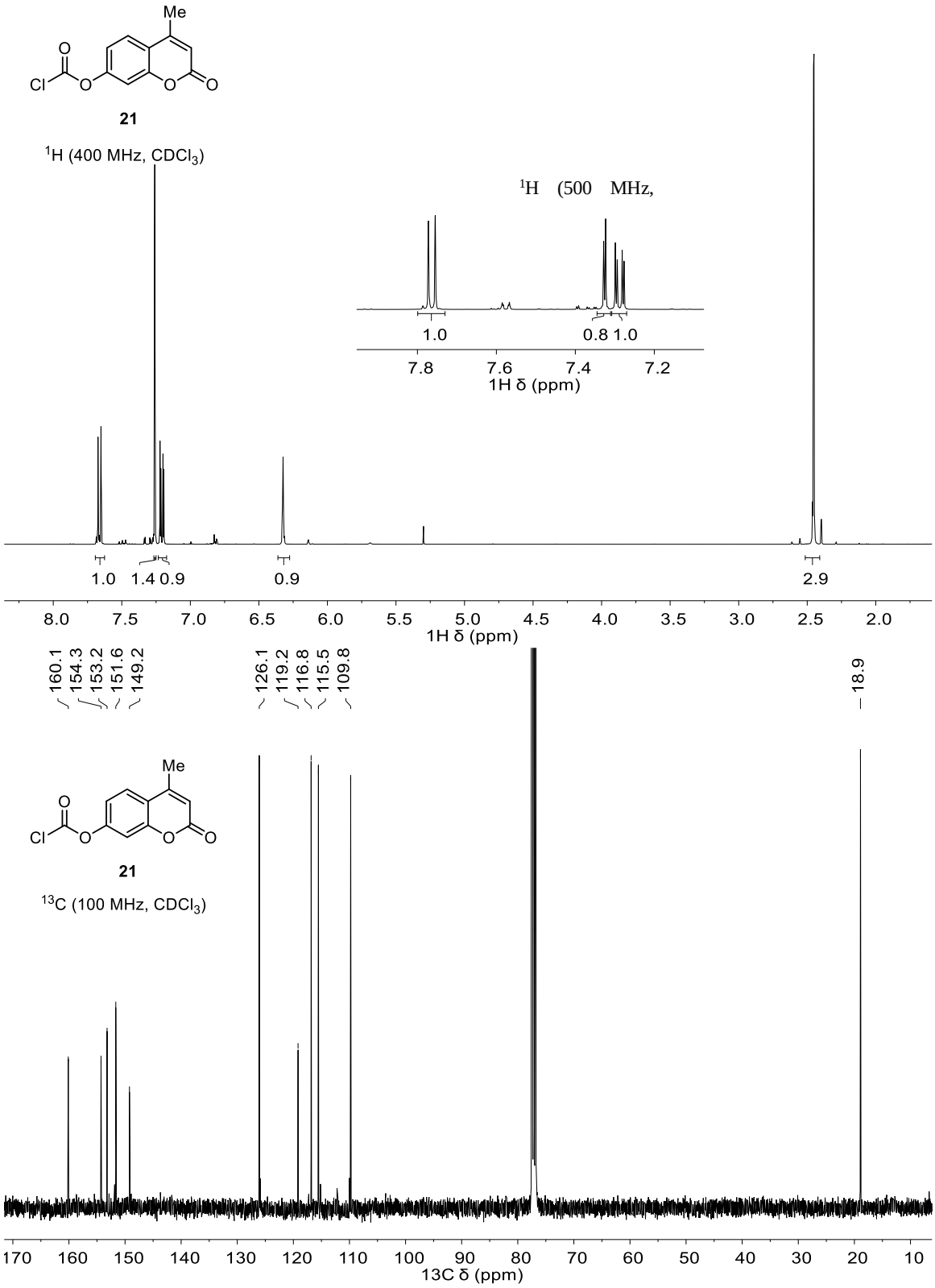
Me
O
Cl
O
O
O
21
1H (400 MHz, CDCl3)
1H (500 MHz,
1.0
0.8 1.0
7.8
7.6
7.4
7.2
1H δ (ppm)
1.0
1.4 0.9
0.9
2.9
8.0
7.5
7.0
6.5
6.0
5.5
5.0
4.5
4.0
3.5
3.0
2.5
2.0
1H δ (ppm)
160.1
154.3
153.2
151.6
149.2
126.1
119.2
116.8
115.5
109.8
18.9
Me
O
Cl
O
O
O
21
13C (100 MHz, CDCl3)
170
160
150
140
130
120
110
100
90
80
70
60
50
40
30
20
10
13C δ (ppm)

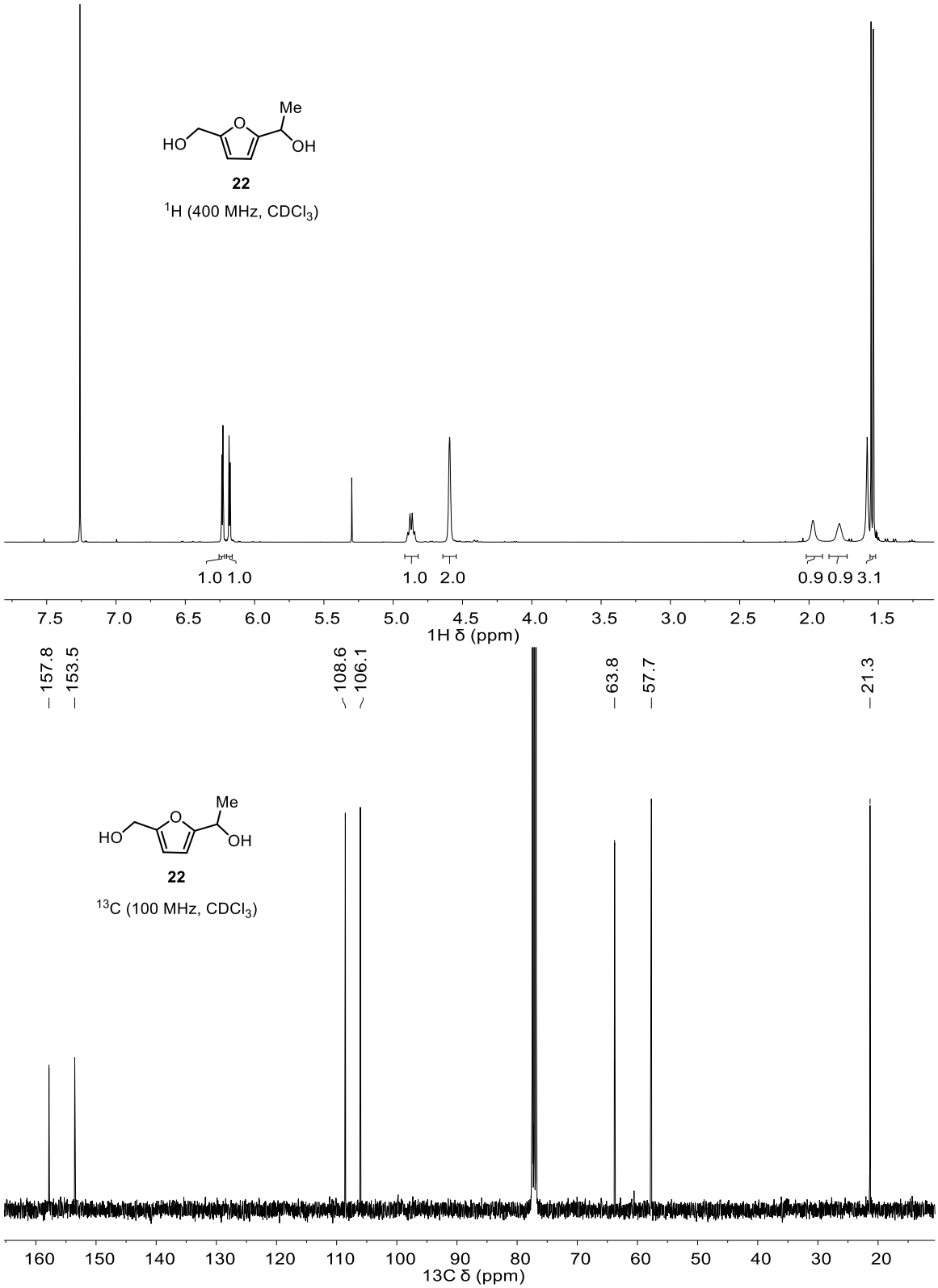
Me
HO
OH
22
1H (400 MHz, CDCl3)
1.0 1.0
1.0 2.0
0.9 0.9 3.1
7.5 7.0 6.5 6.0 5.5 5.0 4.5 4.0 3.5 3.0 2.5 2.0 1.5
1H δ (ppm)
157.8
153.5
108.6
106.1
63.8
57.7
21.3
Me
HO
OH
22
13C (100 MHz, CDCl3)
160 150 140 130 120 110 100 90 80 70 60 50 40 30 20
13C δ (ppm)

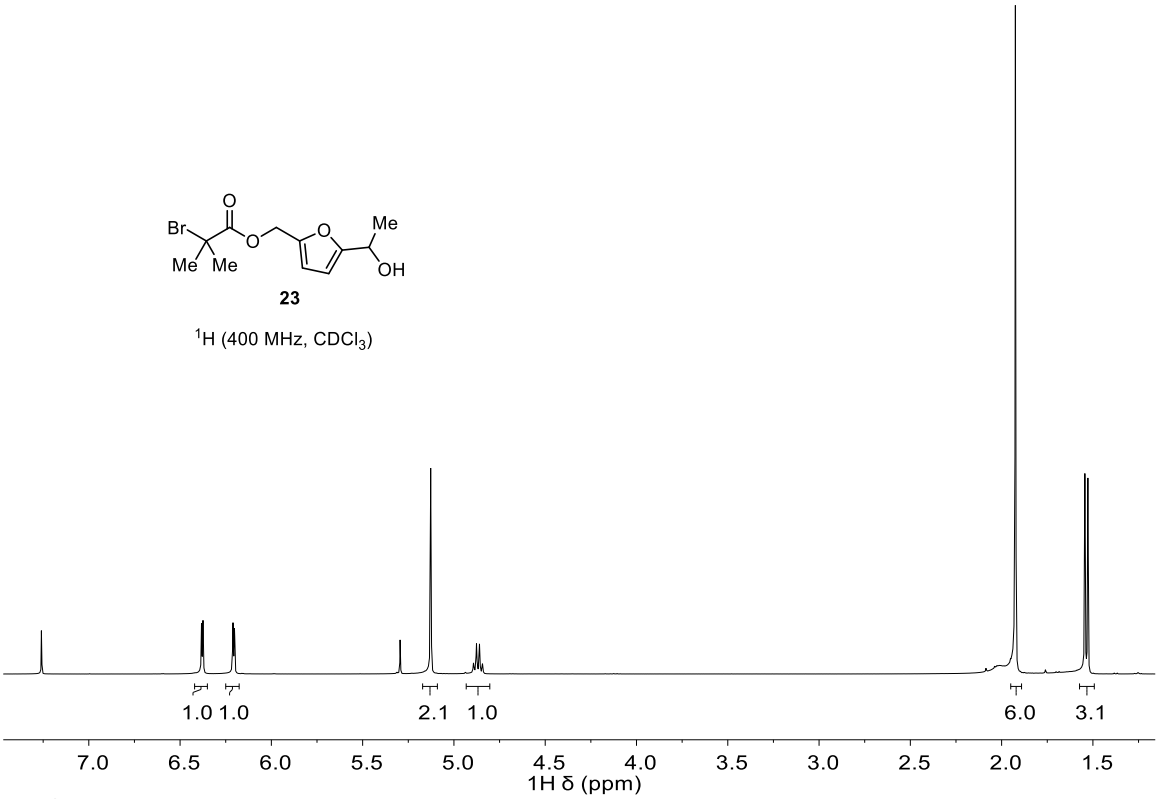
Br
O
O
Me
Me
Me
O
OH
23
1H (400 MHz, CDCl3)
1.0 1.0
2.1
1.0
6.0
3.1
7.0
6.5
6.0
5.5
5.0
4.5
4.0
3.5
3.0
2.5
2.0
1.5
1H δ (ppm)

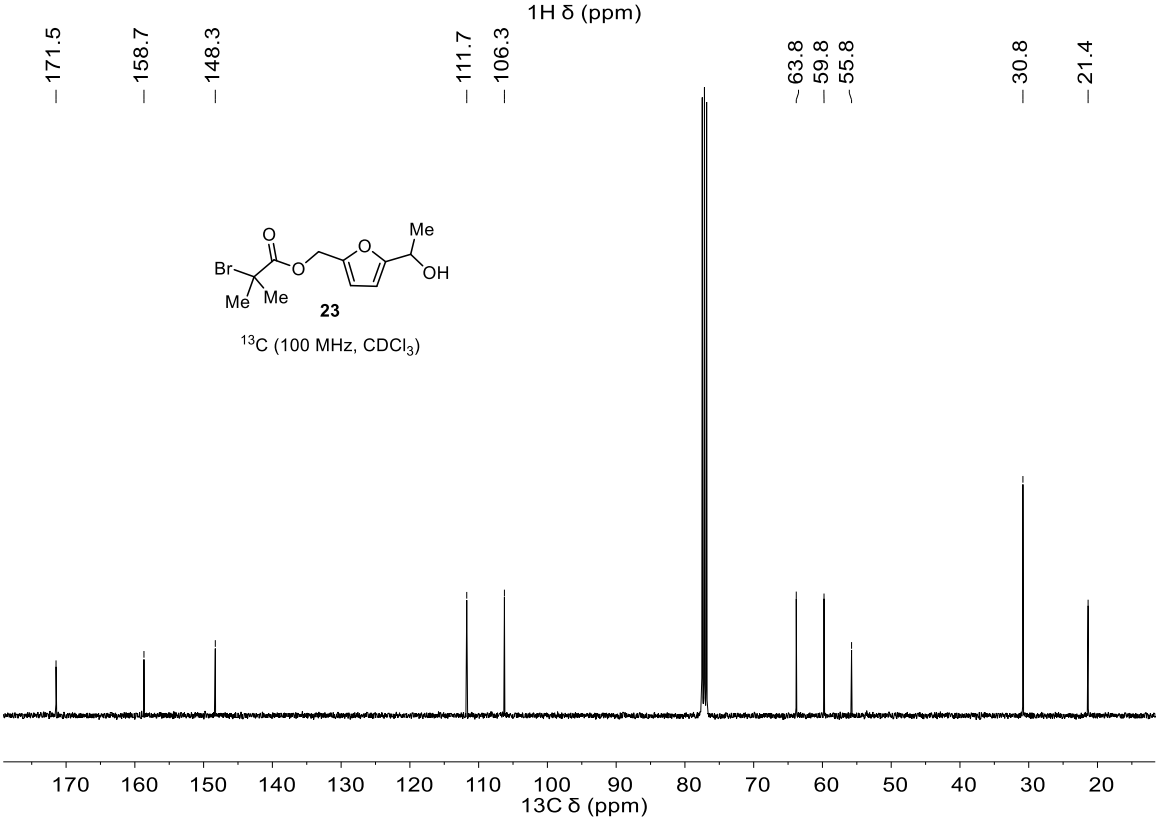
171.5
158.7
148.3
111.7
106.3
63.8
59.8
55.8
30.8
21.4
Br
O
O
Me
Me
Me
O
OH
23
13C (100 MHz, CDCl3)
170
160
150
140
130
120
110
100
90
80
70
60
50
40
30
20
13C δ (ppm)

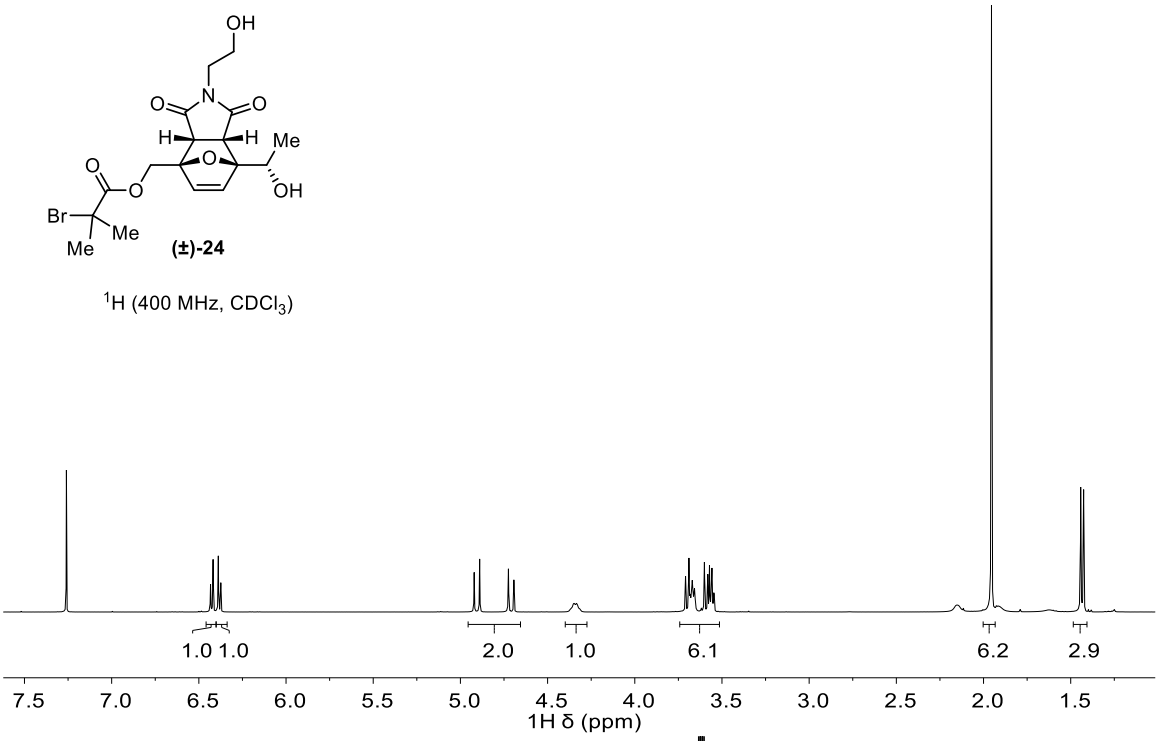
OH
N
O
O
H
H
Me
O
O
O
OH
Br
Me
Me
(±)-24
1H (400 MHz, CDCl3)
1.0 1.0
2.0
1.0
6.1
6.2
2.9
7.5 7.0 6.5 6.0 5.5 5.0 4.5 4.0 3.5 3.0 2.5 2.0 1.5
1H δ (ppm)

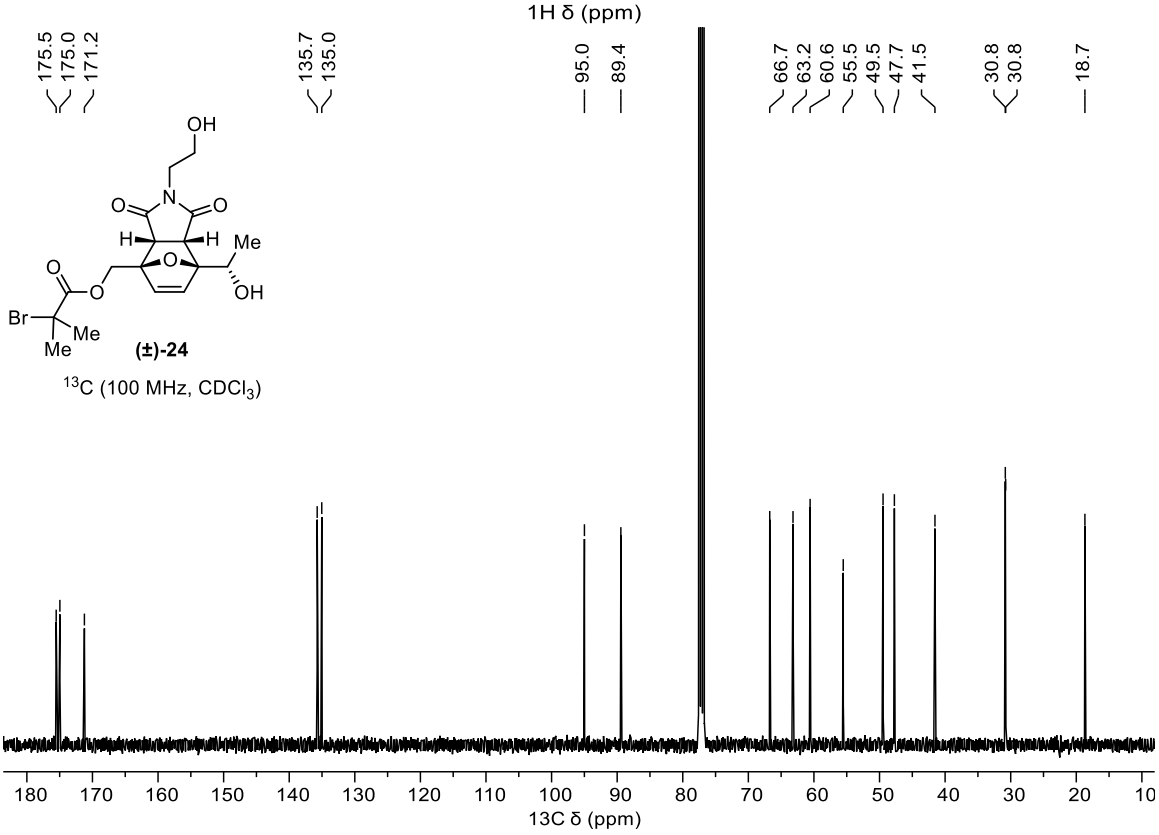
175.5
175.0
171.2
135.7
135.0
95.0
89.4
66.7
63.2
60.6
55.5
49.5
47.7
41.5
30.8
30.8
18.7
OH
N
O
O
H
H
Me
O
O
O
OH
Br
Me
Me
(±)-24
13C (100 MHz, CDCl3)
180 170 160 150 140 130 120 110 100 90 80 70 60 50 40 30 20 10
13C δ (ppm)

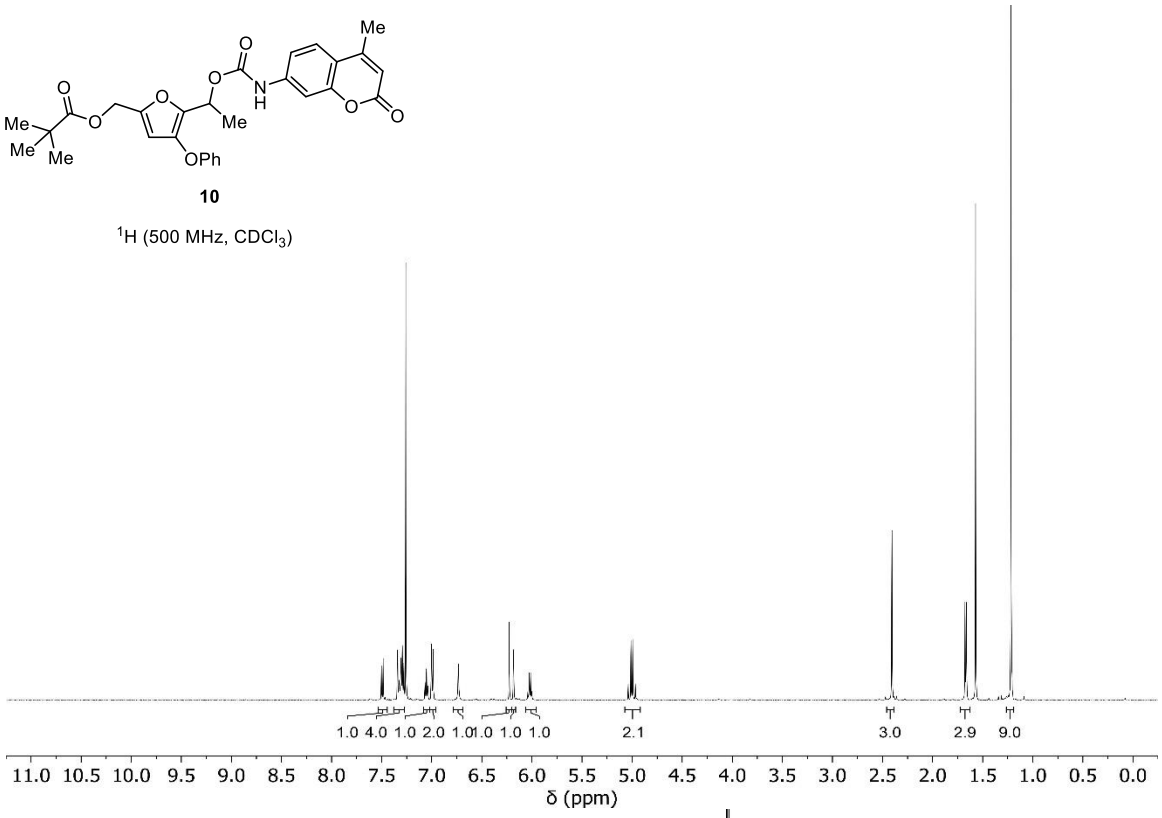

10

^{1}H (500 MHz, $CDCl_3$)

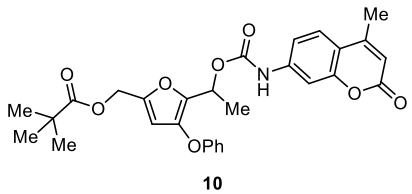

10

^{13}C (125 MHz, $CDCl_3$)

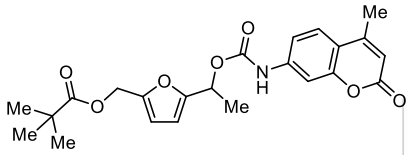

11

^{1}H (400 MHz, $CDCl_3$)

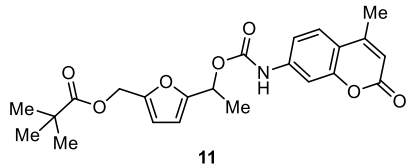

11

^{13}C (100 MHz, $CDCl_3$)

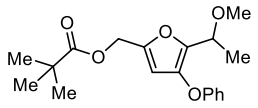

13

^{1}H (400 MHz, $CDCl_3$)

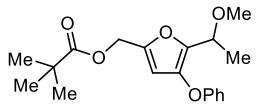

13

^{13}C (100 MHz, $CDCl_3$)

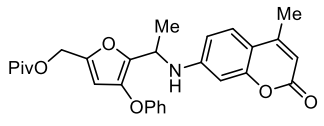

13N

^{1}H (400 MHz, $CDCl_3$)

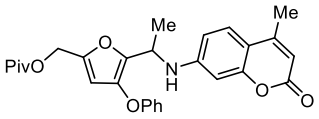

13N

^{13}C (100 MHz, $CDCl_3$)

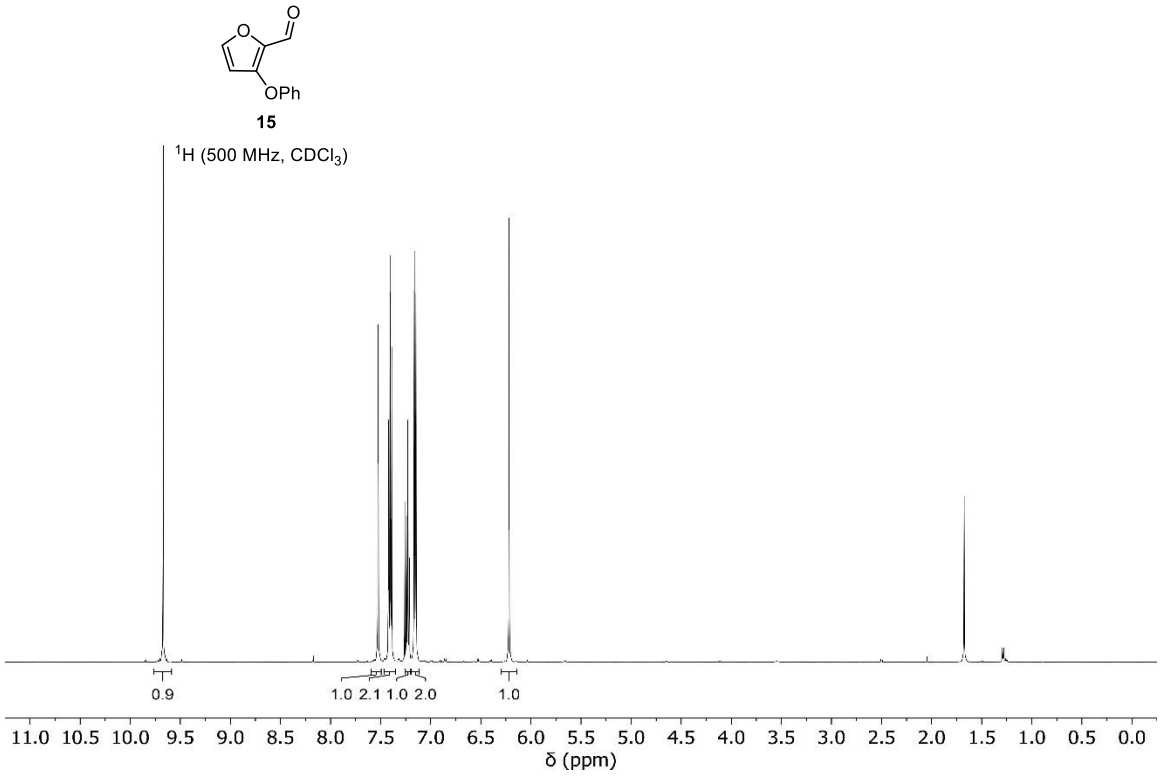
O
O
OPh
15
^{1}H (500 MHz, CDCl$_3$)
0.9
1.0 2.1 1.0 2.0
1.0
11.0 10.5 10.0 9.5 9.0 8.5 8.0 7.5 7.0 6.5 6.0 5.5 5.0 4.5 4.0 3.5 3.0 2.5 2.0 1.5 1.0 0.5 0.0
δ (ppm)

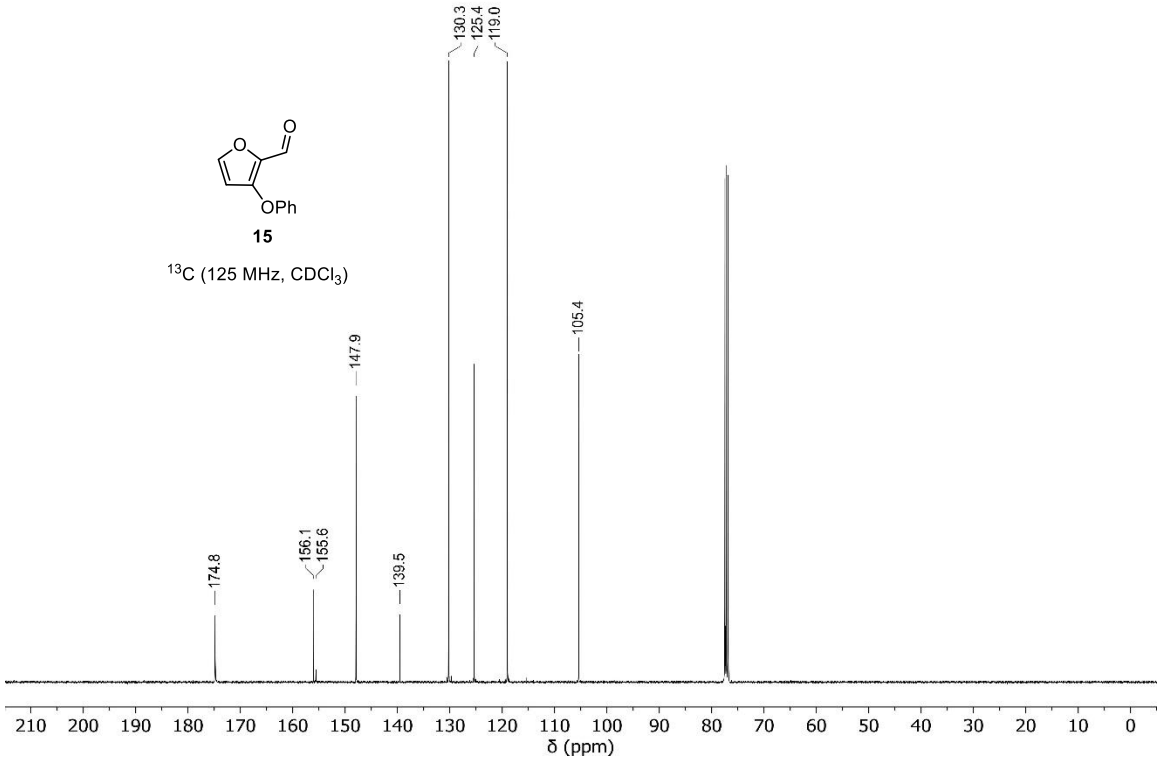
130.3
125.4
119.0
O
O
OPh
15
^{13}C (125 MHz, CDCl$_3$)
147.9
105.4
174.8
156.1
155.6
139.5
210 200 190 180 170 160 150 140 130 120 110 100 90 80 70 60 50 40 30 20 10 0
δ (ppm)

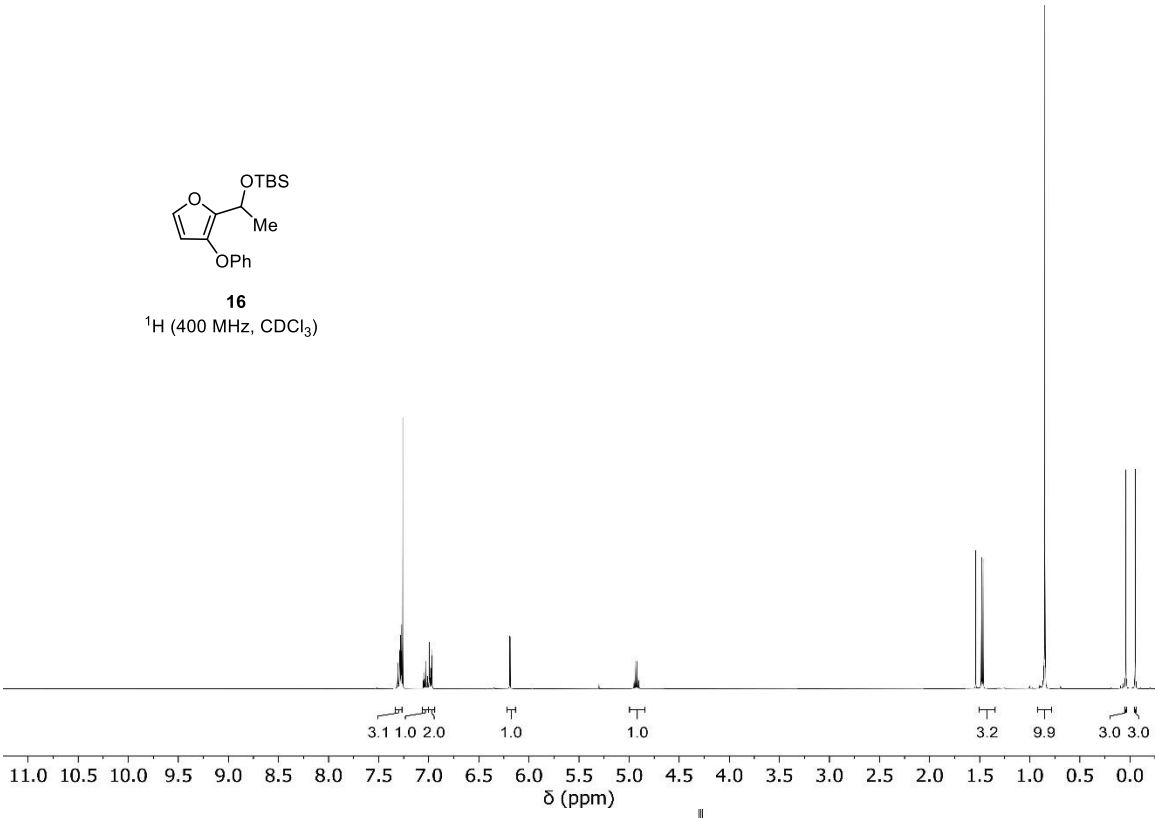
OTBS
Me
OPh
16
1H (400 MHz, CDCl3)
3.1 1.0 2.0
1.0
1.0
3.2
9.9
3.0 3.0
δ (ppm)

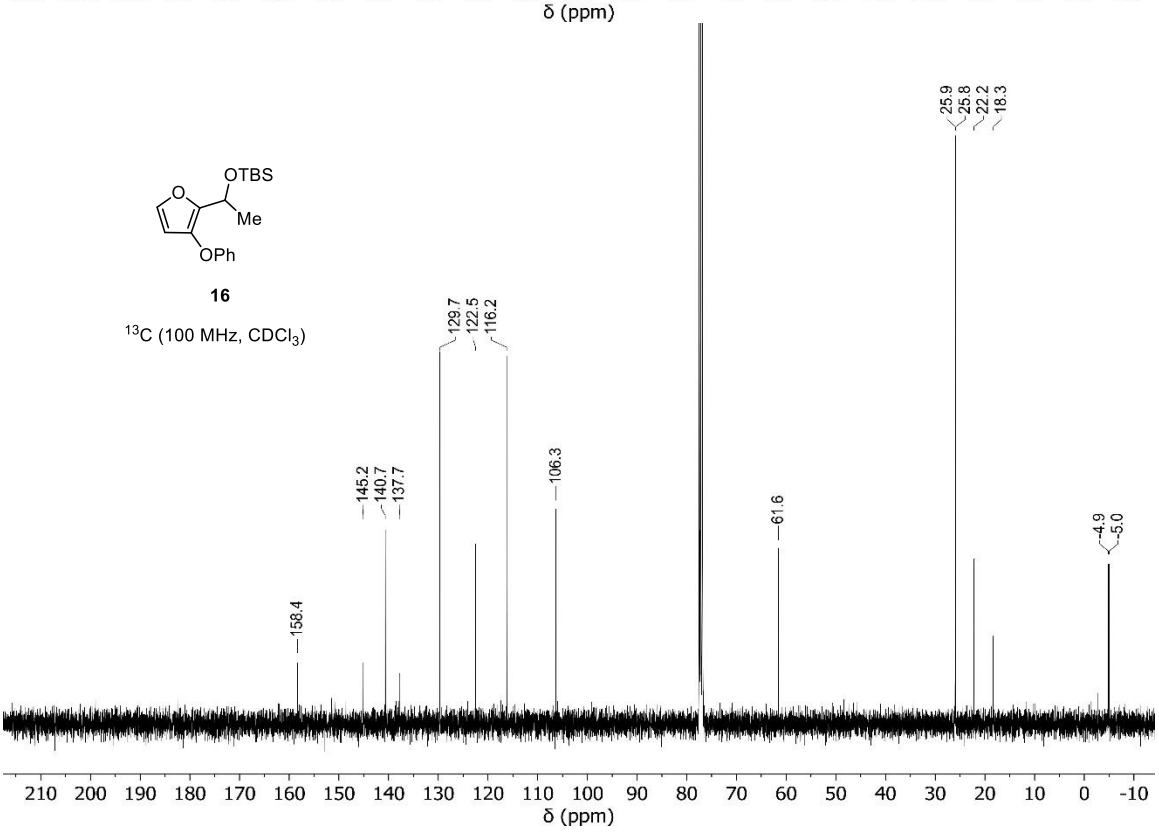
OTBS
Me
OPh
16
13C (100 MHz, CDCl3)
158.4
145.2
140.7
137.7
129.7
122.5
116.2
106.3
61.6
25.9
25.8
22.2
18.3
-4.9
-5.0
δ (ppm)

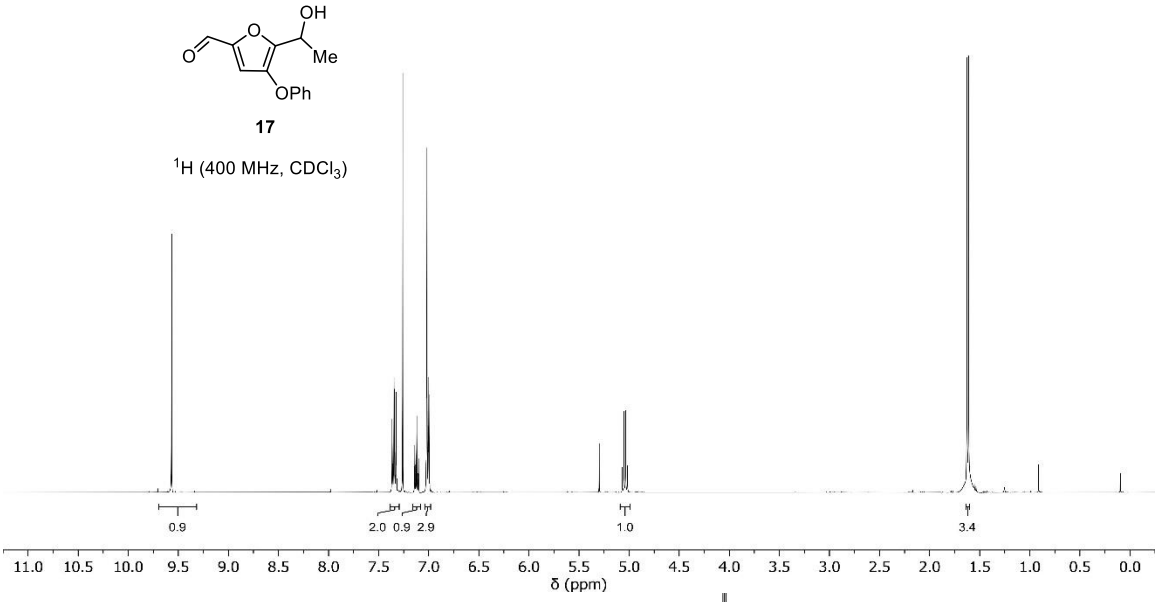
OH
O
Me
OPh
17
^{1}H (400 MHz, $CDCl_3$)
0.9
2.0 0.9 2.9
1.0
3.4
δ (ppm)

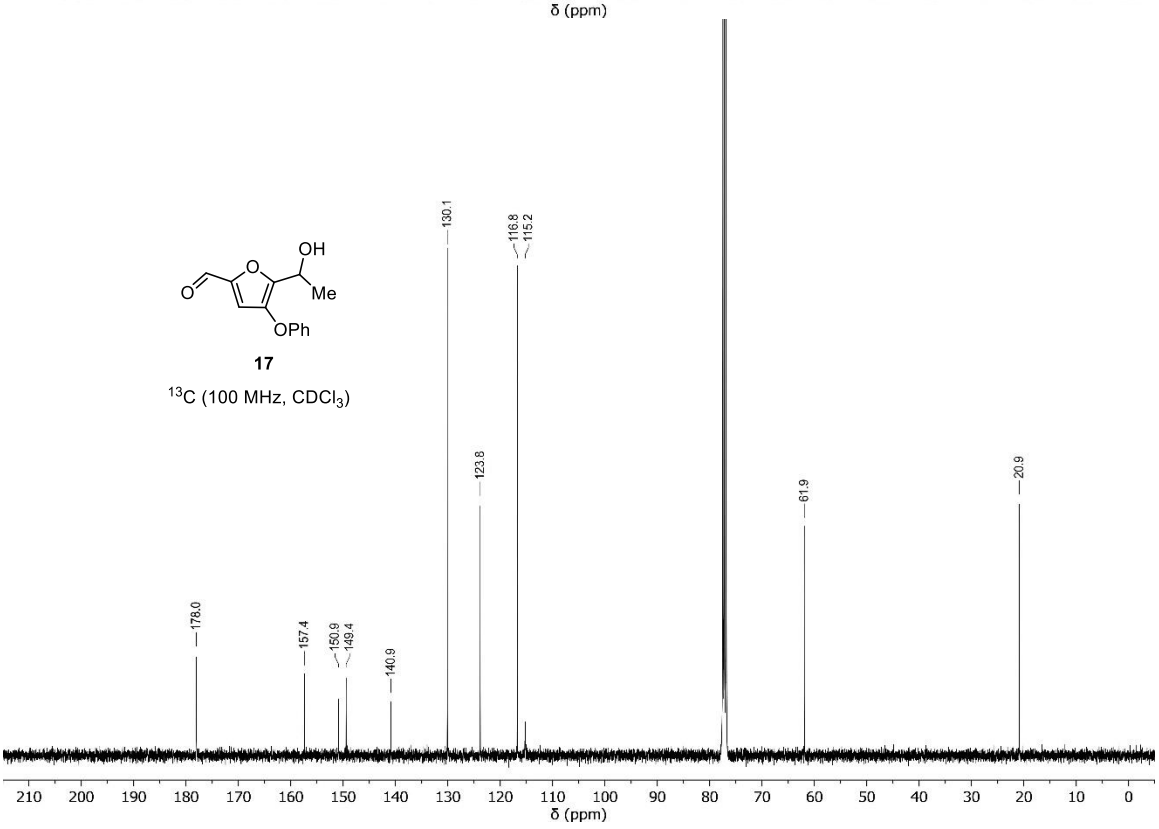
OH
O
Me
OPh
17
^{13}C (100 MHz, $CDCl_3$)
178.0
157.4
150.9
149.4
140.9
130.1
123.8
116.8
115.2
61.9
20.9
δ (ppm)

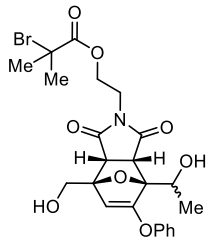

(±)-18

^{1}H (400 MHz, $CDCl_3$)

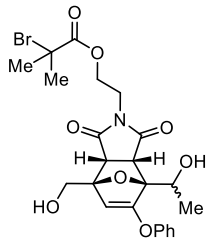

(±)-18

^{13}C (100 MHz, $CDCl_3$)

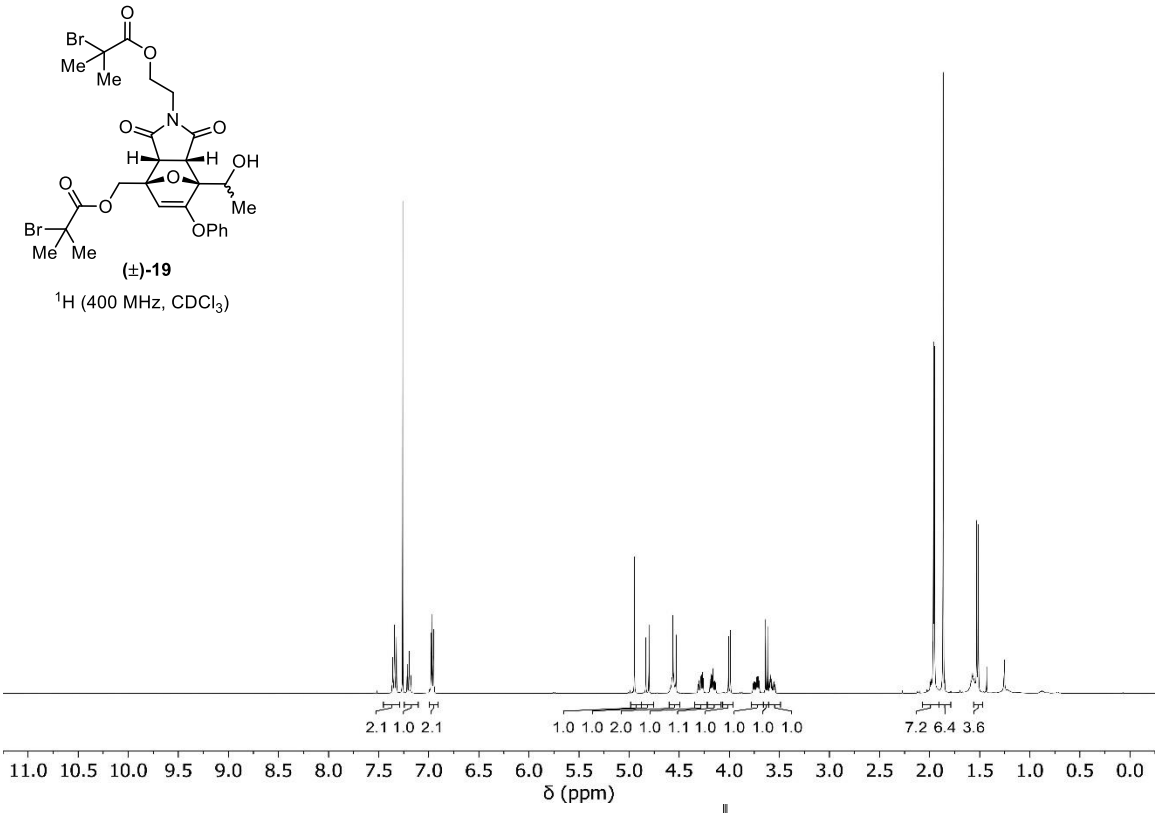
(±)-19
^{1}H (400 MHz, CDCl$_3$)
2.1 1.0 2.1
1.0 1.0 2.0 1.0 1.1 1.0 1.0 1.0 1.0
7.2 6.4 3.6
δ (ppm)

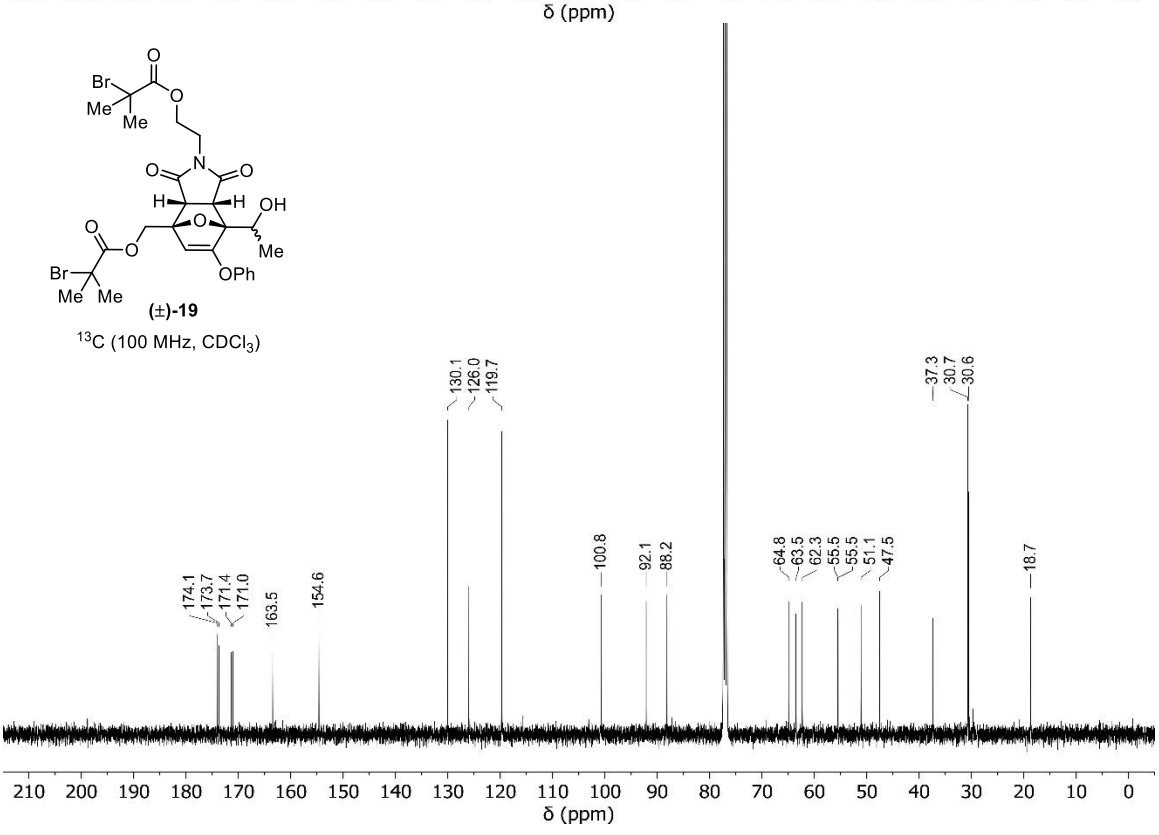
(±)-19
^{13}C (100 MHz, CDCl$_3$)
174.1
173.7
171.4
171.0
163.5
154.6
130.1
126.0
119.7
100.8
92.1
88.2
64.8
63.5
62.3
55.5
55.5
51.1
47.5
37.3
30.7
30.6
18.7
δ (ppm)

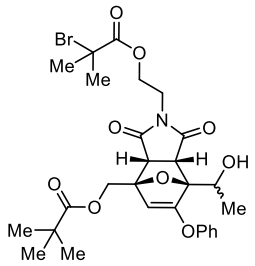

(±)-19-control

^{1}H (400 MHz, $CDCl_3$)

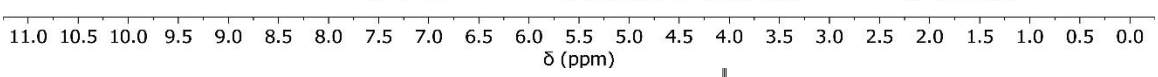

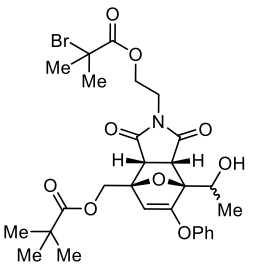

(±)-19-control

^{13}C (100 MHz, $CDCl_3$)

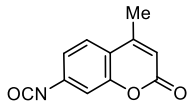

coumNCO

^{1}H (400 MHz, $CDCl_3$)

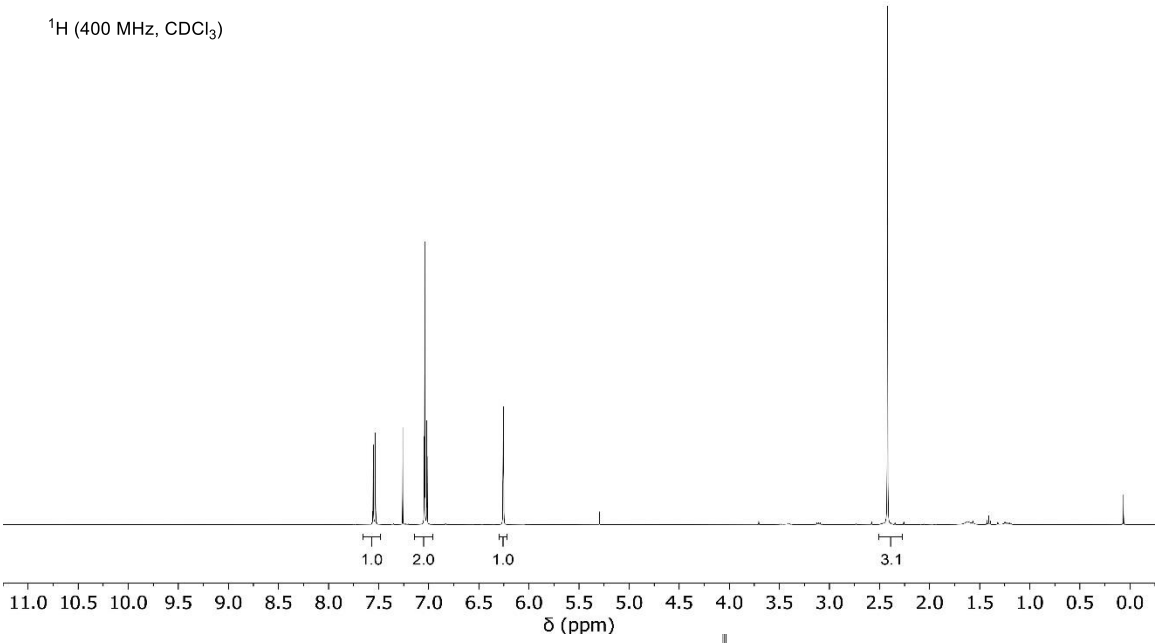

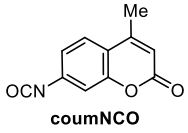

coumNCO

^{13}C (100 MHz, $CDCl_3$)

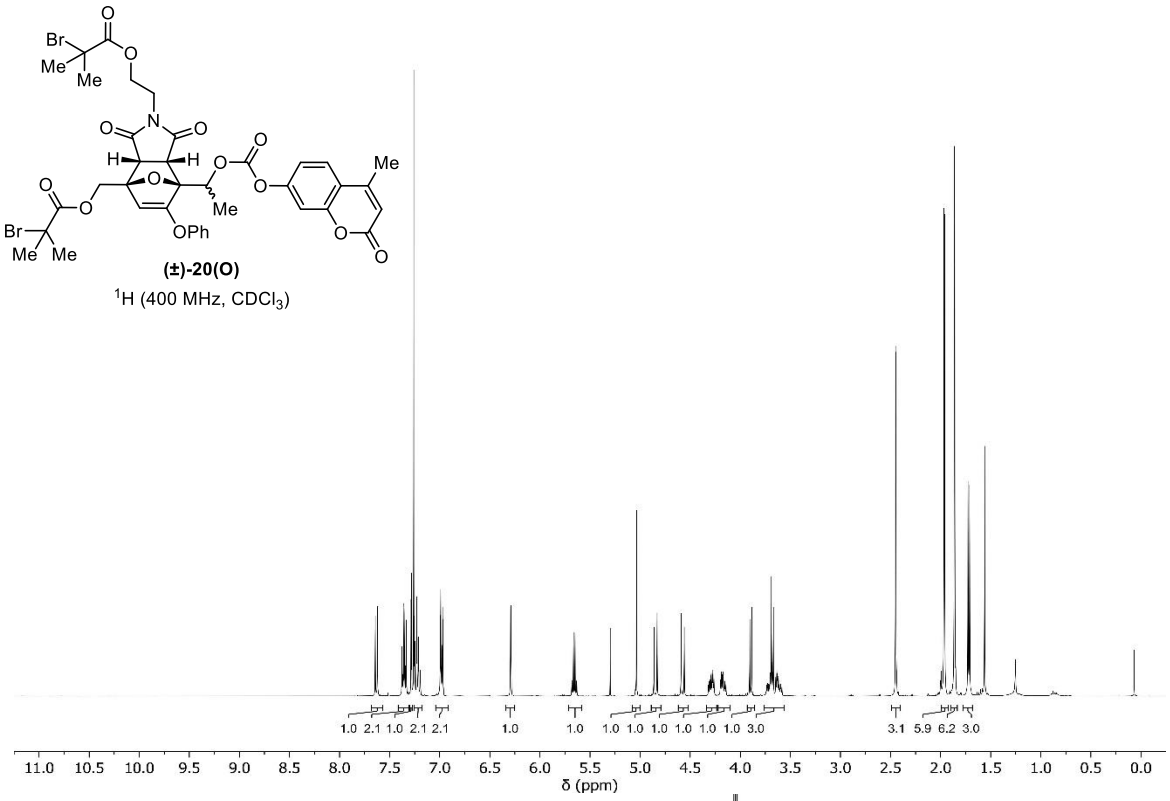
(±)-20(O)
^{1}H (400 MHz, $CDCl_3$)
δ (ppm)

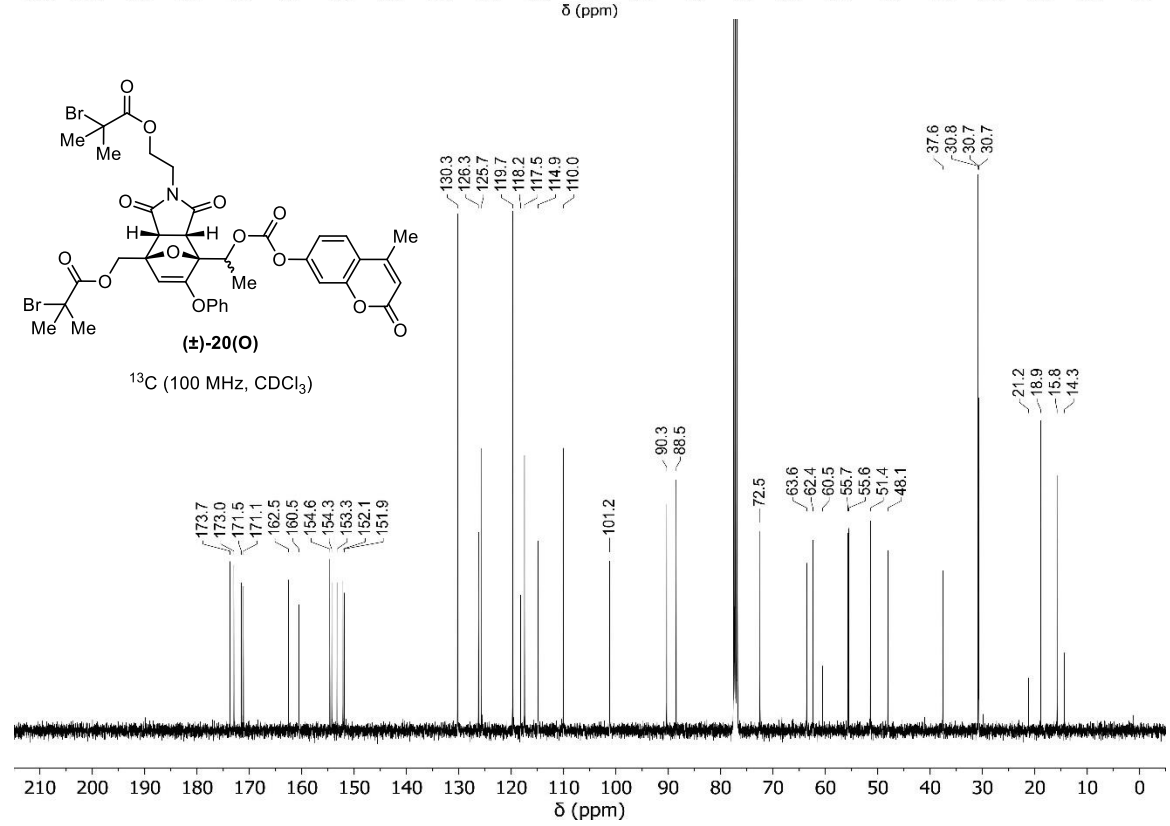
(±)-20(O)
^{13}C (100 MHz, $CDCl_3$)
δ (ppm)

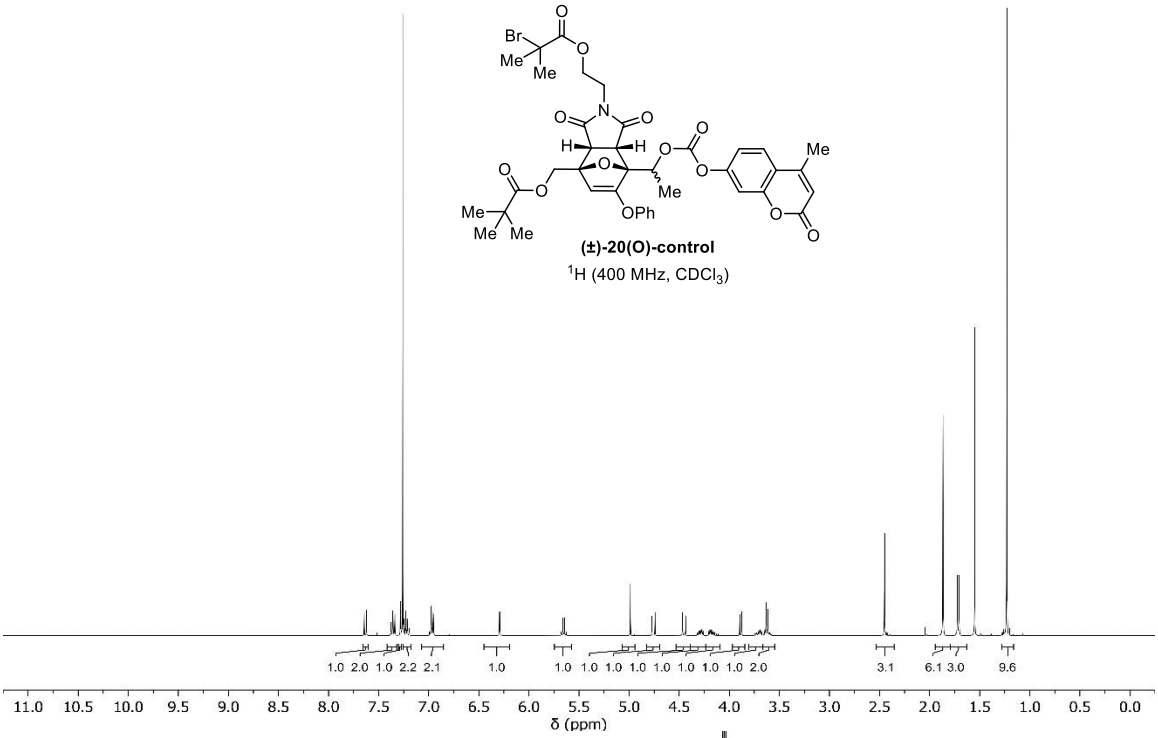
(±)-20(O)-control
^{1}H (400 MHz, $CDCl_3$)
δ (ppm)

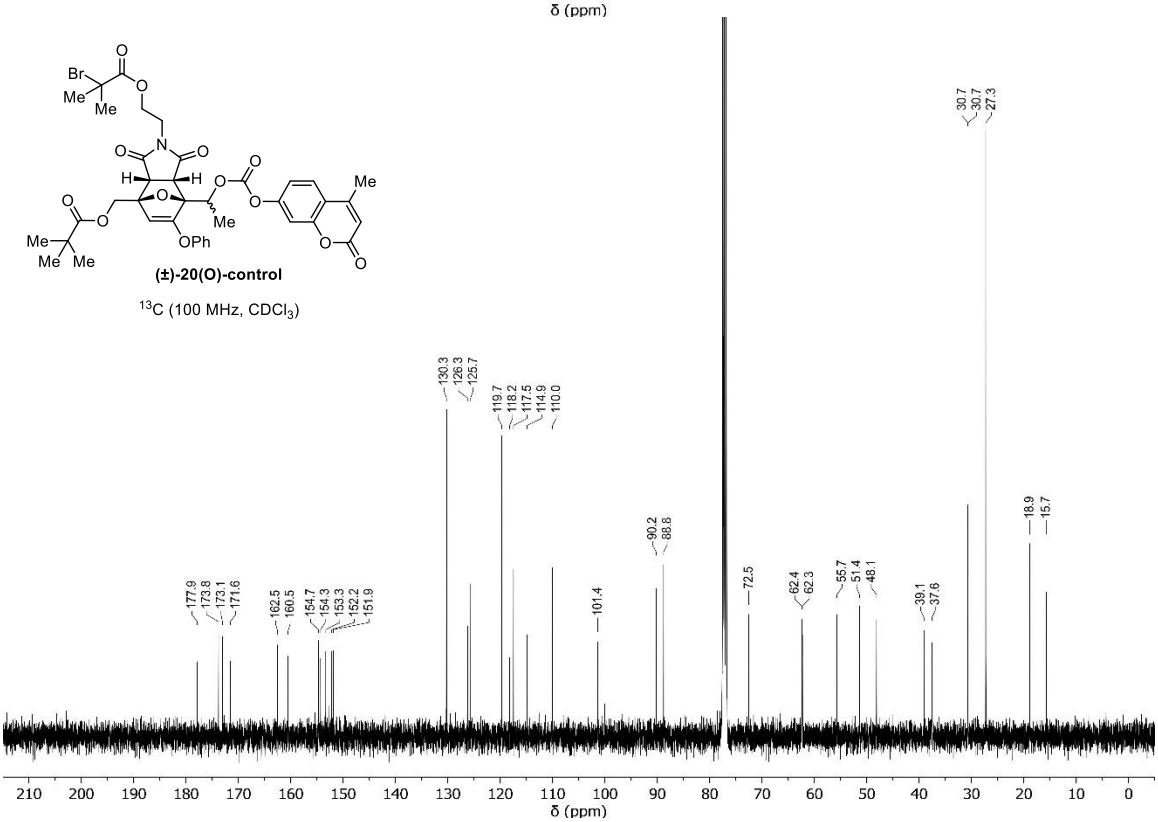
(±)-20(O)-control
^{13}C (100 MHz, $CDCl_3$)
δ (ppm)

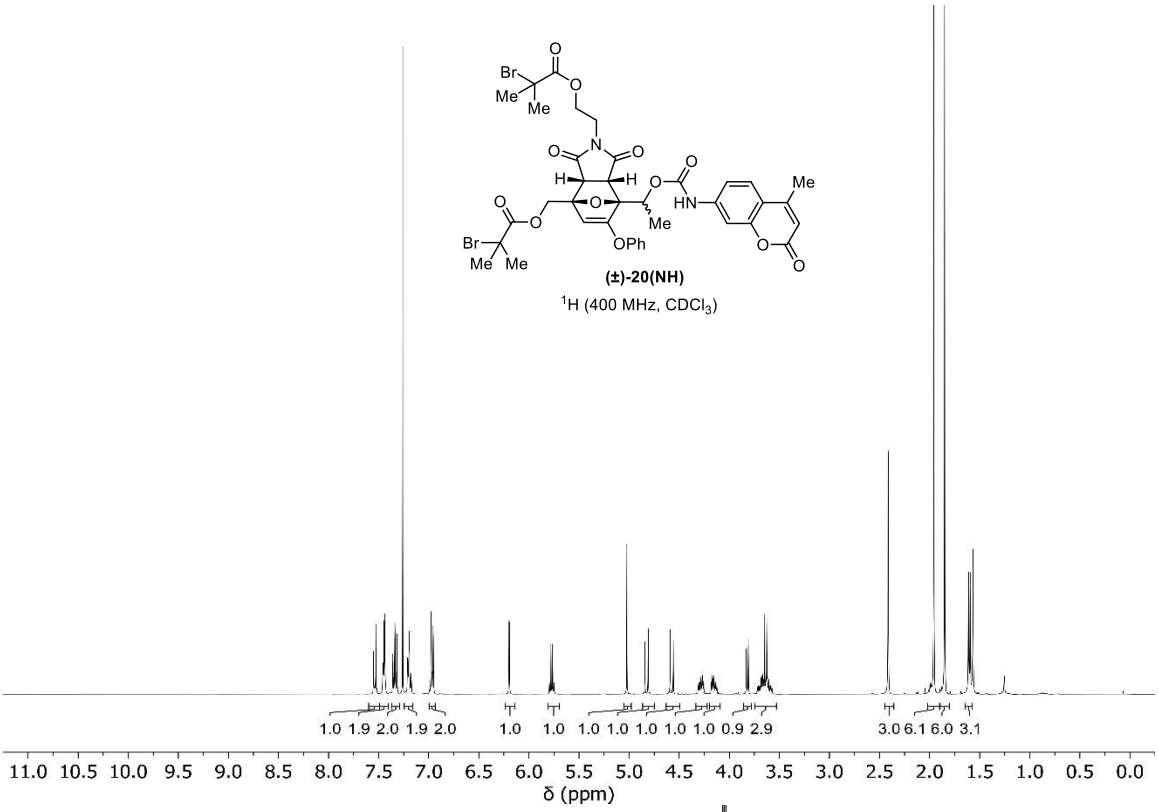
(±)-20(NH)
^{1}H (400 MHz, $CDCl_3$)
1.0 1.9 2.0 1.9 2.0 1.0 1.0 1.0 1.0 1.0 1.0 1.0 0.9 2.9 3.0 6.1 6.0 3.1
δ (ppm)

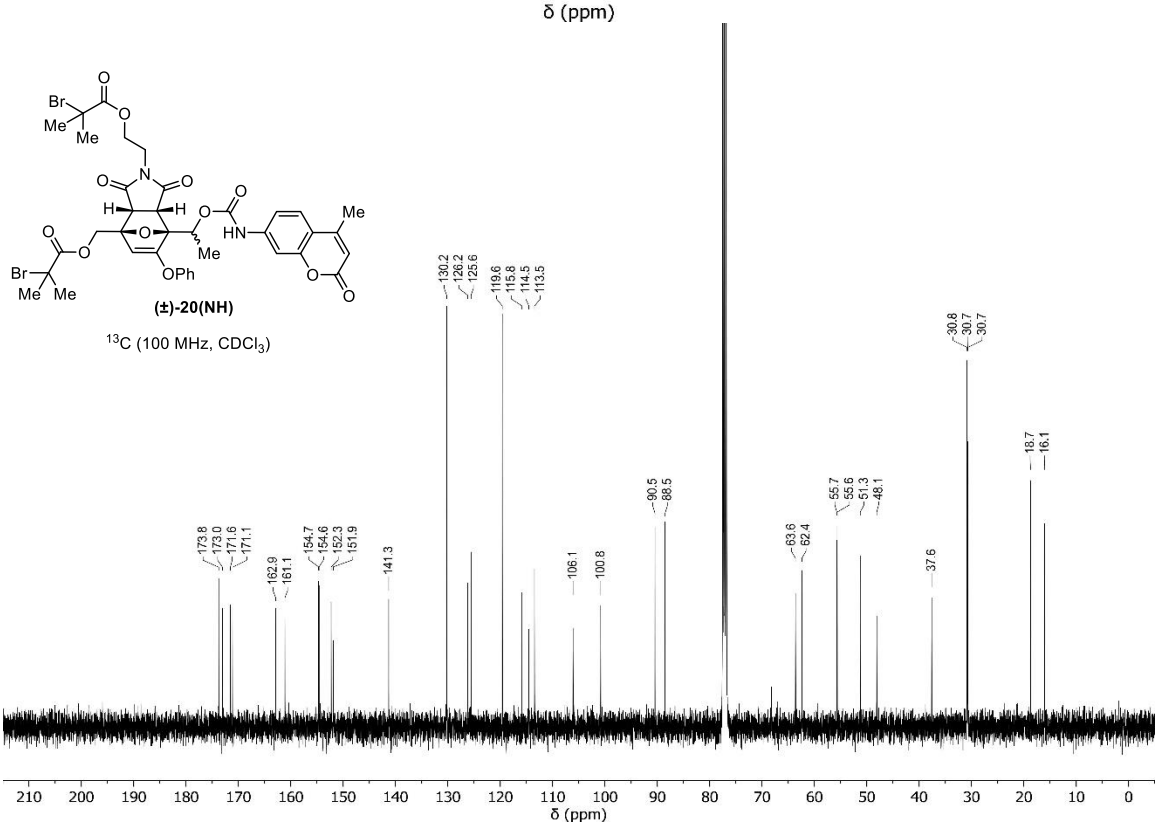
(±)-20(NH)
^{13}C (100 MHz, $CDCl_3$)
173.8 173.0 171.6 171.1 162.9 161.1 154.7 154.6 152.3 151.9 141.3 130.2 126.2 125.6 119.6 115.8 114.5 113.5 106.1 100.8 90.5 88.5 63.6 62.4 55.7 55.6 51.3 48.1 37.6 30.8 30.7 30.7 18.7 16.1
δ (ppm)

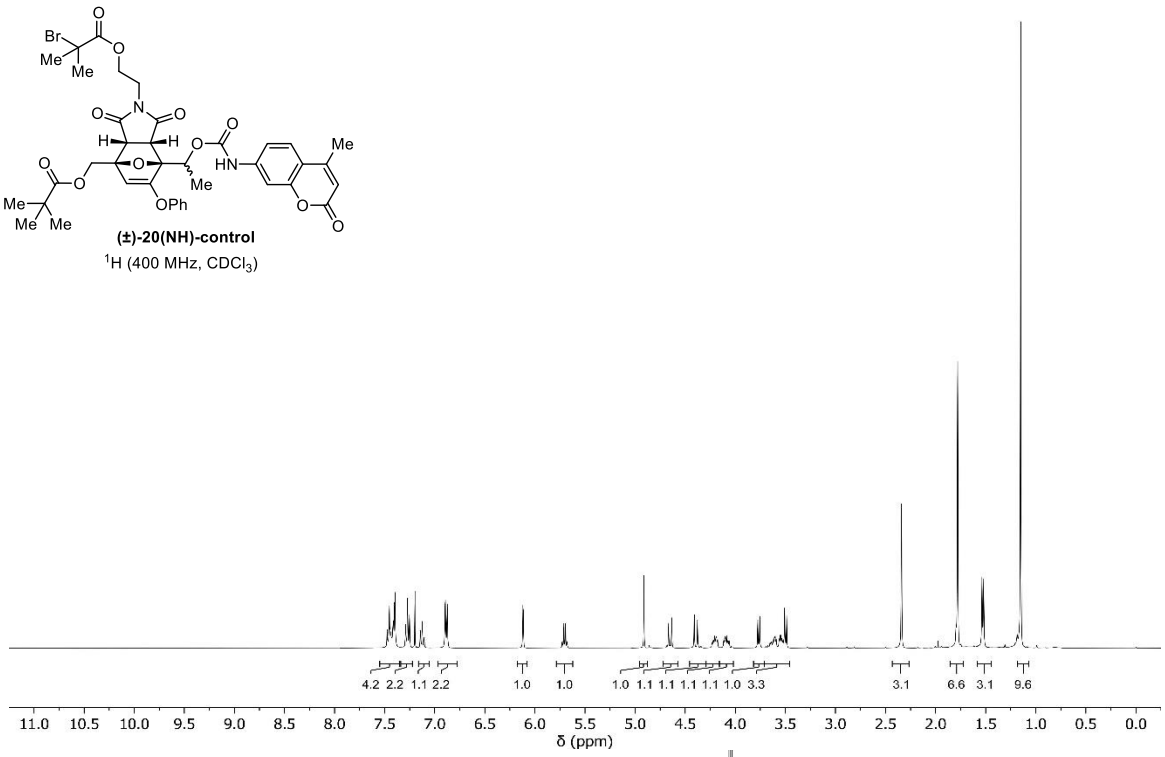
(±)-20(NH)-control
1H (400 MHz, CDCl3)
4.2 2.2 1.1 2.2
1.0
1.0
1.0 1.1 1.1 1.1 1.1 1.0 3.3
3.1
6.6
3.1
9.6
δ (ppm)

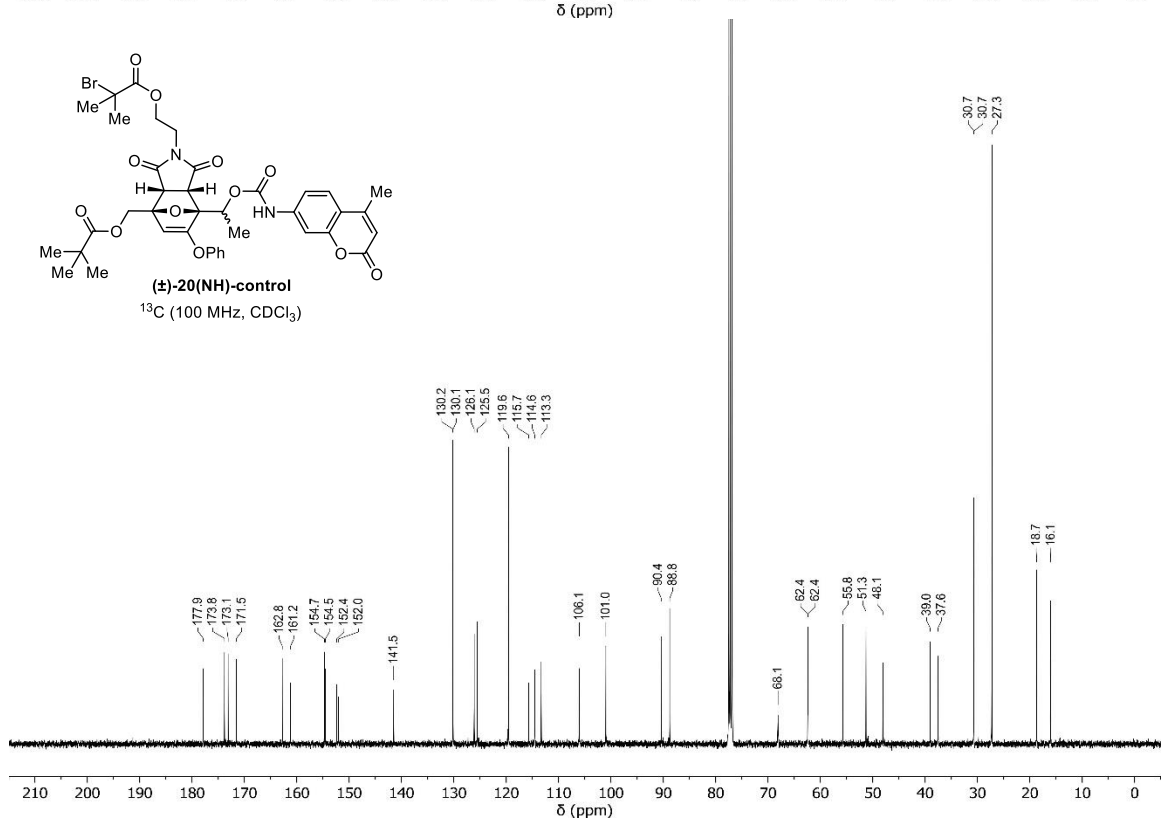
(±)-20(NH)-control
13C (100 MHz, CDCl3)
177.9
173.8
173.1
171.5
162.8
161.2
154.7
154.5
152.4
152.0
141.5
130.2
130.1
126.1
125.5
119.6
115.7
114.6
113.3
106.1
101.0
90.4
88.8
68.1
62.4
62.4
55.8
51.3
48.1
39.0
37.6
30.7
30.7
27.3
18.7
16.1
δ (ppm)

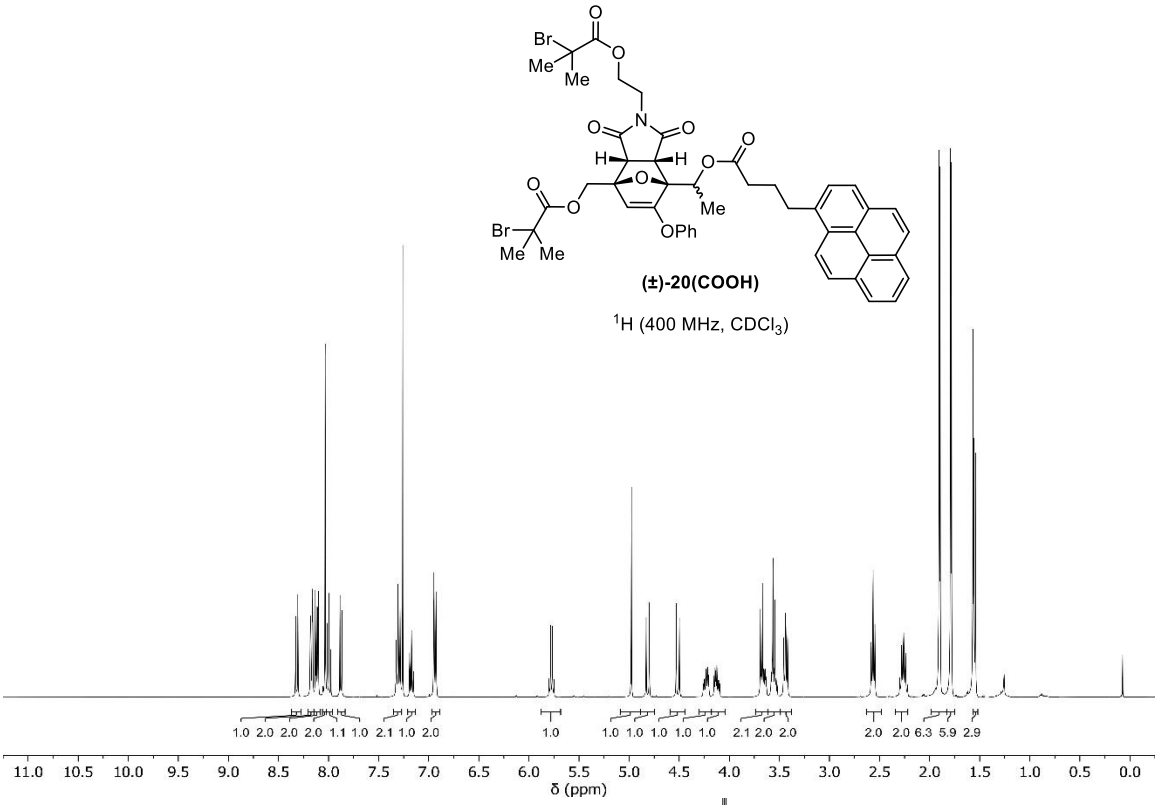
(±)-20(COOH)
^{1}H (400 MHz, CDCl$_3$)
δ (ppm)

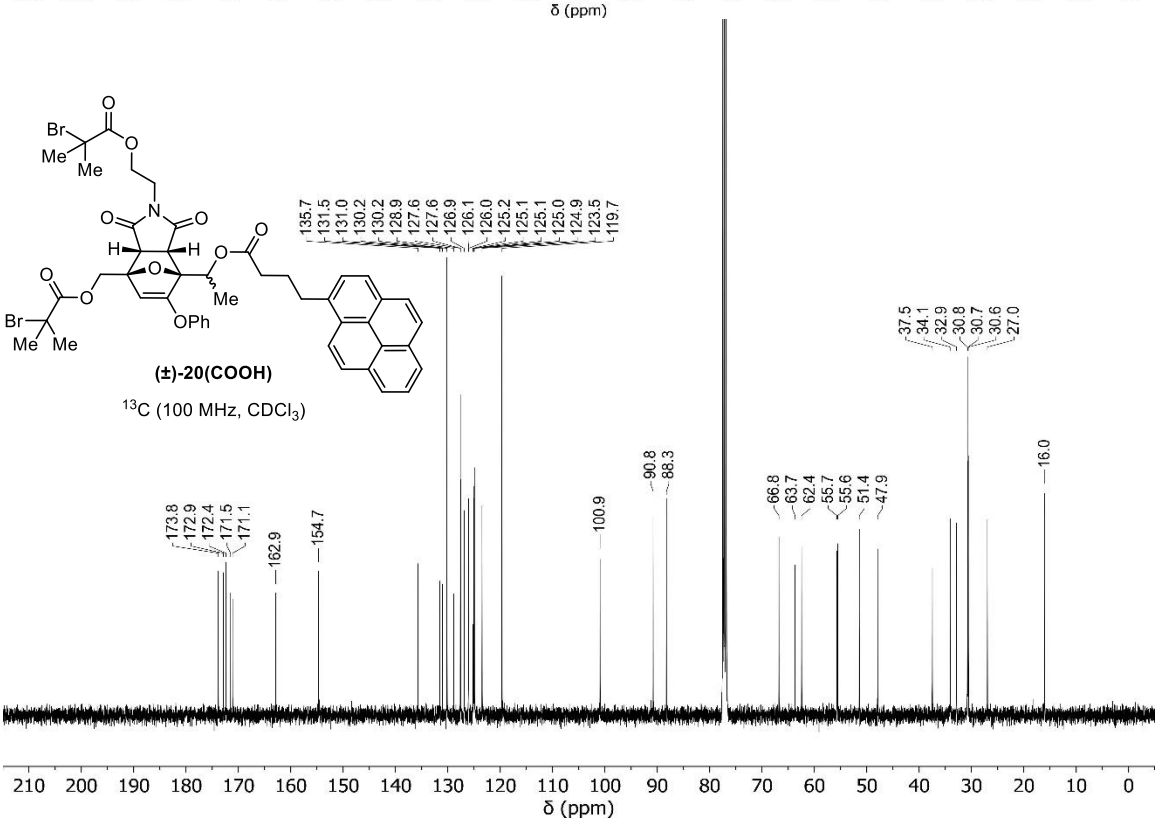
(±)-20(COOH)
^{13}C (100 MHz, CDCl$_3$)
δ (ppm)

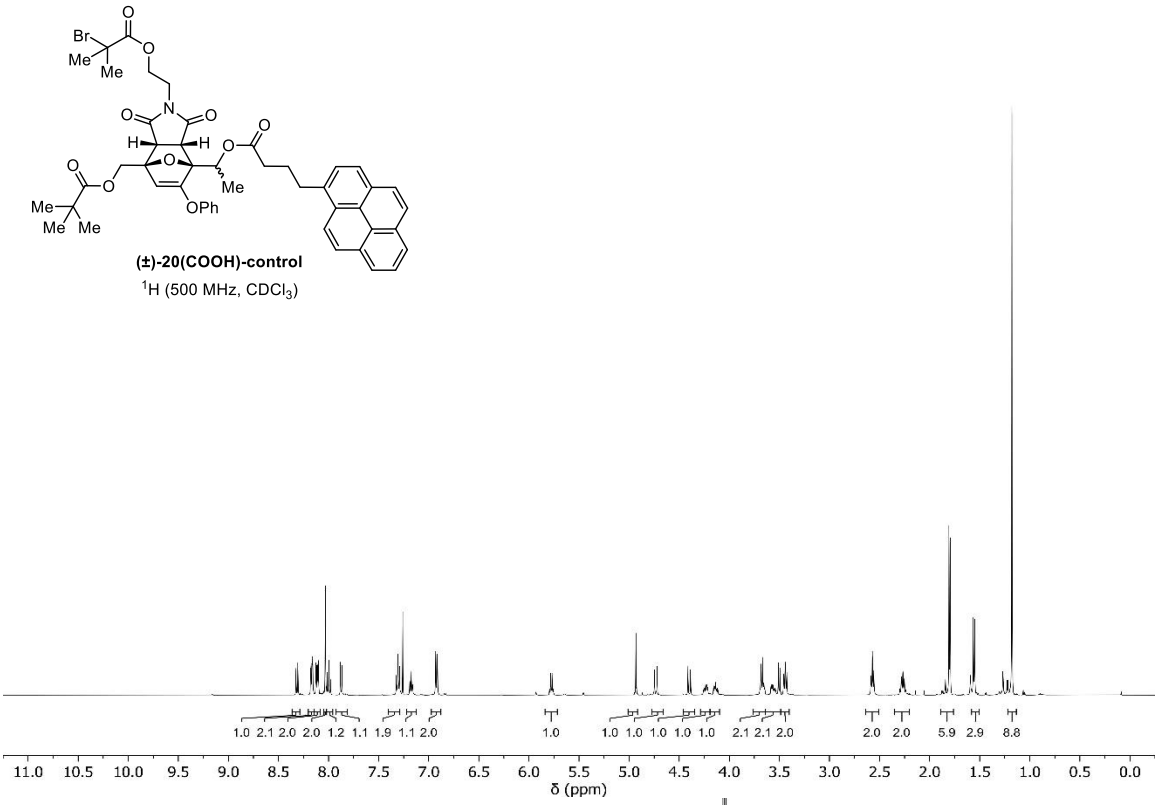
(±)-20(COOH)-control
1H (500 MHz, CDCl3)
δ (ppm)

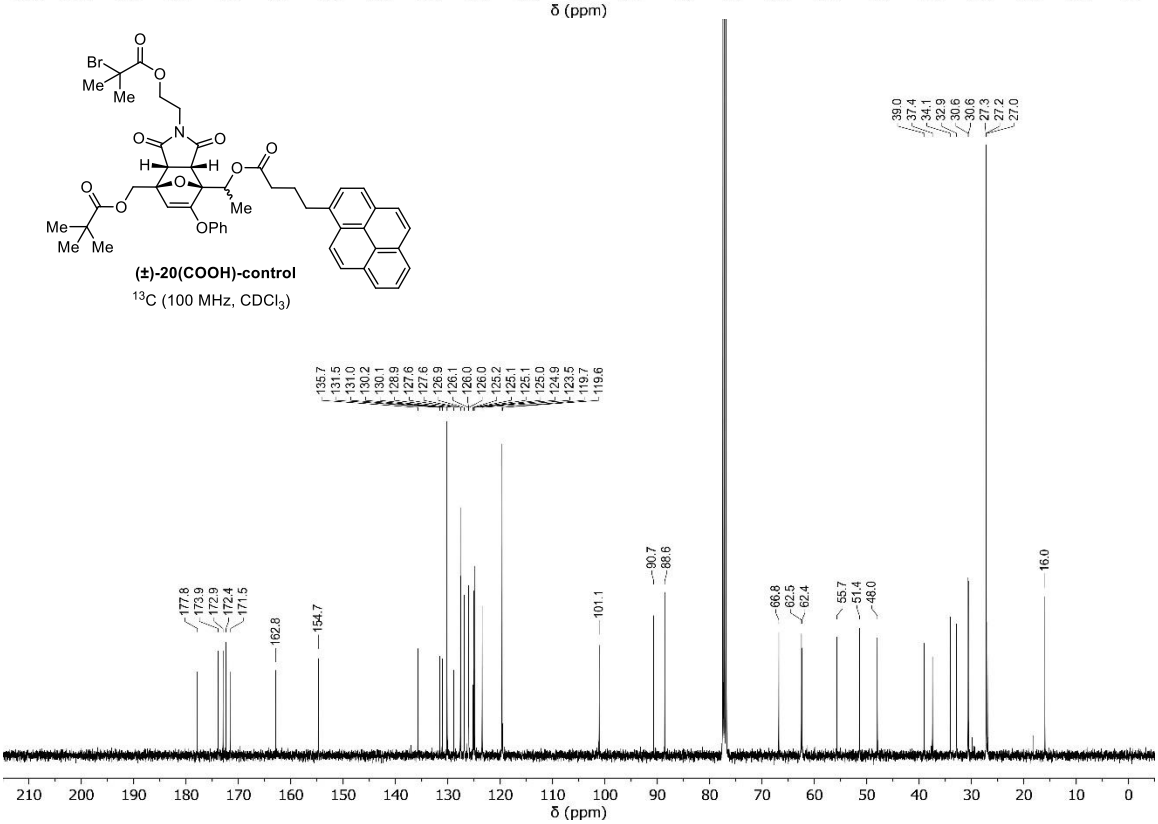
(±)-20(COOH)-control
13C (100 MHz, CDCl3)
δ (ppm)

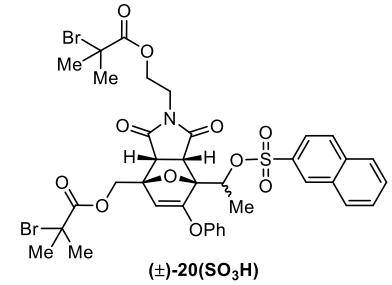

(±)-20(SO_3H)

^1H (400 MHz, $CDCl_3$)

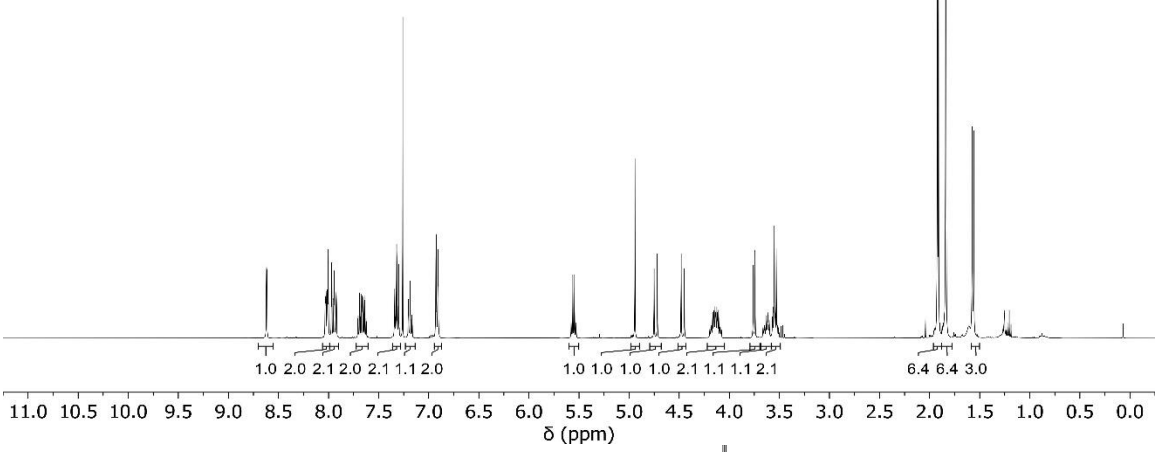

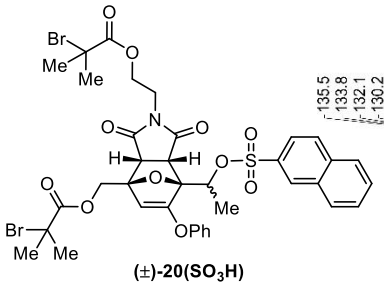

(±)-20(SO_3H)

^{13}C (100 MHz, $CDCl_3$)

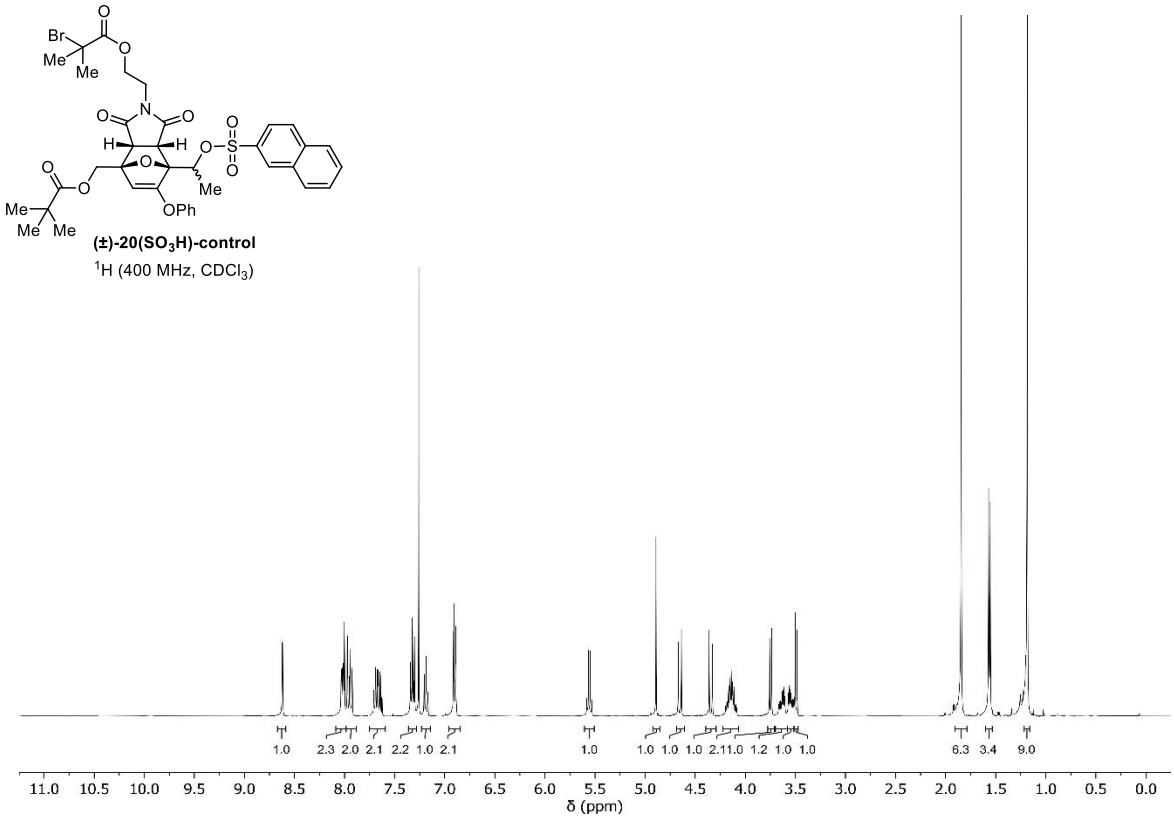
(±)-20(SO3H)-control
1H (400 MHz, CDCl3)
δ (ppm)

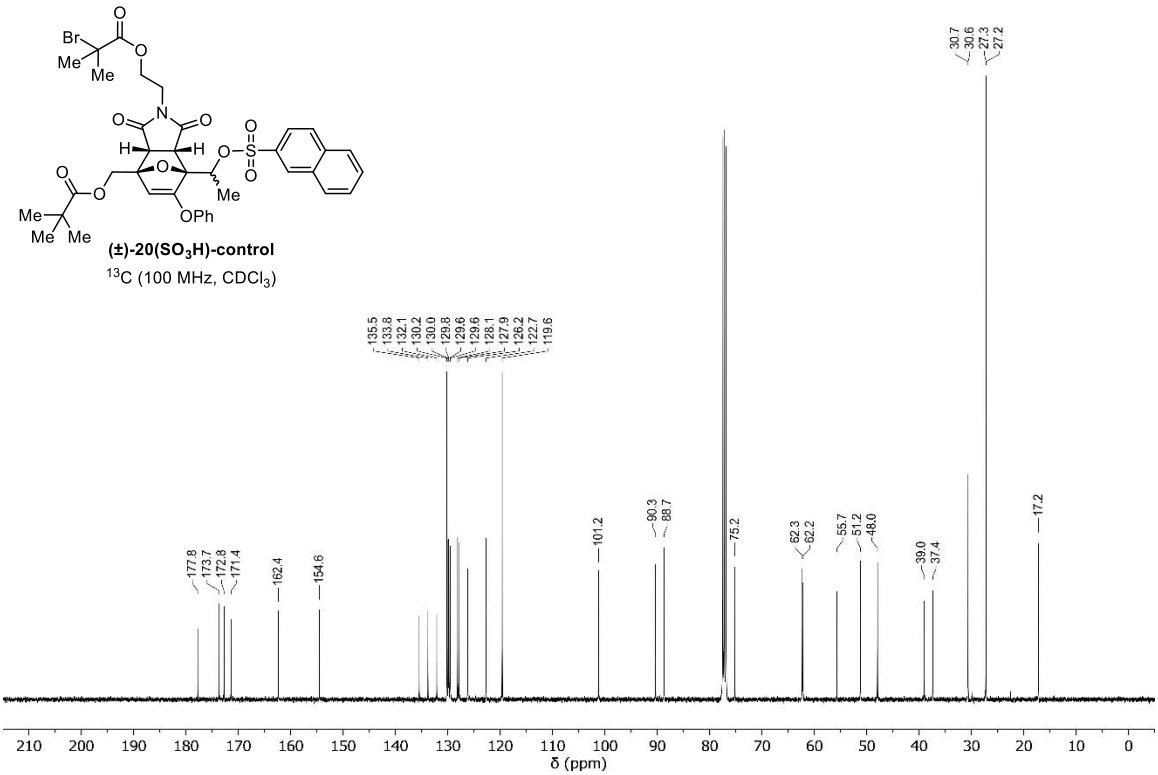
(±)-20(SO3H)-control
13C (100 MHz, CDCl3)
δ (ppm)

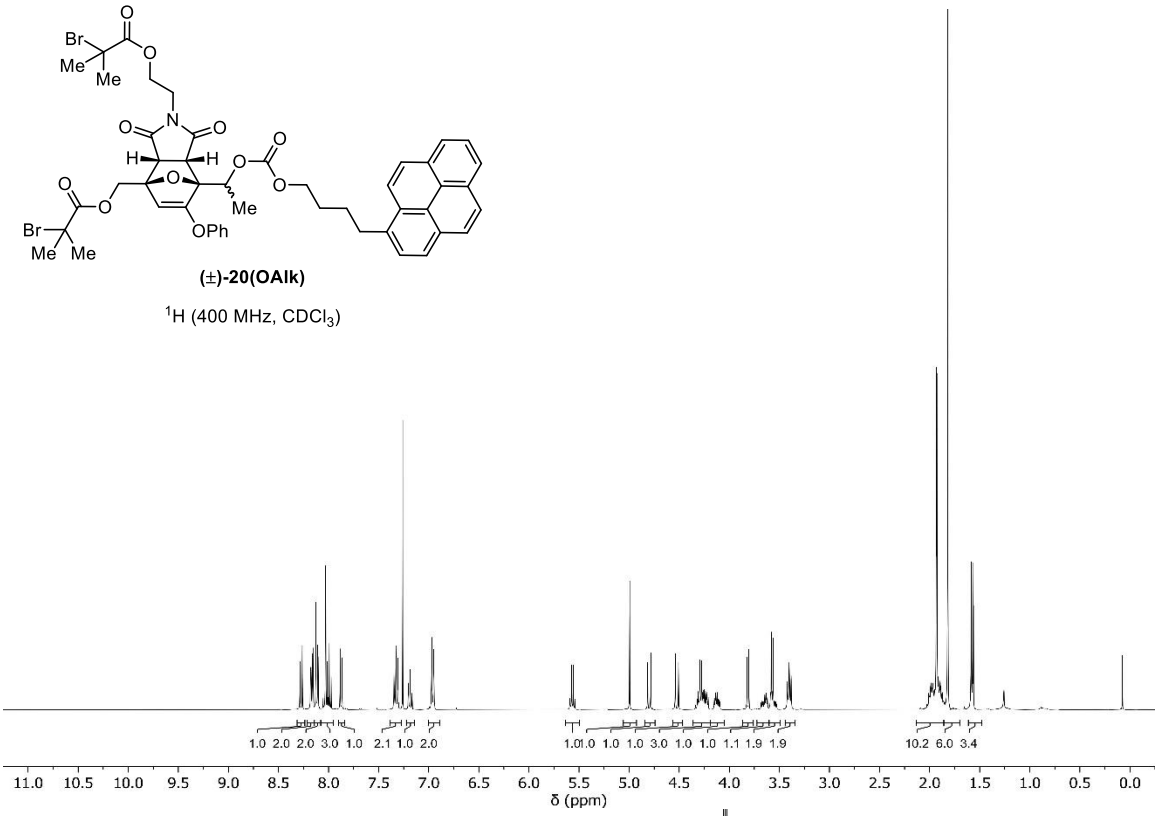
(±)-20(OAlk)
^{1}H (400 MHz, $CDCl_3$)
δ (ppm)

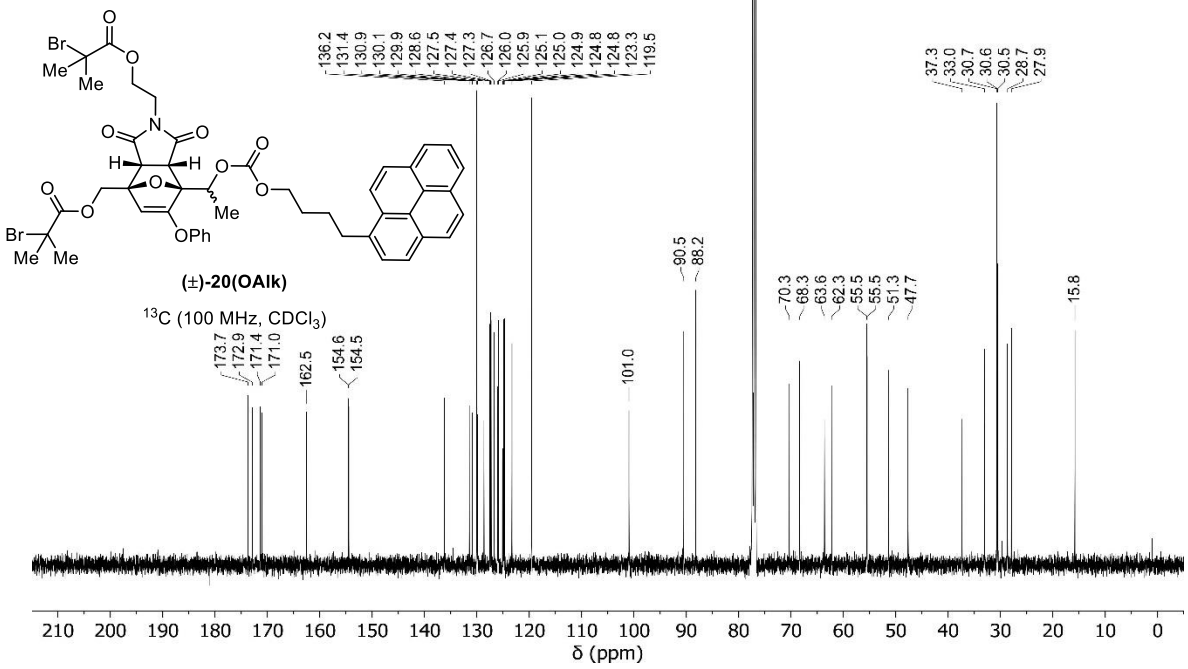
(±)-20(OAlk)
^{13}C (100 MHz, $CDCl_3$)
δ (ppm)

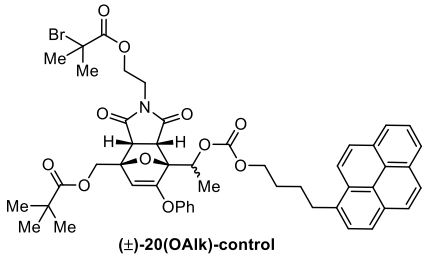

(±)-20(OAlk)-control

^{1}H (400 MHz, $CDCl_3$)

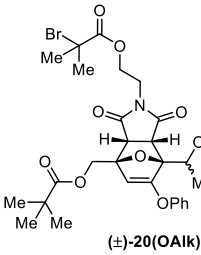

(±)-20(OAlk)-control

^{13}C (125 MHz, $CDCl_3$)

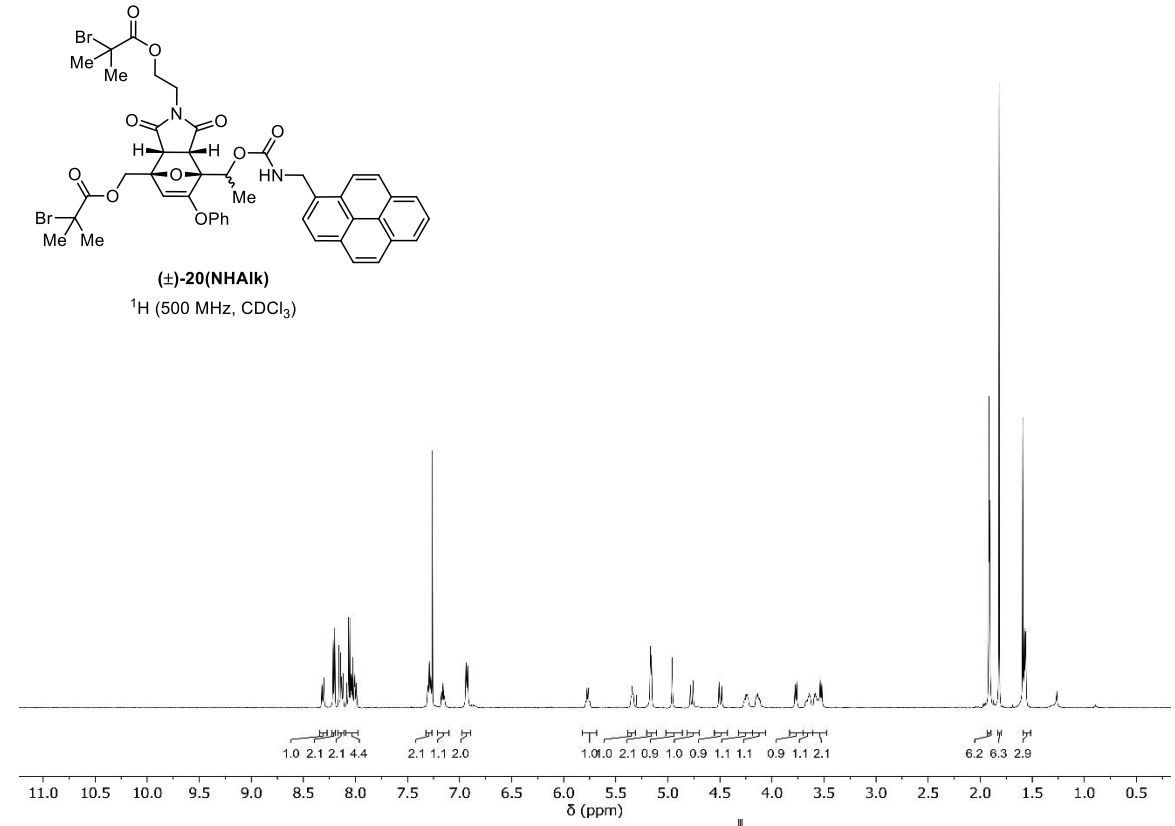
(±)-20(NHAlk)
^{1}H (500 MHz, $CDCl_3$)
δ (ppm)

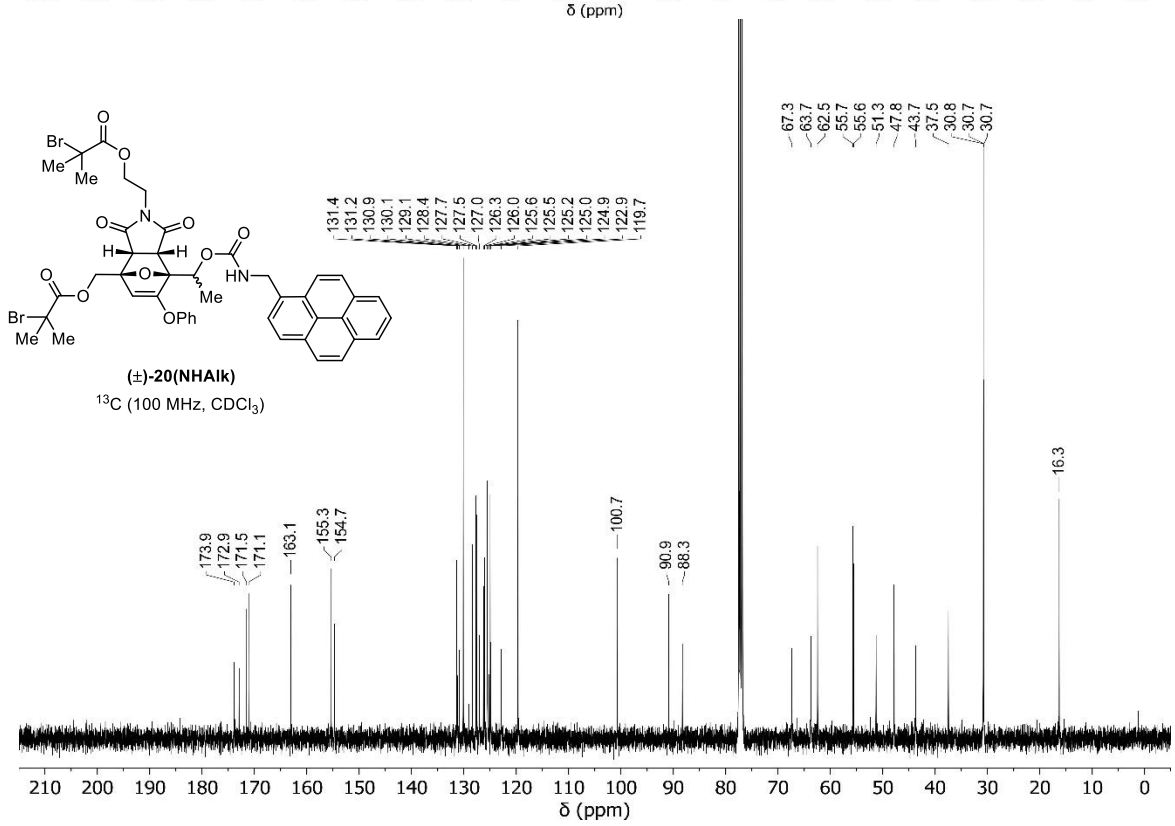
(±)-20(NHAlk)
^{13}C (100 MHz, $CDCl_3$)
δ (ppm)

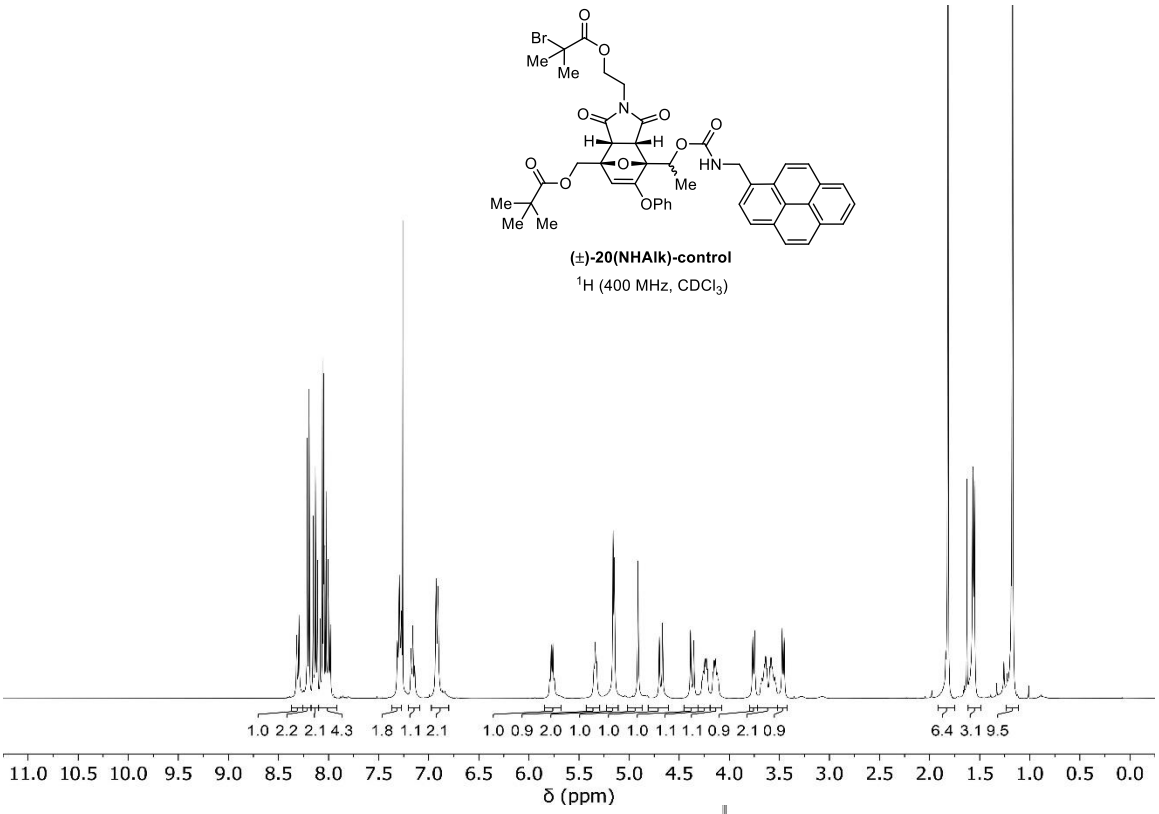
(±)-20(NHAlk)-control
1H (400 MHz, CDCl3)
1.0 2.2 2.1 4.3
1.8 1.1 2.1
1.0 0.9 2.0 1.0 1.0 1.0 1.1 1.1 0.9 2.1 0.9
6.4 3.1 9.5
δ (ppm)

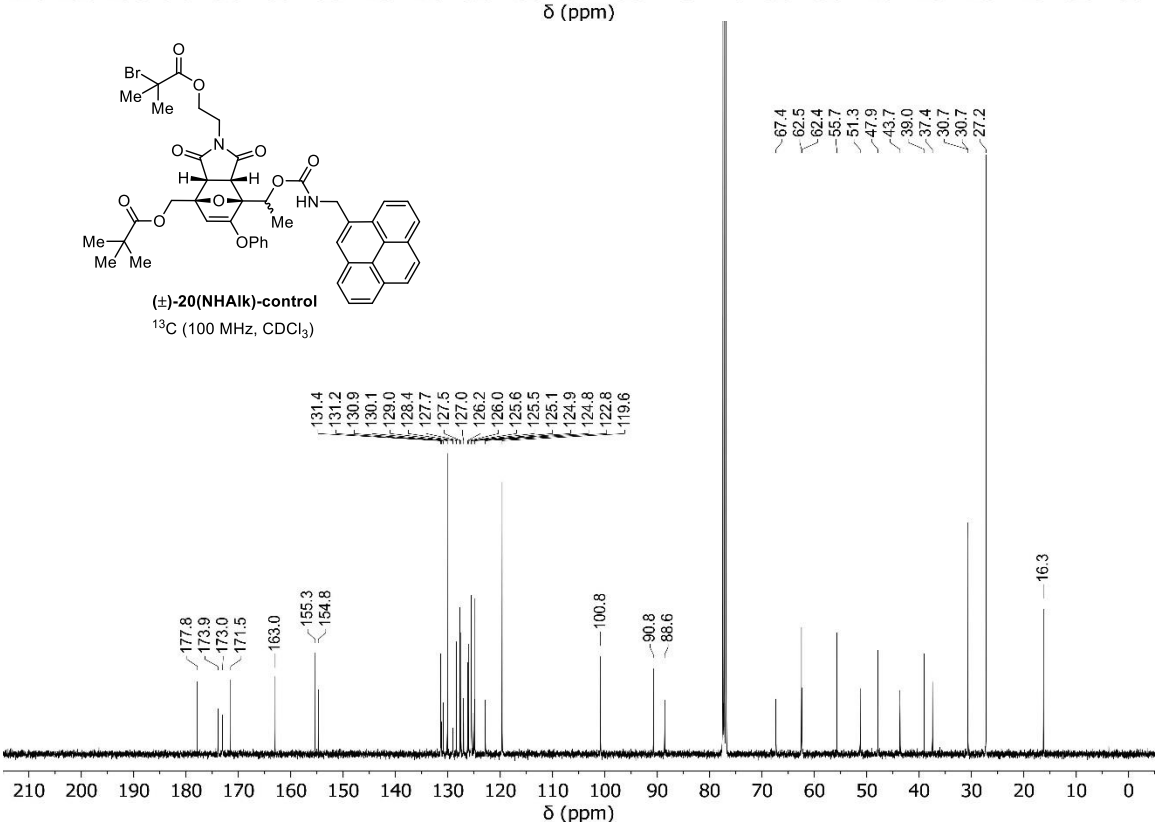
(±)-20(NHAlk)-control
13C (100 MHz, CDCl3)
67.4
62.5
62.4
55.7
51.3
47.9
43.7
39.0
37.4
30.7
30.7
27.2
131.4
131.2
130.9
130.1
129.0
128.4
127.7
127.5
127.0
126.2
126.0
125.6
125.5
125.1
124.9
124.8
122.8
119.6
177.8
173.9
173.0
171.5
163.0
155.3
154.8
100.8
90.8
88.6
16.3
δ (ppm)

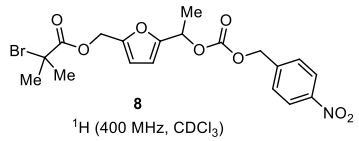

8

^{1}H (400 MHz, $CDCl_3$)

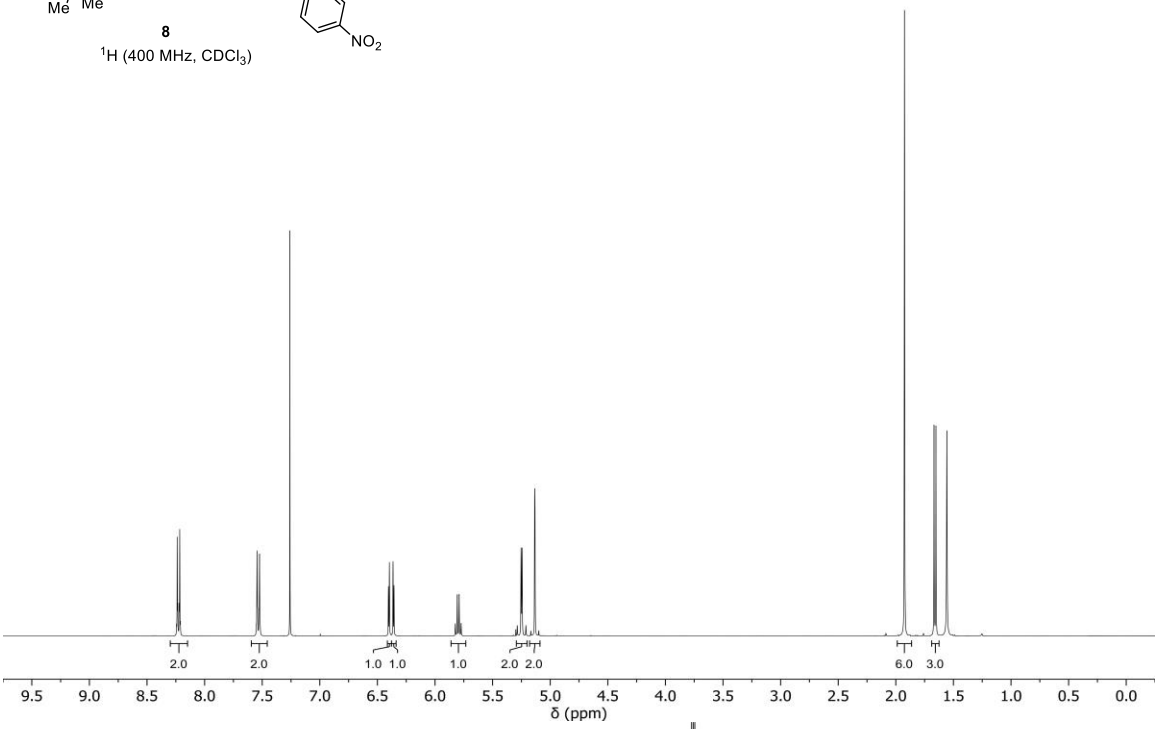

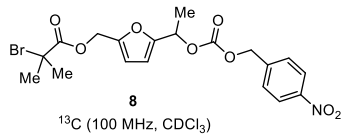

8

^{13}C (100 MHz, $CDCl_3$)

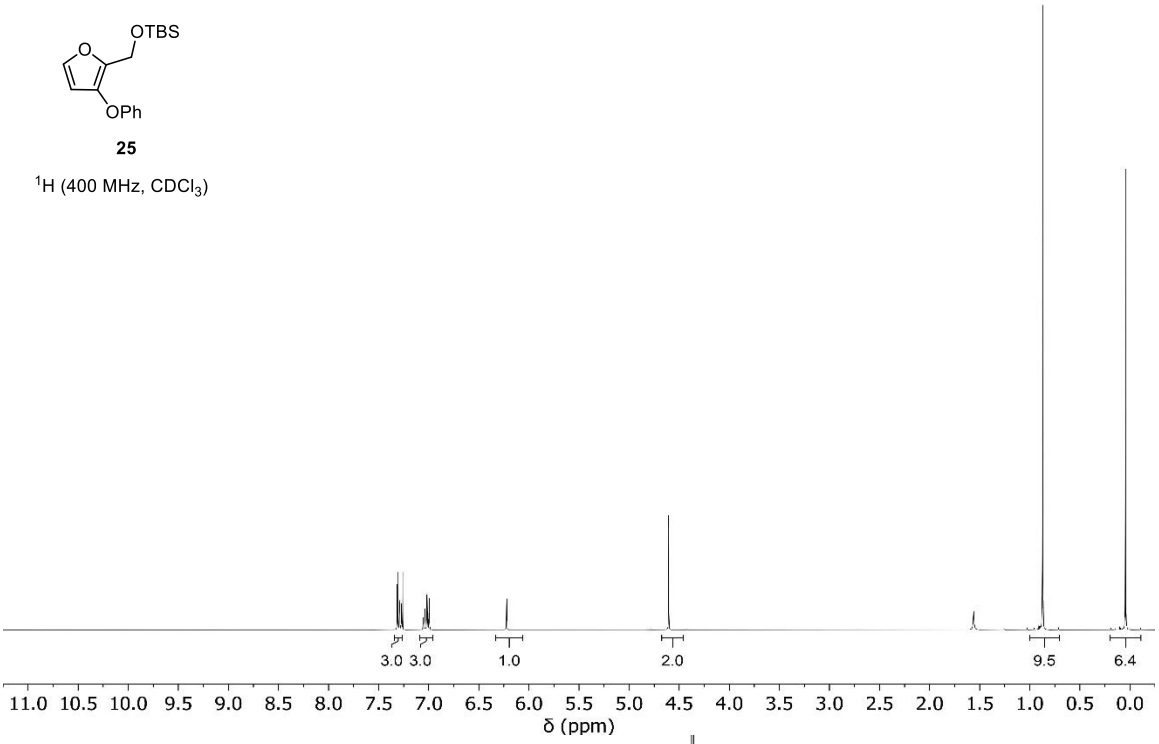
OTBS
OPh
25
1H (400 MHz, CDCl3)
3.0
3.0
1.0
2.0
9.5
6.4
δ (ppm)

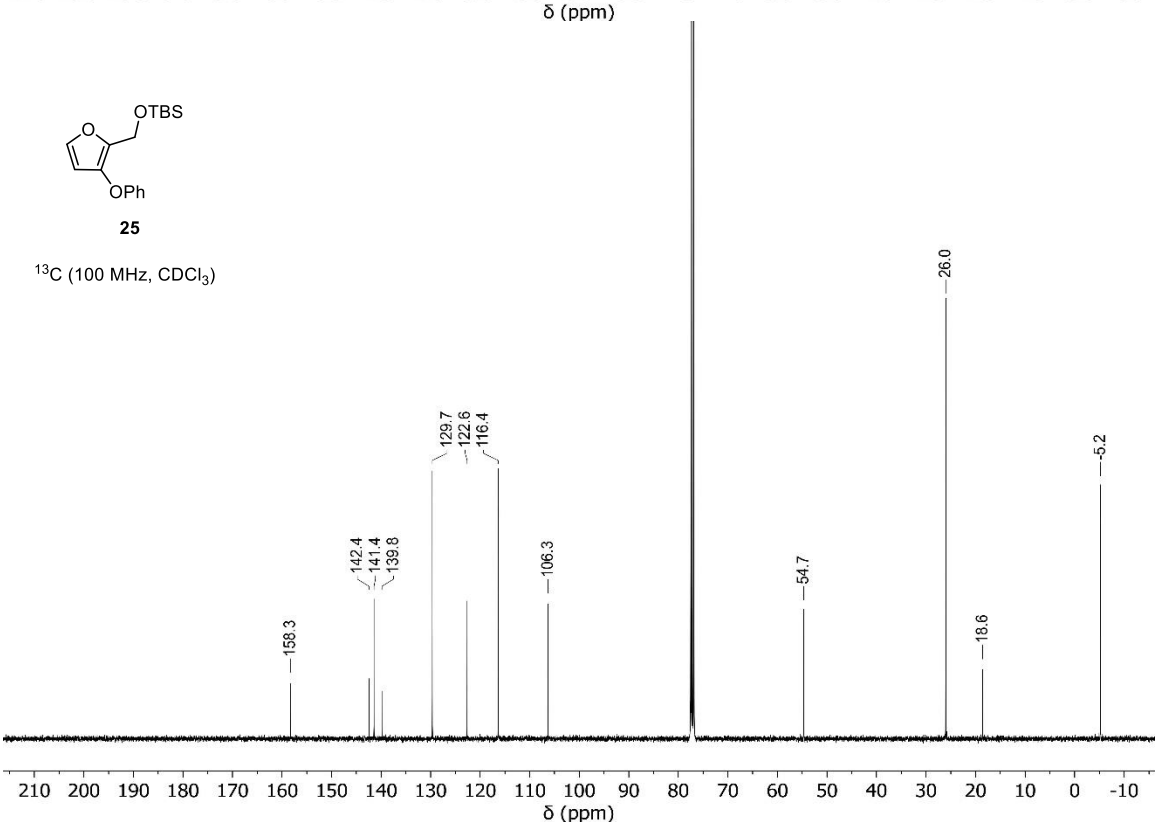
OTBS
OPh
25
13C (100 MHz, CDCl3)
158.3
142.4
141.4
139.8
129.7
122.6
116.4
106.3
54.7
26.0
18.6
-5.2
δ (ppm)

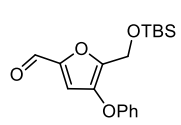

26

^{1}H (400 MHz, $CDCl_3$)

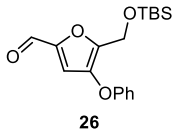

26

^{13}C (100 MHz, $CDCl_3$)

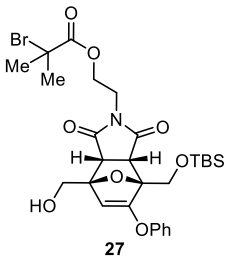

27

^{1}H (400 MHz, $CDCl_3$)

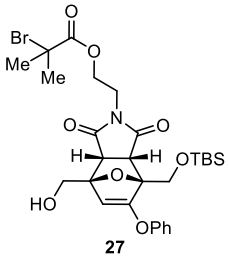

27

^{13}C (100 MHz, $CDCl_3$)

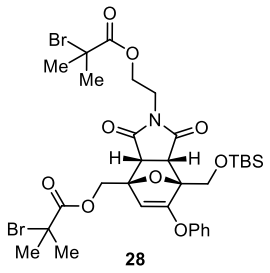

28

^{1}H (400 MHz, $CDCl_3$)

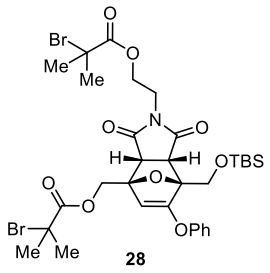

28

^{13}C (100 MHz, $CDCl_3$)

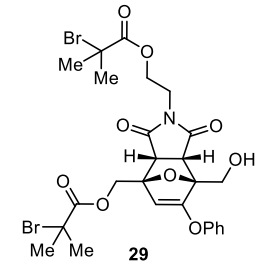

29

^{1}H (400 MHz, $CDCl_3$)

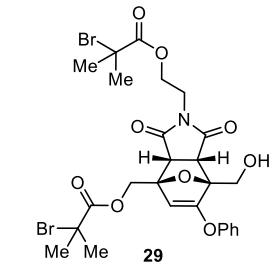

29

^{13}C (100 MHz, $CDCl_3$)

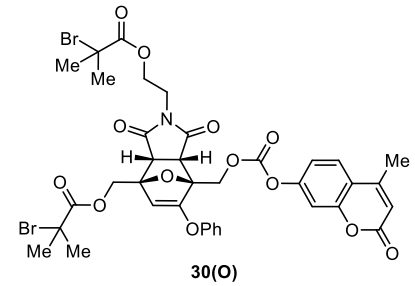

30(O)

^{1}H (400 MHz, $CDCl_3$)

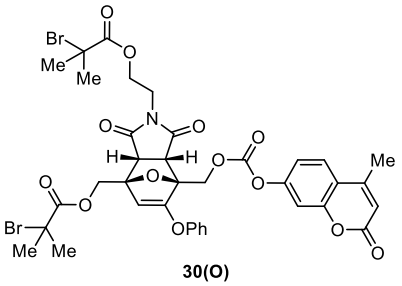

30(O)

^{13}C (100 MHz, $CDCl_3$)

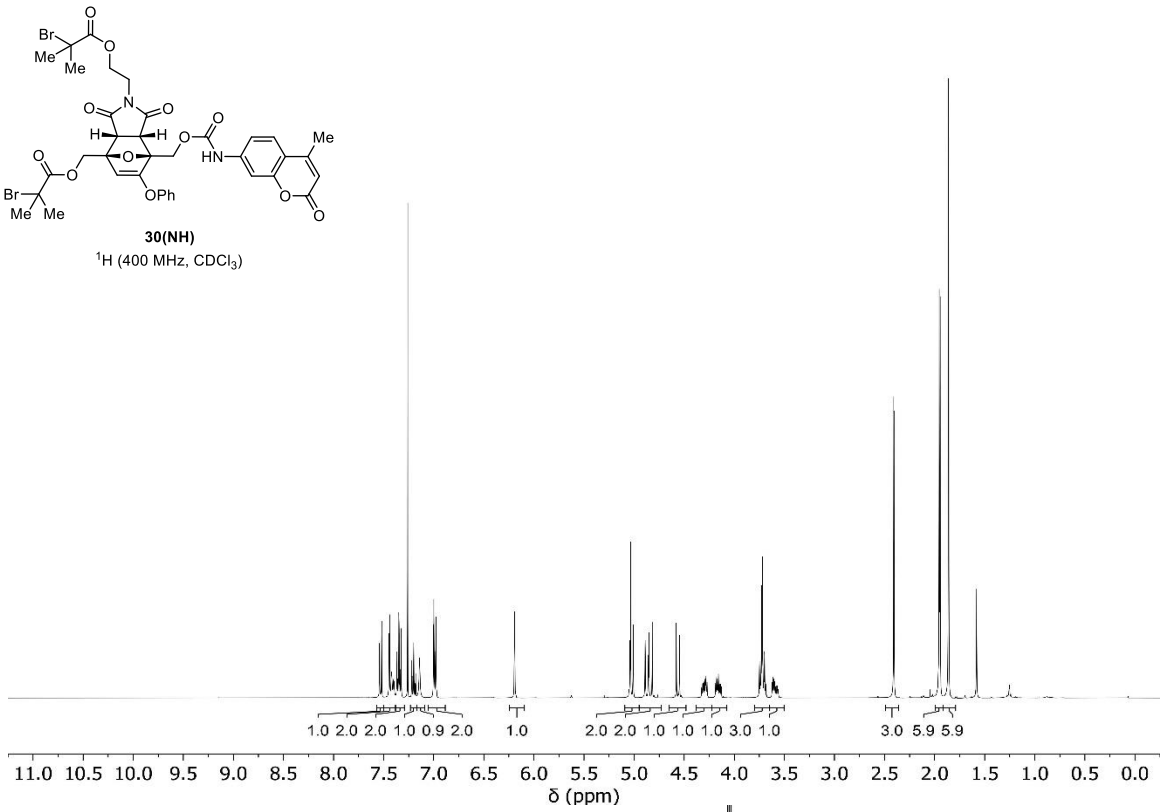
30(NH)
1H (400 MHz, CDCl3)
1.0 2.0 2.0 1.0 0.9 2.0 1.0 2.0 2.0 1.0 1.0 1.0 3.0 1.0 3.0 5.9 5.9
δ (ppm)

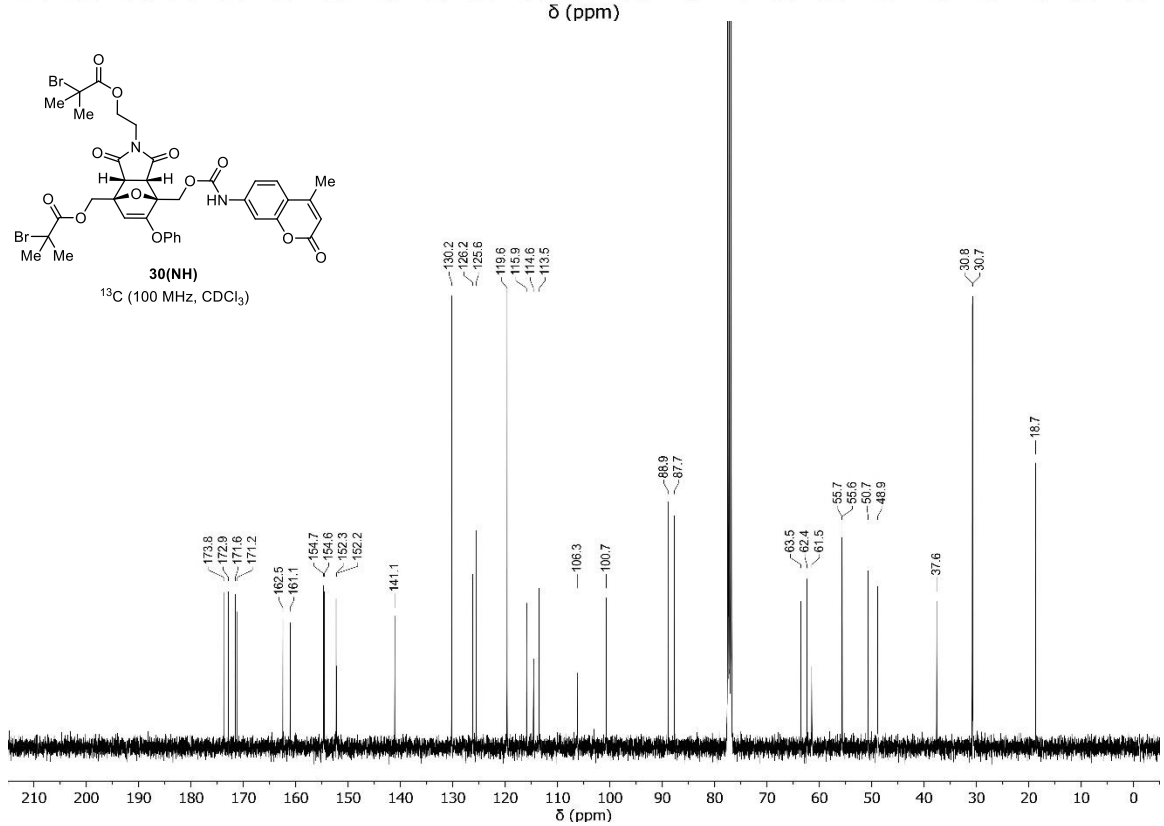
30(NH)
13C (100 MHz, CDCl3)
173.8
172.9
171.6
171.2
162.5
161.1
154.7
154.6
152.3
152.2
141.1
130.2
126.2
125.6
119.6
115.9
114.6
113.5
108.3
100.7
88.9
87.7
63.5
62.4
61.5
55.7
55.6
50.7
48.9
37.6
30.8
30.7
18.7
δ (ppm)

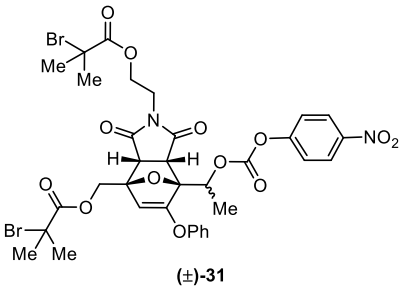

(±)-31

^{1}H (400 MHz, $CDCl_3$)

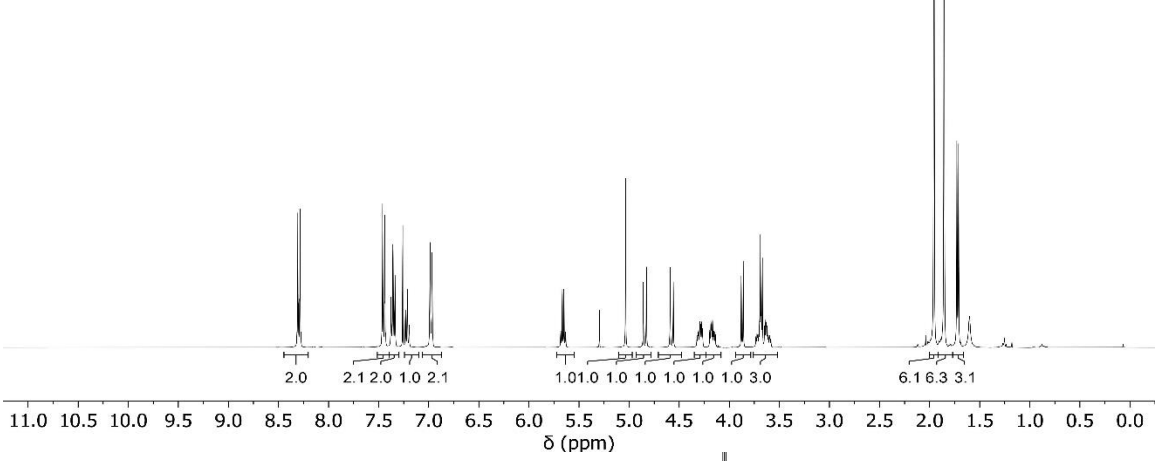

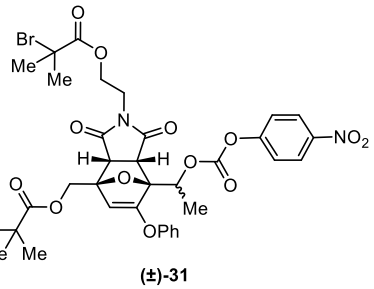

(±)-31

^{13}C (100 MHz, $CDCl_3$)

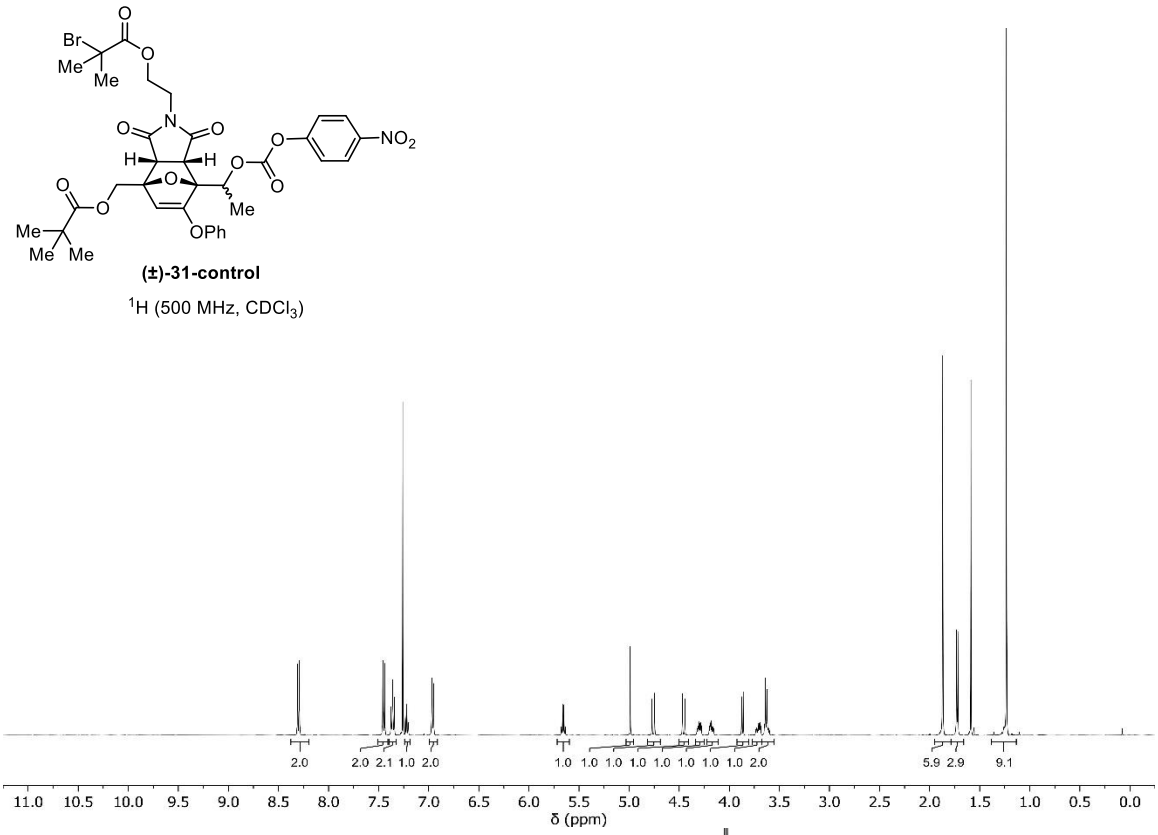
Br
Me
Me
O
O
N
O
O
H
H
O
O
O
O
NO2
Me
OPh
Me
Me
Me
O
O
(±)-31-control
1H (500 MHz, CDCl3)
2.0
2.0 2.1 1.0 2.0
1.0 1.0 1.0 1.0 1.0 1.0 1.0 2.0
5.9 2.9
9.1
δ (ppm)

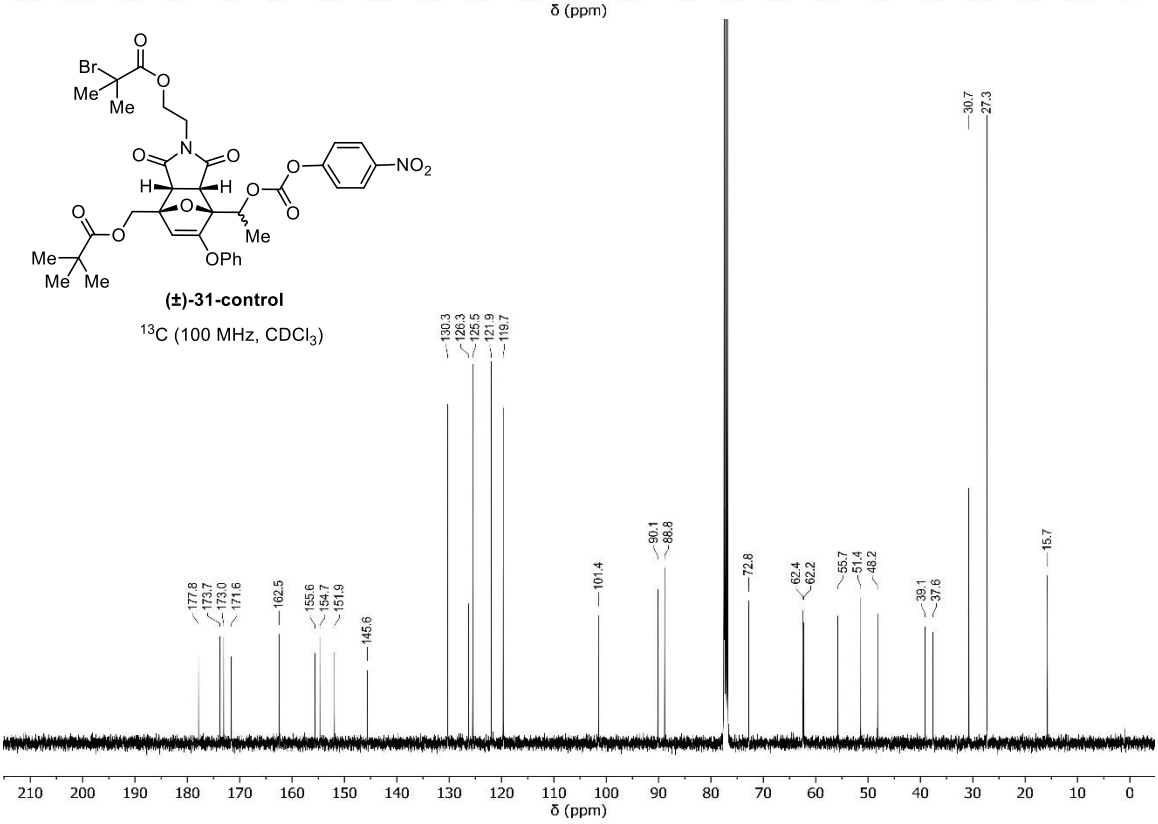
(±)-31-control
13C (100 MHz, CDCl3)
177.8
173.7
173.0
171.6
162.5
155.6
154.7
151.9
145.6
130.3
126.3
125.5
121.9
119.7
101.4
90.1
88.8
72.8
62.4
62.2
55.7
51.4
48.2
39.1
37.6
30.7
27.3
15.7
δ (ppm)

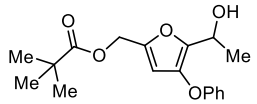

32

^{1}H (400 MHz, $CDCl_3$)

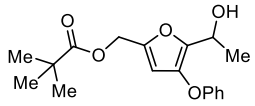

32

^{13}C (100 MHz, $CDCl_3$)

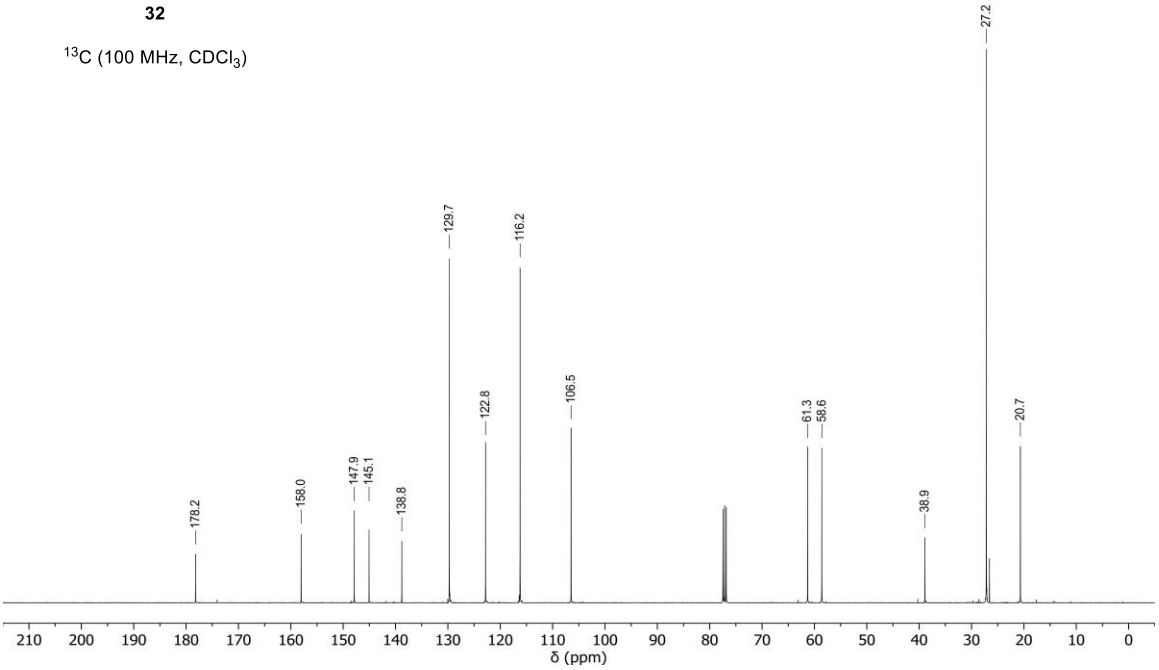

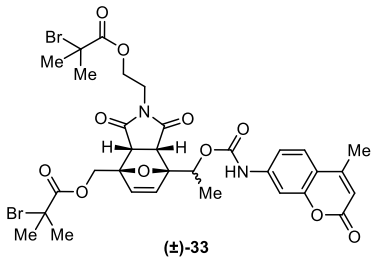

(±)-33

^{1}H (400 MHz, $CDCl_3$)

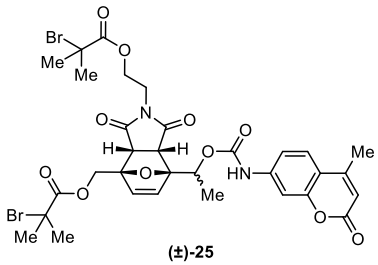

(±)-25

^{13}C (100 MHz, $CDCl_3$)

Chapter 3

5-ARYLOXY SUBSTITUTION ENABLES EFFICIENT MECHANICALLY TRIGGERED RELEASE FROM A SYNTHETICALLY ACCESSIBLE MASKED 2-FURYLCARBINOL MECHANOPHORE

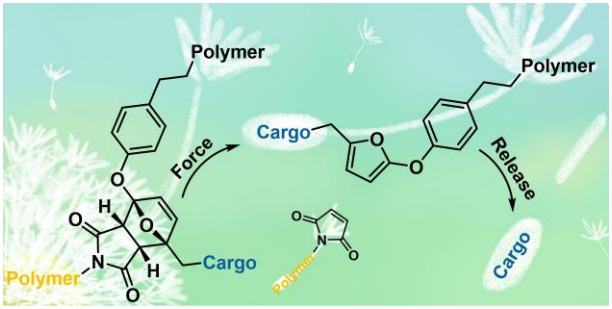

Abstract: Polymers that release small molecules in response to mechanical force are attractive materials for a wide variety of applications. Here, we report a new mechanophore platform based on a masked 2-furylcarbinol derivative that incorporates a 5-aryloxy group, which serves as both an electron-rich substituent to accelerate molecular release and the position of polymer attachment proximal to the furan–maleimide junction. The mechanophore is readily synthesized and efficiently releases both phenol and arylamine payloads in response to mechanical activation.

This chapter has been adapted with permission from
Zeng, T.; Hu, X.; Robb, M *Chem. Commun.* **2021**, 57, 11173–11176.

3.1 Investigation

Polymers that release small molecules in response to mechanical force are attractive for a variety of applications including drug delivery, self-healing materials, sensing, and catalysis.[1–5] To this end, force-sensitive molecules known as mechanophores have been designed to release a covalently-bound cargo molecule upon mechanochemical activation, whereby mechanical force is transduced by attached polymer chains.[6–8] Molecular release from mechanophores has been achieved via mechanically triggered cycloreversion,[9–11] rearrangement,[12,13] and various other cascade reactions.[14–17] In the last category, our group has recently developed a series of furan–maleimide Diels–Alder adducts that undergo mechanically-promoted retro-[4+2] cycloaddition reactions, unmasking reactive 2-furylcarbinol derivatives that spontaneously decompose under mild conditions to release a covalently-bound cargo molecule (Figure 3.1).[18,19] For the fluorogenic hydroxycoumarin and aminocoumarin payloads depicted in Figure 3.1, the cargo molecules are conjugated to the furan–maleimide mechanophore through carbonate and carbamate linkages, respectively, with release occurring through a retro-Diels–Alder/fragmentation–decarboxylation cascade.

The modularity of the latent 2-furylcarbinol scaffold enables the release of functionally diverse cargo molecules and highly tunable release kinetics through strategic structural modifications.[19] For example, an α-methyl substituent like the one in mechanophore **3-H (2°)** promotes the release of a hydroxycoumarin cargo with a half-life of 46 min at room temperature in a mixture of acetonitrile/methanol (3:1 v/v) following

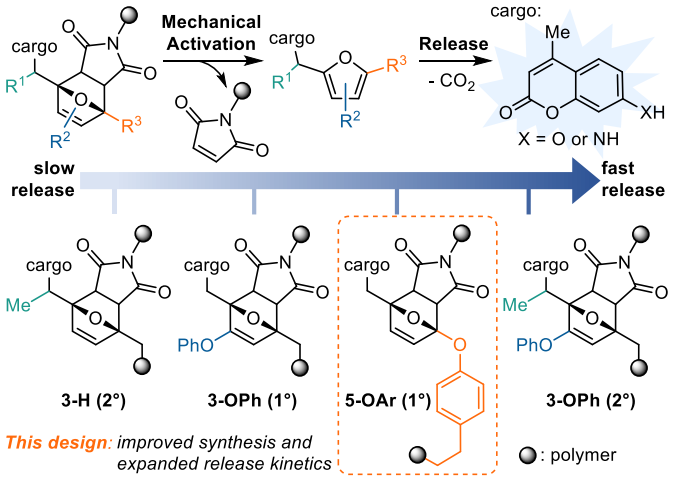

Figure 3.1. Mechanophore platforms for mechanically triggered small molecule release from masked 2-furylcarbinol derivatives.

mechanical activation. As exemplified by mechanophore **3-OPh (2°)**, installation of an electron-donating phenoxy substituent at the 3-position of the furan, in combination with an α-methyl group, significantly accelerates decomposition of the 2-furylcarbinol derivative resulting in nearly instantaneous release of hydroxycoumarin as well as a relatively short half-life of 41 min for the more challenging aminocoumarin cargo. Release of hydroxycoumarin also occurs rapidly from phenoxy-substituted mechanophore **3-OPh (1°)**, which does not contain an α-methyl group, while the release of aminocoumarin occurs much more slowly with a half-life of ~6 days. These results highlight how the nature of the leaving group as well as the stability of the putative furfuryl cation intermediate effect the reactivity of 2-furylcarbinol derivatives.[20]

While an electron-donating phenoxy substituent has proved important for enabling the release of more challenging payloads like amines on reasonable time scales, installation of the 3-phenoxy group in previous mechanophore designs is synthetically onerous and inefficient.[19] Here, we report a new mechanophore that incorporates a 5-aryloxy substituent on the 2-furylcarbinol scaffold that also serves as the point of polymer attachment. The synthesis of mechanophore **5-OAr (1°)** is straightforward and efficient. In addition, this new platform is competent with amine payloads, achieving release rates that are significantly faster than mechanophore **3-OPh (1°)**. These features provide an attractive mechanophore design for mechanically triggered release applications.

Structural features that stabilize the developing positive charge at the α-position in the transition state increase the rate of molecular release from 2-furylcarbinol derivatives. For furfuryl carbonates and carbamates, we have previously demonstrated that an α-methyl substituent reduces the activation barrier for fragmentation by 3–4 kcal/mol compared to the primary 2-furfylcarbinol derivatives. In addition, an electron-donating 3-phenoxy group was found to reduce the activation barrier by 4–5 kcal/mol.[19] Increasing the electron density of the furan was a key parameter for enabling the rapid release of more challenging cargo molecules including amines. The synthetic challenges posed by installation of the 3-phenoxy group, however, prompted us to pursue an alternative design that is more easily accessible, as represented by mechanophore scaffold **5-OAr (1°)**. Importantly, introduction of the phenoxy substituent at the 5-position of the furan preserves a proximal pulling geometry on

the Diels–Alder adduct mechanophore, which has been shown to result in greater mechanochemical activity compared to other regioisomers.[21] Density functional theory (DFT) calculations using the constrained geometries simulate external force (CoGEF) method[22,23] predict the desired retro-[4+2] cycloaddition reaction upon molecular elongation of a truncated model of the **5-OAr (1°)** mechanophore (Figure 3.2). The mechanochemical reaction is predicted to occur with a maximum force (F_{max}) of 4.2 nN for the carbonate model and 4.4 nN for the carbamate model, which are similar to the F_{max} values of 4.0–4.1 nN computed for our previously reported mechanophores based on masked 2-furylcarbinol derivatives.[23]

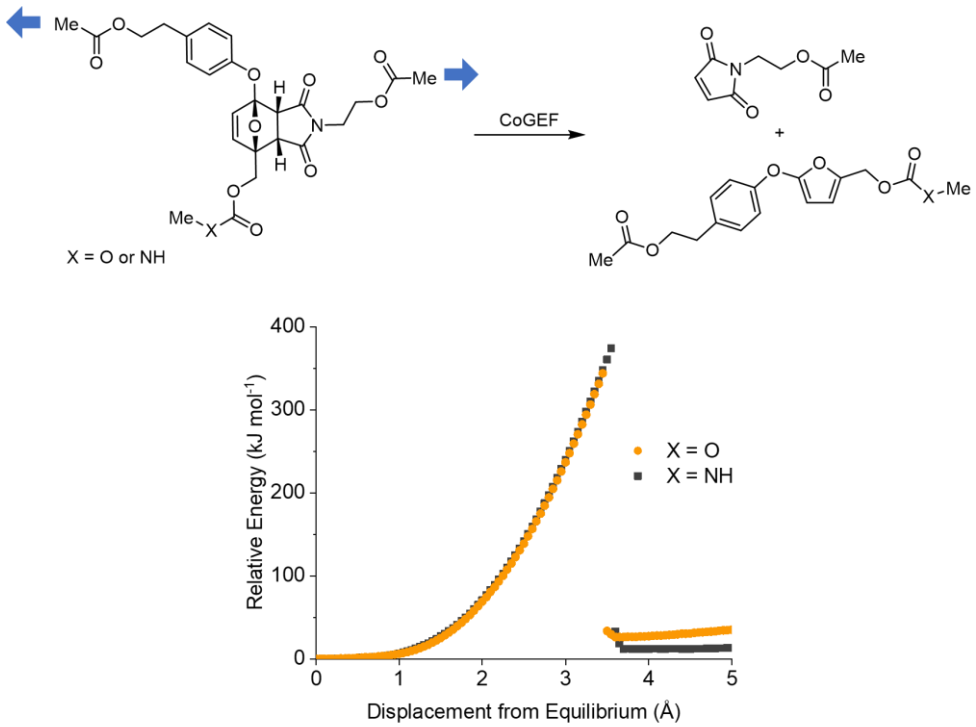

Figure 3.2. Density functional theory (DFT) calculations performed on truncated furan–maleimide Diels–Alder adducts using the constrained geometries simulate external force (CoGEF) method at the B3LYP/6-31G* level of theory. The F_{max} value calculated for the carbonate model (X = O) is 4.2 nN and that for the carbamate model (X = NH) is 4.4 nN. CoGEF calculations predict a retro-Diels–Alder reaction to generate the expected furan and maleimide products upon mechanical

Synthesis of the **5-OAr (1°)** mechanophore scaffold is accomplished in four steps from commercially available reagents (Scheme 3.1). Furaldehyde derivative **1** was first established by a nucleophilic substitution reaction between tyrosol and 5-bromofurfural using Cs_2CO_3 as the base in 86% yield, which represents a two-fold improvement compared

to the installation of a phenoxy group at the 3-position of the furan.[19] Esterification by DCC coupling with α-bromoisobutyric acid produced **2** in 88% yield. This furaldehyde was then reduced with $NaBH_4$ at −78 °C, which was necessary to avoid reduction of the ester, and subsequently reacted with a pre-functionalized maleimide dienophile at room temperature to form *endo*-Diels–Alder adduct bis-initiator (±)-**3**. Under these conditions, *endo*:*exo* stereoselectivity was ~97:3 and achieved an overall yield of 78% over the two steps. Installation of hydroxycoumarin or aminocoumarin payloads proceeded efficiently via reaction of the primary alcohol on (±)-**3** with the corresponding chloroformate or isocyanate to yield mechanophore bis-initiators (±)-**4O** and (±)-**4NH**, respectively. The bis-initiators were then employed in the controlled radical polymerization[24] of methyl acrylate using Cu wire/Me_6TREN in DMSO to give **PMA(O)** (M_n = 88 kg/mol; $Đ$ = 1.06) and **PMA(NH)** (M_n = 90 kg/mol; $Đ$ = 1.15) incorporating the mechanophores near the chain midpoint. Notably, the thermal stability of the **5-OAr (1°)** platform is comparable to that of the **3-OPh** design and significantly greater than the original **3-H** mechanophore (Figure 3.3).[19] Heating compound (±)-**3** in toluene-d_8 at 70 °C for 5 h results in only ~10% retro-Diels–Alder reaction. In comparison, conversions of ~46% for **3-H** and < 2% for **3-OPh** were observed previously under the same conditions. At room temperature, no retro-Diels-Alder reaction of compound (±)-**3** was detectable after nearly two months.

Scheme 3.1. Synthesis of Poly(Methyl Acrylate) (PMA) Polymers Containing a Chain-Centered **5-OAr (1°)** Mechanophore with Fluorogenic Coumarin Payloads.

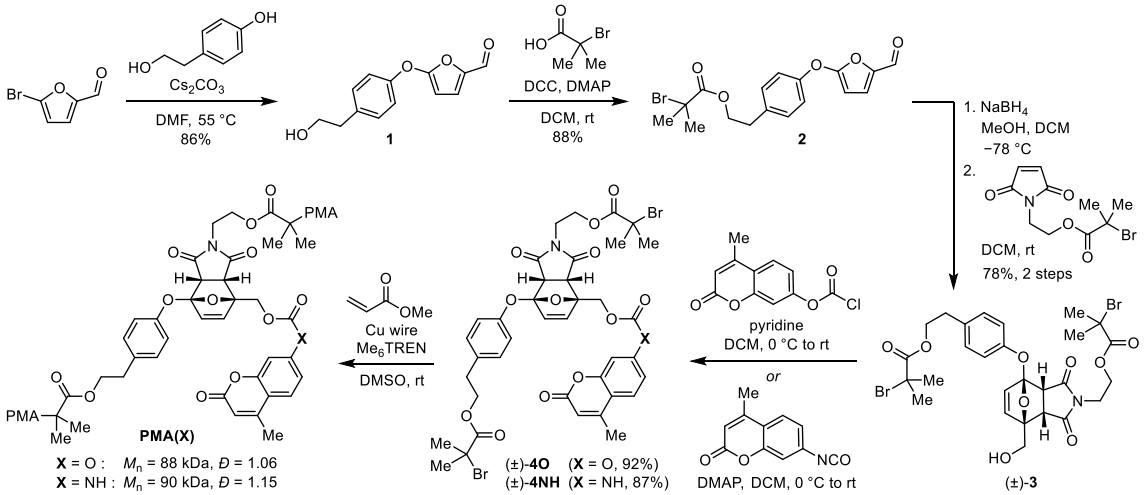

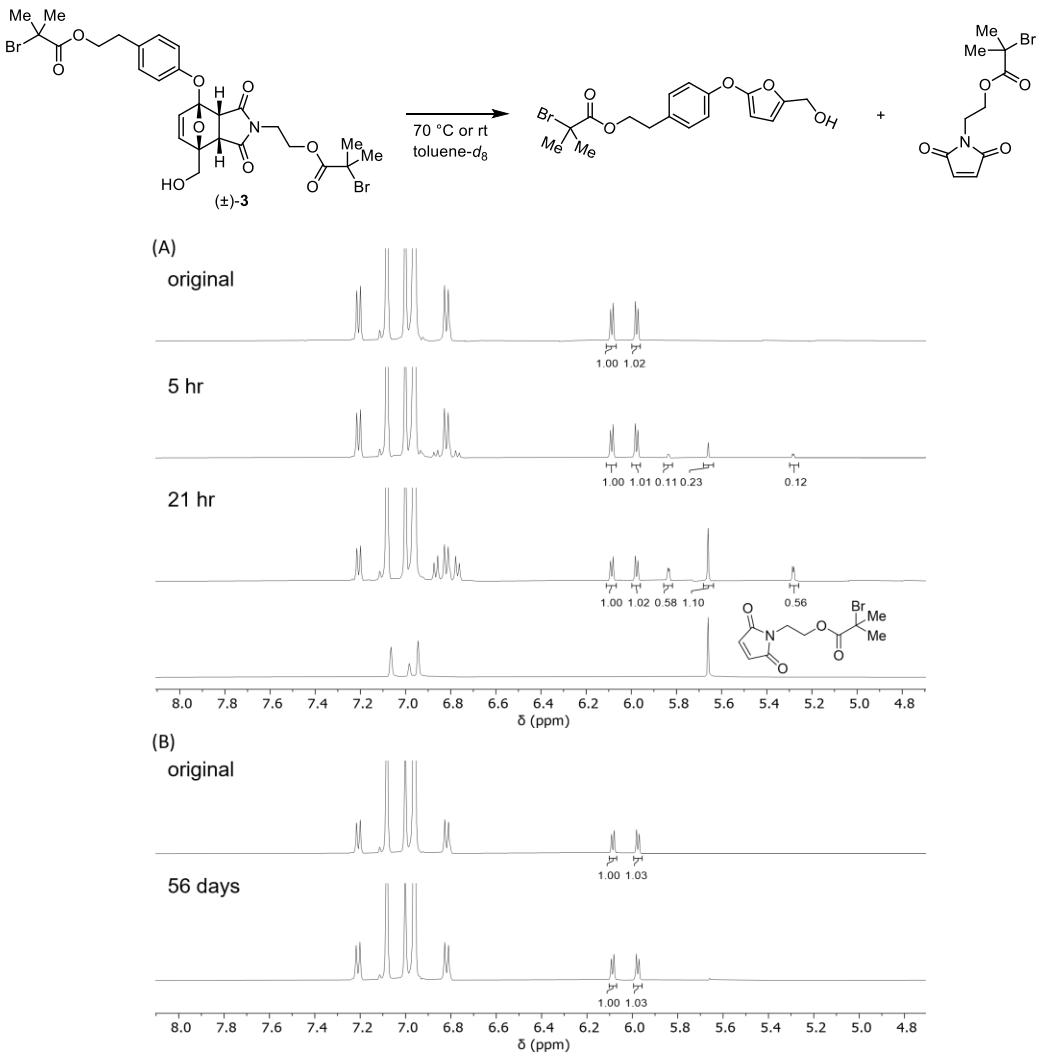

Figure 3.3. Thermal stability study of Diels–Alder adduct **3** in toluene-d_8 (7.7 mM). (A) Partial ^{1}H NMR spectra (500 MHz) of (±)-**3** (A) after heating at 70 °C for the indicated amount of time. Compound (±)-**3** undergoes a retro-Diels–Alder reaction upon heating at 70 °C with a conversion of approximately 10% after 5 h and 35% after 21 h. The ^{1}H NMR spectrum of the maleimide fragment in toluene-d_8 is shown for reference. (B) Partial ^{1}H NMR spectra of (±)-**3** after being kept at room temperature for the indicated amount of time, demonstrating negligible reaction.

Mechanically triggered release from the **5-OAr (1°)** mechanophore platform was investigated using ultrasonication, which produces high stretching forces on polymer chains in solution maximized near the center of the chain where the mechanophore is located.[25] Polymers **PMA(O)** and **PMA(NH)** were subjected to pulsed ultrasound (1 s on/1 s off, 8–10°C, 20 kHz, 30% amplitude, 8.2 W/cm^2) in acetonitrile/methanol (3:1 v/v) and aliquots were periodically removed for characterization by gel permeation chromatography (GPC)

and photoluminescence (PL) spectroscopy (Figure 3.4). Each aliquot was kept at room temperature for a period of time prior to analysis to allow complete decomposition of the mechanically generated 2-furylcarbinol derivative. For the furfuryl carbonate derived from **PMA(O)**, 30 min was found to be sufficient, while 3 days were required for the furfuryl carbamate derived from **PMA(NH)** (*vide infra*). The fluorogenic response of the coumarin payloads facilitates the straightforward determination of molecular release using PL spectroscopy. Increasing exposure of **PMA(O)** and **PMA(NH)** to ultrasonication results in a predictable increase in cargo release, reaching approximately 70% and 51% of the theoretical yield after 300 min of sonication "on" time for hydroxycoumarin and aminocoumarin payloads, respectively (Figures 3.4B and 3.4C). By fitting the sonication time-dependent release data to a first-order rate expression, the maximum release is projected to reach 92% from **PMA(O)** and 58% from **PMA(NH)**. GPC measurements using an in-line UV detector also reflect the increasing production of small molecules consistent with the coumarin cargos as well as the expected decrease in molecular weight over the course of the sonication experiments (Figure 3.5 and 3.6). While attenuation of the original polymer peak

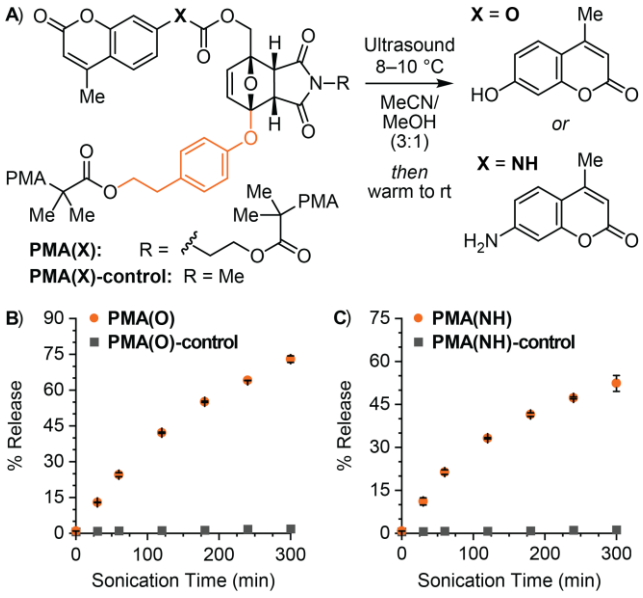

Figure 3.4. (A) Mechanically triggered release of hydroxycoumarin and aminocoumarin from **PMA(X)** and chain-end functional **PMA(X)-control** polymers subjected to ultrasound-induced mechanochemical activation (2 mg/mL in 3:1 acetonitrile/methanol). The total percent release of (B) hydroxycoumarin and (C) aminocoumarin as a function of sonication time was determined by PL spectroscopy after incubation at room temperature post-activation. Data for **PMA(O)** and **PMA(NH)** are the average from two experiments with error bars denoting the range of the two measurements.

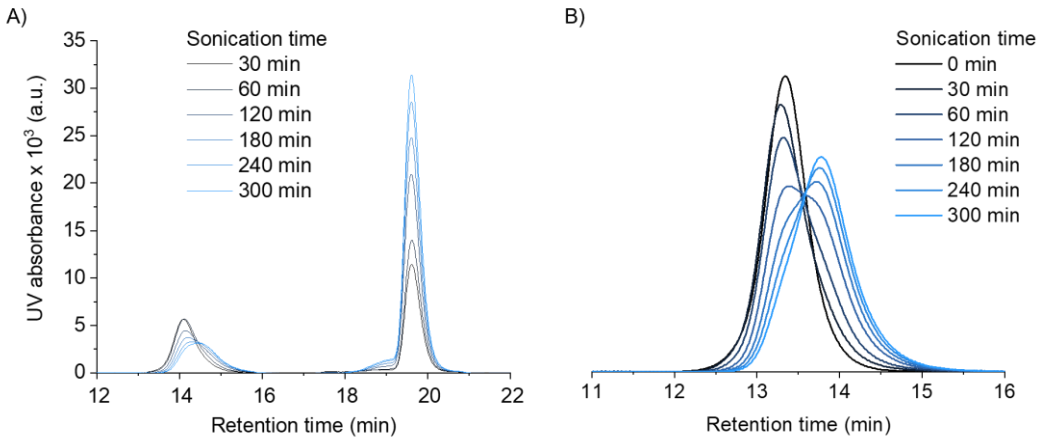

Figure 3.5. GPC traces as a function of ultrasonication time for **PMA(O)** monitored using a (A) UV-vis detector (λ = 322–338 nm) and (B) refractive index (RI) detector. Measurements were performed after incubation at room temperature for 30 mins post-sonication. The growth of the small molecule peak at an elution time of ~20 min in the UV-detected chromatograms is indicative of hydroxycoumarin generation. The M_n decreases steadily from 88 kg/mol to 49 kg/mol over 300 min of ultrasonication, with the GPC-RI chromatograms exhibiting characteristic features of midchain scission. Note that the GPC-RI chromatogram for the unactivated polymer (0 min) was acquired separately resulting in slight differences in retention time.

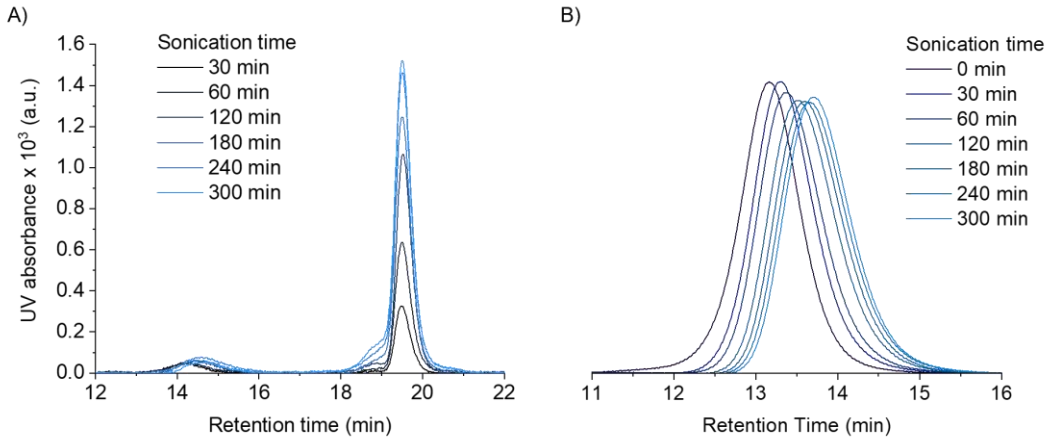

Figure 3.6. GPC traces as a function of ultrasonication time for **PMA(NH)** monitored using a (A) UV-vis detector (λ = 357–373 nm) and (B) refractive index (RI) detector. Measurements were performed after incubation at room temperature for 3 days post-sonication. The growth of the small molecule peak at an elution time of ~20 min in the UV-detected chromatograms is indicative of aminocoumarin generation. The M_n decreases steadily from 90 kg/mol to 50 kg/mol over 300 min of ultrasonication; however, unlike the behavior of **PMA(O)**, the GPC-RI peaks shift continuously to longer retention times without the characteristic features of midchain scission. This behavior is attributed, at least in part, to the broader molecular weight distribution of **PMA(NH)** ($Đ$ = 1.15) and greater competition between mechanophore activation and nonspecific backbone scission. Note that the GPC-RI chromatogram for the unactivated polymer (0 min) was acquired separately resulting in slight differences in retention time.

and generation of a new lower molecular weight peak is observed for the ultrasound-induced mechanical activation of **PMA(O)** characteristic of mid-chain scission, a more continuous shift in average molecular weight is observed upon ultrasonication of **PMA(NH)**. We attribute the difference in behavior to the broader molecular weight distribution of **PMA(NH)**, which we also suspect is responsible, at least in part, for the lower mechanophore activation efficiency compared to **PMA(O)**.[26] Indeed, experiments performed on an isolated small molecule furfuryl carbamate model demonstrate nearly quantitative release of aminocoumarin under similar conditions as those in the sonication experiments, implicating the mechanical activation step as a bottleneck (Figure 3.7). Importantly, no cargo release is observed upon ultrasonication of control polymers **PMA(O)-control** and **PMA(NH)-control** that incorporate the cargo-loaded mechanophores at the chain-end, confirming the mechanical origin of molecular release from **PMA(O)** and **PMA(NH)**.[6]

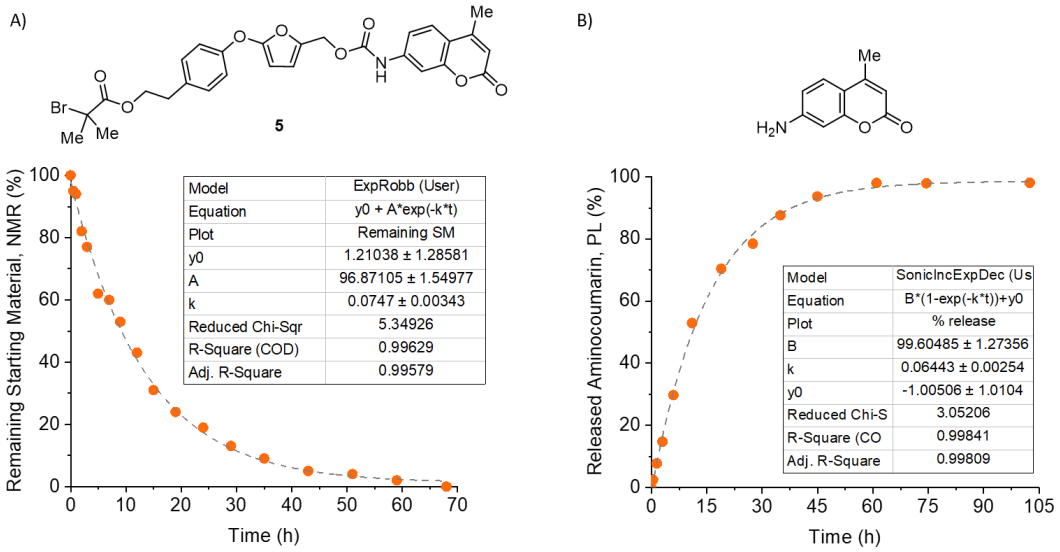

Figure 3.7. Results of small molecule model experiments measuring the room temperature decomposition of furfuryl carbamate **5** in acetonitrile/methanol (3:1 v/v). Time course experiments following (A) the conversion of model compound **5** by ^{1}H NMR spectroscopy (3:1 acetonitrile-d_3/methanol; $[\mathbf{5}]_0$ = 21 mM), and (B) the generation of aminocoumarin by photoluminescence spectroscopy (3:1 acetonitrile/methanol; λ_{ex} = 365 nm; λ_{em} = 424 nm; $[\mathbf{5}]_0$ = 7.0 μM). The concentration of aminocoumarin from PL spectroscopy was calculated based on a standard calibration curve (Figure 3.11). Fitting the curves to a first-order rate expression (dashed grey lines) gives half-lives for consumption of **5** (NMR) and generation of aminocoumarin (PL) of $t_{1/2}$ = 9.3 and 10.8 h, respectively.

To compare the release kinetics from the **5-OAr (1°)** platform with our previously studied furfuryl carbonates and carbamates,[19] solutions of **PMA(O)** and **PMA(NH)** were subjected to ultrasonication for 60 min ("on" time) as above and then coumarin release from the mechanically liberated 2-furylcarbinol derivatives was monitored by PL spectroscopy after warming the solutions to room temperature (Figure 3.8). The initial fluorescence intensity (t = 0) was subtracted from each measurement and the data were normalized to emphasize the relative rates of molecular release. The fluorescence emission from **PMA(O)** reached a maximum prior to the first measurement, indicating that the release of hydroxycoumarin completed nearly instantaneously ($t_{1/2}$ < 5 min), similar to our previously reported **3-OPh** scaffolds. In comparison, release of hydroxycoumarin from the **3-H** platform occurs with a significantly longer half-life of ~46 min. The release of aminocoumarin from mechanically activated **PMA(NH)** occurs with a half-life of 15 h, which is much faster than that from the **3-OPh (1°)** design ($t_{1/2} \approx 6.5$ days) but slower than aminocoumarin release from the **3-OPh (2°)** mechanophore platform ($t_{1/2}$ = 41 min).

Small molecule model experiments were performed to interrogate the mechanism of release from the **5-OAr (1°)** platform. A furfuryl carbamate small molecule corresponding to the unmasked furan component of compound **4NH** was isolated and its decomposition behavior evaluated in acetonitrile/methanol (3:1 v/v) at room temperature. Consistent with the results above, the half-life associated with furfuryl carbamate consumption and

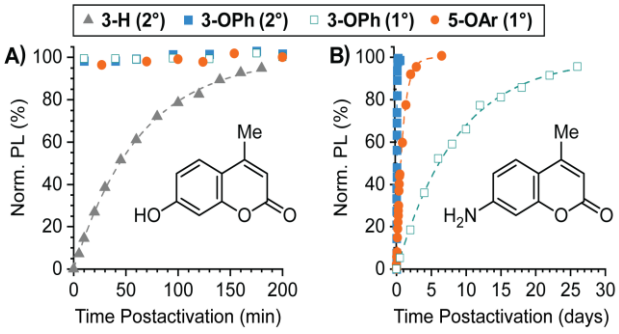

Figure 3.8. Mechanically triggered release of (A) hydroxycoumarin and (B) aminocoumarin from the **5-OAr (1°)** mechanophore platform compared to previously reported systems.[19] Polymer solutions (2 mg/mL in 3:1 acetonitrile/methanol) were sonicated for 60 min ("on" time), warmed to room temperature, and the release of coumarin cargo from the mechanically liberated 2-furylcarbinol derivatives was monitored by PL spectroscopy (see the ESI for details). The initial PL intensity was subtracted from each measurement and the data were normalized to the plateau value. Data for aminocoumarin release from **3-H (2°)** are not shown.

aminocoumarin generation was determined to be ~10 h by ^{1}H NMR and PL spectroscopy, respectively (Figure 3.7). Again, aminocoumarin is produced in nearly quantitative yield. Previously studied 2-furylcarbinol derivatives from the **3-H** and **3-OPh** platforms decompose under these same conditions to produce a furfuryl methyl ether as a major product, which is thought to be generated by nucleophilic attack of the furfuryl cation intermediate by methanol.[18,19] Interestingly, decomposition of the 5-aryloxy substituted furfuryl carbamate does not appear to generate a similar furfuryl methyl ether, but rather an alkyl ester tyrosol derivative as a major product (Figure 3.9). We hypothesize that after the initial fragmentation reaction to release the small molecule cargo, methanol attacks the 5-position of the furfuryl cation to form an orthoester, which closes down to eject the tyrosol fragment (Figure 3.10). A more detailed mechanistic investigation is currently in progress,

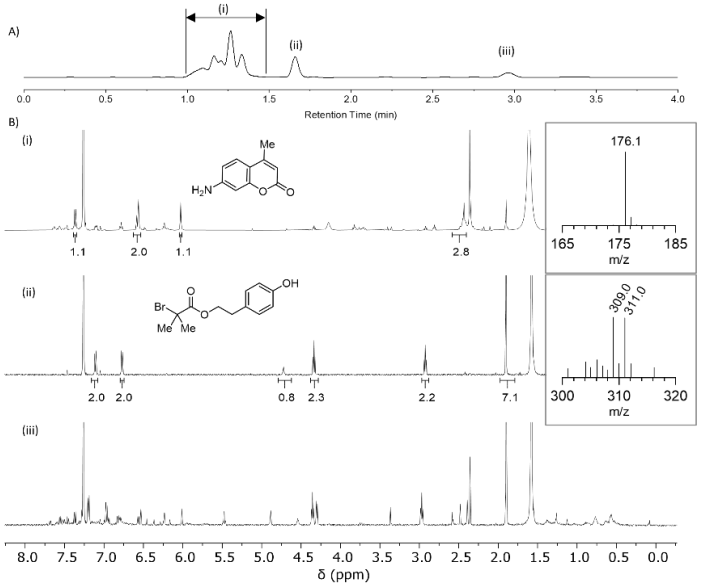

Figure 3.9. Product analysis of the decomposition of model compound **5** in 3:1 acetonitrile-d_3/methanol ([**5**]$_0$ = 7.0 μM). (A) The preparatory-HPLC trace of the mixture after 3 days of decomposition monitored at 285 nm. HPLC conditions: 80% acetonitrile in water, 8 mL/min. (B) ^{1}H NMR spectra (500 MHz, $CDCl_3$) of the fractions isolated after HPLC separation. (i) ^{1}H NMR spectrum corresponding to the retention times 1.0–1.5 min in the HPLC chromatogram showing aminocoumarin as a major product. The assignment is further supported by LCMS measurements. The mass of the analyte (m/z= 176.1 amu) matches the calculated m/z for 7-amino-4-methylcoumarin, $[C_{10}H_{10}NO_2]^+$ $(M+H)^+$ (176.1). (ii) ^{1}H NMR spectrum corresponding to the peak at 1.7 min in the HPLC chromatogram identified as a tyrosol alkyl ester derivative. The assignment is further supported by LCMS measurements. The mass of the analyte (m/z= 309.0 amu) matches the calculated m/z for 4-hydroxyphenethyl 2-bromo-2-methylpropanoate, $[C_{12}H_{15}BrO_3Na]^+$ $(M+Na)^+$ (309.0). (iii) ^{1}H NMR spectrum corresponding to the peak at 3.0 min in the HPLC chromatogram representing a mixture of products that was not identified.

but these preliminary results suggest that the unique fragmentation mechanism could be leveraged to achieve auxiliary functionality with this system.

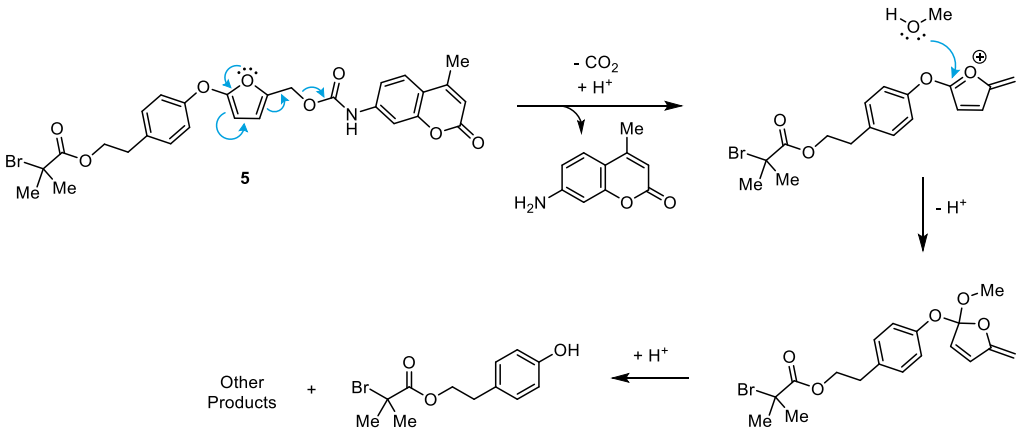

Figure 3.10. Proposed mechanism for the generation of major products aminocoumarin and the tyrosol alkyl ester via the room temperature decomposition of furfuryl carbamate **5** in 3:1 acetonitrile/methanol.

In summary, we have developed a new mechanophore for mechanically triggered small molecule release based on a masked 2-furylcarbinol scaffold incorporating 5-aryloxy substitution. This design combines an electron-rich aryloxy group on the furan ring that accelerates molecular release, while simultaneously serving as the site of polymer attachment for efficient force transfer proximal to the furan–maleimide junction. The efficient synthesis and demonstrated competence of the mechanophore for releasing both phenol and arylamine payloads on reasonable time scales makes this design attractive for a variety of triggered molecular release applications. A unique decomposition mechanism relative to previously studied 2-furylcarbinol derivatives may also provide added functionality.

We acknowledge the Center for Catalysis and Chemical Synthesis of the Beckman Institute at Caltech for access to equipment. Financial support for this work was provided by the Arnold and Mabel Beckman Foundation through a Beckman Young Investigator Award and the Donors of the American Chemical Society Petroleum Research Fund through a Doctoral New Investigator Award (Grant No. 61638-DNI7).

3.2 Experimental Details

Reagents from commercial sources were used without further purification unless otherwise stated. Methyl acrylate was passed through a short plug of basic alumina to remove inhibitor immediately prior to use. Dry THF, diethyl ether, MeCN, and DMF were obtained from a Pure Process Technology solvent purification system. All reactions were performed under a N2 atmosphere unless specified otherwise. Column chromatography was performed on a Biotage Isolera system using SiliCycle SiliaSep HP flash cartridges.

NMR spectra were recorded using a 400 MHz Bruker Avance III HD with Prodigy Cryoprobe, a 400 MHz Bruker Avance Neo, or Varian Inova 500 MHz spectrometers. All ^{1}H NMR spectra are reported in δ units, parts per million (ppm), and were measured relative to the signals for residual chloroform (7.26 ppm), dichloromethane (5.32 ppm), methanol (3.31 ppm), acetone (2.05 ppm), toluene (2.08 ppm) or acetonitrile (1.94 ppm) in deuterated solvent. All ^{13}C NMR spectra were measured in deuterated solvents and are reported in ppm relative to the signals for chloroform (77.16 ppm). Multiplicity and qualifier abbreviations are as follows: s = singlet, d = doublet, t = triplet, q = quartet, dd = doublet of doublets, dq = doublet of quartets, ABq = AB quartet, m = multiplet, br = broad.

High resolution mass spectra (HRMS) were analyzed by Fast Atom Bombardment (FAB) using a JEOL JMS-60H Double-focusing high resolution magnetic sector mass spectrometer operated in the positive ion mode. The instrument was calibrated with PEG clusters over the mass range of interest.

Analytical gel permeation chromatography (GPC) was performed using an Agilent 1260 series pump equipped with two Agilent PLgel MIXED-B columns (7.5 x 300 mm), an Agilent 1200 series diode array detector, a Wyatt 18-angle DAWN HELEOS light scattering detector, and an Optilab rEX differential refractive index detector. The mobile phase was THF at a flow rate of 1 mL/min. Molecular weights and molecular weight distributions were calculated by light scattering using a dn/dc value of 0.062 mL/g (25 °C) for poly(methyl acrylate).

Photoluminescence spectra were recorded on a Shimadzu RF-6000 spectrofluorophotometer using a quartz microcuvette (Starna Cells 18F-Q-10-GL14-C, 10 x 2 mm). Excitation and emission slit widths were 5 nm and 3 nm, respectively.

Preparatory High-Performance Liquid Chromatography (HPLC) was performed with an Agilent Eclipse XDB-C18 column (990967-202) using a single-wavelength UV-vis detector.

Ultrasound experiments were performed inside of a sound abating enclosure using a 500 watt Vibra Cell 505 liquid processor (20 kHz) equipped with a 0.5-inch diameter solid probe (part #630-0217), sonochemical adapter (part #830-00014), and a Suslick reaction vessel made by the Caltech glass shop (analogous to vessel #830-00014 from Sonics and Materials).

LCMS measurements were performed with an Agilent 6140 Series Quadrupole LCMS Spectrometer System equipped with an Agilent Eclipse Plus C18 column using MeCN/water as the eluent.

3.3 Characterization of Molecular Release Using PL Spectroscopy

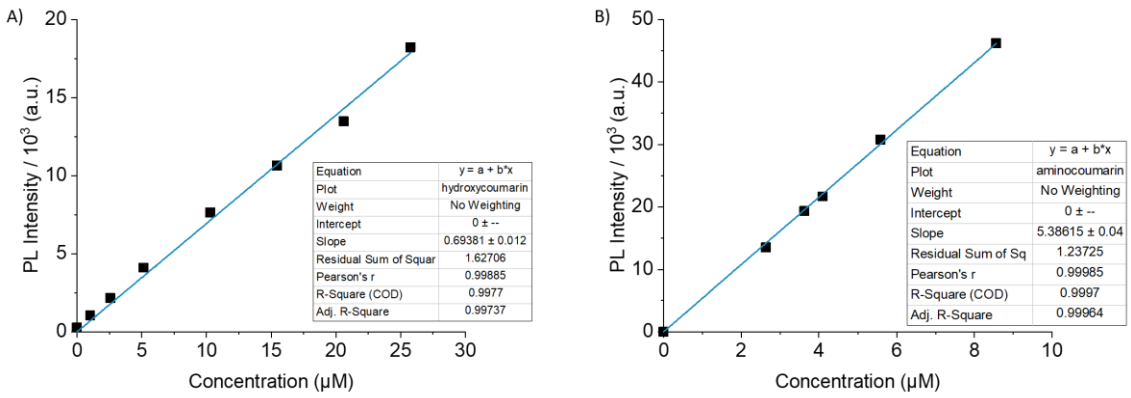

Figure 3.11. Calibration curves for experimental determination of the concentration of (A) 7-hydroxy-4-methylcoumarin (λ_{ex} = 330 nm, λ_{em} = 380 nm), and (B) 7-amino-4-methylcoumarin (λ_{ex} = 365 nm, λ_{em} = 424 nm) in acetonitrile/methanol (3:1 v/v).

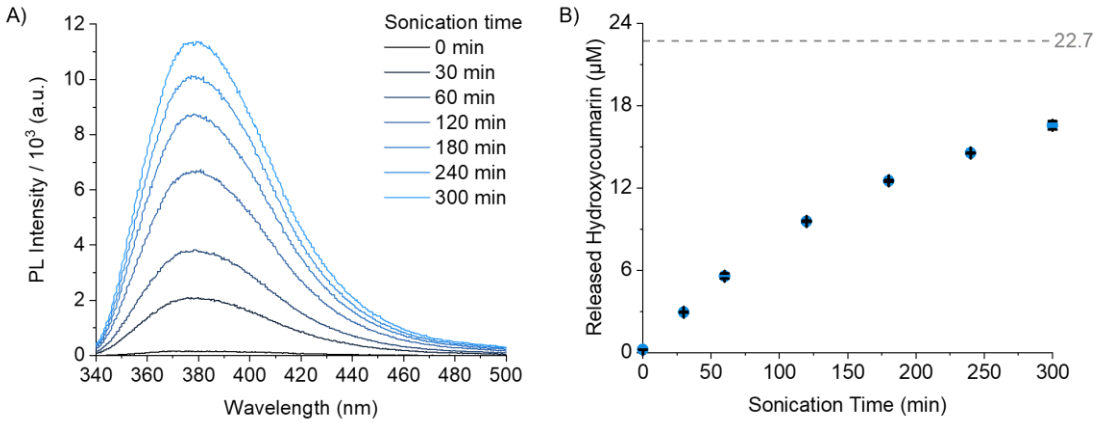

Figure 3.12. (A) Representative PL spectra of a 2.0 mg/mL solution of **PMA(O)** in acetonitrile/methanol (3:1 v/v) after being subjected to ultrasonication for the indicated amount of time. Aliquots were kept at room temperature for 30 min prior to analysis. λ_{ex} = 330 nm. (B) Concentrations of hydroxycoumarin released from **PMA(O)** as a function of ultrasonication time calculated from the fluorescence intensity at 378 nm using a standard calibration curve. The theoretical concentration of hydroxycoumarin based on 100% release from the mechanophore is 22.7 μM. Each data point is the average of two measurements with the error bars denoting the range of the two values.

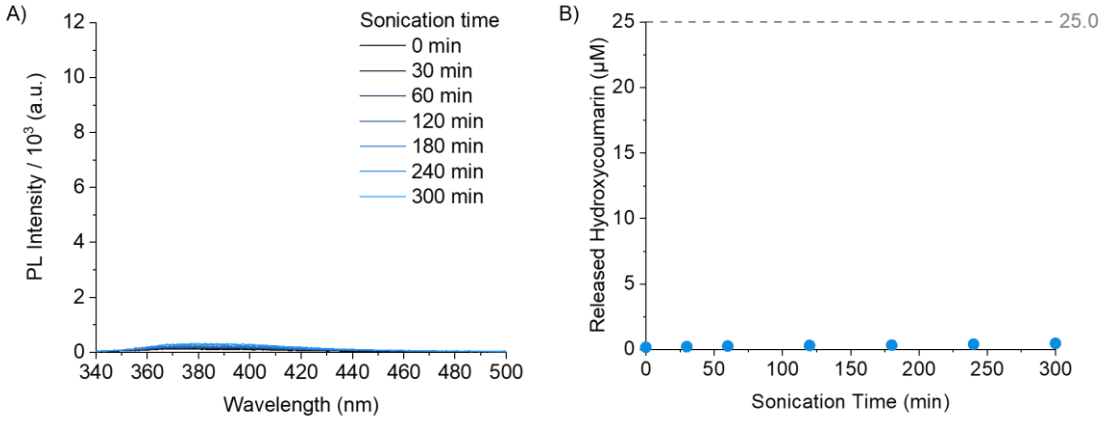

Figure 3.13. (A) PL spectra of a 2.0 mg/mL solution of chain-end functional control polymer **PMA(O)-control** in acetonitrile/methanol (3:1 v/v) after being subjected to ultrasonication for the indicated amount of time. Aliquots were kept at room temperature for 30 min prior to analysis. λ_{ex} = 330 nm. (B) Concentrations of hydroxycoumarin released from **PMA(O)-control** as a function of ultrasonication time calculated from the fluorescence intensity at 378 nm using a standard calibration curve. The theoretical concentration of hydroxycoumarin based on 100% release from the mechanophore is 25.0 μM.

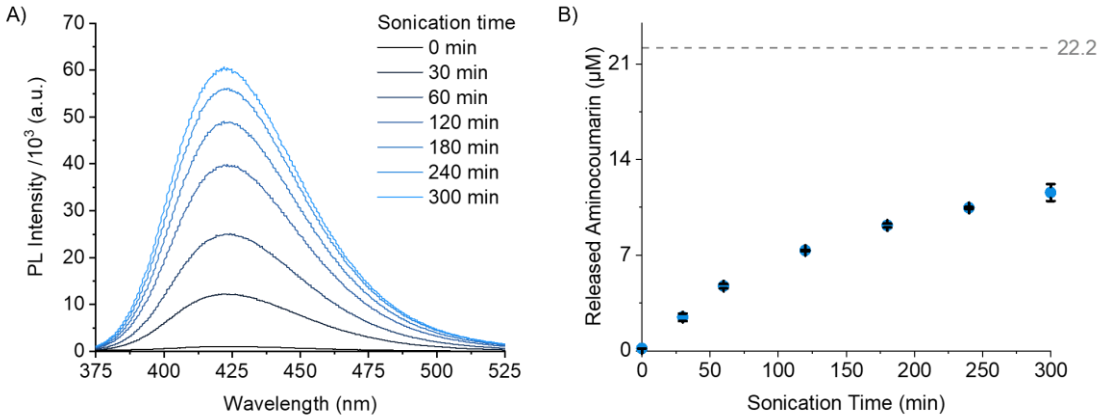

Figure 3.14. (A) Representative PL spectra of a 2.0 mg/mL solution of **PMA(NH)** in acetonitrile/methanol (3:1 v/v) after being subjected to ultrasonication for the indicated amount of time. Aliquots were kept at room temperature for 3 days prior to analysis. λ_{ex} = 365 nm. (B) Concentrations of aminocoumarin released from **PMA(NH)** as a function of ultrasonication time calculated from the fluorescence intensity at 424 nm using a standard calibration curve. The theoretical concentration of hydroxycoumarin based on 100% release from the mechanophore is 22.2 μM. Each data point is the average of two measurements with the error bars denoting the range of the two values.

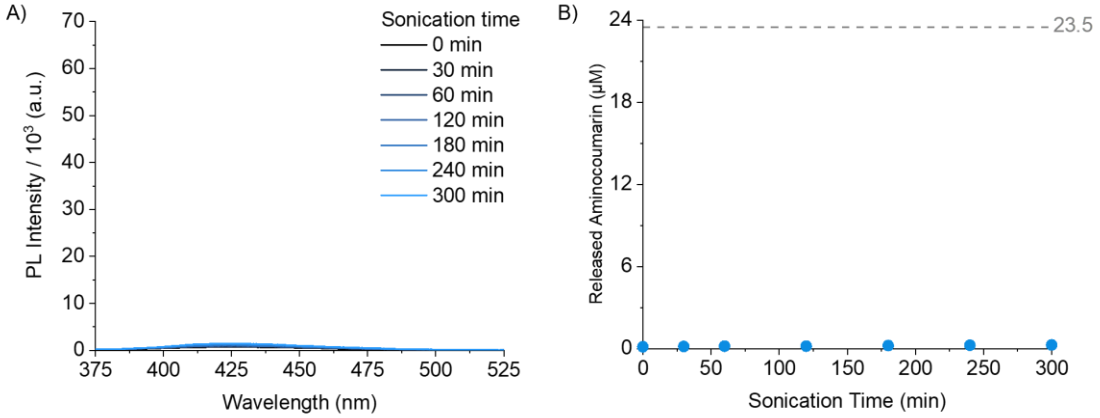

Figure 3.15. (A) PL spectra of a 2.0 mg/mL solution of chain-end functional control polymer **PMA(NH)-control** in acetonitrile/methanol (3:1 v/v) after being subjected to ultrasonication for the indicated amount of time. Aliquots were kept at room temperature for 3 days prior to analysis. λ_{ex} = 365 nm. (B) Concentrations of aminocoumarin released from **PMA(NH)-control** as a function of ultrasonication time calculated from the fluorescence intensity at 424 nm using a standard calibration curve. The theoretical concentration of hydroxycoumarin based on 100% release from the mechanophore is 23.5 μM.

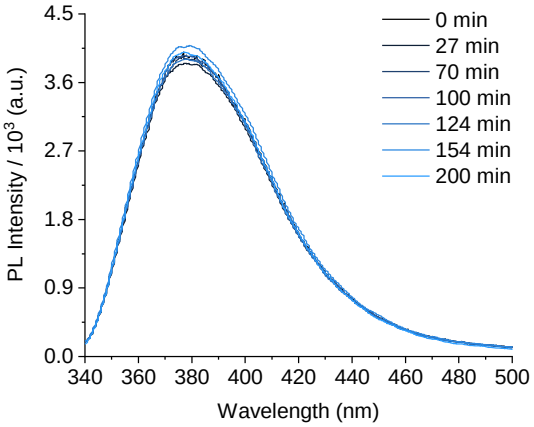

Figure 3.16. Characterization of hydroxycoumarin release from a 2.0 mg/ml solution of **PMA(O)** in acetonitrile/methanol (3:1 v/v) after ultrasound-induced mechanochemical activation for 60 min (sonication "on" time). The sonicated solution was warmed to room temperature and PL spectra were recorded at the indicated times after sonication ended. λ_{ex}= 330 nm. The data indicate that hydroxycoumarin release was completed prior to the first measurement.

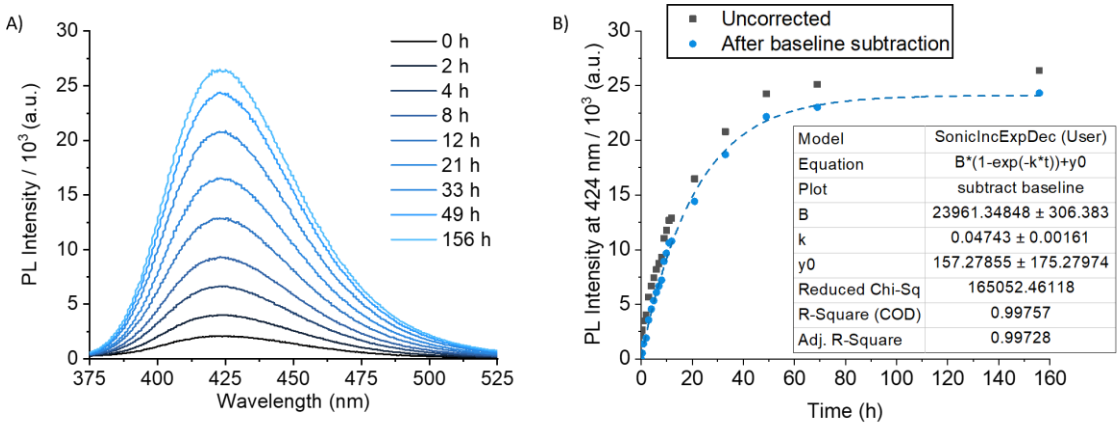

Figure 3.17. Characterization of aminocoumarin release from a 2.0 mg/ml solution of **PMA(NH)** in acetonitrile/methanol (3:1 v/v) after ultrasound-induced mechanochemical activation for 60 min (sonication "on" time). (A) Representative PL spectra of the sonicated solution at room temperature recorded at the indicated times after sonication ended. (B) PL intensity at 424 nm as a function of time post-sonication. The background fluorescence at the start of the experiment (resulting from the release of aminocoumarin cargo during ultrasonication) was subtracted from each subsequent measurement. λ_{ex}= 365 nm. Fitting the baseline corrected data to a first-order rate expression (dashed blue line) gives a half-life of $t_{1/2}$ = 14.6 h.

3.4 Synthetic Details

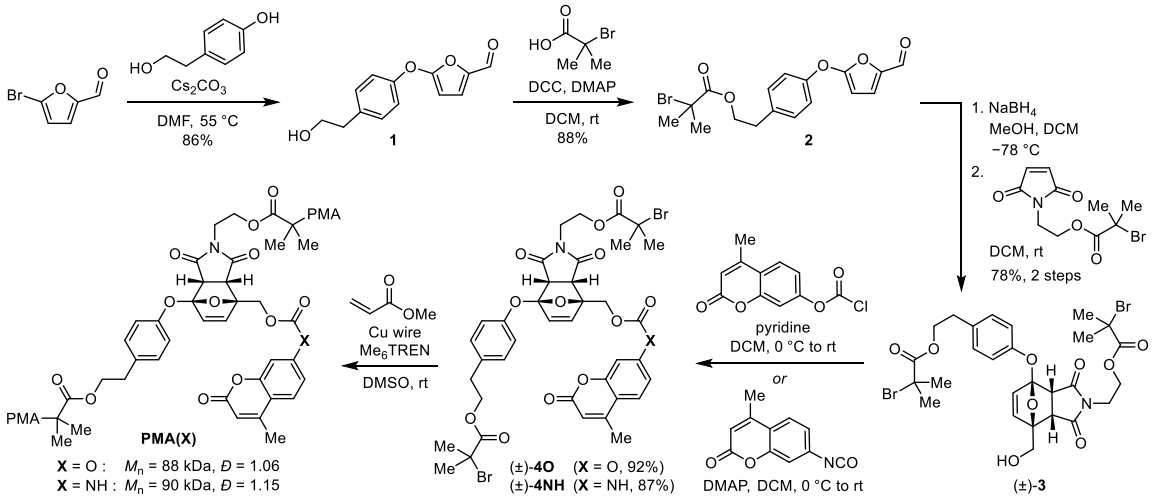

5-(4-(2-hydroxyethyl)phenoxy)furan-2-carbaldehyde (1). A round bottom flask equipped with a stir bar was charged with 5-bromo-2-furaldehyde (1.0 g, 5.7 mmol), 4-(2-hydroxyethyl)phenol (1.0 g, 7.4 mmol), and Cs_2CO_3 (2.4 g, 7.4 mmol). The flask was purged with N_2 before DMF (11 mL) was added. The solution was then heated and kept at 55 °C in an oil bath for 4 h. The reaction was then cooled to room temperature before 10% NH_4Cl (50 mL) was added. The mixture was then extracted with Et_2O (3 x 50 mL) and the combined organic phase was washed with brine (150 mL). The organic layer was dried over $MgSO_4$, filtered, and concentrated under reduced pressure. The crude mixture was then purified by column chromatography (30–60% EtOAc/hexanes) to afford the title compound as a yellow oil, which solidified upon storage in the freezer (1.14 g, 86% yield). ^{1}H NMR (400 MHz, $CDCl_3$) δ: 9.38 (s, 1H), 7.30 – 7.23 (m, 1H), 7.21 (d, *J* = 3.8 Hz, 1H), 7.15 – 7.06 (m, 1H), 5.55 (d, *J* = 3.8 Hz, 1H), 3.87 (t, *J* = 6.6 Hz, 2H), 2.88 (t, *J* = 6.6 Hz, 2H), 1.68 (s, 1H) ppm. ^{13}C{^{1}H} NMR (100 MHz, $CDCl_3$) δ: 175.7, 163.1, 152.8, 144.8, 136.6, 130.6, 125.2, 119.1, 89.8, 63.4, 38.4 ppm. HRMS (FAB, *m/z*): calcd for $[C_{13}H_{13}O_4]^+$ $(M+H)^+$, 233.0808; found, 233.0814.

4-((5-formylfuran-2-yl)oxy)phenethyl 2-bromo-2-methylpropanoate (2). A round bottom flask equipped with a stir bar was charged with **1** (100 mg, 0.431 mmol), DCC (107 mg, 0.517 mmol), DMAP (13.1 mg, 0.108 mmol), and DCM (1 mL). The solution was then stirred to dissolve all reagents before α-bromoisobutyric acid was added (79.0 mg, 0.473 mmol). The solution was stirred at room temperature overnight and then the solid precipitate

was filtered off and discarded. The filtrate was diluted with Et_2O (10 mL) and washed consecutively with 10% NH_4Cl (5 mL) and brine (5 mL). The organic layer was then dried over Na_2SO_4, filtered, and concentrated under reduced pressure. The crude mixture was purified by column chromatography (20–40% EtOAc/hexanes) to afford the title compound as a dark yellow oil, which solidified upon storage in the freezer (143 mg, 88% yield). ^{1}H NMR (400 MHz, $CDCl_3$) δ: 9.40 (s, 1H), 7.28 (app d, *J* = 8.3 Hz, 2H), 7.21 (d, *J* = 3.8 Hz, 1H), 7.12 (app d, *J* = 8.3 Hz, 2H), 5.54 (d, *J* = 3.7 Hz, 1H), 4.38 (t, *J* = 6.8 Hz, 2H), 3.01 (t, *J* = 6.8 Hz, 2H), 1.89 (s, 6H) ppm. ^{13}C{^{1}H} NMR (100 MHz, $CDCl_3$) δ: 175.9, 171.7, 163.0, 153.2, 145.0, 135.5, 130.8, 125.5 119.3, 89.9, 66.3, 55.8, 34.3, 30.9 ppm. HRMS (FAB, *m/z*): calcd for $[C_{17}H_{18}BrO_5]^+$ $(M+H)^+$, 381.0332; found, 381.0335.

4-((2-(2-((2-bromo-2-methylpropanoyl)oxy)ethyl)-7-(hydroxymethyl)-1,3-dioxo-1,2,3,3a,7,7a-hexahydro-4H-4,7-epoxyisoindol-4-yl)oxy)phenethyl 2-bromo-2-methylpropanoate ((±)-3). A flame-dried round bottom flask equipped with a stir bar was charged with **2** (152 mg, 0.40 mmol), DCM (2 mL), and MeOH (2 mL). The solution was cooled to −78 °C in an acetone/dry ice bath before adding $NaBH_4$ (82.0 mg, 2.17 mmol) in three portions. The mixture was kept at −78 °C overnight before being quenched with 10% NH_4Cl (10 mL) and subsequently warmed to room temperature. The solution was then extracted with EtOAc (2 x 10 mL) and the organic phase was washed with brine (10 mL). The organic layer was dried over Na_2SO_4, and filtered. 2-(2,5-dioxo-2,5-dihydro-1H-pyrrol-1-yl)ethyl 2-bromo-2-methylpropanoate[27] (150 mg, 0.52 mmol) was then added to the filtrate, which was then concentrated under reduced pressure until ~2 mL of viscous solution remained. The solution was then reacted at room temperature for 12 h, and the crude mixture was purified by column chromatography (40–70% EtOAc/hexanes). A racemic mixture of the *endo* diastereomer of the title compound was isolated as a foamy white solid (210 mg, 78% yield). ^{1}H NMR (400 MHz, $CDCl_3$) δ: 7.17 (s, 4H), 6.45 (d, *J* = 5.8 Hz, 1H), 6.41 (d, *J* = 5.8 Hz, 1H), 4.35 (m, 2H), 4.31 – 4.12 (m, 4H), 3.73 – 3.64 (m, 4H), 2.96 (t, *J* = 6.9 Hz, 2H), 2.05 (m, 1H), 1.90 (d, *J* = 1.2 Hz, 6H), 1.88 (s, 6H) ppm. ^{13}C{^{1}H} NMR (125 MHz, $CDCl_3$) δ: 174.4, 173.4, 171.7, 171.5, 153.2, 135.7, 135.7, 134.0, 130.1, 120.9, 113.5, 86.7,

66.4, 62.6, 61.9, 55.9, 55.6, 50.6, 48.9, 37.7, 34.2, 30.9, 30.8 ppm. HRMS (FAB, *m/z*): calcd for $[C_{27}H_{32}Br_2NO_9]^+$ $(M+H)^+$, 672.0438; found, 672.0459.

4-((2-(2-((2-bromo-2-methylpropanoyl)oxy)ethyl)-7-(((((4-methyl-2-oxo-2H-chromen-7-yl)oxy)carbonyl)oxy)methyl)-1,3-dioxo-1,2,3,3a,7,7a-hexahydro-4H-4,7-epoxyisoindol-4-yl)oxy)phenethyl 2-bromo-2-methylpropanoate ((±)-4O). A round bottom flask equipped with a stir bar was charged with (±)-**3** (188 mg, 0.282 mmol) and DCM (15 mL). The solution was cooled to 0 °C in an ice bath before adding 4-methylcoumarin-7-chloroformate[18] (153 mg, 0.845 mmol) in DCM (10 mL) then anhydrous pyridine (68 μL, 0.85 mmol). The mixture was then warmed to room temperature, and stirred for 1 h. The mixture was then washed with 10% NH_4Cl (10 mL), extracted with EtOAc (10 mL) and washed with brine (10 mL). The organic layer was dried over Na_2SO_4, and filtered. The crude mixture was purified by column chromatography (40–70% EtOAc/hexanes) to afford the titled compound as a white foamy solid (228 mg, 92% yield). ^{1}H NMR (400 MHz, $CDCl_3$) δ: 7.64 (d, *J* = 8.7 Hz, 1H), 7.29 (d, *J* = 2.3 Hz, 1H), 7.23 (dd, *J* = 8.7, 2.4 Hz, 1H), 7.19 (s, 4H), 6.51 (d, *J* = 5.8 Hz, 1H), 6.46 (d, *J* = 5.8 Hz, 1H), 6.30 (d, *J* = 1.4 Hz, 1H), 4.89 (ABq, $\Delta\nu_{AB}$ = 87.2 Hz, J_{AB} = 12.0 Hz, 2H), 4.43 – 4.31 (m, 2H), 4.25 (t, *J* = 5.1 Hz, 2H), 3.78 – 3.67 (m, 4H), 2.97 (t, *J* = 6.9 Hz, 2H), 2.45 (d, *J* = 1.2 Hz, 3H), 1.90 (s, 6H), 1.88 (s, 6H) ppm. ^{13}C{^{1}H} NMR (100 MHz, $CDCl_3$) δ: 173.6, 173.0, 171.7, 171.5, 160.5, 154.3, 153.2, 153.2, 152.8, 151.9, 136.1, 135.0, 134.2, 130.2, 125.8, 121.1, 118.4, 117.5, 115.0, 113.6, 110.2, 83.7, 66.4, 66.3, 62.6, 55.9, 55.6, 50.1, 49.7, 37.8, 34.3, 30.9, 30.8, 18.9 ppm. HRMS (FAB, *m/z*): calcd for $[C_{38}H_{38}Br_2NO_{13}]^+$ $(M+H)^+$, 874.0704; found, 874.0719.

4-((2-(2-((2-bromo-2-methylpropanoyl)oxy)ethyl)-7-((((4-methyl-2-oxo-2H-chromen-7-yl)carbamoyl)oxy)methyl)-1,3-dioxo-1,2,3,3a,7,7a-hexahydro-4H-4,7-epoxyisoindol-4-yl)oxy)phenethyl 2-bromo-2-methylpropanoate ((±)-4NH). A round bottom flask equipped with a stir bar was charged with (±)-**3** (100 mg, 0.149 mmol) and DCM (2 mL). The solution was cooled to 0 °C in an ice bath before adding 4-methylcoumarin-7-isocyanate[19] (38.9 mg, 0.845 mmol) and then DMAP (1.8 mg, 0.015 mmol). The mixture was warmed to room temperature and stirred for 1 h. The mixture was then washed with 10% NH_4Cl (10 mL), extracted with EtOAc (10 mL), and the organic phase was washed with brine (10 mL). The organic layer was dried over Na_2SO_4 and filtered. The crude mixture was purified by column chromatography (70–100% EtOAc/hexanes) to afford the title compound

as a white foamy solid (113 mg, 87% yield). ^{1}H NMR (400 MHz, $CDCl_3$) δ: 7.55 (d, *J* = 8.7 Hz, 1H), 7.49 (d, *J* = 2.2 Hz, 1H), 7.43 (dd, *J* = 8.7, 2.2 Hz, 1H), 7.30 (s, 1H), 7.16 (s, 4H), 6.47 (d, *J* = 5.7 Hz, 1H), 6.43 (d, *J* = 5.8 Hz, 1H), 6.22 – 6.19 (m, 1H), 4.82 (ABq, Δν*AB* = 79.1 Hz, J_{AB} = 12.0 Hz, 2H), 4.34 (t, *J* = 6.9 Hz, 2H), 4.28 – 4.15 (m, 2H), 3.78 – 3.61 (m, 4H), 2.94 (t, *J* = 6.9 Hz, 2H), 2.41 (d, *J* = 1.2 Hz, 3H), 1.89 (d, *J* = 1.3 Hz, 6H), 1.87 (s, 6H) ppm. ^{13}C{^{1}H} NMR (100 MHz, $CDCl_3$) δ: 173.5, 173.1, 171.7, 171.5, 161.1, 154.6, 153.1, 152.3, 152.3, 141.2, 135.8, 135.4, 134.2, 130.2, 125.6, 121.1, 115.9, 114.6, 113.6, 113.5, 106.3, 84.3, 66.4, 63.2, 62.6, 55.9, 55.7, 50.1, 49.6, 37.7, 34.2, 30.9, 30.8, 18.7 ppm. HRMS (FAB, *m/z*): calcd for $[C_{38}H_{39}Br_2N_2O_{12}]^+$ $(M+H)^+$, 873.0864; found, 873.0898.

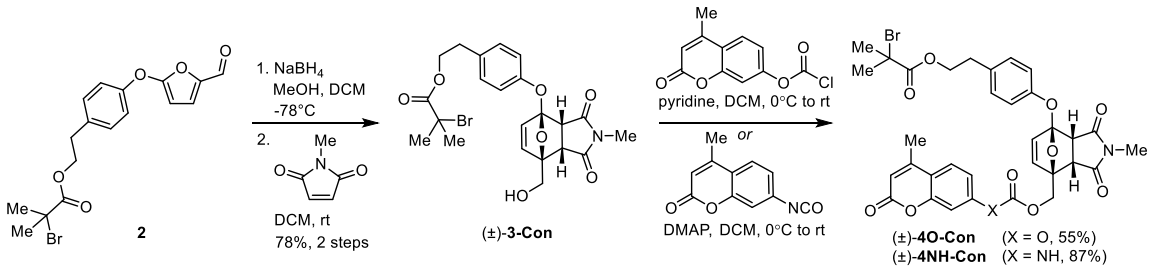

4-((7-(hydroxymethyl)-2-methyl-1,3-dioxo-1,2,3,3a,7,7a-hexahydro-4H-4,7-epoxyisoindol-4-yl)oxy)phenethyl 2-bromo-2-methylpropanoate ((±)-3-Con). The title compound was prepared following a similar procedure as that for compound (±)-**3**, with compound **2** (500 mg, 1.32 mmol), $NaBH_4$ (100 mg, 2.63 mmol), and N-methylmaleimide (175 mg, 1.58 mmol). The crude mixture was purified by column chromatography (40–70% EtOAc/hexanes). A racemic mixture of the *endo* diastereomer of the title compound was isolated as a foamy white solid (566 mg, 87% yield). ^{1}H NMR (400 MHz, $CDCl_3$) δ: 7.17 (s, 4H), 6.39 (d, *J* = 5.8 Hz, 1H), 6.35 (d, *J* = 5.8 Hz, 1H), 4.39 – 4.31 (m, 2H), 4.28 (dd, *J* = 12.6, 5.4 Hz, 1H), 4.17 (dd, *J* = 12.6, 7.0 Hz, 1H), 3.72 – 3.62 (m, 2H), 2.95 (t, *J* = 6.9 Hz, 2H), 2.85 (s, 3H), 2.22 – 2.14 (m, 1H), 1.88 (s, 6H) ppm. ^{13}C{^{1}H} NMR (100 MHz, $CDCl_3$) δ: 174.8, 173.8, 171.7, 153.3, 135.7, 135.6, 133.9, 130.1, 120.9, 113.5, 86.6, 66.4, 61.9, 55.9, 50.6, 49.0, 34.2, 30.9, 24.9 ppm. HRMS (FAB, *m/z*): calcd for $[C_{22}H_{25}BrNO_7]^+$ $(M+H)^+$, 494.0809; found, 494.0799.

4-((2-methyl-7-(((((4-methyl-2-oxo-2H-chromen-7-yl)oxy)carbonyl)oxy)methyl)-1,3-dioxo-1,2,3,3a,7,7a-hexahydro-4H-4,7-epoxyisoindol-4-yl)oxy)phenethyl 2-bromo-2-methylpropanoate ((±)-4O-Con). The title compound was prepared following a similar procedure as that for compound (±)-**4O**, with compound (±)-**3-Con** (44 mg, 0.089 mmol), 4-

methylcoumarin-7-chloroformate[18] (30.0 mg, 0.125 mmol), anhydrous pyridine (13 μL, 0.13 mmol), and DCM (6 mL). The crude mixture was purified by column chromatography (40–70% EtOAc/hexanes) to afford the title compound as a foamy white solid (34 mg, 55% yield). ^{1}H NMR (500 MHz, $CDCl_3$) δ: 7.64 (d, *J* = 8.7 Hz, 1H), 7.29 (d, *J* = 2.3 Hz, 1H), 7.22 (dd, *J* = 8.7, 2.3 Hz, 1H), 7.19 (s, 4H), 6.45 (d, *J* = 5.8 Hz, 1H), 6.40 (d, *J* = 5.8 Hz, 1H), 6.29 (s, 1H), 4.89 (ABq, $\Delta\nu_{AB}$ = 99.5Hz, J_{AB} = 10.0 Hz, 2H), 4.39 – 4.31 (m, 2H), 3.73 (s, 2H), 2.96 (t, *J* = 6.9 Hz, 2H), 2.88 (s, 3H), 2.45 (s, 3H), 1.88 (s, 6H) ppm. ^{13}C{^{1}H} NMR (100 MHz, $CDCl_3$) δ: 173.9, 173.4, 171.7, 160.5, 154.3, 153.2, 153.2, 152.8, 151.9, 136.0, 134.9, 134.1, 130.2, 125.7, 121.0, 118.4, 117.5, 114.9, 113.5, 110.2, 83.6, 66.4, 66.4, 55.9, 50.1, 49.7, 34.2, 30.9, 25.0, 18.9 ppm. HRMS (FAB, *m/z*): calcd for $[C_{33}H_{31}BrNO_{11}]^+$ $(M+H)^+$, 696.1075; found, 696.1060.

4-((2-methyl-7-((((4-methyl-2-oxo-2H-chromen-7-yl)carbamoyl)oxy)methyl)-1,3-dioxo-1,2,3,3a,7,7a-hexahydro-4H-4,7-epoxyisoindol-4-yl)oxy)phenethyl 2-bromo-2-methylpropanoate ((±)-4NH-Con). The title compound was prepared following a similar procedure as that for compound (±)-**4NH**, with compound (±)-**3-Con** (100 mg, 0.2 mmol), 4-methylcoumarin-7-isocyanate[19] (52.9 mg, 0.263 mmol), DMAP (2.4 mg, 0.020 mmol), and DCM (3 mL). The crude mixture was purified by column chromatography (50–100% EtOAc/hexanes) to afford the title compound as a foamy white solid (121 mg, 87% yield). ^{1}H NMR (400 MHz, $CDCl_3$) δ: 7.55 (d, *J* = 8.7 Hz, 1H), 7.48 (d, *J* = 2.1 Hz, 1H), 7.43 (dd, *J* = 8.6, 2.2 Hz, 1H), 7.29 (s, 1H), 7.19 – 7.13 (m, 4H), 6.41 (d, *J* = 5.8 Hz, 1H), 6.38 (d, *J* = 5.8 Hz, 1H), 6.22 – 6.19 (m, 1H), 4.83 (ABq, $\Delta\nu_{AB}$ = 66.9 Hz, J_{AB} = 12.0 Hz, 2H), 4.34 (t, *J* = 6.9 Hz, 2H), 3.73 (d, *J* = 7.9 Hz, 1H), 3.66 (d, *J* = 7.9 Hz, 1H), 2.94 (t, *J* = 6.9 Hz, 2H), 2.86 (s, 3H), 2.41 (d, *J* = 1.3 Hz, 3H), 1.87 (s, 6H) ppm. ^{13}C{^{1}H} NMR (100 MHz, $CDCl_3$) δ: 174.0, 173.6, 171.7, 161.1, 154.6, 153.2, 152.3, 141.2, 135.8, 135.3, 134.1, 130.2, 125.6, 121.0, 116.0, 114.6, 113.5, 106.3, 84.2, 66.4, 63.3, 55.9, 50.2, 49.6, 34.2, 30.9, 25.0, 18.7 ppm. HRMS (FAB, *m/z*): calcd for $[C_{33}H_{32}BrN_2O_{10}]^+$ $(M+H)^+$, 695.1235; found, 695.1262.

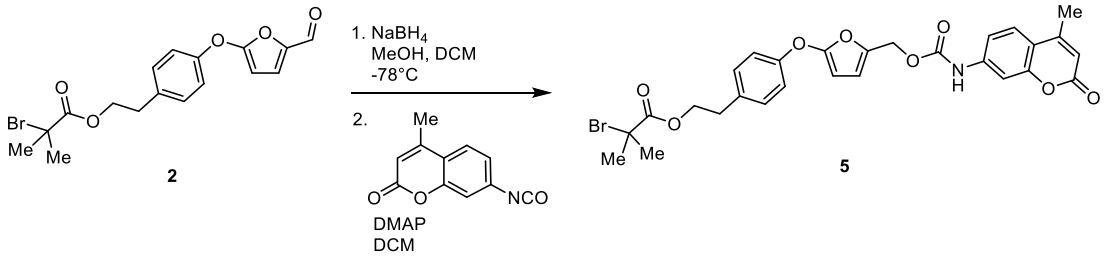

4-((5-((((4-methyl-2-oxo-2H-chromen-7-yl)carbamoyl)oxy)methyl)furan-2-yl)oxy)phenethyl 2-bromo-2-methylpropanoate (5). A 20 mL flame-dried vial equipped with a stir bar was charged with **2** (104 mg, 0.272 mmol), MeOH (2 mL), and DCM (2 mL). The solution was cooled to −78 °C in an acetone/dry ice bath before adding $NaBH_4$ (82.0 mg, 2.17 mmol) in three portions. The mixture was kept at −78 °C overnight before being quenched with 10% NH_4Cl (10 mL) and warmed up to room temperature. The solution was then extracted with EtOAc (2 x 10 mL) and the organic phase was washed with brine (10 mL). The organic layer was dried over Na_2SO_4, filtered, and concentrated under vacuum. The crude product was then redissolved in DCM (2 mL) and cooled to 0 °C in an ice bath before adding 4-methylcoumarin-7-isocyanate[19] (72.8 mg, 0.353 mmol), followed by DMAP (1.0 mg, 0.031 mmol). The reaction mixture was warmed to room temperature and stirred for 2 h before being quenched by adding a solution of glucose (35.0 mg, 0.194 mmol) in 3 mL DMF. The mixture was stirred at room temperature for 2 h to consume the excess isocyanate, then diluted with diethyl ether (20 mL) and hexane (5 mL). A precipitate appeared immediately and the suspension was filtered to remove the excess glucose and other insoluble products. The filtrate was washed with aqueous $NaHCO_3$ solution and brine, dried over Na_2SO_4, then concentrated. The crude material was again dispersed into a mixture of diethyl ether (5 mL) and hexane (10 mL), and then filtered to remove insoluble 7-amino-4-methylcoumarin. The filtrate was concentrated, dissolved in a small amount of DCM (0.3 mL), and then added into a mixture of diethyl ether (3 mL) and hexane (7 mL). The mixture was slowly concentrated to around half the original volume using a rotary evaporator causing an off-white precipitate to form. The off-white solid was collected carefully by removing the liquid using a pipet, and then the solid was washed with hexane and finally dried under high vacuum to yield metastable compound **5** a fluffy white solid (53 mg, 34% yield). ^{1}H NMR (500 MHz, $CDCl_3$) δ 7.52 (d, *J* = 8.7 Hz, 1H), 7.47 – 7.44 (m, 1H), 7.35 (app d, *J* = 8.5 Hz, 1H), 7.23 – 7.19 (m, 2H), 7.04 – 6.99 (m, 3H), 6.44 (d, *J* = 3.2 Hz, 1H), 6.19 (s, 1H), 5.49 (d, *J* = 3.3 Hz, 1H), 5.09 (s, 2H), 4.36 (t, *J* = 6.8 Hz, 2H), 2.97 (t, *J* = 6.8 Hz, 2H), 2.41 (s, 3H), 1.90 (s, 6H) ppm. $^{13}C\{^1H\}$ NMR (100 MHz, $CDCl_3$) δ 171.7, 161.2, 157.5, 155.2, 154.6, 152.5, 152.3, 141.3, 133.7, 130.5, 125.5, 121.7, 117.6, 115.8, 114.5, 113.4, 113.2, 106.1,

89.5, 66.5, 59.5, 55.9, 34.2, 30.9, 18.7 ppm. HRMS (FAB, *m/z*): calcd for $[C_{28}H_{27}BrNO_8]^+$ $(M+H)^+$, 584.0915; found, 584.0916.

General Polymerization Procedure. Polymers were synthesized following the procedure reported previously.[18] A 10 mL Schlenk flask equipped with a stir bar was charged with the initiator (1 equiv), methyl acrylate (~1,500 equiv), Me_6TREN (2 equiv), and DMSO (equal volume to methyl acrylate). The flask was sealed, the solution was deoxygenated via three freeze-pump-thaw cycles, and then backfilled with nitrogen. The flask was opened briefly under a flow of N_2, and freshly cut copper wire (1.0 cm length, 20 gauge) was added on top of the frozen mixture. The flask was resealed, evacuated for an additional 15 min, warmed to room temperature, and then backfilled with nitrogen. The mixture was stirred at room temperature until the solution became sufficiently viscous, indicating that the desired monomer conversion was reached (ca. 1–2 h). The flask was then opened to air and the solution was diluted with DCM. The polymer was precipitated into cold methanol (2x) and the isolated polymer was thoroughly dried under vacuum and characterized by GPC-MALS. Molecular weight characterization data for all polymers studied are reported below (Table 3.1.).

Table 3.1. Characterization of the polymers used in this study.

	M_n (kg/mol)	$Đ$
PMA(O)	88	1.06
PMA(NH)	90	1.15
PMA(O)-control	80	1.21
PMA(NH)-control	85	1.22

3.5 General Procedure for Ultrasonication Experiments

An oven-dried sonication vessel was fitted with rubber septa, placed onto the sonication probe, and allowed to cool under a stream of dry argon. The vessel was charged with a solution of the polymer in anhydrous acetonitrile/methanol (3:1 v/v, 2.0 mg/mL, 20 mL) and submerged in an ice bath. The solution was sparged continuously with argon beginning 20 min prior to sonication and for the duration of the sonication experiment. Pulsed ultrasound (1 s on/1 s off, 30% amplitude, 20 kHz, 8.2 W/cm^2) was then applied to the system. The

solution temperature during sonication was measured to be 8–10 °C. Sonicated solutions were filtered through a 0.45 μm syringe filter prior to analysis. Ultrasonic intensity was calibrated using the method described by Berkowski *et al*.[28]

3.6 . Procedure for CoGEF calculations

CoGEF calculations were performed using Spartan ′18 Parallel Suite according to previously reported methods.[22,23] Ground state energies were calculated using DFT at the B3LYP/6-31G* level of theory. Starting from the equilibrium geometry of the unconstrained molecule (relative energy = 0 kJ/mol), the distance between the terminal methyl groups of the truncated structure was increased in increments of 0.05 Å and the energy was minimized at each step. The maximum force associated with the retro-Diels–Alder reaction was calculated from the slope of the curve immediately prior to bond cleavage.

3.7 References

(1) Patrick, J. F.; Robb, M. J.; Sottos, N. R.; Moore, J. S.; White, S. R. Polymers with autonomous life-cycle control. *Nature* **2016**, *540*, 363–370.

(2) Swager, T. M. Sensor Technologies Empowered by Materials and Molecular Innovations. *Angew. Chem. Int. Ed.* **2018**, *57*, 4248–4257.

(3) Zhang, Y.; Yu, J.; Bomba, H. N.; Zhu, Y.; Gu, Z. Mechanical Force-Triggered Drug Delivery. *Chem. Rev.* **2016**, *116*, 12536–12563.

(4) Groote, R.; Jakobs, R. T. M.; Sijbesma, R. P. Mechanocatalysis: forcing latent catalysts into action. *Polym. Chem.* **2013**, *4*, 4846.

(5) Esser-Kahn, A. P.; Odom, S. A.; Sottos, N. R.; White, S. R.; Moore, J. S. Triggered Release from Polymer Capsules. *Macromolecules* **2011**, *44*, 5539–5553.

(6) Li, J.; Nagamani, C.; Moore, J. S. Polymer Mechanochemistry: From Destructive to Productive. *Acc. Chem. Res.* **2015**, *48*, 2181–2190.

(7) Beyer, M. K.; Clausen-Schaumann, H. Mechanochemistry: The Mechanical Activation of Covalent Bonds. *Chem. Rev.* **2005**, *105*, 2921–2948.

(8) Caruso, M. M.; Davis, D. A.; Shen, Q.; Odom, S. A.; Sottos, N. R.; White, S. R.; Moore, J. S. Mechanically-Induced Chemical Changes in Polymeric Materials. *Chem. Rev.* **2009**, *109*, 5755–5798.

(9) Larsen, M. B.; Boydston, A. J. "Flex-Activated" Mechanophores: Using Polymer Mechanochemistry To Direct Bond Bending Activation. *J. Am. Chem. Soc.* **2013**, *135*, 8189–8192.

(10) Shen, H.; Larsen, M. B.; Roessler, A.; Zimmerman, P.; Boydston, A. J. Mechanochemical Release of N-heterocyclic Carbenes from Flex-Activated Mechanophores. *Angew. Chem. Int. Ed.* **2021**, *60*, 13559–13563.

(11) Jayathilaka, P. B.; Molley, T. G.; Huang, Y.; Islam, M. S.; Buche, M. R.; Silberstein, M. N.; Kruzic, J. J.; Kilian, K. A. Force-mediated molecule release from double network hydrogels. *Chem. Commun.* **2021**, DOI: 10.1039/D1CC02726C.
(12) Diesendruck, C. E.; Steinberg, B. D.; Sugai, N.; Silberstein, M. N.; Sottos, N. R.; White, S. R.; Braun, P. V.; Moore, J. S. Proton-Coupled Mechanochemical Transduction: A Mechanogenerated Acid. *J. Am. Chem. Soc.* **2012**, *134*, 12446–12449.
(13) Lin, Y.; Kouznetsova, T. B.; Craig, S. L. A Latent Mechanoacid for Time-Stamped Mechanochromism and Chemical Signaling in Polymeric Materials. *J. Am. Chem. Soc.* **2020**, *142*, 99–103.
(14) Shi, Z.; Wu, J.; Song, Q.; Göstl, R.; Herrmann, A. Toward Drug Release Using Polymer Mechanochemical Disulfide Scission. *J. Am. Chem. Soc.* **2020**, *142*, 14725–14732.
(15) Shi, Z.; Song, Q.; Göstl, R.; Herrmann, A. Mechanochemical activation of disulfide-based multifunctional polymers for theranostic drug release. *Chem. Sci.* **2021**, *12*, 1668–1674.
(16) Huo, S.; Zhao, P.; Shi, Z.; Zou, M.; Yang, X.; Warszawik, E.; Loznik, M.; Göstl, R.; Herrmann, A. Mechanochemical bond scission for the activation of drugs. *Nat. Chem.* **2021**, *13*, 131–139.
(17) Shi, Z.; Song, Q.; Göstl, R.; Herrmann, A. The Mechanochemical Release of Naphthalimide Fluorophores from β-Carbonate and β-Carbamate Disulfide-Centered Polymers. *CCS Chem.* **2021**, 2333–2344.
(18) Hu, X.; Zeng, T.; Husic, C. C.; Robb, M. J. Mechanically Triggered Small Molecule Release from a Masked Furfuryl Carbonate. *J. Am. Chem. Soc.* **2019**, *141*, 15018–15023.
(19) Hu, X.; Zeng, T.; Husic, C. C.; Robb, M. J. Mechanically Triggered Release of Functionally Diverse Molecular Payloads from Masked 2-Furylcarbinol Derivatives. *ACS Cent. Sci.* **2021**, *7*, 1216–1224.
(20) Alouane, A.; Labruère, R.; Le Saux, T.; Schmidt, F.; Jullien, L. Self-Immolative Spacers: Kinetic Aspects, Structure–Property Relationships, and Applications. *Angew. Chem. Int. Ed.* **2015**, *54*, 7492–7509.
(21) Stevenson, R.; De Bo, G. Controlling Reactivity by Geometry in Retro-Diels–Alder Reactions under Tension. *J. Am. Chem. Soc.* **2017**, *139*, 16768–16771.
(22) Beyer, M. K. The mechanical strength of a covalent bond calculated by density functional theory. *J. Chem. Phys.* **2000**, *112*, 7307–7312.
(23) Klein, I. M.; Husic, C. C.; Kovács, D. P.; Choquette, N. J.; Robb, M. J. Validation of the CoGEF Method as a Predictive Tool for Polymer Mechanochemistry. *J. Am. Chem. Soc.* **2020**, *142*, 16364–16381.
(24) Nguyen, N. H.; Rosen, B. M.; Lligadas, G.; Percec, V. Surface-Dependent Kinetics of Cu(0)-Wire-Catalyzed Single-Electron Transfer Living Radical Polymerization of Methyl Acrylate in DMSO at 25 °C. *Macromolecules* **2009**, *42*, 2379–2386.
(25) Berkowski, K. L.; Potisek, S. L.; Hickenboth, C. R.; Moore, J. S. Ultrasound-Induced Site-Specific Cleavage of Azo-Functionalized Poly(ethylene glycol). *Macromolecules* **2005**, *38*, 8975–8978.

(26) Kean, Z. S.; Gossweiler, G. R.; Kouznetsova, T. B.; Hewage, G. B.; Craig, S. L. A Coumarin Dimer Probe of Mechanochemical Scission Efficiency in the Sonochemical Activation of Chain-Centered Mechanophore Polymers. *Chem. Commun.* **2015**, *51*, 9157–9160.
(27) Ronn, M.; Lim, N.-K.; Hogan, P.; Zhang, W.-Y.; Zhu, Z.; Dunwoody, N. An Expedient Route to 3-Methoxy-2-furaldehyde. *Synlett* **2012**, *2012*, 134–136.
(28) Berkowski, K. L.; Potisek, S. L.; Hickenboth, C. R.; Moore, J. S. Ultrasound-Induced Site-Specific Cleavage of Azo-Functionalized Poly(ethylene glycol). *Macromolecules* **2005**, *38*, 8975–8978.

3.8 ^{1}H and ^{13}C NMR spectra

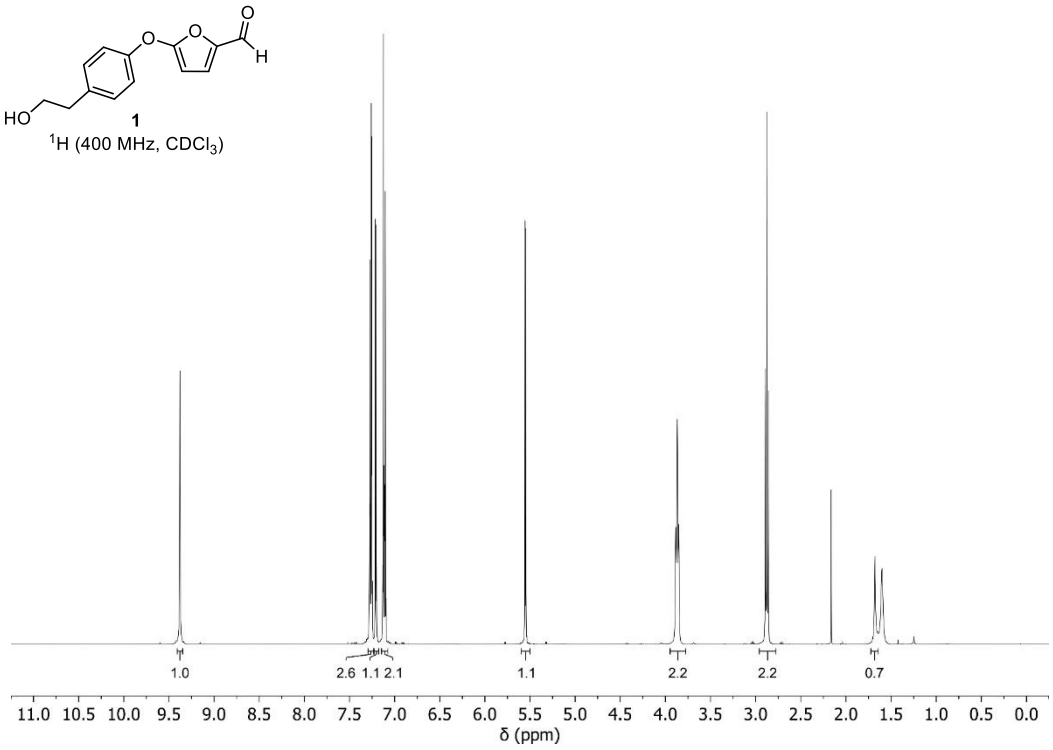

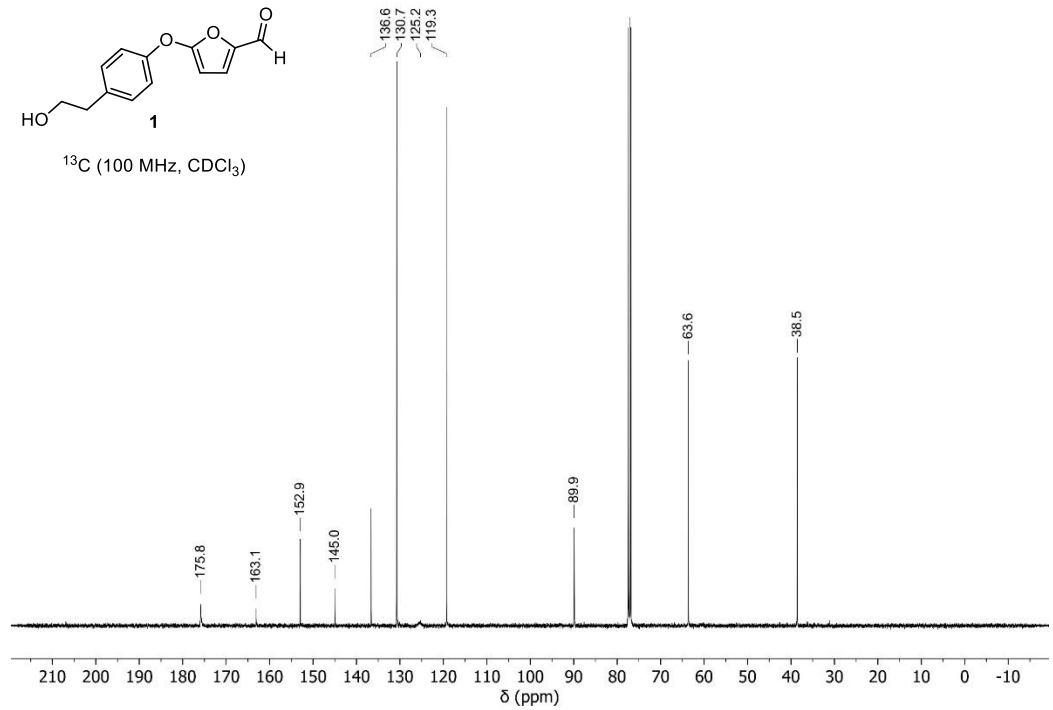

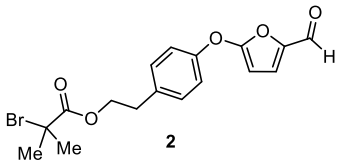

2

^{1}H (400 MHz, $CDCl_3$)

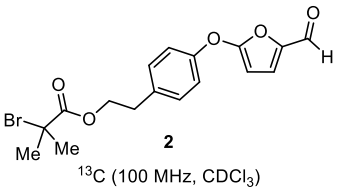

2

^{13}C (100 MHz, $CDCl_3$)

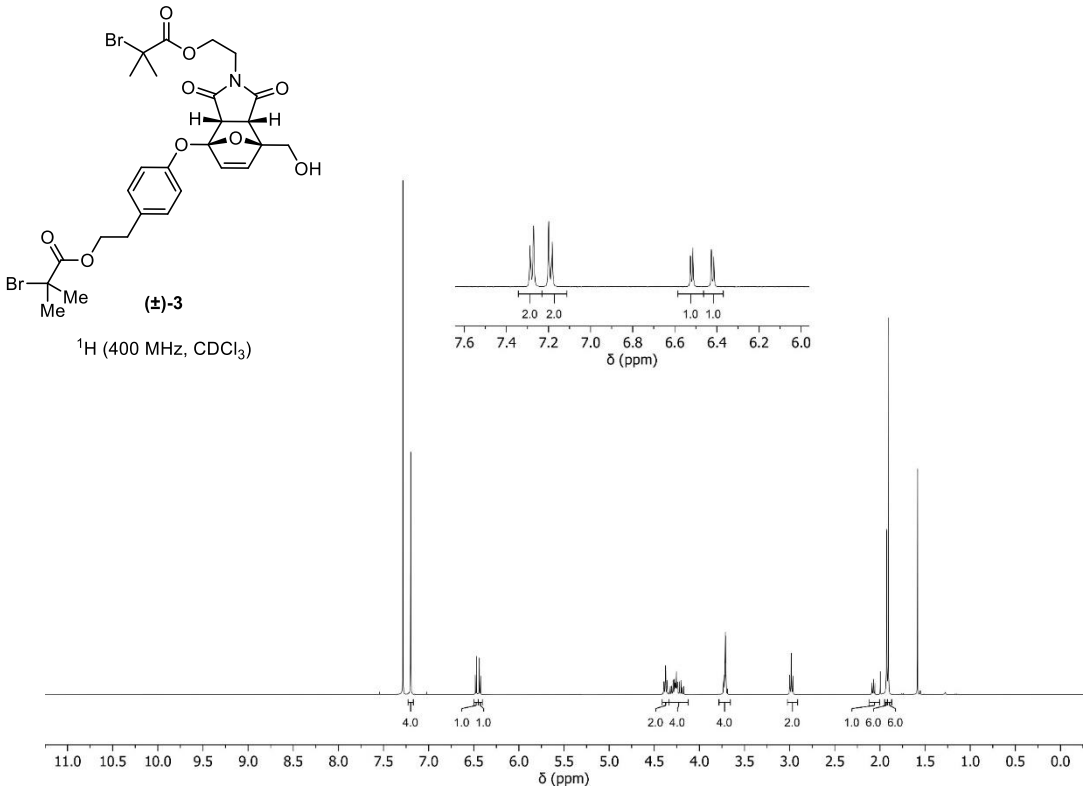
(±)-3
^{1}H (400 MHz, $CDCl_3$)
δ (ppm)

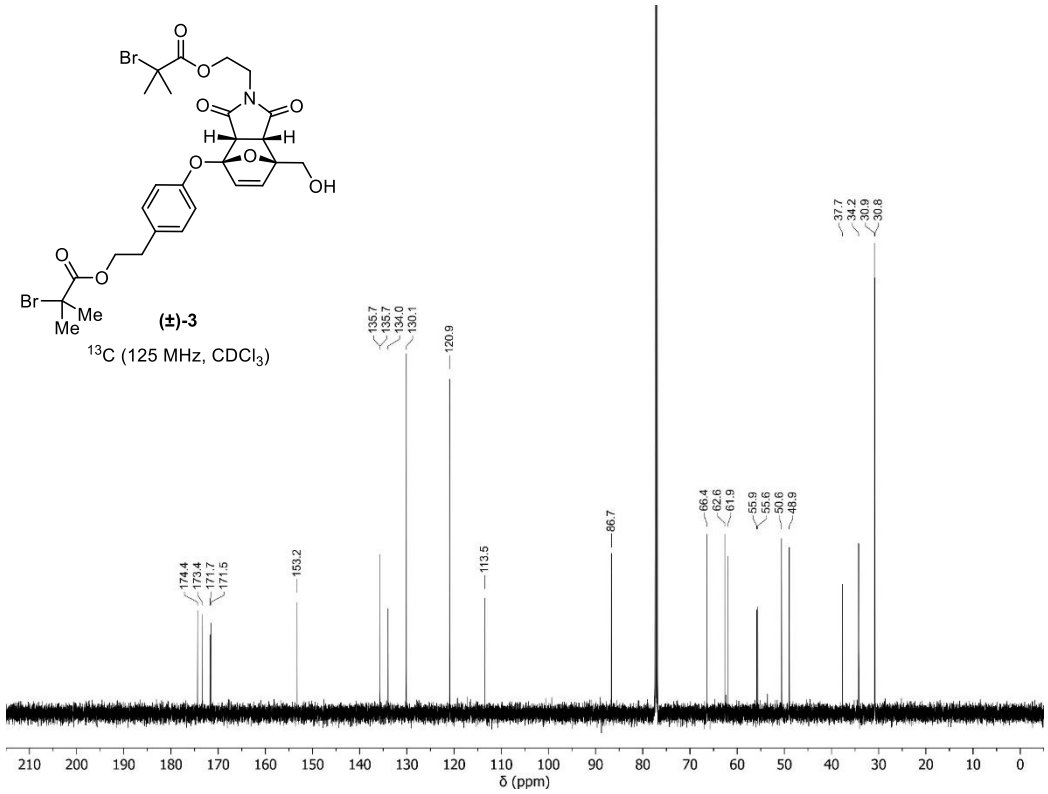
(±)-3
^{13}C (125 MHz, $CDCl_3$)
δ (ppm)

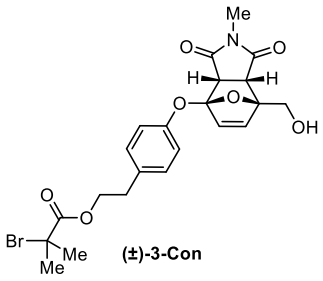

(±)-3-Con

^{1}H (400 MHz, $CDCl_3$)

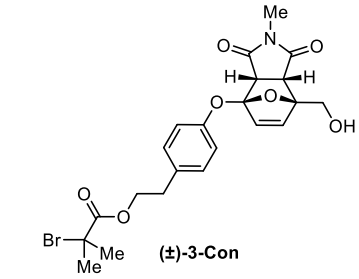

(±)-3-Con

^{13}C (100 MHz, $CDCl_3$)

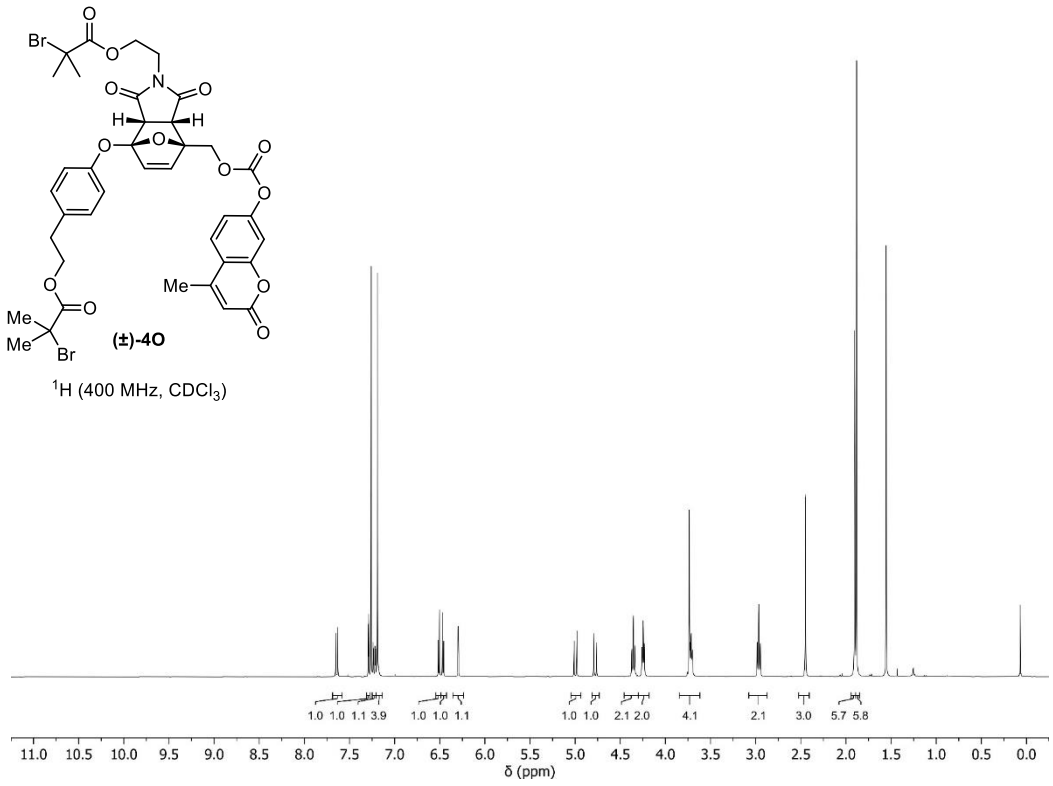
(±)-4O
1H (400 MHz, CDCl3)
1.0 1.0 1.1 3.9
1.0 1.0 1.1
1.0 1.0
2.1 2.0
4.1
2.1
3.0
5.7 5.8
δ (ppm)

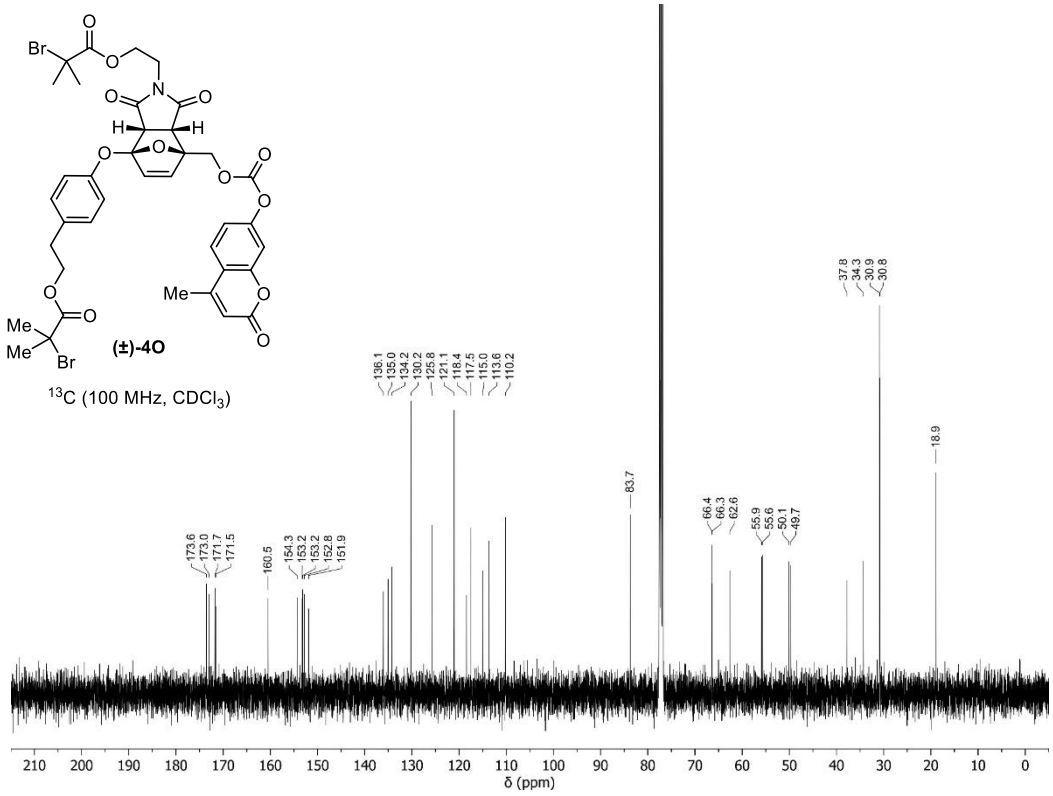
(±)-4O
13C (100 MHz, CDCl3)
173.6
173.0
171.7
171.5
160.5
154.3
153.2
153.2
152.8
151.9
136.1
135.0
134.2
130.2
125.8
121.1
118.4
117.5
115.0
113.6
110.2
83.7
66.4
66.3
62.6
55.9
55.6
50.1
49.7
37.8
34.3
30.9
30.8
18.9
δ (ppm)

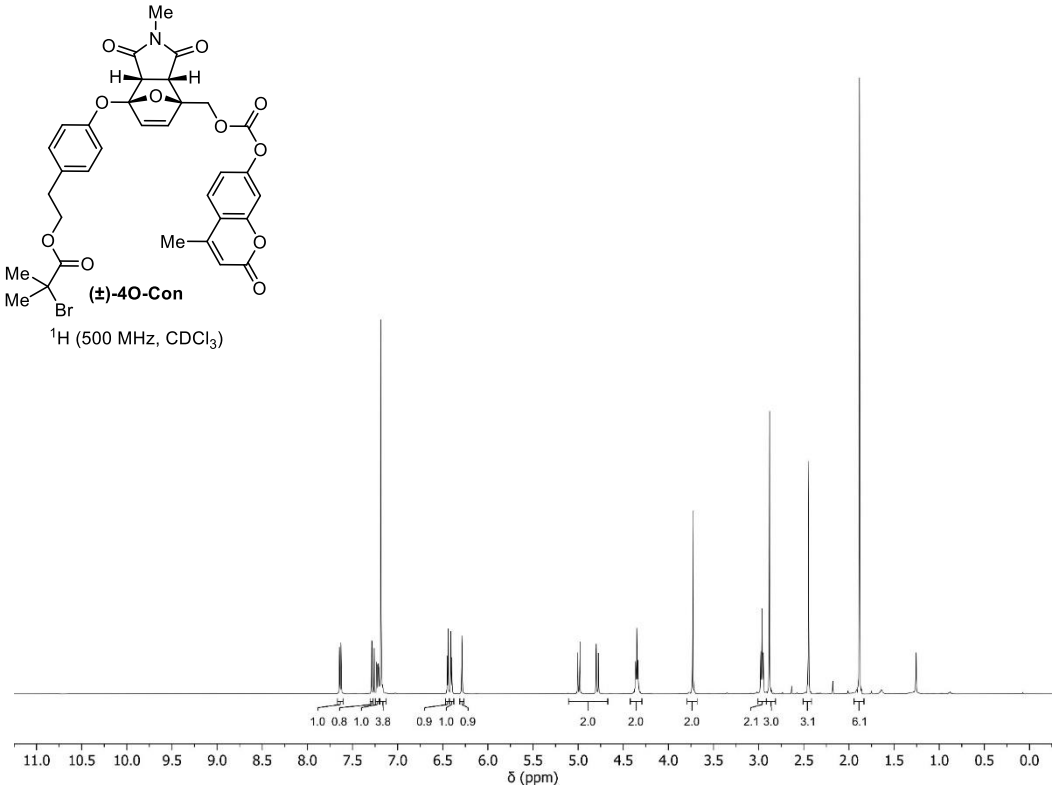
(±)-4O-Con
^{1}H (500 MHz, CDCl$_3$)
1.0 0.8 1.0 3.8
0.9 1.0 0.9
2.0
2.0
2.0
2.1 3.0
3.1
6.1
δ (ppm)

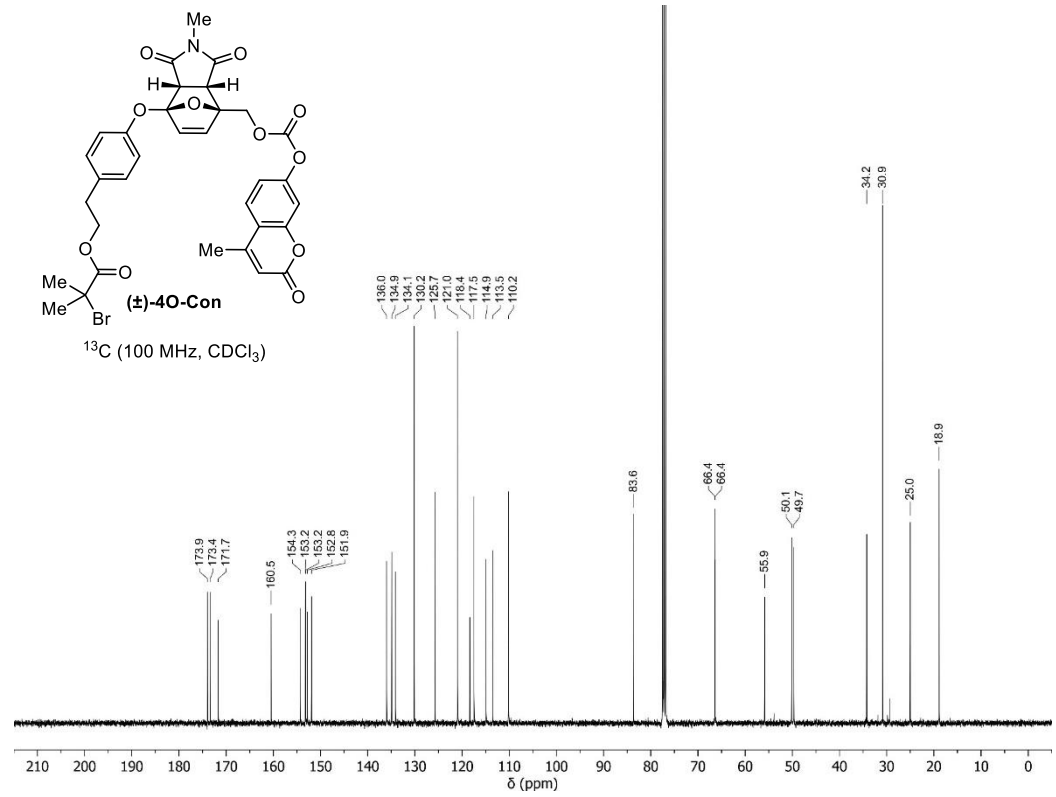
(±)-4O-Con
^{13}C (100 MHz, CDCl$_3$)
136.0
134.9
134.1
130.2
125.7
121.0
118.4
117.5
114.9
113.5
110.2
173.9
173.4
171.7
160.5
154.3
153.2
153.2
152.8
151.9
83.6
66.4
66.4
55.9
50.1
49.7
34.2
30.9
25.0
18.9
δ (ppm)

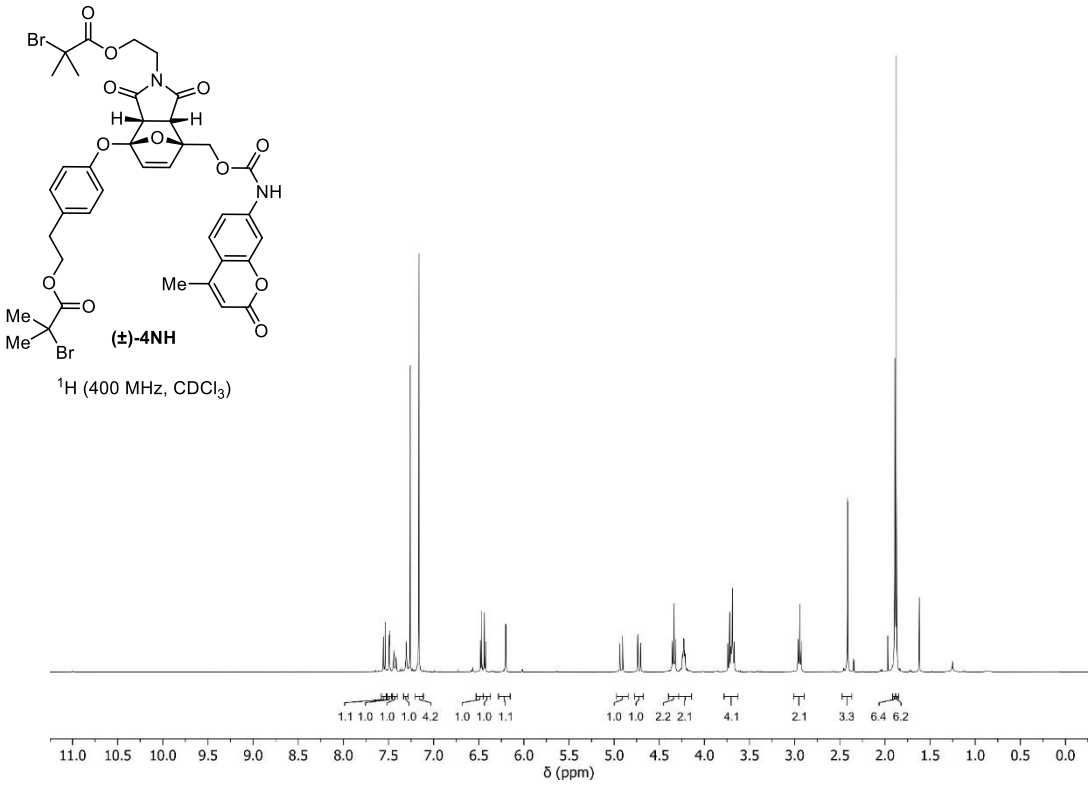
(±)-4NH
1H (400 MHz, CDCl3)
1.1 1.0 1.0 1.0 4.2 1.0 1.0 1.1 1.0 1.0 2.2 2.1 4.1 2.1 3.3 6.4 6.2
δ (ppm)

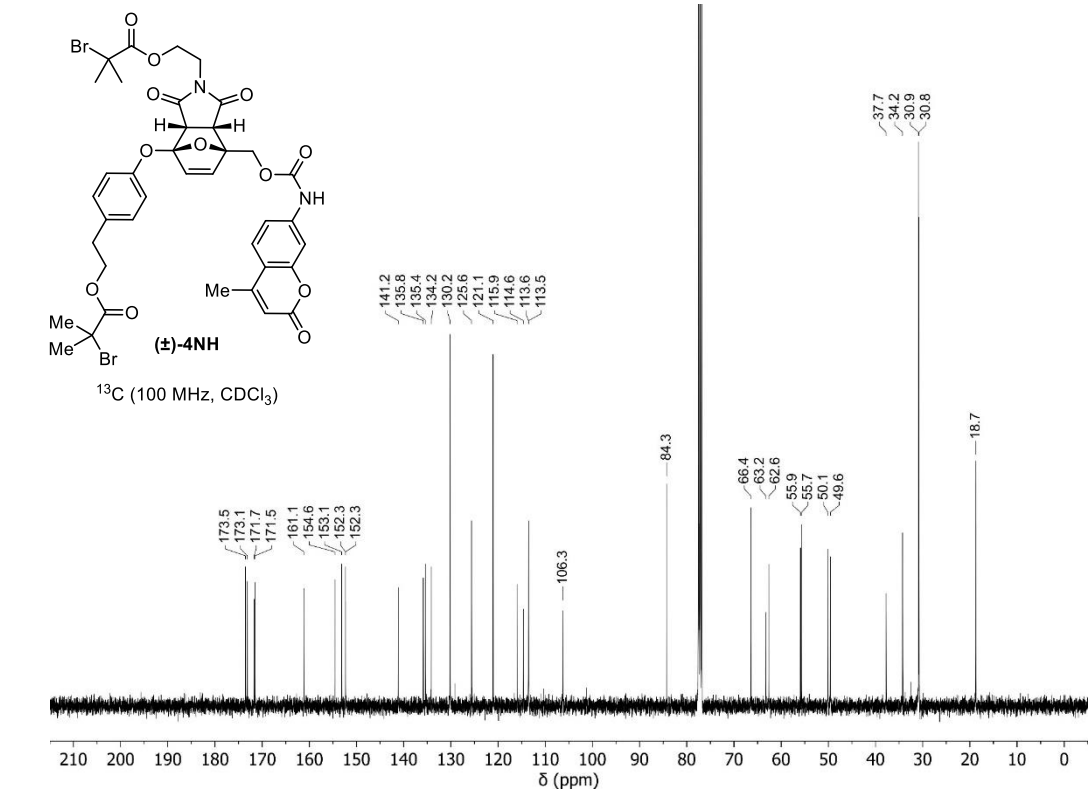
(±)-4NH
13C (100 MHz, CDCl3)
173.5 173.1 171.7 171.5 161.1 154.6 153.1 152.3 152.3 141.2 135.8 135.4 134.2 130.2 125.6 121.1 115.9 114.6 113.6 113.5 106.3 84.3 66.4 63.2 62.6 55.9 55.7 50.1 49.6 37.7 34.2 30.9 30.8 18.7
δ (ppm)

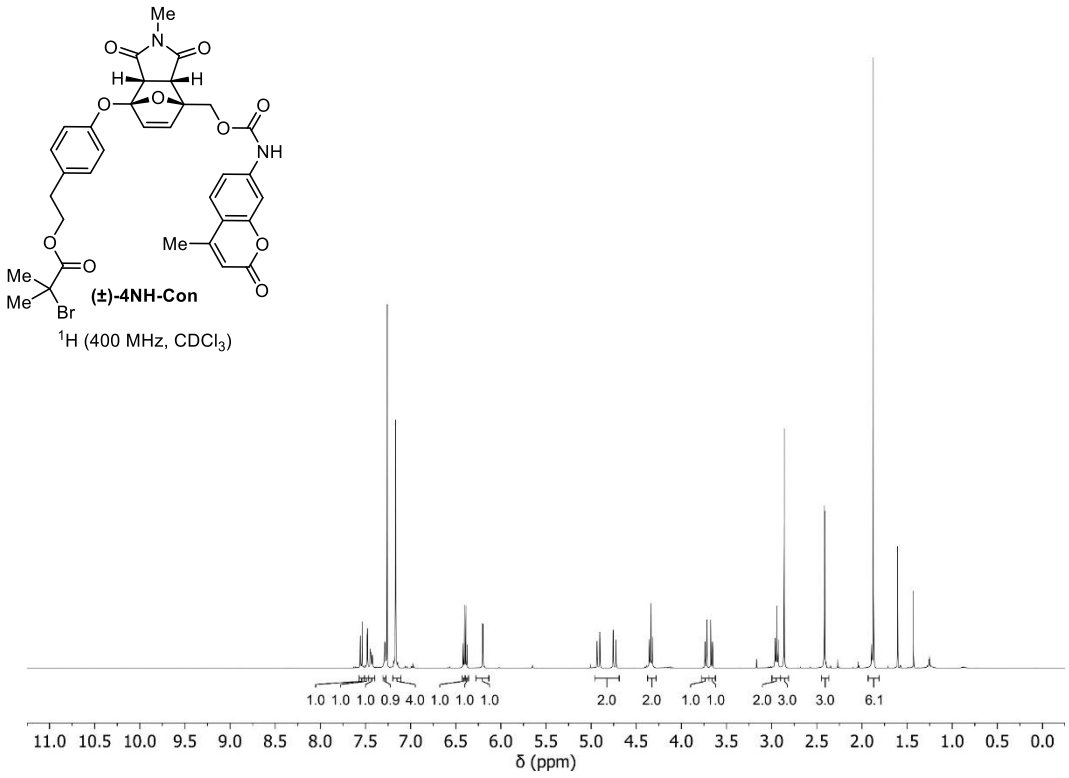
(±)-4NH-Con
^{1}H (400 MHz, $CDCl_3$)
1.0 1.0 1.0 0.9 4.0 1.0 1.0 1.0
2.0
2.0
1.0 1.0
2.0 3.0
3.0
6.1
11.0 10.5 10.0 9.5 9.0 8.5 8.0 7.5 7.0 6.5 6.0 5.5 5.0 4.5 4.0 3.5 3.0 2.5 2.0 1.5 1.0 0.5 0.0
δ (ppm)

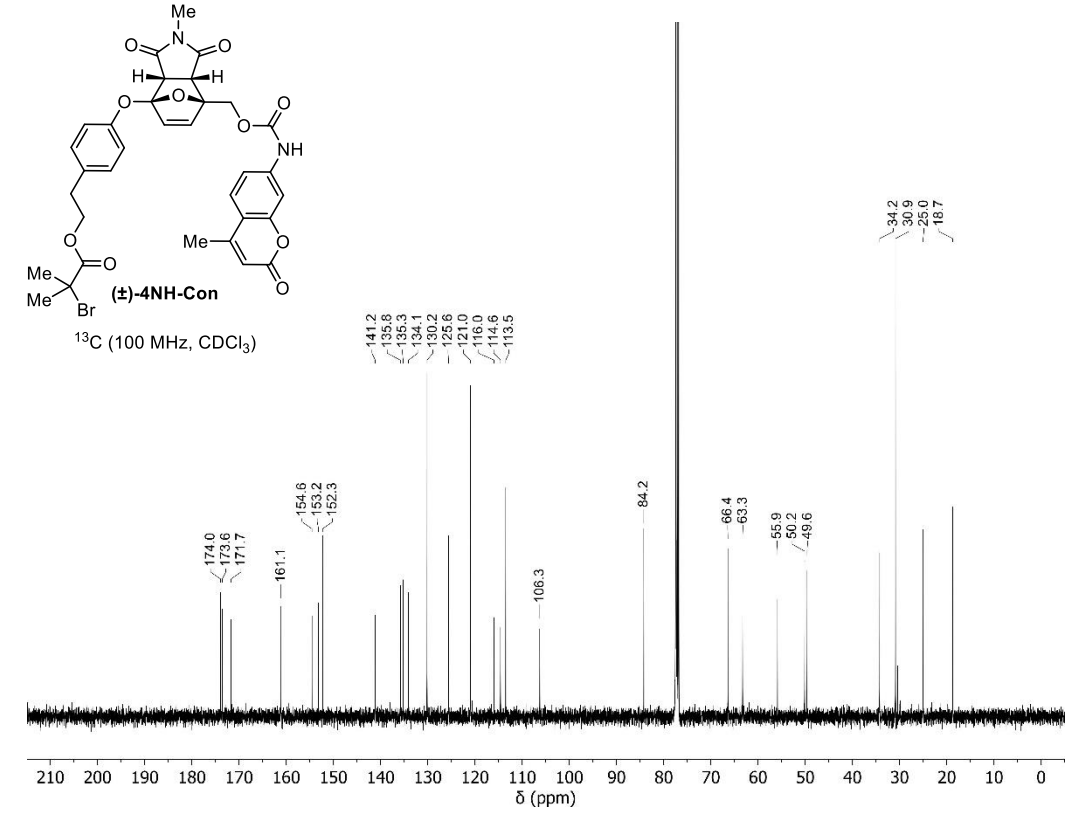
(±)-4NH-Con
^{13}C (100 MHz, $CDCl_3$)
174.0
173.6
171.7
161.1
154.6
153.2
152.3
141.2
135.8
135.3
134.1
130.2
125.6
121.0
116.0
114.6
113.5
106.3
84.2
66.4
63.3
55.9
50.2
49.6
34.2
30.9
25.0
18.7
210 200 190 180 170 160 150 140 130 120 110 100 90 80 70 60 50 40 30 20 10 0
δ (ppm)

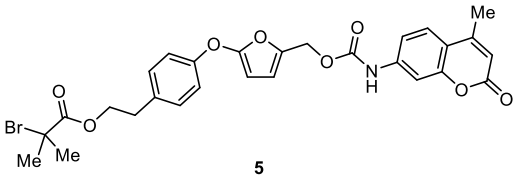

5

^{1}H (500 MHz, $CDCl_3$)

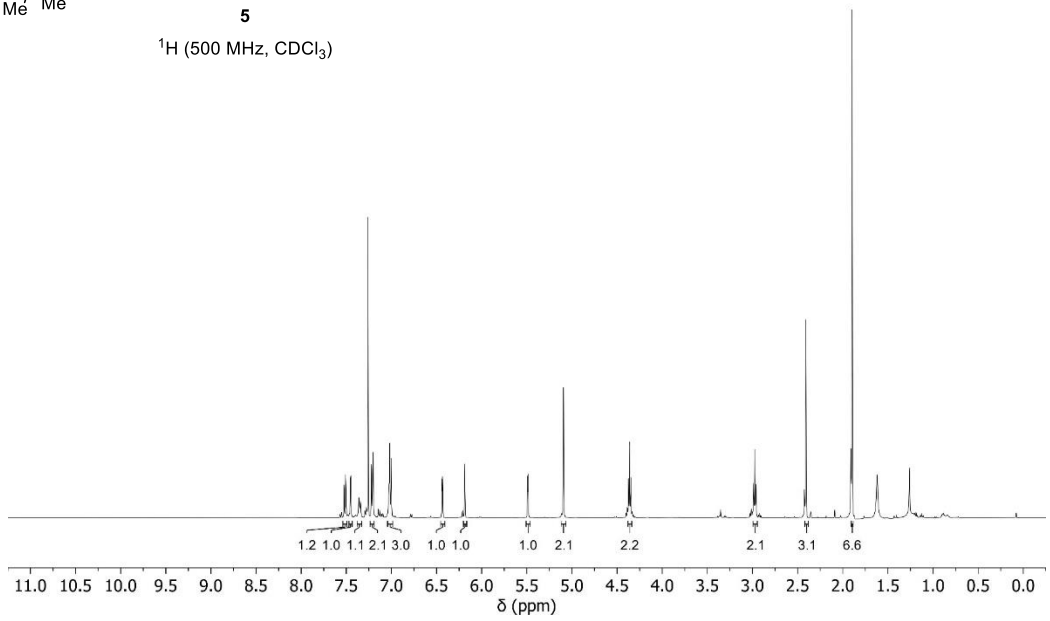

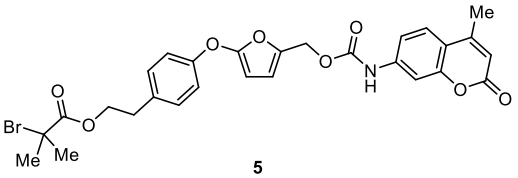

5

^{13}C (100 MHz, $CDCl_3$)

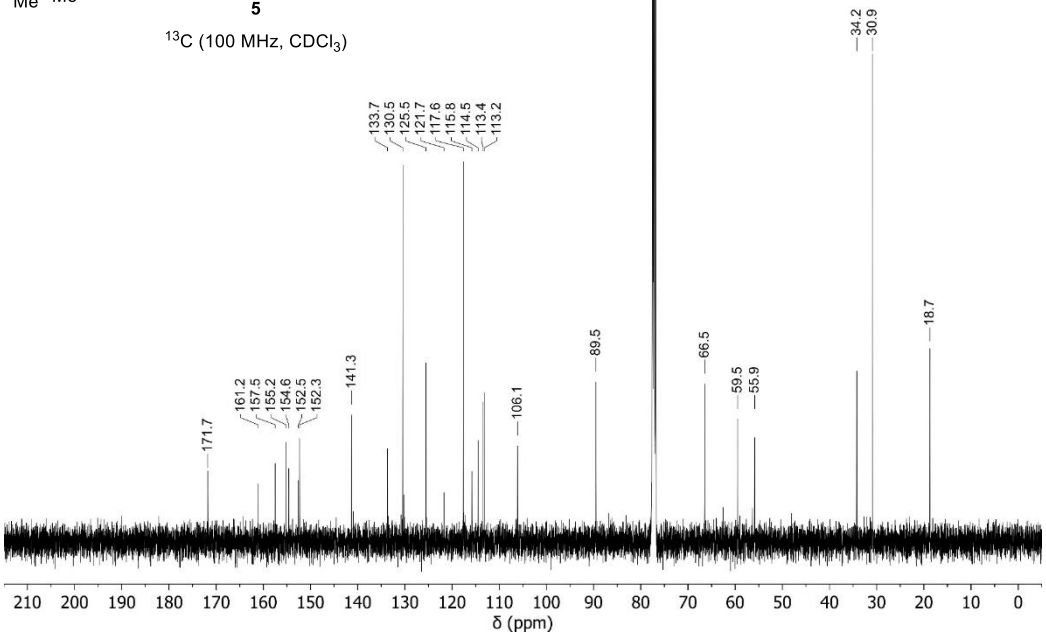

Chapter 4

MULTI-MECHANOPHORE POLYMERS FOR MECHANICALLY TRIGGERED SMALL MOLECULE RELEASE WITH ULTRAHIGH PAYLOAD CAPACITY

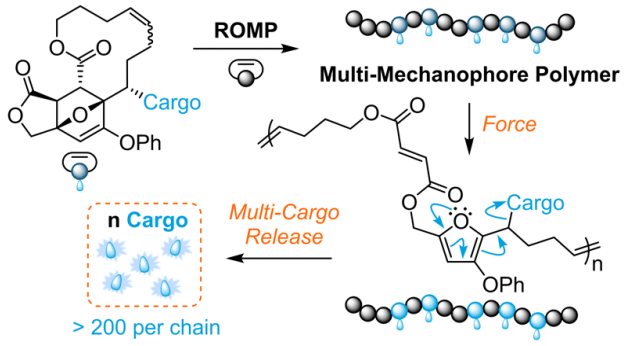

Abstract: Polymers that release small molecules in response to mechanical force are promising for a variety of applications including drug delivery, catalysis, and sensing. While a number of mechanophores have been developed for the release of covalently bound payloads, existing strategies are either limited in cargo scope, or in the case of more general mechanophore designs, are restricted to the release of one or two cargo molecules per polymer chain. Herein, we introduce a non-scissile mechanophore based on a masked 2-furylcarbinol derivative that enables the preparation of multi-mechanophore polymers with ultrahigh payload capacity. We demonstrate that polymers prepared via ring-opening metathesis polymerization are capable of releasing hundreds of small molecule payloads per polymer chain upon ultrasound-induced mechanochemical activation. This non-scissile masked 2-furylcarbinol mechanophore overcomes a major challenge in cargo loading capacity associated with previous 2-furylcarbinol mechanophore designs, enabling applications that benefit from much higher concentrations of delivered cargo.

This chapter has been adapted with permission from
Zeng, T., Ordner, L. A., Liu, P., Robb, M. J. *J. Am. Chem. Soc*. **2023**, DOI: 10.1021/jacs.3c11927.

4.1 Investigation

Stimuli-responsive polymers that release small molecule payloads in response to an external trigger are enabling materials for applications including drug delivery, catalysis, and sensing.[1–3] In particular, mechanical force is an appealing stimulus because of its ubiquity in materials systems as well as the broad range of available methods for applying mechanical force,[4] which include tension and compression in bulk polymeric materials and techniques using ultrasound that afford remote control.[5–7] In the emergent field of polymer mechanochemistry, mechanical force is transduced to force-sensitive moieties termed mechanophores that are covalently incorporated into polymers to achieve specific chemical transformations.[8] The development of mechanophores enabling the mechanically triggered release of covalently bound payloads has recently attracted significant attention.[9–11] Mechanophores have been judiciously designed for the liberation of a wide range of small molecules including CO,[12,13] HCl,[14,15] furans,[16,17] *N*-heterocyclic carbenes,[18] ammonium compounds,[19] 9-fluorenone,[20] and others.

In contrast to the examples above, systems that leverage mechanically gated cascade reactions have been developed to decouple the mechanochemical activation step from cargo release resulting in more general and modular mechanophore platforms.[9] For example, Göstl and Herrmann introduced a disulfide mechanophore that undergoes a mechanically facilitated disulfide reduction triggering the efficient release of various alcohols.[21,22] Our group has developed a system based on furan–maleimide Diels–Alder mechanophores in which a mechanically triggered formal retro-[4+2] cycloaddition reaction unveils a reactive 2-furylcarbinol derivative that spontaneously fragments to release a covalently bound cargo molecule.[23–26] The cargo scope and release kinetics are systematically modulated through substitution of the masked 2-furylcarbinol derivative enabling the mechanically triggered release of functionally diverse payloads including phenols, alcohols, arylamines, alkylamines, sulfonic acids, and carboxylic acids.[24] Polymers are synthesized via a typical controlled radical polymerization (CRP) strategy that positions the mechanophore near the chain midpoint where mechanical force is greatest during ultrasonication (Figure 4.1a).[27] Critically, however, the scissile nature of this Diels–Alder mechanophore generally precludes the mechanochemical activation of more than one unit per polymer chain, which

significantly restricts the amount of deliverable payload and represents a limitation of this design.

Non-scissile mechanophores can be incorporated into multi-mechanophore polymers (MMPs) containing many repeats that are activated mechanochemically along a substantial portion of the polymer chain.[28,29] Craig has pioneered a strategy for the synthesis of MMPs that leverages the ring-opening metathesis polymerization (ROMP) of mechanophores containing macrocyclic olefins.[30] This methodology has been employed extensively, including in the two examples mentioned above enabling the mechanically triggered release of hundreds of equivalents of HCl and CO.[12,15] Inspired by these reports, here we introduce a novel non-scissile masked 2-furylcarbinol mechanophore that capitalizes on the modularity of the 2-furylcarbinol system and enables the preparation of MMPs with significantly higher deliverable payload capacity for mechanically triggered small molecule release (Figure 4.1b). The mechanophore design is based on the intramolecular Diels−Alder reaction of a furfuryl fumarate ester, which upon macrocyclization can be copolymerized via ROMP to

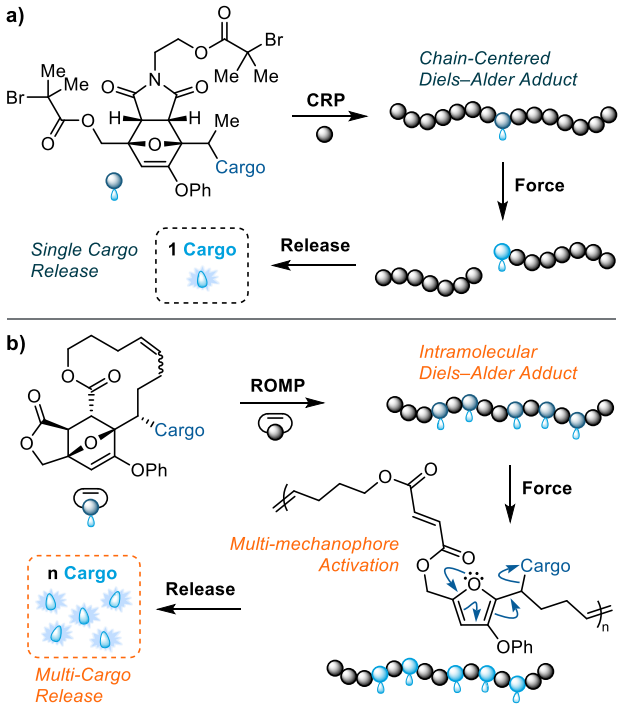

Figures 4.1. Mechanically triggered small molecule release from polymers containing a masked 2-furylcarbinol mechanophore via a retro-Diels–Alder/fragmentation cascade. (a) Mechanochemical activation of a typical chain-centered mechanophore releases up to one cargo per polymer chain. (b) A multi-mechanophore polymer design incorporating a non-scissile mechanophore capable of releasing hundreds of cargo molecules per chain.

afford MMPs capable of multi-mechanophore activation and efficient payload release. In addition to facilitating small molecule release,[24] the phenoxy substituent renders the Diels–Alder adduct more thermally stable and protects the alkene against undesired olefin metathesis. The mechanochemical reactivity of the Diels–Alder adduct was validated by density functional theory (DFT) calculations using the constrained geometries simulate external force (CoGEF) method,[31,32] which predict that the formal retro-Diels–Alder reaction occurs with a relatively low rupture force of 3.4 nN (Figure 4.2).

Encouraged by the computationally predicted mechanochemical reactivity, we targeted the synthesis of a Diels−Alder macrocycle loaded with aminocoumarin (**CoumNH$_2$**) as a model fluorogenic cargo (Scheme 4.1). Starting from 3-phenoxyfurfural, a two-step

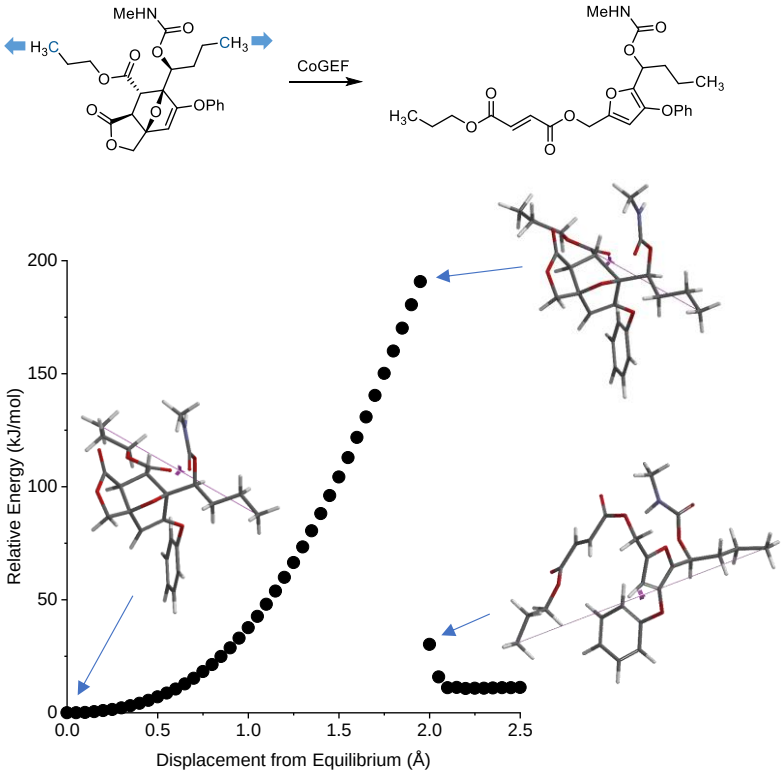

Figures 4.2. Results of density functional theory calculations performed on a truncated model of Diels–Alder adduct **6** using the constrained geometries simulate external force (CoGEF) method at the B3LYP/6-31G* level of theory. Pulling points were defined as the carbon atoms in the terminal methyl groups (colored blue) with a step size of 0.05 Å. A formal retro-Diels–Alder reaction is predicted to occur upon mechanical elongation at a maximum rupture force (F_{max}) of 3.4 nN to generate the expected furfuryl carbamate product. The corresponding computed structures at various points of elongation indicted in the CoGEF plot are shown.

Scheme 4.1. Synthesis of the Non-Scissile Masked 2-Furylcarbinol Mechanophore Macrocycle Loaded with an Aminocoumarin Payload.

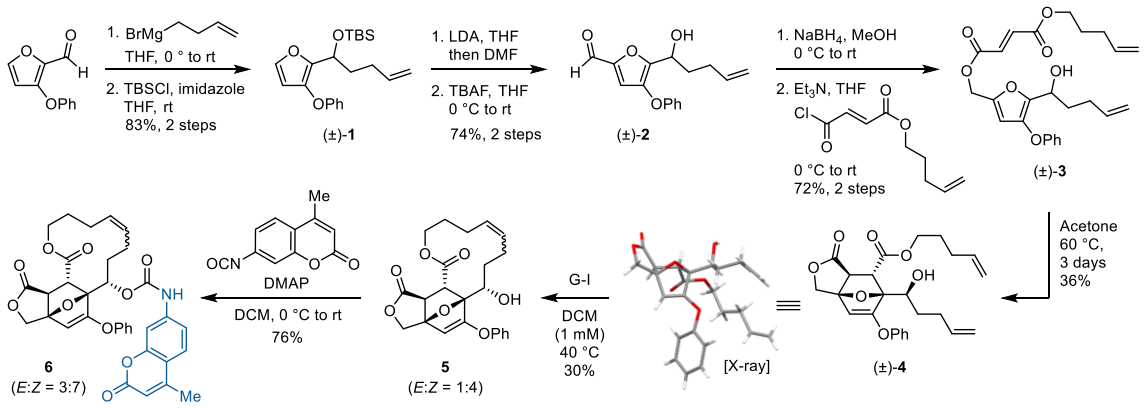

sequence involving Grignard addition and TBS protection afforded furfuryl silyl ether (±)-**1** in 83% yield. Next, a formylation reaction with LDA/DMF followed by removal of the TBS group with TBAF provided furfuryl alcohol (±)-**2** in 74% yield. Subsequent reduction of the aldehyde with $NaBH_4$ followed by selective esterification of the primary alcohol with a fumaric acid monoester chloride derivative gave furfuryl alcohol (±)-**3** in 72% yield. An intramolecular Diels–Alder reaction was then carried out at 60 °C in acetone and the major diastereomer (±)-**4** was isolated in 36% yield and characterized by X-ray crystallography. We note that the maleate isomer resulted in a less stable Diels–Alder adduct. Formation of the 12-membered ring was accomplished by a ring-closing metathesis reaction using Grubbs' 1st generation catalyst in DCM (1 mM) to afford macrocycle **5** in 30% isolated yield. Use of G2 or HG2 catalysts resulted in substantial polymer product or no conversion, respectively. Finally, the aminocoumarin payload was installed by reaction of the secondary alcohol with 4-methylcoumarin-7-isocyanate[24] to afford macrocyclic monomer **6** in 76% yield.

Polymers were synthesized via ROMP of macrocycle **6** with 5-acetoxycyclooctene (**COE_{OAc}**) as a comonomer in $CHCl_3$ (2 M) using Grubbs' 2nd generation catalyst (Figure 4.5a). The **COE_{OAc}** comonomer was selected due its better solubility in polar solvents.[10] Three different MMPs were prepared with varying molar mass and comonomer composition, which were characterized using gel permeation chromatography coupled with multi-angle light scattering (GPC-MALS) and ^{1}H NMR spectroscopy, respectively (Table 4.1 and Figures 4.3 and 4.4). We also prepared small molecule model compound (±)-**7**, which closely resembles the expected mechanophore-containing repeat unit structure in the MMPs (Figure

4.5b). Comparison of the ^{1}H NMR spectra of **MMP$_{80}$** (M_n = 80.3 kDa, $Đ$ = 2.40) and (±)-**7** confirms that the characteristic features of the Diels–Alder motif and the aminocoumarin payload were retained upon polymerization. Importantly, the signal corresponding to the alkenyl proton of the Diels–Alder adduct is also clearly observed in the ^{1}H NMR spectrum of **MMP$_{80}$**, confirming that ROMP was selective towards the macrocyclic alkene. The phenoxy substituent also enhances the thermal stability of the Diels–Alder adduct,[24] which was stable at room temperature for more than two weeks (Figure 4.7). The composition of each MMP was determined by integrating the tertiary proton resonance at ~4.8 ppm on the **COE$_{OAc}$** repeat unit relative to the signals corresponding to the Diels–Alder adduct (see Table 4.1 and Figure 4.3)**.** For **MMP$_{80}$**, approximately 9% of the total repeat units comprise the Diels–Alder motif, which translates to an average of 34 aminocoumarin payloads per chain.

Table 4.1. Characterization of Multi-Mechanophore Polymers (**MMP$_x$**) and a Poly(Methyl Acrylate) Polymer Containing a Chain-Centered Mechanophore (**PMA$_{center}$**).

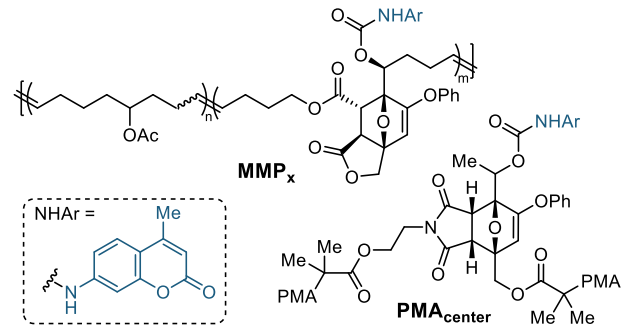

	M_n (kDa)[a]	$Đ$[a]	DP[b]	m : n[c]	cargo / chain[c]	release (%)[d]
MMP$_{23}$	22.5	1.36	103	12 : 88	12	8
MMP$_{80}$	80.3	2.40	383	9 : 91	34	65
MMP$_{295}$	295	2.25	851	40 : 60	340	60
PMA$_{center}$	83.9	1.17	976	–	1	96

[a]Determined by GPC-MALS. [b]Average total number of repeat units per chain (n + m). [c]Determined by ^{1}H NMR spectroscopy. Monomer feed ratios (**6**:**COE$_{OAc}$**): 28:72 (**MMP$_{23}$**), 13:87 (**MMP$_{80}$**), 50:50 (**MMP$_{295}$**). [d]Average cargo release after extended sonication quantified by PL spectroscopy.

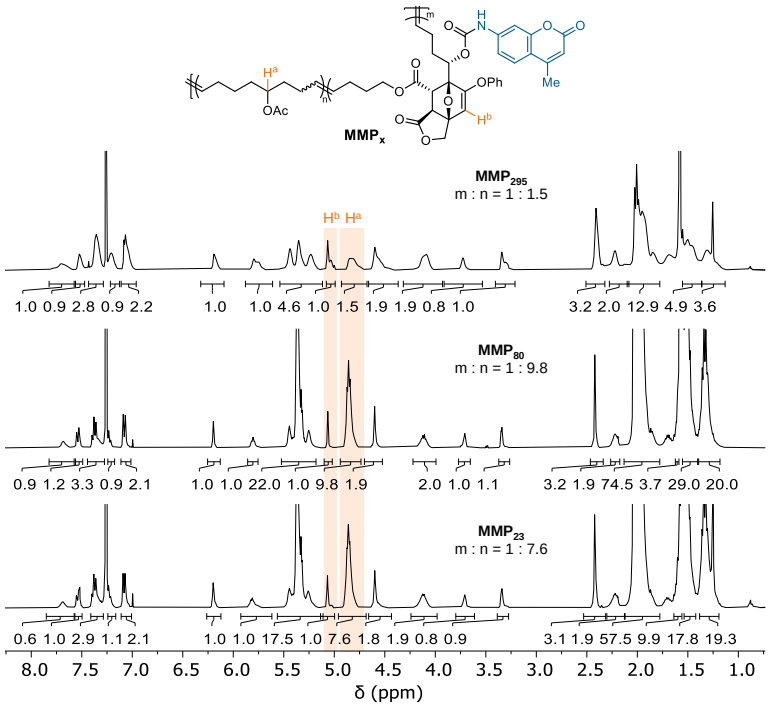

Figures 4.3. ^{1}H NMR spectra ($CDCl_3$, 400 MHz) of MMPs used in the determination of copolymer composition. Repeat unit ratios (m : n) were determined by integration of the signals at ~4.8 and ~5.1 ppm, corresponding to the tertiary proton (H^a) on the cyclooctene repeat unit and the alkenyl proton (H^b) on the mechanophore, respectively.

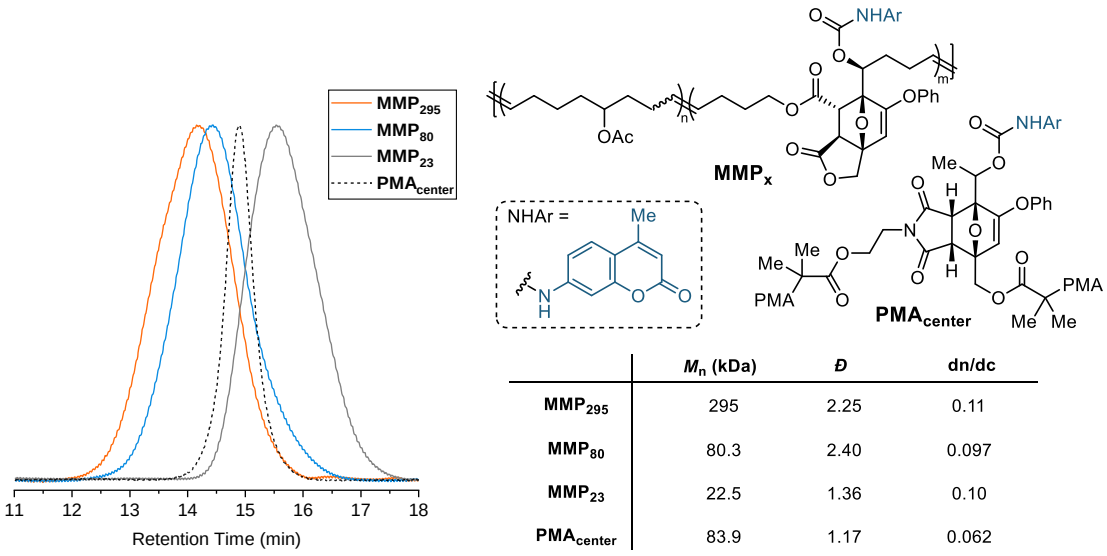

	M_n (kDa)	$Đ$	dn/dc
MMP$_{295}$	295	2.25	0.11
MMP$_{80}$	80.3	2.40	0.097
MMP$_{23}$	22.5	1.36	0.10
PMA$_{center}$	83.9	1.17	0.062

Figures 4.4. Chemical structures, normalized GPC chromatograms (RI response), and characterization data for multi-mechanophore polymers (**MMP$_x$**) and poly(methyl acrylate) polymer **PMA$_{center}$**.

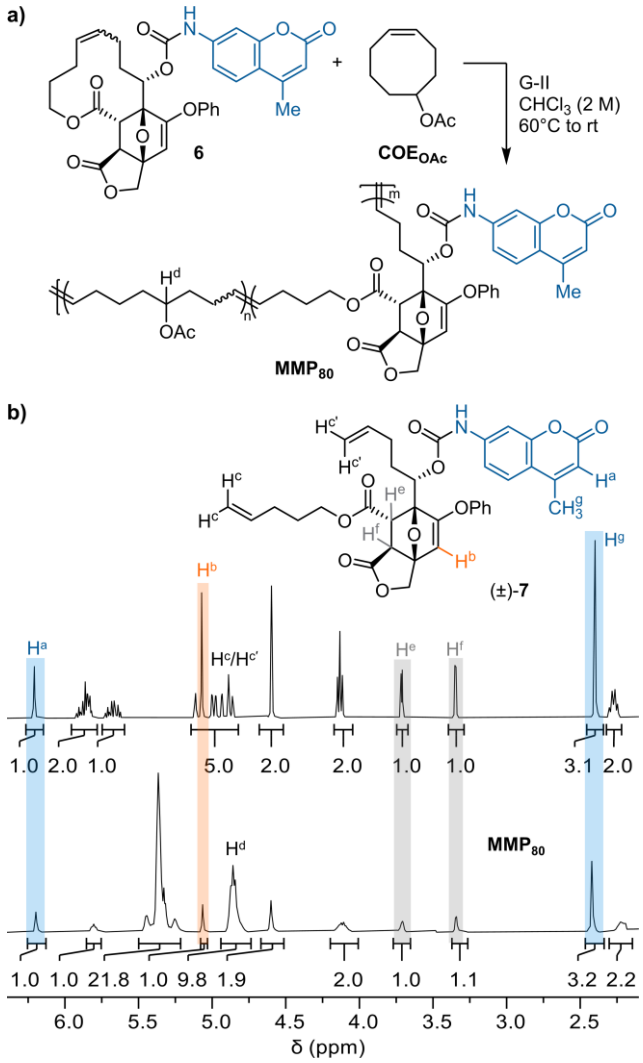

Figures 4.5. (a) Synthesis of multimechanophore polymer **MMP$_{80}$** (M_n = 80.3 kDa, $Đ$ = 2.40) via ROMP of macrocycle **6** and **COE$_{OAc}$**. (b) ^{1}H NMR spectra (400 MHz, $CDCl_3$) comparing small molecule model compound (±)-**7** (*top*) and **MMP$_{80}$** (*bottom*) with diagnostic protons labeled for the polymer backbone, mechanophores, and cargo.

To evaluate the mechanochemical reactivity of the MMPs, we first subjected **MMP$_{80}$** (0.1 mg/mL in 3:1 THF/MeOH) to pulsed ultrasonication (1s on/1s off, 9–13 °C, 20 kHz, 13.9 W/cm^2) and aliquots were removed periodically for analysis by photoluminescence (PL) spectroscopy to quantify the release of **CoumNH$_2$** (Figure 4.6a). THF was used as the cosolvent in these experiments due to improved solubility of the polymers compared to acetonitrile mixtures employed previously,[23–25] despite slower fragmentation kinetics of the 2-furylcarbinol derivatives (Figure 4.8). Samples were allowed to incubate at room

temperature for ~5 days after sonication to ensure complete fragmentation of the furfuryl carbamate intermediate prior to characterization (Figure 4.9). Fluorescence intensity increased systematically with increasing sonication time indicating the successful release of **CoumNH2** upon mechanochemical activation. The PL intensity reached a maximum after ~35 min of sonication corresponding to 65% release, or ~22 cargo molecules per chain

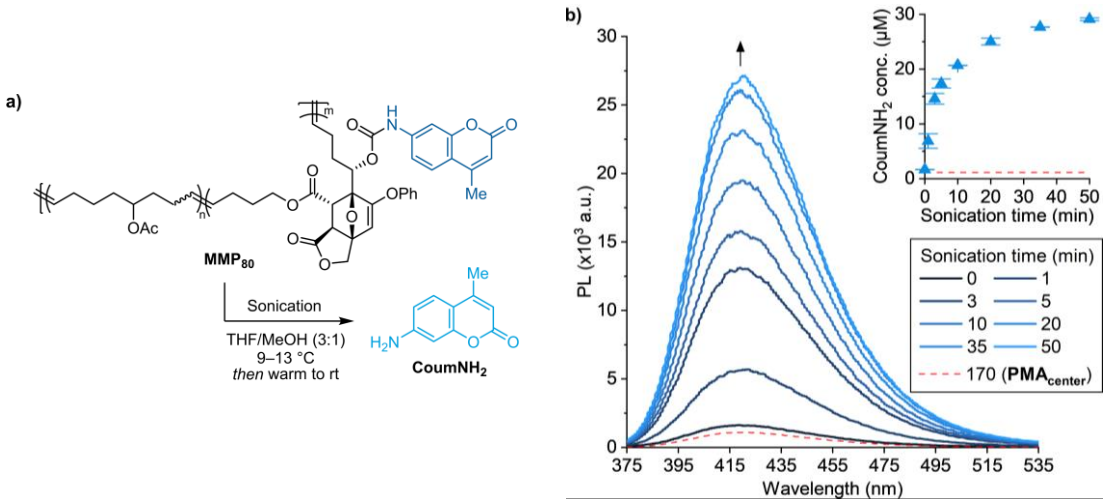

Figures 4.6. (a) Ultrasound-induced mechanochemical activation of **MMP80** (0.1 mg/mL in 3:1 THF/MeOH), and (b) release of aminocoumarin (**CoumNH2**) characterized by PL spectroscopy (λ_{ex} = 365 nm). Inset shows concentration of released **CoumNH2** as a function of sonication time. Data are compared to the mechanochemical activation of **PMAcenter** under identical conditions. The red dashed line in the inset represents the maximum release of **CoumNH2** from **PMAcenter** after sonication for 170 min. Error bars denote the range from two replicate experiments.

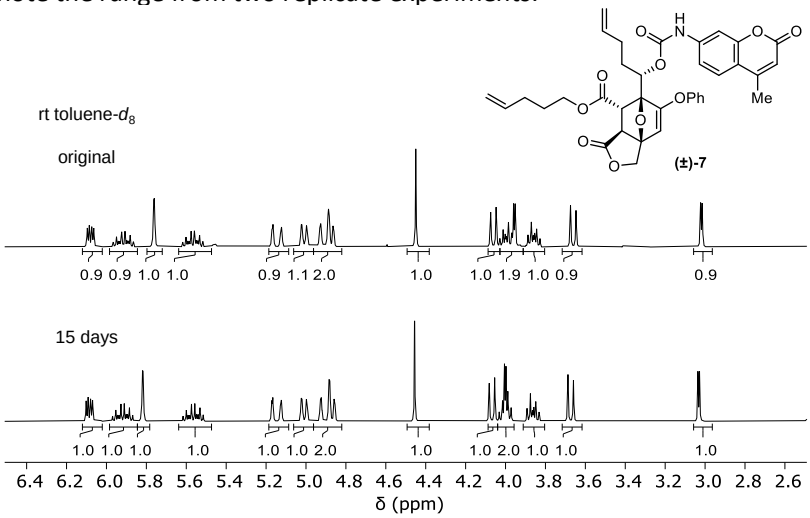

Figures 4.7. Partial ^{1}H NMR spectra (400 MHz) of (±)-**7** after being maintained at room temperature in toluene-d_8 (4.8 mM) for the indicated amount of time. No significant changes are observed after 15 days at room temperature, demonstrating negligible reaction under these conditions.

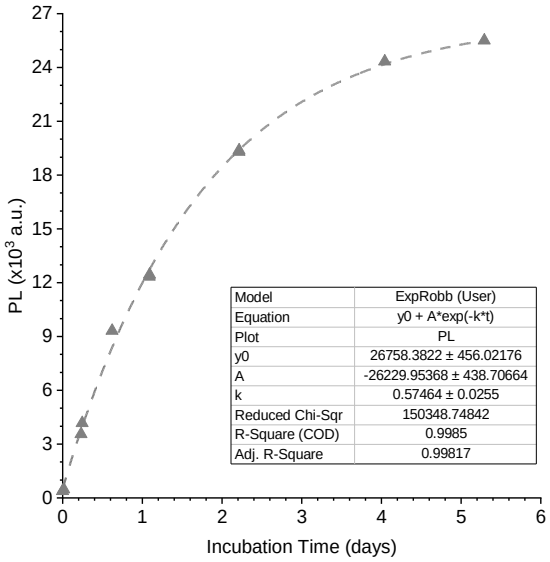

Figures 4.8. PL spectra characterizing the rate of release of **CoumNH$_2$** from **MMP$_{80}$** (0.1 mg/mL in 3:1 THF/methanol) at room temperature following 50 min of sonication. λ_{ex} = 365 nm, λ_{em} = 424 nm. Fitting the data to an expression of simple first-order kinetics provides a half-life of 29 h for release of **CoumNH$_2$** from the mechanochemically liberated furfuryl carbamate under these conditions.

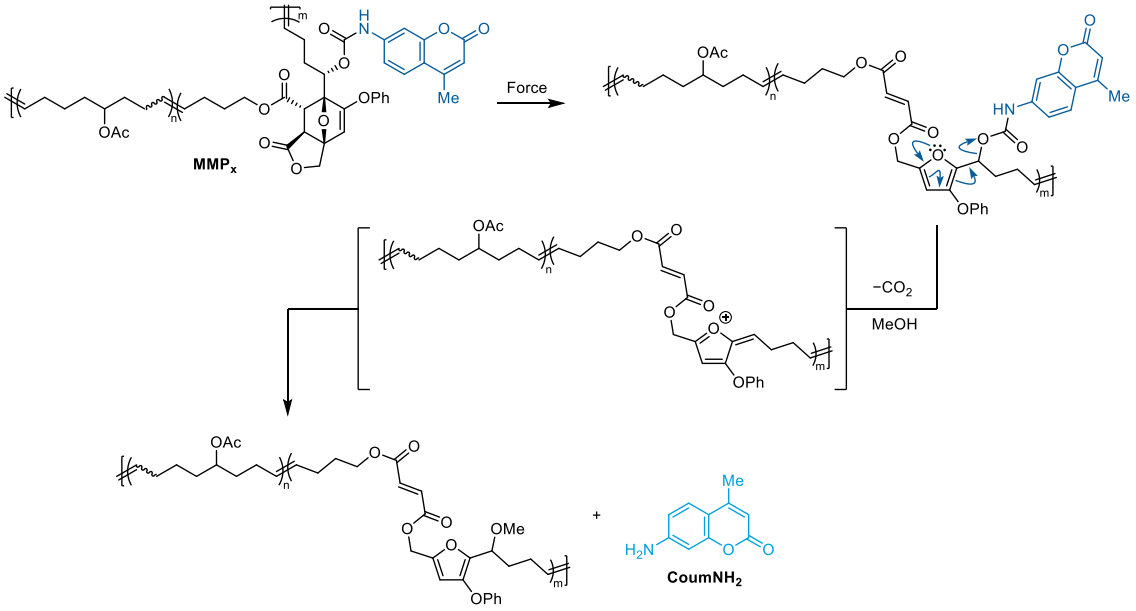

Figures 4.9. Complete reaction scheme depicting the mechanically triggered release of CoumNH$_2$ from a multi-mechanophore polymer (MMPx) in the presence of MeOH. Unreacted mechanophore repeat units are omitted from the polymer product for clarity.

(Figure 4.6b). To compare these results directly with our previous mechanophore design,[24] we prepared poly(methyl acrylate) **PMA$_{center}$** equipped with a single chain-centered furan–maleimide mechanophore (M_n = 83.9 kDa, $Đ$ = 1.17, see Table 4.1). Ultrasonication of **PMA$_{center}$** under identical conditions and with the same initial polymer concentration resulted in 96% release, or ~1 **CoumNH$_2$** molecule per chain (Figure 4.6b and Figure 4.10). As evident from this comparison, the concentration of **CoumNH$_2$** released from **MMP$_{80}$** is ~24 times greater than that from **PMA$_{center}$** for the same initial concentration of polymer on a mass basis. We note that without sonication, a small amount of background fluorescence was observed from **MMP$_{80}$** after 5 days of incubation in 3:1 THF/MeOH that is tentatively ascribed to hydrolysis of the carbamate linkers. Nevertheless, this only corresponds to the release of ~1.4 **CoumNH$_2$** units, or ~4% release per polymer chain (Figure 4.11). Additional control experiments performed on small molecule model (±)-**7** demonstrated no observable changes in the ^{1}H NMR spectrum after 10 days in 3:1 THF-d_8/MeOH solution (Figure 4.12).

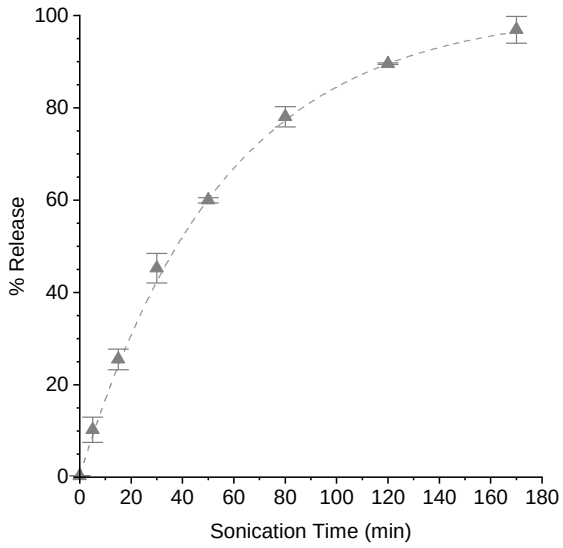

Figures 4.10. Mechanically triggered release of **CoumNH$_2$** from **PMA$_{center}$** (0.10 mg/mL in 3:1 THF/methanol) as a function of sonication time, determined by PL spectroscopy. λ_{ex} = 365 nm, λ_{em} = 424 nm. Error bars denote the range from two replicate experiments. See Section V for additional details.

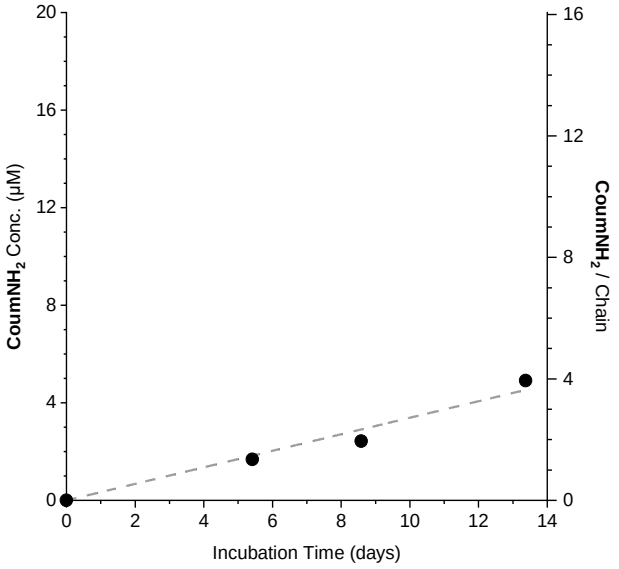

Figures 4.11. Characterization of background aminocoumarin ($CoumNH_2$) release by PL spectroscopy after incubating MMP_{80} in 3:1 THF/MeOH (0.1 mg/mL) at room temperature. After 5 days, the concentration of $CoumNH_2$ was determined to be 1.7 μM, corresponding to the release of ~1.4 $CoumNH_2$ units per chain.

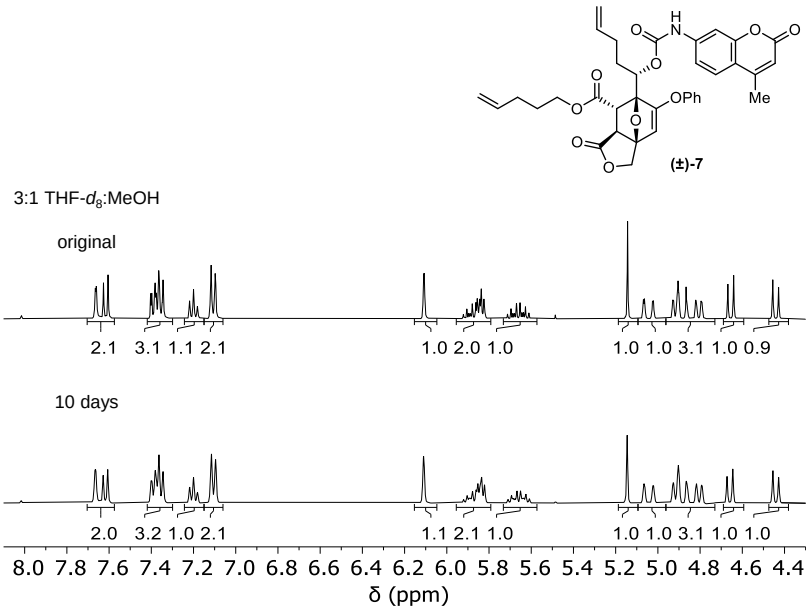

Figures 4.12. Partial ^1H NMR spectra (400 MHz) of (±)-**7** after being maintained at room temperature in THF-d_8/MeOH (3:1 v/v, 7.8 mM) for 10 days. No significant changes are observed, demonstrating negligible reaction under these conditions.

Having demonstrated successful cargo release from **MMP$_{80}$** and the substantially increased payload capacity compared to our previous mechanophore, we next sought to leverage the multi-mechanophore design to control the amount of cargo release and also confirm its mechanochemical origin. To this end, we prepared two additional MMPs following a similar procedure as above with varying molar mass and/or mechanophore incorporation (see Table 4.1). Synthesis of **MMP$_{295}$** (M_n = 295 kDa, $Đ$ = 2.25) was accomplished using a higher feeding ratio of macrocycle **6** to **COE$_{OAc}$**, resulting in 40% mechanophore incorporation and ~340 cargo molecules per chain. On the other hand, **MMP$_{23}$** (M_n = 22.3 kDa, $Đ$ = 1.36) has a similar mechanophore incorporation of ~12% compared to **MMP$_{80}$**, but is significantly smaller (see the SI for details). While faster and greater overall payload release is expected from **MMP$_{295}$**, the molar mass of **MMP$_{23}$** is likely near or below the threshold for mechanophore activation, therefore leading to an insignificant amount of payload release.[33] Following the same experimental conditions as above, all three MMPs were sonicated at the same mass concentration (0.1 mg/mL in 3:1 THF/MeOH) and the release of **CoumNH$_2$** was quantified using PL spectroscopy (Figure 4.13). Notably, mechanochemical activation of **MMP$_{295}$** resulted in 60% release of **CoumNH$_2$**, corresponding to ~203 cargo molecules per chain. As expected, cargo release also occurs significantly faster from **MMP$_{295}$**, achieving maximum release after only ~10 min of sonication. In contrast, only 8% release of **CoumNH$_2$** was achieved upon

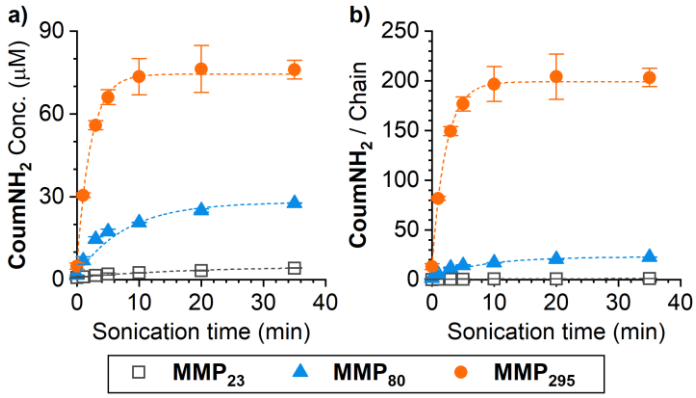

Figures 4.13. (a) Mechanically triggered release of **CoumNH$_2$** from multimechanophore polymers of varying molar mass and composition as a function of sonication time (0.1 mg/mL polymer in 3:1 THF/MeOH). Theoretical cargo concentrations assuming 100% release: [**CoumNH$_2$**]$_{theo}$ = 53 μM (**MMP$_{23}$**), 44 μM (**MMP$_{80}$**), 127 μM (**MMP$_{295}$**). (b) Number of **CoumNH$_2$** units released per chain as a function of sonication time. Error bars denote the range from two replicate experiments.

ultrasonication of **MMP$_{23}$**, corresponding to the release of ~1 payload unit per chain. Taken together, these results are consistent with the expected molar mass dependence on ultrasound-induced mechanochemical activation and provide evidence for the mechanical origin of cargo release.[8]

In summary, we report a non-scissile masked 2-furylcarbinol mechanophore that enables the preparation of multi-mechanophore polymers via ROMP for mechanically triggered small molecule release. Compared to typical chain-centered mechanophore designs that are limited to the release of one or two cargo molecules per polymer chain, we demonstrate that the release of hundreds of small molecule payloads can be triggered from a multi-mechanophore polymer upon ultrasound-induced mechanochemical activation. The substantial increase in deliverable payload capacity overcomes a major existing limitation in mechanophore design and opens the door to applications that require greater concentrations of delivered small molecule cargo.

Financial support from the Arnold and Mabel Beckman Founda-tion through a Beckman Young Investigator Award and the Na-tional Institute of General Medical Sciences of the National Insti-tutes of Health (R35GM150988) is gratefully acknowledged. We thank the Center for Catalysis and Chemical Synthesis of the Beckman Institute at Caltech for access to equipment. We thank Dr. David VanderVelde for assistance with NMR spectroscopy, Dr. Michael K. Takase for assistance with X-ray crystallography, and Yunyan Sun for helpful discussions. L.A.O. thanks the Amgen Scholars program at Caltech for financial support. P.L. thanks the Swiss National Science Foundation for an Early Postdoc Mobility Fellowship. M.J.R. gratefully acknowledges the Alfred P. Sloan Foundation for a Sloan Research Fellowship and the Camille and Henry Dreyfus Foundation for a Camille Dreyfus Teacher-Scholar Award.

4.2 General Experimental Details and Methods

Reagents from commercial sources were used without further purification unless otherwise stated. Methyl acrylate was passed through a short plug of basic alumina to remove inhibitor immediately prior to use. Dry THF, diethyl ether, MeCN, and DMF were obtained from a Pure Process Technology solvent purification system. All reactions were performed

under a N_2 atmosphere unless specified otherwise. Column chromatography was performed on a Biotage Isolera system using SiliCycle SiliaSep HP or SiliaBond C18 cartridges.

NMR spectra were recorded using a 400 MHz Bruker Avance III HD with Prodigy Cryoprobe, a 400 MHz Bruker Avance Neo, or Varian Inova 500 MHz spectrometers. All ^{1}H NMR spectra are reported in δ units, parts per million (ppm), and were measured relative to the signals for residual chloroform (7.26 ppm), dichloromethane (5.32 ppm), methanol (3.31 ppm), acetone (2.05 ppm), toluene (2.08 ppm), or acetonitrile (1.94 ppm) in deuterated solvent. All ^{13}C NMR spectra were measured in deuterated solvents and are reported in ppm relative to the signals for chloroform (77.16 ppm). Multiplicity and qualifier abbreviations are as follows: s = singlet, d = doublet, t = triplet, q = quartet, dd = doublet of doublets, dq = doublet of quartets, ABq = AB quartet, m = multiplet, bs = broad singlet.

High resolution mass spectrometry (HR-MS) was carried out on an Agilent 6230 series time-of-flight mass spectrometer equipped with an Agilent G1958 Jet Stream Electrospray Ionization Source or JEOL JMS-T2000 GC AccuTOF GC-Alpha mass spectrometer interfaced with an Agilent 8890 GC system with samples analyzed by field ionization (FI), which generally resulted in radical cations, $M^{+\bullet}$.

Analytical gel permeation chromatography (GPC) was performed using an Agilent 1260 series pump equipped with two Agilent PLgel MIXED-B columns (7.5 x 300 mm), a Wyatt 18-angle DAWN HELEOS light scattering detector, and an Optilab rEX differential refractive index detector. The mobile phase was THF at a flow rate of 1 mL/min. Molar mass and molar mass distributions were calculated by light scattering using a dn/dc value of 0.062 mL/g (25 °C) for poly(methyl acrylate). For multimechanophore polymers, refractive index increment (dn/dc) values were determined for each injection based on known sample concentration and assuming 100% mass elution.

Photoluminescence spectra were recorded on a Shimadzu RF-6000 spectrofluorophotometer using a quartz microcuvette (Starna Cells 18F-Q-10-GL14-C, 10 x 2 mm). Excitation and emission slit widths were 3 nm.

Ultrasound experiments were performed inside of a sound abating enclosure using a 500 watt Vibra Cell 505 liquid processor (20 kHz) equipped with a 0.5-inch diameter solid

probe (part #630-0217), sonochemical adapter (part #830-00014), and a Suslick reaction vessel made by the Caltech glass shop (analogous to vessel #830-00014 from Sonics and Materials).

4.3 Synthetic Details

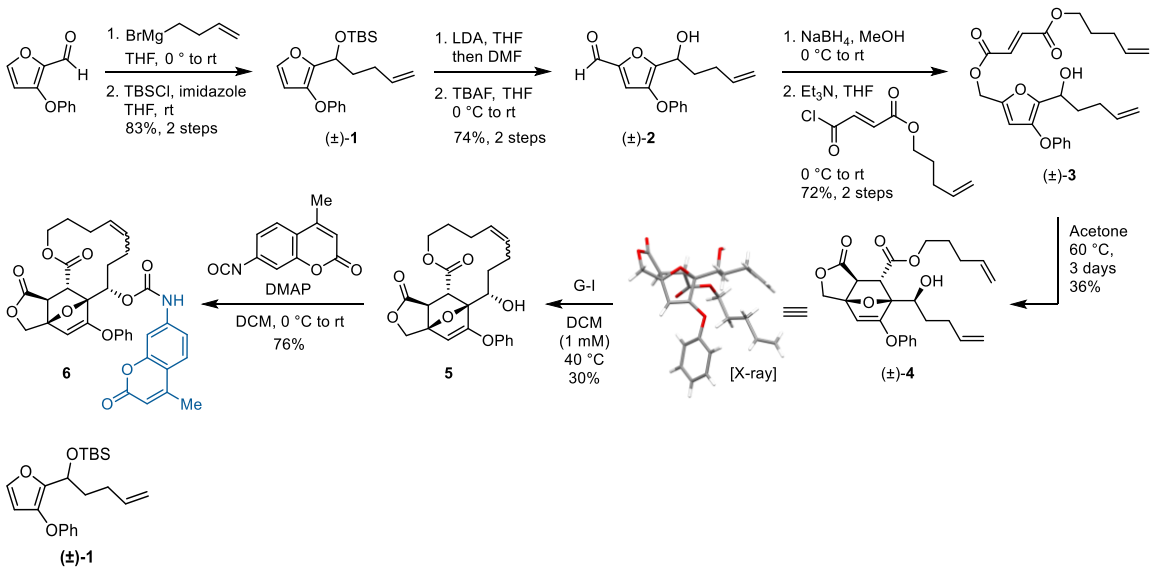

***Tert*-butyldimethyl((1-(3-phenoxyfuran-2-yl)pent-4-en-1-yl)oxy)silane ((±)-1).** A flame-dried round bottom flask equipped with a stir bar was charged with magnesium turnings (0.9 g, 37 mmol) under N_2, and anhydrous ether (70 mL) was added. 4-bromobut-1-ene (5.0 mL, 48 mmol) was then added and the mixture was sonicated in a room temperature water bath under N_2 until all solids reacted and dissolved. The resulting 0.5 M butenylmagnesium bromide ether solution was kept under N_2 in the fridge until ready to be used.

A flame-dried round bottom flask equipped with a stir bar was charged with 3-phenoxyfuran-2-carbaldehyde[24] (2.3 g, 12 mmol) and anhydrous THF (20 mL). The solution was cooled to 0°C before butenylmagnesium bromide (0.5 M in ether, 32 mL, 16 mmol) was added dropwise. The reaction was then slowly warmed to room temperature and stirred for 2 h before 10% NH_4Cl (50 mL) was added to quench the reaction. The mixture was then extracted with EtOAc (3 x 50 mL) and the combined organic phase was washed with brine (150 mL). The organic layer was dried over $MgSO_4$, filtered, and concentrated under reduced pressure to yield 1-(2-phenoxyfuran-2-yl)pent-4-en-1-ol as a light yellow oil. The crude product was then redissolved in THF (50 mL) followed by the addition of imidazole (1.7 g,

24 mmol) and TBSCl (4.7 g, 24 mmol). The reaction was stirred at room temperature overnight and then the mixture was filtered through a cotton pad. The filtrate was diluted with EtOAc (30 mL) and then washed consecutively with 10% NH_4Cl (100 mL), 10% $NaHCO_3$ (100 mL), and brine (100 mL). The organic phase was dried over Na_2SO_4, filtered, and concentrated under reduced pressure. The crude product was purified by column chromatography (0–50% EtOAc/Hex) to yield the title compound as a yellow oil (3.6 g, 83% over two steps). ^{1}H NMR (500 MHz, $CDCl_3$) δ: 7.32 – 7.27 (m, 3H), 7.04 (ddt, *J* = 8.5, 7.4, 1.1 Hz, 1H), 6.99 (dt, *J* = 7.7, 1.0 Hz, 2H), 6.20 (d, *J* = 2.0 Hz, 1H), 5.82 – 5.70 (m, 1H), 5.01 – 4.88 (m, 2H), 4.74 (t, *J* = 6.7 Hz, 1H), 2.16 – 2.06 (m, 1H), 2.06 – 1.94 (m, 2H), 1.90 – 1.80 (m, 1H), 0.86 (s, 9H), 0.04 (s, 3H), -0.09 (s, 3H). ^{13}C{^{1}H} NMR (100 MHz, $CDCl_3$) δ: 158.2, 144.1, 140.8, 138.8, 138.2, 129.7, 122.6, 116.4, 114.9, 106.1, 64.7, 35.3, 30.0, 26.0, 18.3, -4.9, -5.1. HRMS (ESI, *m/z*): calcd for $[C_{21}H_{30}O_3Si]^+$ $(M+H)^+$, 359.2037; found, 359.2050.

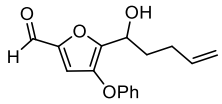

(±)-2

5-(1-hydroxypent-4-en-1-yl)-4-phenoxyfuran-2-carbaldehyde ((±)-2). A flame-dried round bottom flask equipped with a stir bar was charged with diisopropylamine (1.3 g, 13 mmol) and THF (100 mL). The solution was cooled to −78 °C in an acetone/dry ice bath before adding n-BuLi (2.5 M in hexanes, 5.2 mL, 13 mmol) dropwise. After stirring the mixture for ~5 min, a solution of (±)-**1** (3.1 g, 8.7 mmol) in THF (10 ml) was added to the mixture dropwise at −78 °C. The mixture was kept at −78 °C for 30 min prior to adding DMF (1.3 mL, 17 mmol) dropwise. The mixture was then allowed to slowly warm up to room temperature for ~3 h before 10% NH_4Cl (200 mL) was added slowly to the mixture to quench the reaction. The mixture was then extracted with Et_2O (2 x 100 mL), washed with brine (200 mL), and the organic layer was dried over $MgSO_4$, filtered, and concentrated under reduced pressure. The crude mixture was purified by column chromatography (0–30% EtOAc/Hexanes) to yield an inseparable 10:1 mixture of 5-(1-hydroxypent-4-en-1-yl)-4-phenoxyfuran-2-carbaldehyde and 5-(1-hydroxypent-4-en-1-yl)-4-phenoxyfuran-3-

carbaldehyde as a colorless oil (2.7 g, 82% yield), which was used in the next step without further purification.

The above mixture was then dissolved in THF (100 mL) and cooled to 0 °C before adding a 1 M solution of tetrabutylammonium fluoride in THF (8.5 mL, 8.5 mmol) dropwise. The mixture was allowed to slowly warm up to room temperature and stirred for 1 h. The reaction mixture was then diluted with Et_2O (100 mL), washed consecutively with NH_4Cl (200 mL) and brine (200 mL), and the organic fraction was dried over Na_2SO_4, filtered, and concentrated under reduced pressure. The crude product was purified by column chromatography (20–40% EtOAc/Hexanes) to yield the title compound as an orange oil (1.9 g, 79% over two steps). ^{1}H NMR (400 MHz, $CDCl_3$) δ: 9.57 (s, 1H), 7.38 – 7.30 (m, 2H), 7.17 – 7.09 (m, 1H), 7.04 – 6.98 (m, 3H), 5.85 – 5.72 (m, 1H), 5.08 – 4.94 (m, 2H), 4.88 (dt, *J* = 7.4, 6.3 Hz, 1H), 2.24 – 1.94 (m, 5H). ^{13}C{^{1}H} NMR (100 MHz, $CDCl_3$) δ: 178.0, 157.3, 150.4, 149.6, 141.5, 137.3, 130.1, 123.9, 116.9, 115.8, 115.0, 65.3, 34.1, 29.8. HRMS (FI, *m/z*): calcd for $[C_{16}H_{16}O_4]^{+\bullet}$ $(M)^{+\bullet}$, 272.1043; found, 272.1058.

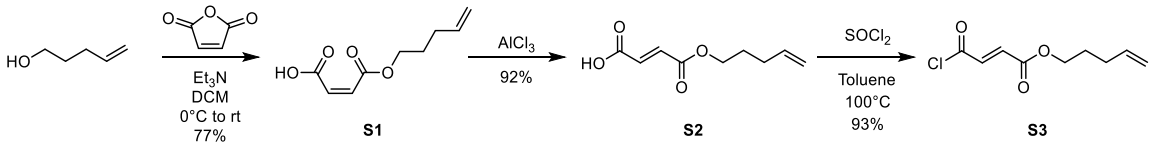

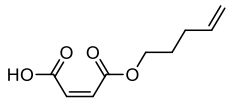

(*Z*)-4-oxo-4-(pent-4-en-1-yloxy)but-2-enoic acid (S1). A round bottom flask equipped with a stir bar was charged with pent-4-en-1-ol (10 mL, 97 mmol), maleic anhydride (9.5 g, 97 mmol), and DCM (20 mL). The solution was cooled to 0 °C in an ice bath before adding triethylamine (14.8 mL, 110 mmol) dropwise. The mixture was slowly warmed to room temperature for 1 h before being quenched with 2 M HCl dropwise until the pH of the solution was < 3. The solution was then diluted with DCM (100 mL) and washed with water (150 mL) and then brine (2 x 100 mL). The organic layer was dried over Na_2SO_4, filtered, and concentrated under reduced pressure to afford the title compound as a colorless oil (13.8

g, 77% yield). ^{1}H NMR (400 MHz, $CDCl_3$) δ: 6.46 (d, *J* = 12.7 Hz, 1H), 6.35 (d, *J* = 12.7 Hz, 1H), 5.79 (ddt, *J* = 16.9, 10.2, 6.6 Hz, 1H), 5.11 – 4.97 (m, 2H), 4.28 (t, *J* = 6.6 Hz, 2H), 2.21 – 2.10 (m, 2H), 1.88 – 1.77 (m, 2H). $^{13}C\{^{1}H\}$ NMR (100 MHz, $CDCl_3$) δ: 168.0, 167.1, 137.6, 137.2, 125.8, 115.7, 65.6, 30.0, 27.6. HRMS (ESI, *m/z*): calcd for $[C_9H_{11}O_4]^-$ $(M-H)^-$, 183.0663; found, 183.0678.

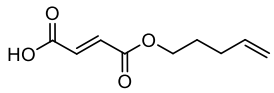

S2

(*E*)-4-oxo-4-(pent-4-en-1-yloxy)but-2-enoic acid (S2). A round bottom flask equipped with a stir bar was charged with **S1** (11.9 g, 64.5 mmol) and $AlCl_3$ (0.43 g, 3.2 mmol). The mixture was heated to 70 °C overnight and then cooled to room temperature, upon which the mixture solidified. The solid was then dissolved in EtOAc (100mL) and washed consecutively with 10% NH_4Cl (100 mL) and then brine (100 mL). The organic layer was dried over Na_2SO_4, filtered, and concentrated under reduced pressure to afford the title compound as a white waxy solid (10.9 g, 92% yield). ^{1}H NMR (400 MHz, $CDCl_3$) δ: 6.95 (d, *J* = 15.8 Hz, 1H), 6.85 (d, *J* = 15.8 Hz, 1H), 5.81 (ddt, *J* = 16.9, 10.2, 6.6 Hz, 1H), 5.11 – 4.97 (m, 2H), 4.24 (t, *J* = 6.6 Hz, 2H), 2.21 – 2.11 (m, 2H), 1.80 (dq, *J* = 8.4, 6.6 Hz, 2H). $^{13}C\{^{1}H\}$ NMR (100 MHz, $CDCl_3$) δ: 170.06, 164.79, 137.28, 135.94, 132.69, 115.72, 65.14, 30.08, 27.75. HRMS (ESI, *m/z*): calcd for $[C_9H_{11}O_4]^-$ $(M-H)^-$, 183.0663; found, 183.0672.

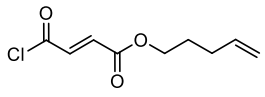

S3

Pent-4-en-1-yl (*E*)-4-chloro-4-oxobut-2-enoate (S3). A round bottom flask equipped with a stir bar was charged with **S2** (10.6 g, 57.8 mmol) and toluene (40 mL). Thionyl chloride was then added slowly to the mixture before heating the reaction to 100 °C for 2 h. The reaction was then cooled to room temperature, concentrated under reduced pressure, and used immediately in synthesis of (±)-**3** (10.9 g, 93% yield).

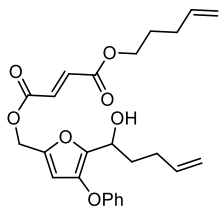

(±)-3

(5-(1-hydroxypent-4-en-1-yl)-4-phenoxyfuran-2-yl)methyl pent-4-en-1-yl fumarate ((±)-3). A flame-dried round bottom flask equipped with a stir bar was charged with (±)-**2** (1.9 g, 6.9 mmol) and methanol (15 mL). The solution was cooled to 0 °C in an ice bath before slowly adding $NaBH_4$ (340 mg, 8.9 mmol). The mixture was kept at 0 °C for 1 h followed by the addition of 10% NH_4Cl (50 mL). The mixture was then extracted with EtOAc (2 x 20 mL) and washed with brine (50 mL). The organic layer was dried over Na_2SO_4, filtered, and concentrated under reduced pressure. The crude mixture was then redissolved in THF (30 mL) and cooled to 0 °C in an ice bath. Triethylamine (1.1 mL, 7.6 mmol) and **S3** (1.5 g, 7.2 mmol) were then added in sequence to the solution slowly. The reaction was allowed to warm to room temperature slowly and stirred for 4 h. The mixture was then diluted with EtOAc (50 mL) and washed consecutively with 10% NH_4Cl (2 x 50 mL) and brine (100 mL), and the organic layer was dried over Na_2SO_4, filtered, and concentrated under reduced pressure. The crude product was purified by column chromatography (10–50% EtOAc/Hexanes) to yield the title compound as a yellow oil (2.1 g, 72% yield over two steps). ^{1}H NMR (400 MHz, $CDCl_3$) δ: 7.35 – 7.28 (m, 2H), 7.10 – 7.03 (m, 1H), 7.03 – 6.97 (m, 2H), 6.93 – 6.83 (m, 2H), 6.29 (s, 1H), 5.86 – 5.73 (m, 2H), 5.11 (s, 2H), 5.09 – 4.91 (m, 4H), 4.77 (t, *J* = 6.9 Hz, 1H), 4.22 (t, *J* = 6.6 Hz, 2H), 2.21 – 2.10 (m, 4H), 2.10 – 1.89 (m, 3H), 1.83 – 1.73 (m, 2H). ^{13}C{^{1}H} NMR (100 MHz, $CDCl_3$) δ: 164.9, 164.6, 157.9, 146.9, 144.7, 139.8, 137.7, 137.3, 134.6, 133.0, 129.9, 123.1, 116.5, 115.7, 115.4, 107.6, 65.0, 64.9, 59.2, 34.0, 30.1, 30.0, 27.8. HRMS (ESI, *m/z*): calcd for $[C_{25}H_{27}O_6]^+$ $(M\text{-}OH)^+$, 423.1802; found, 423.1808.

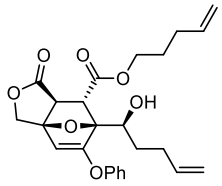

(±)-4

Pent-4-en-1-yl 6-(-1-hydroxypent-4-en-1-yl)-1-oxo-5-phenoxy-1,6,7,7a-tetrahydro-3H-3a,6-epoxyisobenzofuran-7-carboxylate ((±)-4). A round bottom flask equipped with a stir bar was charged with (±)-**3** (2.1 g, 4.8 mmol) and acetone (100 mL). The solution was then refluxed at 60 °C for 3 days before being cooled to room temperature and concentrated. The crude mixture was then purified by column chromatography (15–40% EtOAc/hexanes) to remove unreacted starting material, followed by reverse-phase column chromatography (75% MeCN/H_2O) to afford a single diastereomer of the title compound as a white solid (0.77 g, 36% yield). ^{1}H NMR (500 MHz, $CDCl_3$) δ: 7.40 – 7.33 (m, 2H), 7.25 – 7.20 (m, 1H), 7.10 – 7.04 (m, 2H), 5.94 – 5.84 (m, 1H), 5.79 – 5.68 (m, 1H), 5.16 – 4.93 (m, 5H), 4.57 (s, 2H), 4.46 – 4.39 (m, 1H), 4.24 (dt, *J* = 10.8, 6.6 Hz, 1H), 4.16 (dt, *J* = 10.8, 6.6 Hz, 1H), 3.95 (d, *J* = 3.2 Hz, 1H), 3.35 (d, *J* = 3.2 Hz, 1H), 2.49 – 2.39 (m, 1H), 2.37 – 2.26 (m, 1H), 2.17 – 2.09 (m, 2H), 1.97 – 1.86 (m, 1H), 1.84 – 1.73 (m, 4H). ^{13}C{^{1}H} NMR (100 MHz, $CDCl_3$) δ: 174.7, 170.1, 164.0, 154.9, 138.0, 13z7.2, 130.1, 126.2, 120.5, 115.7, 115.6, 100.7, 94.6, 91.7, 69.5, 67.0, 65.4, 52.8, 46.7, 32.4, 30.3, 30.1, 27.8. HRMS (ESI, *m/z*): calcd for $[C_{25}H_{29}O_7]^+$ $(M+H)^+$, 441.1908; found, 441.1922.

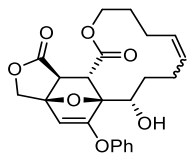

5

6-hydroxy-5-phenoxy-6,7,8,11,12,13,15a,15b-octahydro-3H-3a,5a-epoxy[1]oxacyclododecino[3,4-e]isobenzofuran-1,15-dione (5). A flame-dried round bottom flask equipped with a stir bar was charged with (±)-**4** (0.80 g, 1.8 mmol) and anhydrous DCM (1.2 L). The solution was then sparged with nitrogen for 10 min before adding Grubbs 1st generation catalyst (0.30 g, 3.6 mmol) under stream of nitrogen. The reaction was then refluxed at 40 °C overnight before ethyl vinyl ether (1 mL) was added and

refluxed for 30 additional min. The reaction was then cooled to room temperature and concentrated under reduced pressure. The crude mixture was purified by column chromatography (5–50% EtOAc/hexanes) to afford the title compound as a white solid (220 mg, 30% yield). The product consisted of a 1:4 (*E:Z*) isomeric mixture, which was used directly in the next step. A small amount of the major *Z* stereoisomer was isolated and characterized separately (see Figure 4.14). ^{1}H NMR (500 MHz, $CDCl_3$) δ (**isomeric mixture**): 7.43 – 7.32 (m, 2H), 7.28 – 7.24 (m, 1.6H), 7.24 – 7.19 (m, 1H), 7.11 – 7.04 (m, 0.4H), 5.65 – 5.49 (m, 1H), 5.43 – 5.30 (m, 0.8H), 5.20 (dd, *J* = 11.2, 7.2 Hz, 0.2H), 5.13 (d, *J* = 1.0 Hz, 0.8H), 5.02 (s, 0.2H), 4.58 (s, 1.6H), 4.56 (s, 0.4H), 4.35 (dd, *J* = 11.4, 5.0 Hz, 0.2H), 4.29 – 4.24 (m, 0.8H), 4.06 (q, *J* = 4.0 Hz, 0.8H), 4.02 – 3.95 (m, 0.2H), 3.95 – 3.87 (m, 0.8H), 3.78 (d, *J* = 3.0 Hz, 0.2H), 3.37 (d, *J* = 2.9 Hz, 0.2H), 3.31 (d, *J* = 3.7 Hz, 0.8H), 3.16 (d, *J* = 3.7 Hz, 0.8H), 2.76 – 2.66 (m, 0.8H), 2.55 – 2.42 (m, 1H), 2.40 – 2.15 (m, 2H), 2.11 – 1.90 (m, 3.2H), 1.75 – 1.58 (m, 2H). ^{1}H NMR (500 MHz, $CDCl_3$) δ (**major *Z* isomer**): 7.42 – 7.32 (m, 2H), 7.28 – 7.26 (m, 2H), 7.24 – 7.18 (m, 1H), 5.61 (td, *J* = 10.8, 5.0 Hz, 1H), 5.35 (td, *J* = 10.8, 5.1 Hz, 1H), 5.13 (d, *J* = 1.0 Hz, 1H), 4.58 (s, 2H), 4.31 – 4.22 (m, 1H), 4.10 – 4.04 (m, 1H), 3.97 – 3.85 (m, 1H), 3.31 (d, *J* = 3.7 Hz, 1H), 3.16 (d, *J* = 3.7 Hz, 1H), 2.77 – 2.66 (m, 1H), 2.56 – 2.44 (m, 1H), 2.32 – 2.24 (m, 2H), 2.13 – 1.94 (m, 3H), 1.61 (t, *J* = 14.1 Hz, 2H). ^{13}C{^{1}H} NMR (100 MHz, $CDCl_3$) δ (**major *Z* isomer**): 174.7, 170.5, 164.4, 155.2, 130.9, 129.9, 128.1, 125.9, 121.1, 101.5, 95.6, 91.6, 74.0, 69.4, 63.9, 55.5, 48.6, 34.0, 27.0, 25.9, 22.9. HRMS (ESI, *m/z*): calcd for $[C_{23}H_{25}O_7]^+$ $(M+H)^+$, 413.1595; found, 413.1602.

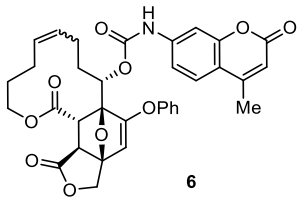

6

1,15-dioxo-5-phenoxy-1,6,7,8,11,12,13,15,15a,15b-decahydro-3H-3a,5a-epoxy[1]oxacyclododecino[3,4-e]isobenzofuran-6-yl (4-methyl-2-oxo-2H-chromen-7-yl)carbamate (6). A round bottom flask equipped with a stir bar was charged with **5** (220 mg, 0.53 mmol), 4-methylcoumarin-7-isocyanate[24] (129 mg, 0.64 mmol), and DCM (4 mL).

After the solids were fully dissolved, DMAP (6.6 mg, 0.053 mmol) was added. The solution was then stirred at room temperature for 1 h. The crude mixture was then filtered through a cotton pad and concentrated under reduced pressure before being purified by column chromatography (30–60% EtOAc/hexanes) to afford the title compound as a white solid (250 mg, 76% yield). The product was then recrystallized from hexanes/ethyl acetate to afford a 3:7 (*E:Z*) isomeric mixture, which was used directly in the next step. A small amount of the major *Z* stereoisomer was isolated and characterized separately.^{1}H NMR (500 MHz, $CDCl_3$) δ (**isomeric mixture**): 7.64 (s, 0.3H), 7.56 – 7.50 (m, 1H), 7.47 (s, 0.7H), 7.44 – 7.35 (m, 3H), 7.34 – 7.26 (m, 2H), 7.26 – 7.21 (m, 0.7H), 7.12 – 7.09 (m, 0.3H), 6.97 – 6.89 (m, 0.7H), 6.68 – 6.63 (m, 0.3H), 6.22 – 6.17 (m, 1H), 6.05 – 5.96 (m, 0.3H), 5.60 – 5.51 (m, 0.7H), 5.46 – 5.31 (m, 1.3H), 5.26 (t, *J* = 4.0 Hz, 0.7H), 5.21 (s, 0.7H), 5.06 (s, 0.3H), 4.65 – 4.54 (m, 2H), 4.45 – 4.39 (m, 0.3H), 4.31 – 4.25 (m, 0.7H), 4.05 – 3.97 (m, 0.3H), 3.96 – 3.86 (m, 0.7H), 3.52 (d, *J* = 2.8 Hz, 0.3H), 3.46 – 3.39 (m, 1H), 3.15 (d, *J* = 3.7 Hz, 0.7H), 2.83 – 2.71 (m, 0.7H), 2.71 – 2.58 (m, 0.7H), 2.56 – 2.48 (m, 0.3H), 2.46 – 2.35 (m, 4H), 2.32 – 2.22 (m, 0.7H), 2.20 – 1.84 (m, 3.6H), 1.75 – 1.57 (m, 1.4H). ^{1}H NMR (500 MHz, $CDCl_3$) δ (**major *Z* isomer**): 7.53 (d, *J* = 8.5 Hz, 1H), 7.47 (bs, 1H), 7.43 – 7.35 (m, 3H), 7.31 (d, *J* = 7.9 Hz, 2H), 7.25 – 7.22 (m, 1H), 6.96 (s, 1H), 6.20 (s, 1H), 5.56 (td, *J* = 10.9, 4.5 Hz, 1H), 5.35 (td, *J* = 11.0, 5.1 Hz, 1H), 5.26 (t, *J* = 4.1 Hz, 1H), 5.21 (s, 1H), 4.62 – 4.53 (m, 2H), 4.31 – 4.25 (m, 1H), 3.94 – 3.86 (m, 1H), 3.43 (d, *J* = 3.8 Hz, 1H), 3.15 (d, *J* = 3.7 Hz, 1H), 2.81 – 2.71 (m, 1H), 2.71 – 2.57 (m, 1H), 2.46 – 2.33 (m, 4H), 2.16 – 1.98 (m, 3H), 1.75 – 1.58 (m, 2H). ^{13}C{^{1}H} NMR (125 MHz, $CDCl_3$) δ (**major *Z* isomer**): 174.3, 170.3, 163.7, 161.2, 155.1, 154.4, 152.5, 141.5, 130.7, 129.9, 127.8, 125.9, 125.5, 121.0, 115.7, 114.7, 113.2, 106.2, 101.2, 93.2, 91.5, 75.5, 69.3, 63.9, 55.4, 48.8, 33.2, 26.5, 25.5, 22.8, 18.7. HRMS (ESI, *m/z*): calcd for $[C_{34}H_{32}NO_{10}]^{+}$ $(M+H)^{+}$, 614.2021; found, 614.2034.

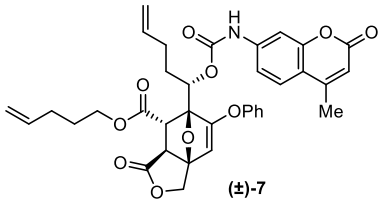

(±)-7

Pent-4-en-1-yl 6-(1-(((4-methyl-2-oxo-2H-chromen-7-yl)carbamoyl)oxy)pent-4-en-1-yl)-1-oxo-5-phenoxy-1,6,7,7a-tetrahydro-3H-3a,6-epoxyisobenzofuran-7-carboxylate ((±)-7). A round bottom flask equipped with a stir bar was charged with (±)**-4** (41.9 mg, 0.095 mmol), 4-methylcoumarin-7-isocyanate[24] (35 mg, 0.17 mmol), and DCM (2 mL). After the solids were fully dissolved, DMAP (1.1 mg, 0.0095 mmol) was added. The solution was then stirred at room temperature for 1 h. The crude mixture was then filtered through a cotton pad and concentrated under reduced pressure before being purified by column chromatography (10–50% EtOAc/hexanes) to afford the title compound as a white solid (45.3 mg, 74% yield). ^{1}H NMR (400 MHz, $CDCl_3$) δ: 7.68 (bs, 1H), 7.54 (d, *J* = 8.6 Hz, 1H), 7.43 – 7.35 (m, 2H), 7.35 – 7.29 (m, 1H), 7.26 – 7.20 (m, 2H), 7.12 – 7.04 (m, 2H), 6.21 (d, *J* = 1.4 Hz, 1H), 5.96 – 5.80 (m, 2H), 5.68 (ddt, *J* = 16.9, 10.2, 6.6 Hz, 1H), 5.15 – 5.05 (m, 2H), 5.03 – 4.96 (m, 1H), 4.96 – 4.86 (m, 2H), 4.61 (s, 2H), 4.14 (t, *J* = 6.7 Hz, 2H), 3.73 (d, *J* = 3.2 Hz, 1H), 3.36 (d, *J* = 3.2 Hz, 1H), 2.42 (d, *J* = 1.3 Hz, 3H), 2.35 – 2.24 (m, 2H), 2.12 – 2.03 (m, 2H), 2.02 – 1.93 (m, 2H), 1.81 – 1.69 (m, 2H). ^{13}C{^{1}H} NMR (100 MHz, $CDCl_3$) δ: 174.8, 169.4, 163.3, 161.3, 154.9, 154.7, 152.3, 152.0, 141.4, 137.6, 137.3, 130.2, 126.3, 125.5, 120.4, 115.8, 115.4, 115.4, 114.5, 113.4, 106.1, 100.4, 93.2, 91.8, 69.4, 69.3, 65.7, 52.7, 47.1, 31.3, 29.9, 29.7, 27.5, 18.7. HRMS (ESI, *m/z*): calcd for $[C_{36}H_{36}NO_{10}]^+$ $(M+H)^+$, 642.2334; found, 642.2349.

General procedure for the synthesis of multi-mechanophore polymers, MMP_x. All reagents were kept in the glovebox in a nitrogen environment. Stock solutions of Grubbs' 2nd generation catalyst (G2) in $CHCl_3$ (2.2 mg/mL) were prepared in the glovebox and used immediately after preparation. Polymerization reactions were carried out in the glovebox. Upon completion, ethyl vinyl ether (0.1 mL) was added to the mixture inside the glove box and allowed to stir for 30 min at room temperature before the vial was removed from the glovebox. The reaction was then opened to air and the solution was diluted with DCM. The polymer was precipitated into methanol (2x) and collected by centrifugation. The isolated polymer was thoroughly dried under vacuum and characterized by NMR spectroscopy and GPC-MALS. GPC data are provided in Figure 4.4.

MMP$_{80}$. Macrocycle **6** (8.3 mg, 0.014 mmol), **COE$_{OAc}$** (20 mg, 0.12 mmol), and $CHCl_3$ (66 μL, 2.0 M) were added to a 2 mL vial equipped with a stir bar. The mixture was heated gently at 60 °C on a hotplate until all solids dissolved. The solution was then cooled to room temperature followed by addition of a stock solution of G2 catalyst in $CHCl_3$ (5.2 μL, 0.013 μmol). The vial was sealed and stirred at room temperature. Polymerization for 3 h provided the title polymer as a white solid (24 mg, 85%). M_n = 80.3 kDa, $Đ$ = 2.40.

MMP$_{295}$. Macrocycle **6** (15 mg, 0.024 mmol), **COE$_{OAc}$** (4.1 mg, 0.024 mmol), and $CHCl_3$ (0.24 mL, 0.20 M) were added to a 2 mL vial equipped with a stir bar. The mixture was heated gently at 60 °C on a hotplate until all solids dissolved. The stock solution of G2 catalyst in $CHCl_3$ (4.0 μL, 0.010 μmol) was then added to the mixture maintained at 60 °C, and the reaction was stirred under a gentle flow of nitrogen to partially concentrate the solution while maintaining homogeneity. When the monomer concentration reached approximately 2 M, as determined by the total mass of the reaction mixture, the vial was sealed and stirred at room temperature. Polymerization for 3 h provided the titled polymer as a white solid (17 mg, 90%). M_n = 2953 kDa, $Đ$ = 2.25.

MMP$_{23}$. Macrocycle **6** (10 mg, 0.016 mmol), **COE$_{OAc}$** (12 mg, 0.074 mmol), and $CHCl_3$ (0.88 mL, 0.1 M) were added to a 2 mL vial equipped with a stir bar. Stock solution of G2 catalyst in $CHCl_3$ (6.2 μL, 0.016 mmol) was then added to the mixture and the vial was sealed and stirred at room temperature. Polymerization for 3 days provided the title polymer as a white solid (7.0 mg, 32%). M_n = 22.5 kDa, $Đ$ = 1.36.

Polymerization procedure for PMA$_{center}$. The synthesis of **PMA$_{center}$** was carried out according to the literature procedure.[24,34] A freshly cut copper wire (1.1 cm length, 20 gauge) was treated with 1 M HCl for approximately 5 min and then rinsed thoroughly with DI water and acetone, and then allowed to dry in air. A 10 mL Schlenk flask equipped with a stir bar was charged with the bis-initiator (8.9 mg, 0.010 mmol), methyl acrylate (1.4 mL, 15 mmol), Me_6TREN (5.4 μL, 0.020 mmol), and DMSO (1.4 mL). The flask was sealed and the solution was deoxygenated via three freeze-pump-thaw cycles, and then backfilled with nitrogen. The flask was opened briefly under a strong flow of nitrogen,

and the copper wire was added on top of the frozen mixture. The flask was resealed, evacuated for an additional 15 min, warmed to room temperature, and then backfilled with nitrogen. The reaction mixture was stirred at room temperature until the solution became sufficiently viscous, indicating that the desired monomer conversion was reached (1.5 h). The flask was then opened to air and the solution was diluted with DCM. The polymer was precipitated into cold methanol (2x) and then thoroughly dried under vacuum to provide a tacky white polymer (0.61 g, 45%). GPC data are provided in Figure 4.4. M_n = 83.9 kDa, $Đ$ = 1.17.

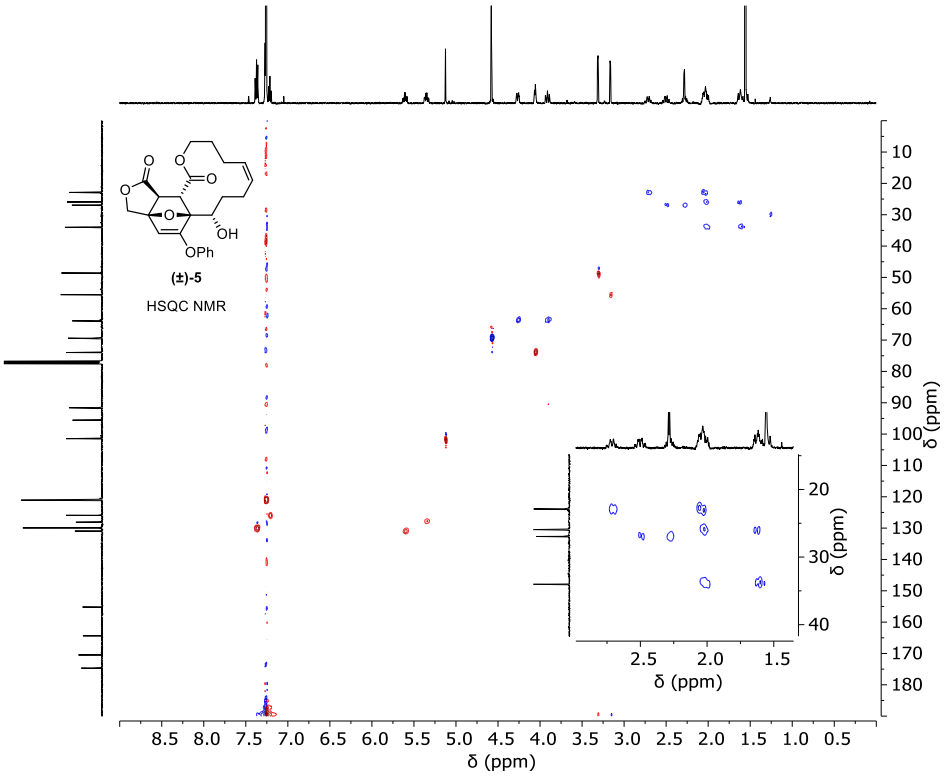

4.4 General Procedure for Ultrasonication Experiments

An oven-dried sonication vessel was fitted with rubber septa, placed onto the sonication probe, and allowed to cool under a stream of dry argon. The vessel was charged with a solution of the polymer in anhydrous THF/methanol (3:1 v/v, 0.1 mg/mL, 20 mL) and

Figures 4.14. HSQC analysis (500 MHz, $CDCl_3$) of (±)-**5** for stereochemical determination. The allylic carbon atoms in the macrocycle resonate at 23.0 and 26.9 ppm, indicating (*Z*) configuration of the macrocyclic olefin.

submerged in an ice bath. The solution was sparged continuously with argon beginning 20 min prior to sonication and for the duration of the sonication experiment. Pulsed ultrasound (1 s on/1 s off, 30% amplitude, 20 kHz, 13.9 W/cm^2) was then applied to the system. The solution temperature during sonication was measured to be 9–13 °C. Sonicated solutions were filtered through a 0.45 μm syringe filter prior to analysis. Ultrasonic intensity was calibrated using the method described by Berkowski *et al*.[35]

4.5 Characterization of Cargo Release Using Photoluminescence Spectroscopy

Aliquots were removed during sonication experiments and characterized using photoluminescence spectroscopy to quantify release of aminocoumarin (**CoumNH$_2$**) according to established procedures.[24] Samples were first allowed to incubate for 5 days, after which the fluorescence emission reached a plateau indicating complete conversion of the intermediate furfuryl carbamate (see Figure 4.8). Emission spectra were recorded using an excitation wavelength of 365 nm. A standard calibration curve was constructed using the emission maximum at 424 nm to determine the concentration of **CoumNH$_2$** (Figure 4.15).

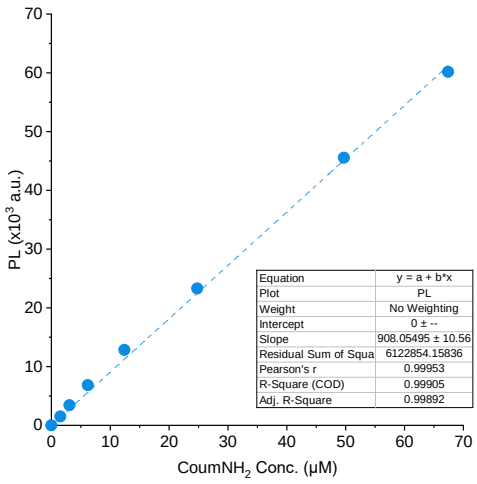

Figures 4.15. Calibration curve for experimental determination of the concentration of 7-amino-4-methylcoumarin (**CoumNH$_2$**) (λ_{ex} = 365 nm, λ_{em} = 424 nm) in THF/methanol (3:1 v/v). A linear regression of the data gives the calibration function Y = 908X.

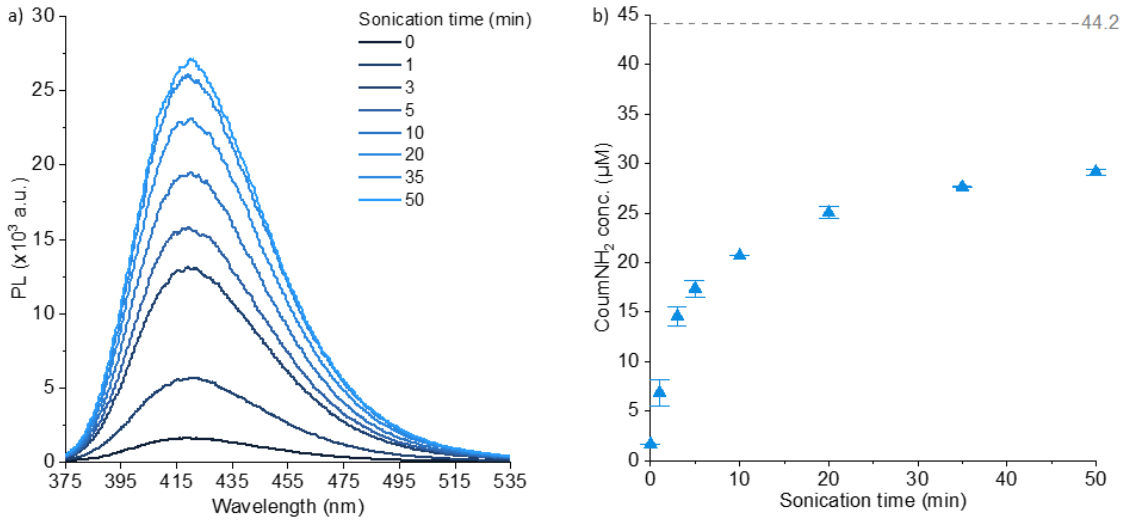

Figures 4.16. a) Representative PL spectra characterizing the release of **CoumNH$_2$** from a 0.1 mg/mL solution of **MMP$_{80}$** in THF/methanol (3:1 v/v). λ_{ex} = 365 nm. b) Concentration of **CoumNH$_2$** released from **MMP$_{80}$** as a function of sonication time calculated from the fluorescence intensity at 424 nm using the calibration curve. The theoretical concentration of **CoumNH$_2$** based on 100% release from the mechanophore is 44.2 μM. Each data point is the average of two replicate measurements with the error bar denoting the range of the two values.

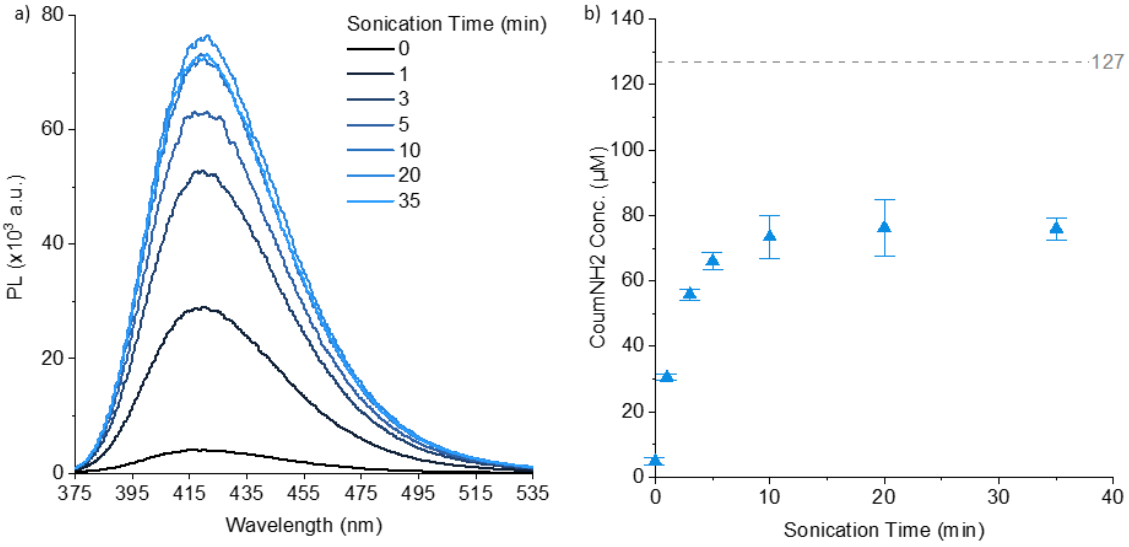

Figures 4.17. a) Representative PL spectra characterizing the release of **CoumNH$_2$** from a 0.1 mg/mL solution of **MMP$_{295}$** in THF/methanol (3:1 v/v). λ_{ex} = 365 nm. b) Concentration of **CoumNH$_2$** released from **MMP$_{295}$** as a function of sonication time calculated from the fluorescence intensity at 424 nm using the calibration curve. The theoretical concentration of **CoumNH$_2$** based on 100% release from the mechanophore is 127 μM. Each data point is the average of two replicate measurements with the error bar denoting the range of the two values.

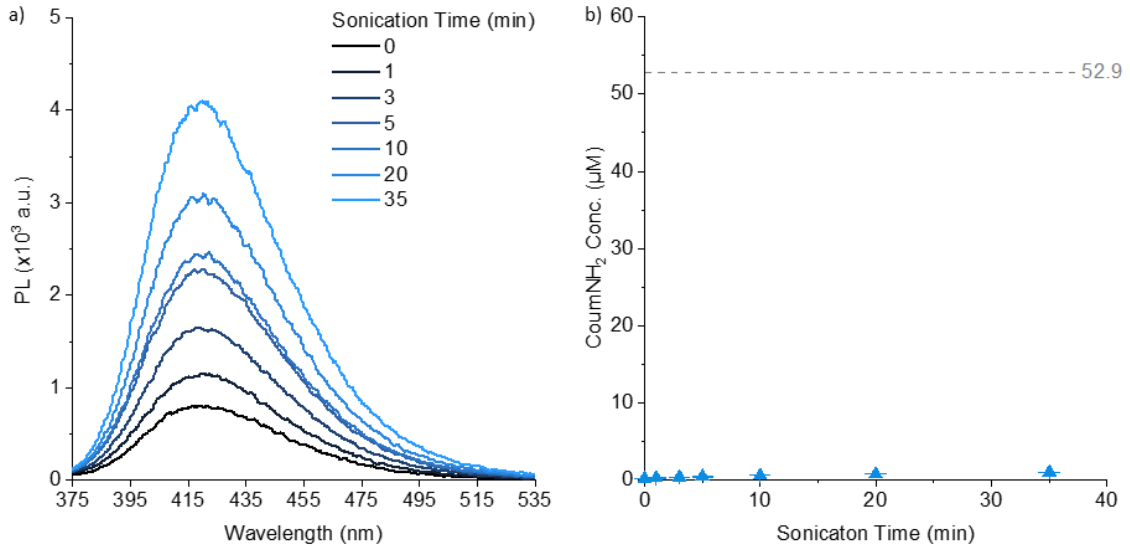

Figures 4.18. a) Representative PL spectra characterizing the release of **CoumNH$_2$** from a 0.1 mg/mL solution of **MMP$_{23}$** in THF/methanol (3:1 v/v). λ_{ex} = 365 nm. b) Concentration of **CoumNH$_2$** released from **MMP$_{23}$** as a function of sonication time calculated from the fluorescence intensity at 424 nm using the calibration curve. The theoretical concentration of **CoumNH$_2$** based on 100% release from the mechanophore is 52.9 μM. Each data point is the average of two replicate measurements with the error bar denoting the range of the two values.

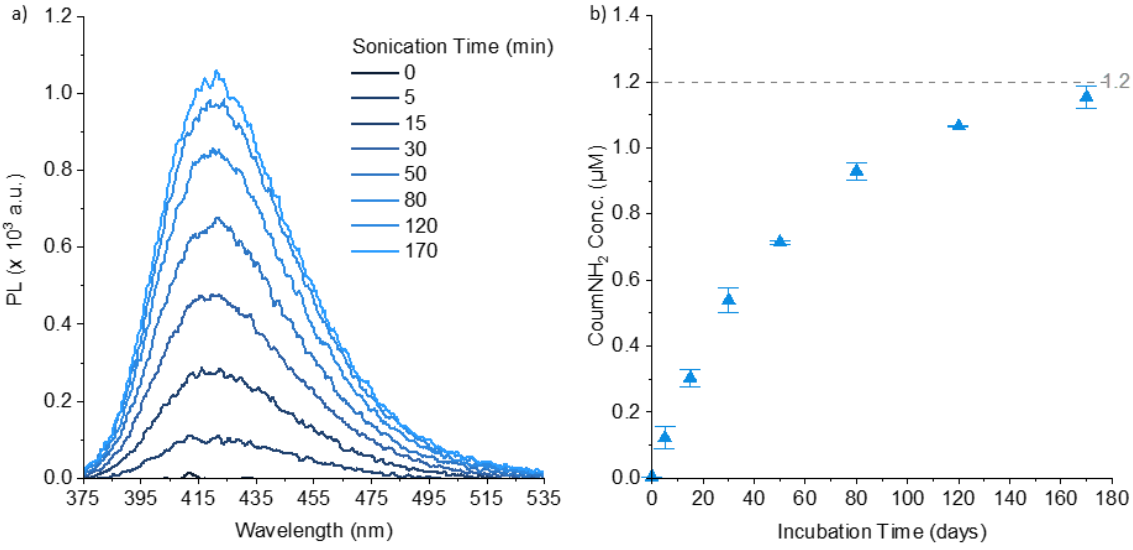

Figures 4.19. a) Representative PL spectra characterizing the release of **CoumNH$_2$** from a 0.10 mg/mL solution of **PMA$_{center}$** in THF/methanol (3:1 v/v). λ_{ex} = 365 nm. b) Concentration of **CoumNH$_2$** released from **PMA$_{center}$** as a function of sonication time calculated from the fluorescence intensity at 424 nm using the calibration curve. The theoretical concentration of **CoumNH$_2$** based on 100% release from the mechanophore is 1.2 μM. Each data point is the average of two replicate measurements with the error bar denoting the range of the two values.

4.6 . Characterization of Multimechanophore Polymers

To investigate the distribution of mechanophores in the MMPs, a hydrolysis experiment was performed and the size of the product fragments was analyzed by GPC (Figure 4.20). A sample of **MMP$_{80}$** (5 mg) was dissolved in 1 mL of THF/MeOH (1:1) and 12 mg of LiOH was added (0.5 M). The mixture was stirred at 60 °C for 9 h. The reaction was then cooled to room temperature and 1 M HCl was added dropwise until the pH was ~1 according to a pH test strip. The mixture was concentrated under reduced pressure and lyophilized overnight. The crude product mixture was then suspended in DCM and then filtered to remove insoluble salt. The filtrate was concentrated and dried under high vacuum, and then analyzed by GPC-MALS. The chain fragments produced via hydrolysis are small with polystyrene-equivalent molar mass substantially < ~4 kDa. These results indicate that the mechanophore is relatively well distributed along the length of the polymer chain in the MMPs, consistent with a random copolymerization without significant blocky structure. This conclusion is further supported by the high mechanophore activation efficiencies (> 60%) achieved upon sonication of **MMP$_{80}$** and **MMP$_{295}$**.

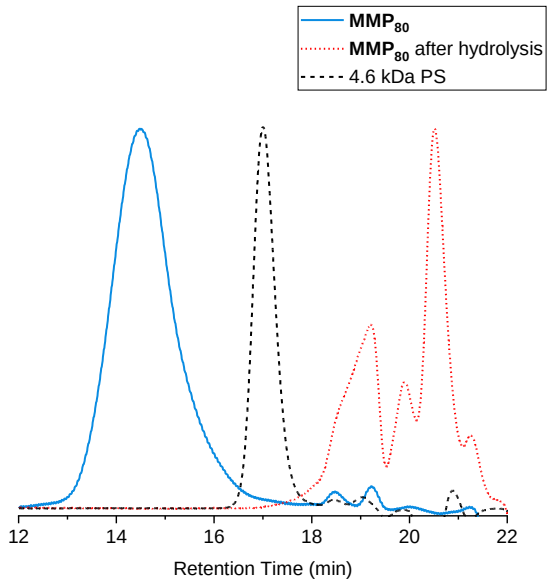

Figures 4.20. GPC traces (RI response) of **MMP$_{80}$** before (blue trace) and after hydrolysis using lithium hydroxide (red trace). A polystyrene standard (M_n = 4.6 kDa, $Đ$ = 1.05) is used as a reference. Hydrolysis of **MMP$_{80}$** produces only low molar mass fragments, indicating that the ester-containing mechanophore repeat units are relatively well distributed along the length of the polymer chain consistent with a random copolymer.

To characterize the structure of the polymer product after ultrasound-induced mechanochemical activation, a sample of **MMP$_{295}$** was subjected to sonication and subsequently analyzed by ^{1}H NMR spectroscopy (Figure 4.21). BHT radical inhibitor (30 mM) was added to the polymer solution in order to preserve the double bonds in the polymer backbone and avoid radical side reactions.[36,37] A sample of **MMP$_{295}$** was dissolved in 3:1 THF/MeOH (0.1 mg/mL, 20 mL) and was sonicated for 35 min. The solution was incubated for 5 days to allow complete reaction of the intermediate furfuryl carbamates, after which it was concentrated under reduced pressure. The residue was redissolved in a small amount of DCM and precipitated into methanol (×2), collected by ultracentrifugation, and then thoroughly dried under vacuum before analysis by ^{1}H NMR spectroscopy using a Shigemi tube. The ^{1}H NMR spectrum of the polymer after sonication exhibits characteristic signals corresponding to the fumarate ester alkene protons, the furan proton, and the furfuryl ester methylene protons, consistent with the expected polymer structure (see Figure 4.9).

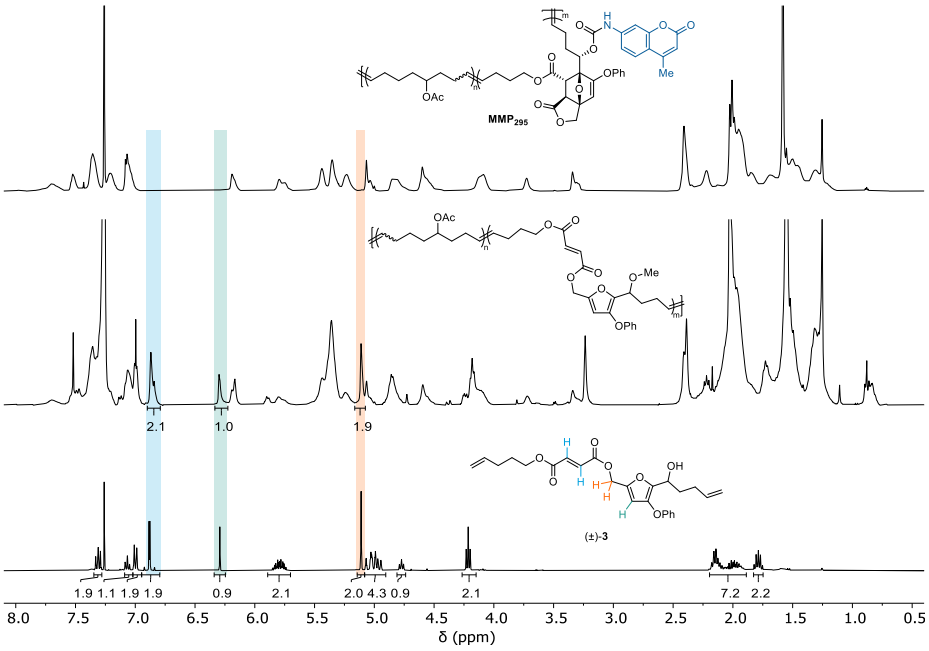

Figures 4.21. ^{1}H NMR spectra (400 MHz, $CDCl_3$) of **MMP$_{295}$** before (*top*) and after sonication (*middle*) compared to (±)-**3** (*bottom*). After sonication of **MMP$_{295}$** (3:1 THF/MeOH, 30 mM BHT, 35 min), characteristic signals corresponding to the fumarate alkene protons (~6.9 ppm), the furan proton (~6.3 ppm), and the furfuryl ester methylene protons (5.1 ppm) are observed, consistent with the expected polymer product. Unreacted mechanophore repeat units are omitted from the structure of the polymer product for clarity.

4.7 Procedure for CoGEF Calculations

CoGEF calculations were performed using Spartan ′18 Parallel Suite according to previously reported methods.[31,38] Ground state energies were calculated using DFT at the B3LYP/6-31G* level of theory. Starting from the equilibrium geometry of the unconstrained molecule (relative energy = 0 kJ/mol), the distance between the terminal methyl groups of the truncated structure was increased in increments of 0.05 Å and the energy was minimized at each step. The maximum force associated with the retro-Diels–Alder reaction was calculated from the slope of the curve immediately prior to bond cleavage.

4.8 Single Crystal X-Ray Diffraction

Crystals for X-ray diffraction analysis were grown by slow diffusion of hexanes into a solution of compound (±)-**4** in DCM. Low-temperature diffraction data (*f*-and *w*-scans) were collected on a Bruker AXS D8 VENTURE KAPPA diffractometer coupled to a PHOTON II CPAD detector with Cu K_a radiation (l = 1.54178 Å) from an IμS micro-source for the structure of compound V22298. The structure was solved by direct methods using SHELXS[39] and refined against F^2 on all data by full-matrix least squares with SHELXL-2019[40] using established refinement techniques.[41] All non-hydrogen atoms were refined anisotropically. Unless otherwise noted, all hydrogen atoms were included into the model at geometrically calculated positions and refined using a riding model. The isotropic displacement parameters of all hydrogen atoms were fixed to 1.2 times the U value of the atoms they are linked to (1.5 times for methyl groups). All disordered atoms were refined with the help of similarity restraints on the 1,2- and 1,3-distances and displacement parameters as well as enhanced rigid bond restraints for anisotropic displacement parameters.

Compound (±)-**4** crystallizes in the monoclinic space group *C*2/*c* with one molecule in the asymmetric unit. The crystal cracked or underwent a phase change upon cooling to low temperatures so the data was collected at 200 K. The coordinates for the hydrogen atoms bound to O6 were located in the difference Fourier synthesis and refined semi-freely with the help of a restraint on the O-H distance (0.84(4) Å). One of the carbon chains was highly disordered and modeled as a three-component disorder.

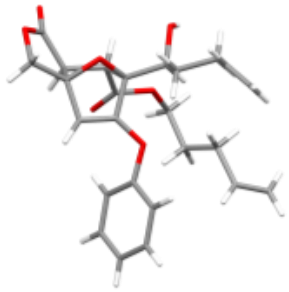

Identification code	V22298	
Empirical formula	C25 H28 O7	
Formula weight	440.47	
Temperature	200(2) K	
Wavelength	1.54178 Å	
Crystal system	Monoclinic	
Space group	C2/c	
Unit cell dimensions	a = 36.804(4) Å	a= 90°.
	b = 8.4725(12) Å	b= 116.172(5)°.
	c = 16.7600(19) Å	g = 90°.
Volume	4690.4(10) $Å^3$	
Z	8	
Density (calculated)	1.248 Mg/m^3	
Absorption coefficient	0.749 mm^{-1}	
F(000)	1872	
Crystal size	0.400 x 0.150 x 0.150 mm^3	
Theta range for data collection	2.675 to 74.613°.	
Index ranges	-45<=h<=45, -10<=k<=9, -20<=l<=20	
Reflections collected	36207	
Independent reflections	4807 [R(int) = 0.0775]	
Completeness to theta = 67.679°	100.0 %	
Absorption correction	Semi-empirical from equivalents	
Max. and min. transmission	0.7538 and 0.5279	
Refinement method	Full-matrix least-squares on F^2	
Data / restraints / parameters	4807 / 521 / 403	
Goodness-of-fit on F^2	1.035	
Final R indices [I>2sigma(I)]	R1 = 0.0549, wR2 = 0.1427	
R indices (all data)	R1 = 0.0713, wR2 = 0.1601	
Extinction coefficient	n/a	
Largest diff. peak and hole	0.289 and -0.272 $e.Å^{-3}$	

4.9 References

(1) Zhang, H.; Gao, F.; Cao, X.; Li, Y.; Xu, Y.; Weng, W.; Boulatov, R. Mechanochromism and Mechanical-Force-Triggered Cross-Linking from a Single Reactive Moiety Incorporated into Polymer Chains. *Angew. Chem. Int. Ed.* **2016**, *55*, 3040–3044.

(2) Swager, T. M. Sensor Technologies Empowered by Materials and Molecular Innovations. *Angew. Chem. Int. Ed.* **2018**, *57*, 4248–4257.

(3) Patrick, J. F.; Robb, M. J.; Sottos, N. R.; Moore, J. S.; White, S. R. Polymers with autonomous life-cycle control. *Nature* **2016**, *540*, 363–370.

(4) Stratigaki, M.; Göstl, R. Methods for Exerting and Sensing Force in Polymer Materials Using Mechanophores. *ChemPlusChem* **2020**, *85*, 1095–1103.

(5) Davis, D. A.; Hamilton, A.; Yang, J.; Cremar, L. D.; Van Gough, D.; Potisek, S. L.; Ong, M. T.; Braun, P. V.; Martínez, T. J.; White, S. R.; Moore, J. S.; Sottos, N. R. Force-induced activation of covalent bonds in mechanoresponsive polymeric materials. *Nature* **2009**, *459*, 68–72.

(6) Yao, Y.; McFadden, M. E.; Luo, S. M.; Barber, R. W.; Kang, E.; Bar-Zion, A.; Smith, C. A. B.; Jin, Z.; Legendre, M.; Ling, B.; Malounda, D.; Torres, A.; Hamza, T.; Edwards, C. E. R.; Shapiro, M. G.; Robb, M. J. Remote control of mechanochemical reactions under physiological conditions using biocompatible focused ultrasound. *Proc. Natl. Acad. Sci. U.S.A.* **2023**, *120*, e2309822120.

(7) Kim, G.; Lau, V. M.; Halmes, A. J.; Oelze, M. L.; Moore, J. S.; Li, K. C. High-intensity focused ultrasound-induced mechanochemical transduction in synthetic elastomers. *Proc. Natl. Acad. Sci. USA* **2019**, *116*, 10214–10222.

(8) Li, J.; Nagamani, C.; Moore, J. S. Polymer Mechanochemistry: From Destructive to Productive. *Acc. Chem. Res.* **2015**, *48*, 2181–2190.

(9) Versaw, B. A.; Zeng, T.; Hu, X.; Robb, M. J. Harnessing the Power of Force: Development of Mechanophores for Molecular Release. *J. Am. Chem. Soc.* **2021**, *143*, 21461–21473.

(10) Küng, R.; Göstl, R.; Schmidt, B. M. Release of Molecular Cargo from Polymer Systems by Mechanochemistry. *Chemistry A European J* **2022**, *28*, e202103860.

(11) Shen, H.; Cao, Y.; Lv, M.; Sheng, Q.; Zhang, Z. Polymer mechanochemistry for the release of small cargoes. *Chem. Commun.* **2022**, *58*, 4813–4824.

(12) Sun, Y.; Neary, W. J.; Burke, Z. P.; Qian, H.; Zhu, L.; Moore, J. S. Mechanically Triggered Carbon Monoxide Release with Turn-On Aggregation-Induced Emission. *J. Am. Chem. Soc.* **2022**, *144*, 1125–1129.

(13) Nijem, S.; Song, Y.; Schwarz, R.; Diesendruck, C. E. Flex-activated CO mechanochemical production for mechanical damage detection. *Polym. Chem.* **2022**, *13*, 3986–3990.

(14) Diesendruck, C. E.; Steinberg, B. D.; Sugai, N.; Silberstein, M. N.; Sottos, N. R.; White, S. R.; Braun, P. V.; Moore, J. S. Proton-Coupled Mechanochemical Transduction: A Mechanogenerated Acid. *J. Am. Chem. Soc.* **2012**, *134*, 12446–12449.

(15) Lin, Y.; Kouznetsova, T. B.; Craig, S. L. A Latent Mechanoacid for Time-Stamped Mechanochromism and Chemical Signaling in Polymeric Materials. *J. Am. Chem. Soc.* **2020**, *142*, 99–103.

(16) Larsen, M. B.; Boydston, A. J. "Flex-Activated" Mechanophores: Using Polymer Mechanochemistry To Direct Bond Bending Activation. *J. Am. Chem. Soc.* **2013**, *135*, 8189–8192.
(17) Suwada, K.; Ieong, A. W.; Lo, H. L. H.; De Bo, G. Furan Release via Force-Promoted Retro-[4+2][3+2] Cycloaddition. *J. Am. Chem. Soc.* **2023**, *145*, 20782–20785.
(18) Shen, H.; Larsen, M. B.; Roessler, A.; Zimmerman, P.; Boydston, A. J. Mechanochemical Release of N-heterocyclic Carbenes from Flex-Activated Mechanophores. *Angew. Chem. Int. Ed.* **2021**, *60*, 13559–13563.
(19) Yang, J.; Xia, Y. Force-Triggered Guest Release from Mechanophore Incorporated Rotaxanes. *CCS Chem* **2023**, *5*, 1365–1371.
(20) Lu, Y.; Sugita, H.; Mikami, K.; Aoki, D.; Otsuka, H. Mechanochemical Reactions of Bis(9-methylphenyl-9-fluorenyl) Peroxides and Their Applications in Cross-Linked Polymers. *J. Am. Chem. Soc.* **2021**, *143*, 17744–17750.
(21) Shi, Z.; Song, Q.; Göstl, R.; Herrmann, A. Mechanochemical activation of disulfide-based multifunctional polymers for theranostic drug release. *Chem. Sci.* **2021**, *12*, 1668–1674.
(22) Shi, Z.; Song, Q.; Göstl, R.; Herrmann, A. The Mechanochemical Release of Naphthalimide Fluorophores from β-Carbonate and β-Carbamate Disulfide-Centered Polymers. *CCS Chem.* **2021**, 2333–2344.
(23) Hu, X.; Zeng, T.; Husic, C. C.; Robb, M. J. Mechanically Triggered Small Molecule Release from a Masked Furfuryl Carbonate. *J. Am. Chem. Soc.* **2019**, *141*, 15018–15023.
(24) Hu, X.; Zeng, T.; Husic, C. C.; Robb, M. J. Mechanically Triggered Release of Functionally Diverse Molecular Payloads from Masked 2-Furylcarbinol Derivatives. *ACS Cent. Sci.* **2021**, *7*, 1216–1224.
(25) Zeng, T.; Hu, X.; Robb, M. J. 5-Aryloxy substitution enables efficient mechanically triggered release from a synthetically accessible masked 2-furylcarbinol mechanophore. *Chem. Commun.* **2021**, *57*, 11173–11176.
(26) Husic, C. C.; Hu, X.; Robb, M. J. Incorporation of a Tethered Alcohol Enables Efficient Mechanically Triggered Release in Aprotic Environments. *ACS Macro Lett.* **2022**, *11*, 948–953.
(27) May, P. A.; Moore, J. S. Polymer mechanochemistry: techniques to generate molecular force via elongational flows. *Chem. Soc. Rev.* **2013**, *42*, 7497–7506.
(28) Lenhardt, J. M.; Black Ramirez, A. L.; Lee, B.; Kouznetsova, T. B.; Craig, S. L. Mechanistic Insights into the Sonochemical Activation of Multimechanophore Cyclopropanated Polybutadiene Polymers. *Macromolecules* **2015**, *48*, 6396–6403.
(29) Bowser, B. H.; Craig, S. L. Empowering mechanochemistry with multi-mechanophore polymer architectures. *Polym. Chem.* **2018**, *9*, 3583–3593.
(30) Gossweiler, G. R.; Kouznetsova, T. B.; Craig, S. L. Force-Rate Characterization of Two Spiropyran-Based Molecular Force Probes. *J. Am. Chem. Soc.* **2015**, *137*, 6148–6151.
(31) Beyer, M. K. The mechanical strength of a covalent bond calculated by density functional theory. *J. Chem. Phys.* **2000**, *112*, 7307–7312.

(32) Klein, I. M.; Husic, C. C.; Kovács, D. P.; Choquette, N. J.; Robb, M. J. Validation of the CoGEF Method as a Predictive Tool for Polymer Mechanochemistry. *J. Am. Chem. Soc.* **2020**, *142*, 16364–16381.
(33) Kryger, M. J.; Munaretto, A. M.; Moore, J. S. Structure–Mechanochemical Activity Relationships for Cyclobutane Mechanophores. *J. Am. Chem. Soc.* **2011**, *133*, 18992–18998.
(34) Nguyen, N. H.; Rosen, B. M.; Lligadas, G.; Percec, V. Surface-Dependent Kinetics of Cu(0)-Wire-Catalyzed Single-Electron Transfer Living Radical Polymerization of Methyl Acrylate in DMSO at 25 °C. *Macromolecules* **2009**, *42*, 2379–2386.
(35) Berkowski, K. L.; Potisek, S. L.; Hickenboth, C. R.; Moore, J. S. Ultrasound-Induced Site-Specific Cleavage of Azo-Functionalized Poly(ethylene glycol). *Macromolecules* **2005**, *38*, 8975–8978.
(36) Overholts, A. C.; McFadden, M. E.; Robb, M. J. Quantifying Activation Rates of Scissile Mechanophores and the Influence of Dispersity. *Macromolecules* **2022**, *55*, 276–283.
(37) Yang, J.; Horst, M.; Werby, S. H.; Cegelski, L.; Burns, N. Z.; Xia, Y. Bicyclohexene-peri-naphthalenes: Scalable Synthesis, Diverse Functionalization, Efficient Polymerization, and Facile Mechanoactivation of Their Polymers. *J. Am. Chem. Soc.* **2020**, *142*, 14619–14626.
(38) Klein, I. M.; Husic, C. C.; Kovács, D. P.; Choquette, N. J.; Robb, M. J. Validation of the CoGEF Method as a Predictive Tool for Polymer Mechanochemistry. *J. Am. Chem. Soc.* **2020**, *142*, 16364–16381.
(39) Sheldrick, G. M. Phase annealing in SHELX-90: direct methods for larger structures. *Acta Cryst A* **1990**, *46*, 467–473.
(40) Sheldrick, G. M. SHELXT – Integrated space-group and crystal-structure determination. *Acta Cryst A* **2015**, *71*, 3–8.
(41) Müller, P. Practical suggestions for better crystal structures. *Crystallography Reviews* **2009**, *15*, 57–83.

4.10 ^{1}H and ^{13}C NMR spectra

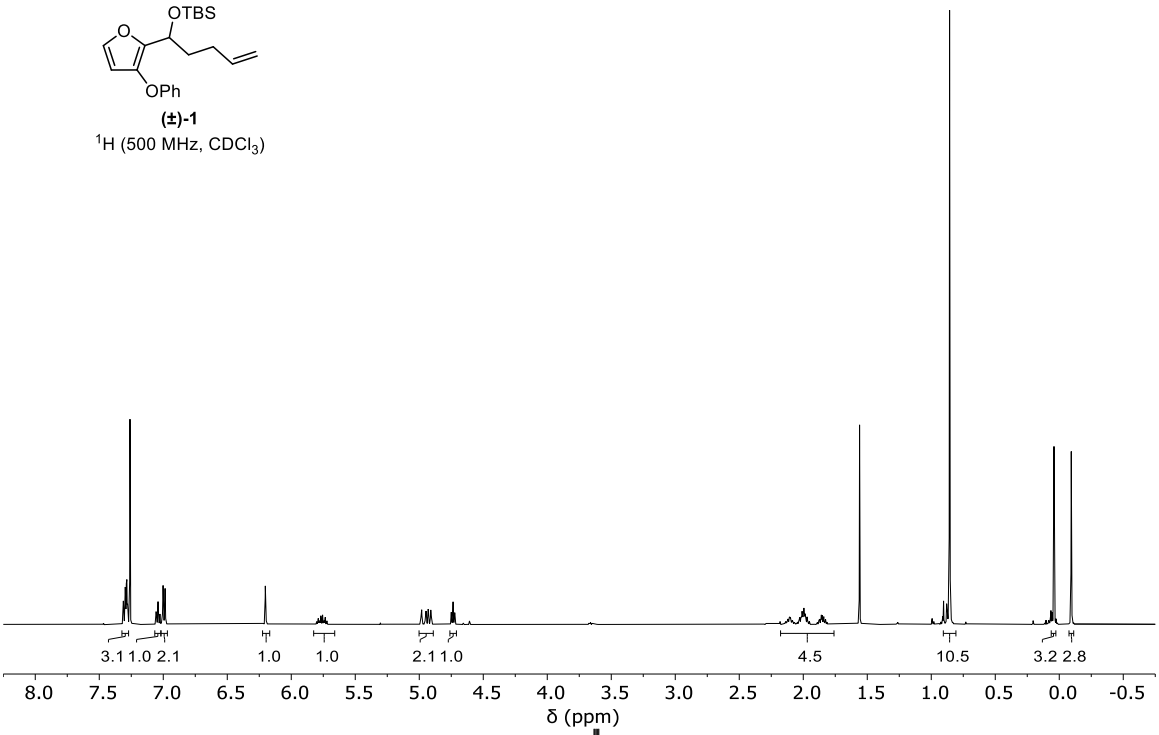

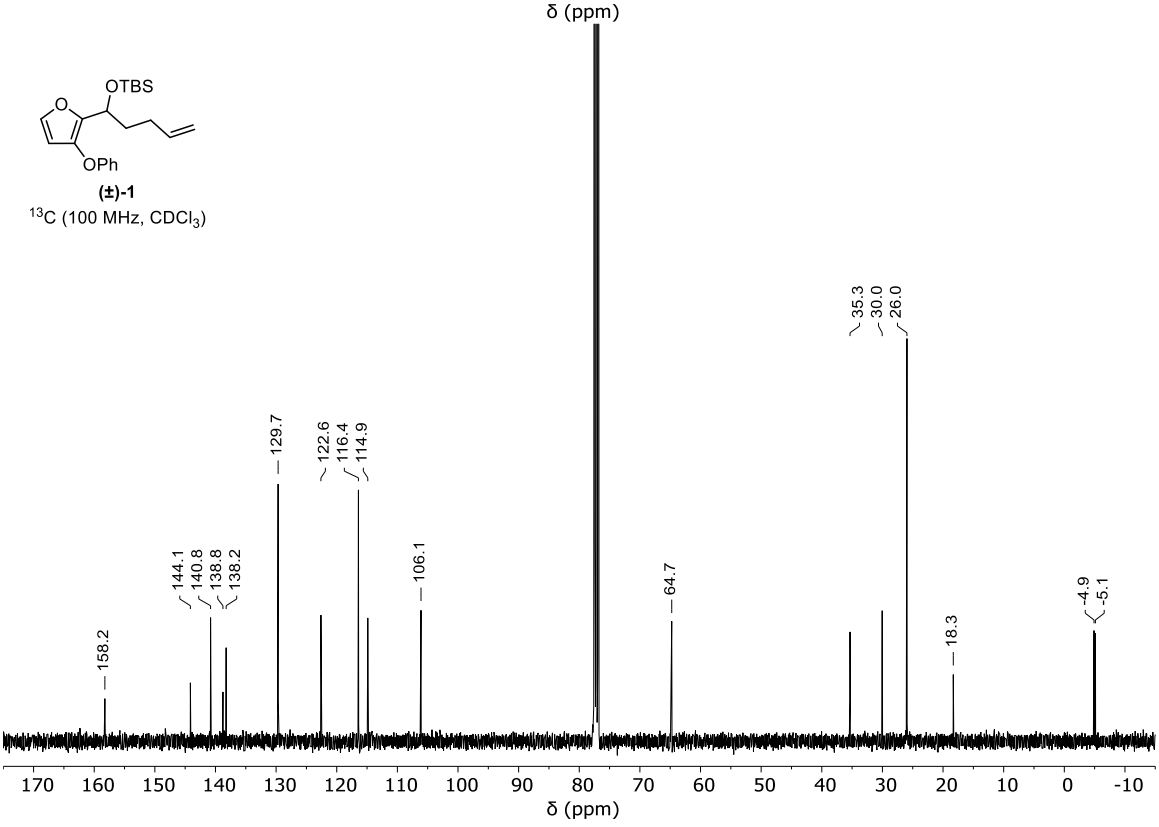

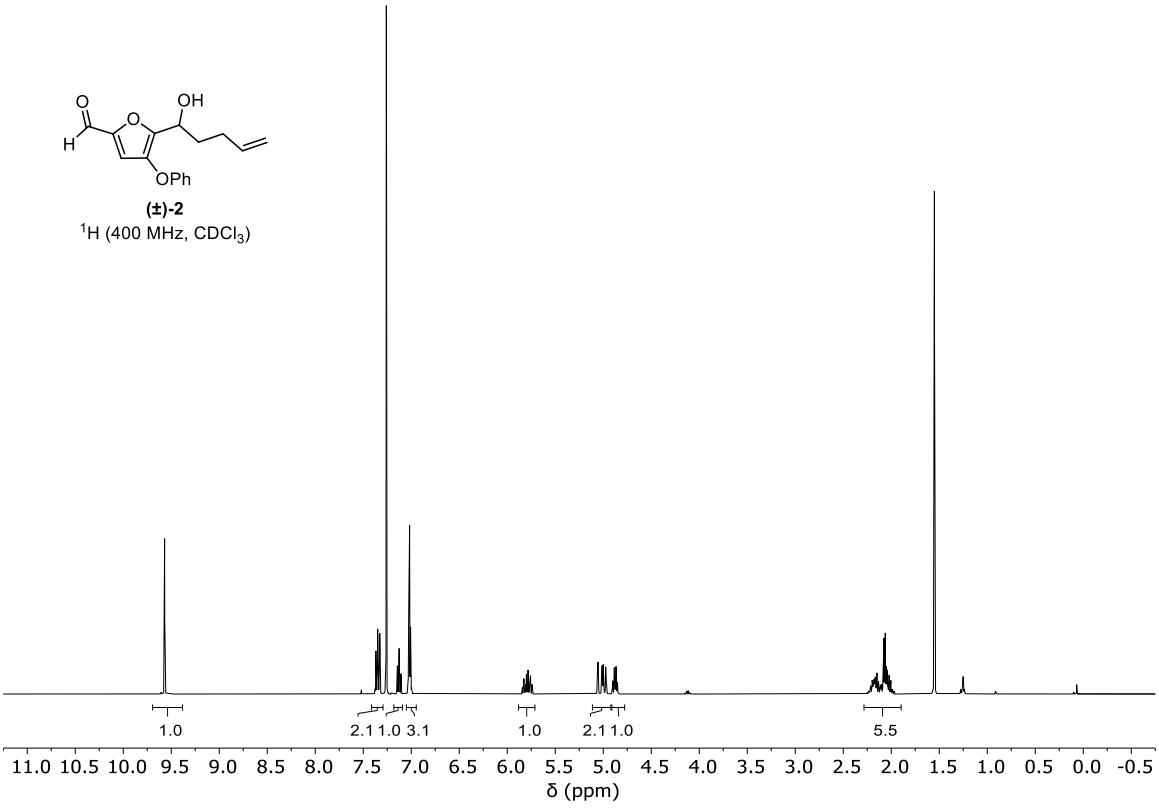
O
H
O
OH
OPh
(±)-2
1H (400 MHz, CDCl3)
1.0
2.1 1.0 3.1
1.0
2.1 1.0
5.5
11.0 10.5 10.0 9.5 9.0 8.5 8.0 7.5 7.0 6.5 6.0 5.5 5.0 4.5 4.0 3.5 3.0 2.5 2.0 1.5 1.0 0.5 0.0 -0.5
δ (ppm)

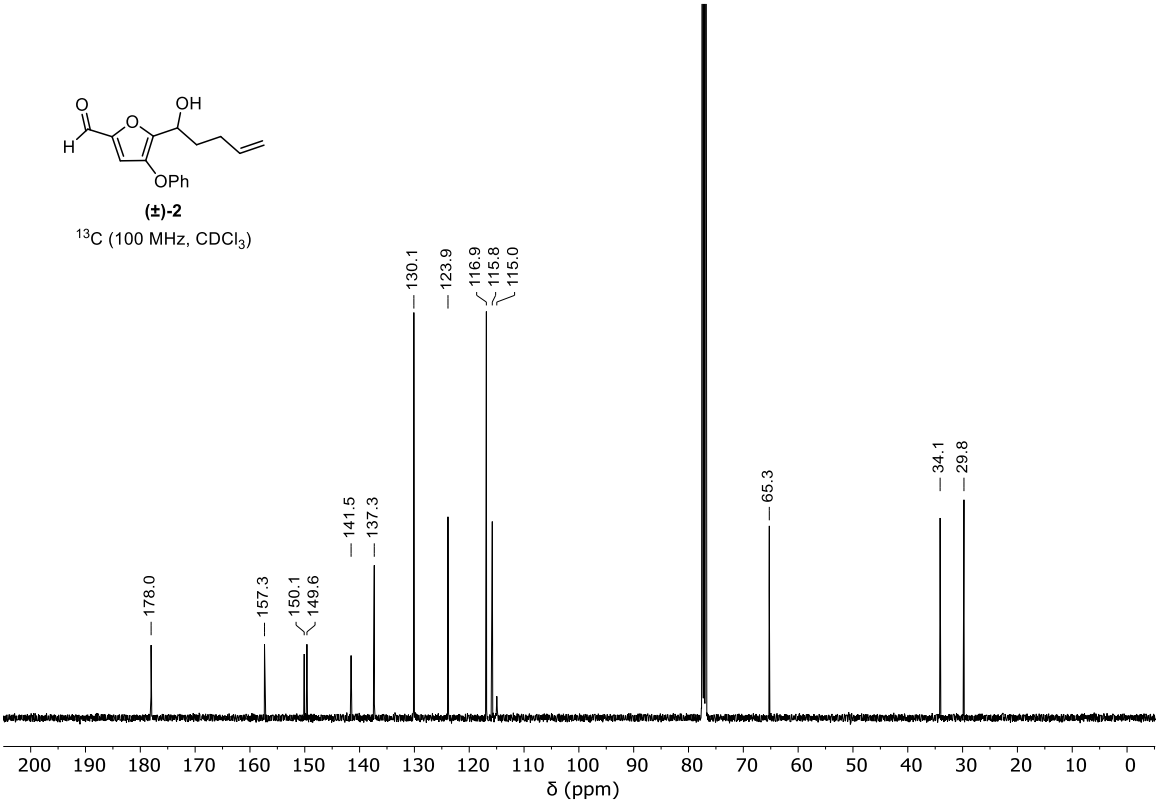
O
H
O
OH
OPh
(±)-2
13C (100 MHz, CDCl3)
178.0
157.3
150.1
149.6
141.5
137.3
130.1
123.9
116.9
115.8
115.0
65.3
34.1
29.8
200 190 180 170 160 150 140 130 120 110 100 90 80 70 60 50 40 30 20 10 0
δ (ppm)

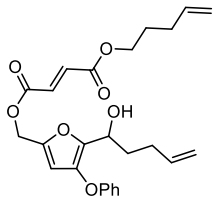

(±)-3

^{1}H (400 MHz, $CDCl_3$)

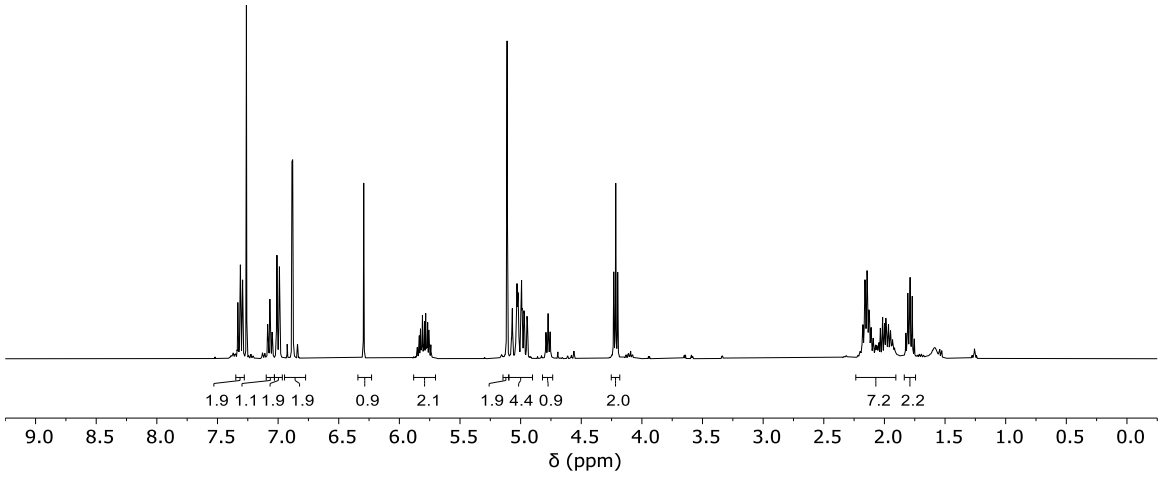

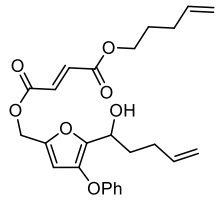

(±)-3

^{13}C (100 MHz, $CDCl_3$)

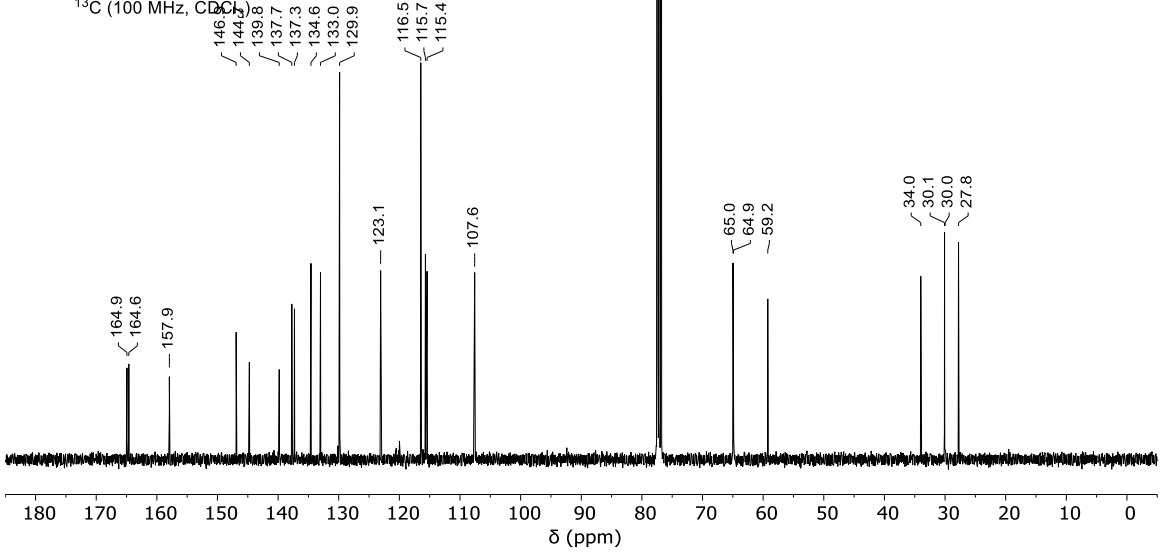

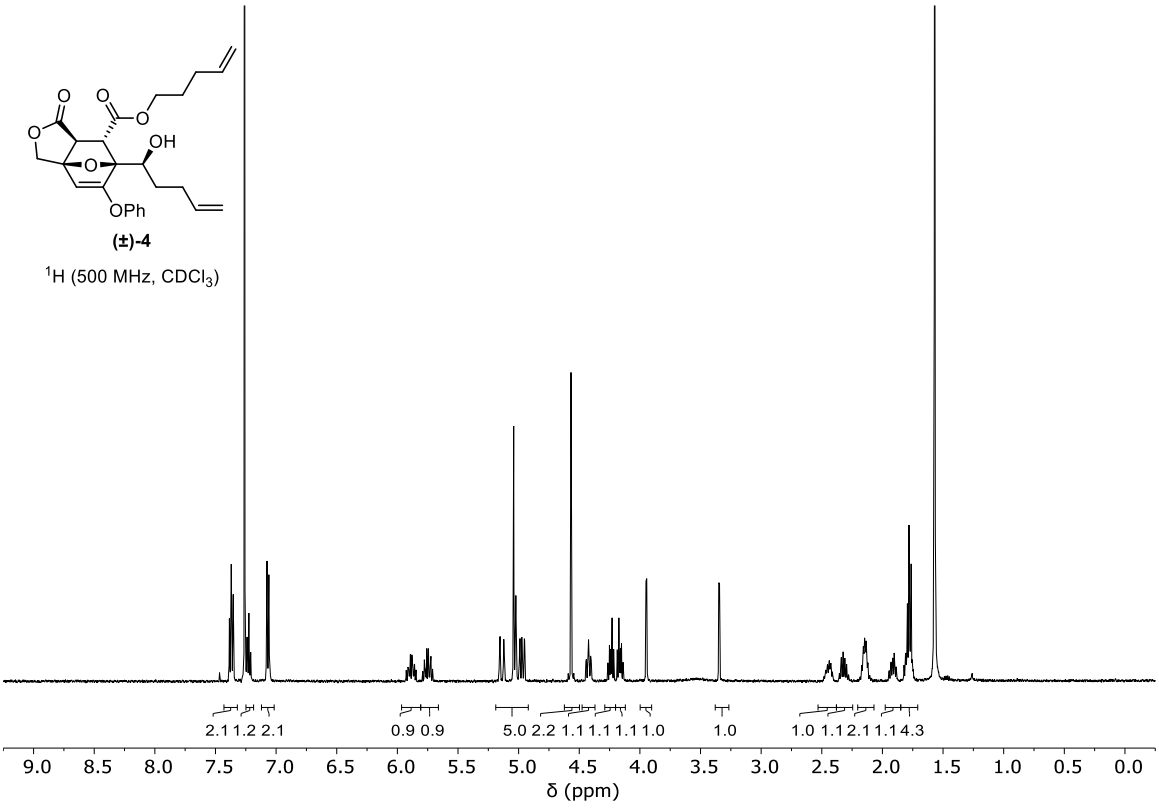
(±)-4
^{1}H (500 MHz, CDCl$_3$)
2.1 1.2 2.1
0.9 0.9
5.0 2.2 1.1 1.1 1.1 1.1 1.0
1.0
1.0 1.1 2.1 1.1 4.3
δ (ppm)

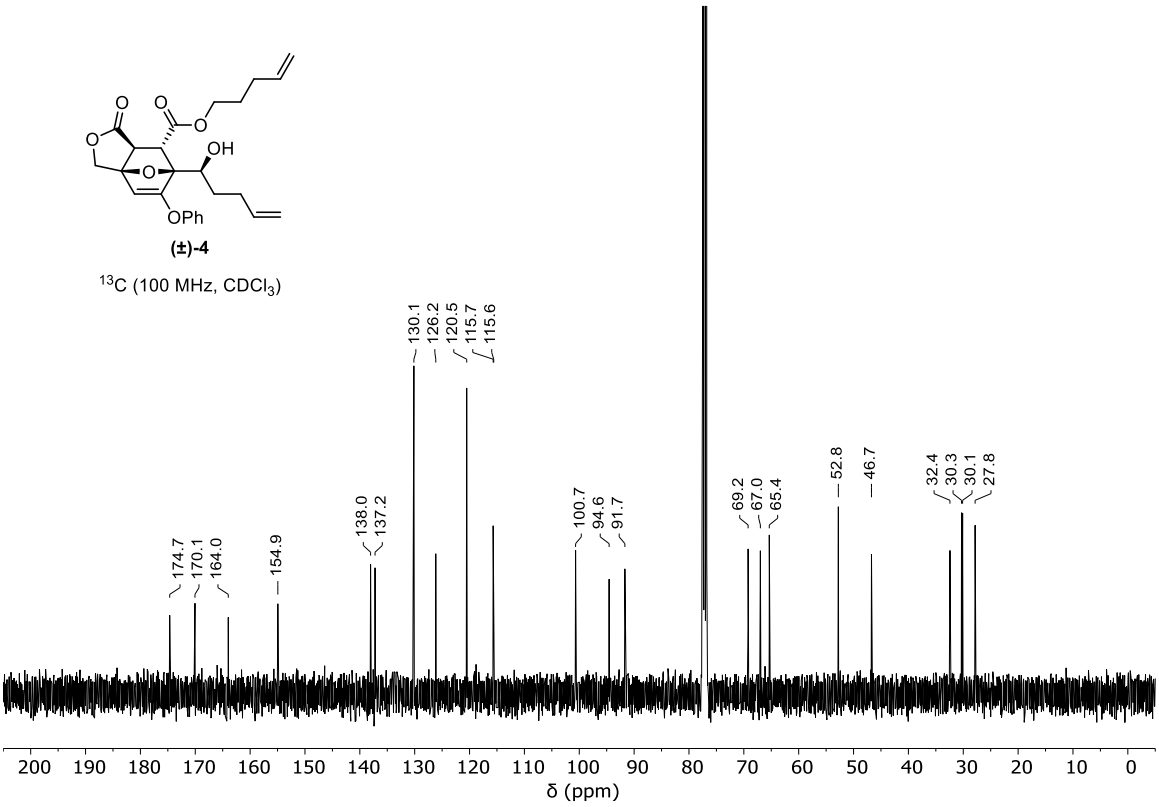
(±)-4
^{13}C (100 MHz, CDCl$_3$)
174.7
170.1
164.0
154.9
138.0
137.2
130.1
126.2
120.5
115.7
115.6
100.7
94.6
91.7
69.2
67.0
65.4
52.8
46.7
32.4
30.3
30.1
27.8
δ (ppm)

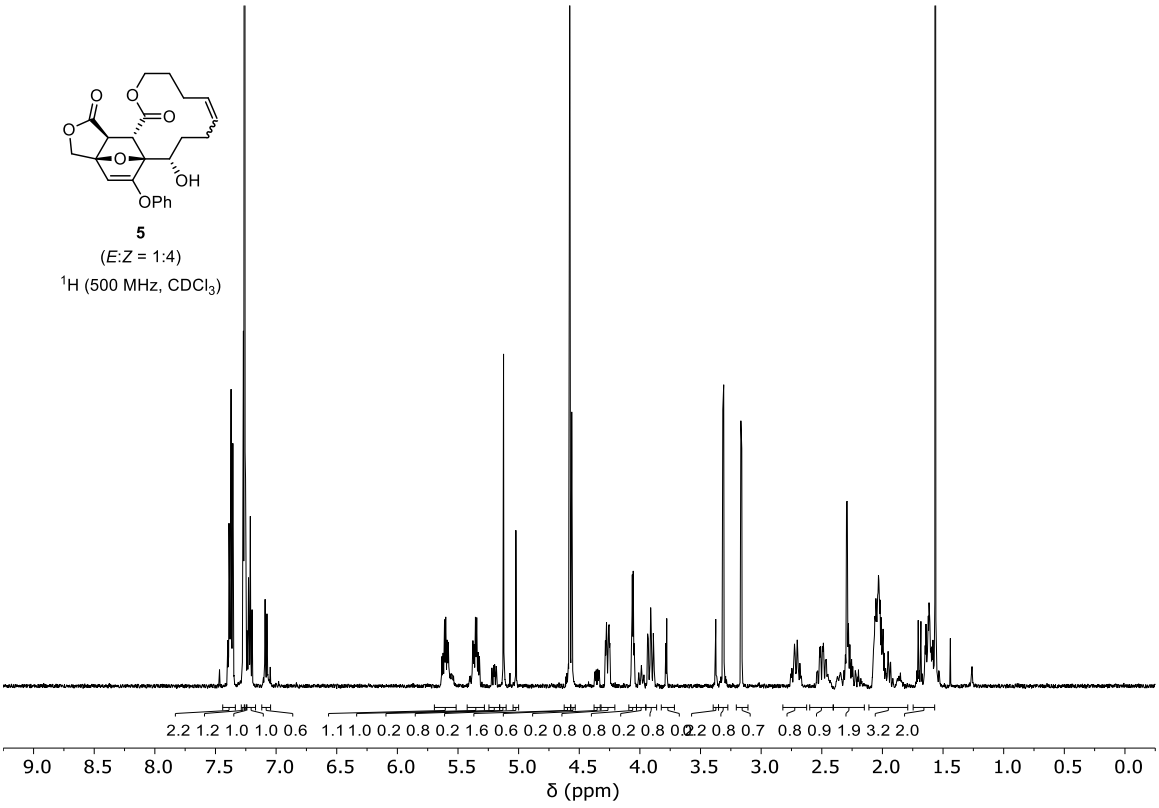
5
(E:Z = 1:4)
1H (500 MHz, CDCl3)
2.2 1.2 1.0 1.0 0.6 1.1 1.0 0.2 0.8 0.2 1.6 0.6 0.2 0.8 0.8 0.2 0.8 0.2 0.8 0.7 0.8 0.9 1.9 3.2 2.0
9.0 8.5 8.0 7.5 7.0 6.5 6.0 5.5 5.0 4.5 4.0 3.5 3.0 2.5 2.0 1.5 1.0 0.5 0.0
δ (ppm)

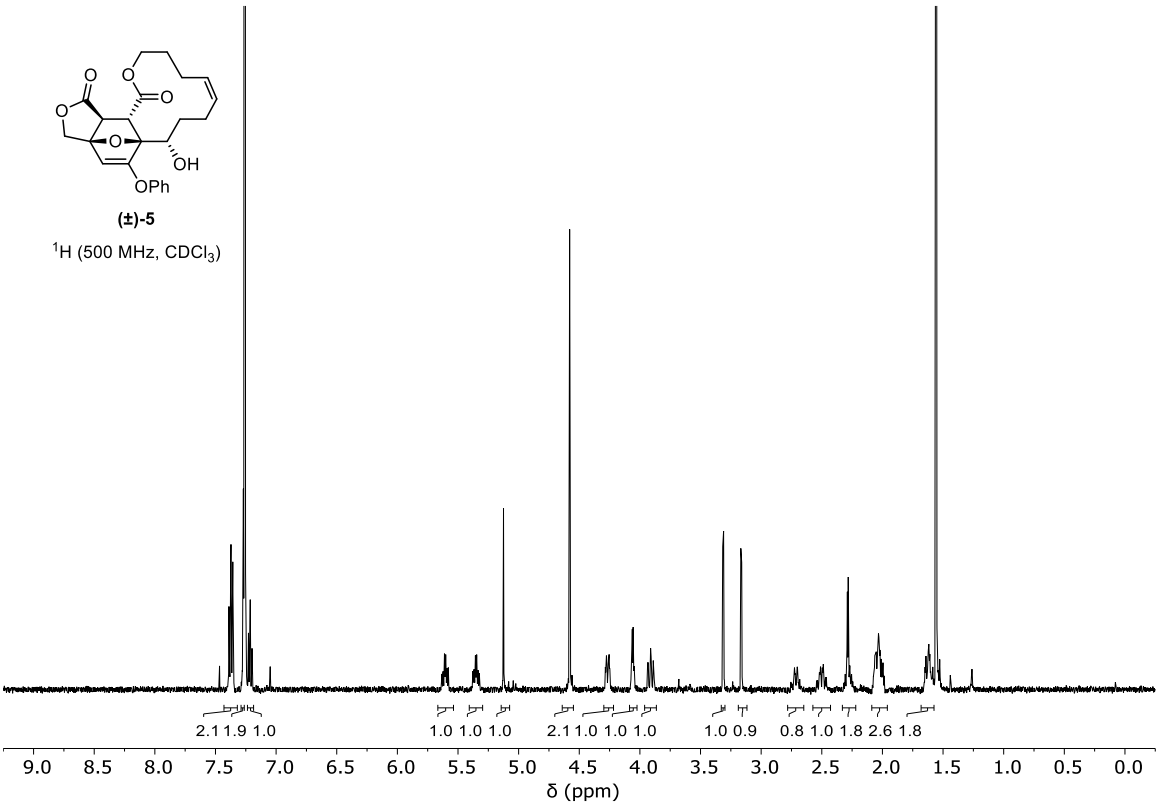
(±)-5
1H (500 MHz, CDCl3)
2.1 1.9 1.0 1.0 1.0 1.0 2.1 1.0 1.0 1.0 1.0 0.9 0.8 1.0 1.8 2.6 1.8
9.0 8.5 8.0 7.5 7.0 6.5 6.0 5.5 5.0 4.5 4.0 3.5 3.0 2.5 2.0 1.5 1.0 0.5 0.0
δ (ppm)

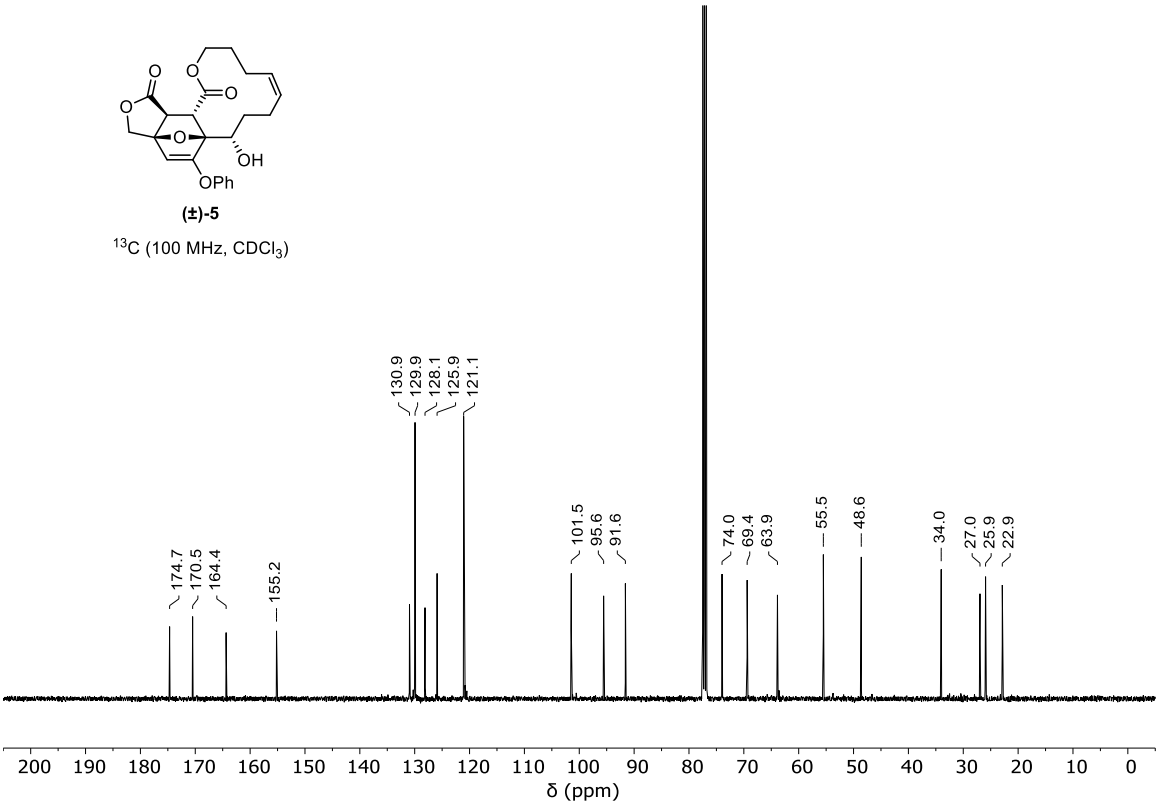
(±)-5
13C (100 MHz, CDCl3)
174.7
170.5
164.4
155.2
130.9
129.9
128.1
125.9
121.1
101.5
95.6
91.6
74.0
69.4
63.9
55.5
48.6
34.0
27.0
25.9
22.9
δ (ppm)

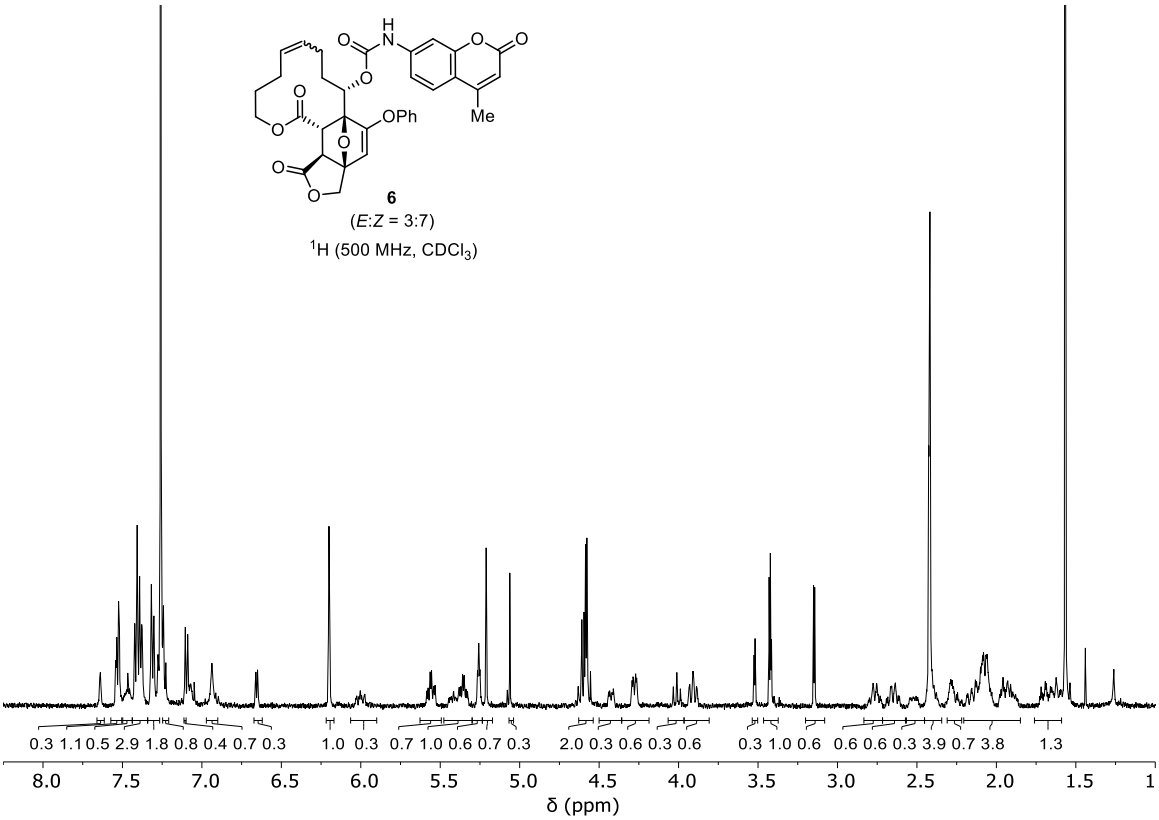
6
(E:Z = 3:7)
1H (500 MHz, CDCl3)
0.3 1.1 0.5 2.9 1.8 0.8 0.4 0.7 0.3
1.0 0.3
0.7 1.0 0.6 0.7 0.3
2.0 0.3 0.6 0.3 0.6
0.3 1.0 0.6
0.6 0.6 0.3 3.9 0.7 3.8
1.3
δ (ppm)

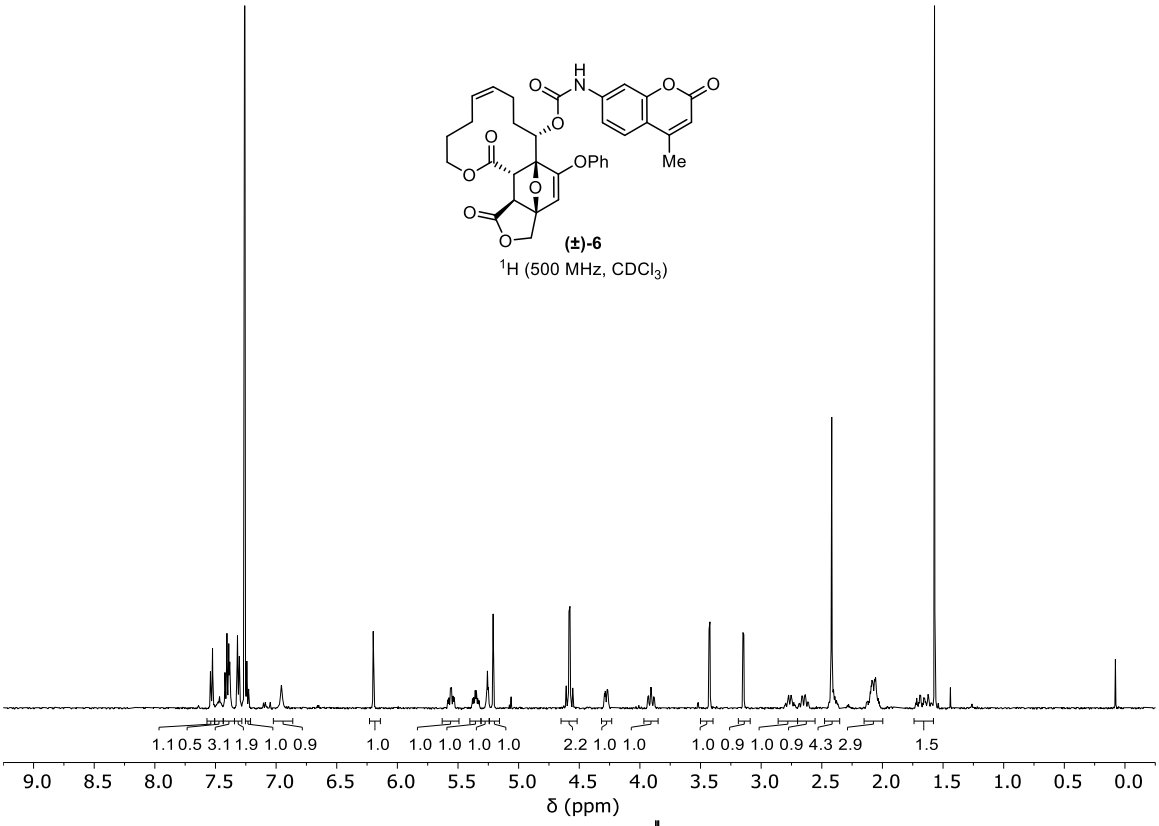
(±)-6
1H (500 MHz, CDCl3)
1.1 0.5 3.1 1.9 1.0 0.9
1.0
1.0 1.0 1.0 1.0
2.2 1.0 1.0
1.0 0.9 1.0 0.9 4.3 2.9
1.5
9.0 8.5 8.0 7.5 7.0 6.5 6.0 5.5 5.0 4.5 4.0 3.5 3.0 2.5 2.0 1.5 1.0 0.5 0.0
δ (ppm)

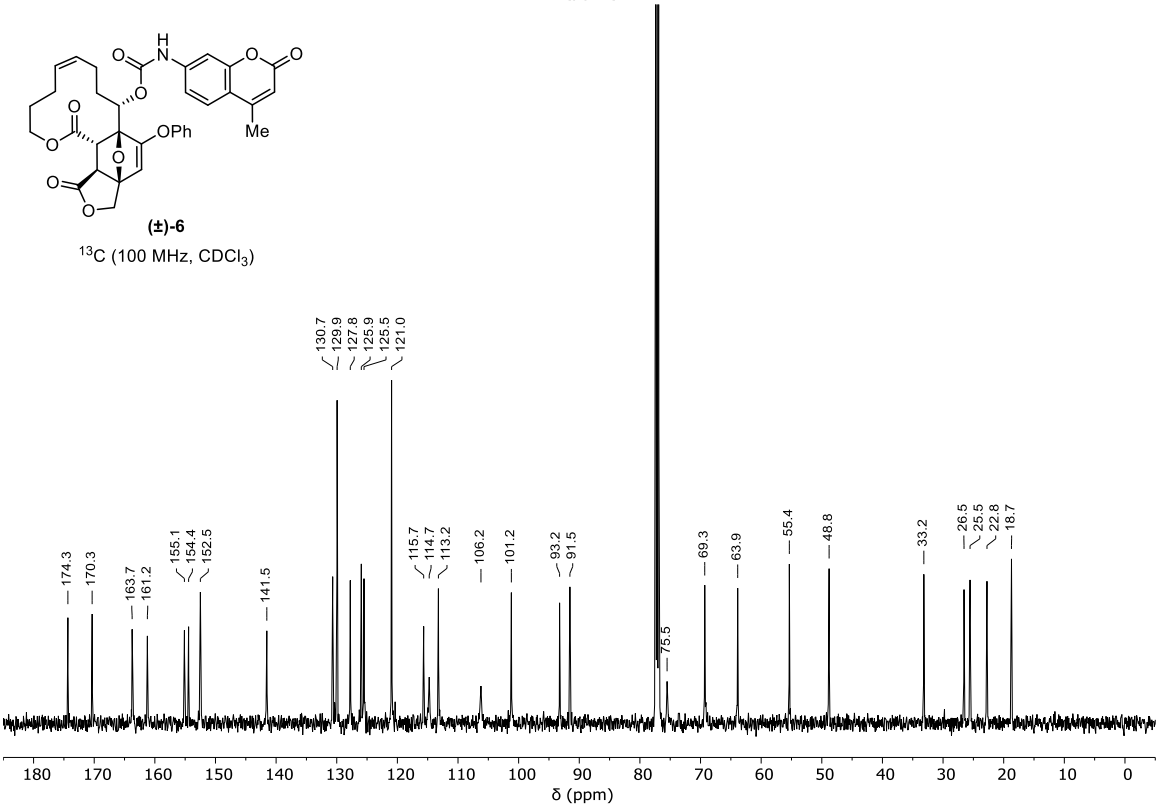
(±)-6
13C (100 MHz, CDCl3)
174.3
170.3
163.7
161.2
155.1
154.4
152.5
141.5
130.7
129.9
127.8
125.9
125.5
121.0
115.7
114.7
113.2
106.2
101.2
93.2
91.5
77.5
69.3
63.9
55.4
48.8
33.2
26.5
25.5
22.8
18.7
180 170 160 150 140 130 120 110 100 90 80 70 60 50 40 30 20 10 0
δ (ppm)

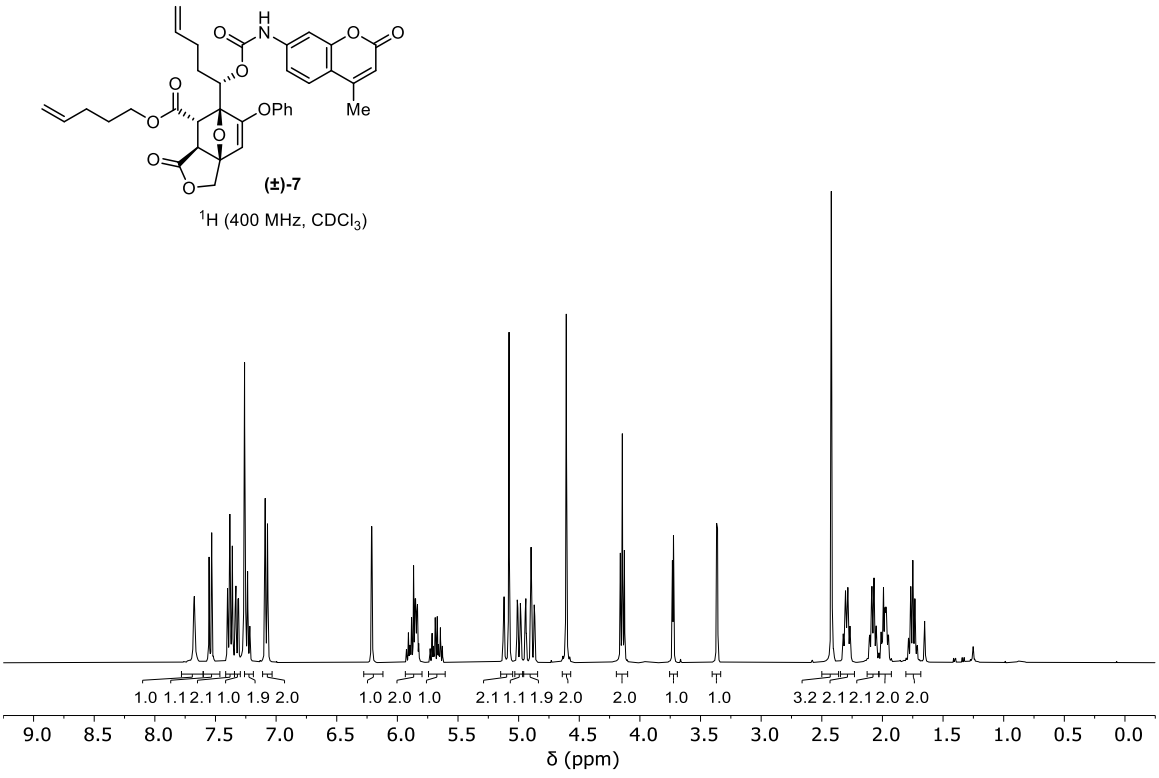
(±)-7
^{1}H (400 MHz, $CDCl_3$)
1.0 1.1 2.1 1.0 1.9 2.0
1.0 2.0 1.0
2.1 1.1 1.9 2.0
2.0
1.0
1.0
3.2 2.1 2.1 2.0 2.0
9.0 8.5 8.0 7.5 7.0 6.5 6.0 5.5 5.0 4.5 4.0 3.5 3.0 2.5 2.0 1.5 1.0 0.5 0.0
δ (ppm)

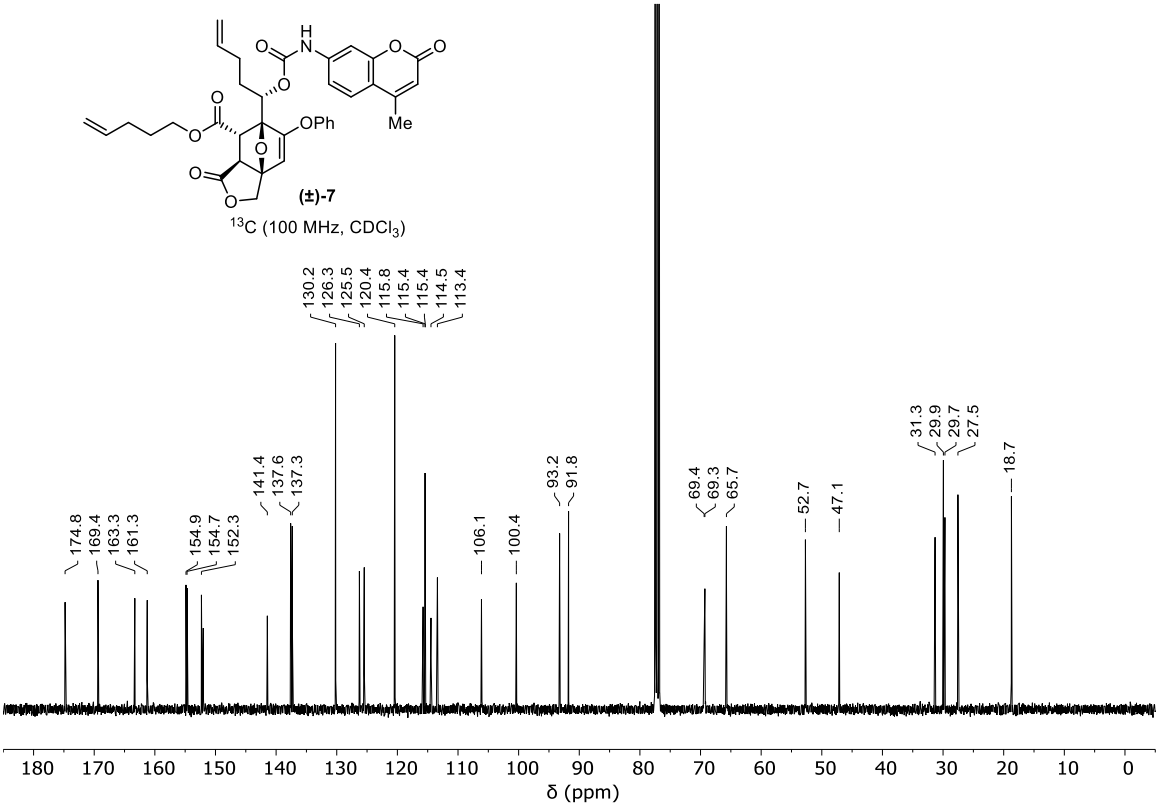
(±)-7
^{13}C (100 MHz, $CDCl_3$)
174.8
169.4
163.3
161.3
154.9
154.7
152.3
141.4
137.6
137.3
130.2
126.3
125.5
120.4
115.8
115.4
115.4
114.5
113.4
106.1
100.4
93.2
91.8
69.4
69.3
65.7
52.7
47.1
31.3
29.9
29.7
27.5
18.7
180 170 160 150 140 130 120 110 100 90 80 70 60 50 40 30 20 10 0
δ (ppm)

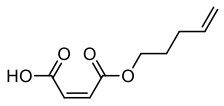

S1

^{1}H (400 MHz, $CDCl_3$)

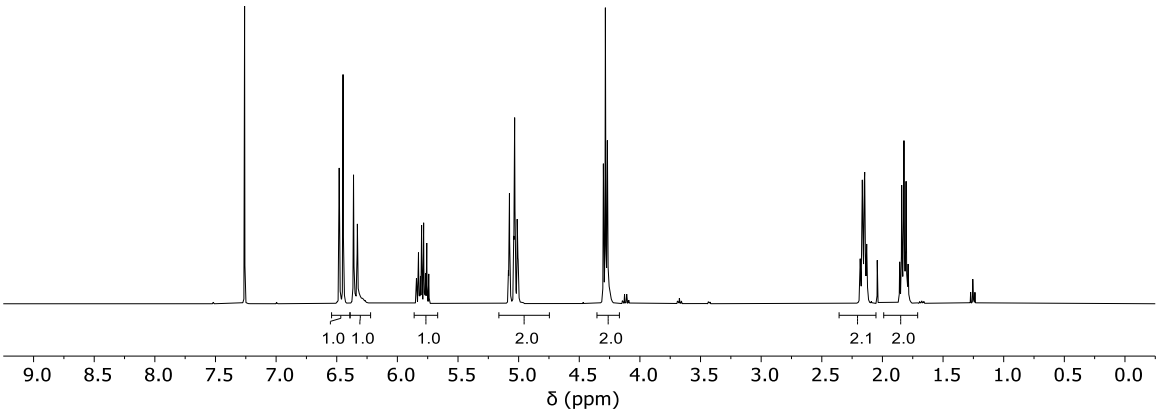

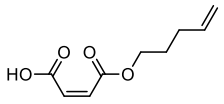

S1

^{13}C (100 MHz, $CDCl_3$)

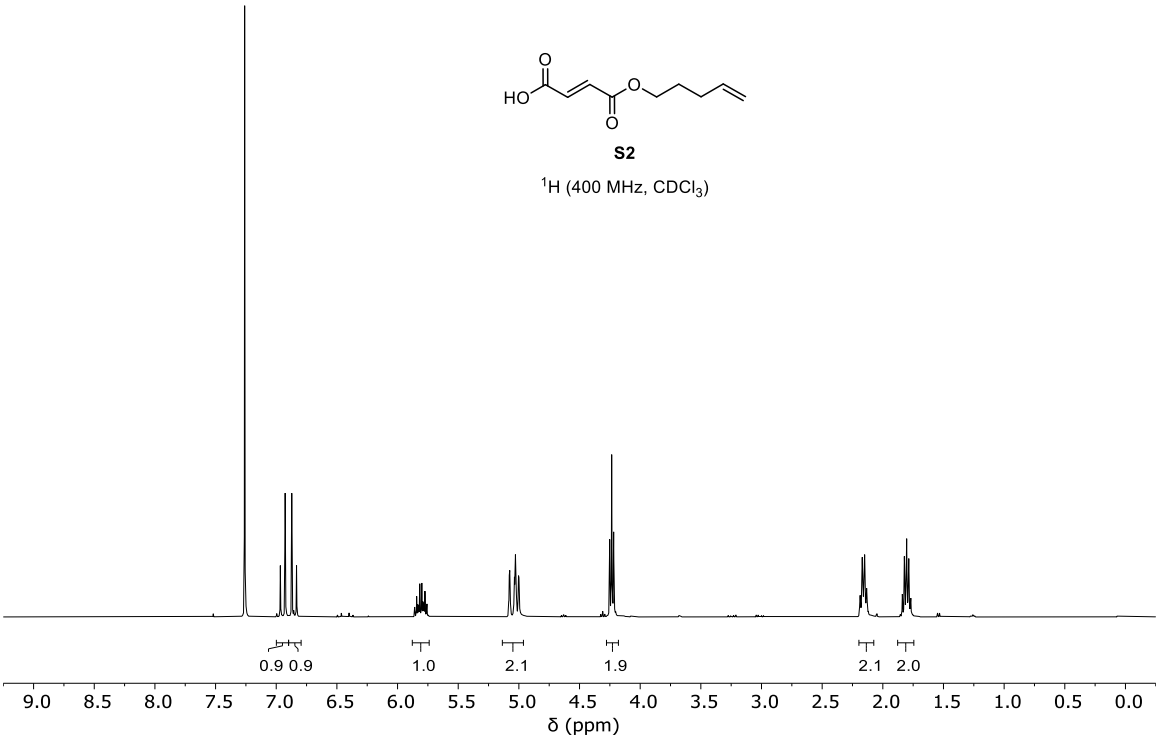
S2
^{1}H (400 MHz, CDCl$_3$)
0.9 0.9
1.0
2.1
1.9
2.1 2.0
δ (ppm)

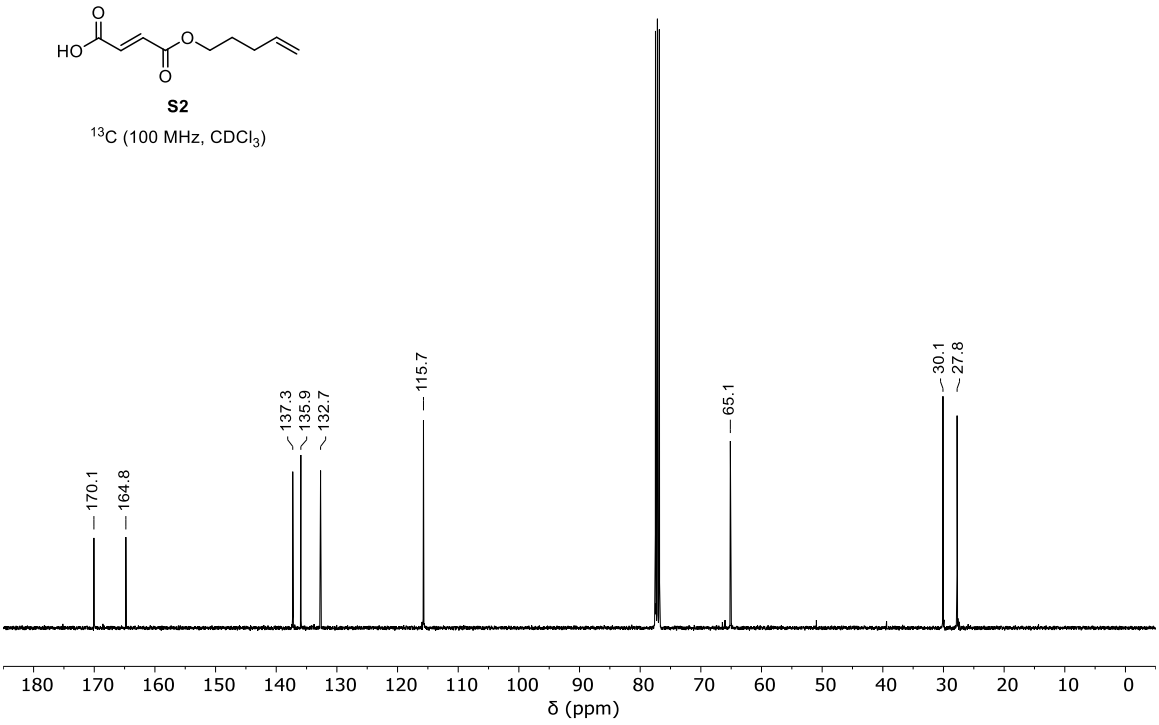
S2
^{13}C (100 MHz, CDCl$_3$)
170.1
164.8
137.3
135.9
132.7
115.7
65.1
30.1
27.8
δ (ppm)

Chapter 5

MECHANICALLY TRIGGERED DEPOLYMERIZATION OF A SELF-IMMOLATIVE POLYMER

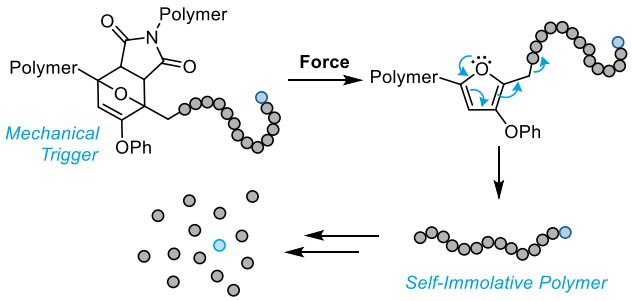

Abstract: Self-immolative polymers are promising materials for applications including sensing, drug delivery, and lithography due to their unique ability to release many small molecules upon a single triggering event. Although many stimuli have been investigated, only one polymer backbone has been explored for mechanically triggered SIP depolymerization. In this work, we demonstrate that using our masked 2-furylcarbinol mechanophore, we can achieve the mechanically triggered de-capping of a self-immolative polymer that leads to its end-to-end depolymerization.

5.1 Investigation

Stimuli-responsive polymers are an emerging class of materials that undergo preprogramed transformations in response to environmental cues or externally applied stimuli. In particular, self-immolative polymers (SIPs) have received significant attention because of their ability to degrade to its monomer make up in response to a triggering event.[1] They are comprised of a kinetically stable chain with an end-capping group that, upon being cleaved by a specific stimulus, undergoes an end-to-end depolymerization cascade. This characteristic of achieving an amplified response to a single molecular signal is highly attractive for applications in sensing, lithography, and drug delivery.[2–5]

Mechanical force is an emerging stimulus for triggering productive chemistry in polymeric materials.[6–8] In polymer mechanochemistry, force is transduced along the polymer chain to judiciously designed stress-sensitive units called mechanophores to trigger a variety of chemical reactions.[9–11] Mechanophore-embedded polymers have been beneficial for understand the mechanism of stress transfer in multi-network elastomers[12] as well as used for a variety of applications including drug-delivery with biocompatible ultrasound in solution[13]. However, only two examples of a mechanically triggered SIP depolymerization have been reported, both of which rely on the heterolytic chain scission of poly(*o*-phthalaldehyde) to release its monomer, phthalaldehyde. [14,15] Despite the elegant design, it is inherently limited in the types of SIPs it can degrade.

Our group recently developed a library of mechanophores for mechanically triggered small molecule release. A kinetically stable Diels–Alder adduct is embedded in the center of a polymer chain which, under force, undergoes mechanically triggered retro-Diels–Alder reaction to reveal a 2-furylcarbinol species. The unstable intermediate then spontaneously decomposes in polar protic solvents to release a covalently bound cargo molecule (Figure 5.1a).[16,17] Furthermore, we have shown that furans with an electron-rich phenoxy substituent can release a wide scope of cargos including phenols, alcohols, arylamines, alkyl amines, sulfonic acids and carboxylic acids.[18] In this work, we aim to leverage this mechanically gated cascade reaction strategy for releasing small molecules to achieve the mechanically triggered depolymerization of SIPs (Figure 5.1). We hypothesized that by capping the SIP with the masked 2-furylcarbinol mechanophore and embedding it into the center of a polymer

chain, mechanochemical activation of the mechanophore would unmask the reactive chain-end and trigger the depolymerization of the SIP. We detect the complete end-to-end depolymerization of the SIP by attaching a fluorogenic reporter unit to the SIP chain end.

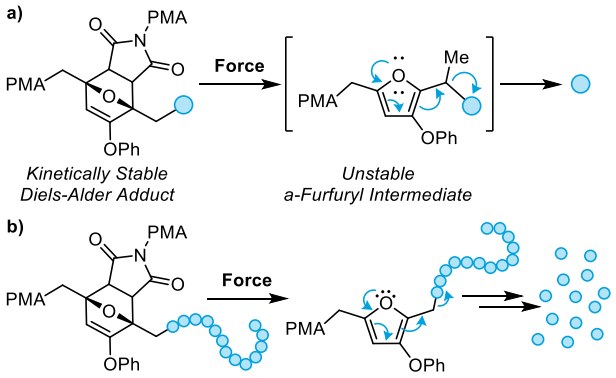

Figure 5.1. (a) Mechanically triggered small molecule release from polymers containing a masked 2-furylcarbinol mechanophore via a retro-Diels–Alder/fragmentation cascade. (b) Mechanically triggered uncapping of a self-immolative polymer (SIP) that leads to the head-to-tail depolymerization of the SIP.

We chose the poly(carboxy pyrrole) as our SIP of study. Following the van Leusen pyrrole synthesis reported by the Phillips group,[19] we prepared pentyl substituted N-phenoxycarbonyl pyrrole monomer **1**. Subjecting monomer **1** to catalytic DBU in THF at 60 °C produced a phenoxycarbonyl capped oligomer, which was then transesterified with our mechanophore by adding Diels–Alder adduct **DA-OH** to form **Olig-1** (Figure 5.2). The 3-phenoxy substituted Diels–Alder adduct was chosen for its facile release of amines,[18] and the primary alcohol design was necessary for efficient transesterification reaction to form **Olig-1** with complete end-capping. Interestingly, exposing **DA-OH** to catalytic amounts of DBU at 60 °C in THF resulted in significant β-elimination of the bromoisobutyrate group. The temperature for end-cap exchange with **DA-OH** was therefore reduced to 55°C, effectively suppressing the undesired elimination reaction. **Olig-1** was then reacted with an excess of 4-methylcoumarin-7-isocyanate which efficiently installed the aminocoumarin (**CoumNH$_2$**) reporter unit on the chain-end of the oligomer to produce **Olig-2**. By integrating the pyrrole proton relative to the signals corresponding to the Diels–Alder adduct in the ^{1}H NMR spectrum, the degree of polymerization (DP) was determined to be 34 and 35 for **Olig-1** and **Olig-2**, respectively (Figure 5.3). The corresponding number average molar mass of **Olig-1** and **Olig-2** is 7.2 and 7.6 kDa, respectively (Table 5.1, Figure 5.3). The dispersity of the two

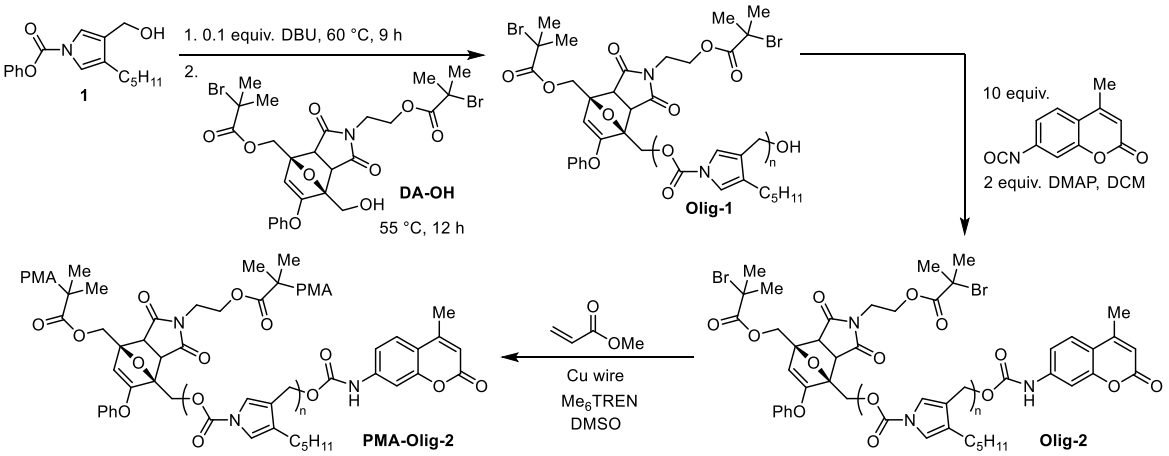

Figure 5.2. Synthesis of poly(carboxy pyrrole) **Olig-1** capped with Diels–Alder adduct DA, **Olig-2** loaded with reporter unit coumNH$_2$, and poly(methyl acrylate)-oligomer conjugate **PMA-Olig-2**.[19]

Table 5.1. Polymer characterizations of **Olig-1**, **Olig-2** and **PMA-Olig-2**.

	n[a]	Mn (kDa)	Đ[b]
Olig-1	34	7.2[a]	1.49
Olig-2	38	8.2[a]	1.29
PMA-Olig-2	38	94.1[b]	1.46

a: determined by NMR
b: determined by GPC

oligomers was determined by GPC to be 1.49 and 1.29, respectively (Table 5.1, Figure 5.4). Finally the oligomer was incorporated into a poly(methyl acrylate) backbone via controlled radical polymerization of methyl acrylate with Cu wire/Me$_6$TREN in DMSO to form polymer-SIP conjugate **PMA-Olig-2** (94.1 kDa, $Đ$ = 1.46) (Table 5.1, Figure 5.4).

To evaluate the mechanically triggered depolymerization of the polymer-SIP conjugate, we subjected solutions of **PMA-Olig-2** (0.5 mg/mL, 5.3 μM in 3:1 THF/MeOH) to pulsed ultrasonication (1s on/1s off, 9–13°C, 20 kHz, 13.9 W/cm^2) and aliquots were removed periodically for analysis by photoluminescence (PL) spectroscopy to calculate the amount of liberated reporter units (Figure 5.5a). Aliquots were allowed to incubate at room temperature for 28 h before evaluation to ensure complete fragmentation of the mechanophore as well as complete depolymerization of the SIP (Figure 5.6). Fluorescence signal corresponding to the free **CoumNH$_2$** increased with sonication time, indicating that the SIP depolymerized head-to-tail upon mechanical uncapping (Figure 5.5b). The PL intensity reached a maximum after 120 min of sonication time corresponding to approximately 10% yield of **CoumNH$_2$** (Figure 5.5c). GPC analysis of the aliquots show

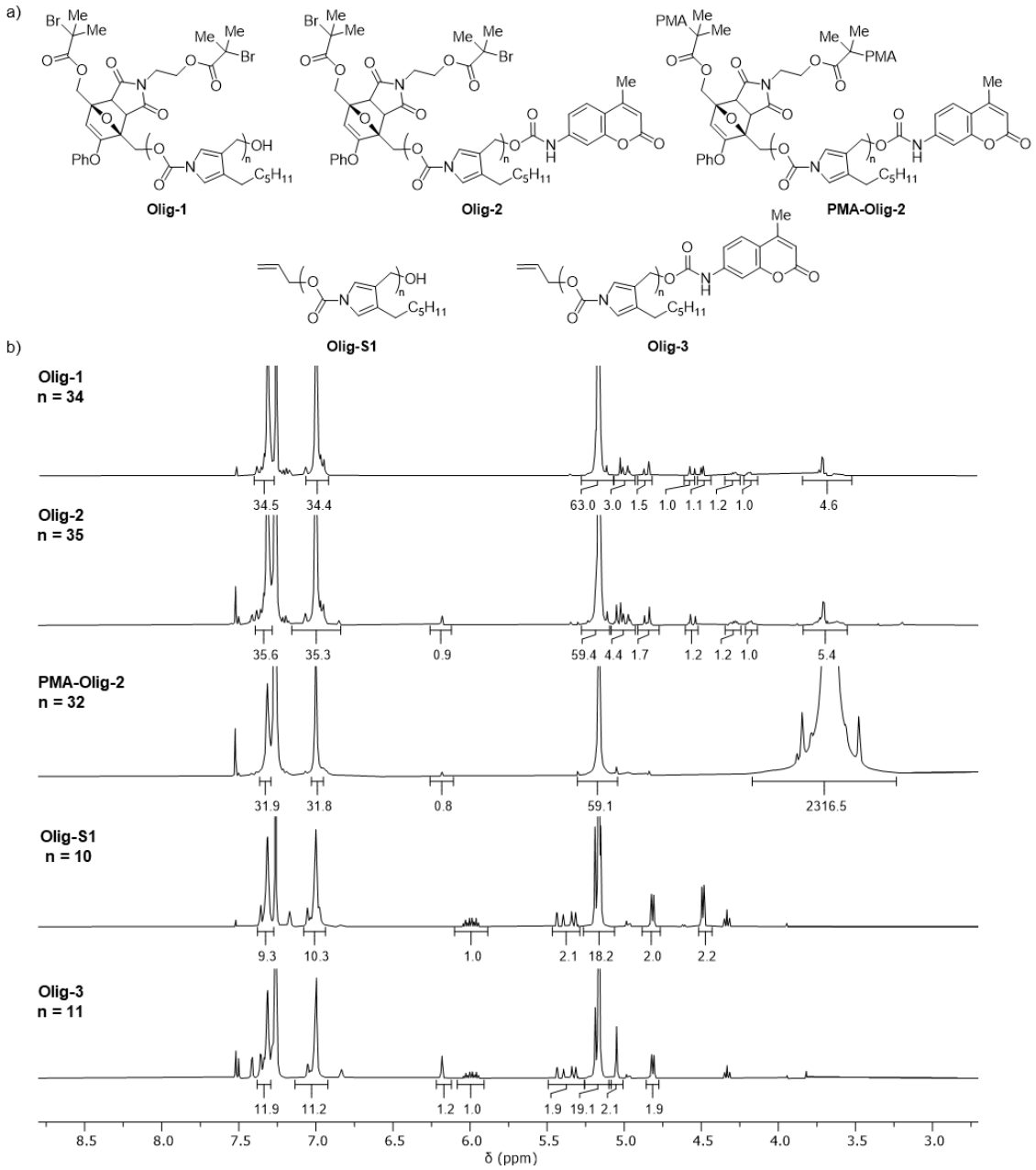

Figure 5.3. Oligomers and polymers studied in this work (a) and their NMR characterizations (b) (400 MHz, $CDCl_3$). For **Olig-1** and **Olig-2**, the repeat unit n was determined by comparing the integrations between 7.0 ppm and 4.2 ppm, which corresponds to 1 proton on the pyrrole backbone and Diels–Alder adduct respectively. For **Olig-S1** and **Olig-3**, the repeat unit n was determined by comparing the integrations between 7.0 ppm and 6.0 ppm, which correspond to 1 proton the pyrrole backbone and the allyl alcohol respectively.

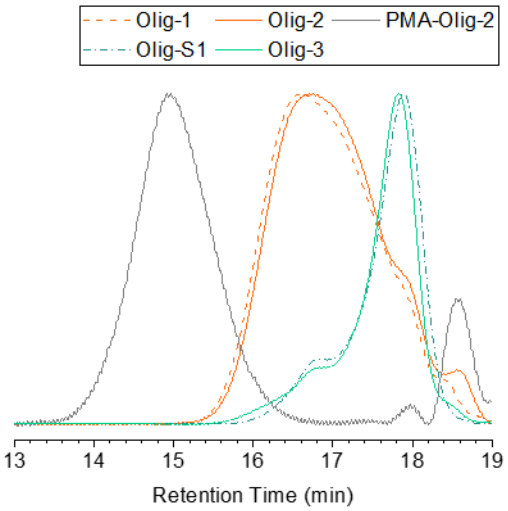

	Mn (kDa)	Đ
Olig-1	4.1	1.49
Olig-2	4.7	1.29
PMA-Olig-2	94.1	1.46
Olig-S1	1.9	1.50
Olig-3	2.1	1.41

Figure 5.4. GPC chromatograms, and characterization data for oligomers and polymers in the study.

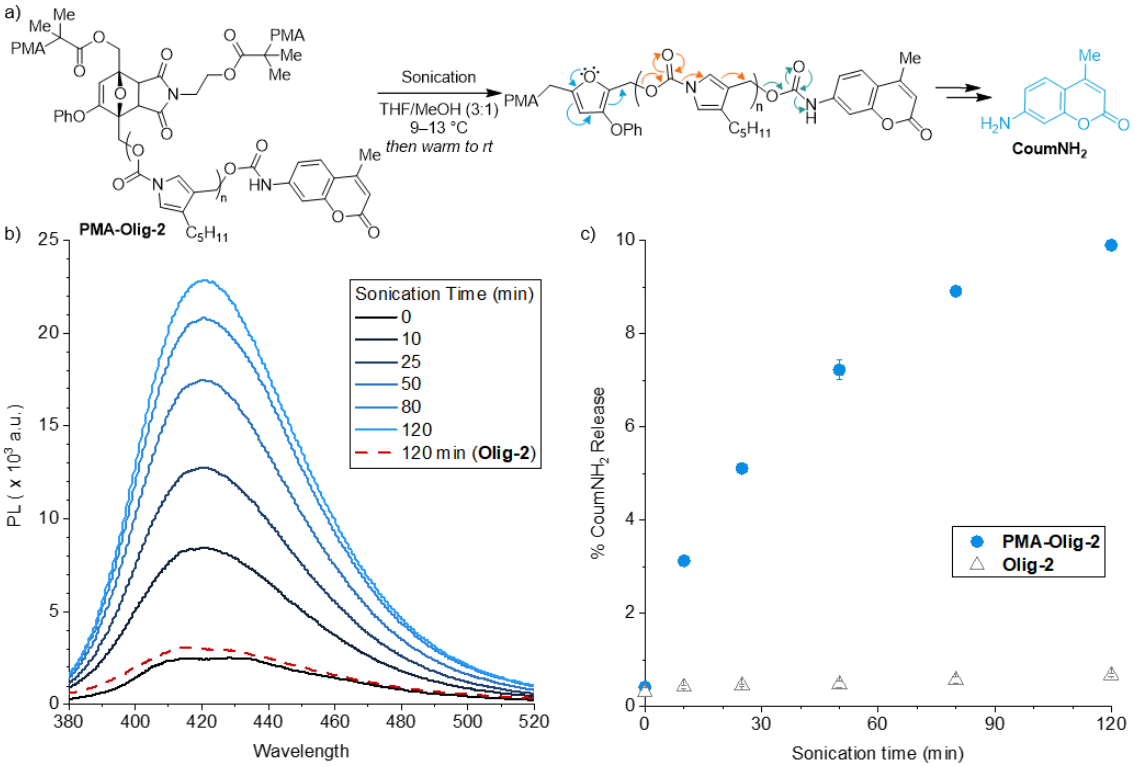

Figure 5.5. Mechanically triggered uncapping of SIP by subjecting **PMA-Olig-2** to ultrasound-induced mechanical activation (0.5 mg mL^{-1} in 3:1 THF/MeOH, 5.3 μM). (a) The proposed mechanism for mechanically triggered uncapping of SIP, followed by head-to-tail depolymerization of SIP to release a free $coumNH_2$ reporter unit. (b) Photoluminescence spectra monitoring the sonicated **PMA-Olig-2** over time (λ_{ex}=365 nm). Red dashed line indicates maximum aminocoumarin released by sonicating **Olig-2** in the same condition (5.0 μM in 3:1 THF:MeOH). (c) Concentration of aminocoumarin released over time by sonicating **PMA-Olig-2** and **Olig-2**.

that the molar mass of PMA decreased steadily from 94 kDa to 44 kDa, which agrees with the proposed mechanism of mechanical activation of the mechanophore at the center of the polymer chain (Figure 5.7a). Subjecting **Olig-2** to the same ultrasonication condition (5.0 μM in 3:1 THF/MeOH) resulted in minimal increase in PL intensity and no change in the average molar mass over 120 min of sonication (Figure 5.5, 5.7b).

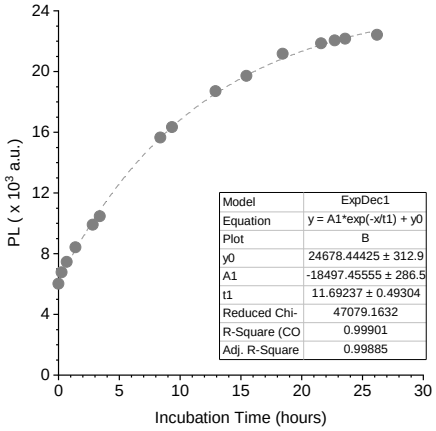

Figure 5.6. Concentration of **CoumNH$_2$** released from incubating 0.5 mg/mL (5.3 μM) solution of **PMA** in THF/methanol (3:1 v/v) at room temperature following 120 min of sonication time. λ_{ex} = 365 nm slit width = 5 nm, λ_{em} = 424 nm slit width = 5 nm. Fitting the data to an expression of simple first-order kinetics provides a half-life of 8.1 h for release of **CoumNH$_2$** from the mechanochemically liberated furfuryl carbamate under these conditions.

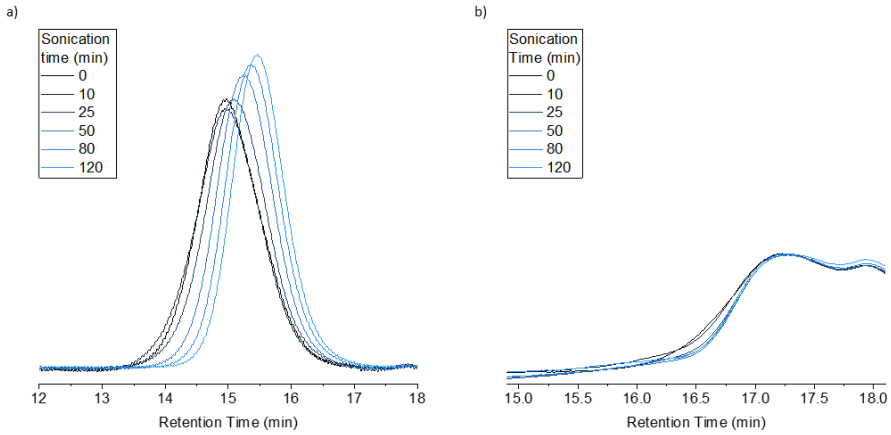

Figure 5.7. GPC traces as a function of ultrasonication time for (a) **PMA** and (b) **Olig-2** monitored with a refractive index (RI) detector. (a) The M_p of **PMA** decreases steadily from 94 kg/mol to 44 kg/mol over 120 min of ultrasonication, indicating mechanically triggered polymer scission. (b) The M_p of **Olig-2** does not change significantly over 120 min of ultrasonication, indicating that the oligomer is below the threshold molecular weight, and does not undergo mechanical activation.

This result illustrates that **Olig-2** has a molar mass below the threshold molecular weight required for mechanical activation, and that the depolymerization of SIP observed from ultrasonication of **PMA-Olig-2** is mechanical in nature.

Although we have successfully demonstrated the mechanically triggered depolymerization of the poly(carboxy pyrrole) SIP, we were initially surprised by the relatively low yield of **CoumNH$_2$**. As opposed to the 50–80% yield observed in previous studies for small molecule release,[17] only 10% yield of **CoumNH$_2$** is observed. We hypothesized that the low yield is due to incomplete depolymerization of uncapped SIPs as only the chains that have undergone complete end-to-end depolymerization will release the fluorescent small molecule reporter. To this end, we prepared a model SIP **Olig-3** (n = 11, M_n = 2.4 kDa, Đ = 1.41) that is capped with an allyl carbamate similar to the compounds reported by Phillips[19].A **CoumNH$_2$** reporter unit was also installed at the opposite chain-end to report on end-to-end depolymerization. Upon exposing **Olig-3** to 1 equiv. of tetrakis(triphenylphosphine) palladium (5.3 μM in 3:1 THF/MeOH), formation of the Pd-allyl complex triggers the SIP to undergo depolymerization. Interestingly, we observed approximately 35% of free reporter unit released from the chemically triggered SIP depolymerization (Figure 5.8). A similar experiment conducted by the Phillips group resulted in approximately 30% residual polymer as detected by NMR and GPC. These results are consistent with the hypothesis that low **CoumNH$_2$**-release from **Olig-3** is due to incomplete depolymerization of the SIP, rather than strictly inefficient mechanophore activation.[19] Since prior work has shown that mechanically triggered small molecule release can be as low as 50% especially for polymers of higher dispersity,[17] only 16% of reporters would be expected to be released from mechanically activating PMA and 35% end-to-end depolymerization of SIP chains. These results are worth considering for future explorations of using mechanical force to trigger polymer and SIP depolymerization. To achieve better amplified signal response from SIP depolymerization, higher efficiency for mechanical activation and better end-to-end SIP depolymerization is required.

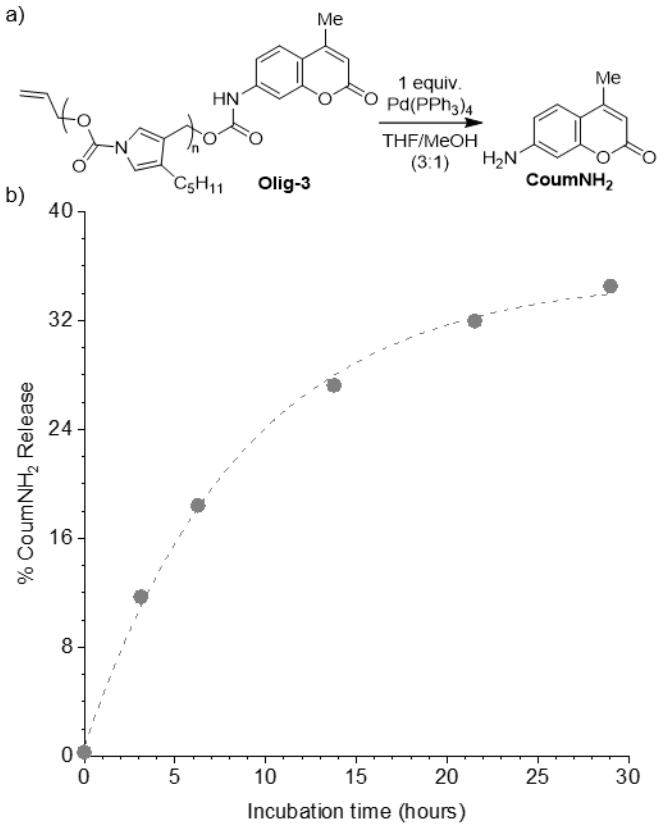

Figure 5.8. (a) Chemically triggered uncapping of SIP by subjecting **Olig-3** (5.3 μM in 3:1 THF/MeOH) with 5.3 μM of $Pd(PPh_3)_4$. (b) Concentration of **CoumNH$_2$** released over time by incubating **Olig-3** with 1 equiv of $Pd(PPh_3)_4$ at room temperature.

In conclusion, we demonstrated that by installing an SIP to the masked 2-furylcarbinol derivative mechanophore, mechanical force can trigger SIP depolymerization. Ultrasonication of a PMA-SIP conjugate containing a masked 2-furylcarbinol mechanophore as a triggering motif results in the end-to-end depolymerization of the SIP, as signified by the release of a fluorogenic reporter unit. In contrast, ultrasonication of the SIP did not lead to a significant increase in fluorescence signal, indicating that mechanical force was responsible for SIP depolymerization. Control experiments demonstrated that both the efficiency of mechanical activation as well as incomplete end-to-end depolymerization led to the low yield of reporter unit observed from mechanically triggered SIP depolymerization. With further optimization, this design could generate promising stimuli-responsive materials through amplified release of drugs or reporter units.

5.2 General Experimental Details and Methods

Reagents from commercial sources were used without further purification unless otherwise stated. Methyl acrylate was passed through a short plug of basic alumina to remove inhibitor immediately prior to use. Dry THF, diethyl ether, MeCN, and DMF were obtained from a Pure Process Technology solvent purification system. All reactions were performed under a N_2 atmosphere unless specified otherwise. Column chromatography was performed on a Biotage Isolera system using SiliCycle SiliaSep HP or SiliaBond C18 cartridges. The pyrrole monomer **1** was synthesized by adapting the procedure described by Kim et al.[19]

NMR spectra were recorded using a 400 MHz Bruker Avance III HD with Prodigy Cryoprobe, a 400 MHz Bruker Avance Neo, or Varian Inova 500 MHz spectrometers. All ^{1}H NMR spectra are reported in δ units, parts per million (ppm), and were measured relative to the signals for residual chloroform (7.26 ppm), dichloromethane (5.32 ppm), methanol (3.31 ppm), acetone (2.05 ppm), toluene (2.08 ppm), or acetonitrile (1.94 ppm) in deuterated solvent. All ^{13}C NMR spectra were measured in deuterated solvents and are reported in ppm relative to the signals for chloroform (77.16 ppm). Multiplicity and qualifier abbreviations are as follows: s = singlet, d = doublet, t = triplet, q = quartet, dd = doublet of doublets, dq = doublet of quartets, ABq = AB quartet, m = multiplet, bs = broad singlet.

High resolution mass spectra (HRMS) were analyzed by direct infusion electrospray ionization (ESI) in the positive ion mode using a Waters LCT Premier XE time-of-flight (TOF) mass spectrometer operated in the V mode. The instrument was externally calibrated with NaI clusters.

Analytical gel permeation chromatography (GPC) was performed using an Agilent 1260 series pump equipped with two Agilent PLgel MIXED-B columns (7.5 x 300 mm), a Wyatt 18-angle DAWN HELEOS light scattering detector, and an Optilab rEX differential refractive index detector. The mobile phase was THF at a flow rate of 1 mL/min. Molecular weights and molecular weight distributions were calculated by light scattering using a dn/dc value of 0.062 mL/g (25 °C) for poly(methyl acrylate). Refractive index increment (dn/dc) values were determined for each injection based on known sample concentration and assuming 100% mass elution.

Photoluminescence spectra were recorded on a Shimadzu RF-6000 spectrofluorophotometer using a quartz microcuvette (Starna Cells 18F-Q-10-GL14-C, 10 x 2 mm).

Ultrasound experiments were performed inside of a sound abating enclosure using a 500 watt Vibra Cell 505 liquid processor (20 kHz) equipped with a 0.5-inch diameter solid probe (part #630-0217), sonochemical adapter (part #830-00014), and a Suslick reaction vessel made by the Caltech glass shop (analogous to vessel #830-00014 from Sonics and Materials).

5.3 Synthetic Details

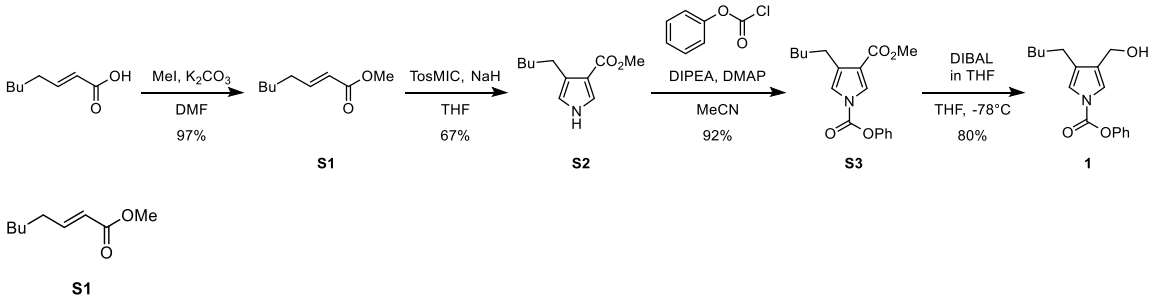

S1

Methyl (*E*)-oct-2-enoate (S1). A flame-dried round bottom flask equipped with a stir bar was charged with (*E*)-oct-2-enoic acid (18.8 g, 0.132 mol), methyl iodide (14 mL, 0.22 mol) and 60 mL of DMF under N_2. Potassium carbonate (36.6 g, 0.265 mol) was then added to the mixture at 0 °C in an ice bath, and the reaction was allowed to warm to room temperature, and stirred for 7 hours. Upon completion, the reaction mixture was diluted with Et_2O (100 mL) and washed with $NaHCO_3$ (3 x 150 mL) and brine (150 mL). The organic layer was dried over $MgSO_4$, filtered, and concentrated under reduced pressure to yield the title compound as a colorless oil (20 g, 97%). ^{1}H NMR (400 MHz, $CDCl_3$) δ: 7.03 – 6.91 (m, 1H), 5.89 – 5.77 (m, 1H), 3.72 (s, 3H), 2.24 – 2.13 (m, 2H), 1.50 – 1.40 (m, 2H), 1.38 – 1.24 (m, 4H), 0.95 – 0.84 (m, 3H) ppm.^{13}C{^{1}H} NMR (100 MHz, $CDCl_3$) δ: 167.4, 150.0, 120.9, 51.5, 32.3, 31.4, 27.8, 22.6, 14.1 ppm. Spectrum matches literature report.[20]

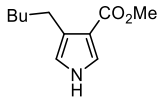

S2

Methyl 4-pentyl-1*H*-pyrrole-3-carboxylate (S2). A flame-dried round bottom flask equipped with a stir bar was charged with 60% NaH dispersed in mineral oil (10.2 g, 128 mmol) and THF (80 mL) and cooled to 0 °C in an ice bath. A solution of **S1** (20.0 g, 128 mmol) and toluenesulfonylmetyl isocyanide (25.0 g, 128 mmol) in THF (100 mL) was then added dropwise via addition funnel over 35 mins. After addition, the reaction was warmed to room temperature and stirred for another hour before being diluted with EtOAc (150 mL). The crude mixture was washed with $NaHCO_3$ (3 x 300 mL) and brine (300 mL), and the organic layer was dried over $MgSO_4$, filtered, and concentrated under reduced pressure. The crude mixture was purified by column chromatography (15–35% EtOAc/Hexanes) to yield the title compound as a white solid (16.8 g, 67% yield). ^{1}H NMR (400 MHz, $CDCl_3$) δ: 8.25 (bs, 1H), 7.40 – 7.34 (m, 1H), 6.57 – 6.52 (m, 1H), 3.79 (s, 3H), 2.76 – 2.59 (m, 2H), 1.62 – 1.54 (m, 2H), 1.43 – 1.27 (m, 4H), 0.96 – 0.83 (m, 3H) ppm.^{13}C{^{1}H} NMR (100 MHz, $CDCl_3$) δ: 165.8, 126.8, 124.5, 116.7, 114.2, 50.8, 32.0, 30.2, 26.2, 22.7, 14.3 ppm. HRMS (FI, *m/z*): calcd for $[C_{11}H_{18}NO_2]^+$ $(M+H)^+$, 196.1332; found, 196.1347.

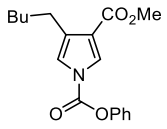

S3

3-methyl 1-phenyl 4-pentyl-1*H*-pyrrole-1,3-dicarboxylate (S3). A round bottom flask equipped with a stir bar was charged with **S2** (17 g, 86 mmol), DMAP (1.0 g, 86 mmol), and MeCN (700 mL). The solution was cooled to 0 °C in an ice bath before adding phenyl chloroformate (11.9 mL, 94.5 mmol) then DIPEA (16.5 mL, 94.5 mmol) dropwise. The mixture was slowly warmed to room temperature and stirred for 6 h before being diluted with EtOAc (200 mL), washed with $NaHCO_3$ (3 x 800 mL) and brine (800 mL), and the organic layer was dried over Na_2SO_4, filtered, and concentrated under reduced pressure. The crude mixture was purified by column chromatography (0–5% EtOAc/Hexanes) to yield the title compound as a waxy white solid (25 g, 92% yield). ^{1}H NMR (400 MHz, $CDCl_3$) δ: 7.99 (d, J = 2.4 Hz, 1H), 7.48 – 7.42 (m, 2H), 7.35 – 7.29 (m, 1H), 7.25 – 7.21 (m, 2H), 7.18 –

7.15 (m, 1H), 3.84 (s, 3H), 2.82 – 2.58 (m, 2H), 1.72 – 1.58 (m, 2H), 1.43 – 1.29 (m, 4H), 1.00 – 0.84 (m, 3H) ppm. $^{13}C\{^{1}H\}$ NMR (100 MHz, $CDCl_3$) δ: 164.7, 150.3, 148.4, 129.9, 129.8, 126.9, 126.4, 121.3, 119.1, 118.4, 51.4, 31.8, 29.4, 26.1, 22.7, 14.2 ppm. HRMS (ESI, *m/z*): calcd for $[C_{18}H_{22}NO_4]^+$ $(M+H)^+$, 316.1543; found, 316.1535.

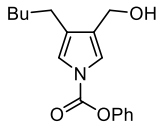

1

Phenyl 3-(hydroxymethyl)-4-pentyl-1*H*-pyrrole-1-carboxylate (1). A round bottom flask equipped with a stir bar was charged with **S3** (3.63 g, 11.5 mmol), and THF (15 mL). The solution was cooled to -78 °C in an acetone/dry ice bath before adding 1.0 M DIBAL in THF (44 mL, 44 mmol) dropwise. The mixture was stirred at -78 °C overnight, before quenching with EtOAc (10 mL) at -78 °C and warming the mixture to room temperature. Rochelle salt solution (10% in water, 100 mL) was then added to the mixture and stirred for 30 mins. The mixture was then extracted with Et_2O (3 x 100 mL), and the organic phase was combined, washed with water (2 x 500 mL) and brine (500 mL). The organic layer was dried over $MgSO_4$, filtered, and concentrated under reduced pressure. The crude mixture was purified by column chromatography (0–50% Acetone/Hexanes) to yield the title compound as a colorless oil (2.6 g, 80% yield). The product was purged with nitrogen and kept in the glove box freezer. Product could slowly degrade over a few months which hinders the following polymerization step. It is recommended to purify the monomer via column again prior to polymerization. ^{1}H NMR (400 MHz, $CDCl_3$) δ: 7.99 (d, J = 2.4 Hz, 1H), 7.49 – 7.41 (m, 2H), 7.35 – 7.28 (m, 1H), 7.26 – 7.21 (m, 2H), 7.18 – 7.13 (m, 1H), 3.84 (s, 3H), 2.75 – 2.67 (m, 2H), 1.66 – 1.57 (m, 2H), 1.42 – 1.34 (m, 4H), 0.93 – 0.87 (m, 3H) ppm. $^{13}C\{^{1}H\}$ NMR (100 MHz, $CDCl_3$) δ: 150.5, 148.9, 129.8, 128.4, 128.0, 126.6, 121.5, 118.8, 118.0, 57.4, 31.8, 29.4, 25.2, 22.7, 14.2 ppm. HRMS (ESI, *m/z*): calcd for $[C_{17}H_{20}NO_2]^+$ $(M-OH)^+$, 270.1489; found, 270.1485.

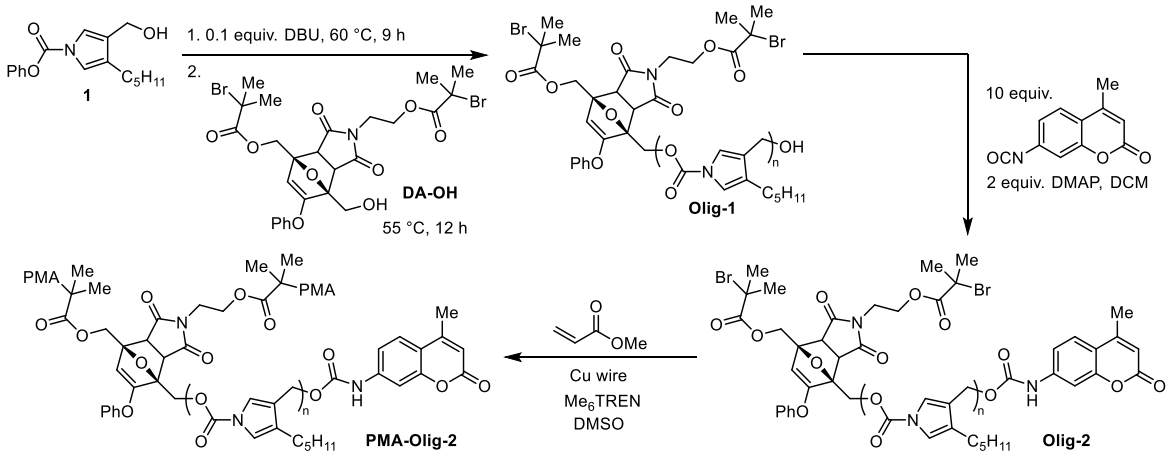

Olig-1. All reagents were kept in the glovebox in a nitrogen environment. DBU was distilled and kept with 4Å molecular sieves in the glove box. A 1-dram vial equipped with a stir bar was charged with monomer **1** (100 mg, 0.34 mmol) and DBU (5.2 μL, 0.034 mmol) in the glove box. THF (0.34 mL) was then added and the vial was sealed with a septum cap. The vial was then heated to 60 °C for 9 hours in an oil bath outside of the glove box before cooling to room temperature and brought back into the glove box. (2-(2-((2-bromo-2-methylpropanoyl)oxy)ethyl)-7-(hydroxymethyl)-1,3-dioxo-6-phenoxy-1,2,3,3a,7,7a-hexahydro-4H-4,7-epoxyisoindol-4-yl)methyl 2-bromo-2-methylpropanoate[21] (220 mg, 0.34 mmol) was then added with 0.17 mL THF in the glove box and ensured full solubility of all solids. The mixture was then heated in an oil bath at 55 °C for 12 hours. After reaction had completed, the reaction was cooled to room temperature and opened to air. It was diluted with THF, precipitated into MeOH x2, collected with centrifugation and dried under reduced pressure before being analyzed with NMR and GPC-MALS. The title oligomer was collected as a white solid (30 mg, 42 %yield).

Olig-2. To a 1-dram vial equipped with a stir bar, **Olig-1** (30 mg, 0.0041 mmol) and **CoumNCO** (10 mg, 0.05 mmol) were dissolved in DCM (1 mL) before DMAP (1 mg, 0.008 mmol) was added. The solution was stirred at room temperature for 1 hour upon which reaction was complete as determined by crude NMR. The reaction was then diluted with DCM, precipitated into MeOH x2, collected with centrifugation and dried under reduced pressure before being analyzed with NMR and GPC-MALS. The title product was collected as a white solid (23 mg, 77% yield)

PMA-Olig-2. The synthesis of **PMA** was carried out according to the literature procedure.[21] A freshly cut copper wire (1.1 cm length, 20 gauge) was soaked in 1 M HCl for approximately 5 min and then rinsed thoroughly with DI water and acetone, and then allowed to dry in air. A 10 mL Schlenk flask equipped with a stir bar was charged with the initiator **Olig-2** (10.0 mg, 0.00122 mmol), methyl acrylate (0.2 mL, 2 mmol), Me_6TREN (0.8 μL, 0.0029mmol), DMSO (0.2 mL), and THF (0.1 mL). The mixture was gently heated to dissolve **Olig-2**. The flask was sealed and the solution was deoxygenated via three freeze-pump-thaw cycles, and then backfilled with nitrogen. The flask was opened briefly under a strong flow of nitrogen, and the copper wire was added on top of the frozen mixture. The flask was resealed, evacuated for an additional 15 min, warmed to room temperature, and then backfilled with nitrogen. The reaction mixture was stirred at room temperature until the solution became sufficiently viscous, indicating that the desired monomer conversion was reached (2 h). The flask was then opened to air and the solution was diluted with DCM. The polymer was precipitated into cold methanol (2x) and was thoroughly dried under vacuum to provide a tacky white (25.6 mg, 13.5%) and characterized by GPC-MALS. Molar mass characterization data are reported in Figure 5.4.

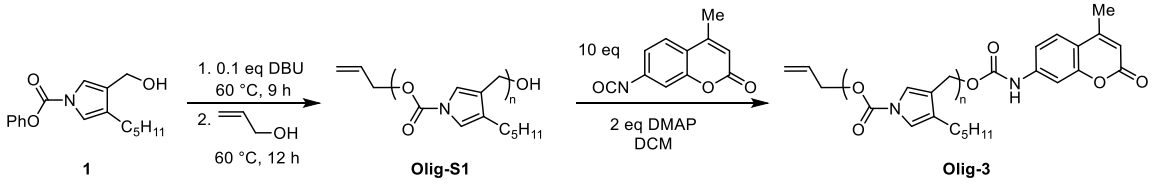

Olig-S1. Olig-S1 was synthesized following the procedure for **Olig-1,** with monomer **1** (143 mg, 0.500 mmol), DBU (7.5 μL, 0.050 mmol), THF (0.5 mL), and allyl alcohol (34 μL, 0.50 mmol). The title oligomer was collected as a white solid (18 mg, 18% yield).

Olig-3. Olig-3 was synthesized following the procedure for **Olig-2,** with **Olig-S1** (17.0 mg, 0.0071 mmol), **CoumNCO** (10 mg, 0.05 mmol), DCM (1 mL), and DMAP (1 mg, 0.008 mmol). The title product was collected as a white solid (20.2 mg, quant.)

5.4 Sonication Experiments and Fluorescence Spectroscopy

An oven-dried sonication vessel was fitted with rubber septa, placed onto the sonication probe, and allowed to cool under a stream of dry argon. The vessel was charged with a solution of the polymer in anhydrous THF/methanol (3:1 v/v, 0.5 mg/mL, 20 mL) and

submerged in an ice bath. The solution was sparged continuously with argon beginning 20 min prior to sonication and for the duration of the sonication experiment. Pulsed ultrasound (1 s on/1 s off, 30% amplitude, 20 kHz, 13.9 W/cm^2) was then applied to the system. The solution temperature during sonication was measured to be 9–13 °C. Sonicated solutions were filtered through a 0.45 μm syringe filter prior to analysis. Ultrasonic intensity was calibrated using the method described by Berkowski *et al.*[22]

5.5 Characterization of Cargo Release Using Photoluminescence Spectroscopy

Aliquots were removed during sonication experiments and characterized using photoluminescence spectroscopy to quantify release of aminocoumarin (**CoumNH$_2$**). Samples were first allowed to incubate for 28 hours, after which the fluorescence emission reached a plateau indicating complete conversion of the intermediate furfuryl carbamate. Emission spectra were recorded using an excitation wavelength of 365 nm. A standard calibration curve was constructed using the emission maximum at 424 nm to determine the concentration of **CoumNH$_2$** (Figure 5.9, 5.10).

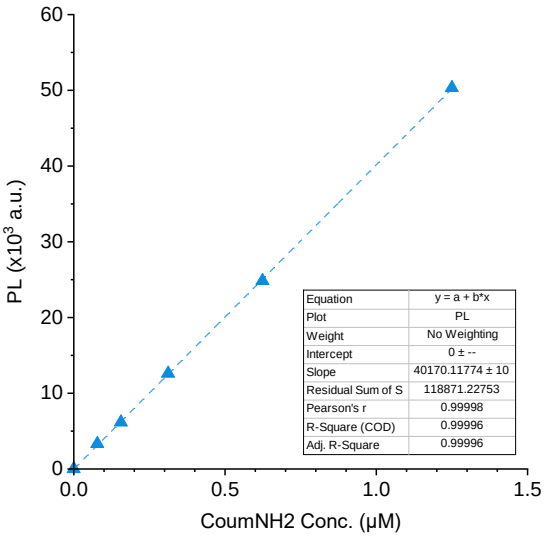

Figure 5.9. Calibration curve for experimental determination of the concentration of 7-amino-4-methylcoumarin (**CoumNH$_2$**) (λ_{ex} = 365 nm slit width = 5 nm, λ_{em} = 424 nm slit width = 5 nm) in THF/methanol (3:1 v/v). A linear regression of the data gives the calibration function Y = 40170X.

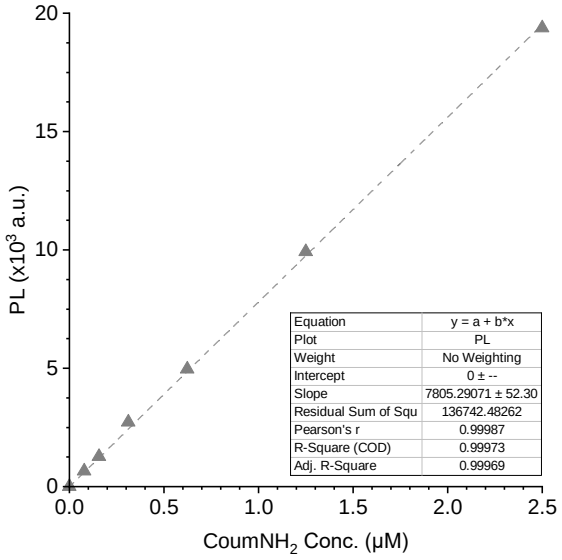

Figure 5.10. Calibration curve for experimental determination of the concentration of 7-amino-4-methylcoumarin (**CoumNH$_2$**) with 5.3 μM of Pd(PPh$_3$)$_4$ added to each sample (λ_{ex} = 365 nm slit width = 5 nm, λ_{em} = 424 nm slit width = 3 nm) in THF/methanol (3:1 v/v). A linear regression of the data gives the calibration function Y = 7805X.

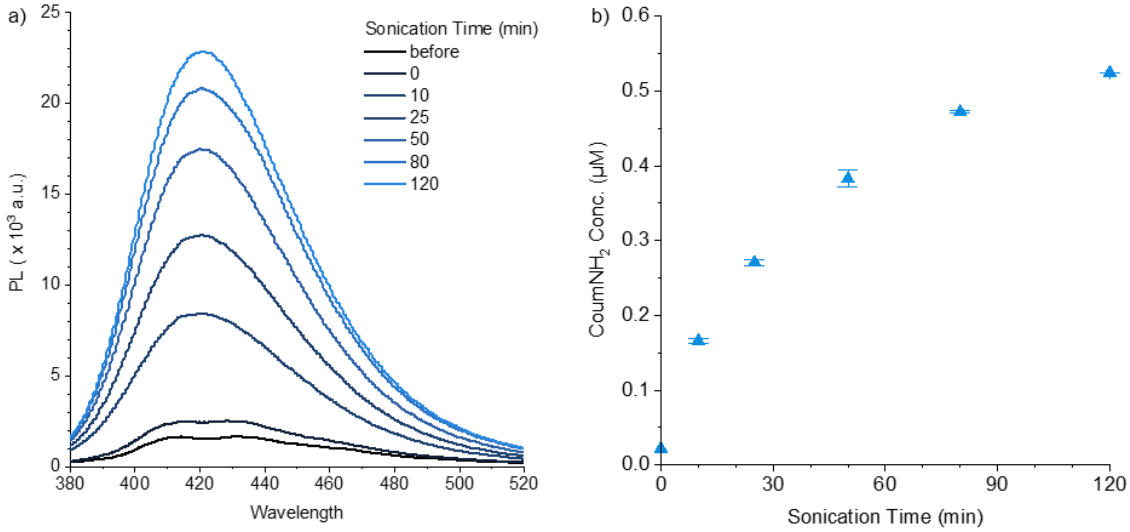

Figure 5.11. a) Representative PL spectra characterizing the release of **CoumNH$_2$** from a 0.5 mg/mL (5.3 μM) solution of **PMA-Olig-2** in THF/methanol (3:1 v/v). λ_{ex} = 365 nm. b) Concentration of **CoumNH$_2$** released from **PMA-Olig-2** as a function of sonication time calculated from the fluorescence intensity at 424 nm using the calibration curve Figure 5.9. The theoretical concentration of **CoumNH$_2$** based on 100% release from the mechanophore is 5.3 μM. Each data point is the average of two replicate measurements with the error bar denoting the range of the two values.

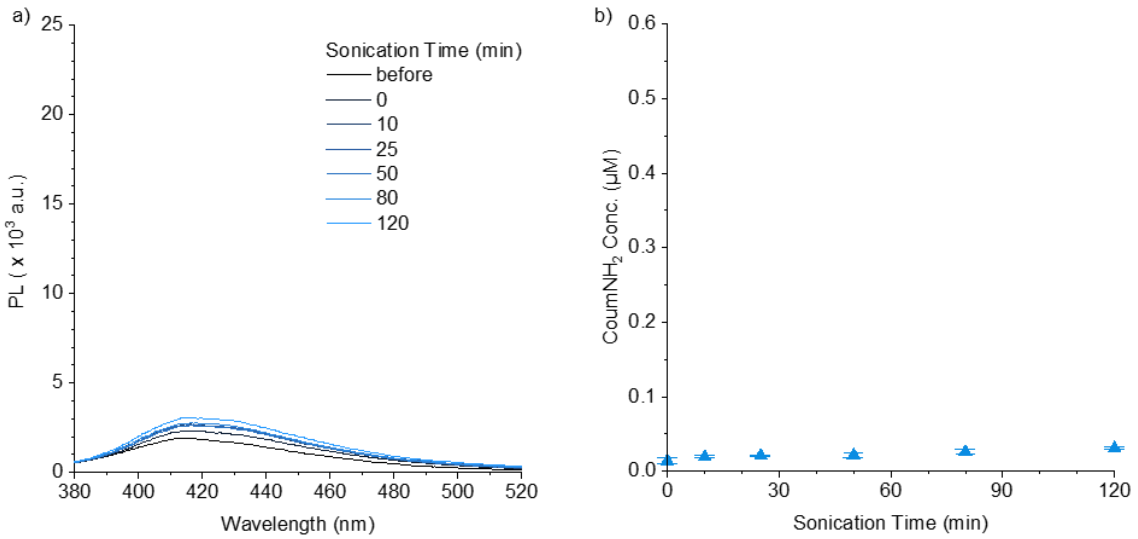

Figure 5.13. a) Representative PL spectra characterizing the release of **CoumNH$_2$** from a 0.037 mg/mL solution of **Olig-2** in THF/methanol (3:1 v/v). λ_{ex} = 365 nm. b) Concentration of **CoumNH$_2$** released from **Olig-2** as a function of sonication time calculated from the fluorescence intensity at 424 nm using the calibration curve Figure 5.9. The theoretical concentration of **CoumNH$_2$** based on 100% release from the mechanophore is 5.0 μM. Each data point is the average of two replicate measurements with the error bar denoting the range of the two values.

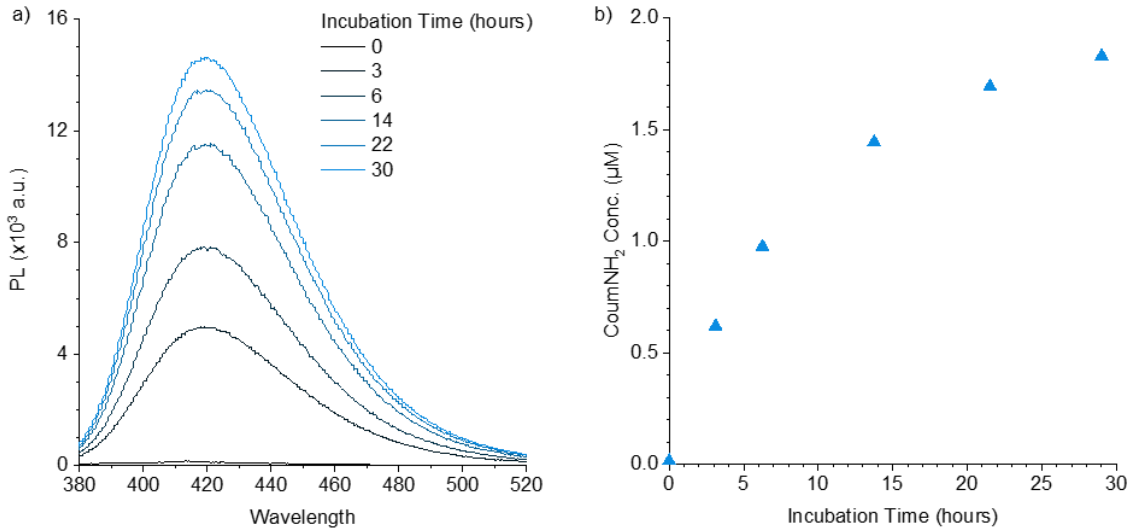

Figure 5.14. a) Representative PL spectra characterizing the release of **CoumNH$_2$** from a 5.3 μM solution of **Olig-3** in THF/methanol (3:1 v/v) with 5.3 μM Pd(PPh$_3$)$_4$ added. λ_{ex} = 365 nm. b) Concentration of **CoumNH$_2$** released from **Olig-3** as a function of sonication time calculated from the fluorescence intensity at 424 nm using the calibration curve Figure 5.10. The theoretical concentration of **CoumNH$_2$** based on 100% release from the mechanophore is 5.3 μM.

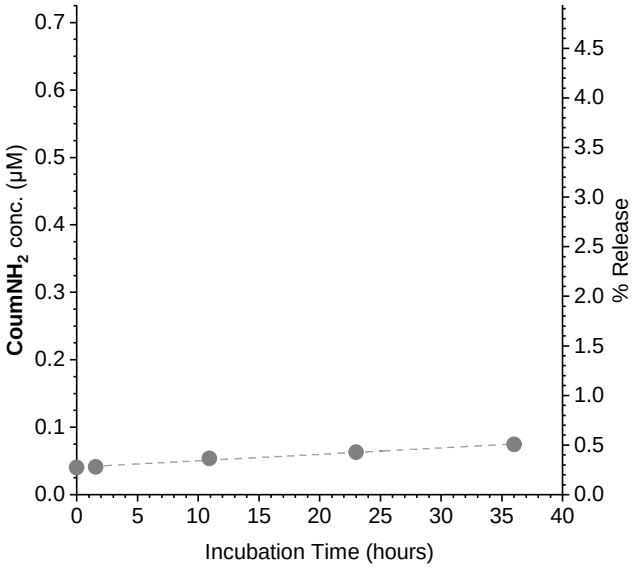

Figure 5.16. Concentration of **$CoumNH_2$** released as a function of time from unsonicated **Olig-2** (14.8 μM) incubated in 3:1 THF/MeOH at room temperature. After 36 hours, 0.5% of **$CoumNH_2$** is liberated presumably due to background hydrolysis.

5.6 References

(1) Sagi, A.; Weinstain, R.; Karton, N.; Shabat, D. Self-Immolative Polymers. *J. Am. Chem. Soc.* **2008**, *130*, 5434–5435.

(2) Scrimin, P.; Prins, L. J. Sensing through signal amplification. *Chem. Soc. Rev.* **2011**, *40*, 4488.

(3) Peterson, G. I.; Larsen, M. B.; Boydston, A. J. Controlled Depolymerization: Stimuli-Responsive Self-Immolative Polymers. *Macromolecules* **2012**, *45*, 7317–7328.

(4) Yardley, R. E.; Kenaree, A. R.; Gillies, E. R. Triggering Depolymerization: Progress and Opportunities for Self-Immolative Polymers. *Macromolecules* **2019**, *52*, 6342–6360.

(5) Deng, Z.; Gillies, E. R. Emerging Trends in the Chemistry of End-to-End Depolymerization. *JACS Au* **2023**, *3*, 2436–2450.

(6) Li, J.; Nagamani, C.; Moore, J. S. Polymer Mechanochemistry: From Destructive to Productive. *Acc. Chem. Res.* **2015**, *48*, 2181–2190.

(7) Zhang, Y.; Yu, J.; Bomba, H. N.; Zhu, Y.; Gu, Z. Mechanical Force-Triggered Drug Delivery. *Chem. Rev.* **2016**, *116*, 12536–12563.

(8) Chen, Y.; Mellot, G.; Luijk, D. van; Creton, C.; Sijbesma, R. P. Mechanochemical tools for polymer materials. *Chem. Soc. Rev.* **2021**, *50*, 4100–4140.

(9) Stratigaki, M.; Göstl, R. Methods for Exerting and Sensing Force in Polymer Materials Using Mechanophores. *ChemPlusChem* **2020**, cplu.201900737.

(10) Versaw, B. A.; Zeng, T.; Hu, X.; Robb, M. J. Harnessing the Power of Force: Development of Mechanophores for Molecular Release. *J. Am. Chem. Soc.* **2021**, *143*, 21461–21473.

(11) Lloyd, E. M.; Vakil, J. R.; Yao, Y.; Sottos, N. R.; Craig, S. L. Covalent Mechanochemistry and Contemporary Polymer Network Chemistry: A Marriage in the Making. *J. Am. Chem. Soc.* **2023**, *145*, 751–768.
(12) Chen, Y.; Sanoja, G.; Creton, C. Mechanochemistry unveils stress transfer during sacrificial bond fracture of tough multiple network elastomers. *Chem. Sci.* **2021**, *12*, 11098–11108.
(13) Yao, Y.; McFadden, M. E.; Luo, S. M.; Barber, R. W.; Kang, E.; Bar-Zion, A.; Smith, C. A. B.; Jin, Z.; Legendre, M.; Ling, B.; Malounda, D.; Torres, A.; Hamza, T.; Edwards, C. E. R.; Shapiro, M. G.; Robb, M. J. Remote control of mechanochemical reactions under physiological conditions using biocompatible focused ultrasound. *Proc. Nat. Acad. Sci. USA* **2023**, *120*, DOI: 10.1073/pnas.2309822120.
(14) Diesendruck, C. E.; Peterson, G. I.; Kulik, H. J.; Kaitz, J. A.; Mar, B. D.; May, P. A.; White, S. R.; Martínez, T. J.; Boydston, A. J.; Moore, J. S. Mechanically triggered heterolytic unzipping of a low-ceiling-temperature polymer. *Nature Chemistry* **2014**, *6*, 623–628.
(15) Peterson, G. I.; Boydston, A. J. Kinetic Analysis of Mechanochemical Chain Scission of Linear Poly(phthalaldehyde). *Macromol. Rapid Commun.* **2014**, *35*, 1611–1614.
(16) Hu, X.; Zeng, T.; Husic, C. C.; Robb, M. J. Mechanically Triggered Small Molecule Release from a Masked Furfuryl Carbonate. *J. Am. Chem. Soc.* **2019**, *141*, 15018–15023.
(17) Zeng, T.; Hu, X.; Robb, M. J. 5-Aryloxy substitution enables efficient mechanically triggered release from a synthetically accessible masked 2-furylcarbinol mechanophore. *Chem. Commun.* **2021**, *57*, 11173–11176.
(18) Hu, X.; Zeng, T.; Husic, C. C.; Robb, M. J. Mechanically Triggered Release of Functionally Diverse Molecular Payloads from Masked 2-Furylcarbinol Derivatives. *ACS Cent. Sci.* **2021**, *7*, 1216–1224.
(19) Kim, H.; Brooks, A. D.; DiLauro, A. M.; Phillips, S. T. Poly(carboxypyrrole)s That Depolymerize from Head to Tail in the Solid State in Response to Specific Applied Signals. *J. Am. Chem. Soc.* **2020**, *142*, 9447–9452.
(20) Hatridge, T. A.; Liu, W.; Yoo, C.; Davies, H. M. L.; Jones, C. W. Optimized Immobilization Strategy for Dirhodium(II) Carboxylate Catalysts for C−H Functionalization and Their Implementation in a Packed Bed Flow Reactor. *Angew Chem Int Ed* **2020**, *59*, 19525–19531.
(21) Hu, X.; Zeng, T.; Husic, C. C.; Robb, M. J. Mechanically Triggered Release of Functionally Diverse Molecular Payloads from Masked 2-Furylcarbinol Derivatives. *ACS Cent. Sci.* **2021**, *7*, 1216–1224.
(22) Berkowski, K. L.; Potisek, S. L.; Hickenboth, C. R.; Moore, J. S. Ultrasound-Induced Site-Specific Cleavage of Azo-Functionalized Poly(ethylene glycol). *Macromolecules* **2005**, *38*, 8975–8978.

5.7 ^{1}H and ^{13}C NMR spectra

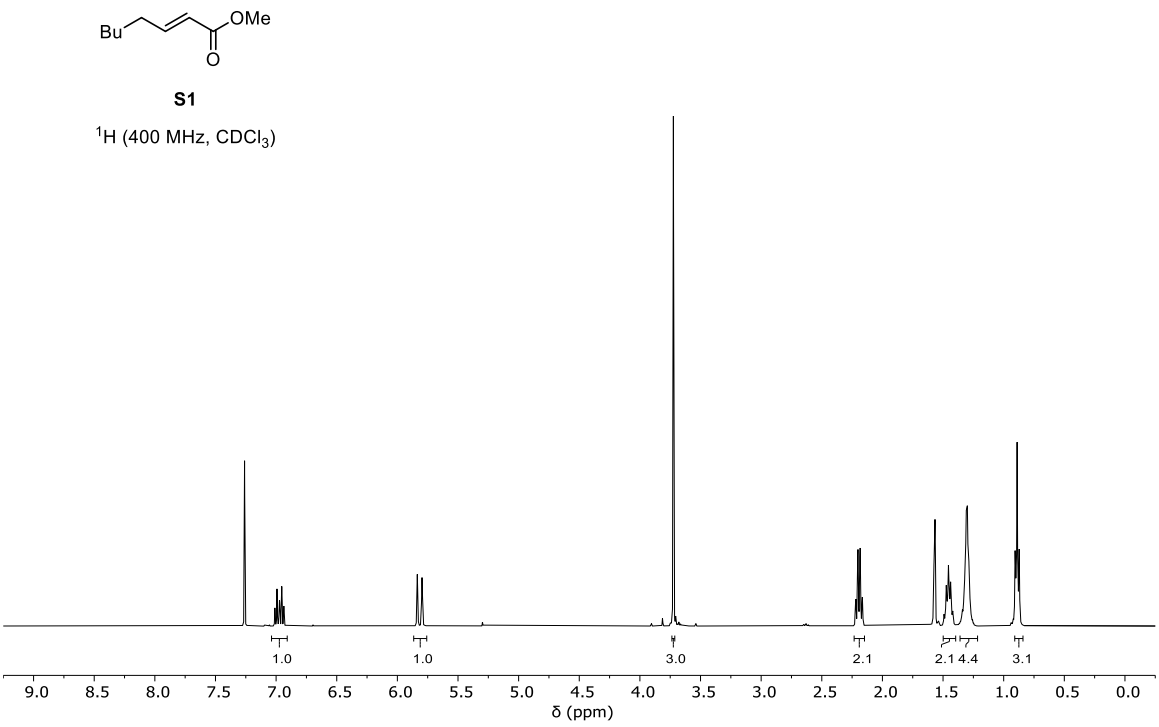

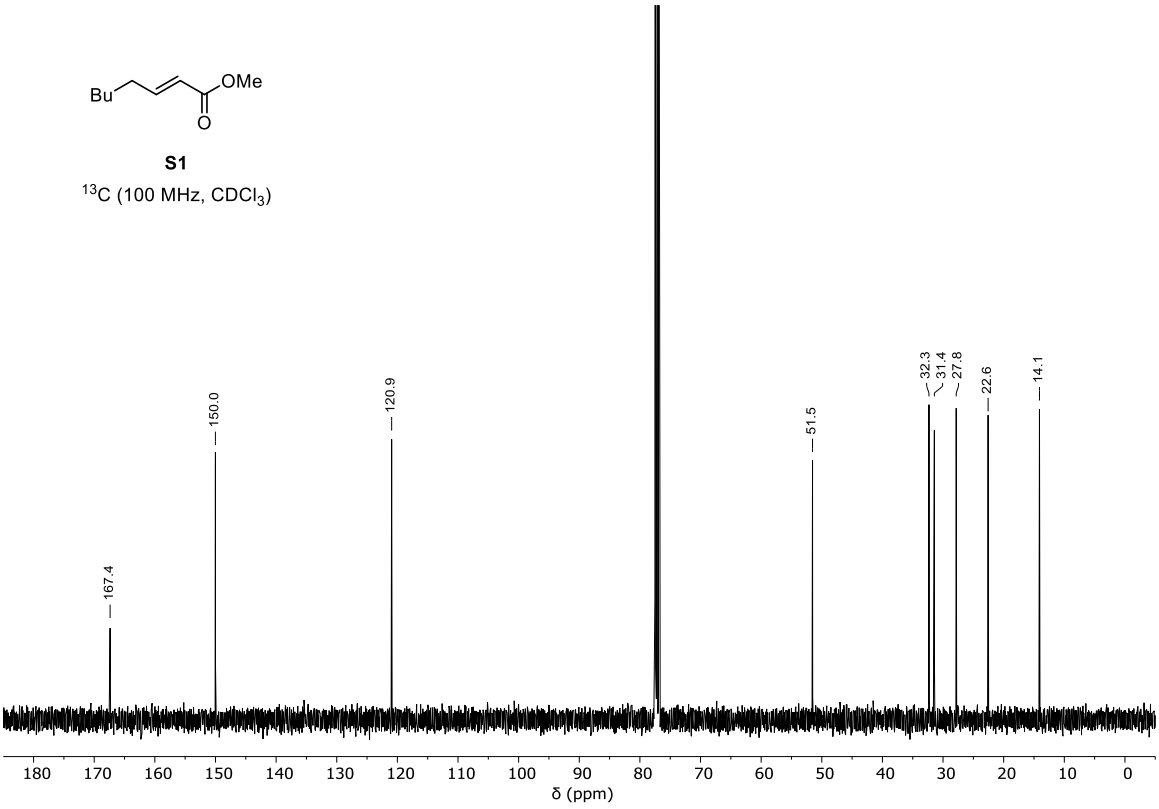

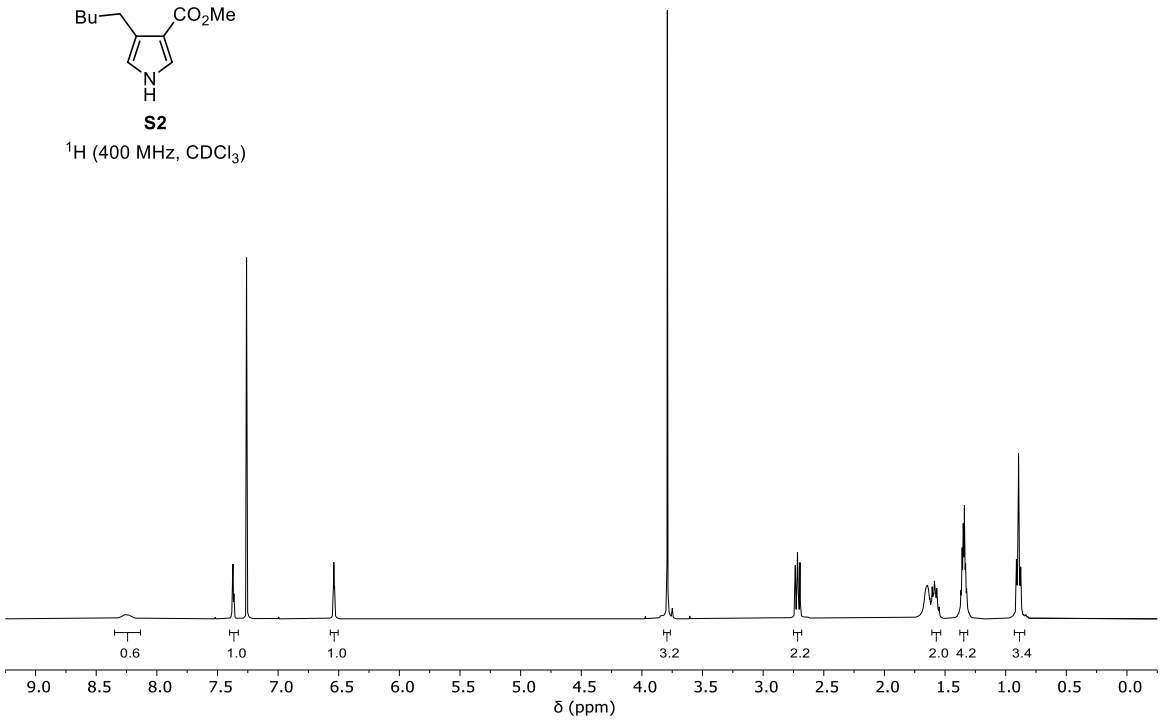
Bu
CO2Me
N
H
S2
1H (400 MHz, CDCl3)
0.6
1.0
1.0
3.2
2.2
2.0
4.2
3.4
9.0 8.5 8.0 7.5 7.0 6.5 6.0 5.5 5.0 4.5 4.0 3.5 3.0 2.5 2.0 1.5 1.0 0.5 0.0
δ (ppm)

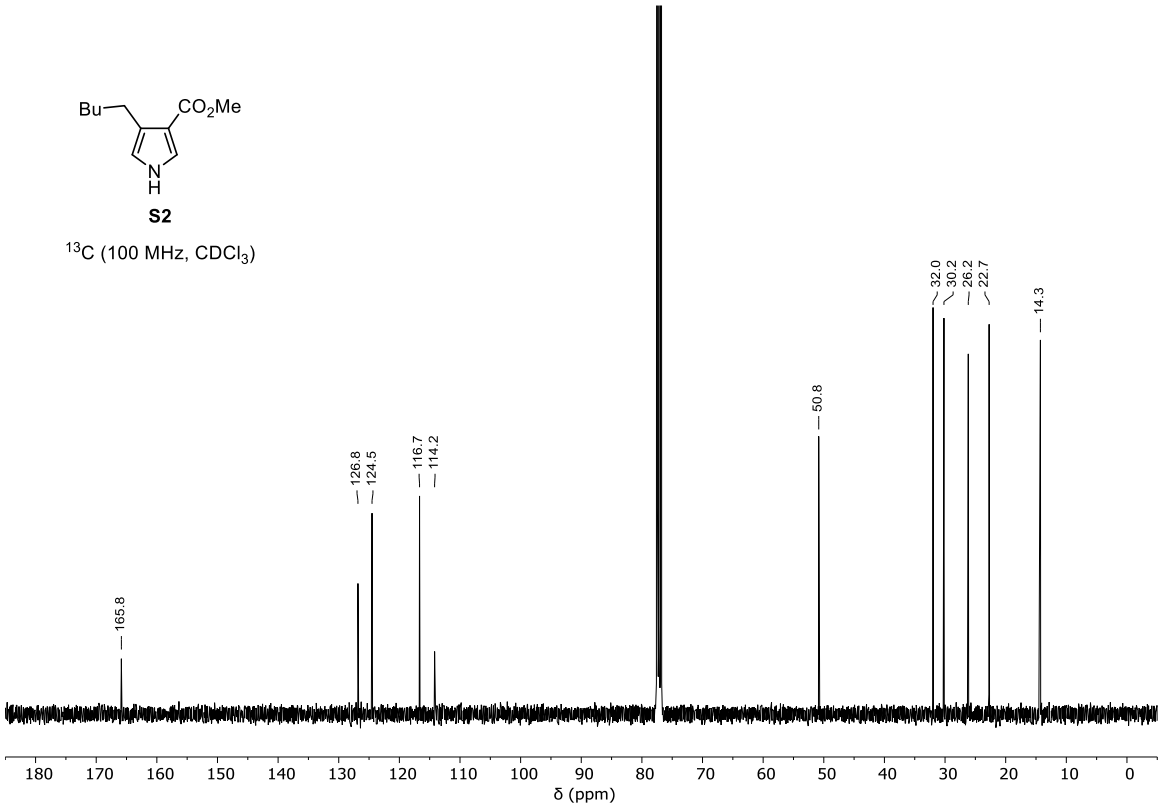
Bu
CO2Me
N
H
S2
13C (100 MHz, CDCl3)
165.8
126.8
124.5
116.7
114.2
50.8
32.0
30.2
26.2
22.7
14.3
180 170 160 150 140 130 120 110 100 90 80 70 60 50 40 30 20 10 0
δ (ppm)

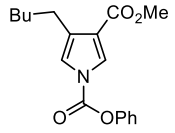

S3

^{1}H (400 MHz, $CDCl_3$)

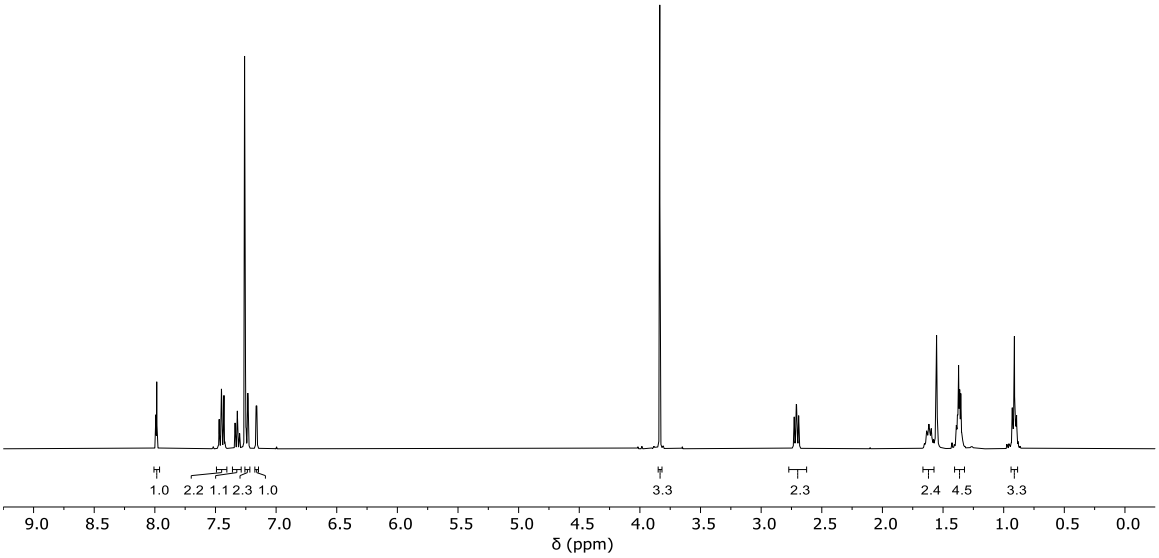

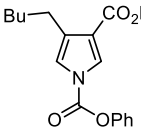

S3

^{13}C (100 MHz, $CDCl_3$)

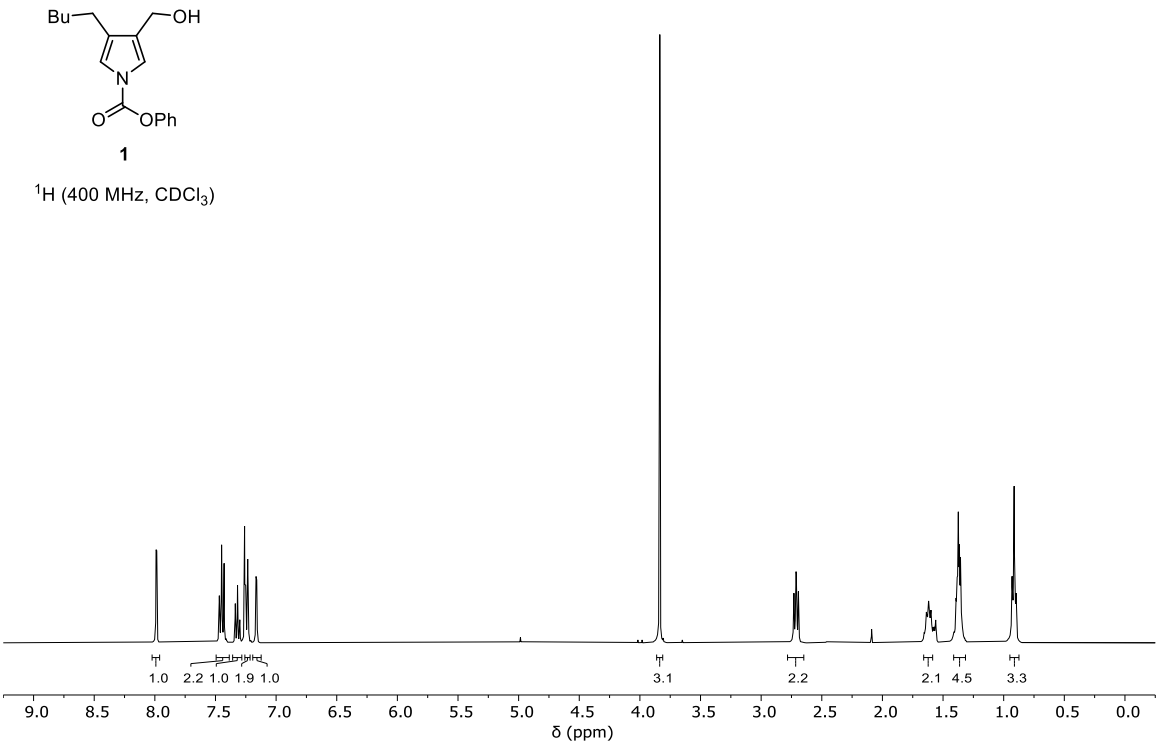
Bu
OH
N
O
OPh
1
1H (400 MHz, CDCl3)
1.0 2.2 1.0 1.9 1.0
3.1
2.2
2.1 4.5
3.3
δ (ppm)

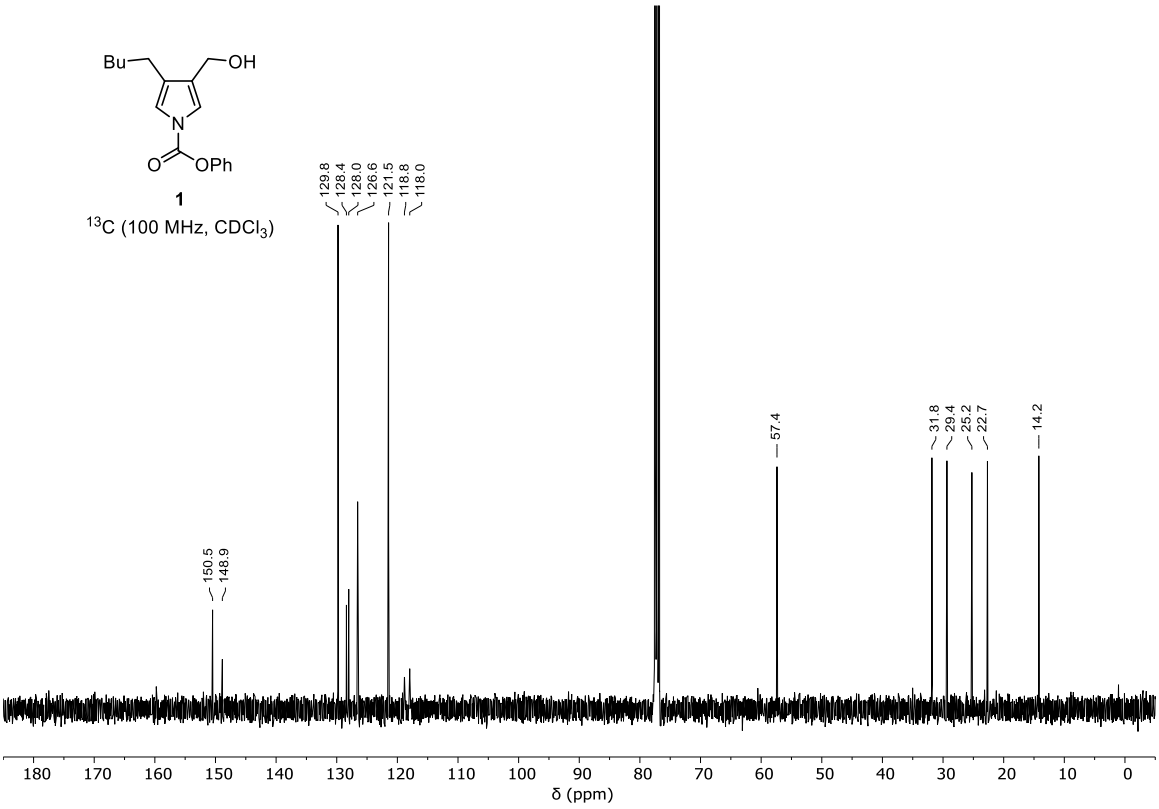
Bu
OH
N
O
OPh
1
13C (100 MHz, CDCl3)
129.8
128.4
128.0
126.6
121.5
118.8
118.0
150.5
148.9
57.4
31.8
29.4
25.2
22.7
14.2
δ (ppm)